

N76-26056

NASA SP-389

X-RAY BINARIES

CASE FILE
COPY

A symposium held at
GODDARD SPACE FLIGHT CENTER
Greenbelt, Maryland
October 20-22, 1975



NATIONAL AERONAUTICS AND SPACE ADMINISTRATION

X-RAY BINARIES

The proceedings of a symposium held at
NASA's Goddard Space Flight Center, Greenbelt, Maryland,
October 20-22, 1975, and associated with
a coordinated campaign (I.A.U. Commissions 42 and 44)
to observe X-ray binaries

Prepared at Goddard Space Flight Center



Scientific and Technical Information Office

NATIONAL AERONAUTICS AND SPACE ADMINISTRATION

1976
Washington, D.C.

The requirement for the use of the International System of Units (SI) has been waived for this document under the authority of NPD 2220.4, paragraph 5.d.

For sale by the National Technical Information Service
Springfield, Virginia 22161
Price - \$17.25

P R E F A C E

This publication of proceedings presents workshop papers in the order of topics on the agenda of the symposium. Introductory and/or summarizing comments by each panel chairman are given at the beginning of the collection of papers from the corresponding panel. Those brief remarks by workshop participants which were submitted in written form are grouped together for each panel and presented after the collection of associated papers. The many comments and questions not exhibited here are covered, to a large extent, by the reviews given by panel chairmen.

Most of the formal presentations at the symposium are represented in this publication of the proceedings either by self-contained papers or by abstracts. Some of the major contributions to the general sessions opening and closing the workshop are not represented here, but involved material which may be found in papers included under the specialized panels.

Elihu Boldt
Goddard Space Flight Center

Yoji Kondo
Johnson Space Center



SCIENTIFIC ORGANIZING COMMITTEE

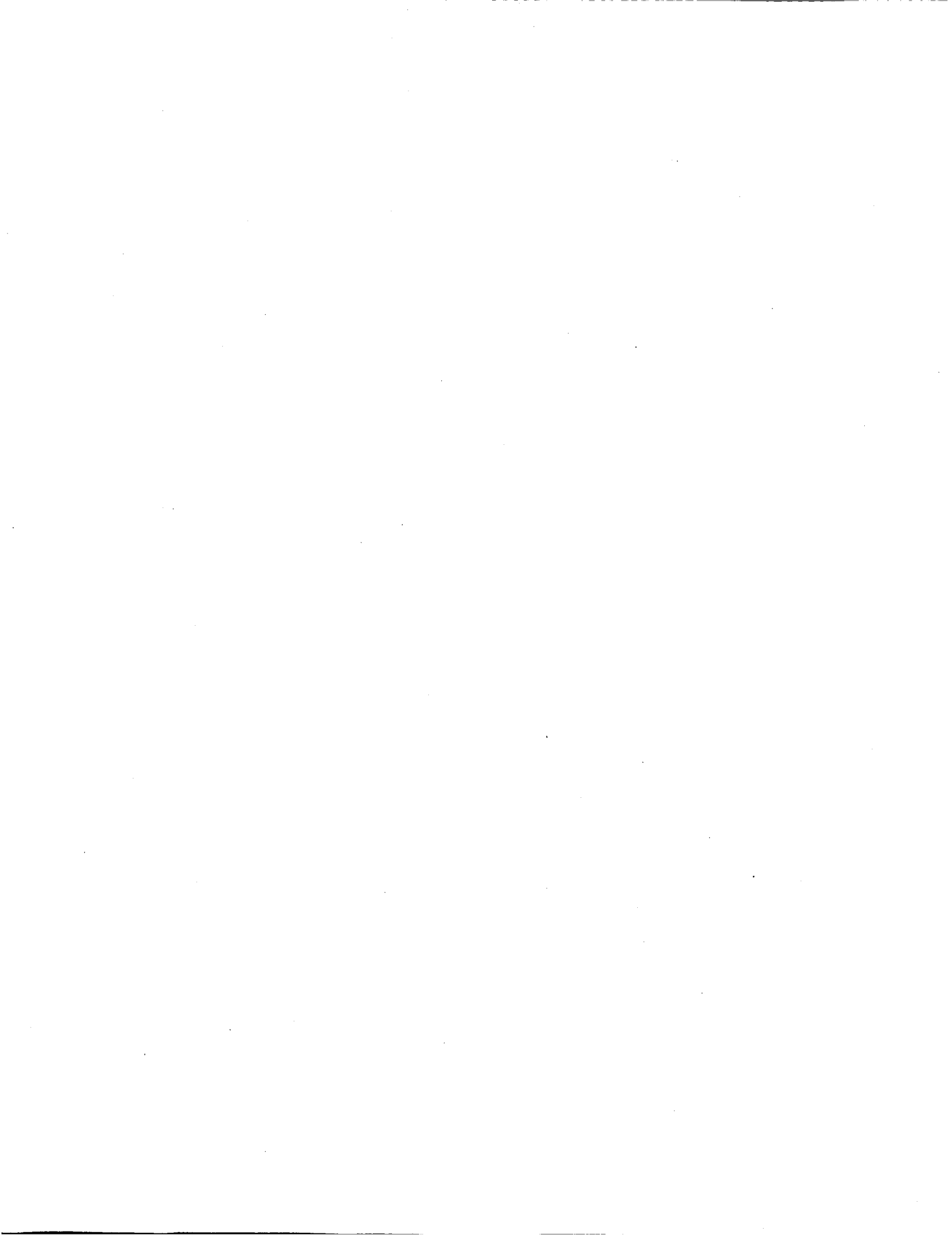
J. N. Bahcall, Institute for Advanced Study	H. Gursky, Center for Astrophysics
E. A. Boldt**, Goddard Space Flight Center	M. Hack, Osservatorio Astronomico (Trieste)
A. C. Brinkman, Space Research Laboratory (Utrecht)	T. Herczeg, University of Oklahoma
G. W. Clark, Massachusetts Institute of Technology	J. B. Hutchings, Dominion Astrophysical Observatory (Victoria)
A. D. Code, University of Wisconsin	M. Kitamura, Tokyo Astronomical Observatory
J. L. Culhane, University College (London)	Y. Kondo*, Johnson Space Center
G. P. Garmire, California Institute of Technology	W. Liller, Harvard College Observatory
	S. P. Maran, Goddard Space Flight Center

LOCAL ORGANIZING COMMITTEE

E. Boldt*, Goddard Space Flight Center	J. Rosendhal, NASA Headquarters
A. Davidsen, Johns Hopkins	R. Rothschild, Goddard Space Flight Center
A. Lazarus, NASA Headquarters	S. Shulman, Naval Research Laboratory
W. Rose, University of Maryland	S. Sobieski, Goddard Space Flight Center

* Chairman

**Co-Chairman



A G E N D A

A SYMPOSIUM ON X-RAY BINARIES

Workshop Program for Coordinated Campaign - IAU Commissions 42 and 44

Goddard Space Flight Center, Greenbelt, Maryland
Building 26, Room 205
October 20-22, 1975

REVIEW OF RECENT X-RAY RESULTS

Y. Kondo*	Introduction
J. L. Culhane	OAQ-Copernicus (MSSL)
K. Pounds	Ariel 5 Binary Studies
A. P. Willmore	Ariel 5 Transient Source Studies
A. C. Brinkman/J. Heise	ANS (Utrecht)
H. Schnopper	Bragg Spectroscopy (ANS-SAO)
H. Kestenbaum	Bragg Spectroscopy (OSO-8 Columbia)
G. Clark	SAS-3 (MIT)
P. Serlemitsos	OSO-8 (GSFC)
M. Weisskopf	Polarimetry (OSO-8 Columbia)

HER X-1 PANEL

J. Bahcall*	HZ Her: Main Features
P. L. Bernacca	Periodical Optical Flickering
E. Boldt	Spectral Evidence for a Strong Magnetic Field
R. C. Catura	Intense Soft X-Ray Flux
R. Henry	Soft X-Rays During the Off State
F. K. Lamb	Information of Accretion Flows from X-Ray Timing
W. Liller	Variability of HZ Her During Optical OFFs
J. A. Petterson	Precessions of the Normal Star in X-Ray Binaries
S. Pravdo	OSO-8 GSFC Results
R. St. John	B-V Curve and White Light Flickering
C. C. Wu/R. J. van Duinen	UV Observations (ANS-Groningen)

CEN X-3 PANEL

H. Mauder*	Interpretation of Optical Light Variations
A. N. Bunner	Wisconsin Soft X-Ray Observations
K. Pounds	Ariel 5 Results
C. E. Ryter	Interstellar Absorption
E. Schreier	Recent UHURU Observations
J. Swank	OSO-8 GSFC Results
I. R. Tuohy	Pulsed X-Ray Observations from Ariel 5

CYG X-3 PANEL

R. M. Hjellming*	Introduction
A. Brinkman	ANS (Utrecht) Results
L. Kaluziński	Ariel 5 GSFC Monitor
G. Ricker	High Energy X-Rays (M.I.T. Balloon Observations)

CYG X-3 PANEL
(continued)

K. O. Mason	OA0 and Ariel 5 (MSSL) Results
G. Garmire (presented by)	Infra-red Observations
D. Parsignault	ANS Observations
K. Founds	Ariel 5 Results
P. Serlemitsos	GSFC Rocket Results
S. Shulman	Soft X-Ray Rocket Observation
R. Staubert/J. Trumper	High Energy X-Rays

SPECIAL PANEL ON THE TRANSIENT SOURCE A0620-00

S. P. Maran*	Introductory Remarks on Nova Monocerotis 1975 AKA A0620-00 and A0621-00, the "Transient X-Ray Source in Orion"
A. P. Willmore	The X-Ray Observations
S. Holt	Decay of the X-Ray Luminosity
H. Bradt	SAS-3 (MIT) Results
P. Serlemitsos	OSO-8 (GSFC) Results
R. Wolfson	Discovery of Optical Counterpart
W. Liller	The Recurrent Nova Associated with A0620-00
H. Duerbeck and K. Walter	UBV Observations
T. Snow/D. York/T. Gull	High Dispersion Spectra of A0620-00
J. Dolan	Measurement of Optical Polarization
F. Owen	Radio Observations of the Source Associated with A0620-00
K. Brecher	Colliding Shells Model
A. S. Endal/E. J. Devinney/ S. Sofia	A Model for the X-Ray Nova A0620-00

CYG X-1 X-RAY PANEL

E. Boldt*	Introduction
C. Canizares	SAS-3 Results
D. M. Eardley	Formation of Hard X-Ray Tails
S. Holt	Ariel 5 GSFC Monitor
J. Matteson	X-Ray Observations from Balloons
P. Murdin	Absorption Events
D. Parsignault	ANS Observations
R. Rothschild	High Resolution Measurements from Rockets
M. Weisskopf	Temporal Variability

HDE 226868 (CYG X-1) PANEL

C. T. Bolton*	Optical Observations - A Review
G. Auriemma	Short Time Transient Periodicities in the Optical Emission
J. F. Dolan	Optical Polarization
R. M. Hjellming	Recent Transient Radio Event
Y. Kondo/G. E. McClusky	Effects of Radiation Pressure on the Equipotential Surfaces in X-Ray Binaries
Y. Kondo/S. Parsons/K. Henize/ J. D. Wray/G. F. Benedict	The Skylab S-019 UV Spectrum
W. Liller	Long-Term Variability
E. N. Walker	Photometry - The Blue Light Curve
C. Wu/R. J. van Duinen	UV Observations (ANS)

HD153919 (3U1700-37) PANEL

J. B. Hutchings*	Introduction
C. T. Bolton	Reddening Distance
A. K. Dupree/J. Lester	High Dispersion Observations
J. Heise	ANS (Utrecht) Results
W. Krzeminski	He II 4686 Photometry
K. O. Mason	OAO Results
E. N. Walker	Broad Emission Features
C. C. Wu/R. J. van Duinen	UV Observations (ANS)
Y. Kondo/S. Parsons/K. G. Henize/ J. D. Wray/G. F. Benedict	The Skylab S-019 UV Spectrum

3U0900-40 (HD77581) PANEL

N. V. Vidal*	Physical Parameters and a Model for HD77581
Y. Avni	Analysis of Ellipsoidal Light Variations and Implications
C. T. Bolton	Reddening Distance
P. A. Charles	OAO-Copernicus Results
J. Heise (presented by)	Mass Determinations for the X-Ray Binary
D. Q. Lamb	Vela X-1 and Neutron Star Original Spin
J. E. McClintock	Masses of the Stars in the Binary System (SAS-3 Results)
K. Pounds	Ariel 5 Results
C. C. Wu/R. J. van Duinen	UV Observations (ANS)

OTHER POSSIBLE X-RAY BINARIES

H. Gursky*	Introduction
D. Bord	Optical Observations of WRA977 (3U1223-62?)
A. Cowley/D. Crampton	The Spectroscopic Binary Sco X-1
A. F. Davidsen	Spectrophotometry of the Unusual Optical Candidate for GX1+4
J. F. Dolan	Optical Polarization of X Persei
S. Holt	Ariel 5 GSFC Monitor of Sco X-1
S. Ilovaisky	Simultaneous X-ray and Optical Observations (Sco X-1, Cyg X-2)
B. Margon	Simultaneous X-ray and Optical Observations of X Persei (3U0352+30)
C. C. Wu/R. J. van Duinen	UV ANS Observations of Sco X-1

OBSERVATIONAL PROGRAMS - PLANS AND PROSPECTS

G. Garmire*	Rocket and Ground-Based Observations (California Institute of Technology)	
R. J. Thomas	GSFC Project	} OSO-8
R. Novick	Columbia	
R. Becker	GSFC X-ray	
B. Dennis	GSFC Hard X-ray	
H. Bradt	SAS-3	
J. L. Culhane	OAO-Copernicus	
A. K. Dupree	IUE and Ground-Based Observations (Center for Astrophysics)	
A. P. Willmore	Ariel 5	
J. Paul	COS B Satellite X-ray Detector	
Y. Kondo	A Coordinated Campaign	

*Panel Chairman



INTRODUCTION

Yoji Kondo
NASA Johnson Space Center
Houston, Texas 77058 USA

This symposium is an outgrowth of a coordinated campaign to observe X-ray binaries sponsored by the IAU (International Astronomical Union) Commission 42 (Close Binary Stars) and Commission 44 (Astronomical Observations from Outside the Terrestrial Atmosphere).

A brief history of the campaign is perhaps in order here. At the IAU General Assembly in Sydney in 1973, the members of the Commission 42 (President, Dr. T. Herczeg) discussed prospective coordinated campaigns for the next triennial period. I suggested a coordinated campaign on X-ray binaries in order to orchestrate the efforts by X-ray experimenters, ground-based observers and theorists. The suggestion was made in part from the realization that many ground-observers were not well acquainted with the current or planned X-ray experiments and that communication among various scientists might be improved by having someone designated as a coordinator. There is a Committee for Coordinated Observing Programs in Commission 42, which is headed by Dr. Kjeld Gyldenkerne, and I hoped that he would find someone for the task. Well, I was selected for the job before I knew what happened. After an exchange of several letters between Kjeld and myself, and with the benefit of his helpful advice, the Coordinated Campaign for Observation of X-ray Binaries went into operation in January of 1974. Prior to announcement of the campaign, the President of Commission 44, Dr. A. D. Code, was also consulted regarding the coordinated campaign and we received an enthusiastic endorsement from him.

The main objectives of the campaign have been: (a) dissemination of information on satellite X-ray experiments and ground-based programs; (b) designation of specific campaign dates for observation of specific objects; and (c) transmission of suggestions and recommendations from campaign participants. These functions have been performed through Campaign Circulars and Special Bulletins; the most recent circular, No. 16, was issued a few weeks ago. Objective (b) is the most difficult task to perform. This is mainly because satellite observing plans are usually made fairly close to the actual time of observation and we cannot provide a sufficient advance notice to the ground-observers. Major observatories tend to schedule their telescope time some six months in advance making it very difficult for astronomers to plan simultaneous observations with satellites. As a result, only a few designated campaign dates were announced. We have merely endeavored to announce X-ray satellite observing schedules in a timely fashion to aid the campaign participants.

As the campaign progressed, I began to realize that it would perhaps be a good idea to provide an opportunity for the campaign participants to gather at one place in a workshop and directly compare notes. In addition, such a meeting might help develop a clearer picture for some X-ray binaries. I discussed this idea with several scientists, among them Dr. Elihu Boldt of Goddard Space Flight Center. We pursued the matter and it was agreed that a good place to host such a meeting would be GSFC. In selecting the date for the workshop, we considered the launch dates of the OSO-8 and SAS-3 as well as the fact that the Ariel 5 and ANS would have been in operation for about a year by then. As it has worked out, we have the unique opportunity of holding this conference while five X-ray satellites are in operation!

I hope and trust that the next three days will prove to be both productive and informative. We look forward to furthering our understanding of these fascinating X-ray binaries if only by a modest amount. We also hope to have developed by the end of those three days a more effective way to wage our coordinated campaign in the future. It is also hoped that this workshop will provide an opportunity for observers, experimenters and theorists to establish direct and personal contacts among themselves in furthering their research.

Finally, I wish to express my sincere thanks to Dr. Elihu Boldt and other members of the Scientific and Local Organizing Committees for their valuable contributions in making this symposium a reality. Dr. Boldt, in particular, dedicated much of his valuable research time toward organization of this meeting. Mrs. S. Shrader and other workers at GSFC also provided valued assistance.

20 October 1975

CONTENTS

	Page
PREFACE	iii
SCIENTIFIC ORGANIZING COMMITTEE	v
LOCAL ORGANIZING COMMITTEE	v
AGENDA	vii
INTRODUCTION, Y. Kondo	xi
COPERNICUS OBSERVATIONS OF A NUMBER OF GALACTIC X-RAY SOURCES, J. L. Culhane, K. O. Mason, P. W. Sanford, and N. E. White	1
ANS RESULTS ON X-RAY BINARIES, J. Heise and A. C. Brinkman	27
X-RAY SPECTROSCOPY WITH THE ANS SATELLITE, H. W. Schnopper, J. P. Delvaile, A. Epstein, H. Gursky, J. Grindlay, K. Kalata, D. R. Parsignault, A. R. Sohval, and E. Schreier	49
STELLAR CRYSTAL X-RAY SPECTROSCOPY ON OSO-8, H. L. Kestenbaum, G. G. Cohen, R. Novick, M. C. Weisskopf, R. S. Wolff, J.R.P. Angel and P. B. Landecker	53
COSMIC X-RAY OBSERVATIONS WITH OSO-8, P. J. Serlemitsos, R, Becker, E. A. Boldt, S. S. Holt, S. Pravdo, R. Rothschild, and J. H. Swank	67
THE X-RAY POLARIZATION EXPERIMENT ON THE OSO-8, M. C. Weiss- kopf, G. G. Cohen, H. L. Kestenbaum, R. Novick, R. S. Wolff and P. B. Landecker	81
Her X-1 PANEL, J. N. Bahcall	99
PERIODIC FLICKERING IN THE OPTICAL SPECTRUM OF HZ HERCULIS, P. L. Bernacca	101
HER X-1 SPECTRAL EVIDENCE FOR A STRONG MAGNETIC FIELD, E. A. Boldt, S. S. Holt, R. E. Rothschild, and P. J. Serlemitsos	113
INTENSE SOFT X-RAY FLUX FROM HER-1, R. C. Catura and L. W. Acton	119
SOFT X-RAYS FROM HER X-1 DURING THE "OFF" PHASE, G. Fritz, S. Shulman, H. Friedman, R. C. Henry, A. F. Davidsen, and W. A. Snyder	127
INFORMATION ABOUT ACCRETION FLOWS FROM X-RAY TIMING OF PULSATING SOURCES, F. K. Lamb, D. Pines, and J. Shaham	141

	Page
VARIABILITY OF HZ HERCULIS DURING THE OPTICAL OFFS, W. Liller	155
PRECESSION OF THE NORMAL STAR IN X-RAY BINARIES, J. A. Petterson .	159
OSO-8 OBSERVATIONS OF HERCULES X-1, S. H. Pravdo, R. H. Becker, E. A. Boldt, S. S. Holt, R. E. Rothschild, P. J. Serlemitsos, and J. H. Swank . .	161
OPTICAL FLICKERING IN HZ HERCULIS, R. H. St. John	169
THE 35 ^d CYCLE DEPENDENCE OF THE 1.7 ^d B-V LIGHT CURVE OF HZ HERCULIS, R. H. St. John and V. H. Regener	171
CENTAURUS X-3: THE OBSERVATIONAL PICTURE, H. Mauder	173
CENTAURUS X-3 PANEL SUMMARY, H. Mauder	177
THE INTERPRETATION OF OPTICAL LIGHT VARIATIONS OF CENTAURUS X-3, H. Mauder	179
WISCONSIN SOFT X-RAY OBSERVATIONS OF CEN X-3, A. N. Bunner and W. T. Sanders	187
THE INTERSTELLAR MATTER COLUMN DENSITY TO CEN X-3, C. Ryter	189
RECENT UHURU RESULTS ON CENTAURUS X-3, E. J. Schreier and G. Fabbiano	197
OSO-8 GSFC RESULTS ON CEN X-3, J. H. Swank, R. Becker, E. Boldt, S. Holt, S. Pravdo, R. Rothschild, and P. J. Serlemitsos	207
PULSED X-RAY OBSERVATIONS OF CEN X-3 FROM ARIEL-5, I. R. Tuohy	219
SUMMARY OF SESSION ON CYG X-3, R. M. Hjellming	229
THE RADIO SOURCES ASSOCIATED WITH CYG X-3, R. M. Hjellming	233
OBSERVATIONS OF CYGNUS X-3 BY ANS, A. C. Brinkman, J. Heise, A.J.F. den Boggende, R. Mewe, E. Gronenschild, and H. Schrijver	241
EVIDENCE FOR A 17d PERIODICITY FROM CYG X-3, S. S. Holt, E. A. Boldt, P. J. Serlemitsos, L. J. Kaluzienski, S. H. Pravdo, A. Peacock, M. Elvis, M. G. Watson, and K. A. Pounds	245
SOME FEATURES OF THE X-RAY SOURCE CYG X-3, K. O. Mason, P. Sanford, and J. Ives	255

	Page
OBSERVATIONS OF CYGNUS X-3 BY ANS, D. R. Parsignault, E. Schreier, J. Grindlay, H. Schnopper, and H. Gursky	267
THE 4.8 H VARIATION OF CYGNUS X-3 AT HIGH X-RAY ENERGIES, W. Pietsch, E. Kendziorra, R. Staubert, and J. Truemper	277
OBSERVATIONS OF CYGNUS X-3 FROM A BALLOON-BORNE X-RAY TELESCOPE, G. R. Ricker, A. Scheepmaker, J. E. Ballantine, J. P. Doty, G. A. Kriss, S. G. Ryckman, and W.H.G. Lewin	279
ABSENCE OF IRON LINE EMISSION IN CYG X-3, S. Shulman, H. Friedman, G. Fritz, D. Yentis, W. A. Snyder, A. F. Davidsen and R. C. Henry.	285
THE TRANSIENT X-RAY SOURCE A0620-00 (NOVA MONOCEROTIS 1975), S. P. Maran	293
THE EARLY LIGHT CURVE OF A0620-00, L. J. Kaluziński, S. S. Holt, E. A. Boldt, and P. J. Serlemitsos	311
OBSERVATIONS OF A0620-00 BY SAS-3, H. Bradt and T. Matilsky	317
OPTICAL IDENTIFICATION OF A0620-00, R. Wolfson and F. Boley	327
A0620-00 AS A RECURRENT NOVA, W. Liller	335
A PERIODIC BRIGHTNESS VARIATION OF THE OPTICAL COUNTERPART OF A0620-00, H. W. Duerbeck and K. Walter	343
SPECTROSCOPIC OBSERVATIONS OF THE CANDIDATE STAR COINCIDENT WITH A0620-00, T. P. Snow, Jr., D. G. York, T. R. Gull and K. G. Henize	347
MEASUREMENTS OF A0620-00 WITH ANS, A. C. Brinkman, J. Heise, A.J.F. den Boggende, R. Mewe, E. Gronenschild, and H. Schrijver	349
A STUDY OF A0620-00 IN THE ULTRAVIOLET, Chi-Chao Wu, J. W. G. Aalders, R. J. van Duinen, D. Kester, and P. R. Wesselius	353
INFRARED MEASUREMENTS OF NOVA MONOCEROTIS 1975 (A0620-00), S. G. Kleinmann, R. R. Joyce, and R. W. Capps	355
COLLIDING SHELLS MODEL, K. Brecher and P. Morrison	359
THE NATURE OF THE X-RAY NOVA A0620-00, A. S. Endal, E. J. Devlinney, and S. Sofia	361
INTRODUCTION TO CYG X-1 X-RAY PANEL, E. Boldt	369

	Page
SAS-3 OBSERVATIONS OF AN X-RAY FLARE FROM CYGNUS X-1, C. R. Canizares, H. Bradt, J. Buff, and B. Laufer	373
FORMATION OF HARD X-RAY TAILS, D. M. Eardley	379
NEW RESULTS FROM LONG-TERM OBSERVATIONS OF CYG X-1, S. S. Holt, E. A. Boldt, P. J. Serlemitsos, and L. J. Kaluziński	391
INTENSITY AND SPECTRAL VARIATIONS OF CYG X-1 OBSERVED FROM BALLOONS, J. L. Matteson, R. F. Mushotsky, W. S. Paciesas, and J. G. Laros	407
ABSORPTION DIPS AT LOW X-RAY ENERGIES IN CYGNUS X-1, P. Murdin	425
OBSERVATIONS OF CYGNUS X-1 IN ITS TWO INTENSITY STATES BY ANS, D. R. Parsignault, J. E. Grindlay, H. Schnopper, E. J. Schreier, and H. Gursky	429
HIGH RESOLUTION MEASUREMENTS OF CYG X-1 FROM ROCKETS, R. E. Rothschild, E. A. Boldt, S. S. Holt, and P. J. Serlemitsos	443
THE TIME VARIABILITY OF CYGNUS X-1, M. C. Weisskopf	453
OPTICAL OBSERVATIONS OF HDE226868 = CYGNUS X-1: A REVIEW, C. T. Bolton	465
SHORT TIME TRANSIENT PERIODICITIES FROM CYG X1, G. Auriemma, D. Cardini, E. Costa, F. Giovannelli, M. Ranieri	485
THE OPTICAL POLARIZATION OF HDE 226868 (=CYG XR-1), J.F. Dolan	493
THE MAY 1975 TRANSIENT RADIO EVENT IN CYG X-1, R. M. Hjellming	495
EFFECTS OF RADIATION PRESSURE ON THE EQUIPOTENTIAL SURFACES IN X-RAY BINARIES, Y. Kondo, G. E. McCluskey, Jr., and S. L. Gulden	499
THE LONG TERM VARIABILITY OF HDE 226868 = CYGNUS X-1, W. Liller	513
BLUE BAND PHOTOMETRY OF CYGNUS X-1, E. N. Walker	521

	Page
INTERSTELLAR REDDENING ESTIMATE OF CYGNUS X-1 FROM THE ULTRAVIOLET, Chi-Chao Wu, R. J. van Duinen, and G. Hammerschlag- Hensberge	539
3U 1700-37 = HD 153919: REVIEW, J. B. Hutchings	531
HIGH DISPERSION SPECTROSCOPIC OBSERVATIONS OF HD153919 (3U 1700-37), A. K. Dupree and J. B. Lester	539
THE SKYLAB S019 ULTRAVIOLET SPECTRA OF HD153919 (=3U1700-37) AND HDE226868 (+CYG X-1), Y. Kondo, S. B. Parsons, K. G. Henize, J. D. Wray, and G. F. Benedict	531
He II λ 4686 PHOTOMETRY OF HD 153919, W. Krzeminski	555
X-RAY OBSERVATIONS OF 3U 1700-37, K. O. Mason, G. Branduardi, and P. Sanford	559
THE BROAD EMISSION FEATURES AND "WAKE" IN HD 153919, E. N. Walker	569
THE X-RAY BINARY HD77581 + 3U 0900-40, N. V. Vidal	575
STATUS OF THE STUDY OF ELLIPSOIDAL LIGHT VARIATIONS IN 3U0900-40 AND OTHER X-RAY BINARIES, Y. Avni and J. N. Bahcall	615
THE X-RAY VARIABILITY OF VELA X-1 (3U0900-40), P. A. Charles, K. O. Mason, J. L. Culhane, P. W. Sanford, and N. E. White	629
MASS DETERMINATION FOR THE X-RAY BINARY SYSTEM VELA X-1 (= 3U 0900-40), J. A. van Paradijs, G. Hammerschlag-Hensberge, E.P.J. van den Heuvel, R. J. Takens, E. J. Zuiderwijk, and C. De Loore	643
VELA X-1 AND NEUTRON STAR ORIGINAL SPIN, D. Q. Lamb, F. K. Lamb, and W. D. Arnett	659
AN X-RAY DETERMINATION OF THE ORBITAL ELEMENTS OF 3U0900-40, J. McClintock, P. C. Joss, and S. Rappaport	661
THE "OTHER" GALACTIC X-RAY SOURCES, H. Gursky	669
OPTICAL OBSERVATIONS OF WRA 977 (3U 1223-62?), D. J. Bord, D. E. Mook, L. Petro, and W. A. Hiltner	677
THE INTERACTING BINARY SCO X-1, A. P. Cowley and D. Crampton	683

	Page
SPECTROPHOTOMETRY OF THE UNUSUAL OPTICAL CANDIDATE FOR 3U 1728-24 (=GX 2+5 = GX 1 + 4): A RECURRENT NOVA?, A. Davidsen, R. Malina, and S. Bowyer	691
LONG-TERM X-RAY STUDIES OF SCO X-1, S. S. Holt, E. A. Boldt, P. J. Serlemitsos, and L. J. Kaluzienski	703
EVIDENCE FOR A 13.6-DAY PERIOD IN CYGNUS X-2 FROM X-RAY AND OPTICAL OBSERVATIONS, C. Chevalier, S. A. Ilovaisky, G. Branduardi, and P. W. Sanford	717
SIMULTANEOUS X-RAY AND OPTICAL OBSERVATIONS OF X PERSEI, B. Margon	719
X-RAY ASTRONOMY PROGRAM AT CIT, G. P. Garmire	727
GO-8 OBSERVING SCHEDULE FOR X-RAY BINARIES, R. J. Thomas	729
THE OBSERVATION PROGRAM FOR THE GSFC COSMIC X-RAY SPECTROSCOPY EXPERIMENT, R. H. Becker, E. A. Boldt, S. S. Holt, S. H. Pravdo, R. E. Rothschild, P. J. Serlemitsos, and J. Swank	737
A STUDY OF THE COSMIC SOURCES OF HARD X-RAYS, B. R. Dennis, J. Beall, C. J. Crannell, K. J. Frost, and L. E. Orwig	739
ULTRAVIOLET OBSERVATIONS FROM IUE, A. K. Dupree	747
CLOSING WORDS, Y. Kondo	749
LIST OF REGISTERED PARTICIPANTS	751
AUTHOR INDEX	755

Copernicus Observations of a Number of
Galactic X-ray Sources

J. L. Culhane, K. O. Mason, P. W. Sanford,
N. E. White.

Mullard Space Science Laboratory,
Department of Physics and Astronomy,
University College London.

INTRODUCTION

The Copernicus satellite was launched on 21 August 1972. The main experiment on board is the University of Princeton UV telescope. In addition a cosmic X-ray package of somewhat modest aperture was provided by the Mullard Space Science Laboratory (MSSL) of University College London. Following a brief description of the instrument, a list of galactic sources observed during the year up to October 1975 is presented. A good deal of the data from these sources has been analysed and much of it will be presented by other speakers at this symposium. Some observations, which will not be discussed in other sessions, will be described in this paper.

Since, in addition to work done by members of the MSSL group, a number of the papers presented at this symposium represent the work of guest investigators, it is important to point out that a continuing guest investigator programme is in progress. Proposals for guest observing time have come from people in many different branches of astronomy and time can still be made available in the course of next year.

Although the X-ray detection aperture is small, as will become clear from the next section, the ability to point the satellite for long periods of time with high accuracy makes Copernicus an ideal vehicle for the study of variable sources. Observing programmes are planned at MSSL two to three months in advance of carrying out the observations. The experiment is operated from the Goddard control centre by a joint team from MSSL and the Appleton Laboratory of the UK Science Research Council.

2. INSTRUMENTATION

The complete MSSL package is illustrated schematically in Figure 1 while the instrument parameters are summarised in table 1. The two grazing incidence X-ray collectors covering the energy range 0.5 to 4.0 keV are unavailable due to the failure, after one year in orbit, of a background shutter. Although the channeltron used in the focal plane of the third reflector suffers from a high background due to a light leak, it is possible to use it for certain observations, (see

for example Margon et al (1974) Henry et al (1975)). The collimated proportional counter detector continues to operate reliably and is at present the main X-ray instrument available in the package. The usual data integration time is 62.5 sec but this can be reduced to between 1 and 16 sec using the computer on board the spacecraft. The particle background rate is variable but averages about 50 counts per minute. The spacecraft pointing precision is better than one arc second while the jitter is less than a fraction of an arc second when the system is under control of the Princeton fine error sensor. When under gyro control, the spacecraft axis drifts at a rate of 2 arc sec. per hour but the star sensors may be used at any time to update the gyros.

3. OBSERVATIONS OF GALACTIC X-RAY SOURCES - GENERAL SURVEY

The galactic X-ray sources which have been observed in the past year are listed in table II under two headings, galactic variable sources and targets of opportunity. In the first category, Cygnus X-1 has been observed extensively by Paul Murdin, a Copernicus guest investigator, together with a number of MSSL co-workers. X-ray and optical data have been obtained by Sergio Ilovaisky and his colleagues, for the Cygnus X-2 source. Results of both Copernicus and Ariel-5 observations of Cygnus X-3 have been analysed by Keith Mason and his co-workers. The work in these three areas will be presented elsewhere in these proceedings. While Ian Tuohy will report on Ariel-5 observations of Centaurus X-3, studies of the accretion wake associated with this source using Copernicus data have already been published (Tuohy and Cruise, (1975)). Similar studies of the source 3U 0900-40 are reported elsewhere in these proceedings by Phil Charles while results obtained for 3U 1700-37 are described by Keith Mason. The sources at the bottom of the first part of the list (3U 1728-16, 3U 1911-17 and 3U 1813-14) have also been observed and analysis of these data is continuing. I will discuss SCO X-1 and 3U 0352+30 in greater detail below and will also mention briefly some recent observations of Her X-1.

In the category of targets of opportunity, the transient source in Centaurus (A 1118-61) was observed by Copernicus. It was suggested by Fabian (1975), that the transient X-ray emission was 'turned on' at a particular phase of the Mira variable RS Centauri. Copernicus observations have showed that X-ray emission did not recur at the appropriate phase of RS Cen and so the association of this star with A 1118-61 can probably be ruled out. The transient X-ray source (A 1742-28) in the galactic centre has been studied with Copernicus by Graziella Branduardi and her colleagues and I will present some preliminary results of their work later. The X-ray source 3U 1908+00 (Aquila X-1) was examined by Copernicus and, prior to June 1975, was found to have strength about 2% of that of the Crab Nebula, a value which is six times below the flux reported in the 3U catalogue (Giacconi et al (1974)). During June 1975 the source increased its X-ray output to a level comparable with the Crab Nebula. Studies of this source are continuing. Finally it was possible at very short notice to arrange for Copernicus X-ray observations of Nova Cygni 1975, an optical nova which was discovered in late August. The X-ray observations set an upper limit of approximately 10^{-10} ergs cm^{-2} sec^{-1}

(or 6 Uhuru counts) on the flux in the 2.5 - 7.5 keV band at the time of optical maximum (Sanford et al(1975)).

4. OBSERVATIONS OF GALACTIC X-RAY SOURCES - SPECIFIC OBJECTS

While most of the sources mentioned in the previous sections will be discussed in greater detail by Copernicus guest investigators and MSSL group members in the panel sessions, I would like to present recent results for several objects which will not be reported elsewhere in these proceedings.

a) SCO X-1

A number of Copernicus observations of this source have been carried out in the period October 1972 to June 1975 and a detailed account of this work is in preparation (White et al (1975a)). Broadly speaking the results reported by earlier observers are confirmed in that the X-ray flux exhibits two states, one active and one quiescent. Data representative of an active phase of the source are shown in Figure 2. The observations were made on 10 July 1974. X-ray intensity in counts per 62.5 sec and spectral slope parameter are plotted against time. The spectral parameter is obtained in the following manner. For the purpose of fitting an expression to the data to represent the source photon spectrum we have assumed that the emission is by the free-free process from a hot spherical plasma cloud of radius $r(\text{cm})$ and having uniform temperature and electron density $T(^{\circ}\text{K})$ and $n(\text{cm}^{-3})$. The source spectrum may then be represented by

$$I(E) = A \exp\left(-\frac{E}{kT}\right) g(E, T) \quad (1)$$

$\text{keV keV}^{-1} \text{cm}^{-2} \text{sec}^{-1}$

where the free-free Gaunt factor is approximated by

$$g(E, T) = 0.84 \left(\frac{kT}{E}\right)^{0.3} \quad (2)$$

and the normalising constant is given by

$$A = \frac{3 \cdot 10^{-15}}{(kT)^{0.5}} \frac{n^2 r^3}{3d^2} \quad (3)$$

Here E is photon energy in keV and d is the distance to the source in Cm . While values of T obtained from the data are limited in their usefulness because of the simplicity of the above model, and cannot be regarded as a true measure of the plasma temperature, it is of interest to examine the variability of the parameter T under both active and quiet conditions. Values of T and A are obtained from the data by fitting equation (1) using a spectral fitting programme which takes account of detector resolution, quantum efficiency and photon escape effects.

As may be seen in Figure 2, the active state involves the occurrence of bursts of typically 5 to 15 minutes duration and with X-ray flux enhancements of up to a factor two. The temperature parameter varied from a baseline

value of about 5.5 keV up to 20 keV or more. The most intense bursts have the longest durations. During active states, in the intervals between flares, the temperature value remains at around 5.5 keV and the flux always returns to a minimum value of 4000 Copernicus counts per minute or 8000 - 9000 Uhuru counts per sec. This minimum value appears stable to within 3% over periods of years at a confidence level of 90%. On one occasion (April, 5th, 1973) a longer lasting flare occurred during which the flux increased by about 25% over a period of approximately one hour.

Data acquired during a typical quiescent period are shown in Figure 3. The X-ray intensity varies by around 20% while the value of the temperature parameter is about 7.5 keV during these intervals. This temperature value is greater during quiescent states than the minimum value reached during the non-flaring portions of the active states.

For the active phase data presented in Figure 2, temperature values have been derived for each 62.5 sec. data sample. These values have been plotted against X-ray counting rates in Figure 4a for the active phase and in Figure 4b for data taken during quiescent phase. In Figure 4c, temperatures have been determined for source intensity intervals of 500 counts. Data from both active and quiescent periods are plotted in this way. The slopes of both plots are similar but it is clear that, for a given source intensity, the quiescent value of the temperature parameter is somewhat higher than the active phase value. Finally the normalising parameter A which represents volume emission measure (see equation (3)) is plotted against temperature in Figure 4d. It is apparent that there is a difference in either plasma density or volume between the two states at a given temperature in agreement with the work of Kitamura et al (1971).

The long term behaviour of the source may therefore be summarised as follows.

During the quiescent phases the flux from SCO X-1 varies by up to 50%, which may be correlated with an associated temperature variability from 5.5 to 8.0 keV. The transition into its active state is heralded by a decline in flux to a minimum level, with a reduction in temperature to 5.5 keV. From this level it then flares with temperatures ranging from 5.5 keV. to above 20 keV that are well correlated with the intensity level. Between flares the flux always returns to the same minimum level. When the active phase terminates the source resumes its quiescent variability and moves away from the base level flux and temperature.

The stability of the underlying flux introduces the problem of how this situation can arise in such an otherwise variable source. The emission may include two components with one component emitting constantly with a temperature of 5.5 keV while a second, more active component, is responsible for the variability seen in both quiescent and active phases. Our data are consistent with a single component spectrum ; however the energy range and the limited number of channels of the detectors do not enable us to resolve a second component. Continuous monitoring over a large energy range will clarify this point.

At present the models for the SCO X-1 system can be divided into two groups ; Close Binary Systems (e.g. Basko and Sunyaev, 1973) and Rotating Degenerate Stars (e.g. Davidson et al, 1971). The 0.7874 day optical periodicity seen in both the light curve (Gottlieb et al (1975) and the radial velocity observation of Cowley and Crampton (1975)), makes it almost certain that the system is a binary. Here the energy source for the X-ray emission is mass accretion from a normal star onto a compact secondary. However among the other X-ray sources known to be contained in binary systems, none exhibit the stable X-ray base level of SCO X-1. Because the initiation of a SCO X-1 binary system must be of the order of 90° the situation is somewhat unique in that we are observing disc or radial accretion 'end on'. The properties reported for this source could well result from this, and may give an indication of which accretion mechanism is operating.

b) 3U 0352 + 30

A considerable amount of Copernicus observing time has been devoted to the study of this source. Positional data from the work of Hawkins, Mason and Sanford (1975) are given in Figure 5. The area of overlap of the Copernicus and Uhuru position boxes is approximately 7 square arc min. Two candidate objects are shown in this region of overlap, one of which is the star X Persei, a peculiar 6th magnitude Be object.

The X-ray source and the star have been studied simultaneously by the Princeton UV telescope and the MSSL X-ray detectors on Copernicus in order to estimate the column density of interstellar material in front of both the star and the X-ray source (Mason et al (1975)). Table III summarises the results of observations with the Princeton instrument. Values of atomic, molecular and total Hydrogen column densities are presented in the table. The high value of the molecular hydrogen column is of particular interest.

The results of X-ray determinations of the gas column density are summarised in table IV. Copernicus data for the energy range 0.5 to 7.5 keV, were employed. While the numbers listed are in equivalent Hydrogen atoms, the absorption is primarily due to elements such as oxygen and neon and the values of N_H determined from X-ray data depend very largely on the element abundances assumed for the interstellar material. Because of this, values of N_H have been deduced from the X-ray data for a number of different models of the interstellar absorption cross sections of Brown and Gould and those of Fireman (1974) which include the effect of grains of different sizes. The result of assuming the Princeton value of the molecular hydrogen column with a consequent increase in the column densities of a number of the heavier elements is also quoted in the table. The range of N_H values derived from the X-ray data (2.6 to $4.0 \cdot 10^{21}$ atoms cm^{-2} column) illustrates the importance of employing an adequately representative model of the interstellar medium. However the UV based column density does lie within the range of values permitted by the X-ray observations and hence the identity of 3U0352 + 30 with the star X Per is not excluded.

Studies of Copernicus X-ray data for the interval October 1972 to January 1975 have lead to the discovery of a 13.9 minute periodicity. Period determinations made at various times during this interval are listed in table V. Data obtained in December 1972 show periods measured for the three Copernicus energy ranges. All other measurements refer to the 2.5 to 7.5 keV band. All the periods determined agree within the errors and so a mean period of 13.9325 ± 0.0047 minutes has been derived. The column headed mean source count per minute indicates the 2.5 - 7.5 keV flux from the source changed by 30% in the interval Feb 1974, to January 1975. Peak to mean amplitude values for the periodic flux are presented in the last column of the table and the 2.5 - 7.5 keV values of this parameter do not appear to vary significantly. Data folded modulo the 13.9325 minute period are presented in Figure 6. Two complete cycles are shown. The observations made in February 1974 were used to generate this light curve. Although only 13 bins can be displayed in each cycle due to the time resolution of the instrument, the light curve is quasi-sinusoidal in shape and does not suggest the sharp cut off that would be associated with binary eclipse. Sharply pulsed emission, such as might arise due to beamed radiation from a neutron star, would also appear to be excluded. A very close binary system has been suggested by Pringle and Webbink involving a pair of compact objects and having the quasi-sinusoidal light curve established by an orbital variation in the electron scattering optical depth could explain the observations using a model similar to that proposed for Cygnus X-3 by Pringle (1974) and Davidson and Ostriker (1974). However six other sources including 0900-40 (Rappaport and McClintock (1975)), two transient sources (Ives et al (1975)), Rosenberg et al (1975)) and three galactic sources (White et al (1975)) have now been found to exhibit periodic behaviour with periods in the range 1.73 to 31.9 minutes and so the possible existence of a class of slow rotators should also be considered. In particular, Fabian (1975) has drawn attention to mechanisms which could lead to the slowing down of a neutron star's rotation and give rise to periods in the range 1 - 100 minutes.

In addition to the pronounced 13.9325 minute periodicity, there is evidence for X-ray modulation at a period of either 11 or 22 hours for at least some of the time during which Copernicus has been observing the source. The general nature of larger term X-ray variability is illustrated by the three samples of data shown in Figure 7. Each data point represents an average taken over 5 integration periods. The data suggest a longer term variability but its nature is not immediately obvious from an inspection of Figure 7. The nature of the data, which includes many time gaps, makes it impossible to use straight forward Fourier analysis techniques. A rather different approach has been developed by Murdin and co-workers for application to data of this kind. A detailed discussion of this work has been submitted to MNRAS by White et al (1975b). The results of this work are summarised in table VI. While no evidence for a 22 hour variation emerges from the power spectral analysis, the 12 hour gaps in some of the data make it possible that a 22 hour period would not have been detected at a level of modulation of as much as 20%. There is further evidence for a 22 hour period in data obtained recently with the MSSL proportional counter on Ariel 5 (Figure 8) but this observation has not yet been subjected to a power spectral analysis.

Thus the X-ray source poses a number of questions particularly if we attempt to establish its association with the star X Per. The positional evidence and the permitted agreement between X-ray and UV column densities are suggestive of an association but not conclusive. Efforts to establish the existence of simultaneous X-ray and optical variability have not yet been successful (see Margon, these proceedings) although further work of this kind will be undertaken in the near future. Hutchings et al (1975) have obtained evidence for periodic radial velocity variations which suggest a 580 day binary period. These authors present evidence for the accretion rate being a factor 2.10^3 lower than that in other X-ray emitting binary systems and it is interesting to note that the X-ray luminosity of 3U0352+30 is lower than that of other systems by a similar factor.

Because of the presently confused situation further studies of X Per and 3U0352 + 30 are urgently required. While a better position determination for the X-ray source could solve a number of problems, an adequate position will probably not become available until after the launch of HEAO-B. In the meantime, a continued search for simultaneous X-ray and optical variability could prove fruitful.

Although a good deal of Copernicus time has been spent in observations of Her X-1, analysis of the data is still in progress. However a particularly sharp exit from binary eclipse is illustrated in Figure 9 (Davison (1975)). The time taken to emerge from occultation is less than one Copernicus integration period or 62.5 seconds. A consideration of the orbital parameters of the Her X-1 system suggests that the size of the X-ray emitting region must be less than 5000 Km.

Reference is made in table II to several observations of 'targets of opportunity'. One of these was the transient X-ray source (A1742-28) which was first detected in the region of the galactic centre by the rotation modulation collimator instrument on Ariel 5 (Eyles et al (1975)). The light curve of this object is shown in Figure 10. Data from a number of satellites including Ariel 5 (Branduardi et al (1975), ANS (Brinkman (1975) and Copernicus, are plotted. The Copernicus observations in particular provide source intensities at between 50 and 200 days after the peak of the light curve. These points suggest that the rate of decay of the X-ray flux is becoming less steep with time.

X-ray spectra of A1742-28 have been obtained with Ariel 5 and Copernicus and are shown in Figure 11. The spectrum of the galactic centre X-ray source (GCX) is plotted for comparison. While the spectral shapes measured in February 1975 by Ariel 5 and March, 1975 by Copernicus are consistent and the Copernicus spectrum for May, 1975 shows a significant hardening. A more detailed account of these observations is in preparation (Branduardi, et al (1975)).

Many other observations have been carried out by Copernicus in the year up to October 1975 as will be apparent from the list presented in table II. It is expected that Copernicus will continue to observe galactic X-ray sources in the course of next year.

References

- Basko, M.M., and Sunyaev, R.A., (1973), *Astrophys. and Space Science*, 23, 117.
- Branduardi, G., Ives, J., Sanford, P., Maraschi, L., (1975), (in preparation).
- Brinkman, A.C., (1975), Private Communication.
- Cowley, A., and Crampton, J., (1975), *Ap. J.*, (Letters), 201, L65.
- Davidson, A., and Ostriker, J.P., (1974), *Ap. J.*, 189, 331.
- Davidson, K., Pacini, F., and Salpeter, E.E., (1971), *Ap. J.*, 168, 45.
- Davison, P.J.N., (1975), Private Communication.
- Fabian, A.C., (1975), *M.N.R.A.S.*, 173, 161.
- Fabian, A.C., Pringle, J.E., and Webbink, R.F., (1975), *Nature*, 255, 208.
- Eyles, C.J., Skinner, G.K., Willmore, A.P., and Rosenberg, F.D., (1975), In press.
- Fireman, E.L., (1974), *Ap. J.*, 187, 57.
- Giacconi, R., Murray, S., Gursky, H., Kellogg, E., Schreier, E., Matilsky, T., Koch, D., and Tananbaum, H., (1974), *Ap. J.*, Suppl., 27, 37.
- Gottlieb, E.W., Wright, E.L., and Liller, W., (1975), *Ap. J.*, 195, L33.
- Hawkins, F.J., Mason, K.O., and Sanford, P., (1975), *Astrophys. Letters*, 16, 19.
- Henry, R.C., Snyder, W.A., Charles, P.A., Culhane, J.L., Sanford, P., Belach, R., and Drake, J., (1975), *Nature*, In press.
- Hutchings, J.B., Crampton, D., and Redman, R.O., (1975), *M.N.R.A.S.*, 170, 313.
- Ives, J.C., Sanford, P., Bell-Burnell, S.J., (1975), *Nature*, 254, 578.
- Kitamura, T., Matsuoka, M., Miyamoto, S., Nakagawa, M., Oda, M., Ogawara, Y., Takagismi, K., Rao, U.R., Chitnis, E.V., Javanthi, U.B., Prakasarao, A.S., and Bhandrao, S.M., (1971), *Astrophys. and Space Sci.*, 12, 378.
- Margon, B., (1975), These Proceedings.
- Margon B., Mason, K.O., Sanford, P., (1974), *Ap. J.*, 194, L75.
- Mason, K.O., White, N.E., Sanford, P.W., Hawkins, F.J., Drake, J.F., and York, D.G., (1975), Submitted to *M.N.R.A.S.*

- Pringle, J.E., (1974), Nature, 247, 21.
- Pringle, J.E., and Webbink, R.F., (1975), M.N.R.A.S., 172, 493.
- Rosenberg, F.D., Eyles, C.J., Skinner, G.K., and Willmore, A.P., (1975),
Nature, 256, 628.
- Rappaport, S., and McClintock, J., (1975), IAU Circular No. 2794.
- Sanford, P., Charles, P.A., and Mason, K.O., (1975), IAU Circular, No. 2828.
- Tuohy, I.R., and Cruise, A.M., (1975), M.N.R.A.S., 171, 33P.
- White, N.E., Huckle, H.E., Mason, K.O., Charles, P.A., Pollard, G., Culhane,
J.L., and Sanford, P., (1975), IAU Circular.
- White, N.E., Sanford, P.W., Mason, K.O., Murdin, P., (1975), Submitted to
M.N.R.A.S.
- White, N.E., Mason, K.O., Sanford, P., Ilovaisky, S.A., and Chevalier, G.,
(1975a), Submitted to M.N.R.A.S.

Table I : Copernicus X-ray Instrument Parameters

Detector	Energy Range (keV)	Field of view
Collimated Proportional Counter	2.5 - 7.5	$3.5^{\circ} \times 3^{\circ}$ (FWHM)
Paraboloidal X-ray reflector and Proportional Counter	1.4 - 4.2	10', 3' and 1'
" " " " " " " "	0.5 - 1.5	10', 6' and 2'
Paraboloidal X-ray reflector and Channel Multiplier	0.1 - 0.6	10'

Table II : Copernicus Observations 1974 - 75

1) GALACTIC SOURCES

CYGNUS X-1	VELA X-1
CYGNUS X-2	3U1700 - 37
CYGNUS X-3	X PERSEI (3U0352 + 30)
CENTAURUS X-3	3U1728 - 16
SCORPIO X-1	3U1811 - 17
HERCULES X-1	3U1813 - 14

2) TARGETS OF OPPORTUNITY

CENTAURUS X-5
 GALACTIC CENTRE TRANSIENT
 3U1908 + 00
 NOVA CYGNI 1975

Table III

X-PERSEUS (3U0352 + 30)

COPERNICUS UV HYDROGEN COLUMN

1) HYDROGEN Ly- α $N_1 = 2.0 \pm 0.5 \cdot 10^{20}$ ATOMS CM⁻²

2) MOLECULAR HYDROGEN $N_2 = 1.1 \pm 0.3 \cdot 10^{21}$ ATOMS CM⁻²

3) TOTAL HYDROGEN $N_T = N_1 + 2N_2$
 $= 2.4 \pm 0.4 \cdot 10^{21}$ ATOMS CM⁻²

4) MOLECULAR FRACTION $f = \frac{2N_2}{N_T} = 0.92 \pm 0.04$

Table IV

X-PERSEUS (3U0352 + 30)

COPERNICUS X-RAY HYDROGEN COLUMN

- 1) BROWN + GOULD (1970) ISM - ALL H ATOMIC

$$N_X = 4.0^{+0.2}_{-0.4} \cdot 10^{21} \text{ ATOMIC CM}^{-2}$$

- 2) FIREMAN (1974) ISM - ALL H ATOMIC

a) NO GRAINS $N_X = 3.3 \pm 0.3 \cdot 10^{21} \text{ ATOMS CM}^{-2}$

- b) 0.15 μ GRAINS

$$N_X = 3.8 \pm 0.1 \cdot 10^{21} \text{ ATOMS CM}^{-2}$$

- 3) FIREMAN (1974) ISM - MOLECULAR FRACTION AS
FROM UV DATA - BROWN + GOULD (1970)
MOLECULAR CROSS SECTION

a) NO GRAINS $N_X = 2.6 \pm 0.3 \cdot 10^{21} \text{ ATOMS CM}^{-2}$

- b) 0.15 μ GRAINS

$$N_X = 2.8 \pm 0.2 \cdot 10^{21} \text{ ATOMS CM}^{-2}$$

Table V

COPERNICUS - PERIODS OF 3U0352 + 30 (X PER)

Date	Period	Duration of observation (DAYS)	No. of 62.5 sec integration periods	Mean source count per min. MEAN CT	Peak to mean Amplitude
Oct 72	13.940 ± 0.010	3.35	908	6.28*	44%*
Dec 72					
2.5 to 7.5 keV	13.927 ± 0.018	1.88	4E0	10.31	30%
1.0 to 3.1 keV	13.933 ± 0.020	1.88	300	3.04	37%
0.6 to 1.4 keV	13.939 ± 0.024	1.88	300	3.55	21%
Mean	13.993 ± 0.012				
Feb 74	13.934 ± 0.010	3.47	912	12.63	35%
Jan 75	13.9228 ± 0.0021	10.77	1788	7.33	34%
Mean	13.9325 ± 0.0047				

Mean 2.5 - 7.5 keV Amplitude = 37%

Sample standard deviation = ± 0.023

* 34% Reduction in flux due to source being offset in collimator.

Table VI

POWER SPECTRA OF 1 - 3Å INTENSITIES

Date	No. of data	Mean intensity (counts)	Duration of data stream (d)	Regular oscillations : Period (h)	Amplitude (counts)	Relative Amplitude
Oct 72	912	7.7*	3.3	0.9*		11
Dec 72	471	14.0	1.9	0.9		6
Feb 74	1050	12.2	5.3	11.2+0.2	2.3	18
Jan 75 (First 3 days (First 3 days)	1000	6.1	2.2	0.8		12
Jan 75 (Last 8 days)	792	7.0	8.5	11.4+0.15	1.4	19
Jan 75 (background)	720	-2.5	3.4	26 ± 7	0.8	--

This data was taken with the source off-axis. Multiply by 1.5 to correct for response function of the detector beam.

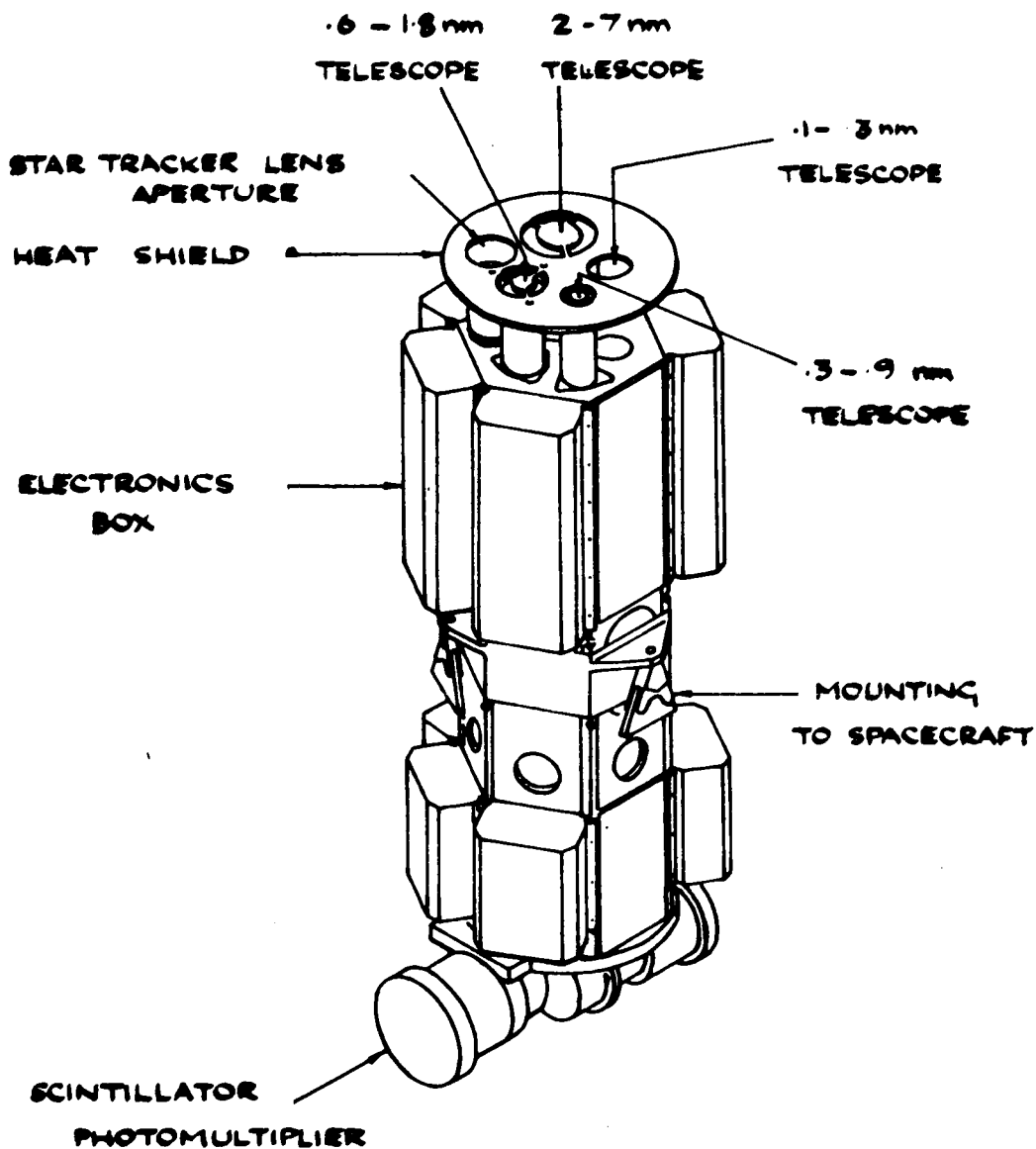


Figure 1

The MSSL X-ray telescope system on Copernicus. Openings in the heat shield permit the three X-ray telescopes, the collimated proportional counter and the instrument star tracker to view the celestial sphere. Detectors and aperture changing mechanisms are located at the base of the package.

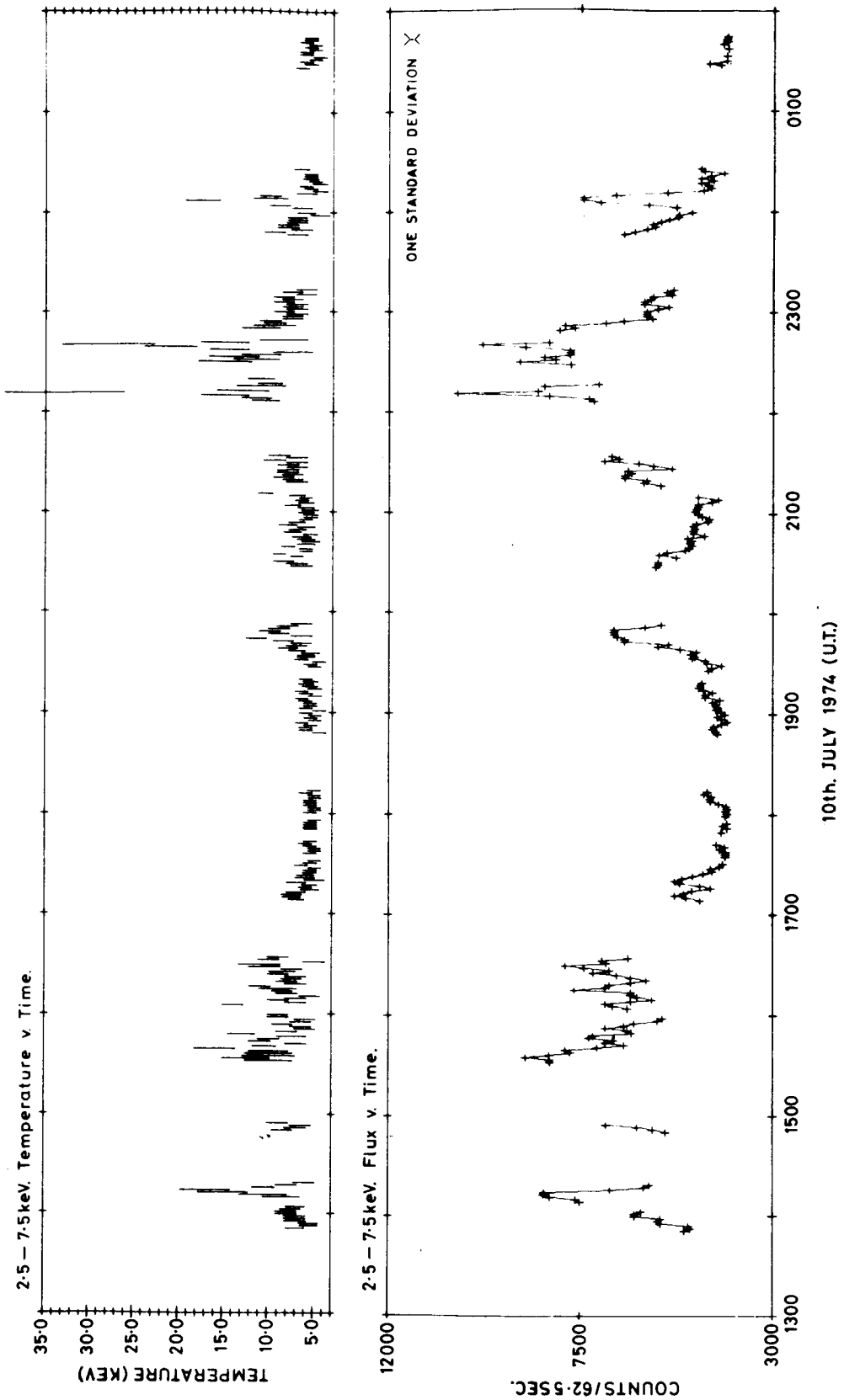


Figure 2 Plots of spectral parameter (temperature) and source intensity against time on July 10th, 1974. Data were obtained during an active phase of SCO X-1.

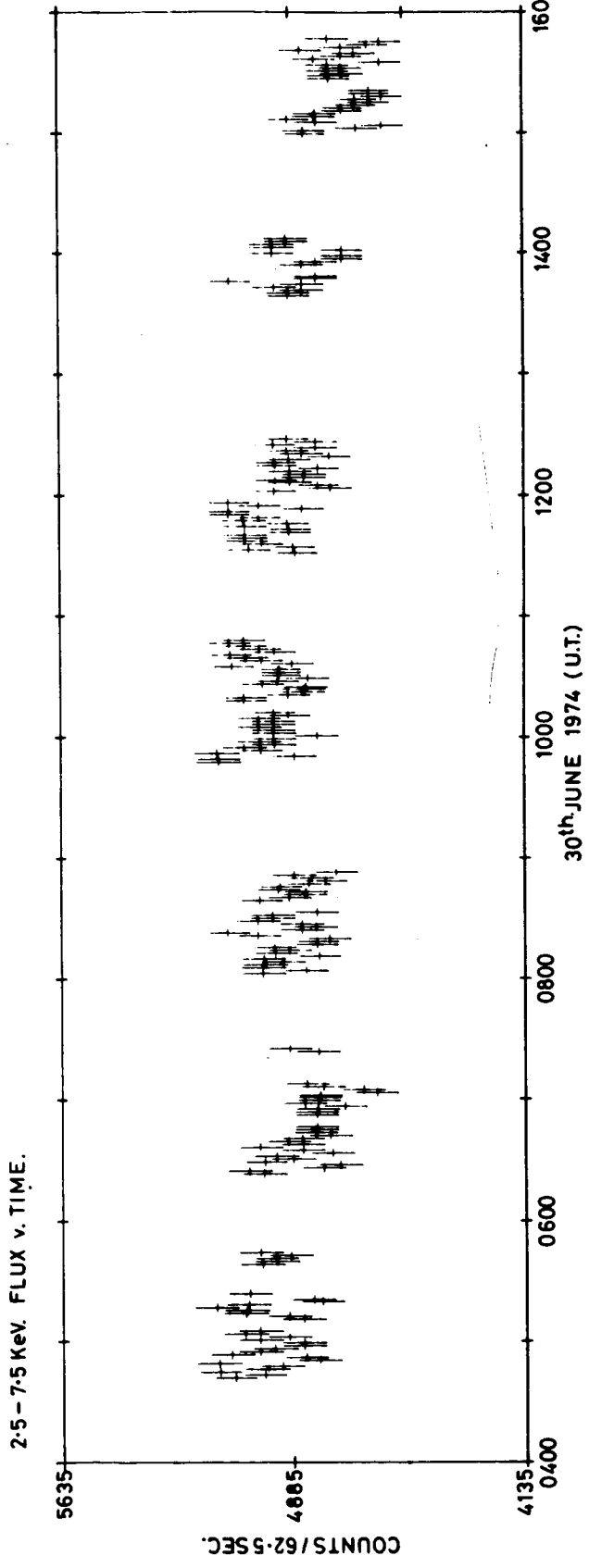
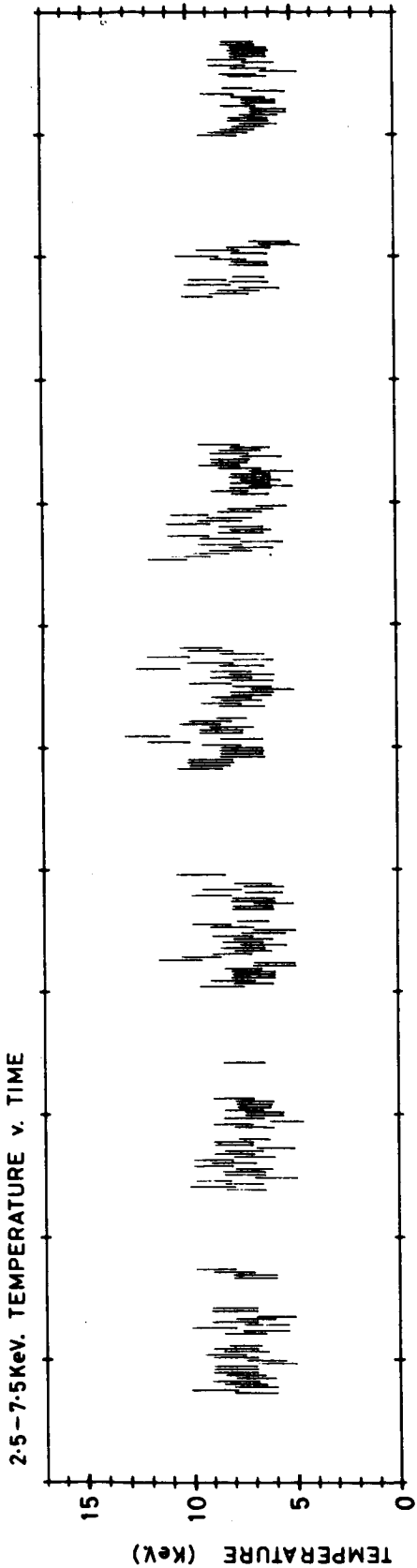


Figure 3 Spectral parameter and source intensity for SCO X-1 plotted against time during a quiescent phase. The intensity scale is expanded by a factor 18 with respect to Figure 2 in order to better illustrate the nature of quiescent variability.

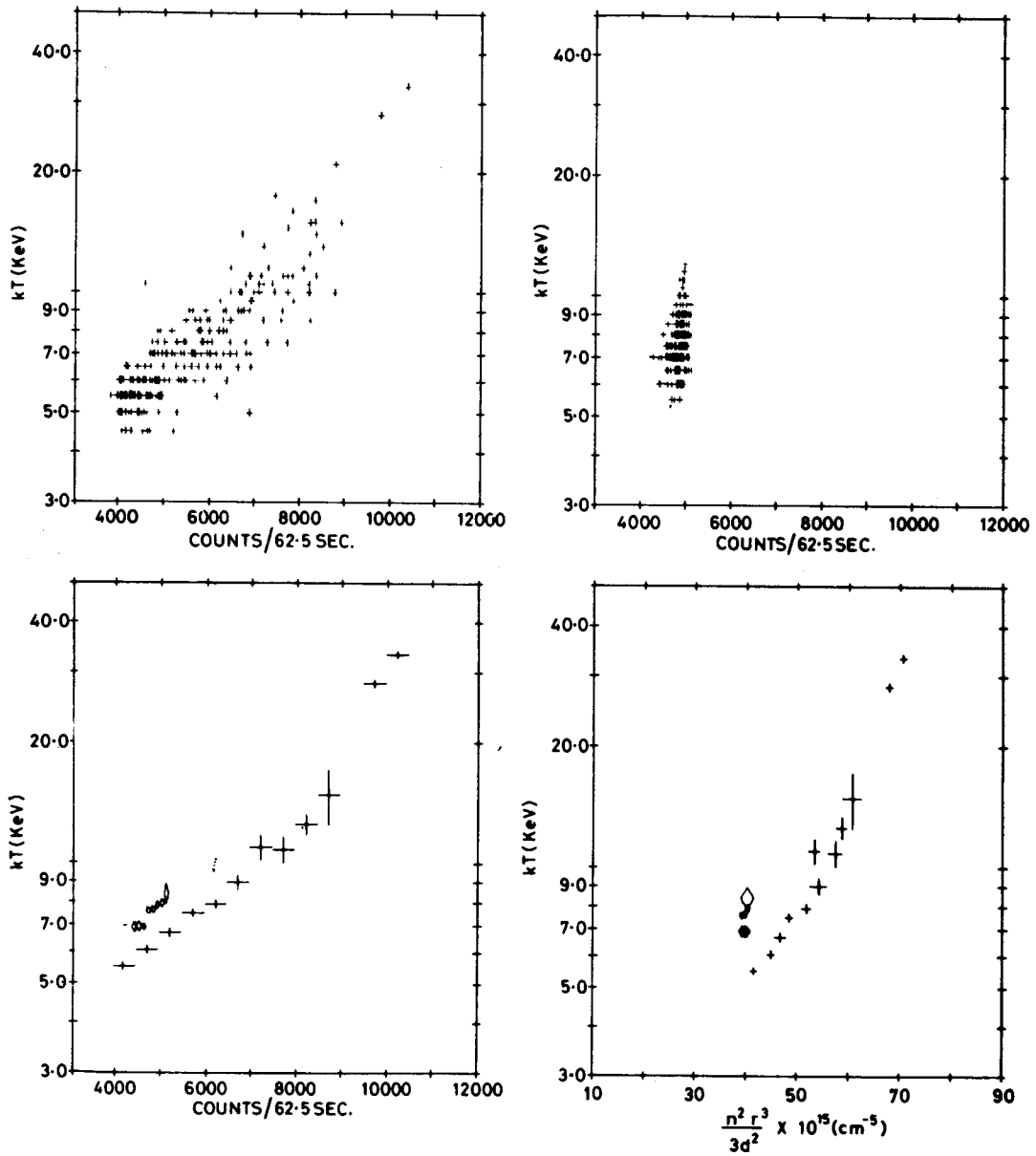
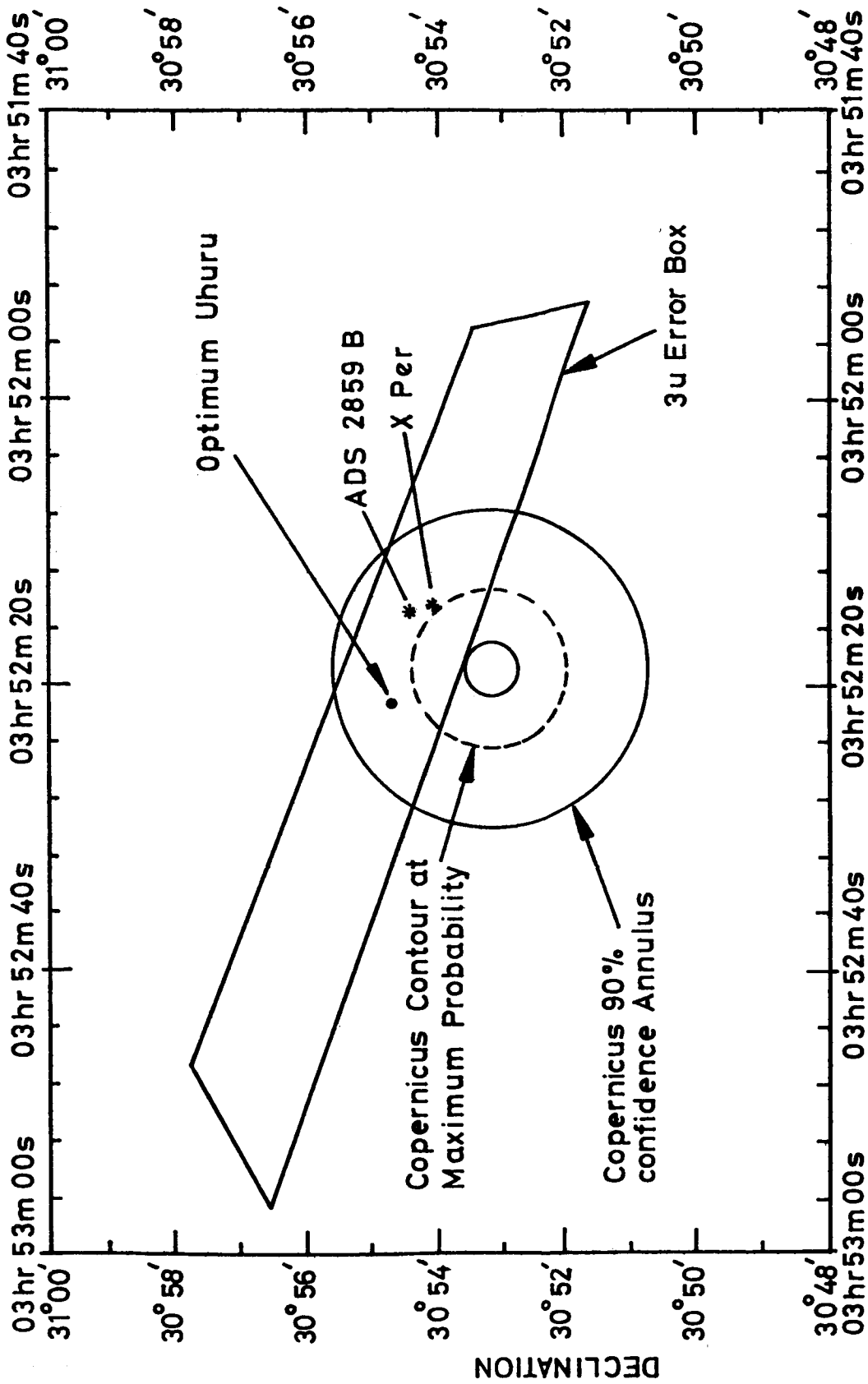


Figure 4 (a) Spectral slope plotted against intensity for the SCO X-1 observations on 10th July, 1974 when the source was in an active phase. Each point refers to a single 62.5 sec data integration period; (b) A plot similar to that of 4a but with the data points from the quiescent phase observation of 30th June 1974; (c) The data from 4a and 4b have been averaged in intensity bins of 500 counts for active data (crosses) and of 300 counts for quiescent data (diamonds).



RIGHT ASCENSION

Figure 5 The Copernicus 90% confidence annulus for the source 3U0352 + 30. The error box from the 3U catalogue is also shown. The area of overlap is approximately 7 square arc min.

3U0352+30 FEB 74

FOLDED MODULO T=13.9325 MINS

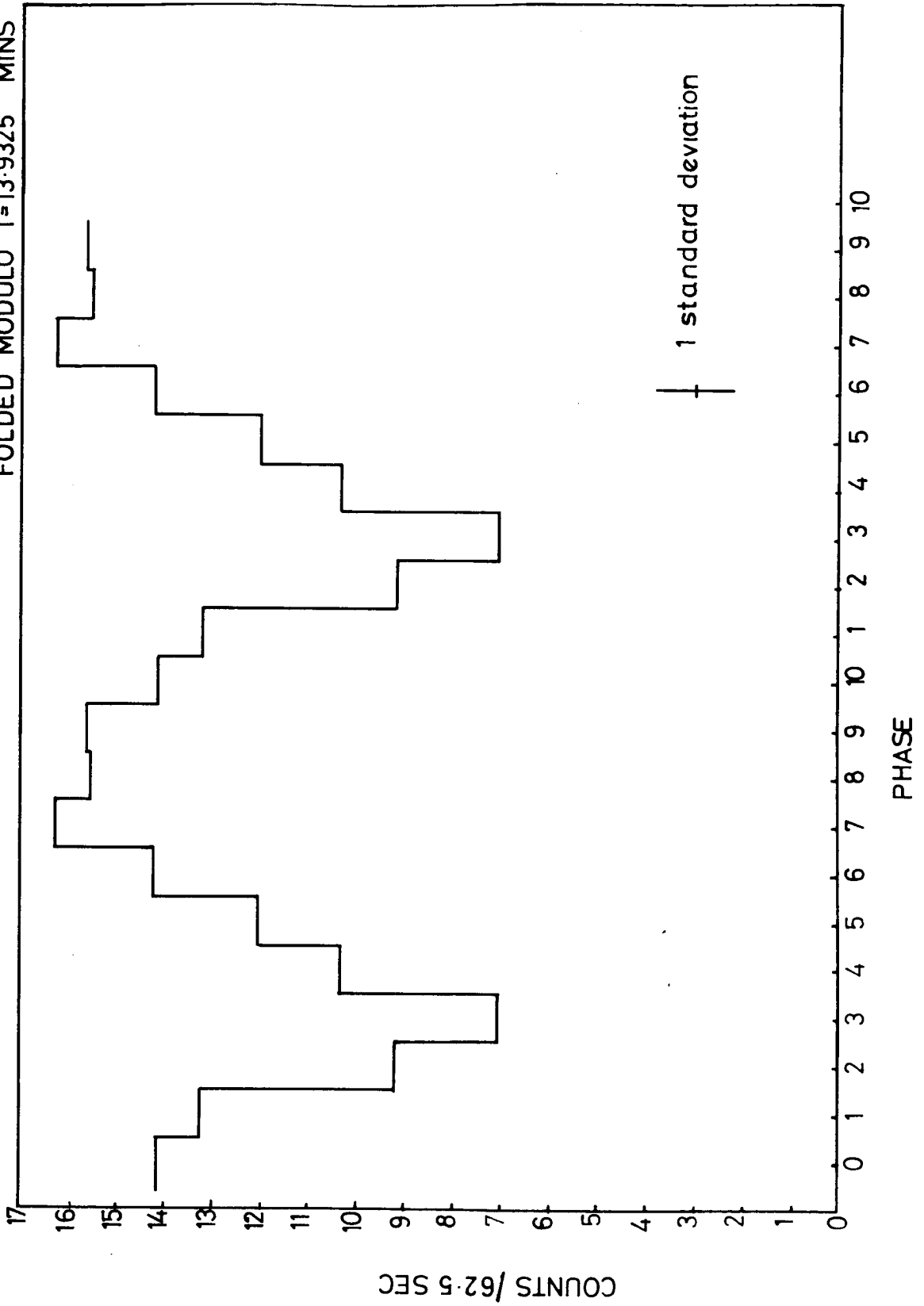


Figure 6 Data from a 2.5 - 7.5 keV Copernicus observation of 3U0352 + 30 folded modulo the period 13.9325 minutes. Two complete

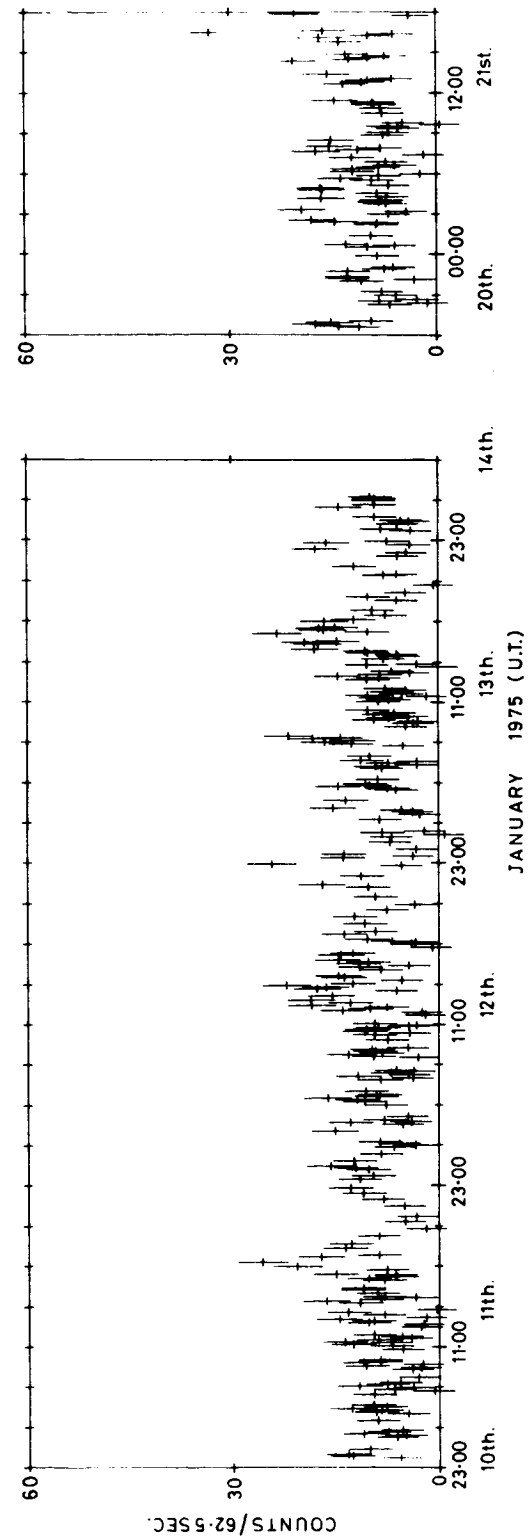
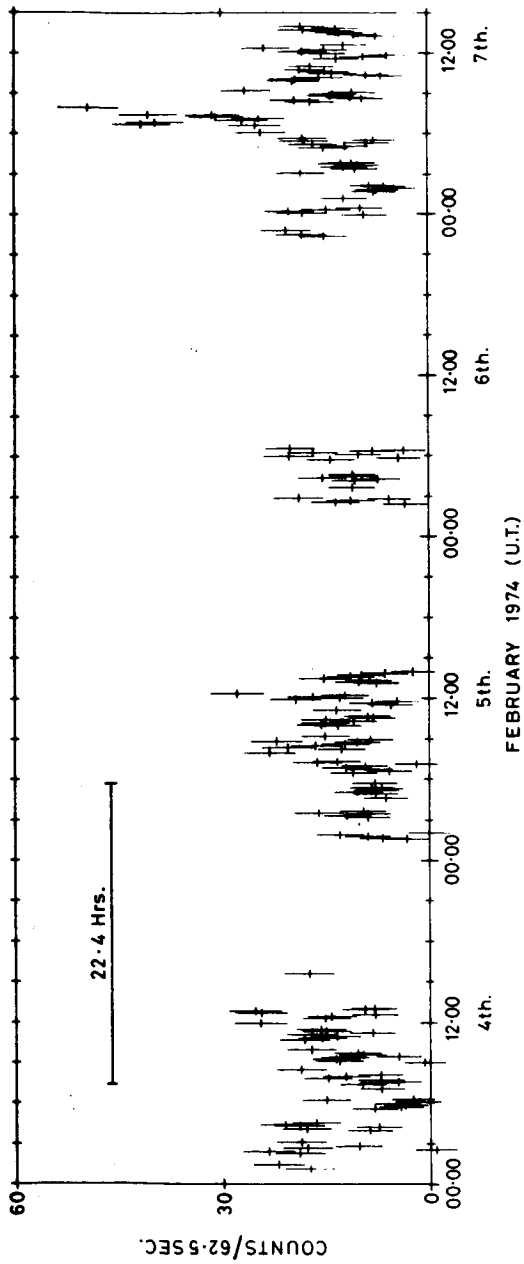


Figure 7 Copernicus counting rates for the 2.5 - 7.5 keV band observed from 3U0352 + 30 during February 1974 and January 1975. Each data point represents the count per 62.5 sec frame averaged over five frames.

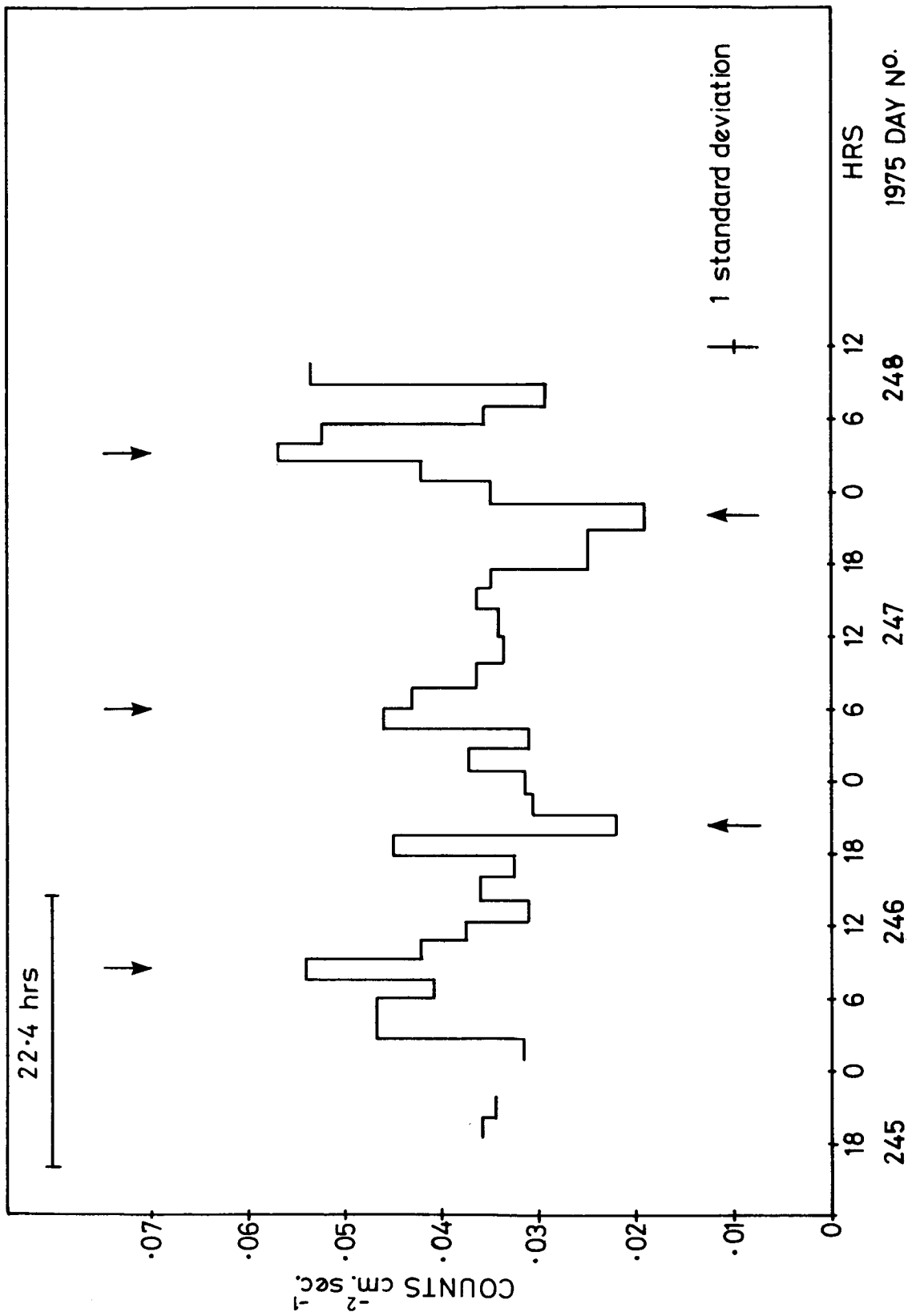


Figure 8 Preliminary data from the MSSL proportional counter on the Ariel 5 spacecraft. The 3U0352 + 30 counting rate is averaged over two orbit intervals and plotted against time. Variability on a 22 hour time scale appears to be present.

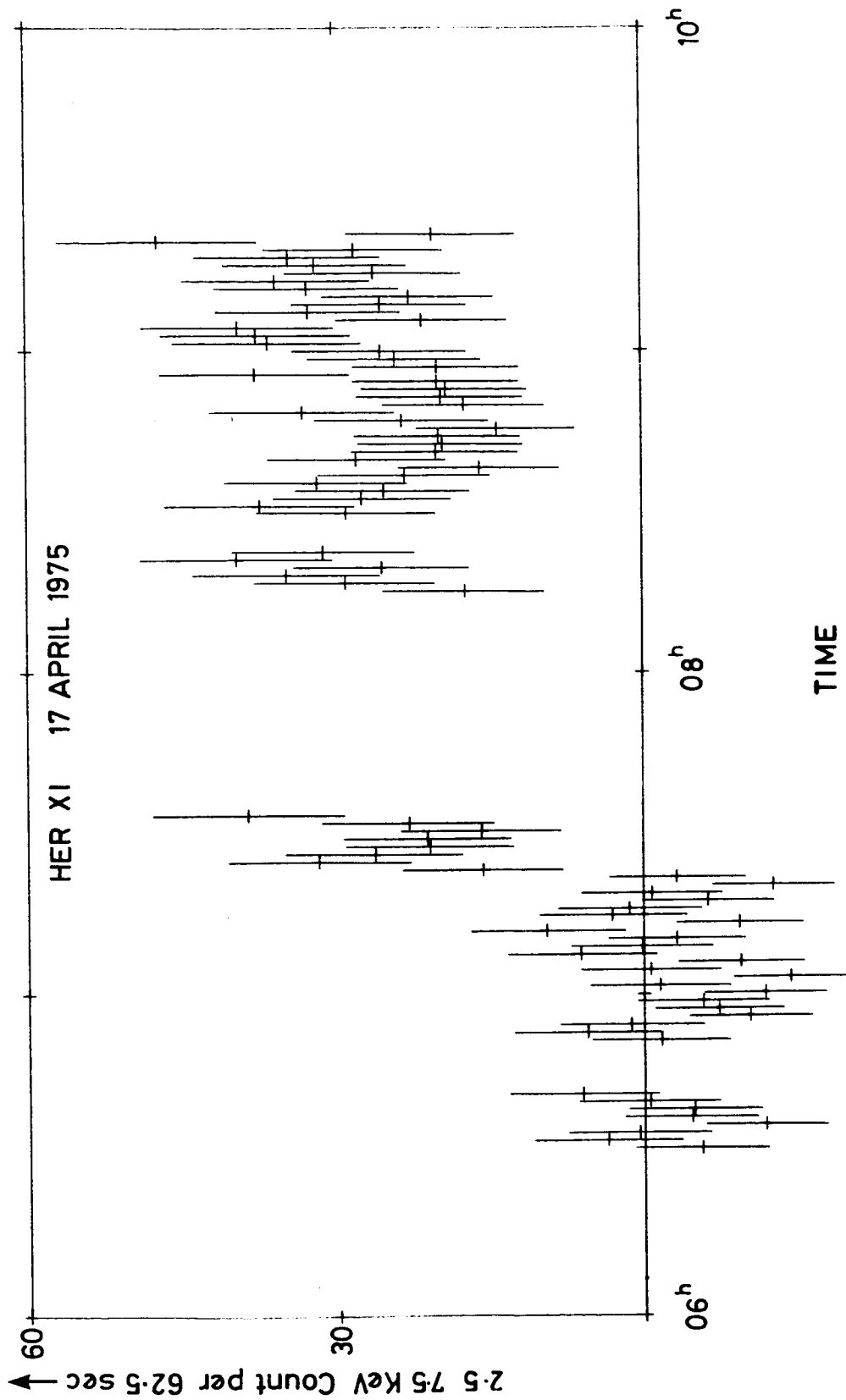


Figure 9 Copernicus data for Her X-1 (2.5 - 7.5 keV) plotted against time during the emergence from a source occultation. The source "turns on" in less than 62.5 seconds.

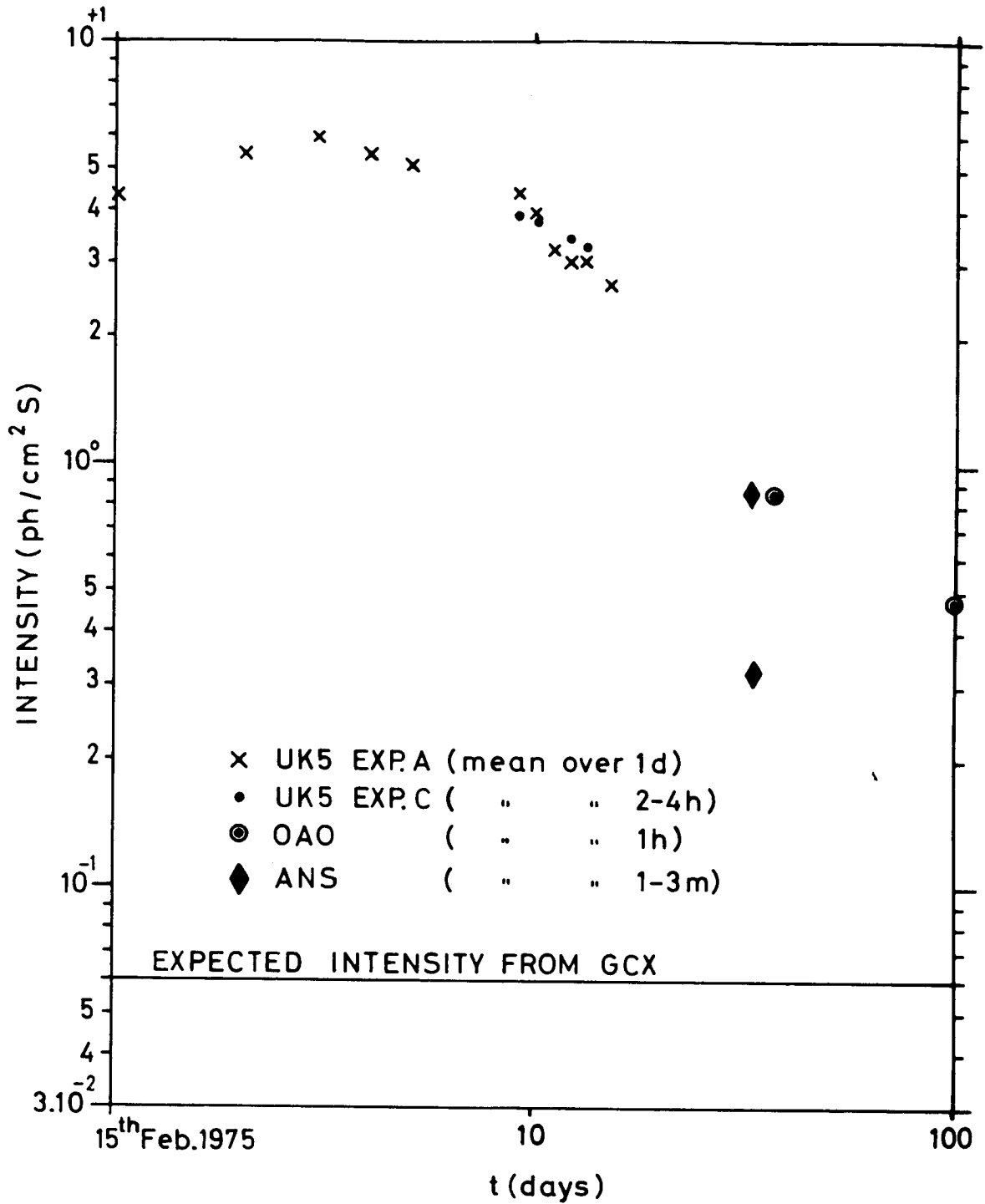


Figure 10

The X-ray light curve of the transient source A1742 - 28 located in the region of the galactic centre. Data were obtained from a number of spacecraft as shown in the figure and discussed in the text. The expected intensity from the source GCX is shown for comparison.

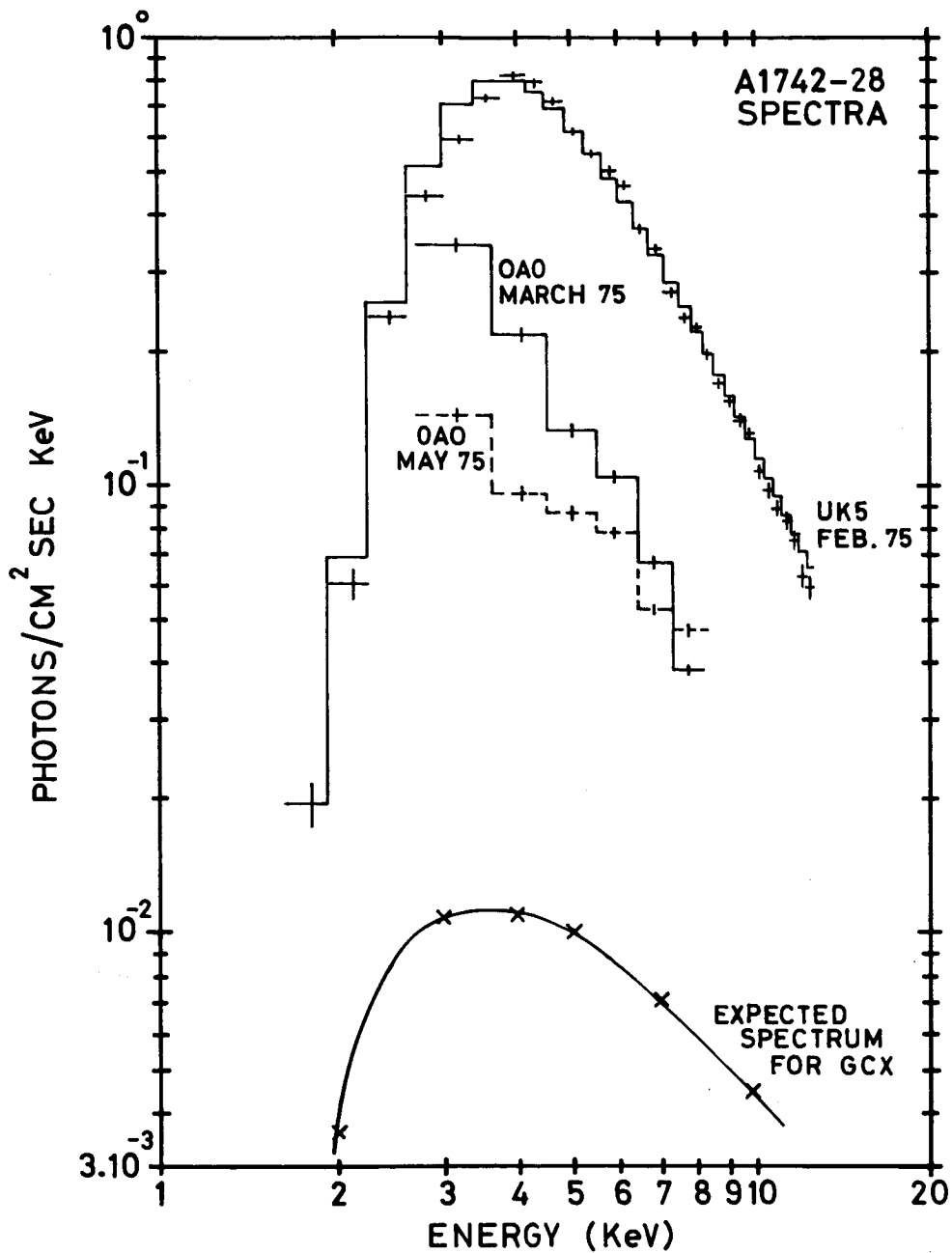


Figure 11

X-ray spectra of A1742 - 28 obtained with the MSSL proportional counter on Ariel 5 and with the 2.5 - 7.5 keV Copernicus detector. The spectrum of GCX is shown for comparison.



ANS RESULTS ON X-RAY BINARIES

J. Heise, A.C. Brinkman
Space Research Laboratory
Utrecht, Holland

ABSTRACT

A short description is given of the Astronomical Netherlands Satellite ANS and the X-ray instruments of the Space Research Laboratory in Utrecht. ANS observed in February 1975 a soft ($\frac{1}{2}$ KeV) X-ray flux in Her-x-1 during the 'off'-state with an intensity of a factor 10 lower than observed previously in the 'on'-state. The measured uncorrected intensity is $(1.1 \pm 0.2)10^{-11}$ ergs/cm² sec in 0.2 - 0.28 keV at earth.

The ANS observations on Cyg-X-1 are summarized. During the May 75 flaring state a very high intensity at 0.5 keV is measured consistent with a power-law photon-spectrum with index 3.5 and an interstellar absorption of 7.10^{21} atoms/cm², but not consistent with spectra that show an additional cut-off below 1 KeV and an absorption of $7 \cdot 10^{21}$ atoms/cm². Intensity changes on a time scale of minutes, as observed in Cyg-X-1 lowstate, are not observed during the flaring state.

INTRODUCTION.

The Astronomical Netherlands Satellite (ANS) was launched on August 30, 1974 in a sun-synchronous polar orbit, with perigee at 265 km and apogee at an unintended height of 1120 km.

The spacecraft carries instruments from three different groups:

- a. a UV-stellar spectrophotometer (University of Groningen)
- b. two X-ray detectors from S.A.O., Cambridge, Massachusetts
- c. two X-ray detectors from Space Research Laboratory, Utrecht.

First we describe shortly some capabilities and limitations of the spacecraft, since that has a great impact on the experiments. Secondly we will mention the main characteristics of the Utrecht X-ray experiments. And then we will describe some of our results on X-ray binaries.

Among the first, elsewhere published, scientific results of the Utrecht instrumentations are the detection of an X-ray flare in YZ-C Mi and in UV Ceti (Heise et al., 1975), the discovery of a soft X-ray flux of Sirius, clearly distinguishable from its UV contamination (Mewe et al., 1975a, 1975b), and the detection of a soft flux from Capella (Mewe et al. 1975b).

SPACECRAFT.

The choice of the polar orbit and the attitude control system were mainly determined by the requirements of the UV-instrument. The nature of this instrument, the observation of a large number of faint stars, requires that the satellite should be pointed accurately and it should be possible to change attitude easily. A three axis stabilized satellite is chosen with an attitude control system such that one axis is continuously pointed towards the sun for a clear and reliable reference necessary for this small satellite (125 kg). See for a full description Bloemendal and Kramer (1973). This attitude control system implies that X-ray objects can only be observed, if they are located within a distance of 2.5 degree from a plane perpendicular to the connecting line with the sun. Because of the annual rotation of the Earth around the sun, every object in

the sky can be observed in principle once per half year for $5/\cos \beta$ days, where β is the ecliptic latitude.

A horizon sensor measures the angle between the horizon and the viewing direction of the scientific instruments. The onboard computer calculates the required torques for the reaction wheels to slew to a desired direction. This can be done with an accuracy of better than 1° . To achieve the 1 arcmin accuracy, a star sensor is used. After a slew manoeuvre the satellite is left in the scanning mode (4° per minute). The star tracker must now recognize a predetermined set of two reference stars within 1.5 degree of the target position and with magnitude brighter than 8.5^m . Also a slow scan can be made after a star recognition with scanspeed of 0.6° per minute. Every 12 hours, when the satellite passes over its main groundstation, a new observing program is loaded and the accumulated data is dumped. If the available memory capacity (7 blocks of 4096 16 bits words) is insufficient for a full 12 hour period, the memory can be dumped over other groundstations.

In summary the spacecraft offers

1. continuous pointing with an accuracy of 1 arcmin;
2. an offset-pointing capability, whereby the viewing direction steps repeatedly on and off the source for maximum 256 sec with a transition time of 16 seconds. The off-source position could be at maximum 1.5 degrees away from the source;
3. a scan mode with scanspeed $4^\circ/\text{min}$;
4. a slow scan mode with scanspeed $0.6^\circ/\text{min}$.

THE UTRECHT X-RAY EXPERIMENTS SXX.

The Utrecht soft X-ray experiments are pictured in fig. They consist of a soft detector (small area proportional counter with 3.8 micron polypropylene) in the focal plane of a circular parabolic reflector with a projected area of 144 cm^2 and a reflection coefficient of around 50%. A filter wheel can select two fields of view (0.5 and 2 degrees FWHM, circular), a UV-filter and a closed, calibrate position. The UV-filter (0.5 mm Mg F_2) blocks out the soft X-ray signal completely and enables us to determine the contribution of the UV-signal to the measured countrate. The overall efficiency of the soft-detector is shown in fig. 2, solid curve. The main efficiency is between .2 and .28 keV, as also determined by the pulse height discriminator limits of .13 and .41 keV, but note the low efficient side lobe at .5 keV, which contributes slightly due to finite counter-resolution into the range .13 - .41 keV. This latter effect is responsible for the soft X-rays in Cygnus-X-1, which I will describe later.

The second instrument consists of a medium energy range X-ray detector with a 1.7 micron Titanium window and an effective area of 40 cm^2 . The field of view is collimated to a rectangular form of $34' \times 90'$ and is sensitive in the range 0.6 - .8 keV with an extra channel around .45 keV (see fig. 2, broken line). Pulse height information of 7 energy channels can be sampled every 1, 4 or 16 seconds.

In the high time resolution mode all photons are binned in 125 msec intervals for either the soft- or medium-energy detector. In the pulsar mode 7 photons per second are registered with an accuracy of 1 msec.

SOFT X-RAYS FROM HERC-X-1 IN THE OFF-STATE.

ANS could observe Herc-X-1 in February and August 1975. In February the source was in the off-state of its 35^d cycle, approximately 7 days before an expected turn-on. In fig. 3 the raw data is shown for a measurement on Her-X-1, with the satellite in an offset-pointing mode, printing alternatively 80 seconds on the source and 80 seconds 50 arcmin away from the source. It is clearly seen that we have detected here with our soft X-ray detector (parabolic reflector system) a definite flux between .2 - .28 keV. The medium energy detector showed no evidence for a X-ray flux between 1 - 7 keV. The soft X-ray countrate is .7 c/s with a statistical significance at a level of 6 sigma (0.66 ± 0.11 c/s). This corresponds to $1.1 \cdot 10^{-11}$ ergs/cm² sec in .2 - .28 keV measured at earth. The radio data of Heiles (1975) and Tolbert (1971) indicate a hydrogen column density of $7 \cdot 10^{20}$ atoms/cm². If we take the source to be at least 2 kpc (Bahcall et al. 1974), then in view of the high galactic latitude of the source the total column density will be between the source and earth. If we correct the measured flux for such an interstellar absorption one would have a flux of $1.5 \cdot 10^{-10}$ ergs/cm² sec at earth. Compared to the X-ray flux between 2 - 6 keV of 10^{-9} ergs/cm² sec this is a rather large fraction. This fraction however is rather

sensitive to the adopted column density of interstellar matter. For example for a density of $3 \cdot 10^{20}$, $5 \cdot 10^{20}$, $7 \cdot 10^{20}$ atoms/cm² the interstellar transmission is 28%, 14%, 7.5% respectively in the .2 - .28 keV band, assuming the Brown and Gould (19) abundances.

Previous observations made in the on-state of Hercules-X-1 35 day cycle by NRL (Shulman et al. 1974) and also Catura and Acton (1975) have measured an intensity in this energy range which is a factor of 10 higher. Our measurement during the OFF-state is consistent with earlier obtained upper limits (Shulman et al. 1974). It follows from our observations that the soft X-ray flux at 1/4 keV of Her-X-1

- a. is not constant throughout the 35^d cycle, but varies with at least a factor of 10
- b. is not always off, when the hard X-ray flux is off
- c. the soft X-ray intensities are remarkable bright.

The interpretation of the soft X-ray flux is rather difficult.

The black body intensity of a neutron star at a temperature of $\sim 10^6$ K, without interstellar absorption would yield $2.6 \cdot 10^{-13} R_{10}^2 / D_{2\text{kpc}}^2$ ergs/cm² sec in the range .2 - .28 keV where R_{10} is the neutron star radius in unit of 10 km and D de distance in units of 2 kpc, and hence is too small to account for the measured luminosities for both ON and OFF-states.

Also, in the usual picture of the accretion disk model, the accretion disk itself could not give rise to such high luminosities in the soft X-ray range compared to the harder X-ray luminosities.

If the emission is caused by an optical thin gas surrounding the X-ray source, the contribution of line radiation is dominant over the continuum by a factor of 20 in our soft X-ray channel. In fig. 4 we plotted the expected countrate of an optical thin source of emission measure $10^{50}/\text{cm}^3$ placed at a distance of 1 pc as a function of temperature. One sees that mainly Si VIII, Si IX, S X are contributing. If the soft Her-X-1 flux were due to such emission, the required emission measure at 2 kpc during the OFF-state would range between $3 \cdot 10^{57}/\text{cm}^3$ and $1.2 \cdot 10^{58}/\text{cm}^3$ for assumed interstellar column densities between $3 \cdot 10^{20}$ and $7 \cdot 10^{20}$ atoms/cm². From the measurements of Shulman et al. (1974) and Catura et al. (1975) one would infer emission measures that are a factor of 10 higher in the ON-state. For a spherical volume with radius 10^3 cm around the neutron star for example, this would imply electron densities of the order of $10^{15}/\text{cm}^3$ in the OFF-state and $5 \cdot 10^{15}/\text{cm}^3$ in the ON-state. At such densities the electron scattering opacity is of the order of unity.

The light curve of the ANS observations of Her-X-1 in August 1975 is shown in fig. 5. The source is seen during a turn-on in its 35 day cycle. The exact turn-on must have happened between binary phase 0.2 and 0.5 on August 28, 1975, as was also reported by Serlemitsos et al. (1975). Unfortunately at this time the window of our soft detector was broken, so that no soft X-ray measurements could be made during the turn-on.

CYGNUS-X-1

Cyg-X-1 has been observed by ANS in November 1975 and in May 1975.

In May 1975 we discovered the source to be in a high intensity state.

The flux around 2 keV was a factor of 10 higher than observed in November 1974 (J. Heise et al. 1975a, 1975b). Fig. 6 shows the complete lightcurve of our May data. One data point is typically 10 to 20 minutes worth of data, hence statistical errors are of the size of the data points. The spectrum has changed to a very steep powerlaw (photon number index 2.5) compared to November 1974 (index ~ 0.5) and did not change markedly during this flare period. The best fit spectrum is shown in fig.7 with powerlaw photon index of 3.5 and a cut-off corresponding to 7.10^{21} atoms/cm². Due to a decrease in opacity of the interstellar medium below the oxygen K-absorption edge around 0.5 keV, a significant flux could be detected in the parabolic section of our instruments. The measured flux around 0.5 keV is entirely consistent with the above mentioned spectrum. As also a column density of 7.10^{21} atoms/cm² is the one expected from purely interstellar matter, this would imply that the intrinsic source spectrum of Cyg-X-1 in the high state is a very steep powerlaw, increasing all the way down to at least 0.5 keV, and this implies that the bulk of the X-ray energy is emitted below 1 keV. Attempts to fit the data with spectra that do not have this energetic soft X-ray component, e.g. a powerlaw with a break to index 1 below 1 keV, always need a lower column density to account for the measured flux around 0.5 keV (typically 4.10^{21} atoms/cm²).

A remarkable difference between the flare data of May 1975 and the low state data of November concerns the time variability of the order of 100 sec.

In November 1974 we often observed intensity changes of 30 to 50 % on a timescale of 100 sec: intensity dips (see fig. 8 as an example) rather symmetric in time and correlated with spectral changes in the sense that at lower intensities the spectrum is harder. In fig.9 the correlation is shown for spectral fits taken with a constant absorption of 7.10^{21} atoms/cm². Significant changes of that sort are not observed in our May data of Cygnus-X-1 during the flaring state, although the total time coverage of the source has been much better.

A qualitative interpretation could be given (Thorne and Price, 1975) on the basis of the standard accretion-disc model for Cyg-X-1. Here the spectrum has two major components. A high energy component originating from a thick, but optically thin inner region and a thin, but optically thick outer region of the accretion disc. The relative contributions to the total spectrum are dependent on the location of the transition radius between those two regions. Variations of the order of the drift time of gas through the X-ray emitting region are to be expected. These are stronger in or near the notch of the spectrum than elsewhere.

If the low and high states of Cyg-X-1 are due to changes in accretion rate, the location of the transition radius is such that the "notch" of the spectrum falls into our energy range, say between 2 and 5 keV. The time scale for variations then is of the order of minutes, as observed, (drift-time through X-ray emitting region) and one would also expect this to be correlated with the hardness of the spectrum measured in the range 1-7 keV.

In the high state, the transition radius in Cyg-X-1 would be much closer to the central object, the "notch" of the spectrum is shifted outside our energy range (> 7 keV) and in this range one does not see any more spectral changes in relation to intensity variations, as is observed. Also the time scale of the variations will be shifted to much shorter times (order of seconds).

OTHER X-RAY BINARY SOURCES.

For completeness we show the lightcurves of other X-ray binary sources as obtained so far from quick-look data. Fig. 10 gives the source 3U 1700-37, Fig. 11 the lightcurve for Cen-X-3 observed in July 1975 in the scan-mode of the satellite (only a few seconds of data per datapoint).

REFERENCES.

- Bahcall, J.N., Joss, P.C. and Avni, Y., 1974, Ap. J. 191, 211.
- Bloemendal, W., Kramer, C., 1973, Philips Tech. Rev. 33, 117.
- Catura, R.C. and Acton, L.W., 1975, Ap. J. 202, L5.
- Heiles, C., 1975, Astron. and Ap. Suppl. 20, 37.
- Heise, J., Brinkman, A.C., Schrijvers, J., Mewe, R., Gronenschild, E., den Boggende, A., 1975, Ap. J. 202,
- Mewe, R., Heise, J., Gronenschild, E., Brinkman, A.C., Schrijver, J., den Boggende, A., 1975a, Ap. J. 202.
- Mewe, R., Heise, J., Gronenschild, E., Brinkman, A.C., Schrijver, J., den Boggende, A., 1975b, Nat. 256, 711.
- Serlemitsos, P.J., 1975, I.A.U.-circular 2824, August 29, 1975.
- Shulman, S., Friedman, H., Fritz, G., Henry, R.C., Yentis, D.J., 1975, Ap. J. 199, L101.
- Thorne, K.S., Price, R.H., 1975, Ap. J. 195, L101.

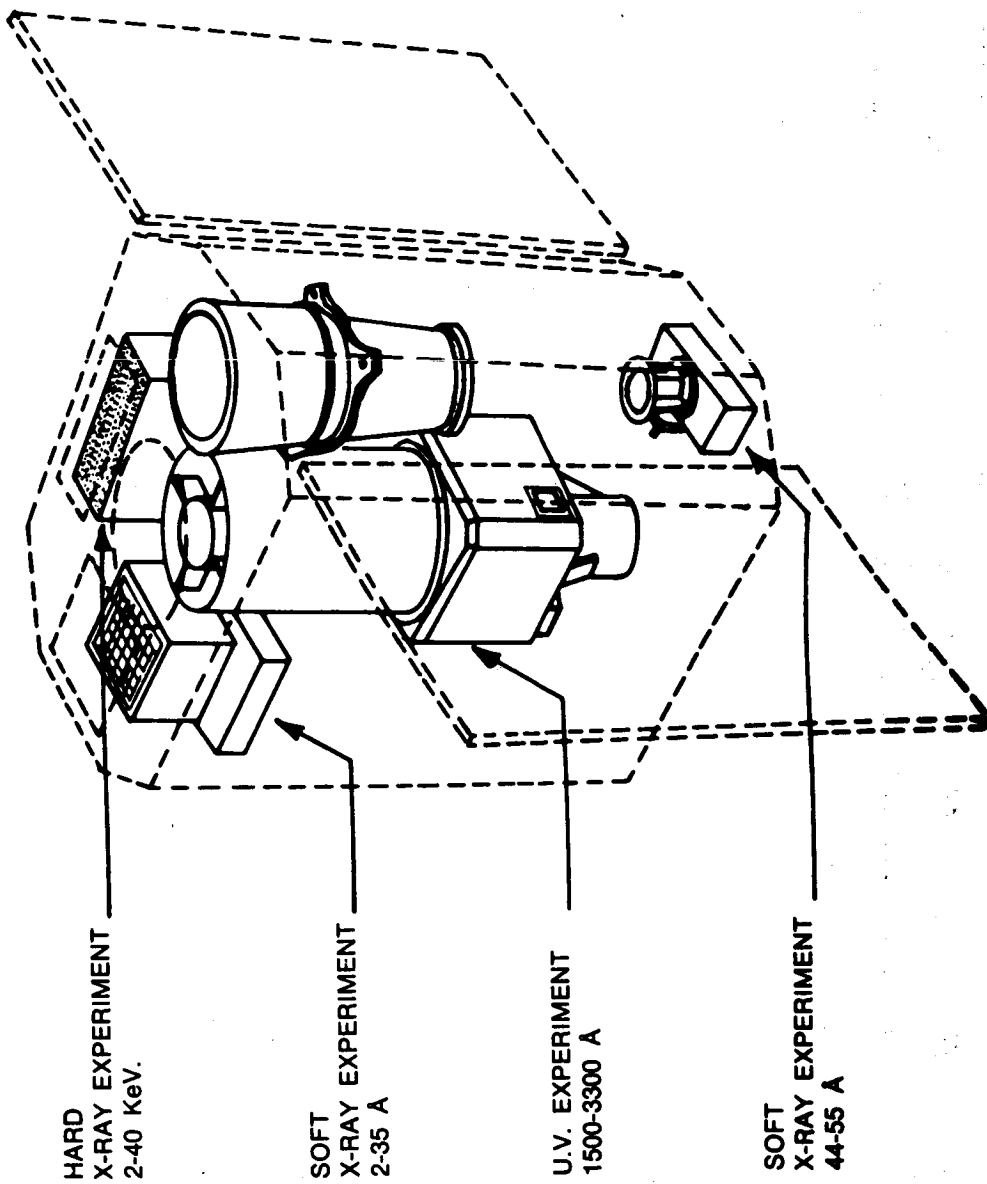


Figure 1. Location of Experiments

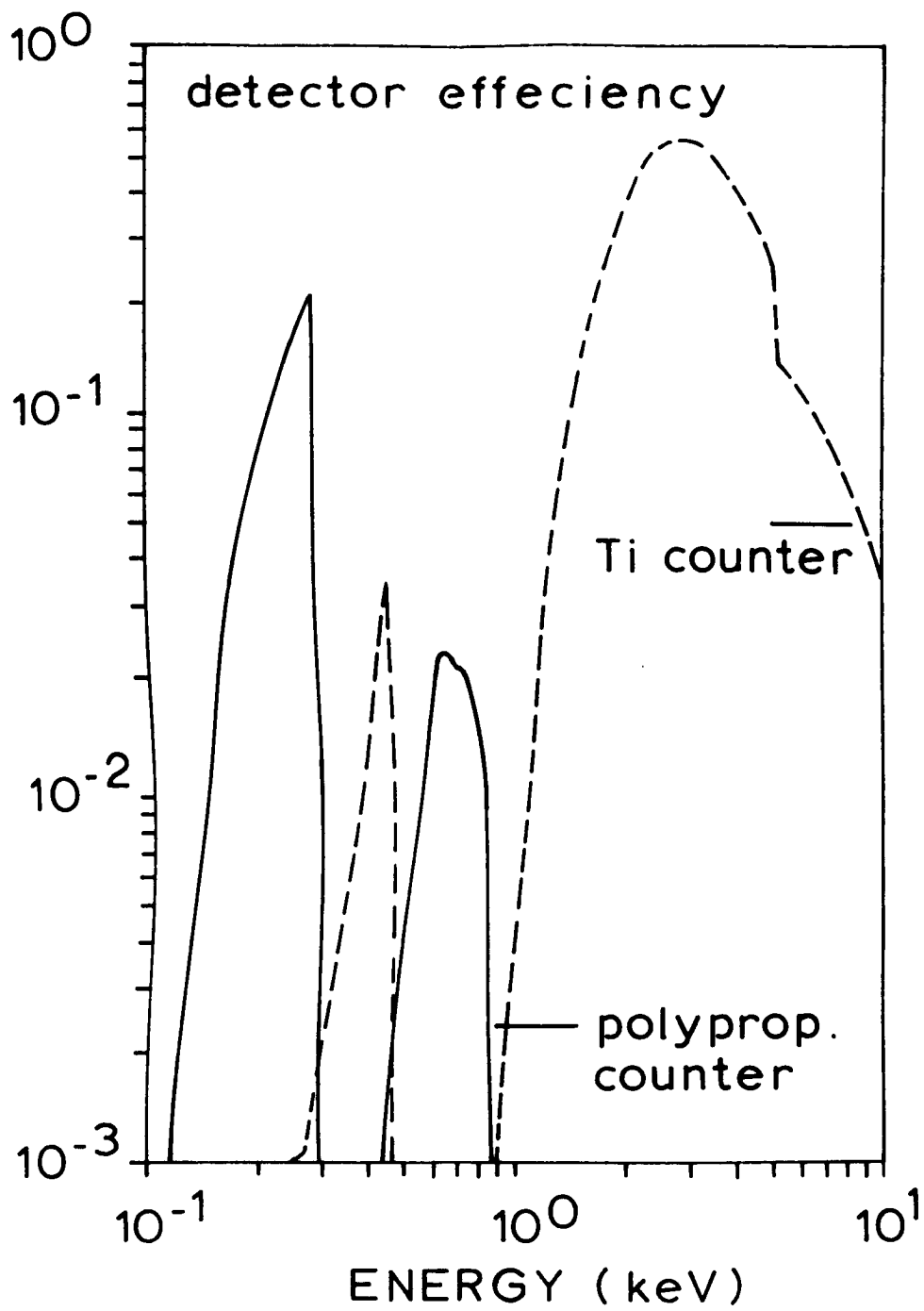


Fig. 2. Overall detector efficiency of the two Utrecht X-ray instruments.

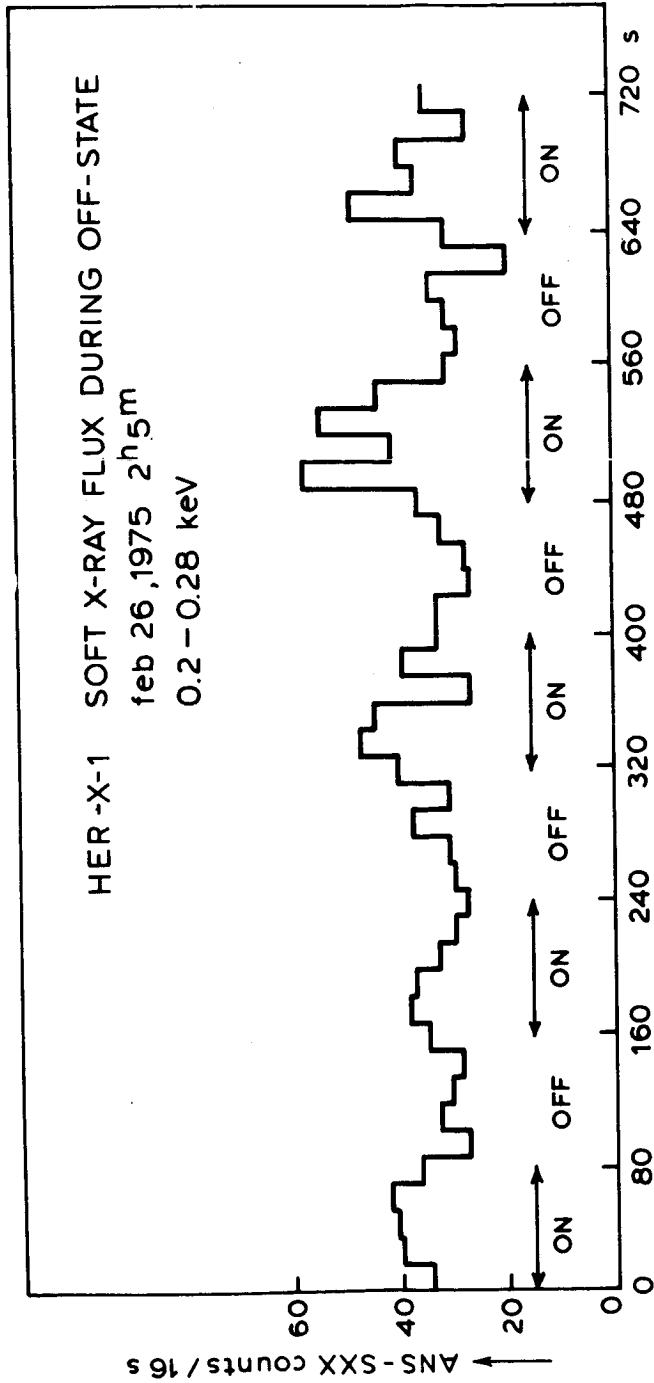


Fig. 3. Raw data of Hercules-X-1 observation in 0.2 - 0.28 keV channel, alternatively pointing on and off the source.

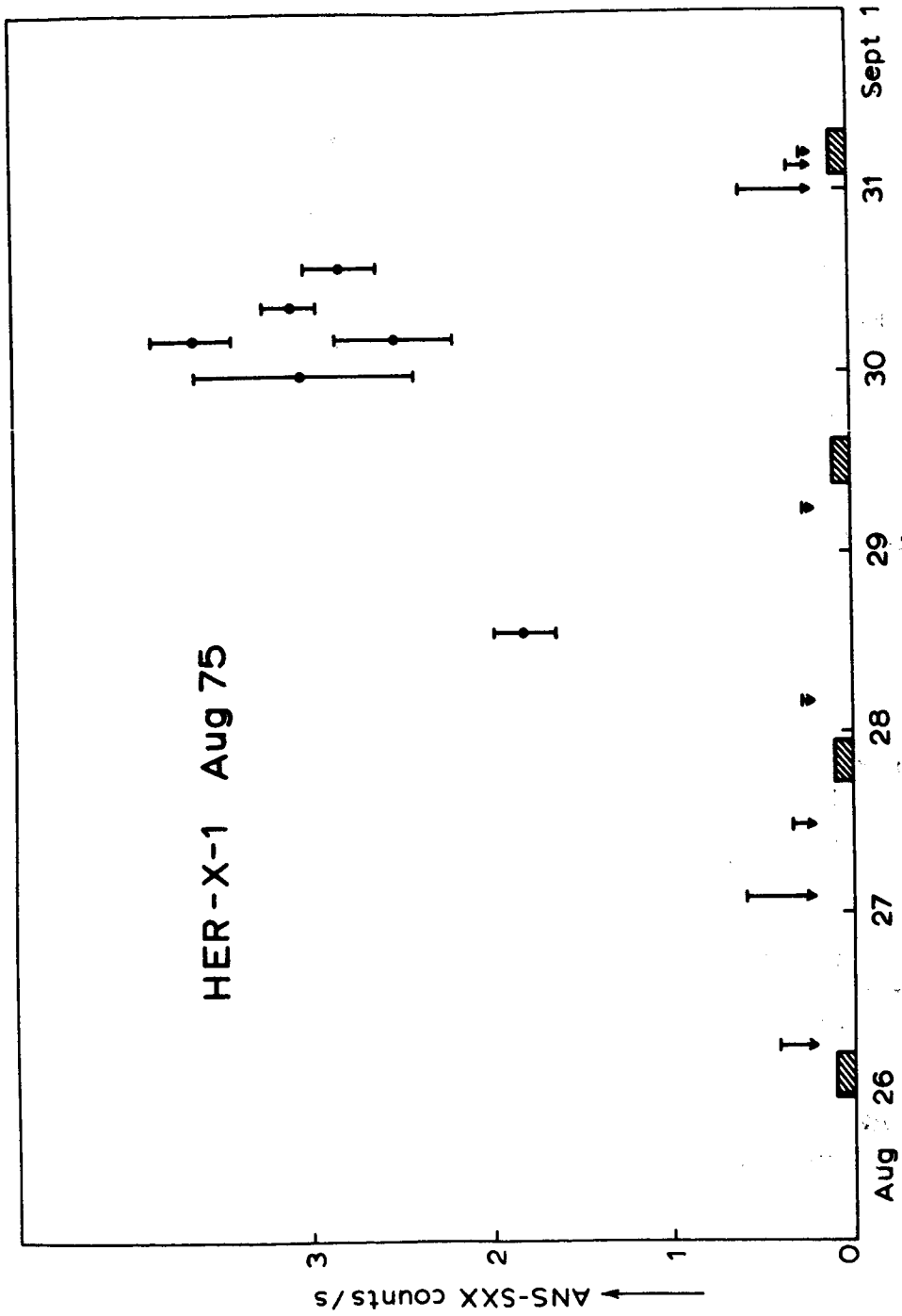


Fig. 5. Her-X-1 preliminary light curve of August 1975 observations.

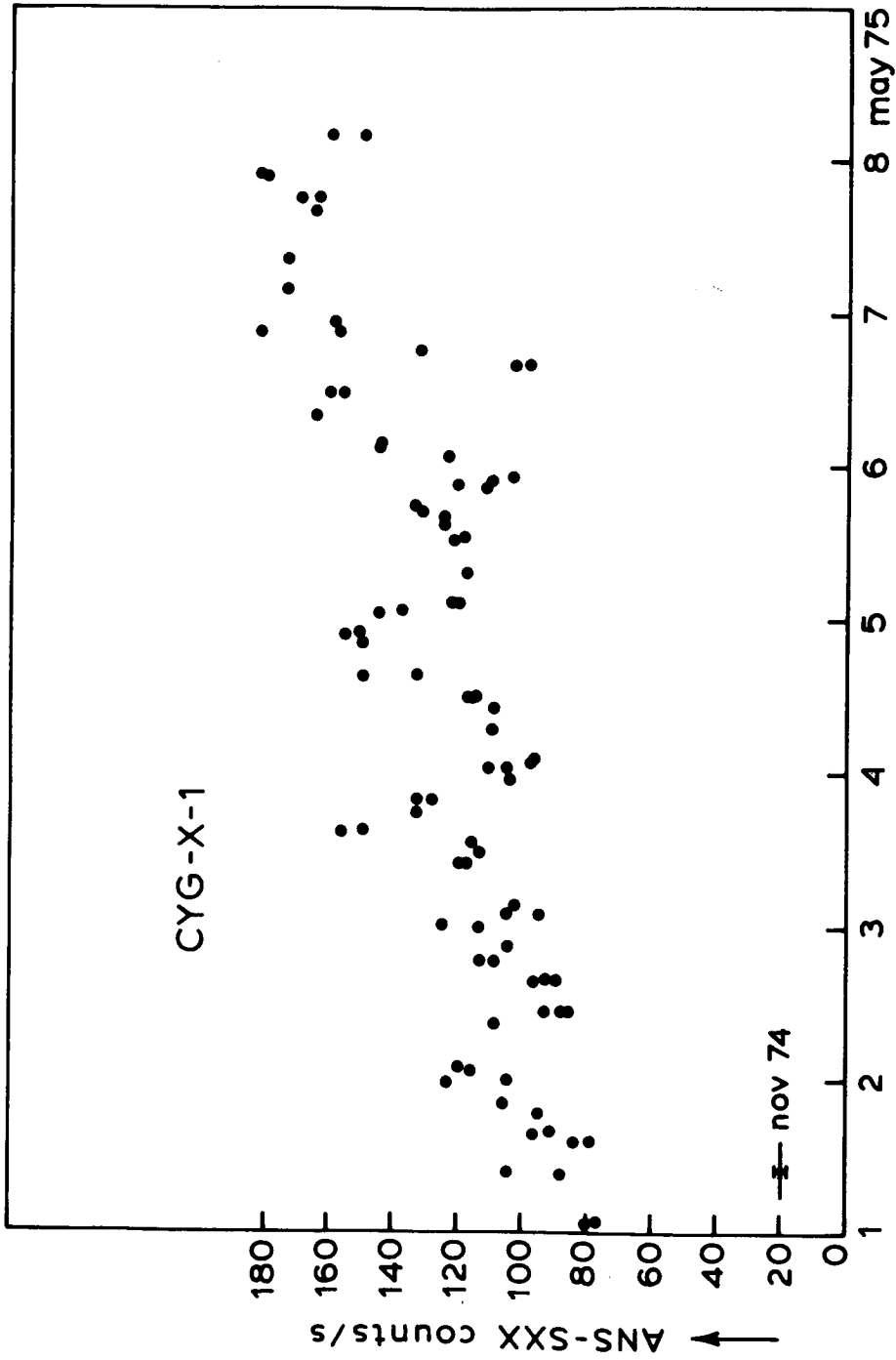


Fig. 6. Light curve of Cyg-X-1 of May 1975. The November 1974 intensity is indicated.

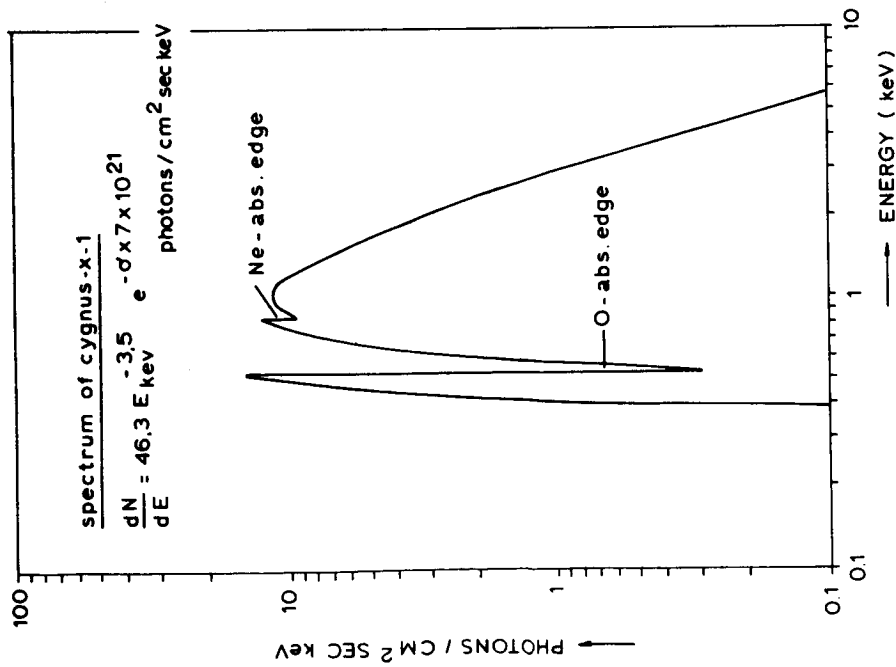
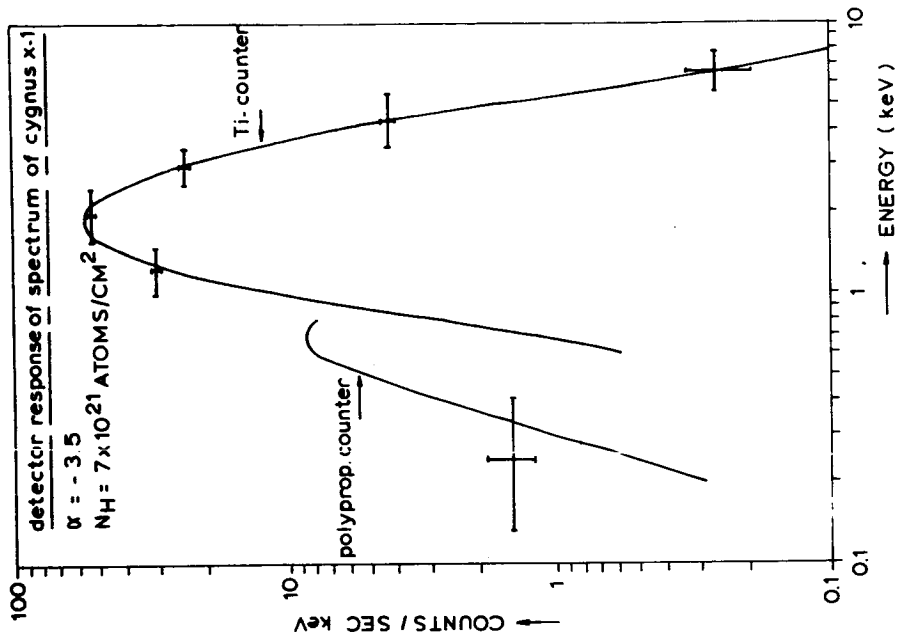


Fig. 7. Spectrum of Cyg-X-1 during flaring state in May 1975.

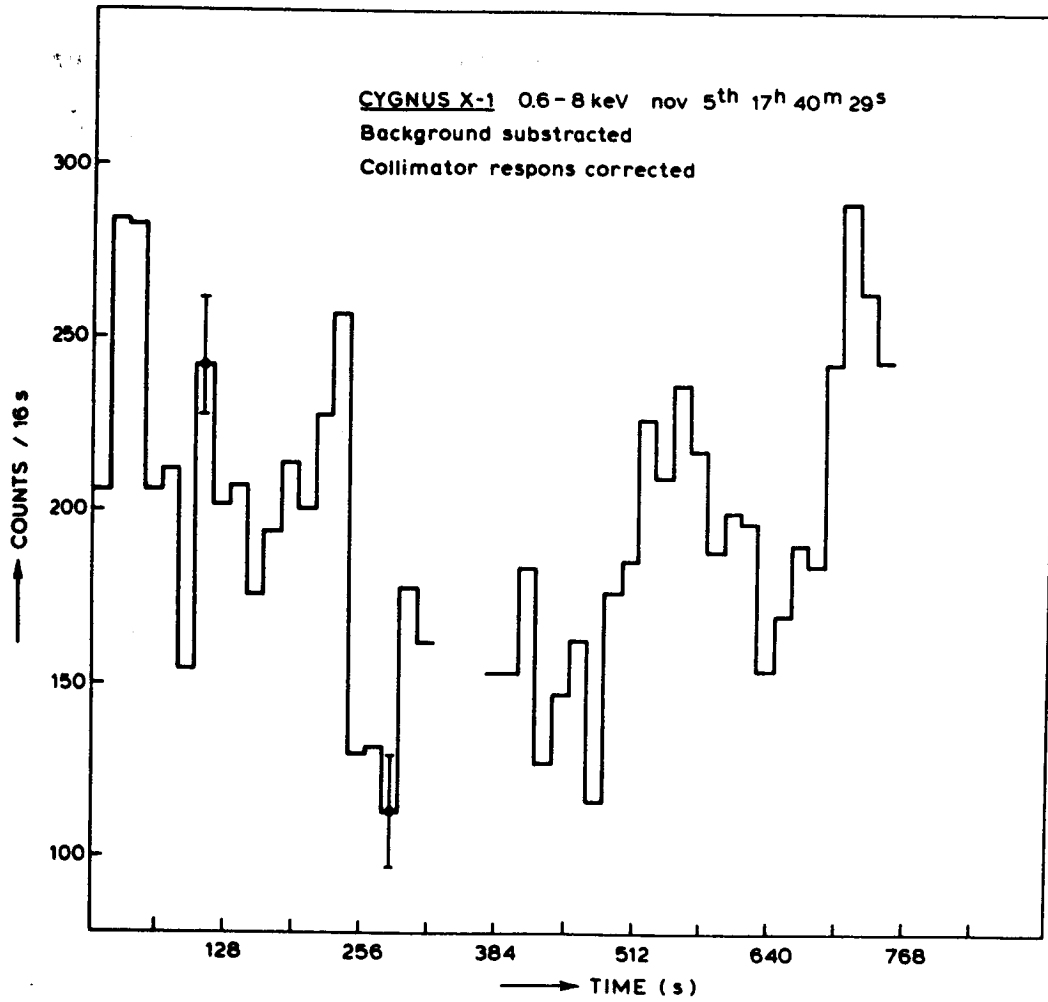


Fig. 8. Intensity change on timescales of minutes in Cyg-X-1 low state (Nov. 1974).

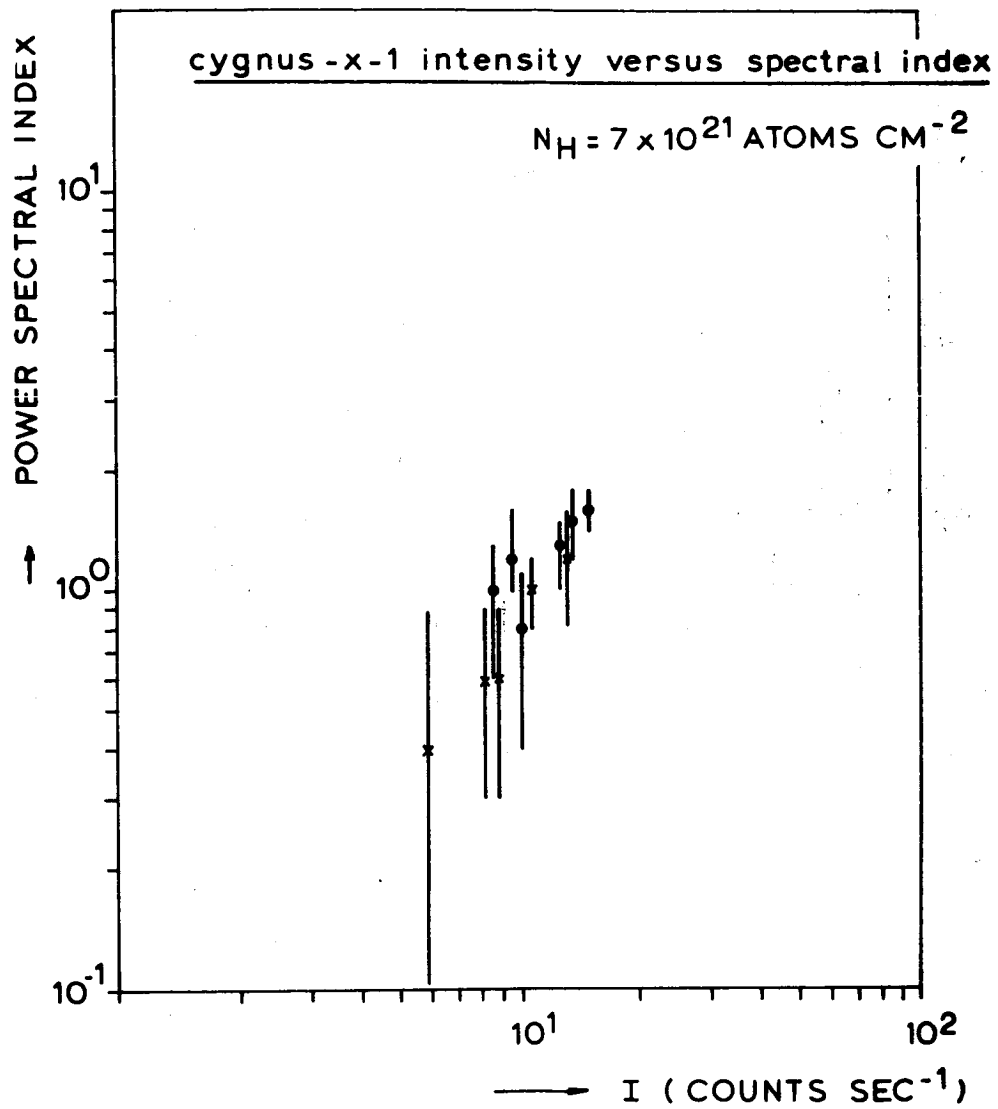


Fig. 9. Spectral shape change as a function of total intensity of Cyg-X-1 for various intensity dips, such as the one in fig. 8.

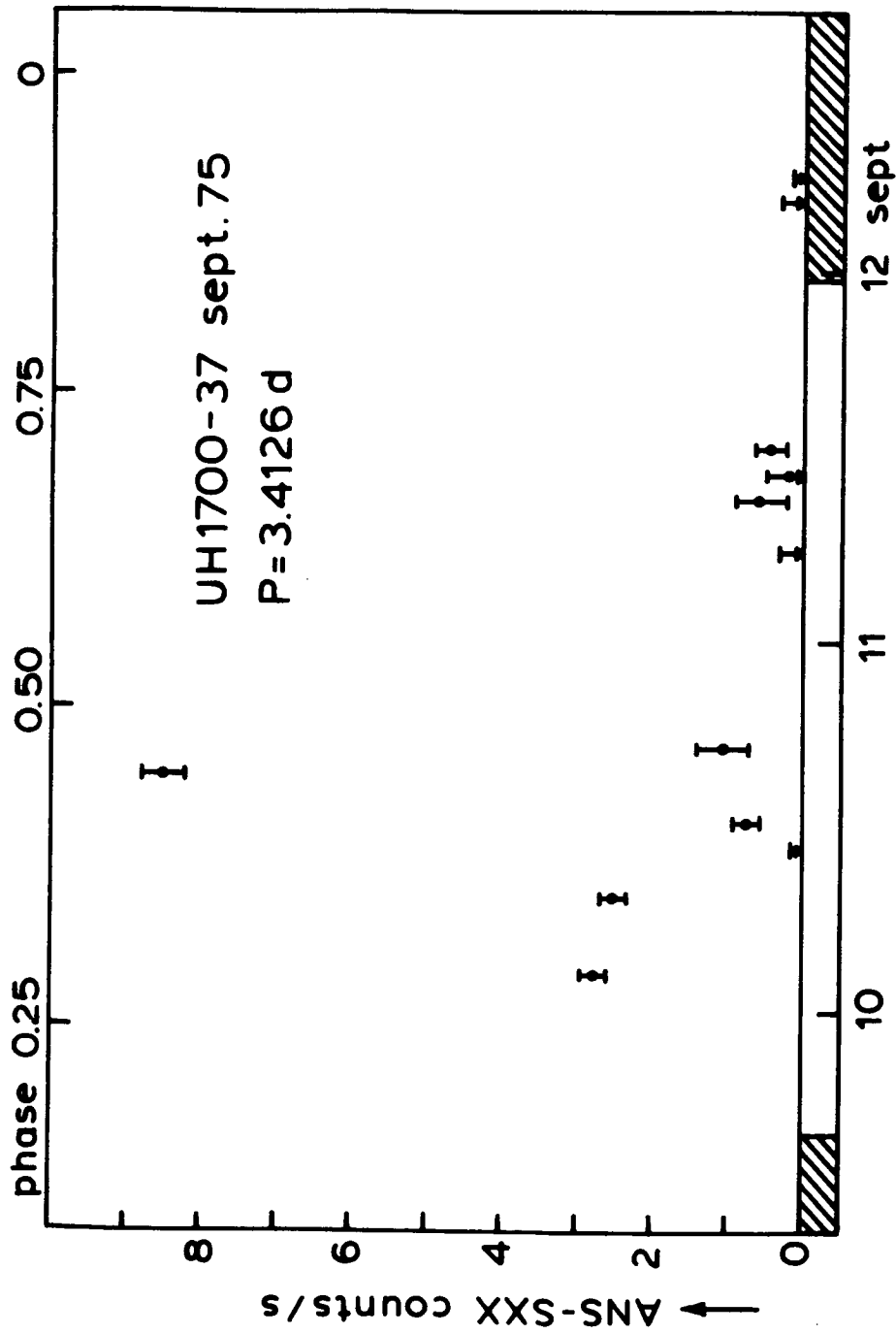


Fig. 10. Preliminary lightcurve of 3U 1700-37 as observed from quick look data by ANS in September 1975.

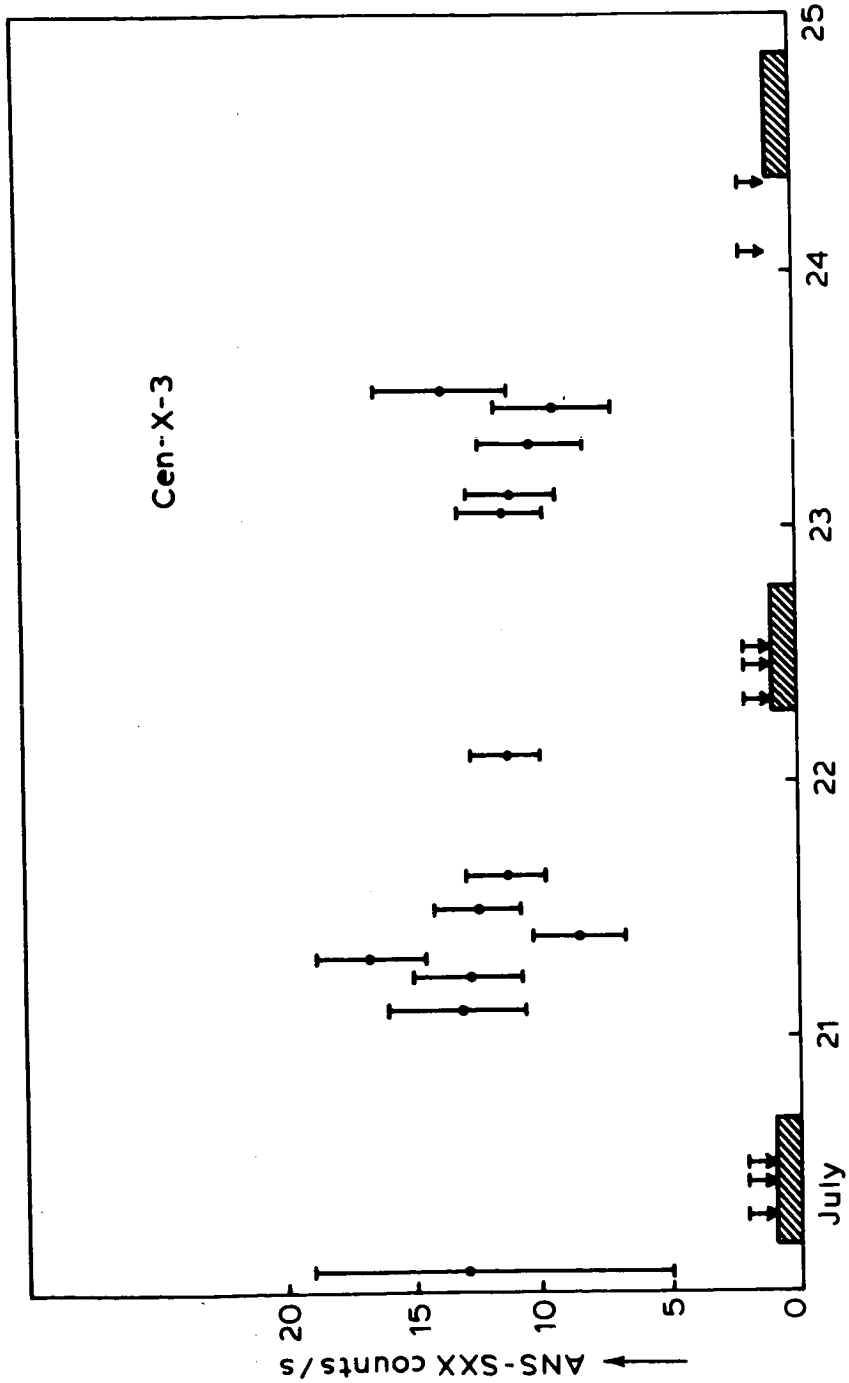


Fig. 11. Lightcurve of Cen-X-3, observed in July 1975.

X-RAY SPECTROSCOPY WITH THE ANS SATELLITE

H. W. Schnopper, J. P. Delville, A. Epstein, H. Gursky, J. Grindlay,
K. Kalata, D. R. Parsignault*, A. R. Sohval and E. Schreier
Center for Astrophysics
60 Garden Street
Cambridge, Massachusetts 02138

ABSTRACT

Preliminary results from the Bragg crystal spectrometer on the ANS satellite are given. No significant Si XIII and Si XIV narrow line emission has been detected from Cygnus X1, 2, or 3.

A small Bragg crystal spectrometer is incorporated in the Hard X-Ray Experiment (HXX) on the Astronomical Netherlands Satellite (ANS). More complete details of the experiment and the satellite are given elsewhere (Gursky et al, 1975; Schnopper et al, 1975).

The spectrometer is designed to observe sources of small angular extent and is sensitive to line emission from highly excited ions Si XIII and Si XIV (see Table I).

Table I. Characteristics of the Silicon Lines to be Observed by ANS

<u>Crystal</u>	<u>Ions</u>	<u>Transition</u>	<u>λ (Å)</u>	<u>θ Bragg</u>	<u>Nominal Reference Offset</u>
Bragg 2	Si XIV	$1s^2 \text{ } ^2\text{S}_{\frac{1}{2}} - 2p \text{ } ^2\text{P}_{\frac{1}{2}, \frac{3}{2}}$	6.184	45°01'	0'.0
Bragg 1	Si XIII	$1s^2 \text{ } ^1\text{S}_0 - 1s2p \text{ } ^1\text{P}_1$	6.649	49°31'	- 12'.6
Bragg 1	Si XIII	$1s^2 \text{ } ^1\text{S}_0 - 1s2p \text{ } ^3\text{P}_{2,1}$	6.684	49°52'	- 33'.9
Bragg 1	Si XIII	$1s^2 \text{ } ^1\text{S}_0 - 1s2s \text{ } ^3\text{S}_1$	6.739	50°26'	- 67'.6

* American Science and Engineering, Cambridge, MA

Two independent PET crystals, offset from each other in Bragg angle, are used to scan both line regions simultaneously. Scanning is accomplished by offset pointing of the spacecraft from the head-on direction to the source. A field of $\pm 75'$ can be scanned.

The satellite is in a sun synchronous polar orbit and a typical source is viewed for about five days before it leaves the field of view of the coarse (3° FWHM) collimation system.

The sensitivity of the spectrometer is measured by $N_{L,m}$, the minimum number of photons in the line which are detectable above the background counting rate. In general, the number of photons observed in the line is given by: (Schnopper et al, 1975)

$$N_L = A T \eta P F(E)_C \Delta E_L$$

where,

- A = effective area (geometry only) for x-ray detection,
- T = time of observation,
- η = net efficiency for detecting an x-ray of energy E (transmission through windows, detector, but not crystal),
- P = peak reflectivity of the crystal,
- $F(E)_C$ = continuum flux from the source at energy E,
- and ΔE_L = equivalent width.

For a minimum detectable signal, $N_L = N_{L,m} = 3 (N_B)^{1/2}$, where N_B is the background counting rate. For the ANS spectrometer, N_B is dominated by nonsource related x-rays and charged particles. Table II lists the parameters relevant to the ANS spectrometer.

Table II. Parameters for N_L and ΔE_L Calculations

<u>SI XIV E = 6.18 keV</u>		<u>ANS flat</u>
disperser		PET $2d = 8.7 \text{ \AA}$
peak efficiency P		0.17
resolution ΔE	eV	1.2
detection efficiency η		0.5
collecting area	cm^2	50
detector area	cm^2	50
background	$\text{cm}^{-2}\text{sec}^{-1}$	6×10^{-3}

Because of the highly elliptical nature of the ANS orbit, N_B can vary over a very wide range of values. In a typical orbit about 10^3 seconds of good data can be obtained during the times when the satellite is not in the polar cap region or in the South Atlantic Anomaly.

Table III gives experimental results for the sources Cygnus X1, X2 and X3.

<u>Source</u>	<u>Date</u>	<u>F(1.9 keV)</u> <u>(photons/</u> <u>cm²-sec-keV)</u>	<u>T</u> <u>sec</u>	<u>N_{L,m}</u> <u>photons/</u> <u>64 sec</u>	<u>Δ E_L</u> <u>eV</u>
Si XIII ¹ P					
3U 1956 + 35 (Cygnus X1)	May 1975	4.6	601	4.4	4.0
	Nov. 1974	0.16	576	4.6	119
3U 2030 + 40 (Cygnus X3)	May 1975	0.02	382	5.8	712
	Nov. 1974	0.05	349	5.9	503
Si XIV ² P					
3U 1956 + 35 (Cygnus X1)	May 1975	4.6	704	3.8	3.5
	Nov. 1974	0.16	1056	3.9	101
3U 2142 + 38 (Cygnus X2)	June 1975	1.2	576	4.7	16.4
	Dec. 1974	0.91	875	3.8	17.5
3U 2030 + 40 (Cygnus X3.)	May 1975	0.02	640	4.1	900
	Nov. 1974	0.05	400	4.5	385

A typical scan covered about 5 eV on either side of the nominal line position in about 10 steps. Although total time T was spent at each step, N_{L,m} is given in units of photons/64 sec since the spectrometer is read out once each 64 sec. In Table III, Δ E_L is the equivalent with corresponding to N_{L,m}.

Tucker and Koren (1971) discuss line emission from a hot thin coronal plasma. They predict values for Δ E_L which can be compared with our data if the ion temperature of the source is known. Given the proper emitting conditions, values for Δ E_L as high as several hundred eV are not unusual.

Our data, however, do not yield a measurable signal N_L above the 3 standard deviation upper limit N_{L,m}. In the case of Cygnus X3 our result lacks a strong significance since the source spectrum is severely cut-off in the region of the line emission. In contrast, Cygnus X1 was observed in a high state during May 1975 and our upper limits for Si XIII and Si XIV preclude any significant narrow line emission. Our results, however, do not rule out significant contributions from broadened line shapes. Furthermore, it is not possible to put meaningful upper limits on Δ E_L for the case where the line is broadened to a value greater than about 10 eV. This value would be expected on the basis of stellar wind models (S. Hatchett, 1975). This line broadening is modest when compared with the values predicted by various electron scattering

theories and by the dynamical effects of accretion onto a large disc. It would require a much greater sensitivity than we have to be able to detect a residual, unbroadened line core.

REFERENCES

- Gursky, H., Schnopper, H., and Parsignault, D. 1975, Ap.J. (Letters) 201, L127, 1975.
- Hatchett, S. 1975, private communication.
- Schnopper, H. W., Delvaille, J. P., Epstein, A., Kalata, K., and Sohval, A. 1975, Space Science Instrumentation in press.
- Tucker, W. H. and Koren, M., 1971, Ap.J. , 168, 283; erratum 170, 621.

STELLAR CRYSTAL X-RAY SPECTROSCOPY ON OSO-8

H. L. Kestenbaum, G. G. Cohen, R. Novick,
M. C. Weisskopf, and R. S. Wolff
Columbia Astrophysics Laboratory
Departments of Astronomy and Physics
Columbia University
New York, New York 10027

J. R. P. Angel
Department of Astronomy
University of Arizona
Tucson, Arizona 85721

and

P. B. Landecker
Space Physics Laboratory
The Aerospace Corporation
El Segundo, California 90245

ABSTRACT

The large-area graphite crystal X-ray spectrometer on the OSO-8 satellite is described, and its response to stellar line and continuum radiation is discussed. A high-resolution X-ray spectrum of Sco X-1 obtained from a preliminary analysis of quick-look data shows a strong, smooth continuum with an absence of emission or absorption features over the energy range 2.2 to 8 keV. Upper limits are set on narrow line emission from highly ionized states of S, Ca, and Fe.

INTRODUCTION

In the past few years numerous groups have measured the X-ray spectra of the stronger galactic sources using proportional counters. For several sources, excesses have been seen in the continuum spectra near 6.7 keV, and these features have been interpreted as line emission from highly ionized iron (Holt, Boldt, and Serlemitsos 1969; Acton *et al.* 1970; Serlemitsos 1975; Pravdo 1975; Mason 1975). However, because the resolution of the best proportional counters at these energies is about 900 eV, it is not possible to make an unambiguous interpretation of the features as emission lines. Crystal spectrometers with high spectral resolution have been flown aboard sounding rockets in search of narrow line emission from Fe⁺²⁴, Fe⁺²⁵ (6.7 keV) and S⁺¹⁵ (2.6 keV) in Sco X-1 (Pounds 1971; Kestenbaum, Angel, and Novick 1971; Griffiths 1972; Stockman *et al.* 1973), but these sensitive searches failed to

detect the expected lines. The 3σ upper limits that were obtained for narrow line emission (equivalent widths of 6.7 eV for S^{+15} and 3 eV for Fe^{+24}) have been used to show that electron scattering and resonance trapping are occurring within the plasma, thus severely broadening the line emission from Sco X-1 (Felten and Rees 1972; Loh and Garmire 1971).

The Columbia graphite crystal spectrometer on OSO-8 is capable of detecting narrow line emission from optically thin sources and of determining detailed shapes for X-ray continua with high spectral resolution over the 2-8 keV band. Strong features which result from broadened line emission will be observable, and the amount of broadening may be used to determine plasma densities and temperatures. In the following section we briefly describe the instrument and discuss the response of the spectrometer to stellar continuum and line radiations. In Section II we present some preliminary results for Sco X-1 obtained from ten orbits of quick-look data.

I. THE SPECTROMETER

The spectrometer is located in the wheel section of OSO-8 and makes use of the wheel rotation to obtain a complete Bragg scan every 10 sec. A schematic diagram of the spectrometer indicating the principle of operation is shown in Figure 1. A feature of the spectrometer, and one that appears strikingly in the data from Sco X-1, is that each proportional counter is illuminated by reflected X-rays over a different range of Bragg angles. This feature allows us to obtain background data during each Bragg scan when the individual detector is not being illuminated. In Figure 2 is shown an exploded view of the instrument. A slat collimator positioned directly in front of the crystal panels limits the spectrometer field of view to within 3° of the OSO-8 wheel plane and has enabled the spectrometer to obtain useful data on stellar sources located in the center of the galaxy where the population density is high. X-rays from an on-axis source enter through the slat collimator and strike the large crystal (2170 cm^2) panels. Graphite mosaic crystals were chosen for their high reflectivity of stellar continuum and line radiation. Those X-rays which satisfy the Bragg condition may be reflected into the central bank of detectors. The detectors are double-sided proportional counters with 1-mil beryllium windows on each side and contain an argon-xenon gas mixture chosen for its high opacity over the 2-8 keV range. A grounded wire grid plane through the center of the bank of counters effectively divides the instrument into two isolated spectrometers. Detected events which pass rise-time and anticoincidence tests and which satisfy pulse-height criteria are encoded as digital words and stored in a tape recorder whose contents are read out over specified ground stations. Each event is assigned three bits of counter location information, five bits of pulse-height data, and 12 bits of azimuth information which allow a determination of the Bragg angle to 0.1° . This accuracy is sufficient for superposition of Bragg scans since the crystal panel rocking curve has a FWHM of 0.7° .

The reflecting properties of large-area graphite crystal panels have been measured in the laboratory using a beam of Cl fluorescent radiation (2.6 keV), collimated to 0.12° (Kestenbaum, Angel, and Novick 1971; Kestenbaum 1972).

At this energy the peak reflectivity is about 6.4 percent, with a FWHM = 0.7° , corresponding to a resolution of 32 eV. At 2 keV, the resolution is 10 eV, and the peak reflectivity is 14 percent, while at 6.7 keV, where the Fe lines are expected, the resolution is 285 eV, and the peak reflectivity is 21 percent. We have measured thoroughly the reflectivity of a graphite crystal sample over the range 2–8 keV and have found that the theoretical curve for integrated reflectivity gives a good representation of the data apart from a normalization constant (Kestenbaum 1973). Thus, in our spectrometer response function, we have used the theoretical curve of reflectivity vs. energy, normalized to the measured data points.

In our data reduction, we use the measured signal counting rate $R_c(E)$ from the continuum as a function of Bragg angle θ to determine an incident continuum spectrum $I_c(E)$ [$\text{keV} (\text{keV cm}^2 \text{ sec})^{-1}$], using the following relation (Kestenbaum 1972):

$$R_c(E) = I_c(E) [A(E) \epsilon(E) \Delta\theta(E) \cot \theta] \quad , \quad (1)$$

where E is the X-ray energy at the center of a resolution element (0.7° width). The area $A(E)$ of the detector illuminated by X-rays has been determined by a complete computer simulation of the spectrometer, where the projected crystal area available for reflection has been taken into account as well as all shadowing effects caused by collimators, strongback, and structural supports. Counter efficiencies $\epsilon(E)$ have been calculated from the known gas pressure and depth, window thickness, and rise-time settings. The integrated reflectivity $\Delta\theta(E)$ has been determined from measured values as discussed above. In this way we have determined an effective area $A_c(E)$ for each counter for each resolution element for continuum radiation over the bandwidth 2–8 keV; $A_c(E)$, represented by the term in brackets in equation (1), is plotted in Figure 3(a). A feature seen in Figure 1, in which each counter is illuminated by reflected radiation over a different range of Bragg angles, can be seen clearly in the response function and is geometrical in nature. The general trend of increasing area with increasing energy is caused by the change in resolving power of the crystals; at higher energies, the resolution is poorer, and a larger fraction of continuum is reflected, yielding a larger effective area.

A relation similar to equation (1) can be written for narrow line emission:

$$R_L(E) = I_L(E) [A(E) \epsilon(E) P_{\text{eff}}(E)] \quad . \quad (2)$$

Here $R_L(E)$ is the net signal counting rate from an X-ray emission line of energy E , $I_L(E)$ is the line strength [$\text{photons} (\text{cm}^2 \text{ sec})^{-1}$], and $P_{\text{eff}}(E)$ is the effective peak reflectivity ($\approx 0.8 \times$ peak reflectivity) over a resolution element. The term in brackets is defined as an effective area for line emission $A_L(E)$ and is plotted from 2–8 keV in Figure 3(b). Clearly, the instrument is most sensitive to detecting narrow line emission in the range from 1.9 to 3 keV, where the crystals reflect a large fraction of incident line radiation [$A_L(E)$ large] and a small fraction of incident continuum radiation [$A_c(E)$ small]. In this energy band, emission lines from highly ionized states of Si and S will predominate.

The determination of the spectrometer response functions $A_C(E)$ and $A_L(E)$ is critical for any determination of continuum shapes and line equivalent widths. To check that our response functions are accurate, we are making several in-flight calibrations of the spectrometer. One test is to observe the Crab Nebula for more than one week and see if we can employ the computed functions to reproduce the well-known power-law spectrum. A second test, already performed, is to observe both the continuum and lines from the optically thin solar corona (Fig. 4). We have used our values of $A_C(E)$ to determine a solar thermal continuum spectrum for which we have calculated the temperature. A second estimate of the temperature has been deduced from the measured ratio of strengths of various Si lines by using the calculations of Mewe (1972) and Tucker and Koren (1971). The temperature for the continuum agrees well with that obtained from the line strengths, and the consistency gives us confidence in the computed response functions.

II. OBSERVATION

Sco X-1 was observed for four days from 1975 July 9 to 13, and we have analyzed quick-look data obtained during ten orbits. The quality of the data can be seen in Figure 5 where we have superposed 155 Bragg scans (26 min of observation) for two counters. The strong signal from Sco X-1, dominant above the background rate, is seen to occur over a different range of Bragg angles in each detector. In Figure 6 are plotted all the quick-look data from counter No. 5 consisting of the superposition of 1459 Bragg scans (~4 hr of observation). The histogram refers to the left-hand scale and represents the counting rate in each resolution element (0.9° bins were chosen) with $\pm 1\sigma$ error bars obtained from counting statistics. The dashed line is the background rate obtained during the same Bragg scans, but when the counter was not being illuminated by reflected X-rays. The crosses (x's) refer to the right-hand vertical scale and represent the effective area per resolution element $A_C(E)$. For each resolution element, we have taken the total counting rate and subtracted the background rate to obtain the net signal rate $R_C(E)$; we then have divided by the effective area for that resolution element to obtain an incident continuum spectrum $I_C(E)$. In Figure 7 we plot as a histogram the spectrum obtained for Sco X-1 with $\pm 1\sigma$ error bars obtained from counting statistics alone. The solid curve is the best fit of the data to an incident thermal spectrum

$$I_C(E) = I_0 E^{-0.3} \exp(-E/kT) \quad . \quad (3)$$

The best-fitting parameters were $I_0 = 83 \text{ keV (keV cm}^2 \text{ sec)}^{-1}$ and $kT = 4.5 \text{ keV}$, yielding a value for χ^2 of 71 for 45 degrees of freedom. Narrow line emission would manifest itself as an excess in one bin, and no such feature is observed. Several bins are marked by arrows on the figure, indicating where one would expect excess events resulting from strong S, Ca, and Fe line emission in a thin, hot plasma. In Table 1 we give upper limits (3σ) on the equivalent widths of these lines. These results, in agreement with previous upper limits for narrow line emission in Sco X-1, indicate that electron scattering of the X-rays is greatly reducing the observable line strengths. Furthermore, no broadened feature at 6.7 keV is seen, but we stress that the

presence of a feature would be indicated by excesses, in several contiguous bins, above the best-fitting spectrum. Thus, the search for a broad feature relies rather heavily on the assumed thermal spectrum used in the fitting procedure. The statistical accuracy of the data will improve by a factor of about four when the production data are analyzed, and any definitive conclusion about the presence or absence of a broadened feature must await the full analysis.

We acknowledge the many contributions of the staff of the Columbia Astrophysics Laboratory without which this work could not have been successfully completed. We thank in particular Ms. D. J. Miller, Mr. D. D. Mitchell, Mr. I. Rochwarger, Mr. M. Sackson, Dr. J. Toraskar, Dr. J. R. Wang, and Dr. B. E. Woodgate. This work was supported by the National Aeronautics and Space Administration under contract NAS5-22408. This paper is Columbia Astrophysics Laboratory Contribution No. 116.

REFERENCES

- Acton, L. W., Catura, R. C., Culhane, J. L., and Fisher, P. C. 1970, *Astrophys. J. (Letters)*, 161, L175.
- Felten, J. E., and Rees, M. J. 1972, *Astron. and Astrophys.*, 17, 226.
- Griffiths, R. E. 1972, *Astron. and Astrophys.*, 21, 97.
- Holt, S. S., Boldt, E. A., and Serlemitsos, P. J. 1969, *Astrophys. J. (Letters)*, 158, L155.
- Kestenbaum, H. L. 1972, Ph. D. Thesis, Columbia University, New York, N. Y.
- Kestenbaum, H. L. 1973, *Appl. Spectry.*, 27, 454.
- Kestenbaum, H., Angel, J. R. P., and Novick, R. 1971, *Astrophys. J. (Letters)*, 164, L87.
- Loh, E. D., and Garmire, G. P. 1971, *Astrophys. J.*, 166, 301.
- Mason, K. O. 1975, in these *Proceedings*.
- Mewe, R. 1972, *Solar Phys.*, 22, 459.
- Pounds, K. A. 1971, *Nature Phys. Sci.*, 229, 175.
- Pravdo, S. 1975, in these *Proceedings*.
- Serlemitsos, P. J. 1975, in these *Proceedings*.
- Stockman, H. S., Jr., Angel, J. R. P., Novick, R., and Woodgate, B. E. 1973, *Astrophys. J. (Letters)*, 183, L63.
- Tucker, W. H., and Koren, M. 1971, *Astrophys. J.*, 168, 283.

TABLE 1
X-Ray Spectral Data of Sco X-1.

Line	Energy (keV)	Type of Crystal Spectrometer	Upper Limit on Equivalent Width at 3σ (eV)	Ref.
S XV	2.45	OSO-8 graphite	18	(a)
S XVI	2.62	Graphite	6.7	(b)
	2.62	OSO-8 graphite	17	(a)
Ca XIX	3.88	OSO-8 graphite	26	(a)
Fe XXV	6.7	Lithium fluoride	25	(c)
	6.7	Lithium fluoride	3	(d)
	6.7	OSO-8 graphite	72	(a)

(a) This work.

(b) Kestenbaum 1972; Kestenbaum *et al.* 1971.

(c) Griffiths 1972.

(d) Stockman *et al.* 1972.

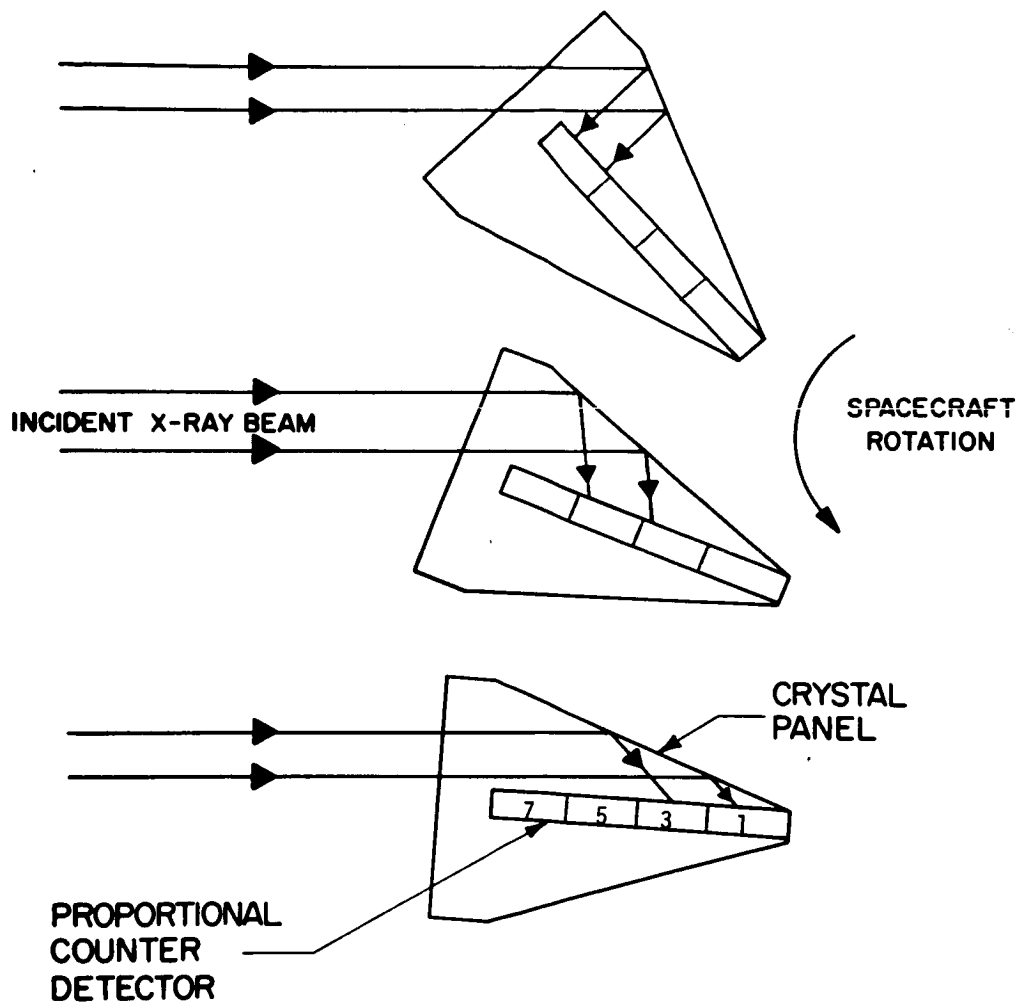


Figure 1. Schematic diagram of the spectrometer showing the principle of operation. A complete Bragg scan for each panel is obtained with every rotation of the OSO-8 wheel. Each of the four proportional counters (Nos. 1, 3, 5, 7) is illuminated over a different range of Bragg angles.

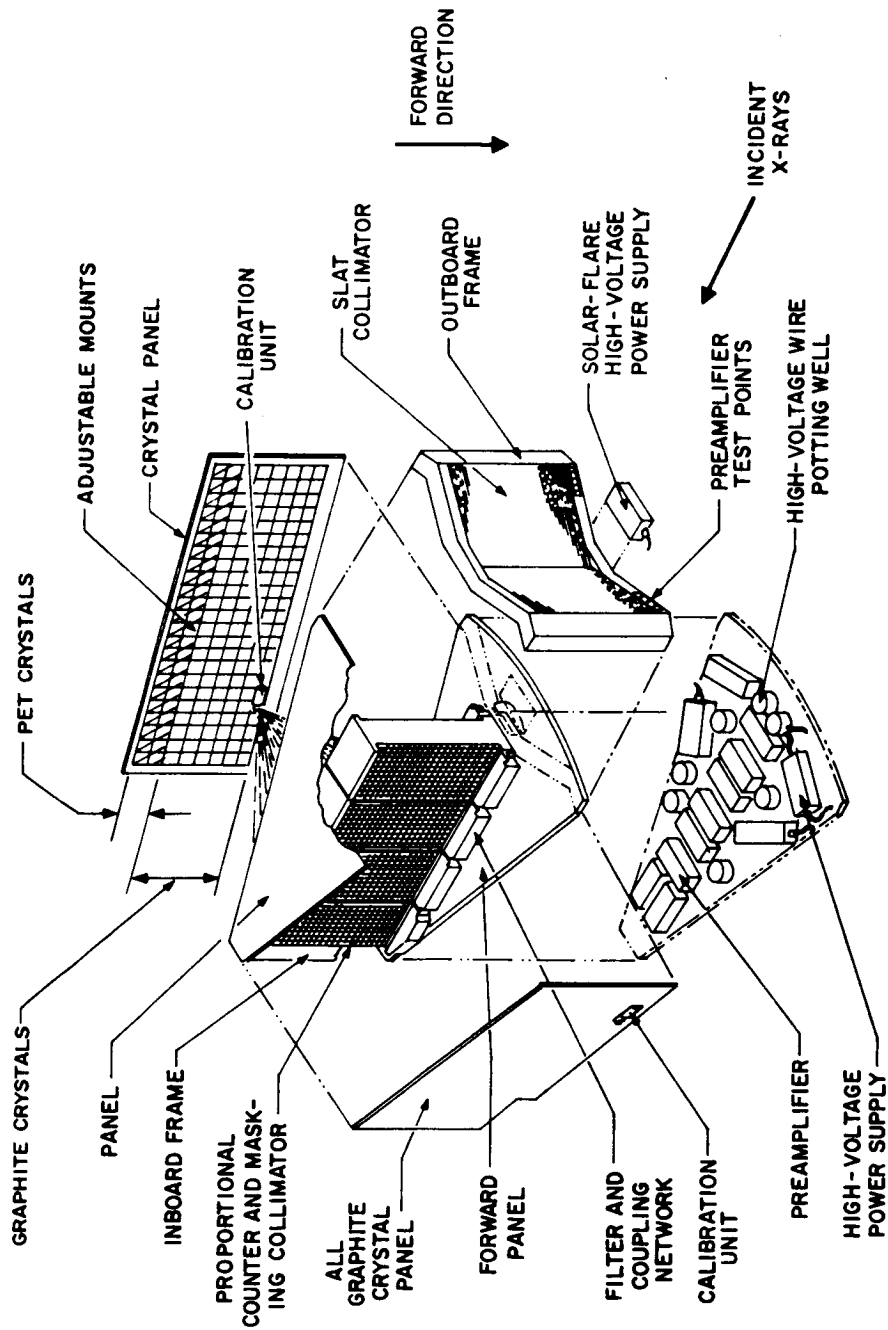


Figure 2. An exploded view of the spectrometer.

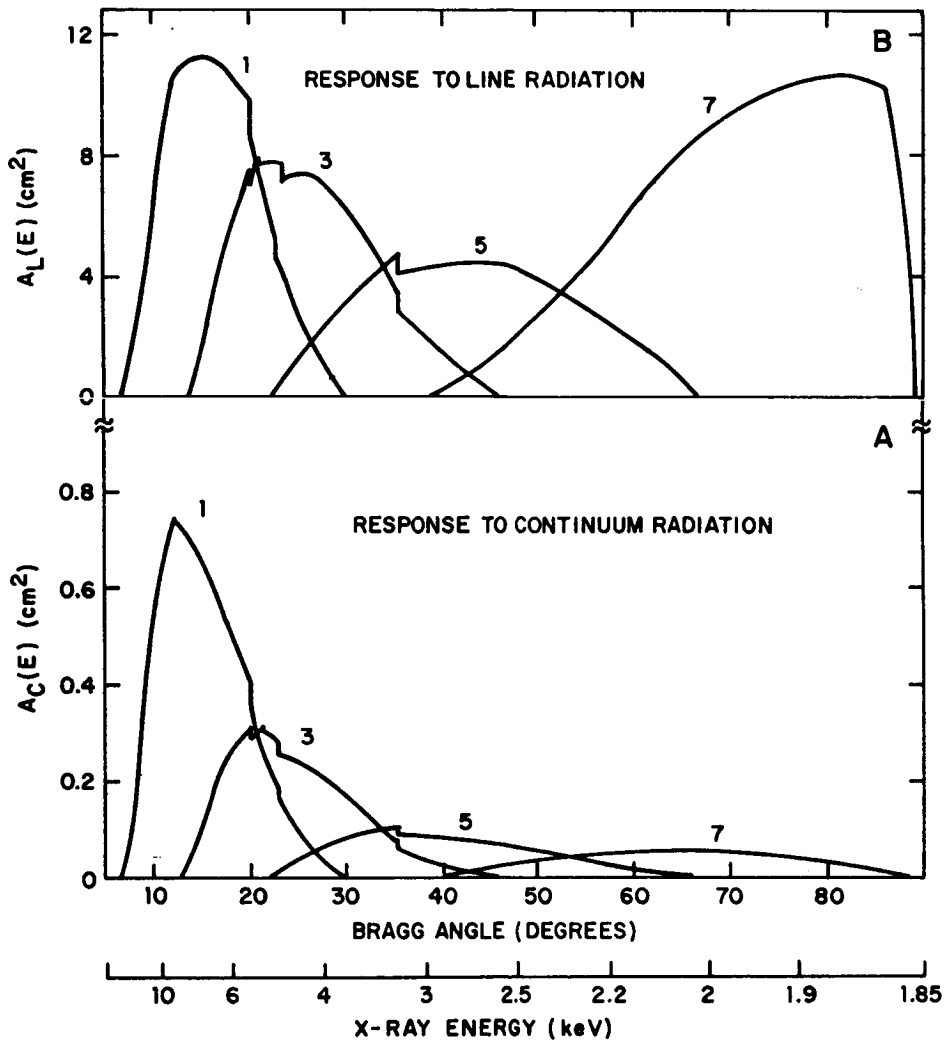


Figure 3. (a) The effective area of the spectrometer in each resolution element (for one crystal panel) for incident continuum radiation. (b) The effective area in each resolution element (for the same panel) for incident line radiation. The numbers next to each curve indicate the proportional counter to which each curve refers.

Year 1975 Day 223 Time 6^h 35^m UT

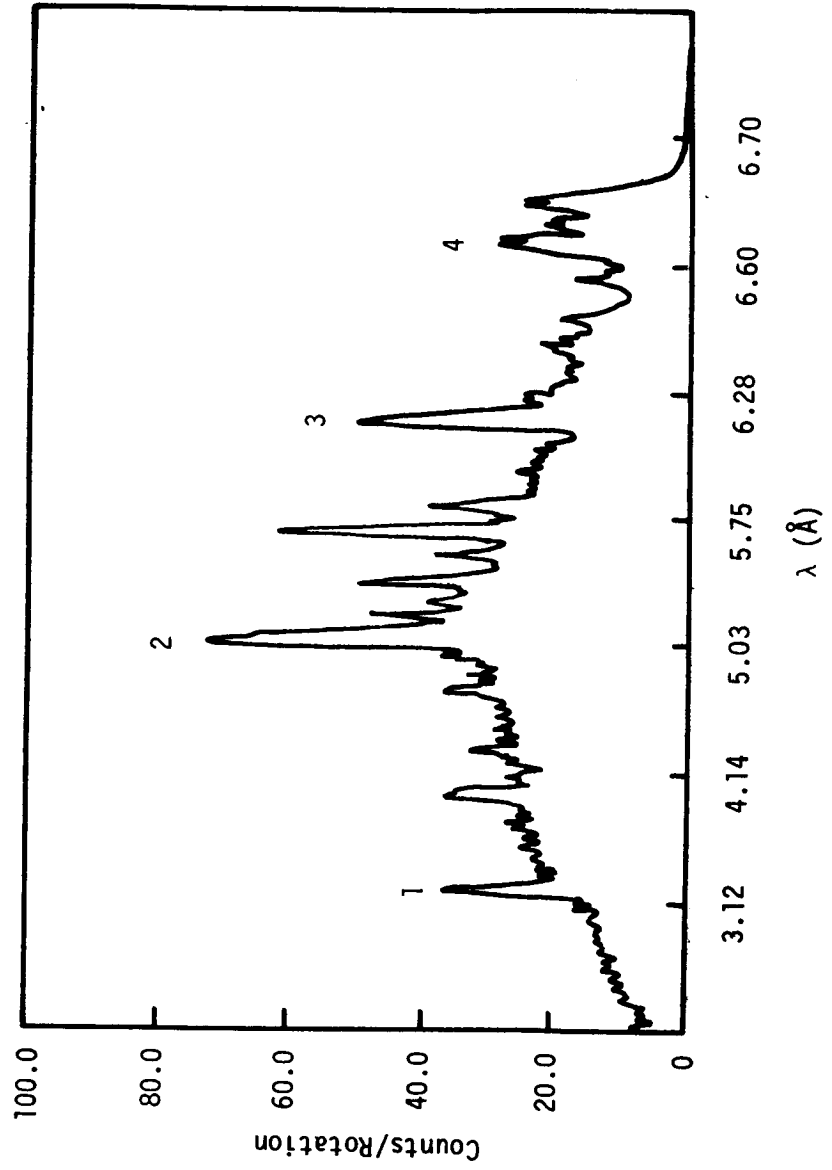


Figure 4. A solar spectrum obtained with the graphite spectrometer, showing strong X-ray line and continuum radiations. Line 1 is Ca XIX [$1s^2-1s2p(^1P)$; $1s^2-1s2p(^3P)$]; $1s^2-1s2p(^3S)$]; line 2 is S XV [$1s^2-1s2p(^1P)$; $1s^2-1s2p(^3P)$; $1s^2-1s2p(^3S)$]; line 3 is Si XIV ($1s-2p$); line 4 is Si XIII [$1s^2-1s2p(^1P)$].

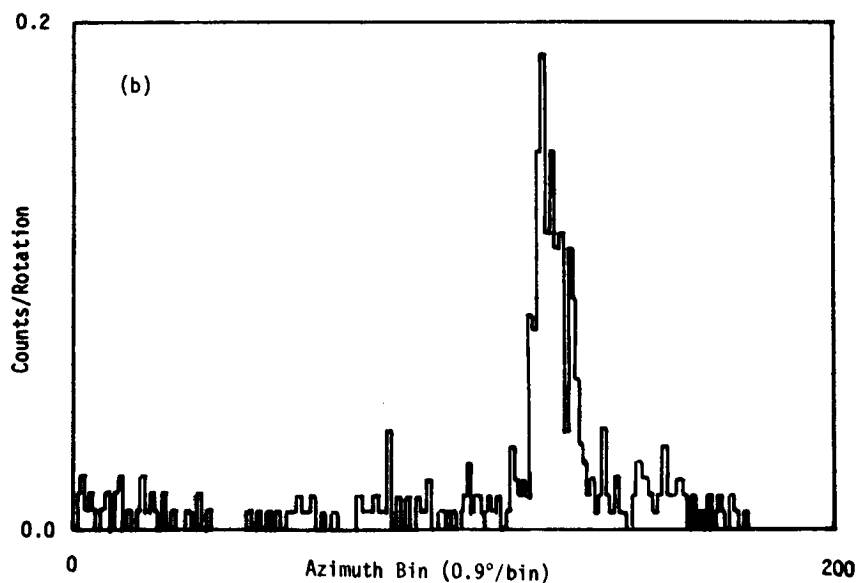
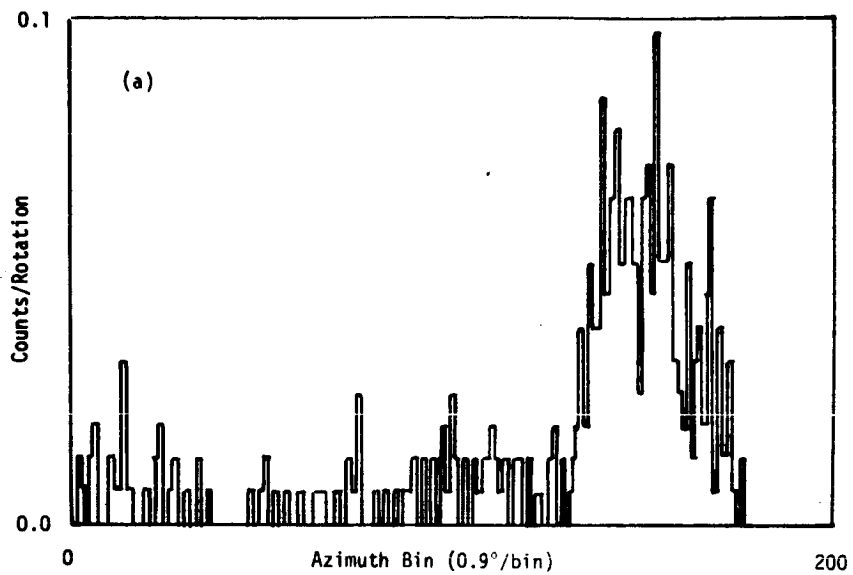


Figure 5. (a) A superposition of 155 Bragg scans, with azimuth bins of 0.9° width, for proportional counter No. 5, with Sco X-1 in the field of view. (b) The same superposition for counter No. 1. Note that each detector is illuminated by reflected X-rays over a different range of Bragg angles.

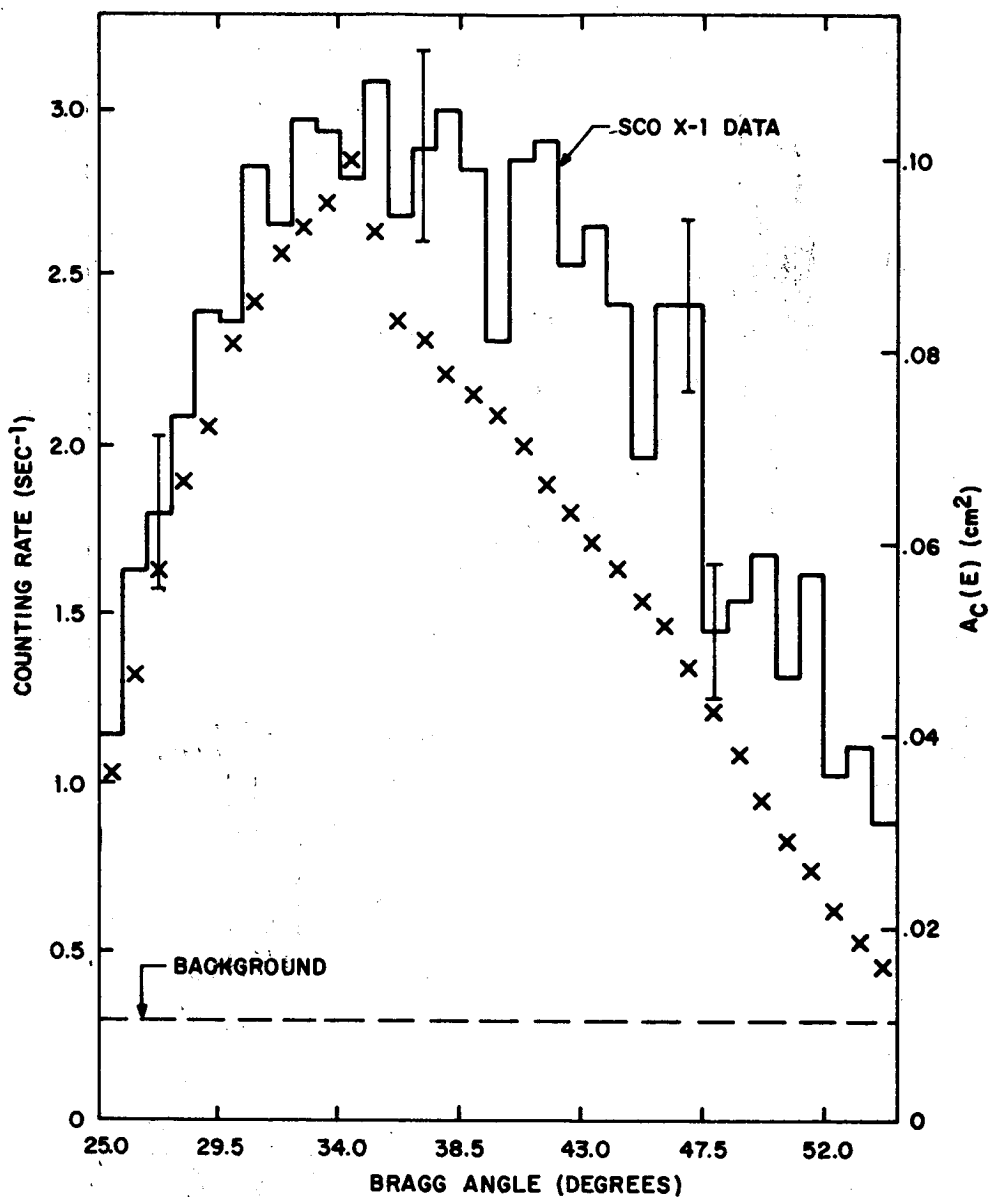


Figure 6. The superposition of Bragg scans for proportional counter No. 5, using data obtained from 4 hr of observation of Sco X-1. The histogram refers to the left vertical scale and shows the counting rate in each resolution element with $\pm 1\sigma$ error bars obtained from counting statistics. The crosses (X's) refer to the right vertical scale and give the effective area of the spectrometer in each resolution element (for counter No. 5) for continuum radiation. The dashed line is the background counting rate when no source is in the field of view.

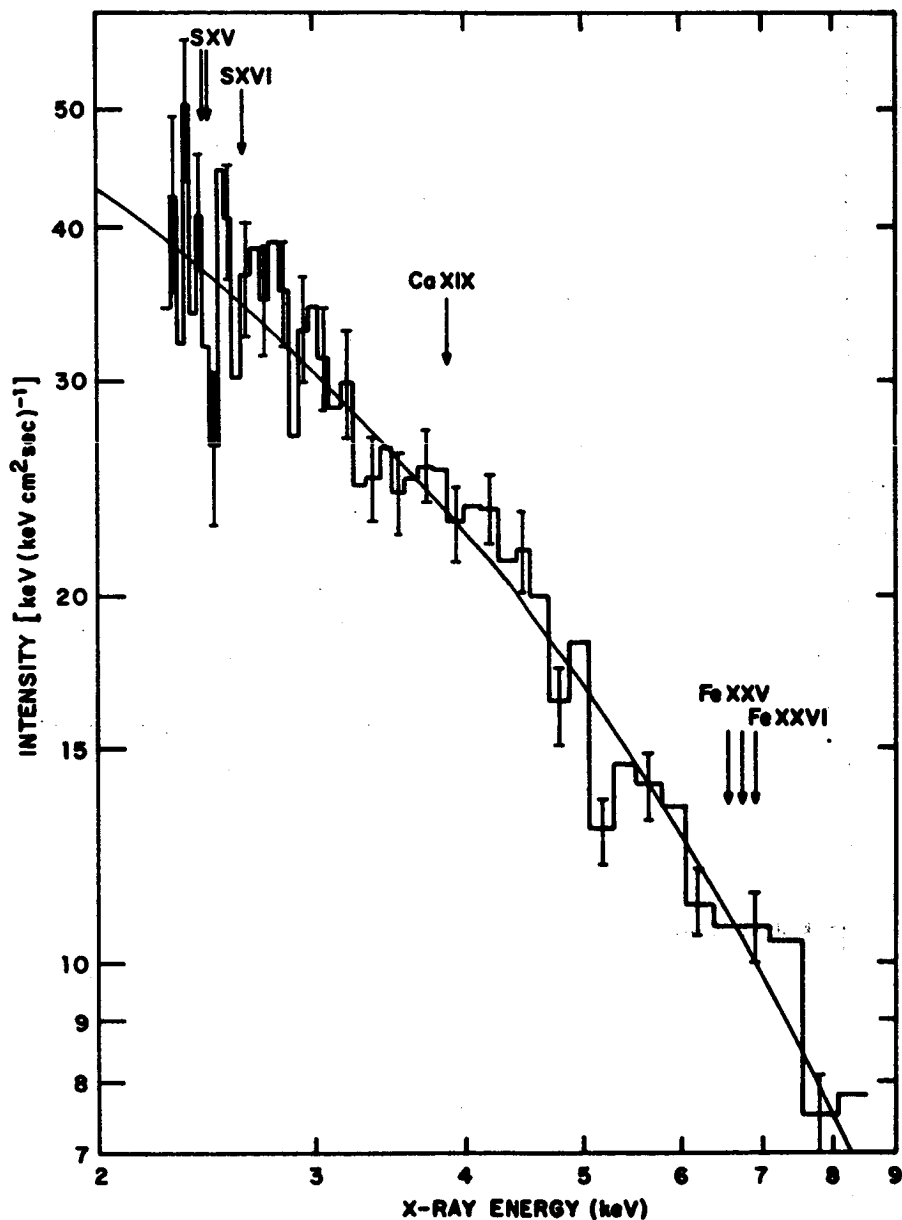
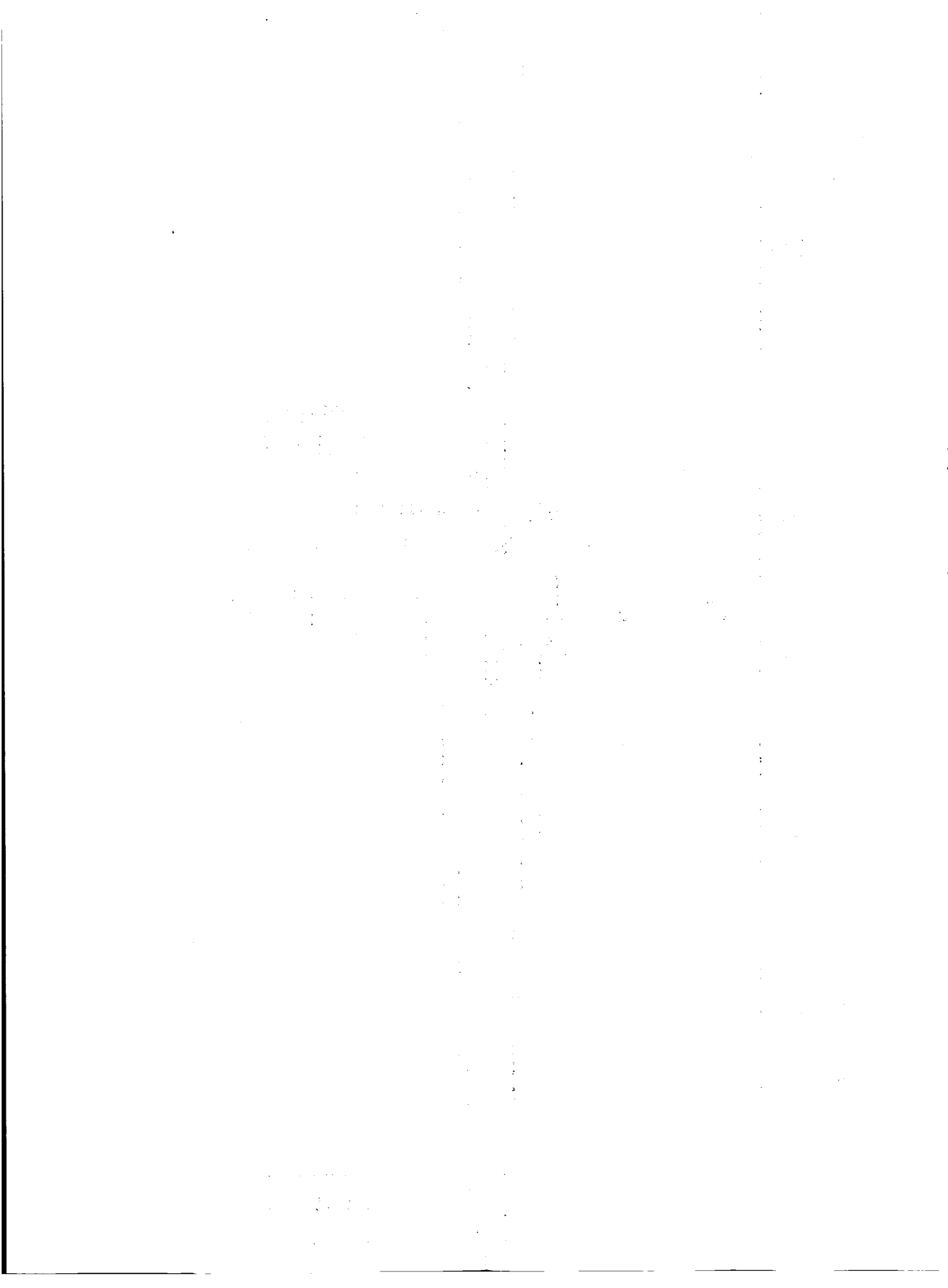


Figure 7. The X-ray spectrum of Sco X-1. The histogram gives the intensity in each resolution element with $\pm 1\sigma$ error bars determined only from counting statistics. The solid line is the best-fitting thermal spectrum. The arrows indicate energies where strong line emission would be expected from an optically thin plasma with an electron temperature of 4.5 keV.



COSMIC X-RAY OBSERVATIONS WITH OSO-8

P. J. Serlemitsos, R. Becker*, E. A. Boldt, S. S. Holt,
S. Pravdo**, R. Rothschild, and J. H. Swank*
NASA-Goddard Space Flight Center
Greenbelt, Maryland 20771

ABSTRACT

The GSFC Cosmic X-ray Spectroscopy experiment aboard OSO-8 has operated successfully since launch providing in this 4-month period spectral and temporal data on X-ray sources in the energy range 2-60 keV. Analysis of "Quick Look" data shows a variety of spectral features, some stable, others variable, which will increase our understanding of the nature of individual sources. In particular, observed emission and absorption features that can be attributed to iron will result in abundance measures of this important element in sources such as some X-ray binaries, the supernova remnant Cas A, and the nucleus of the galaxy Cen A.

The X-ray Group at GSFC has an experiment aboard the 8th Orbiting Solar Observatory (OSO-8), shown in Fig. 1, a satellite launched on June 21, 1975 into a 550 km circular orbit at 33 degrees inclination. The primary objectives of OSO-8 are obviously solar oriented, and they are, for the most part, dictated by the two pointed experiments mounted on the spacecraft spin axis. However, several other experiments are mounted on the rotating portion of the spacecraft (wheel), three of which have exclusively non-solar objectives. Their fields of view are either aligned to the spin axis or they are at small angles to it, hence they always view the portion of the sky at right angles to the earth-sun line.

The objectives of our experiment, somewhat updated in the lengthy period between proposal and launch, are as follows:

1. Spectra of sources and diffuse background in the range 2-60 keV.
2. Source intensity and spectral variations on scales from fractions of a second to several days.
3. Intensity profile and spectrum of the galactic contribution to the diffuse X-ray background.
4. Sensitive search for weak emission from a limited number of objects of importance to astrophysics.

In the four month period since launch, the only data received are of the "Quick Look" variety. These consist of some 10 per cent of all data, with predicted and incomplete orbital information and with spotty spin axis positions. For these reasons, the data analysis conducted thus far cannot

* NAS-NRC Associate

** Permanent Address - Univ. of Maryland

proceed to a reasonable completion, particularly with regard to time variations and weak sources. The purpose of this paper therefore, is to provide a brief description of the experiment, setting the stage for the subsequent papers on Cen X-3 and Her X-1, and to present some preliminary spectra of selected sources for the purpose of discussing the potential of this experiment for extracting information from such spectra, as regards the nature of a source and conditions in the emitting region.

The experiment utilizes two xenon and one argon proportional counters. Two of these have fields of view oppositely aligned with the spacecraft spin axis. The third counter has its 5-degree field of view offset 5 degrees from the aft spin axis so that, with each wheel revolution, it scans the region of the sky within 10 degrees of the aft axis direction. The two aft pointed counters have clear fields of view, whereas, the forward pointed detector has its field of view periodically occulted by the pointed instruments and by occultation shields mounted under the spacecraft sail.

All three detectors are of the same modular construction consisting of stacked wire grids which partition a sealed gas volume into many rectangular cells with grounded boundaries and a central wire anode. The aft pointed detectors have single gas volumes, whereas, the forward pointed detector has two, back-to-back, independent gas volumes, one designed to guard against electrons entering the detector via the collimator opening. The collimator fields of view are circular, effected by BeCu tubing.

There are basically two commandable modes of operation: stored and real time. Stored data consists of 64-channel pulse height information from all three detectors read into the telemetry every ~2.5 sec for the scanning detector, and every ~40 sec for the pointed detectors. Wheel azimuth information relative to the sun pointed instruments is used onboard to (1) sector the data from the scanning detector so as to simultaneously produce, each wheel rotation, source and background histograms; (2) bin the data from the forward pointed detector according to a hard-wired program that makes distinction whether the field of view of that detector is open or occulted. For the two xenon detectors, the 64 channels are arranged in a quasi-logarithmic format that doubles the resolution below about 15 keV.

In the real time mode the same pulse height information from only one of the detectors (chosen by command) is read out, event-by-event, using an 8-bit address. For sources that do not saturate the available telemetry, this mode results in 20 msec temporal resolution. With few exceptions, integral rates from all three detectors are monitored every 160 msec. On rare occasions, the entire spacecraft telemetry can be made available to this experiment, improving the temporal resolution to 1.25 msec.

In Table 1 we summarize some relevant experiment information. In Table 2 we list characteristics of the three detectors. Detectors "B" and "C" are the aft and forward pointed instruments respectively; "A" is the scanning detector.

TABLE 1

Total Area	575 cm ²
Field of View	3 and 5 deg. circular
Observing Method	Small Angle Scan; Point
Energy Range	2-60 keV
Temporal Resolution	160 msec (Normal) 20 msec (Real Time) 1.25 msec (Dwell Mode)
Bit Rate	500 bits/sec
Flight Calibration	Fe ⁵⁵ ; Am ²⁴¹

TABLE 2

DETECTOR	OUTER VOLUME	INNER VOLUME	COLLIMATION	WINDOW	AREA (cm ²)	ENERGY RANGE	VETO
A	--	xenon methane	5°	.002"Be	263	2-60keV	3 sides
B	--	argon methane	3°	.003"Be	76	2-20keV	3 sides
C	propane neon	xenon methane	5°	.002" mylar	237	2-60	4 sides

Non-solar observations with OSO-8 are closely tied to the orientation of the spacecraft spin axis. Spacecraft design demands that the spin axis is always within 3 degrees of the plane normal to the earth-sun line. Typical maneuverability within that narrow band is 3 degrees per day using magnetic torquing with occasional larger excursions effected by the use of gas jets. The requirements of the solar pointed experiments and a limited gas supply severely limit such large maneuvers. These constraints essentially eliminate our capability to respond to a new discovery such as a transient source or a large flare by an interesting object such as Cyg X-1.

By carefully planning the path of the spin axis subject to the above constraints, we, instead, methodically undertake to study most known X-ray objects. For example, at the completion of the first year of observations, we will have observed more than half of the sources in the 3rd UHURU catalogue. Observations may be as short as a few orbits, but for the most part, they extend to several days per source. In the case of X-ray binaries, we have been successful in maintaining a source in the field of view for at least one binary cycle.

The experiment has functioned without flaw during the first four months in orbit. In Figure 2 we show a typical 1-orbit rate profile from all three detectors A, B, C, in that order. Each vertical trace in the plot corresponds to all 64 rate readouts from each detector during one wheel revolution. The galaxy Cen A is in the field of view of the A detector; no known

sources are in view of the other two detectors. We wish to bring to attention several features in connection with this figure.

Electron contamination of the X-ray data causes the frequent rises in the rates. The single volume xenon detector is the most susceptible to this effect. Because of its special design, the second xenon detector is more effectively discriminating against this background. Precipitating electrons have a lesser effect on the argon detector as well, partly because of its smaller field of view and partly because of its thicker window. The data gap in the middle of the figure is caused by a high voltage turn off, a precautionary measure effected automatically by the on-board radiation monitor.

Although a substantial fraction of the data are so contaminated, we find that the detector background rapidly returns to a repeatable low state immediately after the satellite exits the high radiation region. We have seen no build up to the background of our detectors since launch.

In Fig. 3 we show a similar rate plot at a time when Cen X-3 was in the field of view of the A detector. The periodic peaks are due to the beating of the Cen X-3 spin period against the spin period of the spacecraft. The rate distribution during one wheel revolution (i.e. one single vertical trace) is shown in Figure 4.

The spectrum of Cen X-3, in and out of eclipse and during times of pre-eclipse intensity dips, is discussed in a separate paper of these proceedings. We present here in Figure 5 one such spectrum obtained with the A detector at maximum source intensity. The spectrum appears featureless, i.e. there is no evidence of low energy absorption or of any other features, particularly those that could be attributed to iron. The best fit is to an exponential in photon energy than to a thermal. Obviously, the total emission from Cen X-3 cannot be characterized as one from a tenuous plasma at a given temperature.

Not so much consistent with the objectives of the conference, but very much consistent with the scope of this paper, we next present in Figure 6 the spectrum from the galaxy Cen A, obtained with the A detector from about 6 orbits of "Quick Look" data. We find that the spectrum can be fitted with a power law heavily absorbed at low energies. The parameters of the best fit spectrum are given on the figure. We note that the absorption is well described by Brown and Gould abundances if we include iron, roughly, in the amount consistent with a universal abundance. The effect of the iron absorption edge can be seen by inspection of the figure.

Using UHURU data, Tucker et al., 1973, proposed a spectrum similar to the one presented here. Furthermore, they suggested that the emission originates in the central region of the galaxy where the low energy photons are absorbed by dust. With the eventual complete analysis of all the data from this source, (some 20 times the amount presented), we expect to produce an accurate measure of the iron abundance in the absorbing medium in the nucleus of Cen A.

Based on data from OSO-7, Winckler and White, 1975, have found evidence for variability of this source on time scales relevant to our exposure. We find no such large variability with the data at hand. However, a more detailed elaboration of this topic must await the availability of better aspect information.

In Figure 7 we present the spectrum for Cas A obtained with the 2-gas C detector. This is particularly of interest to us since we studied this source with a similar detector flown on a rocket flight (Serlemitsos et al., 1973). The OSO-8 spectrum is generally consistent with that in Serlemitsos et al., including the observed bulge around 7 keV which we have attributed to broadened iron line from charge exchange of energetic iron nuclei. There is one very significant difference in that the OSO-8 spectrum, with better statistics, clearly shows the presence of narrow iron lines near 6.7 keV. This new evidence renders our previous interpretation unlikely. A more plausible explanation is that the high energy broad feature is due to thermal continuum from a higher temperature region, which is also the source of the observed iron lines. We expect that a more detailed analysis of these data based on this new interpretation will result in the abundance iron in this important source.

In a final example, we present in Figure 8 the spectrum obtained for the transient source Nova Monocerotis 1975. We observed this source at a time when its intensity was comparable to Sco X-1. The spectrum is well fitted by a thermal with $kT = 1$ keV. Note the absence of any feature around iron, a significant fact since this is the same detector involved in the Cas A observation.

REFERENCES

- Serlemitsos, P. J., Boldt, E. A., Holt, S. S., Ramaty, R., and Briskin, A. 1973, Ap. J. (Letters), 184, L1.
- Tucker, W., Kellogg, E., Gursky, H., Giacconi, R., and Tananbaum, H. 1973, Ap. J., 180, 715.
- Winckler, P. F. and White A. E. 1975, Ap. J. (Letters), 199, L139.

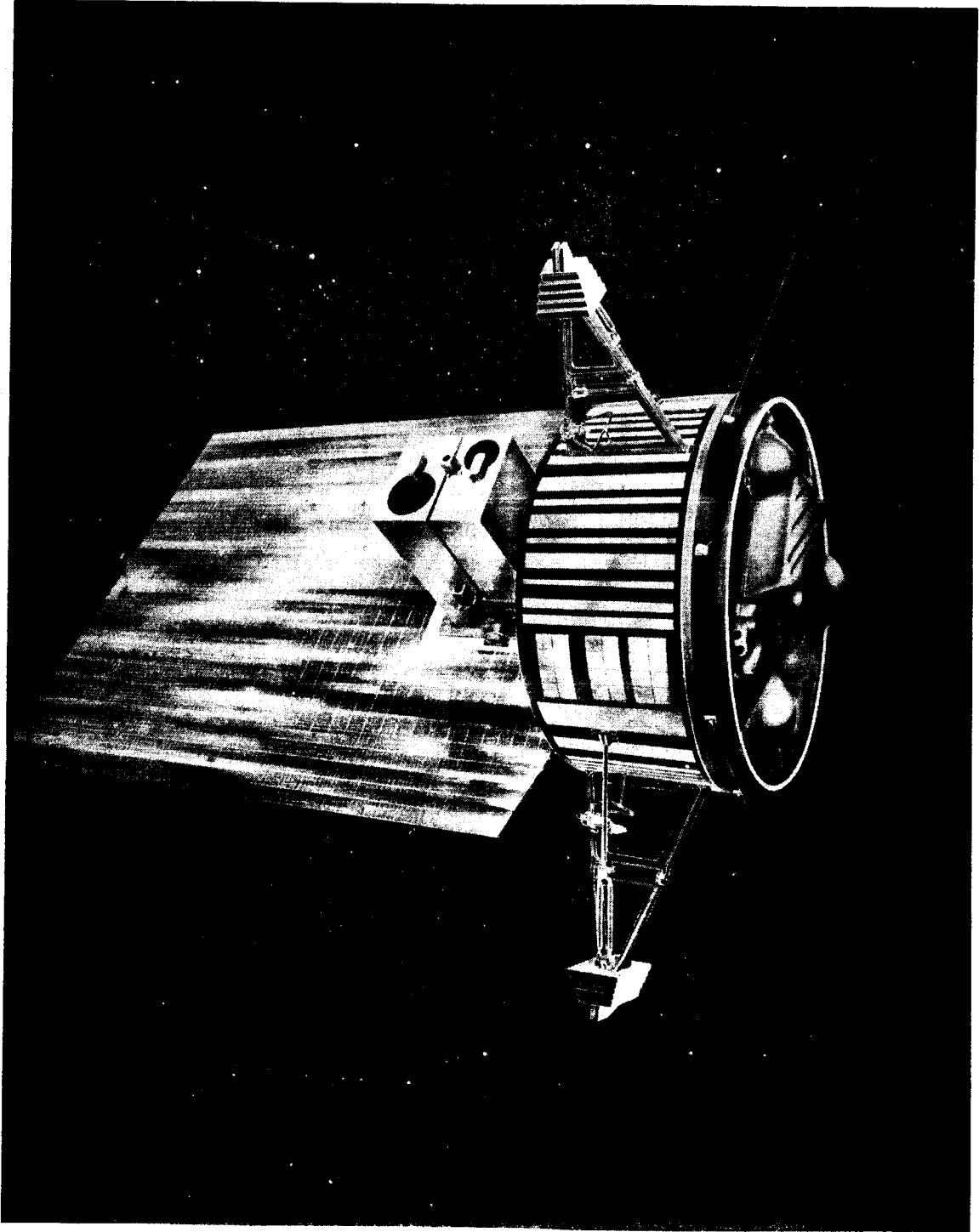


Figure 1. OSO-8

050-1 RATES PLOT
PAGE 21
START TIME 1015 200 02200102
END TIME 1015 200 01200002

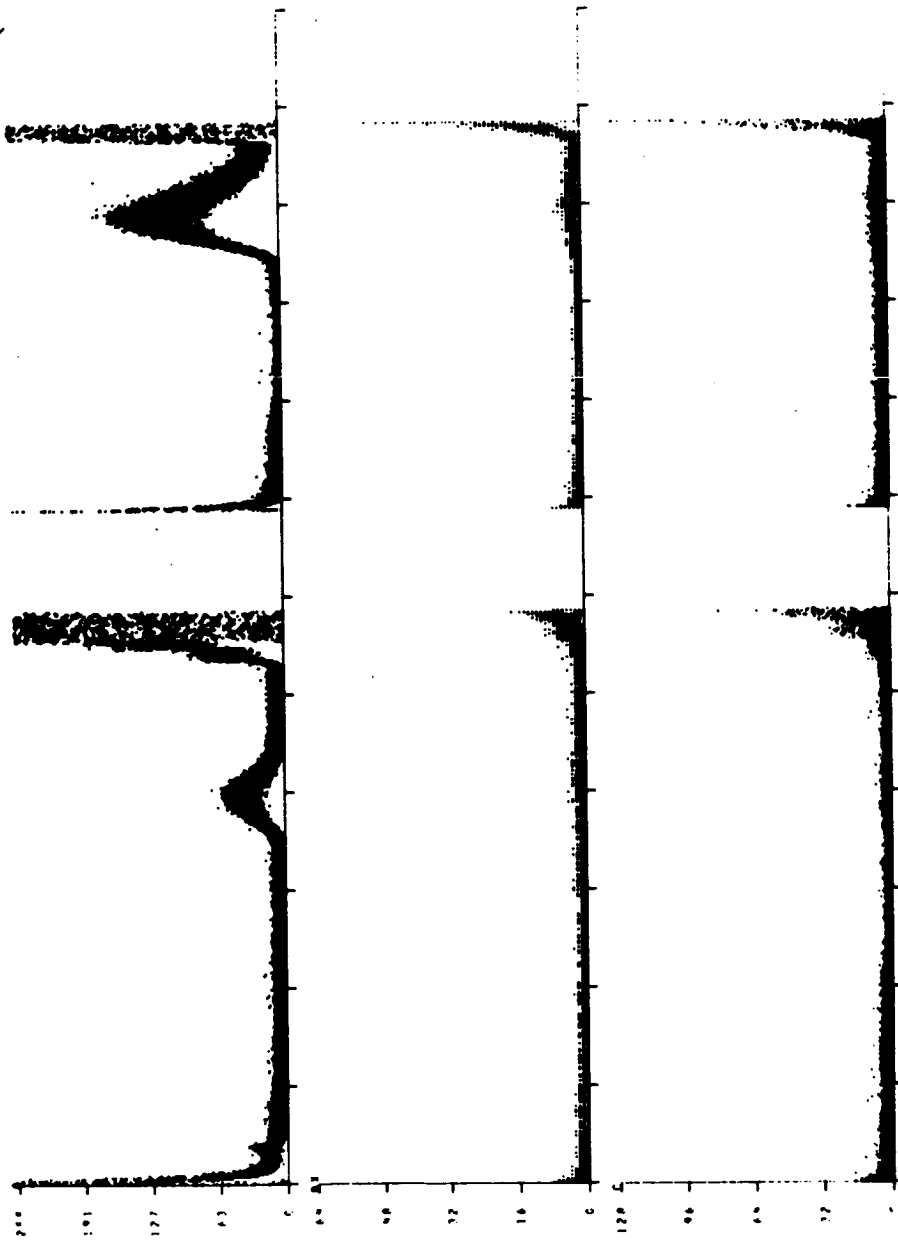


Figure 2. OSO-1 One-Orbit Rate Plot, Detectors A, B, and C

OSO-1 RATES PLOT
Page
START TIME 1975 197 0801000
END TIME 1975 197 7513300

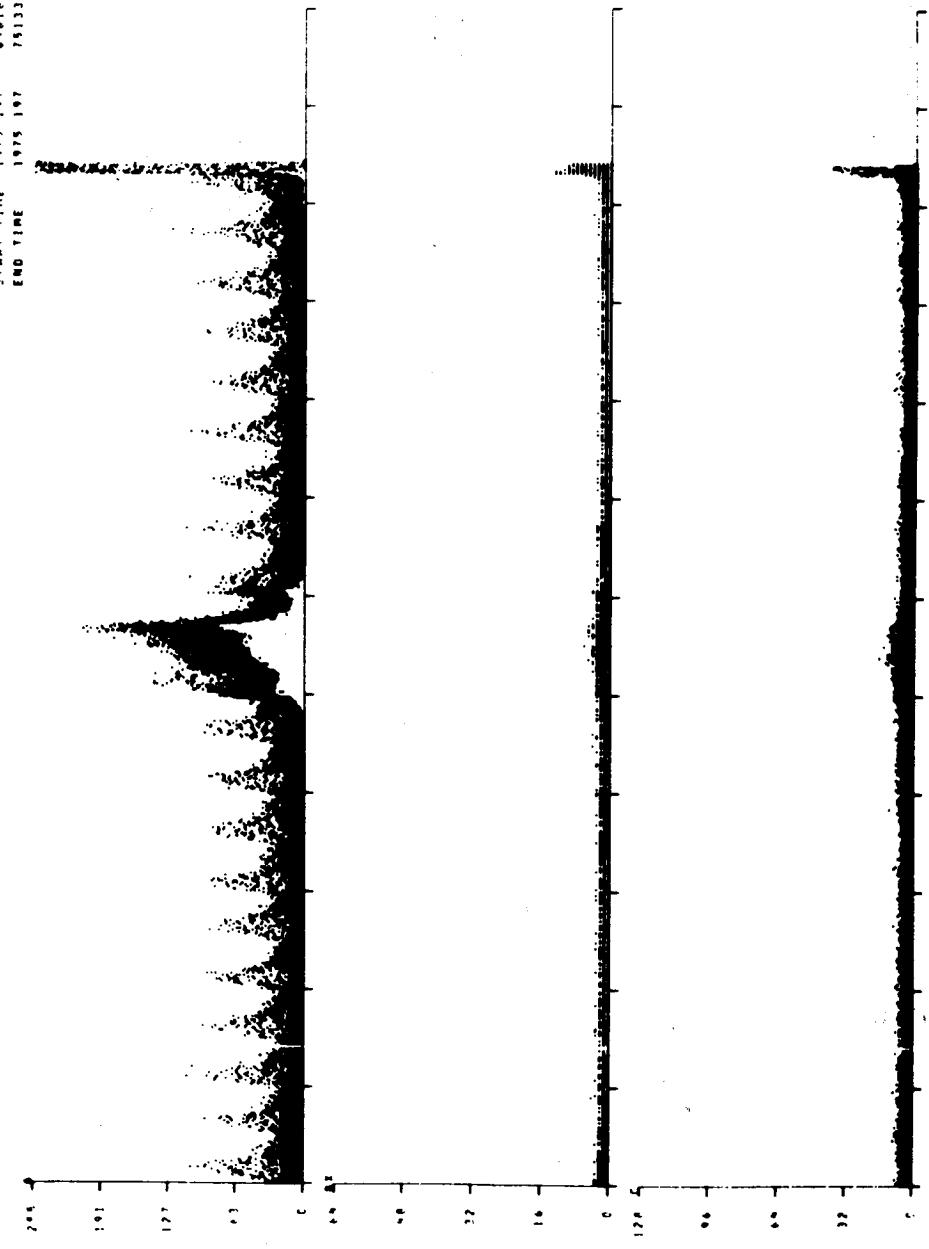


Figure 3. OSO-1 One-Orbit Rate Plot, Detector A Only

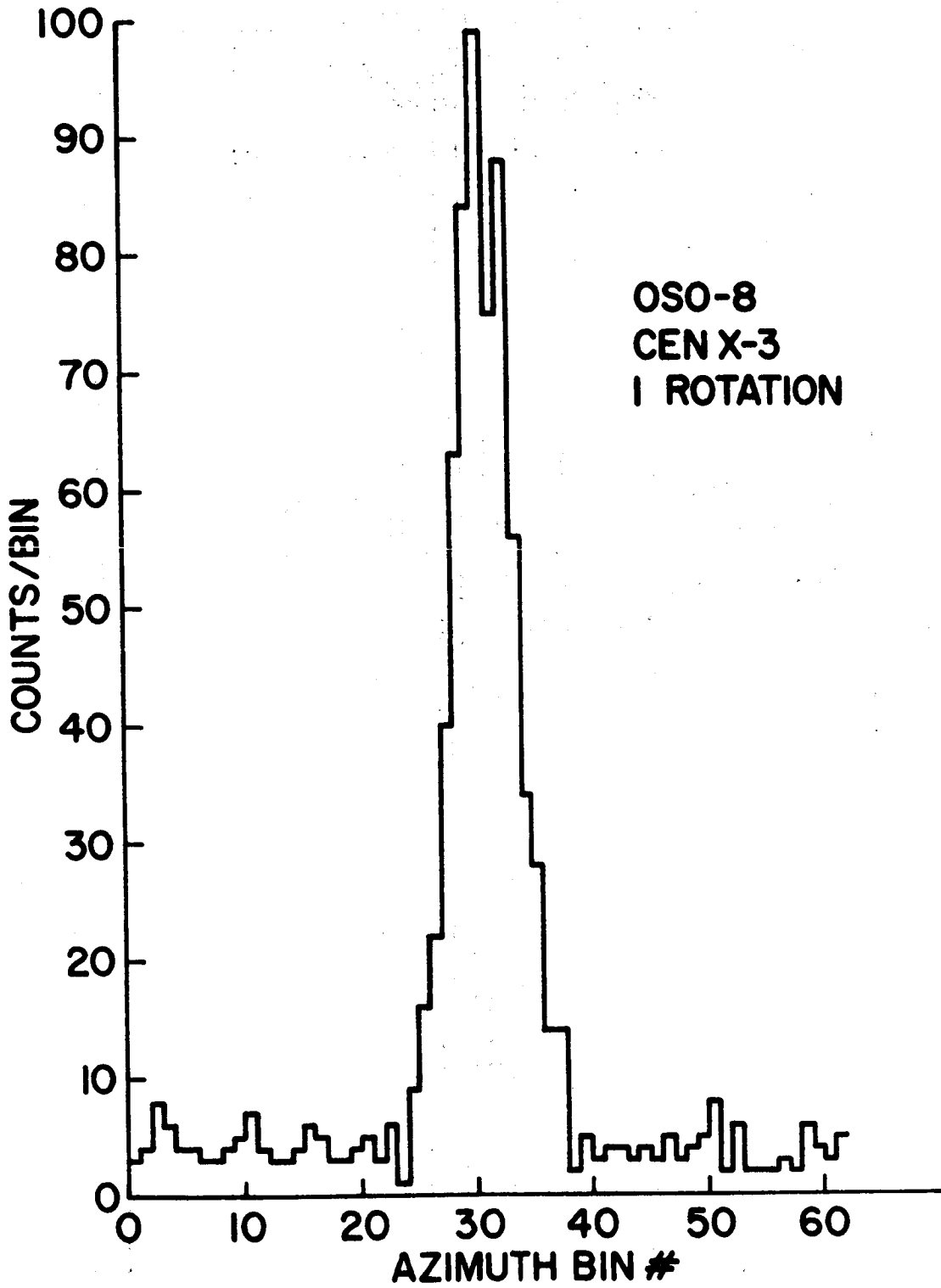


Figure 4. Rate Distribution During One Wheel Revolution

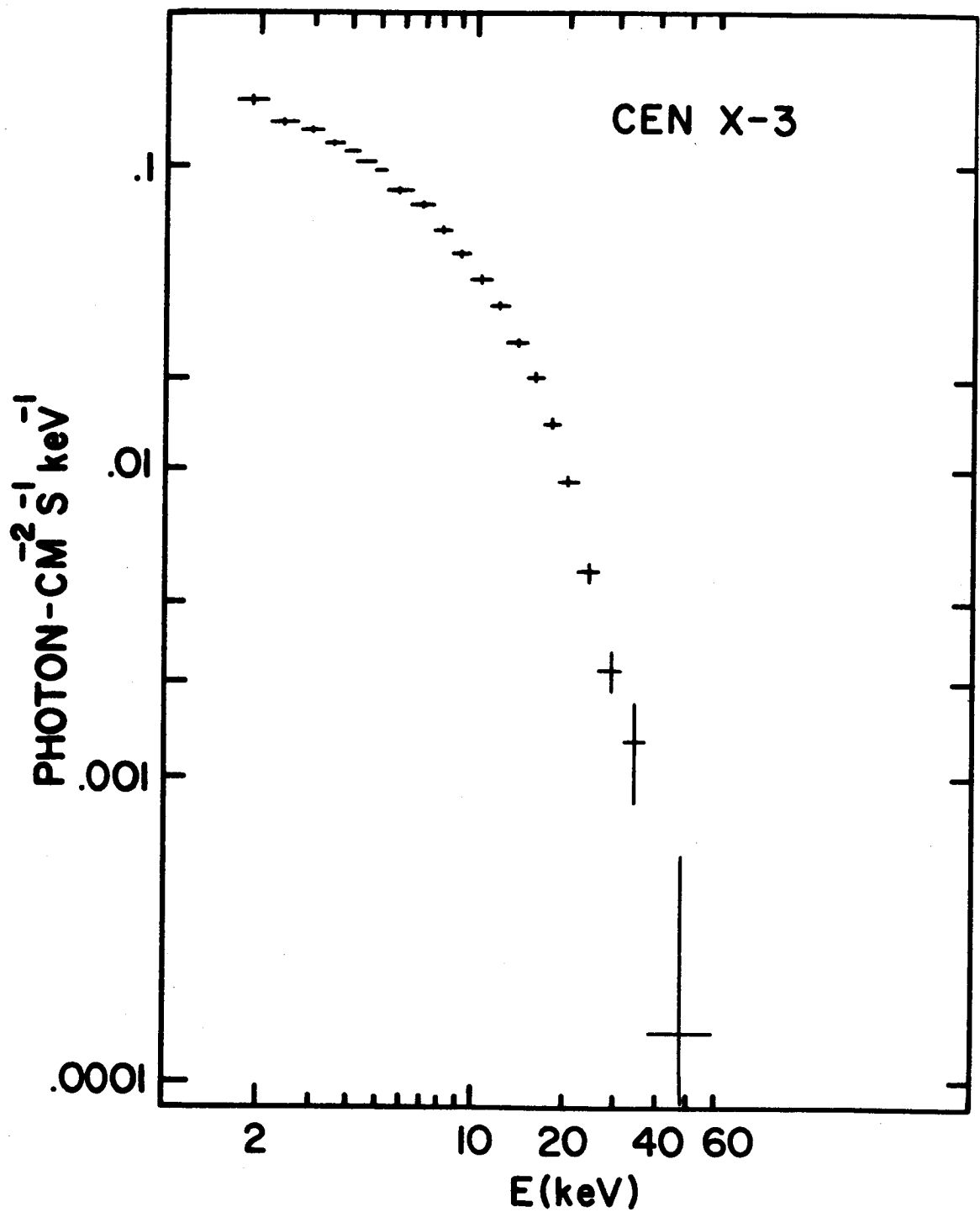


Figure 5. One CEN X-3 Spectrum Obtained with Detector A at Maximum Source Intensity

OSO-8
CEN A SPECTRUM
DAYS 208, 209, 210

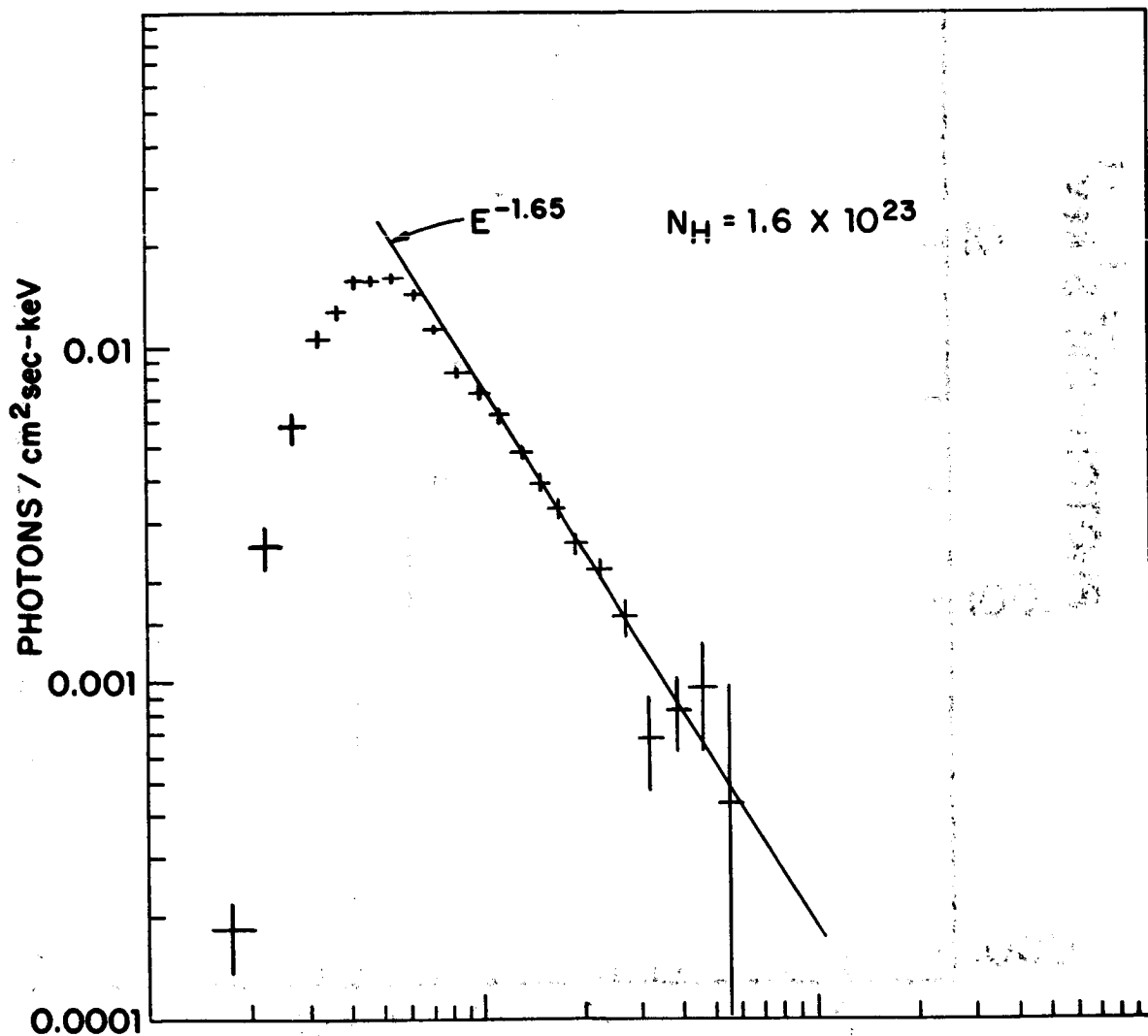


Figure 6. The Spectrum from Galaxy CEN A Obtained with Detector A from about Six Orbits of Quick Look Data

CAS A
OSO-8 FORWARD DETECTOR
OBSERVED: DAYS 199-205

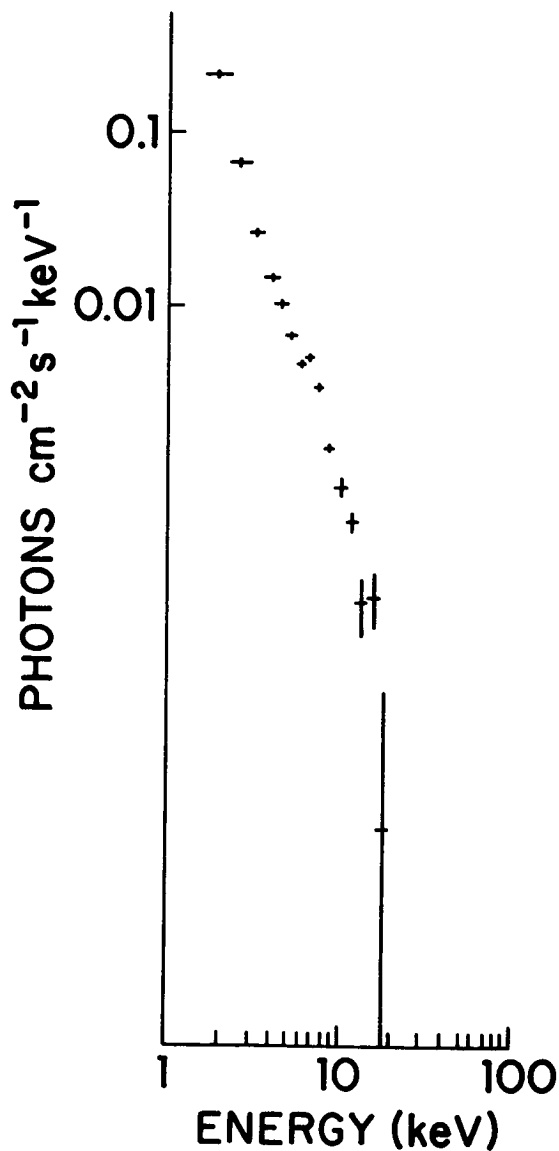


Figure 7. The Spectrum from Cas A Obtained with the 2 gas Detector C

OSO-8
NOVA MONOCEROTIS 1975

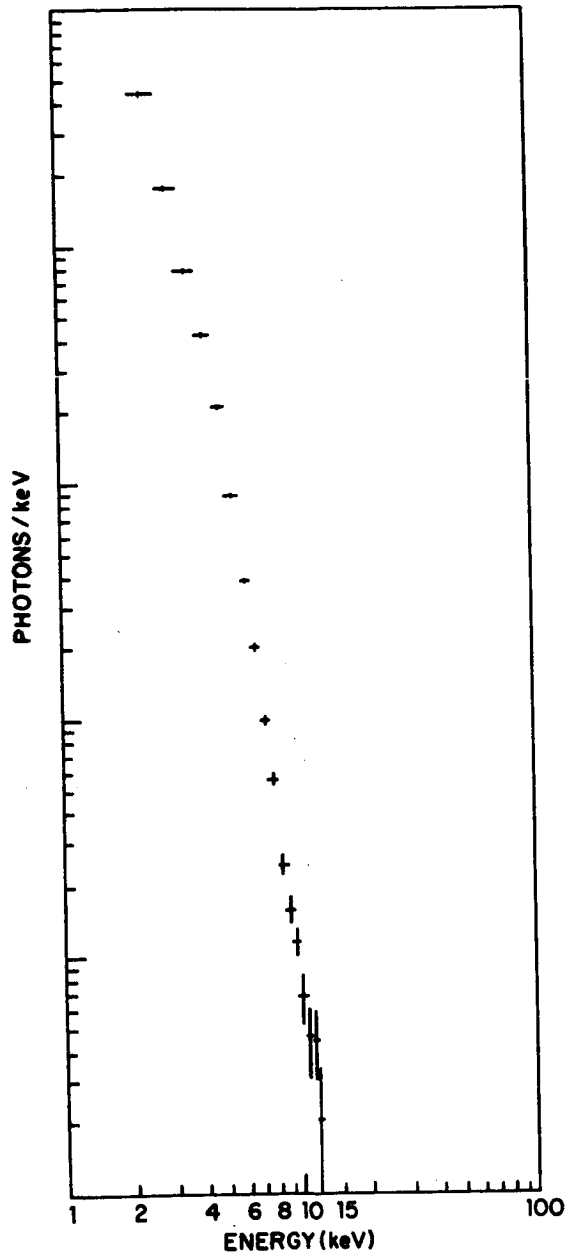


Figure 8. The Spectrum Obtained for the Transient Source Nova Monocerotis 1975



THE X-RAY POLARIZATION EXPERIMENT ON THE OSO-8

M. C. Weisskopf, G. G. Cohen, H. L. Kestenbaum,
R. Novick, and R. S. Wolff
Columbia Astrophysics Laboratory
Departments of Astronomy and Physics
Columbia University
New York, New York 10027

and

P. B. Landecker
Space Physics Laboratory
The Aerospace Corporation
El Segundo, California 90245

ABSTRACT

The OSO-8 satellite, launched on 1975 June 21, contains two X-ray polarimeters built by the Columbia Astrophysics Laboratory. These polarimeters use mosaic crystals of graphite to yield polarization-sensitive Bragg reflection of stellar X-rays. The crystals reflect a narrow energy bandwidth centered at 2.6 and 5.2 keV. The polarimeter background signal is minimized by mounting the crystals on parabolic surfaces which focus the diffracted X-rays onto small-area, beryllium-window proportional counters. This technique permits the observation of low-intensity X-ray sources and reduces the possibility of systematic background effects which could lead to a false signature of polarization. A description of the instrument is given, and the sensitivity to polarization, particularly in regard to binary sources, is discussed. Preliminary results for Cen X-3 and GX5-1 are presented.

INTRODUCTION

The OSO-8 satellite contains two stellar X-ray polarimeters that are capable of providing a sensitive search for polarization in a number of sources. This experiment, together with studies of the energy spectra and time variability, will provide important information in identifying and understanding the underlying X-ray emission mechanisms. For example, in the case of an optically thin, thermal emitter, one expects to observe a thermal bremsstrahlung energy continuum, narrow-line emission, and no linear polarization. The role of polarization experiments in X-ray astronomy was firmly established by the discovery (Novick *et al.* 1972) that the X-ray continuum of the Crab Nebula was linearly polarized with magnitude and direction similar to that observed in the radio and visible regions of the spectrum. This result,

together with the observed power-law spectrum and the discovery of the pulsar as the source of the energy, identified synchrotron radiation as the emission mechanism of this object.

Apart from being able to differentiate synchrotron from optically thin emitters, polarization experiments can also play a role in understanding the emission of X-rays from binary systems. For example, if the electron density in a thermal source is large enough so that the optical depth for Thomson scattering is greater than unity and there are sufficient departures from spherical symmetry, then we expect linear polarization up to 7 percent (Angel 1969). Such conditions may exist in the accretion disk surrounding a black hole. Recently both Rees (1975) and Lightman and Shapiro (1975) have noted that the standard accretion model (Pringle and Rees 1972; Shakura and Sunyaev 1973; Novikov and Thorne 1973) should lead to linear polarization of the X-ray flux above 1 keV of between 1 percent and 11 percent, depending on the inclination angle of the disk.

In the case of accretion onto a magnetic neutron star, both Rees (1975) and Tsuruta (1974) have shown that the pulsed X-ray flux will be strongly polarized and that polarization studies as a function of pulse phase can serve to distinguish between the "fan" beam and "pencil" beam models of these sources. Both authors have noted that the observation of polarization of much greater than 10 percent from Her X-1 would effectively rule out the white-dwarf model (Cameron 1975) for this source.

In the case of the Crab Nebula, we expect to achieve an accuracy of a few percent on both the nebula and pulsar polarization. Roberts *et al.* (1973) and Sturrock *et al.* (1975) have predicted that the pulsar X-ray polarization will be orthogonal to the pulsar optical polarization. In the case of Sco X-1 the sensitivity is so high that we might be able to detect transient polarization effects.

PRINCIPLE OF POLARIMETER OPERATION

A Bragg crystal operating at an angle of 45° acts as a perfect polarization analyzer over the energy bandwidth characteristic of the Bragg reflection. This effect can be thought of as a form of coherent scattering through an angle of 90° . Since the energy bandwidth of nearly perfect crystals is extremely small, such crystals make very inefficient polarimeters for stellar X-ray sources. This limitation can be partially overcome by using mosaic or ideally imperfect crystals. Such crystals exhibit large reflection over a much larger energy bandwidth, and they can be used to construct reasonably efficient stellar X-ray polarimeters. Such mosaic crystals consist of disordered arrays of very small perfect crystals. Each small crystal is thick enough to provide strong reflections for photons that satisfy its Bragg condition but thin enough to cause only small absorption for photons that do not satisfy the Bragg condition. We can visualize each photon in a polychromatic X-ray beam as penetrating the mosaic crystal until it encounters a crystal domain that satisfies the Bragg condition for the precise wavelength of the photon of interest. That photon is then coherently (Bragg) scattered out of the crystal. In this way we can understand how a large range of photon wave-

lengths can be simultaneously reflected by the crystal. The theory of this effect was developed many years ago by Darwin (1914) and Bragg (1914) who showed that mosaic crystals can be characterized by a quantity known as integrated reflectivity. This quantity is defined as follows.

Suppose a crystal is illuminated with radiation from an X-ray source and is rotated with uniform angular velocity ω to scan from Bragg angle θ_1 to θ_2 and that Bragg reflection of wavelength λ takes place within this range. Let $I(\lambda)d\lambda$ be the power at wavelength λ in the spectral range $d\lambda$ incident on the crystal, and let $R(\theta, \lambda)$ be the coefficient of reflection of X-rays of wavelength λ incident at angle θ on the crystal. The total reflected energy in the same spectral range, $W(\lambda)d\lambda$, is given by

$$\begin{aligned} W(\lambda)d\lambda &= \int_{\theta_1}^{\theta_2} I(\lambda)d\lambda R(\theta, \lambda) \frac{d\theta}{\omega} \\ &= \frac{1}{\omega} I(\lambda)d\lambda \cdot \Delta\theta(\lambda) \end{aligned} \quad (1)$$

where

$$\Delta\theta(\lambda) = \int_{\theta_1}^{\theta_2} R(\theta, \lambda) d\theta \quad (2)$$

The quantity $\Delta\theta$ is the integrated reflectivity. Since the number of photons reflected is directly proportional to $\Delta\theta$, the most efficient crystals for Bragg reflection will be those with the highest values of $\Delta\theta$.

The integrated reflectivity of a mosaic crystal is given in the case of unpolarized radiation by the expression derived by Darwin:

$$\Delta\theta = \frac{1 + \cos^2 2\theta}{4 \sin 2\theta} \frac{N^2 \lambda^3 F^2 r_0^2}{\mu} \quad (3)$$

Here θ is the Bragg angle, μ is the absorption coefficient; N is the number of scattering cells per unit volume, F is the crystal structure factor, that is, the effective number of scattering electrons per cell, and r_0 is the classical electron radius. A full account of reflection by crystals is given by James (1948). An examination of equation (3) shows that $\Delta\theta$ is maximized in crystals with well-defined planes of high electron density, and for scattering atoms whose photoelectric absorption cross section is small compared with the cross section for coherent scattering, proportional to $F^2 r_0^2$.

When polarized radiation is reflected by a mosaic crystal, the angular dependence of the integrated reflectivity is given by

$$\Delta\theta = \frac{N^2 \lambda^3 F^2 r_0^2}{2\mu} \left[\frac{1}{\sin 2\theta} - \frac{\sin 2\theta}{2} (1 + P \cos 2\phi) \right] \quad (4)$$

Here P is the polarization of the incident radiation, θ is the Bragg angle, ϕ is the azimuth angle between the plane of incidence and the plane formed by the incident photon direction and polarization vectors, and the other symbols were defined above. In the case of a 45° Bragg angle, $\Delta\theta$ is given by

$$\Delta\theta = \frac{N^2 \lambda^3 F^2 r_0^2}{4\mu} (1 - P \cos 2\phi) \quad (5)$$

If we envision a Bragg-crystal polarimeter as consisting of a flat crystal at 45° , then the detector must have the same area as the intercepted photon beam [see Fig. 1(a)]. Since the signal for even the best crystals and the strongest sources is quite small, the non-X-ray background associated with such a large detector would be excessive and would seriously limit the effectiveness of the polarimeter. The X-ray polarimeter on the Ariel V satellite is of this type, and it can only be used to study the strongest sources. We can overcome the problem of a large detector if we recognize that all presently known X-ray sources are continuum emitters and all models that suggest polarization indicate that, at most, the polarization would be a very slowly varying function of energy. In view of this, we can mount the crystals on a sector of a parabolic surface so that the diffracted rays converge to a small spot that allows us to use a small detector with a small background counting rate [see Fig. 1(b)]. With this construction the focal spot cannot be any smaller than the size of the crystals mounted to the surface. In addition, the mosaic spread of the crystals also contributes to the spot size.

STATISTICAL LIMITATIONS

In this type of polarimetry, the angular dependence of the photon signal is observed as the polarization analyzer is rotated about the line of sight. In view of the photon nature of the signal, it can be readily shown that the angular dependence can *never* be zero; we must *always* obtain a positive indication of polarization. If N signal photons are detected without background contamination and if the analyzer only accepts one state of polarization, then it can be readily shown that the distribution of polarization values is given by

$$f(P)dP = \frac{1}{2} NP dP \exp(-NP^2/4) \quad (6)$$

where P is the fractional polarization, which is assumed to be small, and $f(P)dP$ is the probability of obtaining an apparent polarization in the range from P to $(P + dP)$ due to statistical fluctuations in the signal. The 1σ variance in the apparent polarization is

$$\delta P(1\sigma) = \sqrt{2/N} \quad (7)$$

Real polarimeters are always plagued with background signals, and they generally accept some of the orthogonal polarization components. The acceptance

of the undesired polarization can be expressed as the polarization modulation factor m for the polarimeter. It is defined as the apparent polarization recorded with 100-percent polarized incident radiation. In the case of a polarimeter of the rotating type, then it can be shown that the actual polarization P of a signal of unknown polarization is given by

$$P = \frac{1}{m} \frac{N_{\max} - N_{\min}}{N_{\max} + N_{\min}}, \quad (8)$$

where N_{\max} and N_{\min} are the maximum and minimum signals recorded as the polarimeter is rotated about the line of sight to the source.

In the presence of a background signal and with a polarimeter with modulation factor m , the 3σ or 99.7-percent confidence limit on any measured polarization is given by

$$\delta P(3\sigma) = \frac{3}{mS} [2(S + B)/T]^{1/2}, \quad (9)$$

where S is the signal counting rate, B is the background rate, and T is the observing time.

THE INSTRUMENT

The OSO-8 crystal panel has a projected area of about 140 cm^2 and contains about 450 graphite crystals. The panel is a 30° arc of a parabola of revolution, and the Bragg angles range from about 40° to 50° . With this range of azimuthal and Bragg angles the modulation factor is somewhat reduced below unity. It can be readily shown from equation (5) that a strip of crystals with 45° Bragg angle but a range $\Delta\phi$ of azimuthal angles will yield a modulation m given by

$$m = \frac{\sin \Delta\phi}{\Delta\phi}. \quad (10)$$

In the case of the OSO-8 panels, $\Delta\phi$ is 30° and $m = 0.96$, in very good agreement with the laboratory measurements shown in Figure 2.

The detector in the OSO-8 polarimeter consists of a thin-window, gas proportional counter that utilizes pulse-height analysis, rise-time discrimination, and anticoincidence techniques to reduce the background. Background reduction is necessary not only to improve the sensitivity of the instrument but also to reduce the possibility of false polarization produced by anisotropies in the background. The properties of the detector and the crystal panels are summarized in Table 1.

The OSO-8 satellite is a spinning vehicle. Two crossed graphite polarimeters are coaligned with the spin axis and view the sky along this axis (see Fig. 3). The two orthogonal polarimeters not only provide redundancy but also

allow us to measure the two Stokes parameters simultaneously. This is extremely important in the case of time-variable sources. With the OSO-8 instrument polarization will manifest itself as a modulation of the polarimeter counting rate at twice the rotation frequency of the spacecraft. The amplitude of modulation yields the fractional polarization, and the phase, the position angle. True polarization will lead to antiphase modulation in the two orthogonal polarimeters while temporal variations in the source will cause in-phase time variations.

PRELIMINARY RESULTS

Figures 4 and 5 show the pulse-height spectra obtained from the two OSO-8 polarimeters during observations of the strong source 3U 1758-25 (GX5-1). The first- and second-order reflections centered at 2.6 and 5.2 keV are clearly visible above the background. The background energy spectrum, shown as the solid line in these figures, was obtained when the source was eclipsed by the Earth. The slightly broader pulse-height peaks in Figure 5 are due to the poorer resolution of the second detector as compared with the first. These spectra, and particularly the relative counting rates of the signal versus the background, show the success of employing focusing together with rise-time discrimination and anticoincidence techniques to achieve background suppression. The background rates are approximately 1×10^{-3} events $(\text{cm}^2 \text{ sec keV})^{-1}$ for both detectors.

Figure 6 shows similar spectra obtained from observations of the eclipsing binary 3U 1118-60 (Cen X-3), both in and out of binary eclipse. Although the source is weaker than GX5-1, the first- and second-order reflections from the graphite crystals were clearly observed. The first- and second-order reflection peaks appear in slightly lower pulse-height channels in the second polarimeter than they do for the GX5-1 observations, as the high voltage and therefore the gain were at a lower setting.

We have examined all four data sets shown in Figures 4-6 for evidence of modulation at twice the rotation frequency of the satellite; i.e., the signature of polarization. The results for the two observations where the X-ray sources were in the field of view are listed in Table 2. In all cases, including analysis of the background data, no evidence for modulation was obtained. However, due to the limited amount of data available at this time, the sensitivity to modulation is limited. Nevertheless, when combined with the results of the background data analysis, these results can be used to set upper limits on the polarization of these two X-ray sources at 28 percent for the integrated emission from Cen X-3 and 12 percent for GX5-1, both at the 99 percent confidence level. We caution the reader, however, that these results assume that there are no large systematic background effects which depend on time or the satellite orbit which might mask a strongly polarized signal. This proviso is particularly relevant to the Cen X-3 observation where the signal-to-background ratio is approximately unity.

SENSITIVITY TO POLARIZATION

By the end of November 1975 we will have completed observations of four of the binary X-ray sources, Cen X-3, Her X-1, Cyg X-1, and Cyg X-3, which are being discussed at this Conference. The expected sensitivity to polarization for these sources is listed in Table 3. These estimates are based on the background rates we have observed and assume that we find no significant spurious modulation in the background. By this time we shall also have completed extensive background observations where no known X-ray sources are in the field of view under a variety of satellite environmental conditions. It is also worth noting that the sensitivity to polarization for the Cyg X-1 measurement is somewhat optimistic as the source fluctuations are greatly in excess of those predicted by counting statistics.

The successful launch and operation of a satellite experiment involves the coordinated efforts of a large number of people. The following list is by no means exhaustive, but we would like to acknowledge the contributions of Prof. J. R. P. Angel, Dr. J. R. Wang, Dr. J. Toraskar, Ms. D. J. Miller, Mr. D. D. Mitchell, Mr. I. Rochwarger, M. M. Sackson, and the staff of the Columbia Astrophysics Laboratory. This work was supported by the National Aeronautics and Space Administration under contract NAS5-22408. This paper is Columbia Astrophysics Laboratory Contribution No. 118.

REFERENCES

- Angel, J. R. P. 1969, *Astrophys. J.*, 158, 219.
- Bragg, W. H. 1914, *Phil. Mag.*, 27, 881.
- Cameron, A. G. W. 1975, *Astrophys. and Space Sci.*, 32, 215.
- Darwin, C. G. 1914, *Phil. Mag.*, 27, 315, 675.
- James, R. W. 1948, *The Optical Principles of the Diffraction of X-Rays* (London: G. Bell and Sons, Ltd.).
- Lightman, A. P., and Shapiro, S. L. 1975, *Astrophys. J. (Letters)*, 198, L73.
- Novick, R., Weisskopf, M. C., Berthelsdorf, R., Linke, R., and Wolff, R. S. 1972, *Astrophys. J. (Letters)*, 174, L1.
- Novikov, I. D., and Thorne, K. S. 1973, in *Black Holes, Les Houches*, eds., DeWitt, C., and DeWitt, B. (New York: Gordon and Breach).
- Pringle, J. E., and Rees, M. J. 1972, *Astron. and Astrophys.*, 21, 1.
- Rees, M. J. 1975, *Mon. Not. Roy. Astron. Soc.*, 171, 457.
- Roberts, D. H., Sturrock, P. A., and Turk, J. S. 1973, *Ann. N.Y. Acad. Sci.*, 224, 206.
- Shakura, N. I., and Sunyaev, R. A. 1973, *Astron. and Astrophys.*, 24, 337.

Sturrock, P. A., Petrosan, V., and Turk, J. S. 1975, *Astrophys. J.*, **196**, 73.

Tsuruta, S. 1974, preprint submitted for publication in *Proceedings of the Seventh Texas Symposium on Relativistic Astrophysics, Dallas, Texas, December 16-20.*

TABLE 1
Instrument Parameters of the OSO-8 Polarimeter

Parameter		First Order	Second Order
<i>(a) Crystal Panels</i>			
Material	Graphite (2d = 6.7 Å)		
Projected geometric area	140 cm ²		
$\Delta\theta$		9×10^{-4}	5×10^{-4}
E (keV)		2.6	5.2
ΔE (keV)		0.4	0.8
<i>(b) Proportional Counters</i>			
Window	2-mil beryllium		
Gas composition			
Neon	620 mm Hg		
Xenon	65		
Carbon dioxide	<u>75</u>		
	760		
Efficiency		0.67	0.53
<i>(c) Polarimeters</i>			
Effective area (cm ²)		0.169	0.075

TABLE 2
Search for Modulation at 2.6 keV

Instrument	A [*] (counts sec ⁻¹ × 100)	M ^{**} (%)	φ [†] (°)	Proba- [‡] bility	S [§] (%)
(a) 3U 1758-25 (GX5-1)					
Counter 1	0.98	3.3	53	0.71	12.0
Counter 2	0.49	1.6	208	0.92	11.7
Average	0.50	1.7	68	0.83	8.4
(b) 3U 1118-60 (Cen X-3)					
Counter 1	0.28	3.6	242	0.76	14.6
Counter 2	0.50	6.8	138	0.40	15.2
Average	0.39	5.1	242	0.34	10.5

* A is the average count rate.

** M is the detected amplitude of modulation as a percentage of the average.

† φ is the position angle (in this case, relative to an arbitrary reference point).

‡ Probability of measuring M or greater by chance due to random fluctuations of the data.

§ S is the sensitivity expressed as a percent modulation of the signal. Modulation at this level would have a 1% probability of occurring by chance.

TABLE 3

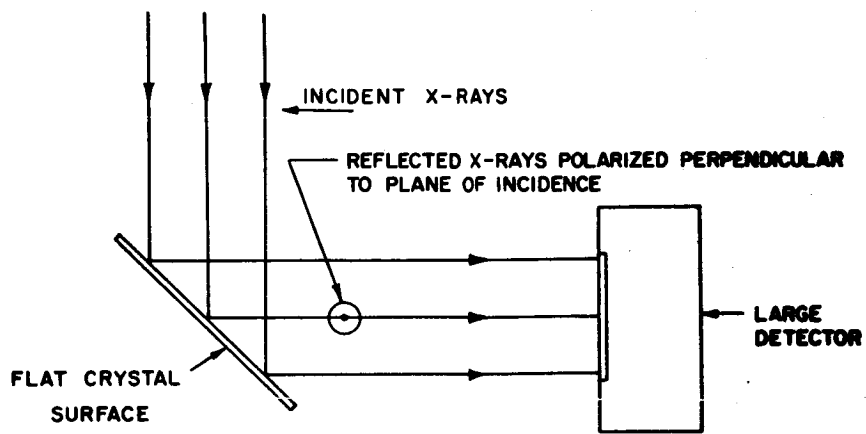
Sensitivity to Polarization of Binary Sources

Source	Minimum Detectable Polarization		
	First Order (%)	Second Order (%)	Combined (%)
Gen X-3	5.0	8.7	4.4
Her X-1*	10.2	13.2	8.1
Cyg X-1 [†]	5.0	12.8	4.8
Cyg X-3 [§]	5.7	12.1	5.3

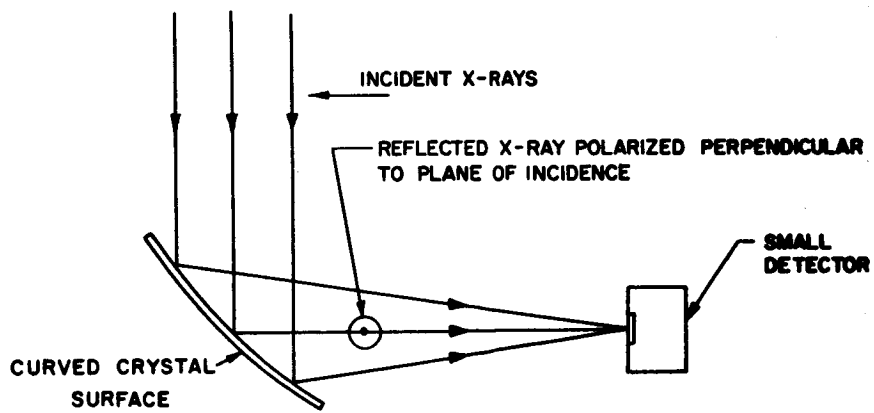
*Observation time known; source strength estimated.

[†]Observation time known; Poisson statistics assumed; source strength estimated.

[§]Observation time and source strength estimated.



A) NON FOCUSING POLARIMETER



B) FOCUSING POLARIMETER

Figure 1. Conceptual diagram of (a) nonfocusing and (b) focusing Bragg-crystal polarimeters.

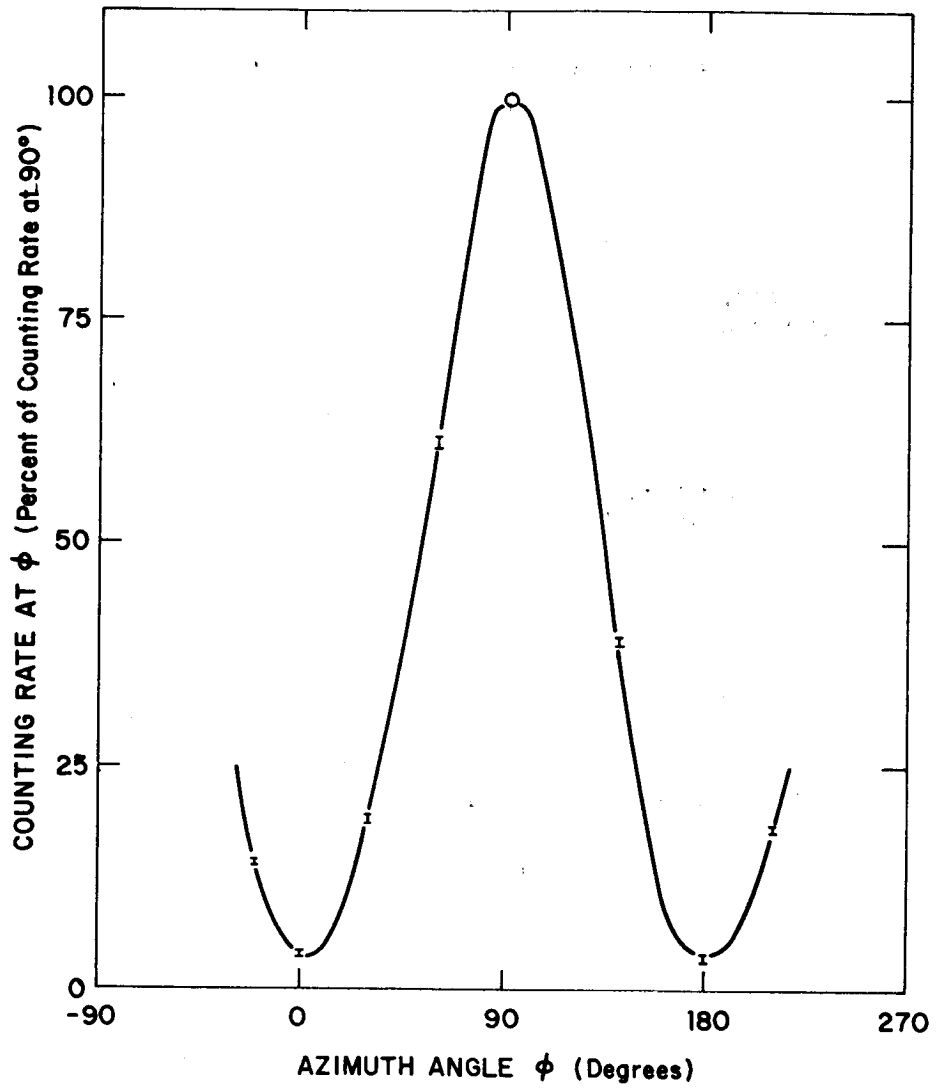


Figure 2. Modulation response of the pre-engineering model OSO-8 polarimeter, measured with a collimated beam of 5.2-keV (second-order) polarized X-rays.

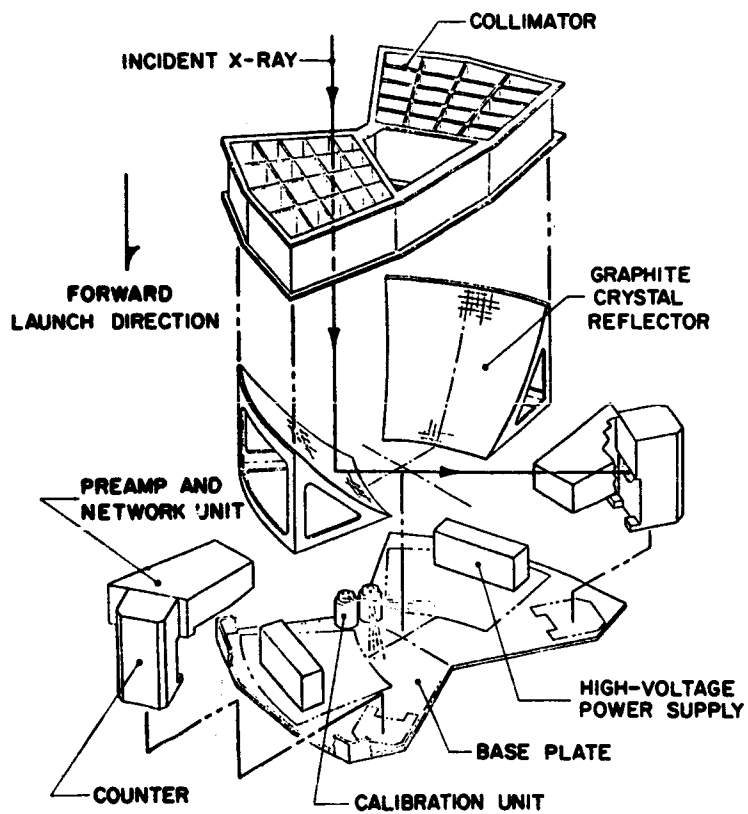


Figure 3. Exploded view of the OSO-8 polarimeter assembly.

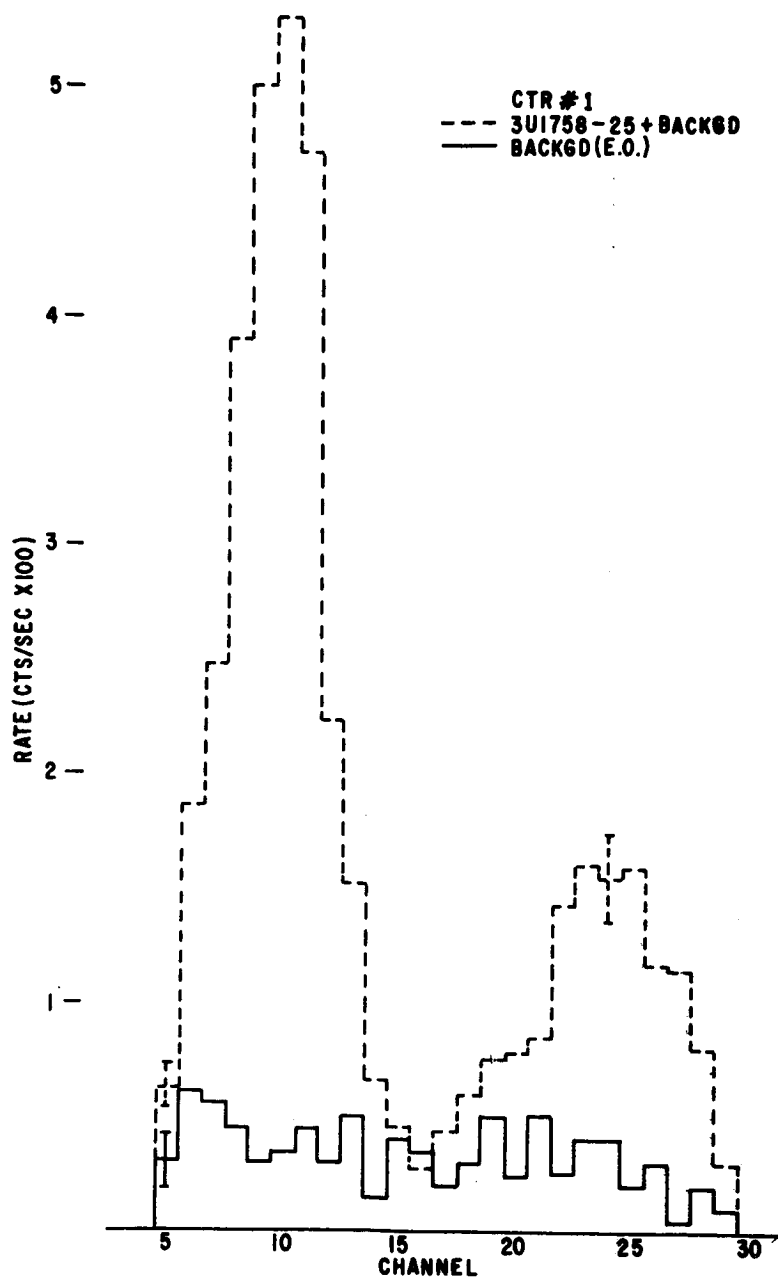


Figure 4. Pulse-height spectrum obtained with polarimeter No. 1 while observing the source 3U 1758-25 (GX5-1). The solid line represents the data obtained while the source was in Earth eclipse.

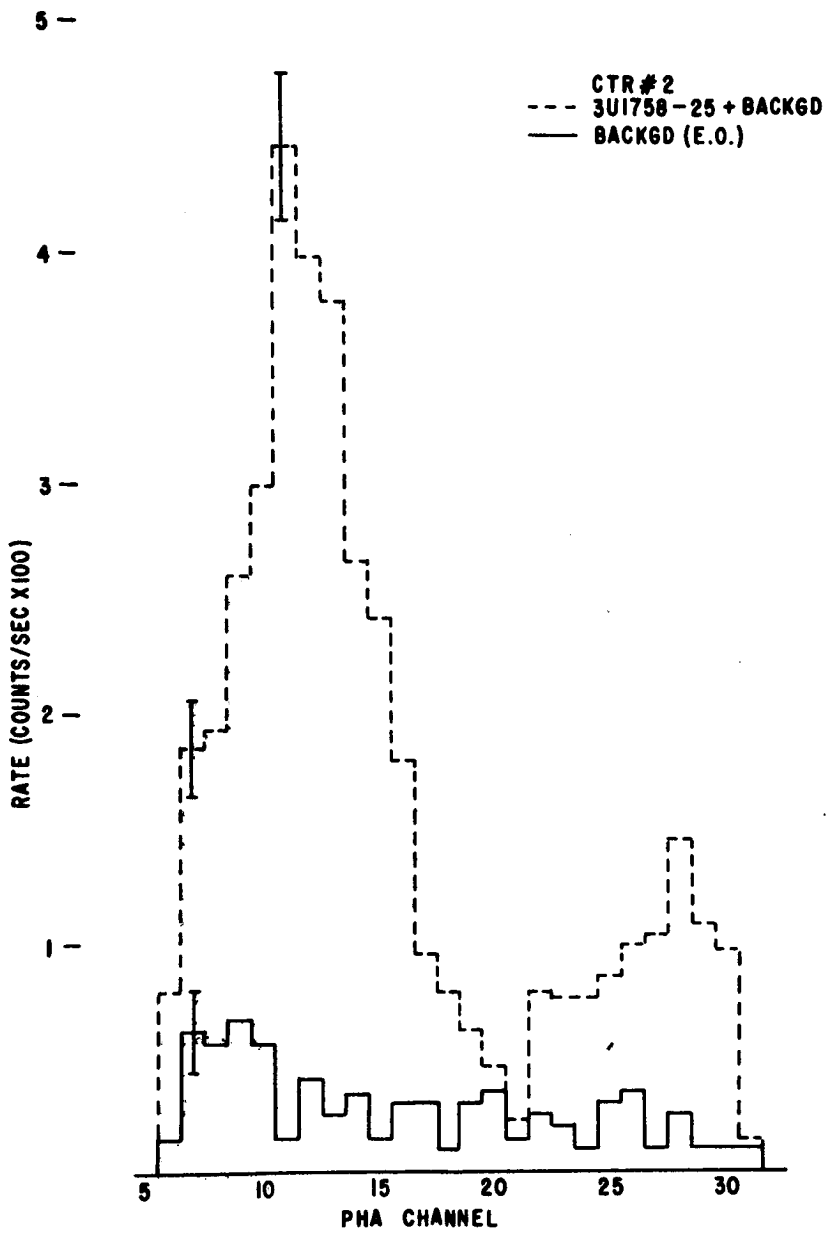


Figure 5. Same as Figure 2, but obtained with polarimeter No. 2.

COUNTER # 2

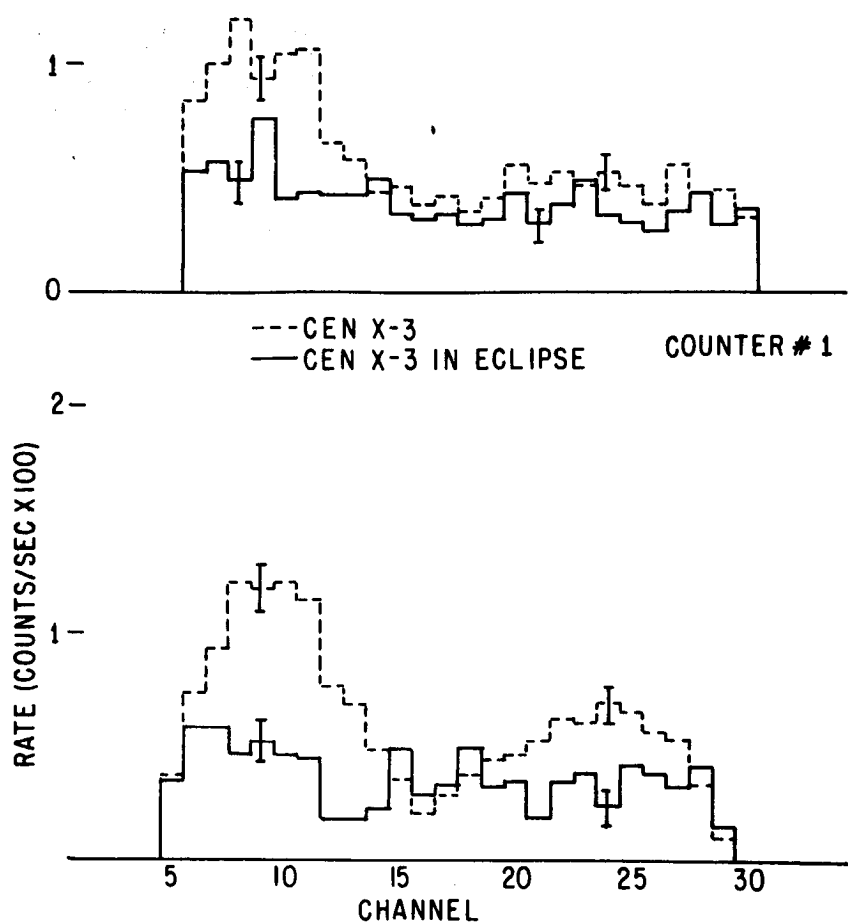


Figure 6. Pulse-height spectra obtained with both polarimeters during the Cen X-3 observations. The first-order peak occurs at 2.6 keV. The dashed lines are data obtained when viewing the source, not in eclipse. The solid lines are the data obtained while the source was in eclipse.

REVIEW OF RECENT X-RAY RESULTS

Discussion

P. Murdin to J. L. Culhane/B. Margon:

Topic: Reality of 22 hr. period in X Per.

When you sample a periodic X-ray source periodically with a satellite which goes behind the Earth every orbit, may pass through high-background regions, or do other duties every day, then the Fourier power spectrum of the intensity of the source contains several peaks in a pattern centered on the source period. The pattern of the peaks in the power spectrum is an aid to recognising the reality of the periodicity.

3U0352+30 has been observed by Copernicus on six occasions and there is periodicity recognisable in the power spectrum of two of these six runs, at a period of 22 hours and peak to mean amplitude about 15%. On the other occasions periodicity of the same amplitude would probably have been seen but wasn't.

F. Winkler to P. Serlemitsos:

What are temperatures of the two thermal components which best fit the observed spectral data for Cas A?

P. Serlemitsos:

Cas A answer: $kT = 0.7$ keV and $kT = 3.9$ keV.

Her X-1 PANEL

John N. Bahcall
Institute for Advanced Study
Princeton, New Jersey 08540

INTRODUCTION

The Hz Herculis/Her X-1 system was the first X-ray pulsar in a binary system to be optically identified and as such it has been the subject of many related X-ray and optical investigations. Several basic properties of this system were understood as an almost immediate result of the epochal UHURU X-ray observations, the optical identification, and the early fundamental theoretical papers. Among the properties we can regard as understood are:

- (1) The origin of the 1.7^d period (cause: binary motion);
- (2) The origin of the 1.2^s period (cause: rotation of a compact star);
- (3) The origin of the X-ray emission (cause: mass accretion onto a compact star);
- (4) The origin of the large optical variations (cause: X-ray heating of the photosphere of Hz Herculis).

Nevertheless we do not yet have a good understanding of some of the elementary properties in this now classical X-ray binary. Future X-ray and optical observations should concentrate, at least in part, on trying to provide clues for understanding these puzzles. I list some of the more obvious incompletely understood phenomena.

- (1) The origin of the 35^d period;
- (2) The origin of the long inactive periods (seen on historical optical plates and presumed to occur likewise in the X-rays) - what turns the X-ray emission on and off;
- (3) The nature and origin of the X-ray spectrum and pulse shape; and
- (4) The systematics of, and quantitative explanation for, the observed occasional optical pulsations.

The most fundamental observation that one can anticipate is the intensive study of Hz Herculis during an X-ray OFF period (extended optical low).

It will then be possible to measure optically reasonably accurately the ellipsoidal light variations and the projected radial velocity of Hz Herculis providing an over-determined system of equations for fixing the binary parameters (the two masses and the inclination angle i). One can then compare the mass of the X-ray source determined in this way with that suggested by the Berkeley group (using a model for the origin of the optical pulsations that, however, does not explain the observed smallness of the optical pulsations). The monitoring of Hz Herculis and Her X-1 ought to be done as often as possible, with an early-warning to other observers if an OFF period is discovered, in order not to lose information on an historical opportunity.

The papers in this panel concern the basic unsolved problems of the Hz Herculis/Her X-1 system listed above. Although they do not provide definitive answers, the present observations do provide valuable clues and hopefully point the way toward the correct solutions.

PERIODIC FLICKERING IN THE OPTICAL SPECTRUM OF HZ HERCULIS

P.L. Bernacca

Asiago Astrophysical Observatory
36012 Asiago (Vicenza) Italy

ABSTRACT

Photometric observations of HZ Herculis in the ultraviolet with a time resolution of 5 seconds show the existence of periodic flickering with a time scale of 115 to 130 seconds. The amplitude modulation is about 3 to 6 percent, larger than that associated with the erratic white flickering. The flickering, either erratic or periodic, occurs, but not always, near orbital phase 0.5, irrespective of the ON and OFF parts of the X-ray cycle.

I. INTRODUCTION

The properties of HZ Herculis in the optical region have been most recently summarized by Bahcall (1975). He has also emphasized the importance of observations directed to detect light flickering and to establish its dependence both on orbital phase and X-ray cycle.

Up to date it is accepted only that HZ Herculis flickers non-periodically with a time scale of 15 to 300 seconds on the basis of dual-channel photometry carried out by Moffet, Nather and VandenBout (1974) in white light. It will now be shown that HZ Her may temporarily also show periodic flickering in ultraviolet light with a time scale of 115 to 130 seconds of larger amplitude than that associated with the white erratic flickering.

II. OBSERVATIONS

HZ Herculis was monitored at Asiago using a one-channel photometer attached to the 122 cm Reflector. The response of the photometer is determined by the EMI 6256/S photomultiplier and a UG2/1-mm filter. The digital signal was apportioned through a multichannel analyzer and recorded on paper tape for data processing. A field diaphragm of 22 seconds of arc (") in diameter was used. Offset guiding allowed to watch continuously that the target be kept within the diaphragm. Average seeing at Asiago is about 3" and guidance errors due to atmospheric turbulence were not larger than about 1 mirror image. Thus, also in bad seeing conditions, when the image could temporarily measure about 6", the target was always well settled on the photocatode. A comparison star, near HZ Her, was frequently monitored before, after and in between.

Of all the observations, only those obtained in good quality nights and stable atmospheric conditions have been considered. The check has been easily made by examining the constancy of the time series of the comparison star. A signal is here conservatively defined to be constant when the actual dispersion is not larger than the poissonian dispersion by a factor 4 and when, after removing possible quadratic trend, its spectrum does not show lines with power exceeding the limit given by the a priori probability of 0.1 percent of having larger or equal power.

The journal of the observations is given in Table 1. Headings are self-explanatory. Indication of the status of Her X-1 during the 35 days X-ray cycle is based on having assumed that turn on occurred sometime between May 29 and May 30, 1974. This estimate is in agreement with estimates by Chevalier and Ilowaisky (1974) and with information recently provided by Fritz et al (1975). A duration of 11 days for the ON phase is assumed.

III. ANALYSIS AND RESULTS

Figure 1 shows the light curve observed on May 29, 1974. The ordinates give the net count rate per channel free from the average sky background. Time is advancing from the top to the bottom. These runs are, however, physically divided by the monitoring of the comparison star. It is evident the progressive increasing of the amplitude of the flickering, starting from run c, until a stage is reached where quasi-periodic attenuations appear with depths of about 0.3 mag. The time scale of these features is around 120 seconds. Runs a and b are typical of a constant signal.

A similar behaviour was already announced by Bernacca (1974) and observed, independently, by Chevalier and Ilowaisky (1974). The latter authors made observations in ultraviolet with an integration time of 8 seconds using a one-channel photometer. The fact they found the same time scale and, as it will be seen, comparable amplitude modulation, confirms the reality of the phenomenon. It is however opinion of the writer that the constancy of the comparison, checked by interrupting the monitoring of HZ Her, is per se evidence of the reality of the flickering.

The observations shown in Figure 1 were Fourier analyzed to search for periodic components. These indeed begin to show up in run d and are clearly present in run e. The power spectrum of run e is shown in Figure 2 where the power is plotted in units of the average noise power of about 1540 counts (the background is included).

The strong line at 128 seconds with its first harmonic at 64 seconds leads to folding the data modulo 130 seconds. The recovered light curve is shown in Figure 3, where we see that the amplitude is about 50 counts on the average or about 6% when referred to an average signal of about 850 counts (Fig. 1). The same amplitude can, of course, be derived from the power spectrum which is based on 128 data points.

Chevalier and Ilowaisky (1974) have reported an amplitude of 3% with temporary excursions up to 13%. The white flickering is known to be at most 1.6% in intensity.

Figure 4 shows the light curve on Jun 3, 1974. The power spectrum of the first part (top), in Figure 5, shows two strong lines at 116 and 61 seconds. Owing to the low resolution of the spectrum, it is not safe to consider them

as two independent lines and we will consider only the signal recovered by folding the data modulo 115 seconds (Figure 6). The amplitude modulation is again about 6%. In the second part of the run dips develop reaching depths of about 0.6 mag. One may question about their reality. We note however that the structure of this 4 minutes lasting attenuation has a time scale of about 120 seconds similar to that of the periodic components discussed above and that the light curve has a smaller variance outside the dips than that associated with the first part of the run. We finally show the power spectrum of the run obtained on July 20, 1974 which is typical of that obtained some hours earlier (July 19). The signal was rather erratic on that night with time scale between 30 and 130 seconds. The amplitude associated with the 128 seconds and 30 seconds components are about 3.2% and 2% respectively. From the observations of the comparison star we derive a maximum amplitude modulation due to atmospheric scintillation of less than 1% in the range of frequencies examined. During the remaining nights no significant differences were found between HZ Her and the comparison star when allowance is made for atmospheric phenomena.

IV. CONCLUDING REMARKS

It is not the scope of the present note to discuss in detail the bearing of this flickering on present theories concerning the mechanism responsible for this behaviour. We simply conclude with the following remarks, which stem from considering the present observations together with those of the authors quoted above.

- 1.- HZ Her presents sometimes in addition to the erratic white flickering periodic flickering in ultraviolet light. The time scale ranges between 115 and 130 seconds. The amplitude modulation, between 3% and 6%, is larger than that associated with the white flickering.
- 2.- The flickering either erratic or periodic, has a larger amplitude near orbital phase 0.5, when present.
- 3.- HZ Her flickers irrespective of the ON and OFF part of the X-Ray cycle. The available data are still too sparse to investigate whether the intensity of the flickering is larger during the ON status. It seems however that the hard (2-20 KeV) pulsed X-Rays are not the only agents responsible for the heating associated with the flickering.

TABLE 1
Journal of observations of HZ Herculis

EPOCH OF OBSERVATIONS		AT	START	ΔT (sec)	LENGTH (bins)	ORBITAL PHASE AT MID-RUN	X-RAY CYCLE	
DATE	U.T.							
1974, May	25 22 ^h	47 ^m	17 ^s	1	1024	.112		
	26 22	34	08	1	1024	.695	OFF	
	29 21	57	26	5	1024	.459	OFF/ON	Fig.1,2,3
Jun	1 21	30	57	5	1024	.213	ON	
	3 21	30	57	5	1024	.389	ON	Fig.4,5,6
	9 01	52	26	5	1024	.436	ON/OFF	
July	19 23	09	19	5	1024	.485	OFF	Fig.7
	20 01	25	10	5	512	.532	OFF	Fig.7
Aug	12 20	58	03	5	512	.539	ON	
	17 22	16	04	5	512	.512	ON/OFF	
	20 20	38	20	5	1024	.246	OFF	
1975 Aug	18 23	57	16	2	1024	.824	OFF	
	27 23	28	46	2	1024	.106	OFF/ON	
Oct	5 19	53	32	2	2048	.964	ON	

REFERENCES

- Bahcall, J.N. 1975, Lectures at the Enrico Fermi Summer School on Physics and Astrophysics of Neutron Stars and Black Holes, Varenna, Italy, July 1975.
- Bernacca, P.L. 1974, I.A.U. Circular No.2685.
- Chevalier, C., Ilowaisky, S.A. 1974, I.A.U. Circular No. 2691.
- Fritz, G., Shulman, S., Friedman, H., Henry, R.C., Davidsen, A., Snyder, W. 1975, Symposium on X-Ray Binaries, Goddard Space Flight Center, October 20-22, 1975.
- Moffet, T.J., Nather, R.E., Vanden Bout, P.A. 1974, Ap.J., 190, L63.

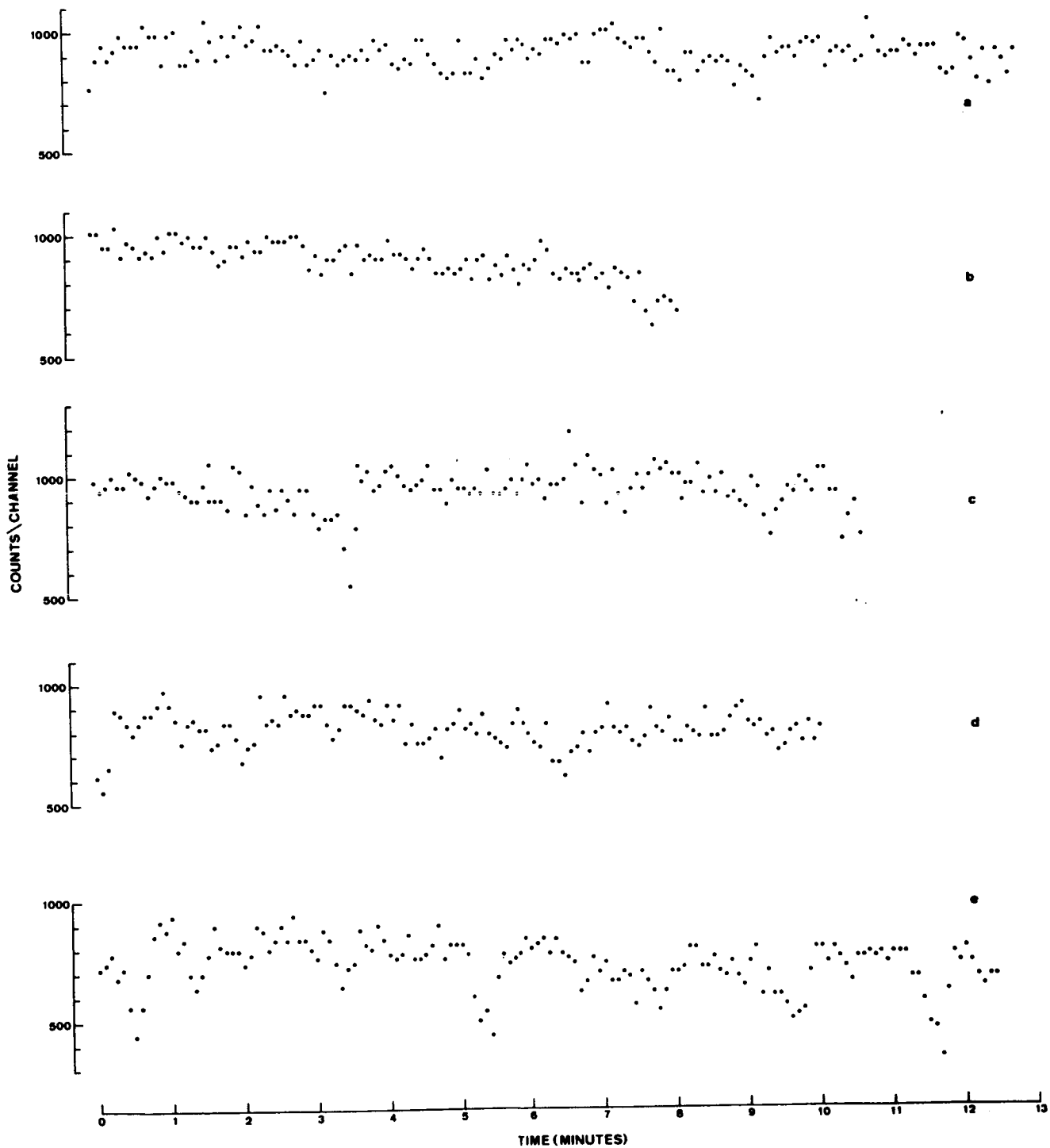


Figure 1. Light curve of HZ Her of May 29, 1974. Each point represents 5 seconds of integration time. Ordinates give the net count rate per channel. Flickering is progressively increasing with advancing time from top to bottom.

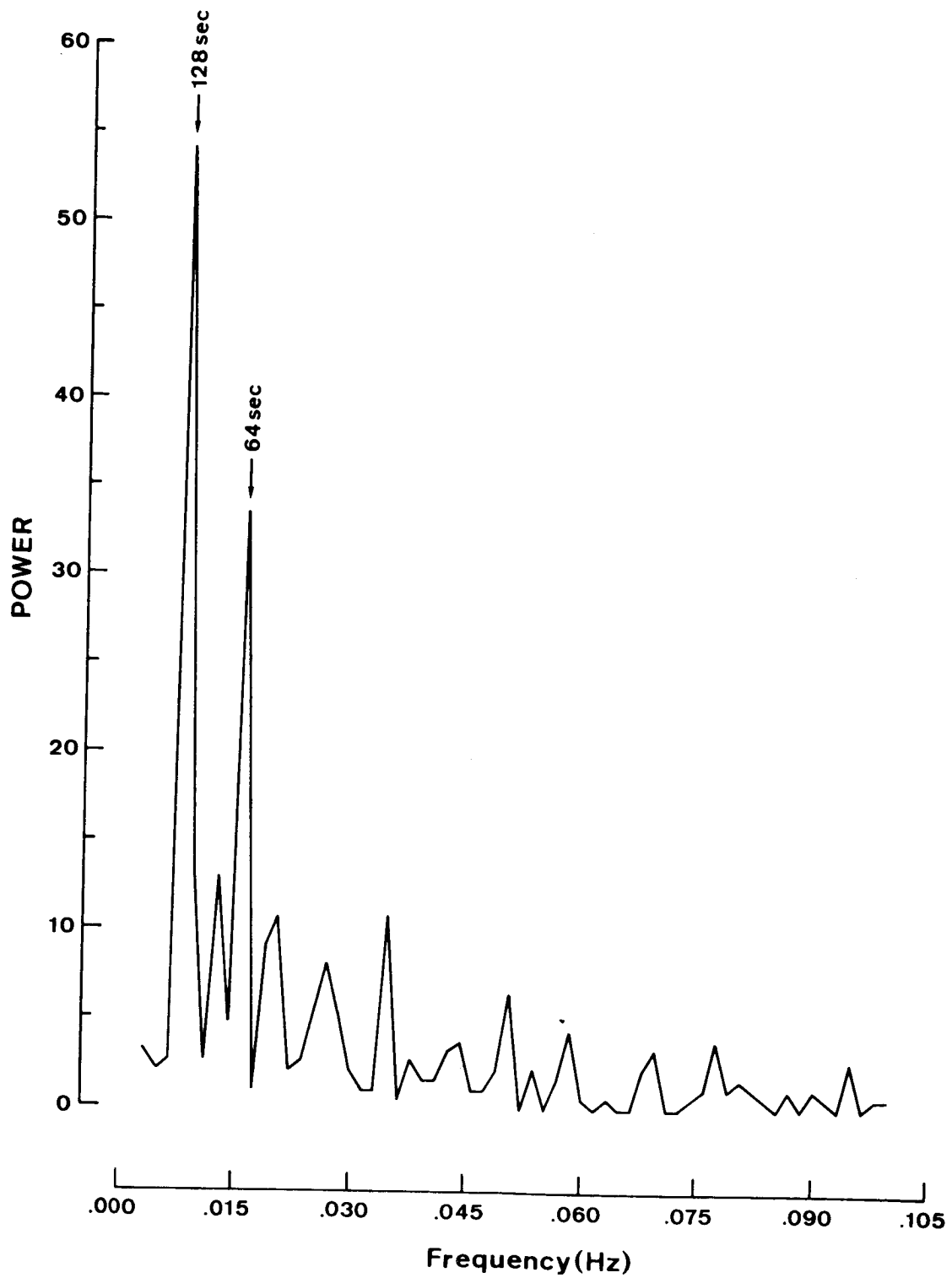


Figure 2. Power spectrum of run e of Figure 1. The power is plotted in units of the average noise power.

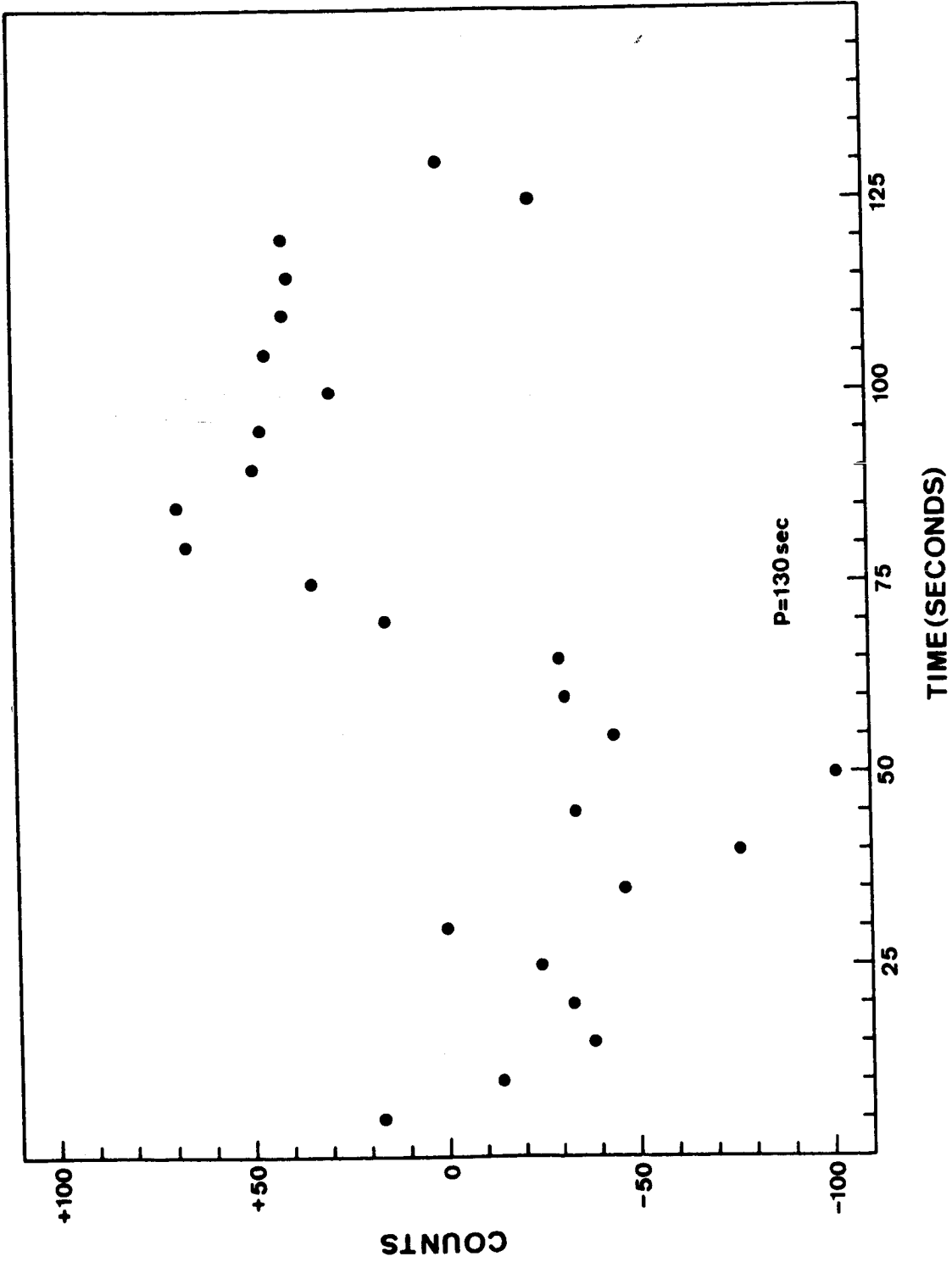


Figure 3. Light curve of HZ Her recovered by folding the data shown in run e of Figure 1 modulo 130 seconds. The amplitude is about 6% of the mean signal.

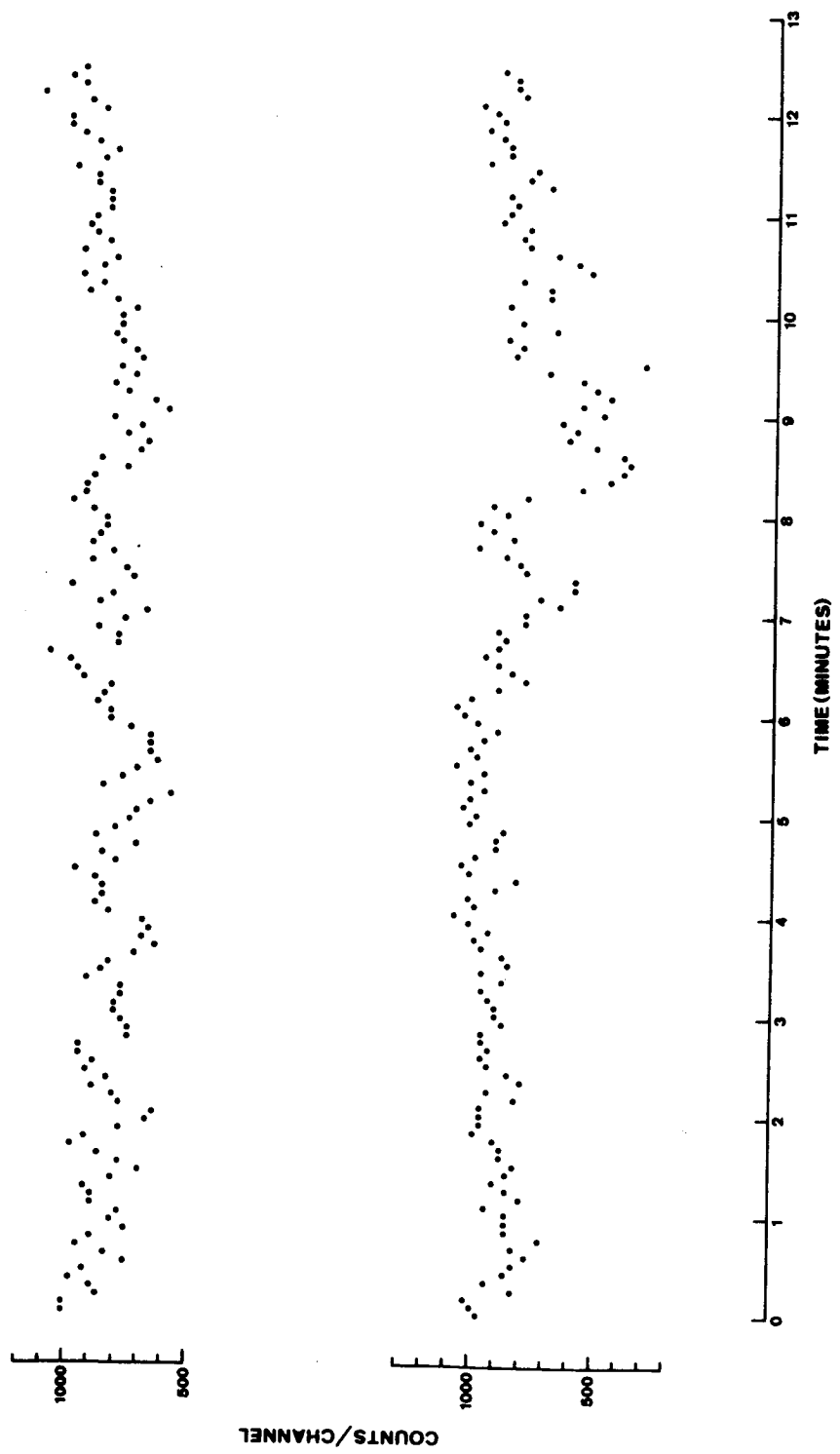


Figure 4. Light curve of HZ Her of June 3, 1974. See the text for details.

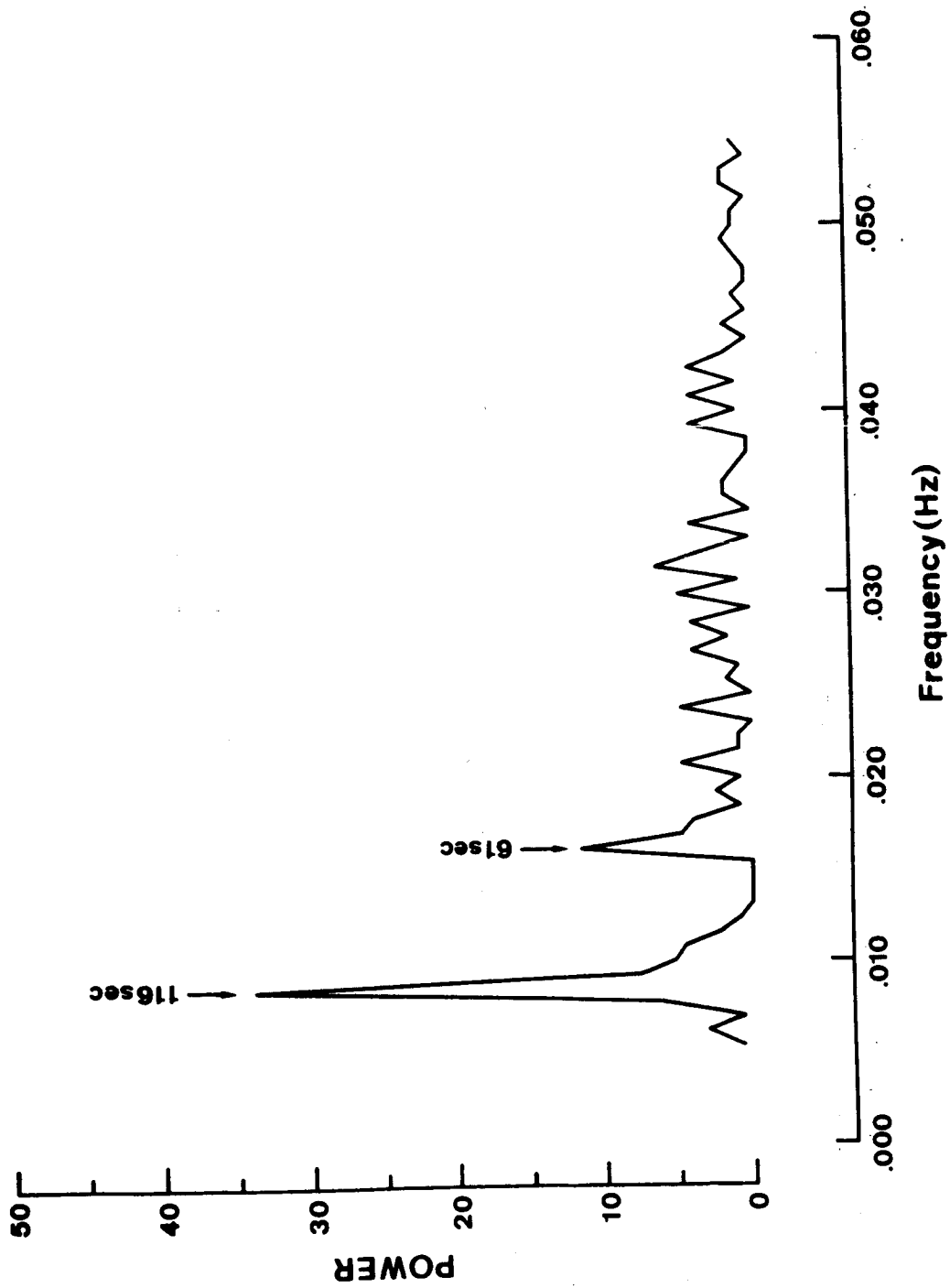


Figure 5. Power spectrum of the first part (top) of the light curve shown in Figure 4.

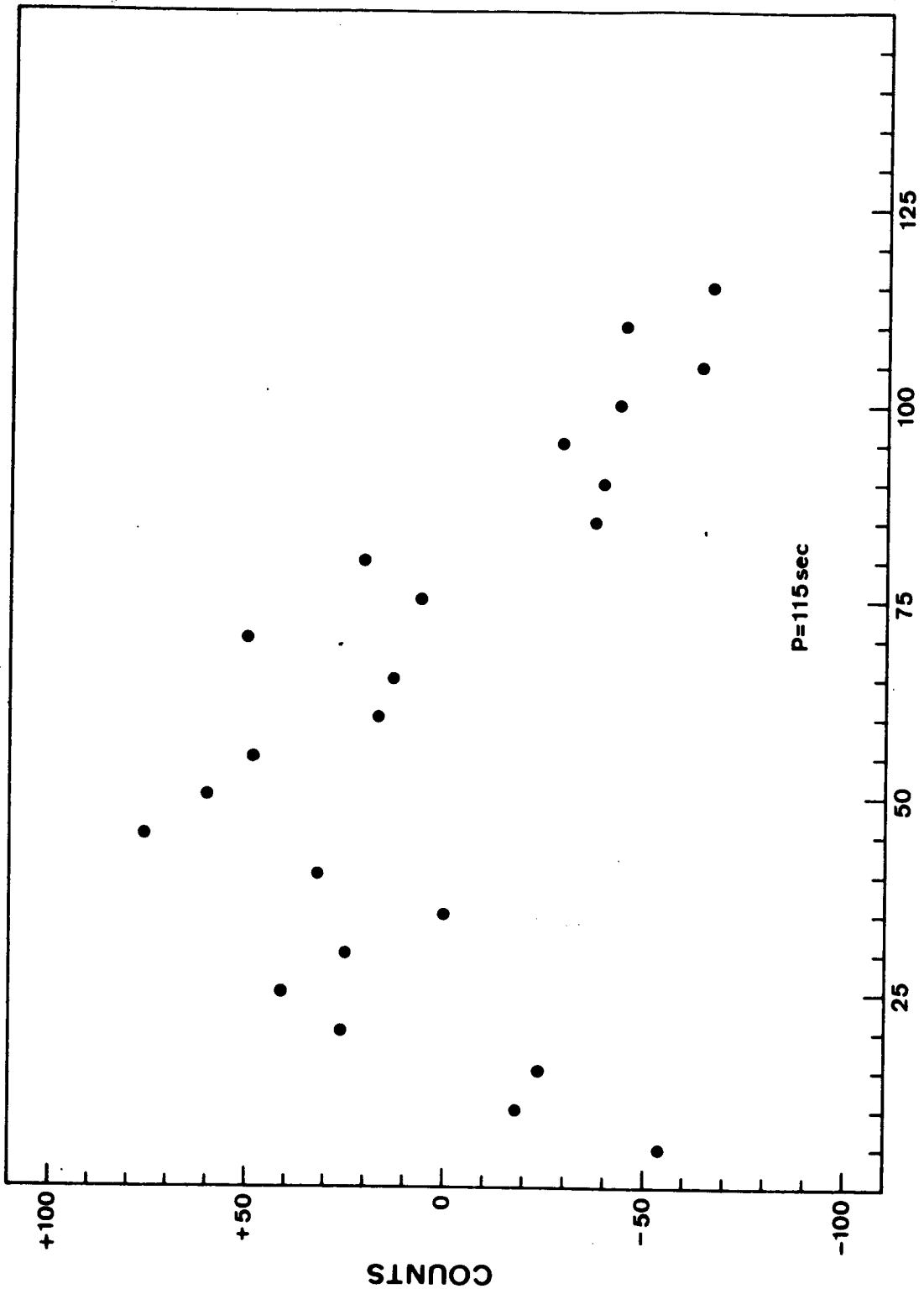


Figure 6. Light curve of HZ Her recovered by folding the data shown in Figure 4 (top) modulo 115 seconds. The amplitude is about 6% of the signal.

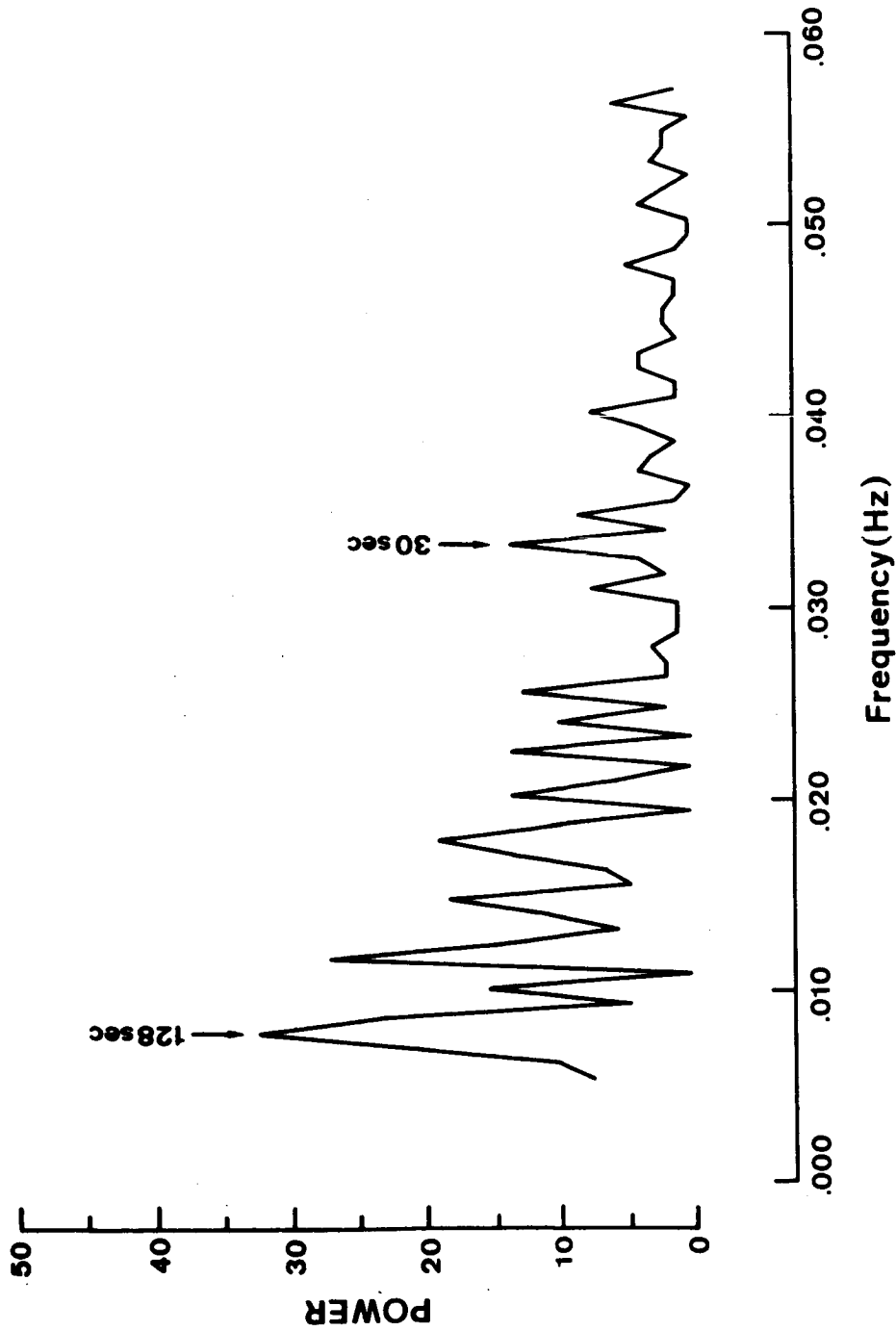
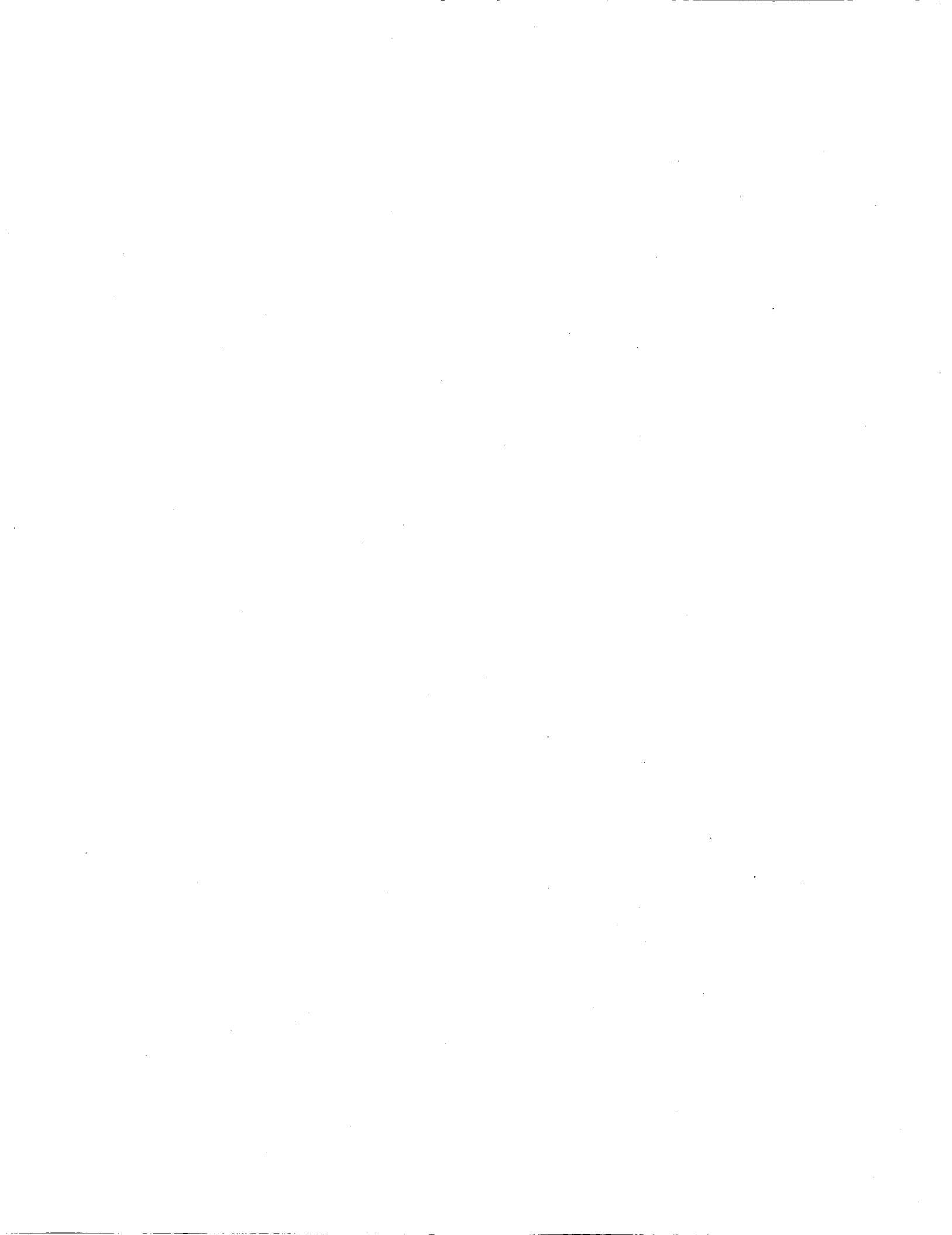


Figure 7. Power spectrum of the run obtained on July 20, 1974 which is similar to that of the observations of July 19, 1974. The amplitude associated to the 128 and 30 seconds Fourier components is about 3.2 and 2 percent respectively.



HER X-1 SPECTRAL EVIDENCE FOR A STRONG MAGNETIC FIELD

Elihu A. Boldt, Stephen S. Holt, Richard E. Rothschild
and Peter J. Serlemitsos
NASA-Goddard Space Flight Center
Greenbelt, Maryland 20771

ABSTRACT

The steep high energy cutoff observed in the spectrum for Her X-1 is analyzed in terms of the severely modified Thomson scattering that dominates the radiative transfer in a highly magnetized plasma near the surface of a neutron star. The data are shown to indicate a field of about 10^{13} G near the magnetic poles and the stopping of accreting matter by nuclear collisions in the neighboring plasma.

INTRODUCTION

From rocket-borne experiments over the last few years and a current experiment aboard OSO-8, we have obtained detailed spectra over a broad band (1.5-40 keV) for several X-ray binary sources. These vary from the featureless power-law spectrum seen repeatedly for Cyg X-1 (Rothschild et al., 1975) to the variable spectrum of Cyg X-3, sometimes a black-body but often more complicated with features such as line emission (Serlemitsos et al., 1975). However, the particular spectrum that stands out as one that is most highly ordered is that measured for Her X-1, observed during a rocket-borne exposure to the source while near inferior conjunction (Holt et al., 1974). This extremely simple spectrum, shown in the figures, has puzzled us for some time. With an energy spectral index close to zero and a remarkably sharp high energy cut-off at about 24 keV, we soon suspected that it must be a rather direct indication of some basic characteristic of a neutron star and yet perhaps unique to Her X-1. For example, is this the spectral signature to be expected for accretion onto a highly magnetized neutron star fed by matter that is freely falling from the companion star, unperturbed by any significant stellar wind? Basco and Sunyaev (1975) and Tsuruta (1974) have recently considered this problem of free-fall accretion onto a magnetized neutron star. They have described how the beaming of X-radiation necessary to explain the Her X-1 pulsar could arise from the anisotropy in the scattering process for photons in a highly magnetized plasma. In this communication, we show that the energy dependence of such scattering could also induce a spectral distortion adequate to explain the sharp high energy cut-off in the Her X-1 pulsar spectrum.

MODEL

In the model of Basco and Sunyaev the magnetic field funnels the accreting matter towards the magnetic poles where free-fall to the surface is stopped mainly via nuclear collisions (i.e. Coulomb collisions in a highly magnetized plasma are considered to be negligible). The radiative transfer of the X-rays produced within this optically thick atmosphere is dominated by Thomson

scattering. As recently demonstrated (Canuto et al., 1971; Lodenquai et al., 1974), the Thomson scattering cross-section in a magnetized plasma (σ_{\pm}) is expected to deviate drastically from the field-free cross-section (σ_0). If θ is the angle between the magnetic field (H) and the wave vector of the incident electromagnetic wave, we have, as $\theta \rightarrow 0$,

$$\left(\frac{\sigma_{\pm}}{\sigma_0}\right)_{\pm} \approx \left[\frac{E}{(E_{\pm} + E)} \right]^2 + \frac{1}{2} \sin^2 \theta \quad (1)$$

where (+) and (-) refer to the ordinary and extraordinary modes of propagation respectively, E is the photon energy and E_H is the cyclotron energy defined as

$$E_H = (h/2\pi) (e/mc) H. \quad (2)$$

The important feature of Eq. (1) for this discussion is that, for $E \ll E_H$, Thomson scattering along the field is much less than expected from the field-free cross-section. Therefore, we pursue the suggestion that an unscattered pencil beam may indeed emerge from well within the optically thick atmosphere near the poles.

Following Basko and Sunyaev, we consider the situation where the rate of energy release by accretion varies in the atmosphere as $\exp(-\tau/\tau_0)$, where τ is the optical depth measured with respect to the field-free Thomson scattering cross-section and τ_0 is that particular value of τ corresponding to a nuclear mean free path. With a cosmic abundance of elements $\tau_0 \approx 10$, whereas for iron $\tau_0 \approx 20$.

Since the source energy spectrum is expected to be essentially constant up to about 30 keV for photons Comptonized in the plasma near the magnetic poles of Her X-1 (Basko and Sunyaev, 1975), the spectral structure of the emerging unscattered beam will be determined mainly by the energy dependence of the modified Thomson scattering that removes photons from this beam. A good approximation to the spectrum of the unscattered radiation should thereby be obtained as follows:

$$dS/dE \propto (\tau_0)^{-1} \int_0^{\infty} \exp[-(\tau/\tau_0) - \tau(\sigma_{\pm}/\sigma_0)] d\tau = [1 + \tau_0(\sigma_{\pm}/\sigma_0)]^{-1} \quad (3)$$

where S is energy flux and (σ_{\pm}/σ_0) is obtained from Eq. (1), neglecting $\sin^2 \theta$.

RESULTS AND DISCUSSION

In making comparisons of Eq. (3) with our spectral data, we have found that $\tau_0 = 10$ and $E_H = 100$ keV (i.e. $H \approx 10^{13}$ G) give results that are adequate for obtaining the behavior characteristic of this effect. The two curves shown in Figure 1, superposed upon the spectral data, correspond to

$$\left(\frac{dN}{dE}\right)_{\pm} = (0.15/E) \{1 + 10[E/(100 \pm E)]^2\}^{-1} \text{ (cm}^2 \text{ sec keV)}^{-1} \quad (4)$$

where (+) and (-) again refer to the ordinary and extraordinary modes, respectively. As analyzed by Basko and Sunyaev, the ratio of intensity in the extraordinary mode to that in the ordinary mode is expected to increase with photon energy, being comparable at about 10 keV for the case considered here. The

data exhibited in Figure (1) show that this behavior may be applicable to the Her X-1 spectrum. The apparent importance of the extraordinary mode at energies higher than about 10 keV indicated by these data might also account for the change in pulse profile (Holt et al., 1974) that sets in for this same energy band. The polarization (electric vector) for this extraordinary mode is normal to the direction of the magnetic field, rotating in the same sense as the revolution of an electron in this field (Ginzburg, 1970).

To check the sensitivity of the pronounced spectral effect exhibited here with respect to the distribution in τ assumed for the source function, we have also considered an extreme situation where the source resides exclusively at the optical depth τ_0 . The curves corresponding to this are shown in Figure (2), superposed upon the same data as shown in Figure (1). The expression used for this computation is

$$(dN/dE)_{\pm} = (0.15/E) \exp\{-\tau_0 [E/E_H \pm E]^2\} \quad (5)$$

where the curves shown in Figure (2) were evaluated for $\tau_0 = 10$ and $E_H = 120$ keV. The results obtained for this case are qualitatively the same as those obtained for the distributed source model used for Eq. (4). We conclude that the spectrum of the emerging unscattered beam depends mainly upon τ_0 and E_H , and that the detailed structure of the source with respect to τ plays a minor role. Hence, the spectral shape we observed for Her X-1 near inferior conjunction is likely to be a feature inherent to the underlying neutron star (i.e. determined by the surface magnetic field strength and nuclear collision length near the magnetic poles), rather than being a direct indicator of the accretion process itself. Specifically, we infer that the magnetic field at the poles is about 10^{13} G and that the nuclear collisions in the nearby plasma are probably not dominated by iron. Ruderman (1975) has pointed out that the field near the neutron star's surface at the poles could be considerably larger than the pure dipole value and that the accretion process prevents the formation of an iron crust.

Since Thomson scattering in a magnetized plasma appears to severely suppress the spectrum of the Her X-1 pulsar emission at $E \geq 24$ keV, we expect that any X-radiation at higher energies might not be pulsed. A balloon-borne experiment for observing hard X-rays from Her X-1 (Iyengar et al., 1974) gives an upper limit of 10% for the pulsating component in the bandwidth 20-45 keV whereas our observation at the lower energies considered here indicates that most of the emission is from the pulsar.

REFERENCES

- Basko, M. M. and Sunyaev, R. A. 1975, *Astron. and Astrophys.* 42, 311.
- Canuto, V., Lodenguai, J. and Ruderman, M. 1971, *Phys. Rev. D.* 3, 2303.
- Ginzburg, V. L. 1970, *The Propagation of Electromagnetic Waves In Plasmas*, Pergamon Press, Oxford, p. 122.
- Holt, S. S., Boldt, E. A., Rothschild, R. E. and Serlemitsos, P. J. 1974, *Ap. J.* 190, L109.

Iyengar V. S., Manchanda, R. K., Durgaprasad, N., Gokhale, G. S., Kunte, P. K. and Sreekantan, B. V. 1974, Nature 251, 292.

Lodenquai, S., Canuto, V., Ruderman, M. and Tsuruta, S. 1974, Ap. J. 190, 141.

Rothschild, R., Boldt, E., Holt, S. and Serlemitsos, P. 1975, this symposium.

Ruderman, M. 1975, private communication.

Serlemitsos, P., Boldt, E., Holt, S., Rothschild, R. and Saba, J. 1975, Ap. J. 201, L9.

Tsuruta, S. 1974, Culham Conference on Cosmic Plasma Physics.

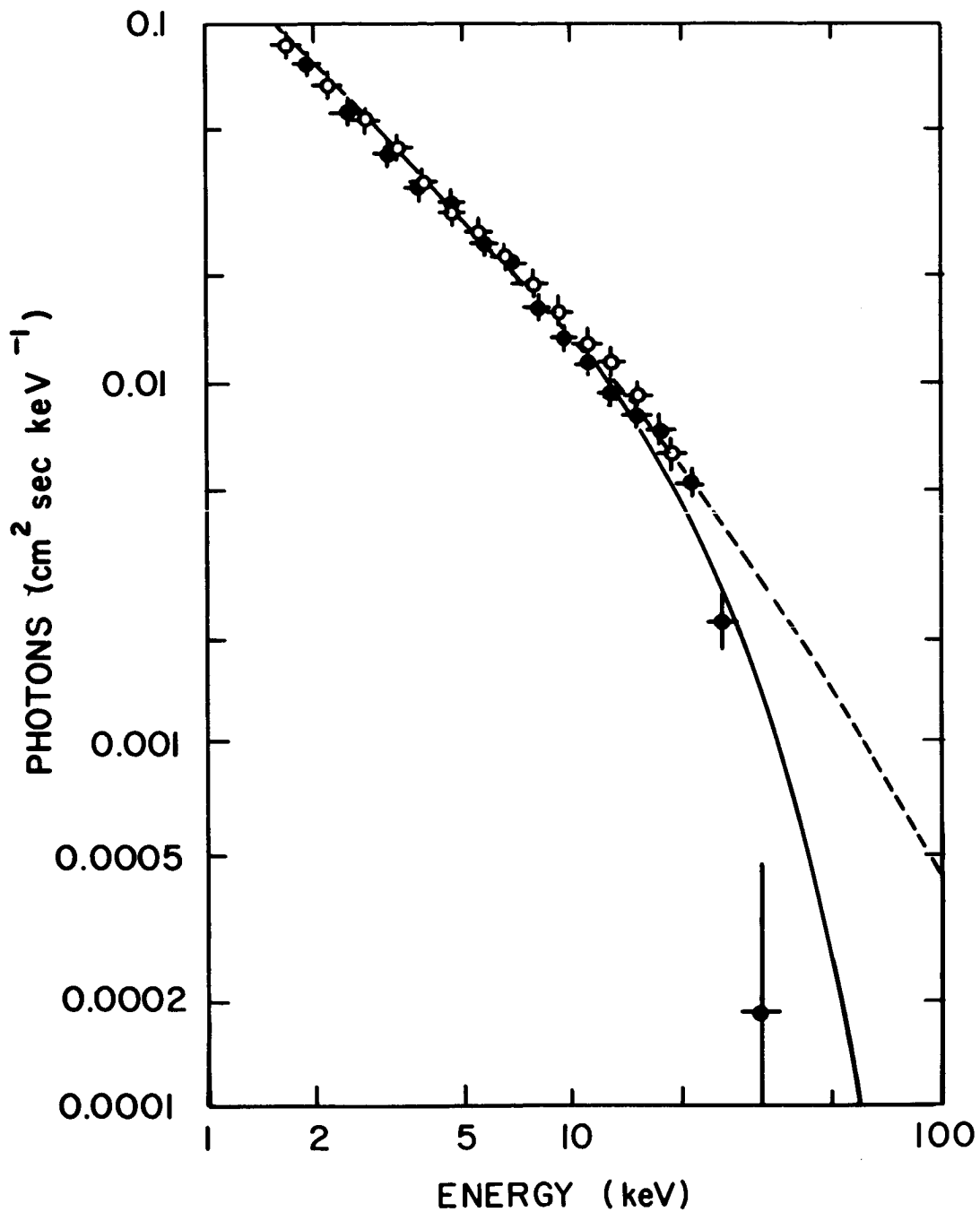


Fig. 1 The Her X-1 spectrum obtained 4 October 1973 (at binary phase 0.6 referenced to eclipse center). The open symbols refer to data from an argon-filled counter, and the closed symbols refer to data from a xenon-filled counter (same experiment; see text). The dashed and solid curves were obtained from Eq. (4) for the ordinary and extraordinary modes, respectively.

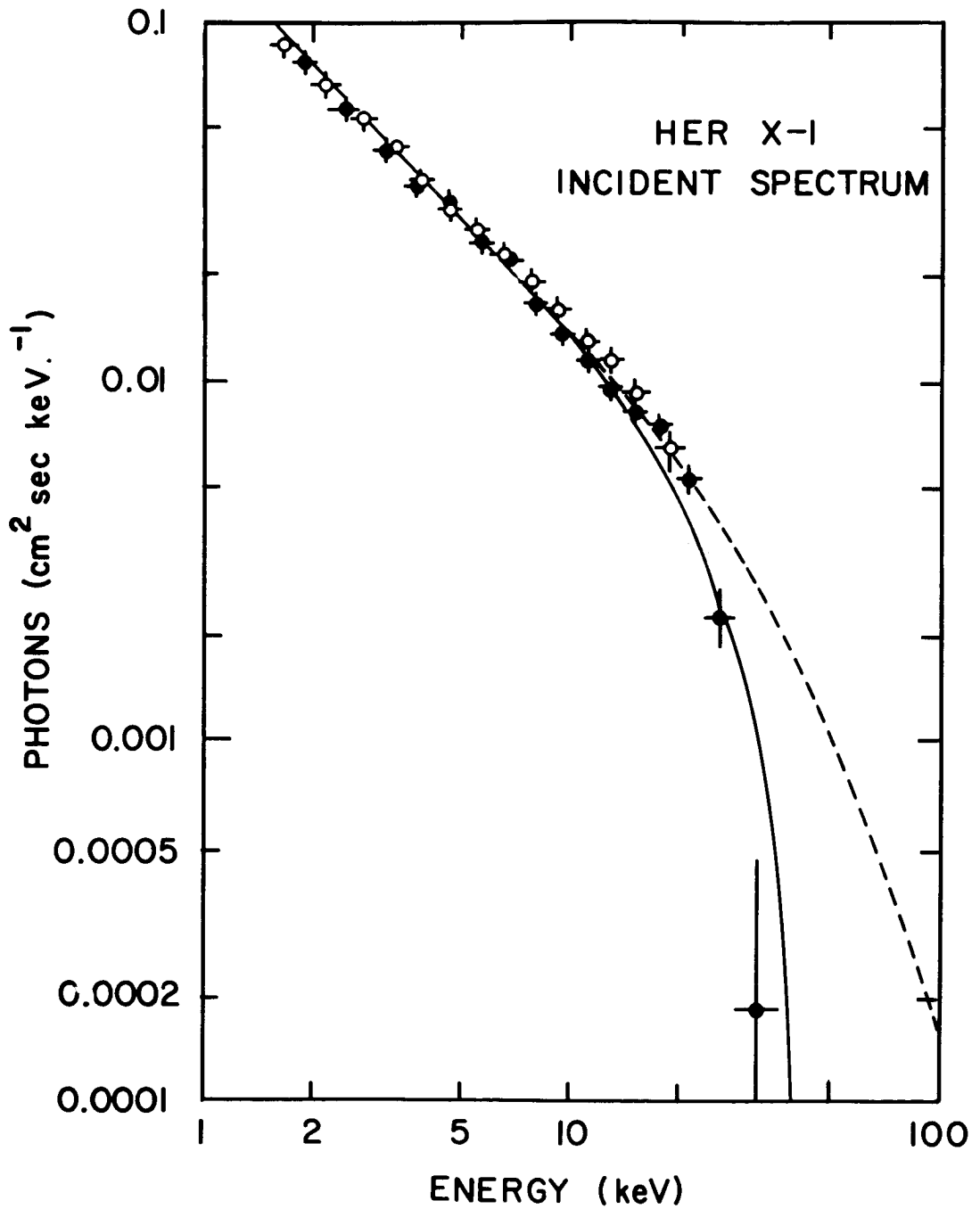


Fig. 2 The same spectral data as in Fig. 1. The dashed and solid curves were obtained from Eq. (5) for the ordinary and extraordinary modes, respectively, with $\tau_0 = 10$ and $E_H = 120$ keV.

INTENSE SOFT X-RAY FLUX FROM HER-1

R. C. Catura and L. W. Acton
Lockheed Palo Alto Research Laboratory
3251 Hanover Street
Palo Alto, California 94304

ABSTRACT

An intense flux of soft X-rays extending up to at least 1 keV has been observed from Her X-1. If the soft X-ray intensity is corrected for interstellar absorption the luminosity between 0.16 and 1 keV is comparable to that from 2-10 keV. The soft X-rays are modulated with the 1.24 sec period observed at higher energies but are approximately 180° out of phase with the high energy flux. These results confirm the conclusions of Shulman et al. (1975) and extend the detection of this flux to higher energy, a different binary phase and to a time 19 periods (of the 35 day cycle) later. These observations suggest that this soft emission is a stable feature in the spectrum of this source during its X-ray "on" state and that this emission is local to Her X-1.

INTRODUCTION

The X-ray spectrum of Her X-1 was observed in the energy range from 0.16 to 6 keV during a rocket flight at 0919 UT on 3 February 1975. Some results obtained from these data have been published (Catura and Acton, 1975) and will only be summarized here. Newly reduced spectral data in the range 0.5-2 keV and results on the 1.24 sec light curve of Her X-1 will be discussed.

The rocket observation was at a binary phase of 0.18, approximately 2 days after X-ray "turn-on", relative to the 35-day cycle of Her X-1. The primary instrument was an X-ray reflector (Catura and Roethig, 1975), focussing in one dimension, with three proportional counters behind apertures at its focus. These apertures defined fields of view of $0.1^\circ \times 9^\circ$ for one detector and $0.23^\circ \times 9^\circ$ for the others. The reflector system covered the energy range from 0.16 to 2.2 keV and was complemented by a collimated proportional counter covering the range 0.75 to 6 keV. This detector had an open area of 100 cm² and two dimensional collimation of 2° FWHM. During the observation the rocket performed a 1° scan over Her X-1 at a rate of 0.02° s⁻¹.

RESULTS

Data from the primary detection system are shown in Figure 1 where counting rates in two energy intervals are plotted throughout the scan for each of the three detectors. At the beginning of the scan, Her X-1 was already within the field of view of detector 3. As the scan progressed, X-rays from Her X-1 were focussed successively into detectors 2 and 1 as indicated by their increase in counting rate. The calculated response of these detectors to a point source of X-rays is shown by the profiles in the 0.16 - 0.28 keV plots for these detectors. Nearly 70% of the X-ray detected from Her X-1 by the reflector system fall within the 0.16 - 0.28 keV band.

Her X-1 remained within the field of view of the collimated proportional counter for a period of 57 s. Spectral data from Her X-1 are shown in Figure 2 for both the reflector system and the collimated proportional counter. These data represent observed fluxes with no correction for X-ray absorption by interstellar matter. The solid line in Figure 2 indicates the result of a least-squares fit of a power-law function to the data above 1 keV. The spectral index of this function is $1.23 \pm .14$, somewhat larger than the values near 1.0 obtained by Giacconi et al. (1973), Ulmer et al. (1973), Holt et al. (1974) and Shulman et al. (1975). It is clear that the data points at low energy fall substantially above the extrapolation of the best fitting power law, indicating the presence of a soft component in the spectrum of Her X-1. It is possible that this component also contributes to the flux at 1.5 keV and is responsible for the large spectral index obtained in the present analysis. Shulman et al. (1975) have also detected a large flux of soft X-rays from Her X-1 but do not observe this component to be appreciably enhanced above 0.7 keV. The soft component of X-ray emission extends to somewhat higher energy in our observation.

The energy flux between 2 and 10 keV, as calculated from the power law function shown in Figure 2, is 10^{-9} erg cm^{-2} s^{-1} while the flux between 0.2 and 1 keV in excess of this power law is 2×10^{-10} erg cm^{-2} s^{-1} . The data of Heiles (1975) and Tolbert (1971) indicate a hydrogen column density of $\sim 5 \times 10^{20}$ cm^{-2} in the direction of Her X-1. If the soft X-ray flux is corrected for absorption by this interstellar matter using the cross sections of Brown and Gould (1970), the data point at 0.25 keV will fall above the power law function in Figure 2 by a factor of 30. The corrected energy flux between .2 and 1 keV in excess of the power law is then 7×10^{-10} erg cm^{-2} s^{-1} . This is comparable to the flux from 2-10 keV, a result which confirms the observations of Shulman et al. (1975). Since the present observation and that of Shulman et al. (1975) are separated by nearly two years, these results suggest the intense soft flux may be a stable feature in the X-ray spectrum of Her X-1. It should be noted, however, that this large flux has so far been detected only in the X-ray "on" portion of the 35-day cycle.

Shulman et al. (1975) have summarized the evidence which suggests that this flux does not persist at the same intensity into the "off" period. Observations presented at this symposium by Heise of the Space Research Center in Utrecht, and also by Henry of the Naval Research Laboratory have detected soft X-rays from Her X-1 during its "off" state but the intensity of this emission is more than a decade below that observed during the "on" period.

In a preliminary analysis, the data acquired in the range 0.16-6 keV have been divided into four energy intervals and folded modulo 1.2375s. The resulting light curves are shown in Figure 3 and exhibit pulsations at all energies. The light curve in the highest energy interval is similar to those observed previously by Shulman et al. (1975), Holt et al. (1974) and Doxsey et al. (1973). As the energy decreases, however, a phase shift occurs such that pulses between 0.16 and 0.75 keV are $\sim 180^\circ$ out of phase with respect to pulses in the 1.25 - 6 keV range. This observation was made at a binary phase of 0.18. A similar shift in phase at low energies has been reported by Shulman et al. (1975) at a binary phase of 0.57. If the soft X-ray flux originates in the atmosphere of Hz Her, the binary companion of Her X-1, by reprocessing of hard X-ray pulses, particular orbital parameters are required to produce similar phase shifts in the two observations. More likely, the observations indicate relative pulse-phase of the hard and soft X-rays is independent of binary phase and the soft emission is local to Her X-1.

We have fitted the flux between 0.25 and 1.0 keV in excess of a power law to a function describing blackbody emission. If the power law of Figure 2 is subtracted and the residual flux corrected for interstellar X-ray absorption equivalent to a hydrogen column density of $5 \times 10^{20} \text{ cm}^{-2}$, the resulting blackbody temperature is $1.1 \times 10^6 \text{ K}$. An upper limit to this temperature of $1.4 \times 10^6 \text{ K}$ is obtained by neglecting the interstellar absorption and subtracting a power law with spectral index of 1.0 which has been normalized to the data above 2 keV. This temperature is a conservative upper limit as experimental errors, which might increase the derived temperature, are considerably smaller than the effect of totally neglecting interstellar absorption.

As discussed by Catura and Acton (1975), it is unlikely that the soft X-rays come from the $1.3 M_\odot$ companion of Hz Her via blackbody emission because the surface area of this neutron star is far too small if the source is as distant as 2 kpc (Bahcall, Joss and Avni, 1974). This has also been pointed out by McCray and Lamb (1975) who discuss a model where the soft X-ray emission originates in an optically thick ring of gas at the Alfvén surface. This gas ring is heated by absorption of the hard X-rays and has sufficient surface area to produce the observed emission. Their model can also qualitatively account for the 180° phase shift between the soft and hard X-rays.

We thank personnel of the Sounding Rocket Division of Goddard Space Flight Center, especially Mr. Rick Erdman, for their contributions and the crew at White Sands Missile Range for launch support. We are indebted to R. Carvalho, E. Laveen and D.T. Roethig of Lockheed Palo Alto Research Laboratories for their invaluable support. This research has been supported by NASA under Contract NASw-2660 and by the Lockheed Independent Research Program.

REFERENCES

- Bahcall, J.N., Joss, P.C. and Avni, Y. 1974, Ap.J. 191, 211.
- Brown, R. and Gould, R. 1970, Phys. Rev. D, 1, 2252.
- Catura, R.C. and Roethig, D.T. 1975, Space Sci. Instr. 1, 141.
- Catura, R.C. and Acton, L.W. 1975, Ap.J. (Letters), Nov. 15 issue, in press.
- Doxsey, R., Bradt, H.V., Levine, A., Murphy, G.T., Rappaport, S. and Spada, G. 1973, Ap.J. (Letters) 182, L25.
- Giacconi, R., Gursky, H., Kellogg, E., Levinson, R., Schreier, E. and Tananbaum, H. 1973, Ap.J. 184, 227.
- Heiles, C. 1975, Astron. and Ap. Suppl. 20, 37.
- Holt, S.S., Boldt, E.A., Rothschild, R.E., Saba, J.L. and Serlemitsos, P.J. 1974, Ap.J. (Letters) 190, L109.
- McCray, R. and Lamb, F.K. 1975, preprint.
- Shulman, S., Friedman, H., Fritz, G., Henry, R.C. and Yentis, D.J. 1975, Ap.J. (Letters) 199, L101.
- Tolbert, C.A. 1971, Astron. and Ap. Suppl. 3, 349.
- Ulmer, M.P., Baity, W.A., Wheaton, W.A. and Peterson, L.E. 1973, Ap.J. (Letters) 181, L33.

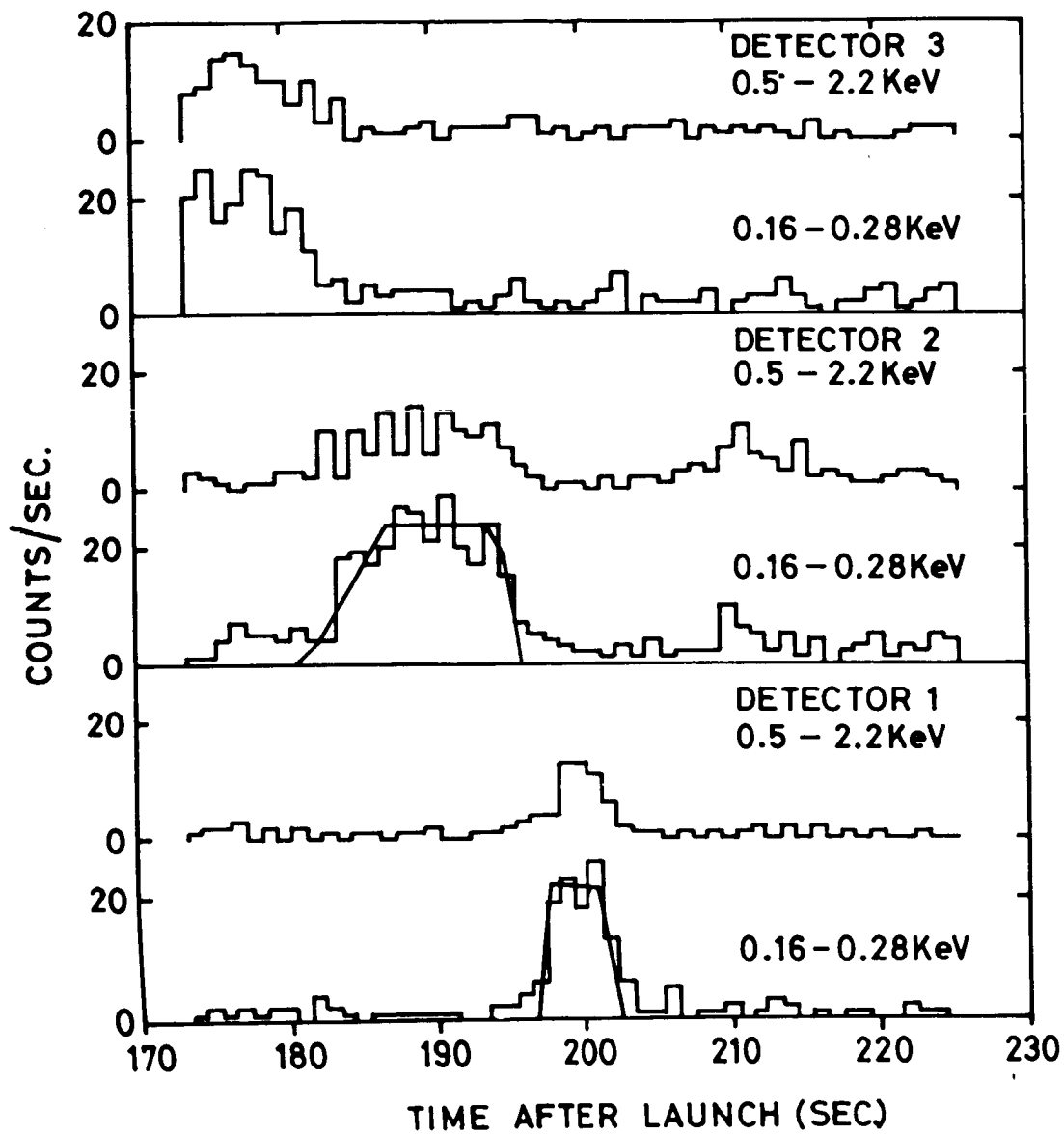


Figure 1 Counting rates observed in detectors at the focus of the X-ray reflector during a scan over Her X-1. The point-source response of Detectors 1 and 2 normalized to the peak counting rates are indicated by the solid lines.

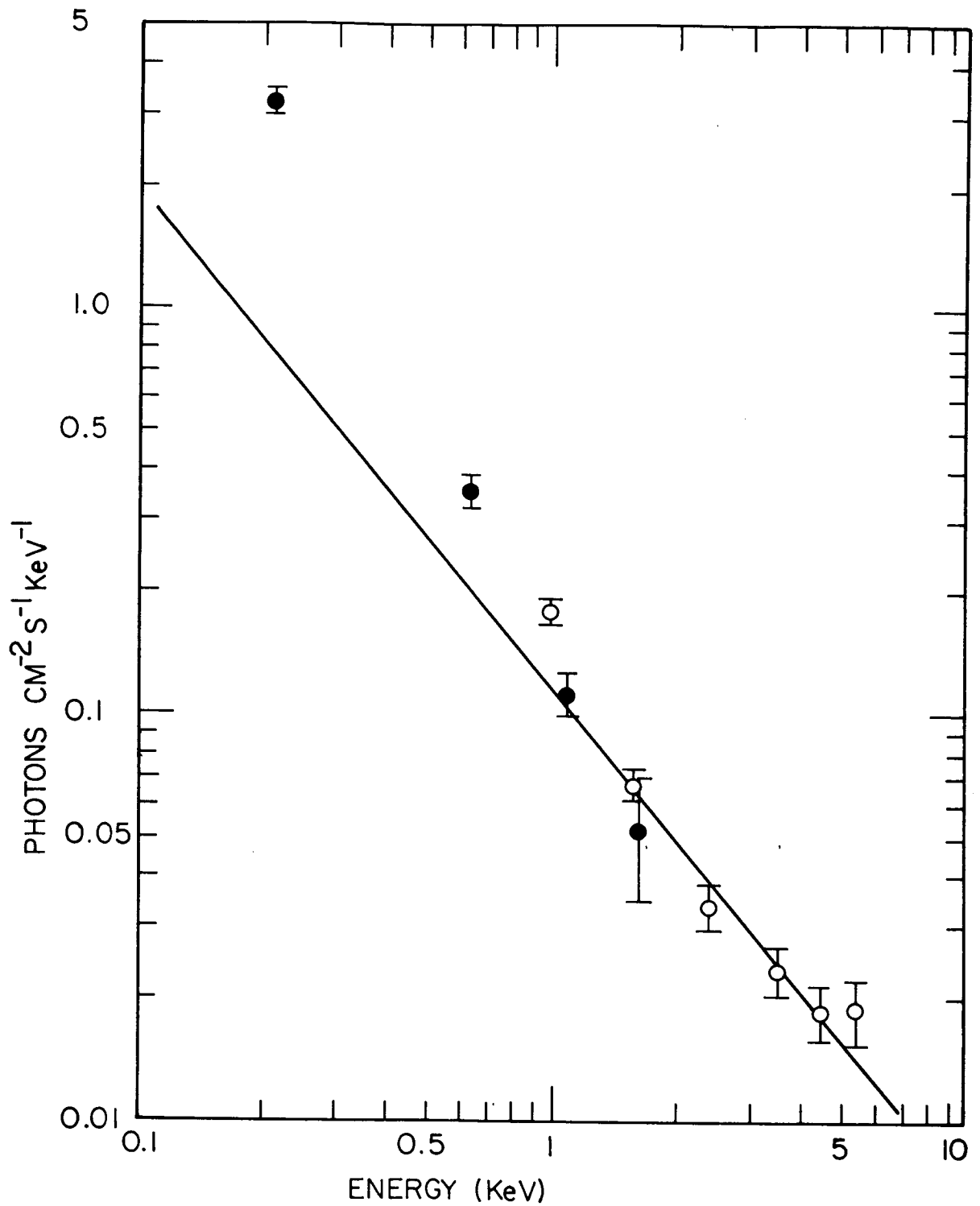


Figure 2 X-ray spectrum of Her X-1. The straight line is a power law function ($\propto E^{-1.23}$) resulting from a least-squares fit to the data above 1 keV. Disks refer to data from the reflector system while circles represent data from the collimated proportional counter.

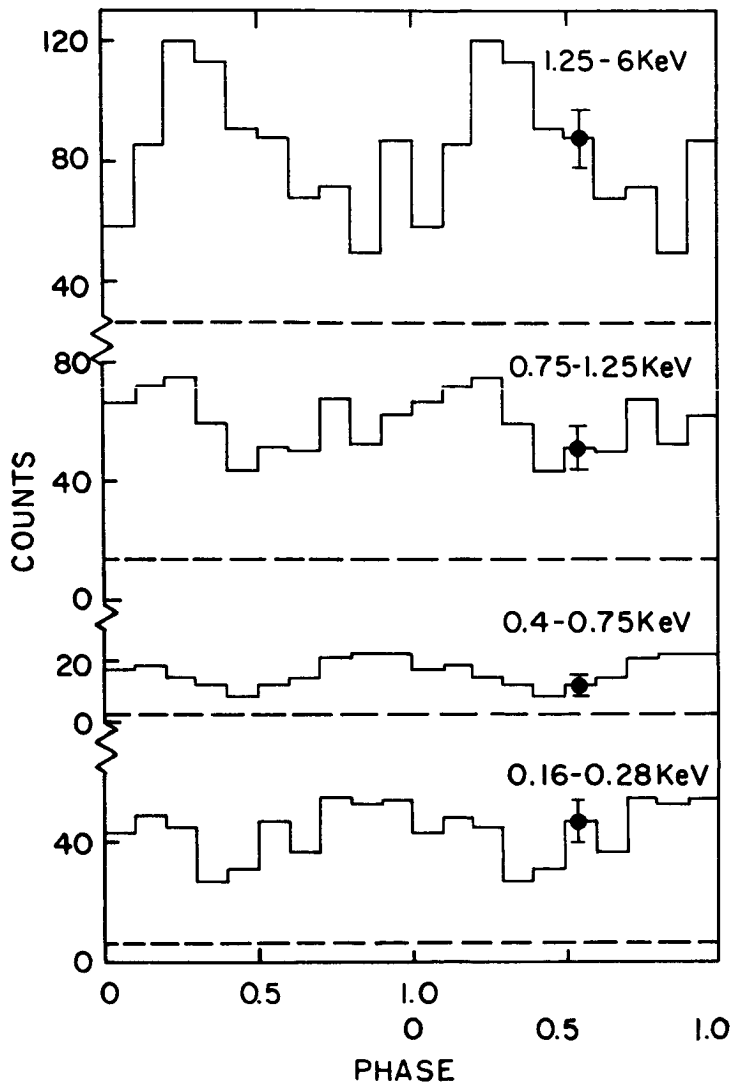


Figure 3 Profiles of the 1.24 s pulse from Her X-1 in four energy intervals. The light curve has been repeated to more clearly show the phase shift with decreasing energy. Detector backgrounds are indicated by the dashed lines.

SOFT X-RAYS FROM HER X-1 DURING THE "OFF" PHASE*

G. Fritz, S. Shulman, and H. Friedman
E. O. Hulburt Center for Space Research,
Naval Research Laboratory, Washington, D. C. 20375

and

R. C. Henry, A. F. Davidsen, and W. A. Snyder
Department of Physics
The Johns Hopkins University, Baltimore, Md. 21218

ABSTRACT

Weak 0.28-keV radiation has been observed from Her X-1 5 days before turn-on in the 35 day cycle. The observations were made from an Aerobee rocket at 0500 UT 1974 September 7. The 0.28-keV intensity is about 1/25 that observed during the "on" phase. Some evidence for x-rays above 1 keV is also present, and it is possible that the spectrum is different only in intensity from the spectrum in the "on" phase. The radiation may be x-rays from the vicinity of the neutron star, scattered by ionized material in the inner accretion disk, or may be thermal radiation from the inner accretion disk, or both. No evidence for pulsation is present in the 0.28-keV radiation, but the upper limit on pulsation is not very restrictive.

INTRODUCTION

Shulman et al. (1975) have presented evidence for an intense flux of x-rays at energies below 1 keV from Hercules X-1. At the time of observation, the source was approximately 3 days past the start of the "on" portion of the 35-day cycle, and the binary system was at phase 0.57 (0.00 is the center of the x-ray eclipse). The low energy flux was pulsed with the 1^s24 period, although the pulse profile differed markedly from that at higher energies. Catura (this symposium) has confirmed all of the essential features of the observation.

A motivation for the search for low-energy (<1 keV) x-rays was the idea (Avni et al. 1973; Pringle 1973) that a

*Read by R. C. Henry

steady low-energy flux could heat the primary star and produce the 1.7 optical modulation that persists in HZ Her throughout the "off" portion of the 35-day x-ray cycle. However, Shulman et al. (1975) cited a number of observations which indicate that the strong low-energy flux which they observed is not present during the "off" phase.

In particular, they reported a new observation made during the "off" period, preliminary analysis of which yielded an upper limit of 10 percent of the soft flux observed during the "on" phase. The observation was made from an Aerobee rocket, at 0500 UT 1974 September 7. More detailed examination of these rocket data has revealed that Her X-1 actually was detected, at about 4 percent of the intensity previously observed during the "on" phase. This paper gives the details of this detection.

THE OBSERVATION

The Aerobee rocket carried two proportional counters, each of 1200 cm² effective area. Each had a 2- μ Kimfol (polycarbonate) window, and was sensitive in the energy ranges 0.18 - 0.28 keV and 0.6 - 10 keV. Each used P10 gas (90% argon, 10% methane). One counter viewed the sky through a mechanical collimator which gave a circular field of view with 5° full-width at half-maximum (FWHM) transmissions, while the other had a collimator that was identical except that the FWHM was only 3°. The two collimators were pointed in the same direction to within 0.2%.

The payload of the rocket was pointed during the flight by an inertial attitude control system, used in conjunction with an optical star tracker. The star ζ Her was observed just before the observation of Her X-1, and aspect photographs indicate that both detectors were pointed approximately 15' away from the x-ray source during a 40 s hold, an error which is negligible compared to the aperture of the mechanical collimators.

The sequence of maneuvers is shown in Figure 1. The detectors were initially pointed perpendicular to the zenith. They were then rapidly scanned to γ Cyg, which was used to remove the errors in the attitude control system, and then to Cygnus X-3 which was observed for 44 seconds (Shulman, et al. 1975). Then a complicated series of maneuvers scanned the detectors through 3U2129+47, 3U2052+47, SS Cygni, and Cygnus X-6 (Davidsen, et al. 1975). Then Cygnus X-2 was observed for 18 seconds (Snyder, et al., 1975), following which the Cygnus Loop was observed, and the detectors were scanned through Cygnus X-1 to ζ Herculis. Then Her X-1 was in the field of view for 61 seconds. After this observation was completed, the detectors were scanned toward the zenith, and then back through Her X-1 toward the horizon, by which time the rocket was quite low in altitude.

The count rate in the 3° FWHM detector over the energy range 0.1 to 10 keV is shown in Figure 2 for virtually the whole flight. Calibrations, consisting of placing an Fe⁵⁵ source briefly in the field of view of each detector, were made twice during the flight. For the 3° FWHM detector, the gain at 5.9 keV changed by 13% between the two calibrations. This change was assumed to occur at a linear rate throughout the flight. One of these calibrations took place about 10 s before the start of the Her X-1 observation. At low energies, near 0.28 keV, the detector system is not linear, and a gain correction has been made to compensate for this effect also.

The time of observation was 5 days before predicted x-ray turn-on in the 35-day cycle, and the binary phase of Hercules X-1 was 0.42. Thus, the neutron star is not eclipsed by HZ Her, but, on the basis of previous observations, no x-rays should be seen.

Many celestial x-ray sources contribute to the data presented in Figure 2, but there is no clear evidence for x-rays from Hercules X-1. When the data for the lowest-energy channels are segregated, however, clear evidence for detection of Her X-1 appears. Figure 3 is identical to Figure 2 except that just the channels which contain only counts due to 0.18 to 0.28 keV photons are summed. Figure 3 is dominated by the Cygnus Loop (off scale). Data taken before the Cygnus Loop were at low galactic latitude, while after the Cygnus Loop, the data were taken at high galactic latitude where the 0.28 keV count rate is expected to be higher (Davidsen, *et al.*, 1972), as is seen. However, the x-ray intensity at the position of Her X-1 itself is about 30% above that at neighboring regions. The precision of the coincidence of the change in x-ray intensity with the detector's arrival at, and departure from, the position of Her X-1, together with the narrowness (3° FWHM) of the field of view of the detector, leads to the conclusion that 0.28 keV x-rays have been detected from Hercules X-1 during the nominal "off" state.

Figure 3 also shows the internal background level that was measured (for 15 seconds) during the up-leg of the rocket flight. The data in the figure suggest that until about 100 seconds (when the rocket was at an altitude of 112 km), terrestrial atmospheric absorption affected the 0.28 keV x-ray intensity. On the down-leg, the rocket had reached an altitude of 120 km at 380 seconds, when the zenith distance of the direction of observation was 52°. This predicts that the 0.28 keV intensity should be 0.81 of its value outside the earth's atmosphere, which is consistent with Figure 3. Atmospheric attenuation should then increase rapidly, both because the rocket is losing altitude and because the direction of observation is rapidly approaching horizontal. The scan path from 383

to 394 seconds passed through Hercules X-1, but the object is not seen, presumably because of the low rocket altitude and the very short observation time.

SPECTRUM OF THE X-RAYS

The spectrum of the x-rays from Hercules X-1 was formed by subtracting the normalized average spectrum observed between 302 and 309 seconds, and between 372 and 382 seconds, from the spectrum obtained during the 309 to 370 second period, when Her X-1 was observed. The result for the 3° FWHM detector is shown in Figure 4 (the 5° FWHM detector yields similar results). The error bars are $\pm 1\sigma$, and include only \sqrt{N} statistical errors in the data and background. Hercules X-1 was clearly detected at 0.28 keV, and probably was detected at somewhat higher energies. A pure thermal bremsstrahlung spectrum, attenuated by a 5.0×10^{20} atoms cm^{-2} column of hydrogen and a "cosmic-abundance" mixture of heavier elements (Shulman et al. 1975), was folded through the efficiency and resolution of the proportional counter, following the method of Meekins et al. (1969) and using a fitting program developed by D. Yentis. This program allows a number of options in the automatic search for a best-fit spectrum, and in the present case, the hydrogen column density was fixed at the value of Shulman et al. (1975) and then the program adjusted the thermal bremsstrahlung temperature and the amplitude for minimum χ^2 . The resulting temperature was 2.0×10^6 °K. The fit, which has a reduced χ^2 of 2.5, is not very satisfactory. In particular, there is quite clear evidence for an excess of x-rays at the highest energy of detection, 1 to 3 keV.

The spectrum which Shulman et al. (1975) found to give a good fit to the x-ray data during the "on" phase involved thermal bremsstrahlung plus a harder component. These data, and the fitted spectrum, are shown in Figure 5. At energies above 2 keV, the power law dominates, and the best-fit value of the photon number spectral index, -1.0 ± 0.2 , agrees quite well with that obtained by Holt et al. (1974). The data below 1 keV are fitted reasonably well by adding a thermal bremsstrahlung component (no lines) with a temperature of 1.4×10^6 °K. An interstellar hydrogen column density of 5.0×10^{20} cm^{-2} was assumed.

The existence of a high-energy excess in the present data suggested the possibility that the present "off"-phase spectrum might be identical to the "on"-phase spectrum, but simply reduced in intensity. This hypothesis is tested in Figure 6, where the fitted spectrum of Figure 5 has been reduced in intensity by a factor of 25.0 and is compared to the data of Figure 4, that is, the present

data. Agreement is clearly better than the agreement that was obtained in Figure 4 between the present data and a pure thermal bremsstrahlung (χ^2 per degree of freedom of 1.9). Clearly, however, the data are not of sufficient quality to confirm the hypothesis with any great degree of certainty. We adopt, then, simply as a working hypothesis, the idea that the spectrum of Her X-1 during the "off" phase is the same as during the "on" phase, but reduced about a factor of 25 in intensity.

In this connection we note with great interest Dr. J. Heise's report at this conference that 0.28 keV x-rays have been detected at times during the "off" phase of Her X-1 by an experiment aboard the Astronomical Netherlands Satellite (ANS). Also clearly of great interest is Dr. K. Pounds' report at this conference that Ariel V has detected Her X-1 in the 2-20 keV energy range at approximately full strength at a time that is halfway through the "off" phase. Clearly all of these observations indicate that sensitive observations will ultimately provide a great deal more information regarding the origin and character of the 35 day period associated with Hercules X-1.

LACK OF PULSATION OF THE X-RAYS

Shulman *et al.* (1975) found that the strong 0.28 keV flux which they observed during the "on" phase was pulsed with the 1.2378 period, but that a phase shift occurs with respect to the pulses at higher energy. The pulsed fraction at 0.28 keV was only 10 to 20%, compared to about 50% in the 2 to 10 keV band. The present data unfortunately involve too few counts to detect a 10 to 20% pulsation if present. Simulations similar to that reported by Shulman *et al.* (1975) lead to an upper limit of 50% on the pulsed fraction of 0.28 keV x-rays which would have been detected with 90% confidence.

DISCUSSION

The fact that a weak 0.28 keV flux is present, at least at times, during the "off" phase of Hercules X-1, does not provide any obvious answer to the question of why the 1.97 optical modulations persist in HZ Her during the "off" phase of the 35 day x-ray period. Rather, it raises the further question of the place of origin of the low-energy flux. Thorne and Price (1975) have shown that heating of the inner part of the accretion disk by x-rays from near the collapsed object will cause the inner part of the accretion disk to expand in the direction perpendicular to its plane. A popular model for the occurrence of a 35-day cycle in Hercules X-1 is the precession of the

accretion disk with this period. During part of the precession cycle, the neutron star and all parts of the accretion disk are visible from earth, but during another part the accretion disk is viewed nearly edge-on, and the neutron star and the innermost portions of the accretion disk are not visible, or at least not directly visible. If the inner part of the accretion disk has a scale height above its plane which is substantially greater than this scale height for outer parts of the accretion disk, however, it would be visible even if the accretion disk were viewed exactly edge-on.

There are difficulties, however, with this model. Thorne and Price (1975) suggest that it is much higher energy photons that originate in the inner, thermally swollen, part of the accretion disk, while lower energy photons originate in the outer part. If the accretion disk is viewed edge-on, this outer part, which is optically thick in this model, would not be seen.

The apparent fact that the spectrum of the x-rays observed during the "off" phase is not a purely thermal spectrum, also suggests that a new model is needed. We have seen in Figure 6 that the spectrum that is observed during the "on" phase fits the data obtained during the "off" phase rather well, if the intensity is substantially reduced. This suggests that the mechanism of reduction of intensity is scattering by free electrons.

CONCLUSION

The work of Catura (1975), of Brinkman and Heise (1975), and of Pounds (1975), together with that of Shulman et al. (1975), and that reported in this paper, lead to the conclusion that a large amount of further observational work remains to be done on the system HZ Her-Her X-1 in the x-ray part of the spectrum, particularly during the nominal "off" portion of the 35-day x-ray cycle. The suggestion by Pounds (1975) that Her X-1 may turn on fully in the middle of each "off" cycle is particularly intriguing. The spectral behaviour during the "off" phase suggests that the observed x-rays are being scattered by a very hot thin ionized cloud surrounding the inner part of the accretion disk of the neutron star.

REFERENCES

- Avni, Y., Bahcall, J. N., Joss, P. C., Bahcall, N. A., Lamb, F. K., Pethick, C. J., and Pines, D. 1973, Nature Phys. Sci., 246, 36.

- Brinkman, A. C., and Heise, J. 1975, this symposium.
- Catura, R. C. 1975, this symposium.
- Dauidsen, A., Shulman, S., Fritz, G., Meekins, J. F.,
Henry, R. C., and Friedman, H. 1972, Ap. J., 177, 629.
- Dauidsen, A., Henry, R. C., Snyder, W. A., Shulman, S.,
Fritz, G., and Friedman, H. 1975, B.A.A.S. (to appear).
- Holt, S. S., Boldt, E. A., Rothschild, R. E., Saba, J. L.,
and Serlemitsos, P. J. 1974, Ap. J. (Letters), 190,
L109.
- Meekins, J. F., Henry, R. C., Fritz, G., Friedman, H.,
and Byram, E. T. 1969, Ap. J., 157, 197.
- Pounds, K. 1975, this symposium.
- Pringle, J. E. 1973, Nature Phys. Sci., 243, 90.
- Shulman, S., Friedman, H., Fritz, G., Henry, R. C., and
Yentis, D. J. 1975, Ap. J. (Letters), 199, L101.
- Snyder, W. A., Dauidsen, A., Henry, R. C., Shulman, S.,
Fritz, G., and Friedman, H. 1975, B.A.A.S. (to appear).
- Thorne, K. S., and Price, R. H. 1975, Ap. J. (Letters),
195, L101.

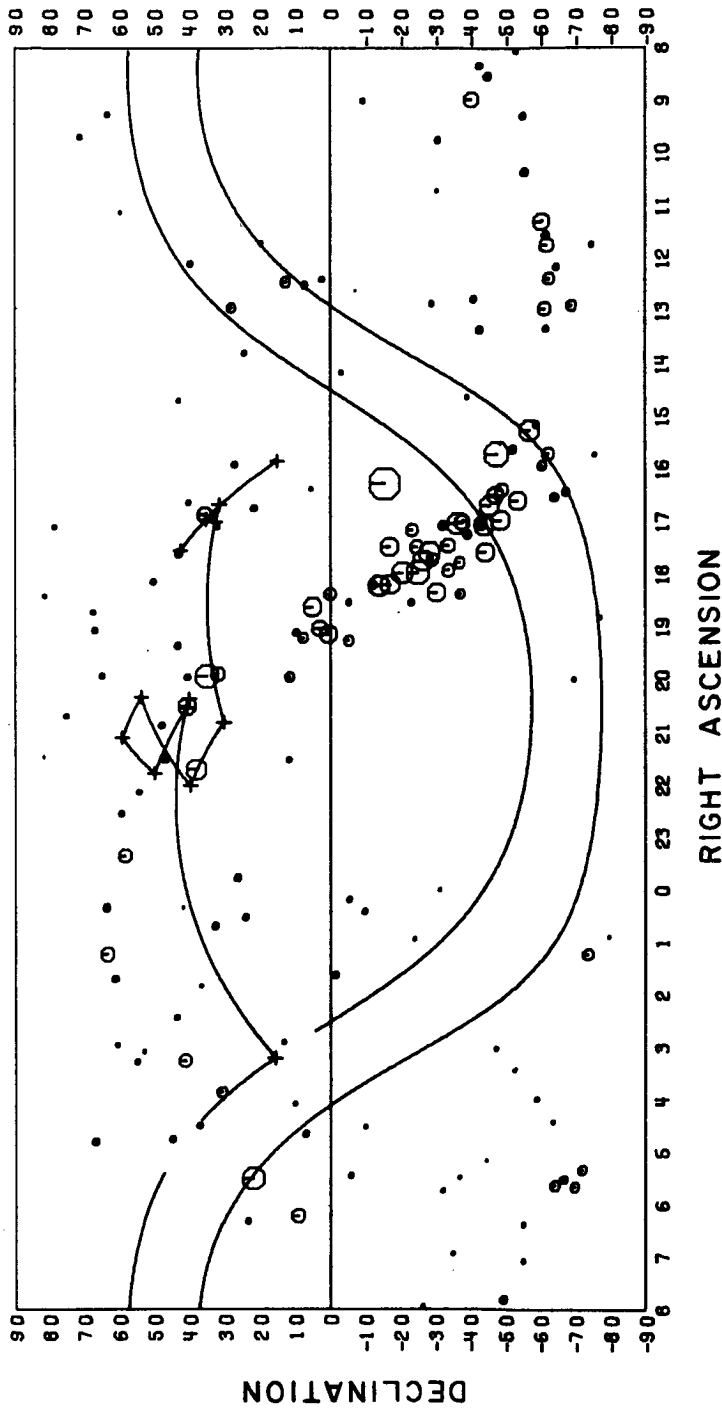


Figure 1. Sequence of attitude-control system maneuvers of the Aerobee rocket. The detectors were pointed first at the horizon, then at a series of targets in Cygnus, and afterward at Hercules X-1. They were then scanned slightly up toward the zenith, and finally down through Her X-1 toward the horizon.

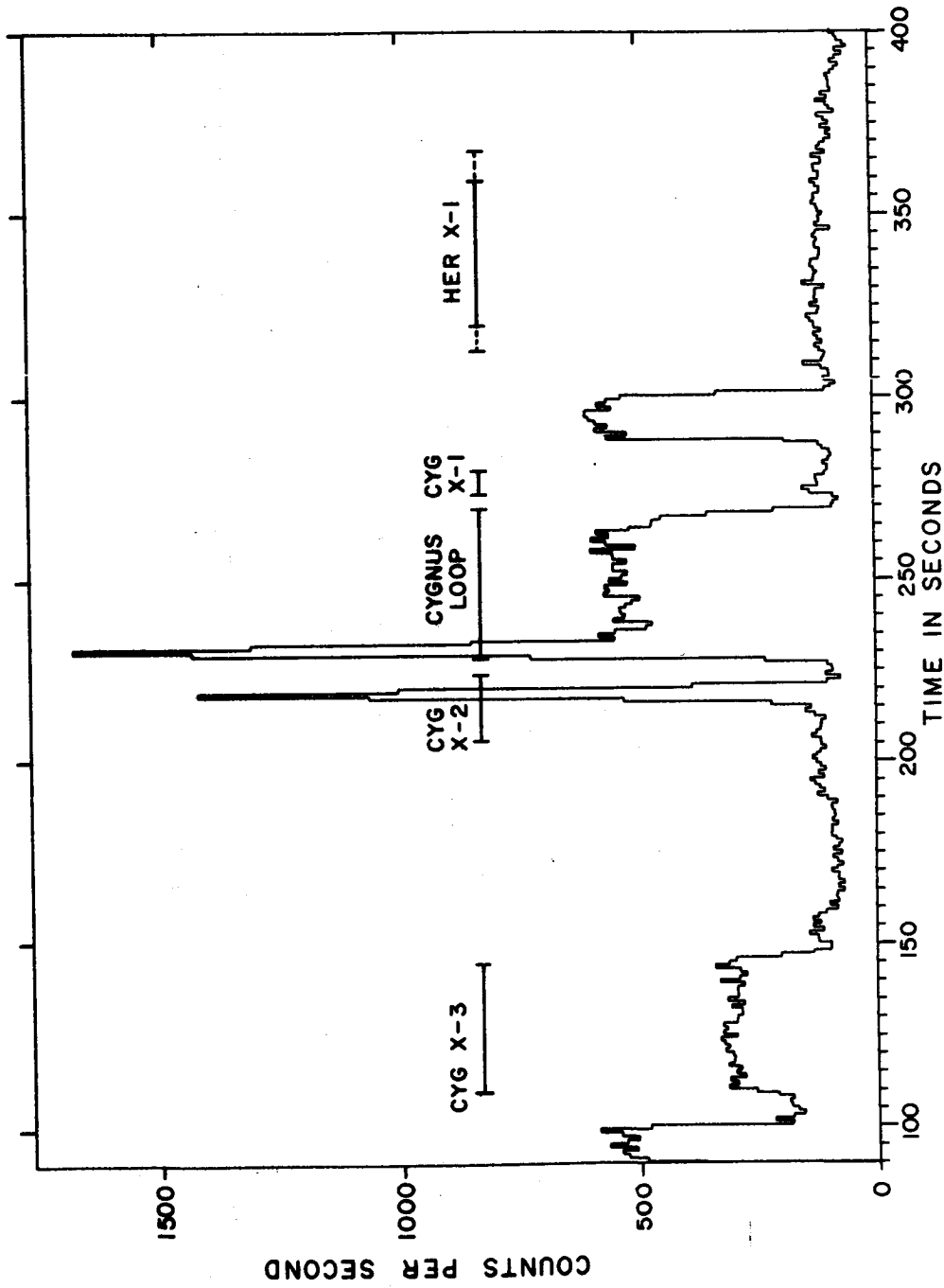


Figure 2. The count rate (0.1-10 keV) observed by the 3° FWHM collimated detector during the sequence of maneuvers shown in Figure 1. Two calibrations (at 85-100 and 286-302 seconds) and many celestial X-ray sources appear, but there is no obvious X-ray emission from Her X-1, which was in its "off" phase of the 35-day cycle at the time of the flight.

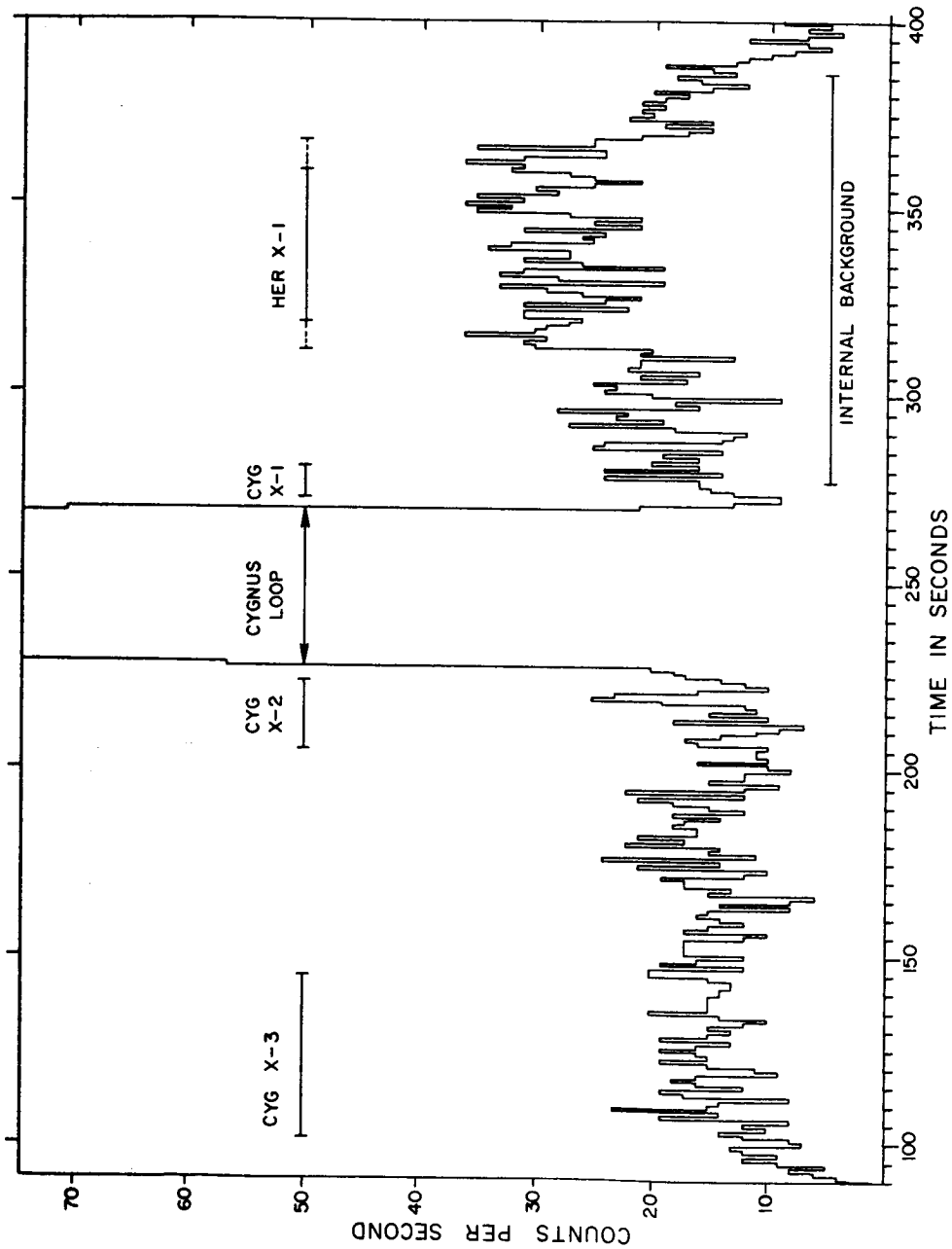


Figure 3. This is the same as Figure 2, but is restricted to counts produced by photons below 0.28 keV. The calibrations produce no counts in this energy range, and all of the sources that were prominent in Figure 2 are absent except the Cygnus Loop, which is off scale. Hercules X-1, however, which was not detectable in Figure 2, is clearly emitting X-rays in this energy range.

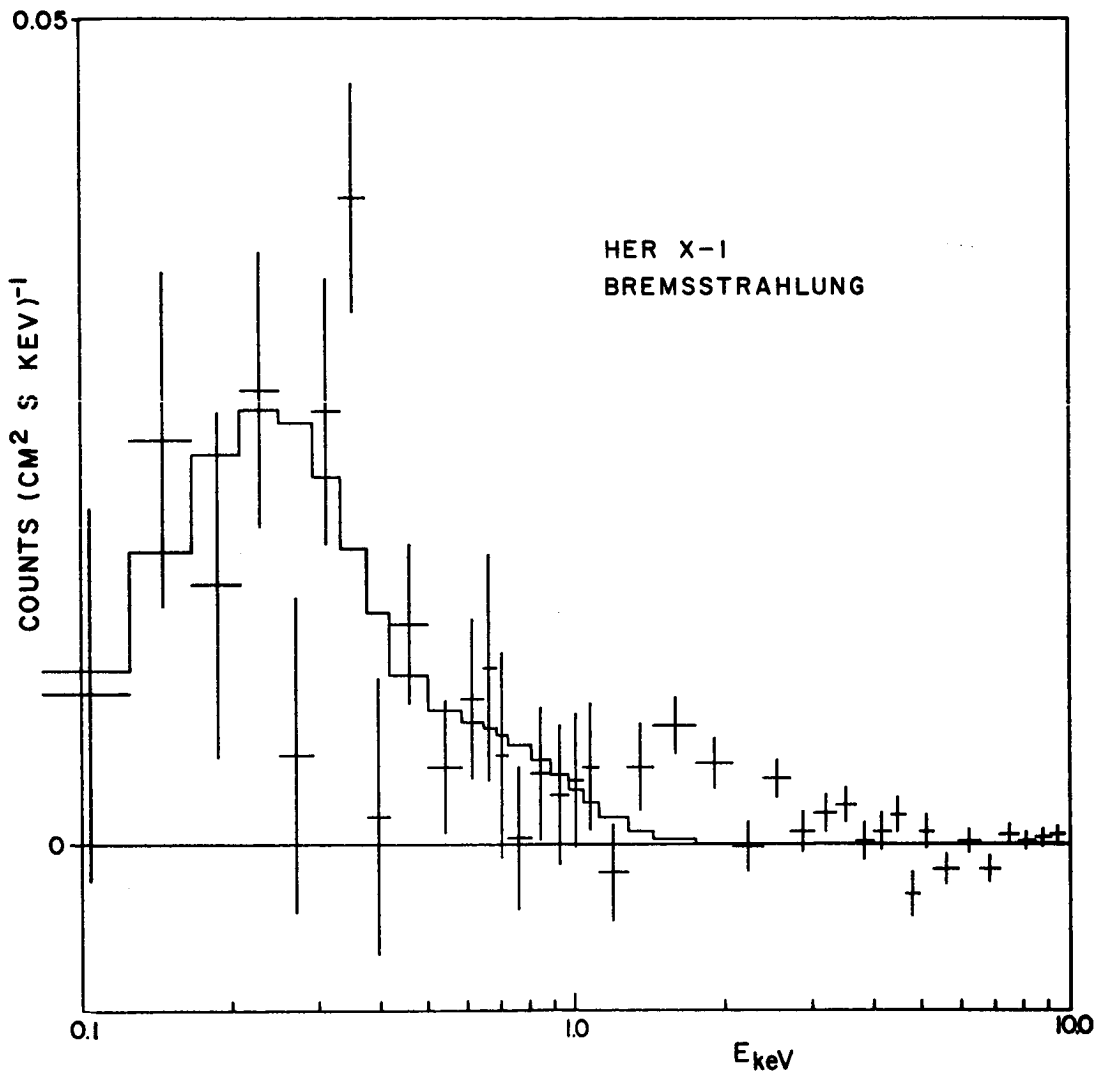


Figure 4. Spectrum of the X-rays from Hercules X-1, with background subtracted, observed with the 3° FWHM detector. A pure thermal bremsstrahlung spectrum, with a temperature of 2.0×10^6 °K, has been fitted to the data, assuming an interstellar hydrogen column density of 5×10^{20} cm $^{-2}$. The fit is not very good between 1 and 3 keV; the data suggest that a harder component may be present in the spectrum.

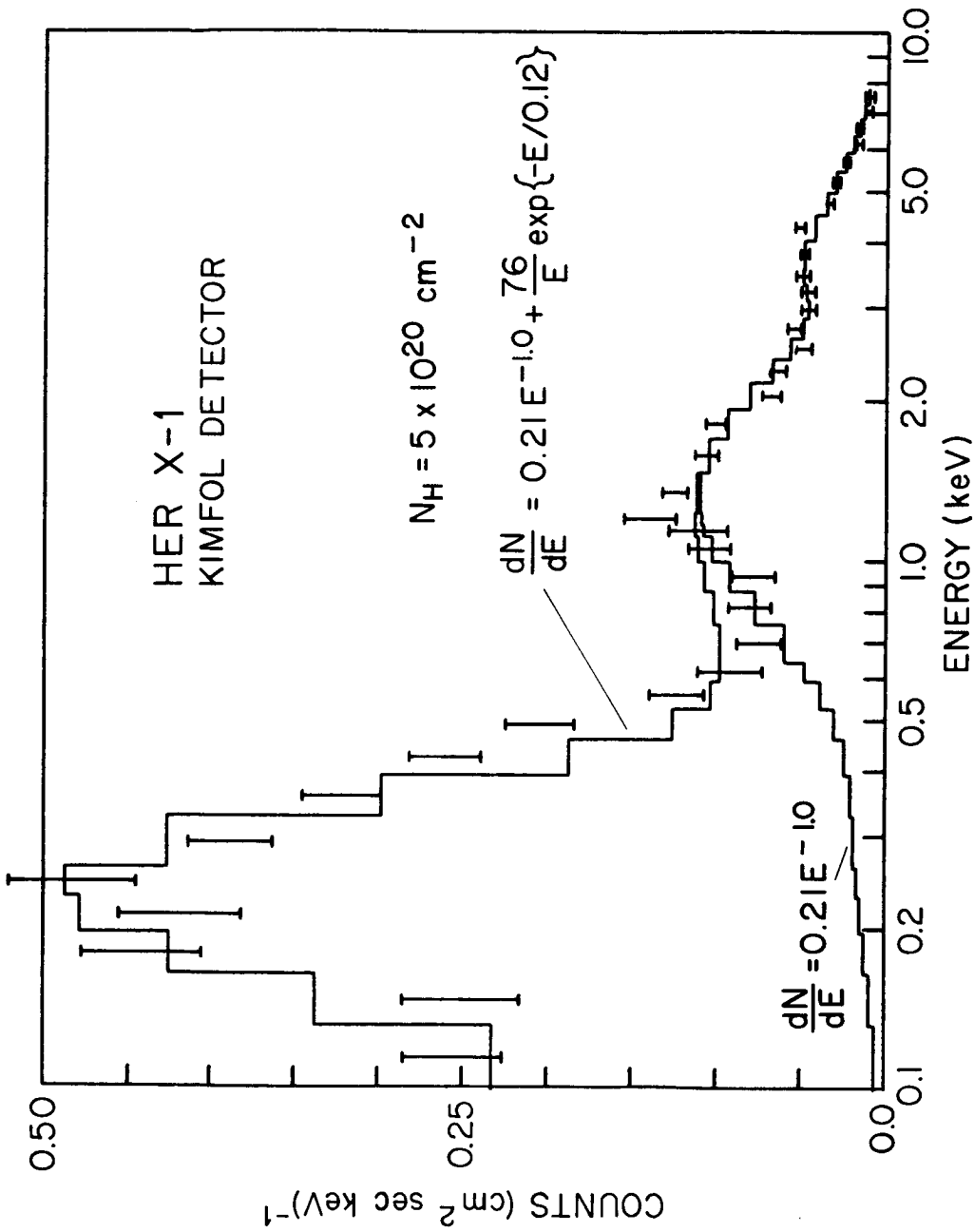


Figure 5. Spectrum of Her X-1 observed by Shulman *et al.* (1975) during the "on" phase. The data are plotted with 2σ error bars for each point. The higher solid line is the best-fit composite power law plus thermal bremsstrahlung spectrum folded through the detector response. The lower line is the same but for the power law alone.

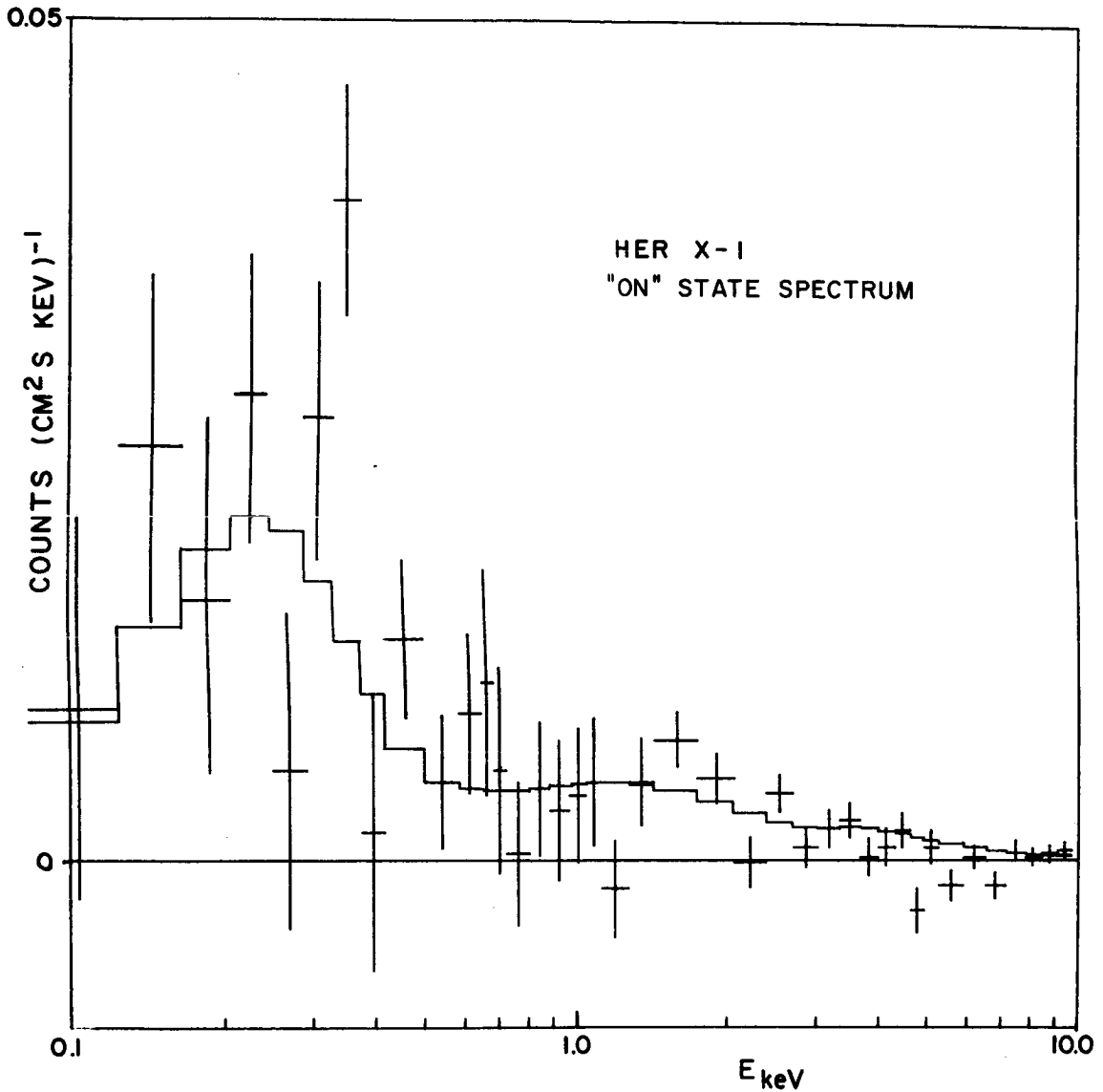


Figure 6. The data for Her X-1 from the present flight, as in Figure 4, but fitted with the "on" phase spectrum of Figure 5, reduced by a factor of 25. The fit is considerably better than that for pure thermal bremsstrahlung in Figure 4, and this suggests that the spectrum of Hercules X-1 may be the same during its "off" phase as during its "on" phase, except for a reduction in intensity. This in turn would imply that the reduction in intensity during the "off" phase is not due to simple absorption of the X-rays, which would affect the lower-energy X-rays more severely.



INFORMATION ABOUT ACCRETION FLOWS FROM X-RAY
TIMING OF PULSATING SOURCES*

F. K. Lamb[†] and D. Pines
Department of Physics
University of Illinois at Urbana-Champaign
Urbana, Illinois 61801

and

J. Shaham
Racah Institute of Physics
Hebrew University
Jerusalem, Israel

ABSTRACT

We have studied the response of a rotating neutron star to fluctuating torques and find that the observed variations in the pulsation periods of the compact X-ray sources Cen X-3 and Her X-1 could be caused by short time scale fluctuations in the accretion torques acting on the neutron stars. The sizes and rates of the required fluctuations are consistent with current accretion models. Such fluctuations can cause period variations either (a) directly, by causing a random walk of the star's angular velocity or (b) indirectly, by exciting a long-period mode of the neutron star, such as the Tkachenko mode of the rotating neutron superfluid. Should torque fluctuations be confirmed as the cause of the period variations, X-ray timing observations may yield valuable information about the flow of accreting matter into neutron star magnetospheres. We draw attention to other phenomena in compact X-ray sources and cataclysmic variables which may be caused by fluctuating mass flow rates.

I. INTRODUCTION

The pulsating compact X-ray sources Her X-1 and Cen X-3 are believed to be rotating magnetic neutron stars that are accreting matter from a close binary companion (for recent summaries of the evidence favoring such an interpretation, see Pines 1974; Rees 1974; and Lamb 1975a,b). In this picture the pulsation period, P , is the rotation period of the neutron star crust.

Unlike pulsars (which spin down), these neutron stars are expected to spin up as a consequence of the torque exerted by the accreting matter (Pringle and Rees 1972; Lamb, Pethick, and Pines 1973). The Uhuru observations (Giacconi 1974) reveal significant variations in the pulsation periods of both sources, as shown in Figure 1. As expected, both show a net decrease in period, amounting to some 6 μ sec over 14 months in the case of Her X-1, and some 3 msec over 21 months in the case of Cen X-3; this overall trend toward decreasing period is indicated by the straight lines in the figure. Elsewhere in these proceedings Tuohy reports more recent data on Cen X-3 from Ariel-5 which show that the de-

* Research supported in part by the National Science Foundation through grants GP 37485X, GP 41560, and MPS 75-08790. A longer version of this report is being submitted to the *Astrophysical Journal*.

† Alfred P. Sloan Foundation Research Fellow

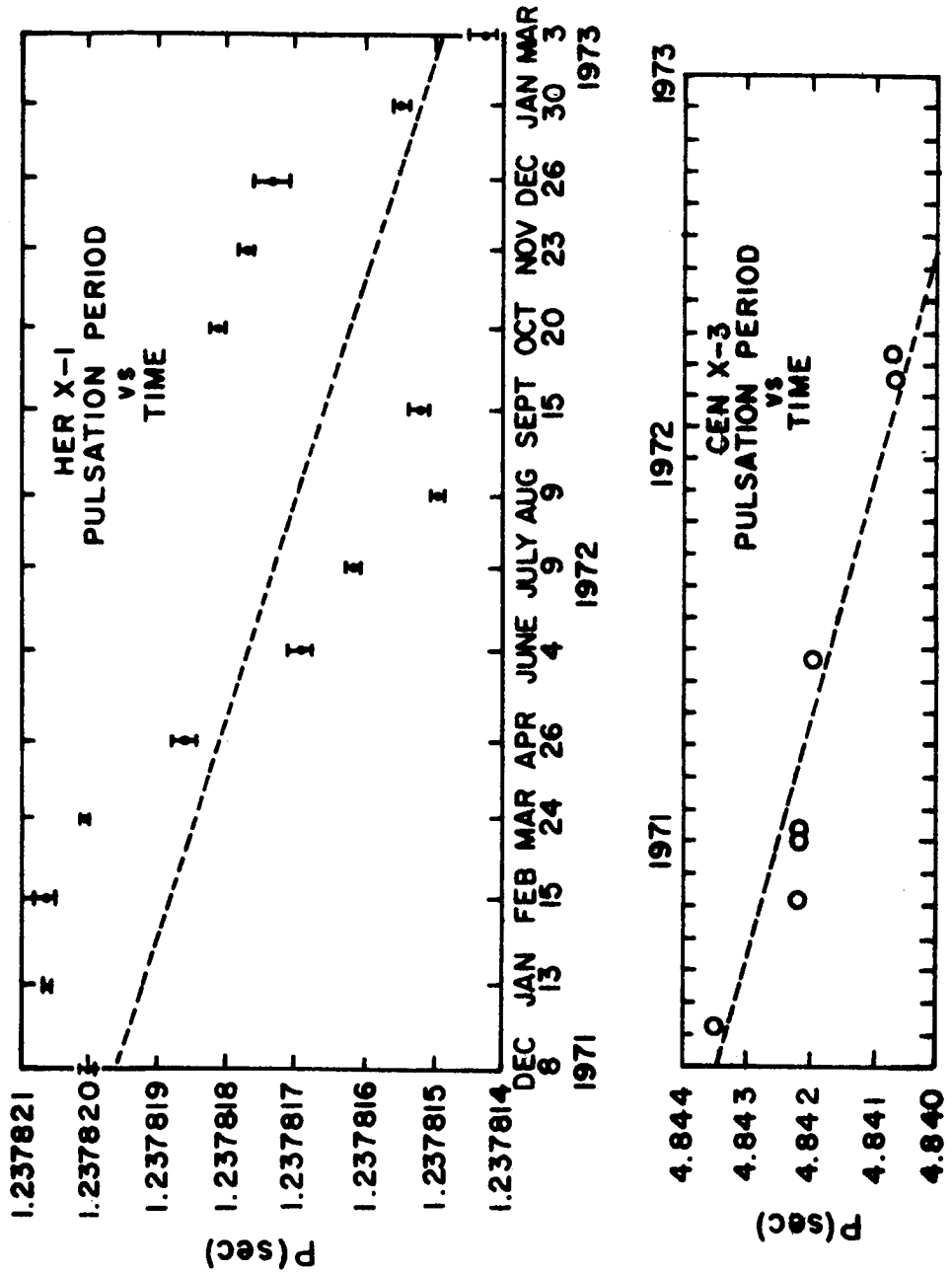


Figure 1. Period changes in Her X-1 and Cen X-3 (after Giacconi 1975). The dashed lines indicate the overall trends toward shorter periods, and emphasize the irregularity of the period changes from month to month. In Her X-1, the relative amplitude of the variation is $\Delta P/P \sim 10^{-6}$, with a characteristic time scale $P \text{ var} \sim 9 \text{ months}$, whereas in Cen X-3, $\Delta P/P \sim 10^{-4}$ with $P \text{ var} \sim 20 \text{ months}$.

crease in period of Cen X-3 has continued at about this same rate up to January, 1975.

On the other hand the period changes are not steady in either source, the period sometimes increasing as well as decreasing from one month to the next. One can interpret the data on both sources as due to a steady decrease in pulse period, characterized by the time scale $T_s = |P/\dot{P}|$, on which is superimposed a quasi-sinusoidal variation in pulse period of relative magnitude $(\Delta P/P)$, characterized by an apparent period, P_{var} . In Table 1 we list the values of these parameters which have been estimated from the data in Figure 1.

What is the cause of these quasi-sinusoidal period variations? In the case of Her X-1 Brecher and Wasserman (1974) have suggested that the HZ Her-Her X-1 system is actually a triple, and that the variations are Doppler shifts due to motions caused by the third, otherwise undetected, member of the system. Here we suggest a different interpretation, namely that they are a direct reflection of variations in the angular velocity of the neutron star crust caused by fluctuations in the accretion torque. In order to account for the observed variations, the accretion torque must change by a factor of $\sim 3-6$ on a time scale of a few months, in Her X-1, or about a year, in Cen X-3. Moreover, Figure 1 clearly shows that the sign of the torque must sometimes be reversed in Her X-1. While the X-ray flux from Her X-1 (and, by inference, the mass accretion rate onto the neutron star) is known to vary on time scales of several months (P. Boynton, private communication), the size of these variations is at most a factor ~ 2 , and there is as yet no evidence that they are in any way correlated with the observed period variations. Therefore this interpretation requires changes by a large factor in the angular momentum per unit mass accreting onto the star, and in some cases a reversal in its sign.

How can such changes come about? A change in the sign of the accretion torque could in principle be caused by a large-scale change of the matter flow-pattern in the binary system, such as a reversal in the sense of rotation of the accretion flow about the neutron star (see the discussion of disk reversals by Shapiro and Lightman 1975). However, the evidence that Her X-1, at least, is fed by Roche lobe overflow is overwhelming (cf. Lamb 1975b) and such a rotation reversal therefore appears exceedingly unlikely in this source. On the other hand, the coupling between the accretion torque and the star occurs at the Alfvén surface, where changes in the accretion flow pattern leading to ejection of a small fraction of the inflowing matter could cause a reversal in the net torque exerted by the flow (Davidson and Ostriker 1973; Lamb, Pethick, and Pines 1973; Lamb and Pethick 1974). If Her X-1 and Cen X-3 are rotating close to, but slower than their equilibrium spin rates, fluctuations in the accretion flow at the Alfvén surface will produce sizeable fluctuations in the accretion torque which can, for a time, lead to spin down, even though the torque will on average lead to spin up.

In this report we show that the observed period variations in both Her X-1 and Cen X-3 could be caused by relatively short time scale fluctuations in accretion torques due to changes in the flow pattern near the Alfvén surface, and that the sizes and rates of the required fluctuations are consistent with current accretion models. The observed X-ray intensities display substantial fluctuations over time scales from seconds to days (Doxsey *et al.* 1973; Giacconi *et al.* 1973; Holt *et al.* 1974; Giacconi 1975) that suggest corresponding fluctuations in the spin

Table 1

Observed Period Variations in Her X-1 and Cen X-3

<u>Parameter*</u>	<u>Her X-1</u>	<u>Cen X-3</u>
T(months)	14	21
P (sec)	1.24	4.84
T_s (years)	3×10^5	3×10^3
$\Delta P/P$	$\sim 10^{-6}$	$\sim 10^{-4}$
P_{var} (months)	~ 9	~ 20

* T is the duration of the observations; P, the pulse period; T_s , the mean spin up time; $\Delta P/P$, the relative amplitude of period variations; and P_{var} , the characteristic time scale of these variations.

up torques acting on the two stars. There are as well strong theoretical grounds for believing that accretion is an unsteady process (Lamb 1975b). We show that torque fluctuations could cause period variations of the observed size either (a) directly, by causing a random walk of the star's angular velocity (shot noise¹) or (b) indirectly, by exciting a long-period mode of the neutron star (such as the Tkachenko mode of the rotating neutron superfluid).

II. MODEL CALCULATIONS

a) Shot Noise

We have studied the response of a rotating neutron star to fluctuating torques and find that such torques could account for the period variations observed in Her X-1 and Cen X-3. To demonstrate this, we assume that the accretion torque may be written $N(t) = N_0 + \delta N(t)$, where N_0 is a constant and the fluctuating part, $\delta N(t)$, results from a stationary random process (δN itself need not be stationary, however). Although the assumption that $\delta N(t)$ results from a stationary process may not be valid on very long time scales (the ~ 10 - 20 year variations observed in HZ Her may be associated with an interruption of the accretion torque, for example), it would seem a reasonable approximation on the time scale of current observations (~ 1 - 2 years). We further assume $\langle \delta N(t) \rangle = 0$, where the sharp brackets denote a time average.

With these assumptions there are still an infinite number of different types of torque noise processes one might consider. Here we discuss two specific models which are plausible in the context of accretion torques:

$$\delta N_1(t) = \sum_i \delta L_i \delta(t-t_i) \quad (1)$$

corresponding to a sequence of steps in the angular momentum of the star, and

$$\delta N_2(t) = \sum_i \delta N_i \theta(t-t_i) \quad (2)$$

corresponding to a sequence of steps in the torque acting on the star. The first model can be described as white noise in the torque N and the second, as white noise in N . Jumps of type (1) could result, for example, from clumping of the matter crossing the Alfvén surface (Lamb *et al.* 1973). Jumps of type (2) could result from steps in the rate at which matter crosses the Alfvén surface. Fluctuations of both types would then be seen as variations in the X-ray intensity. In order to clarify the difference between the two types of fluctuations, consider a particular event at time t_i that includes both: suppose that after a time $T_1 \ll T$ a fraction δN_{i1} of the original torque jump δN_i has died away, but some fraction, δN_{i2} , remains ($\delta N_{i1} + \delta N_{i2} = \delta N_i$). One would then have both types of noise, with $\delta L_i \sim \delta N_{i1} T_1$ and $\delta N_i \sim \delta N_{i2}$ (in this example the two are correlated, and there would be interference between them). Physically, the torque in a type (1) process returns to the reference value N_0 after each event. In a type (2) noise process, on the other hand, each step δN_i must persist for at least as long as the observing period, although it may disappear after a longer time; in this type of process there is no reference torque. In the limit of infrequent torque jumps of large size, this description in terms of noise processes gives the same result as slow but very large amplitude changes in the torque. (As we shall see, torque jumps $\sim 1/10$ the mean torque, for example, occurring ~ 10 times per second and lasting $\sim 10^4$ seconds, would suffice to explain the observations; alternatively,

¹ We use the term 'shot noise' here to refer to any stationary noise process.

if only $\sim 10^{-2} - 10^{-3}$ of each such jump persisted for $\gtrsim 3T \sim 10^8$ seconds, this would also suffice.)

In order to calculate the effect of $N(t)$ on the angular frequency of the neutron star, we adopt the two-component model, in which the solid outer crust, the solid core (if any), and the charged particles in the liquid interior of the star are assumed to rotate together at angular frequency Ω , as a result of the strong magnetic fields which thread the stellar crust and core, and are weakly coupled to the superfluid neutrons (Baym et al. 1969). If we neglect any low-frequency modes, the equations of motion of the system are

$$I_c \dot{\Omega} = N - \frac{I_c}{\tau_c} (\Omega - \Omega_n) \quad (3)$$

and

$$I_n \dot{\Omega}_n = \frac{I_c}{\tau_c} (\Omega - \Omega_n) \quad (4)$$

where I_c and I_n are the moments of inertia of the crust and the neutron superfluid, respectively, and Ω_n is the superfluid angular velocity. The crust angular velocity then obeys the equation

$$\frac{d^2 \Omega}{dt^2} + \frac{1}{\tau} \frac{d\Omega}{dt} = \frac{1}{I_c} \frac{dN}{dt} + \frac{N}{I\tau} \quad (5)$$

where $\tau = \frac{I_n \tau_c}{I}$ is the crust-core coupling time, and $I = I_n + I_c$.

A solution of (5) is

$$\Omega(t) = \Omega_0 + \dot{\Omega}_0 t + \delta\Omega(t) \quad (6)$$

where Ω_0 and $\dot{\Omega}_0$ are constants which satisfy

$$T_s \equiv \Omega_0 / \dot{\Omega}_0 = I \Omega_0 / N_0 \quad (7)$$

and $\delta\Omega(t)$ obeys (5) with $N(t)$ replaced by $\delta N(t)$. A theoretical estimate of T_s may be made by calculating the angular momentum flux carried by particles crossing the Alfvén surface (Lamb et al. 1973). The results are in good qualitative agreement with the values for Her X-1 and Cen X-3 cited in Table 1.

Assuming $\delta N(T) = \delta N(0)$ and $\delta\Omega(T) = \delta\Omega(0)$, $\delta\Omega(t)$ can be calculated from $\delta N(t)$ using discrete Fourier transform techniques. If T is the duration of the observations, the bulk of the response noise power lies in the frequency range $\Delta\omega \sim \pi/T$. Thus the signature of this type of noise is quasiperiodic behavior, with an apparent frequency, $2\pi/T$, determined by the length of the data (cf. Groth 1972, 1975; Boynton et al. 1972).

In the limits of observing periods long and short compared to the crust-core coupling time, the total mean square fluctuation $(\Delta\Omega)^2 = \langle (\delta\Omega)^2 \rangle_T$ is given by

$$\left(\frac{\Delta\Omega}{\Omega}\right)_{NL}^2 = \eta^2 \frac{R_1 \beta^2 T}{12} \left(\frac{1}{R_1 T_s}\right)^2 \quad (8)$$

for model (1) and

$$\left(\frac{\Delta\Omega}{\Omega}\right)^2_{N2} = \eta^2 \frac{R_2 \gamma^2 T}{720} \left(\frac{T}{T_s}\right)^2 \quad (9)$$

for model (2). Here

$$\eta = \begin{cases} I/I_c, & T \ll \tau \\ 1, & T \gg \tau, \end{cases} \quad (10)$$

R_1 and R_2 are the average rates of angular momentum and torque jumps, respectively, and we have introduced the dimensionless constants $\beta = R_1 \langle (\delta L_1)^2 \rangle^{1/2} / N_0$ and $\gamma = \langle (\delta N_1)^2 \rangle^{1/2} / N_0$ to characterize the sizes of the torque fluctuations.

b) Tkachenko Oscillations

If there are low-frequency modes of the neutron star which can be excited by fluctuations in the accretion torque, the response of the star will generally differ from (8) and (9), with some of the noise power concentrated near the resonance frequencies of the modes. One set of low-frequency modes which might be excited are Tkachenko oscillations of the rotating neutron superfluid.

Tkachenko modes are oscillations of the vortex lattice which exists in a rotating superfluid. They obey a sound-wave-like dispersion relation at low frequencies, with phase velocity in a neutron superfluid (Tkachenko 1966; Ruderman 1970)

$$c_{Tk} = \frac{1}{2} (h\Omega/2m_n)^{1/2}, \quad (11)$$

where m_n is the neutron mass. Recently, Tsakadze and Tsakadze (1973) have reported excitation of Tkachenko modes in rotating superfluid helium in an experiment in which a vessel containing superfluid helium was suddenly spun up. The success of this experiment suggests that under laboratory conditions, there exists a liquid boundary layer which strongly couples the container to the rotating superfluid.

If the outer crust of a rotating neutron star is similarly strongly coupled to the interior neutron superfluid, fluctuating accretion torques may excite Tkachenko oscillations in the interior. The lowest frequency such mode, with a wavelength, λ , comparable to the stellar radius, R , would have a period

$$P_{Tk} \sim 20 \left(\frac{R}{10^6 \text{ cm}}\right) \left(\frac{P}{1 \text{ sec}}\right)^{1/2} \text{ months.} \quad (12)$$

To model the response of such a star, we shall use a phenomenological modification of (5), namely

$$\frac{d^2\Omega}{dt^2} + \frac{1}{\tau} \frac{d\Omega}{dt} + \Omega^2_{Tk} = \frac{1}{I_c} \frac{dN}{dt} + \frac{N}{I\tau} + \frac{\Omega^2_{Tk}}{I} \int_0^t dt' N(t'), \quad (13)$$

where Ω_{Tk} is the frequency of the Tkachenko mode (for further discussion, see Shaham 1975).

The $\Omega(t)$ given by (6) and (7) is again a solution, but $\delta\Omega(t)$ obeys (13) with $N(t)$ replaced by $\delta N(t)$. Making the same assumptions as before, $\delta\Omega(t)$ can again be calculated. The resulting general expressions for that part of $(\Delta\Omega)^2$ associated with the Tkachenko mode are quite complicated. However, if we assume that the fluctuating torque has been acting for some time T_N which is long compared to either τ or T , that $\Omega_{Tk} \gtrsim 1$, and furthermore, that the mode is lightly damped, $\Omega_{Tk} \tau \gg 1$, the expressions for torque models (1) and (2) simplify to

$$\left(\frac{\Delta\Omega}{\Omega}\right)_{Tk1}^2 \sim \left(\frac{I_n}{I_c}\right)^2 \frac{1}{2} R_1 \beta^2 \tau \left(\frac{1}{R_1 T_s}\right)^2 \quad (14)$$

and

$$\left(\frac{\Delta\Omega}{\Omega}\right)_{Tk2}^2 \sim \left(\frac{I_n}{I_c}\right)^2 \frac{1}{2} R_2 \gamma^2 \tau \left(\frac{P_{Tk}}{2\pi T_s}\right)^2 \quad (15)$$

If, on the other hand, the mode is heavily damped, $\Omega_{Tk} \tau \ll 1$, the general expressions reduce to (8) and (9), and its existence is no longer apparent.

III. APPLICATIONS TO CEN X-3 AND HER X-1

As may be seen from Figure 1 and Table 1, for both Cen X-3 and Her X-1 the pulsation period shows a deviation from the indicated straight line which, if periodic, has an apparent period, P_{var} , which is comparable to the time, T , over which observations have been made. This suggests that in these two sources one may be observing either shot noise in Ω or a Tkachenko oscillation with period $P_{Tk} \sim T$, excited by torque fluctuations.

a) Accretion Torque Fluctuations

We can place an upper limit on the amplitude of the fluctuations in Ω to be expected within the framework of the accreting neutron star model, as follows. Coupling between the angular momentum of the accreting matter and the neutron star occurs at the Alfvén surface, where the time scale for variations in accretion flows is of the order of the hydrodynamic time scale, $\tau_H \sim (R_A^3/GM)^{1/2}$, and is ~ 0.1 to 1 sec for typical accretion conditions (Lamb 1975a). Therefore, if torque fluctuations are associated with macroscopic fluctuations in the accretion process, we expect the rate of fluctuations to satisfy $R \lesssim 1/\tau_H$. A description in terms of torque noise is only appropriate if there are a large number of fluctuations during the observing period, $RT \gtrsim 10$, say. The torque noise model thus leads us to expect values of RT in the range

$$10 \lesssim RT \lesssim 4 \times 10^8 \left(\frac{R_A}{10^8 \text{ cm}}\right)^{-3/2} \left(\frac{M}{M_\odot}\right)^{1/2} \left(\frac{T}{1 \text{ yr}}\right) \quad (16)$$

b) Shot Noise Interpretation

If we adopt for the moment a shot noise interpretation, we can estimate $RT/\eta^2\beta^2$ (model 1) or $\eta^2\gamma^2RT$ (model 2) for each source from the observed values of $\Delta\Omega$, using (8) and (9). The results are shown in Table 2. The similarity in the product values derived for the two sources is perhaps surprising, in view of the fact that the spin up times for the two stars differ by two orders of magnitude (suggesting comparable differences in the angular momentum fluxes onto the two stars) and the likelihood (Lamb 1975b; Schreier et al. 1975) that the mass transfer modes are different as well (stellar wind in Cen X-3, Roche lobe overflow in Her X-1). However, in both sources one likely has orbital inflow of the accreting matter, and the physical processes by which matter enters the two magnetospheres may well be quite similar. Assuming $\eta \sim 1$, white torque noise (model 1) can account for the observed variations in Ω if $\beta \gg 1$. For example, changes in \dot{M} of size $\sim (1/10) \langle \dot{M} \rangle$ at a rate $R \sim 10 \text{ sec}^{-1}$ and lasting for 10^4 sec would suffice. On the other hand, if a part of each torque fluctuation lasts longer than T (model 2) a fluctuation $\delta\dot{M} \sim (1/10) \langle \dot{M} \rangle$, of which only a fraction $\sim 10^{-3}$ persists, would also suffice, again assuming $R \sim 10 \text{ sec}^{-1}$.

c) Tkachenko Mode Interpretation

If we instead interpret the period variations in terms of Tkachenko oscillations with $P_{\text{TK}} \sim T$, we can estimate $(I_c/I_n)^2(RT^2/\beta^2\tau)$ (model 1) or $(I_n/I_c)^2(\gamma^2R\tau)$ (model 2) for each source using (14) and (15), with the results again shown in Table 2. From (12), a Tkachenko mode with a wavelength $\sim 5 \text{ km}$ has the correct period to explain the observed period variations in both Cen X-3 and Her X-1, provided, of course, that the variations prove to be genuinely periodic. Again, the required level of fluctuations is within the range (16) if angular momentum jumps with $\beta \gg 1$ or torque jumps of duration $> T$ occur (the longer the crust-core coupling time τ , the smaller the required values of β and γ).

d) Discussion

How can we decide among these various possibilities? Our calculations suggest that, for torque fluctuations of a given size and rate, the power in the Tkachenko oscillation will dominate that in the shot noise component if $\tau \gtrsim T$ (model 1) or $360 \Omega_{\text{TK}}\tau \gtrsim (\Omega_{\text{TK}}T)^3$ (model 2). Thus, if the crust-core coupling time τ is of the order of years (the value deduced for the Vela pulsar), and $T \sim P_{\text{TK}}$, as suggested by (12), at the present time the power in the two components will be about the same. Moreover, the power in both will be a maximum at $\omega \sim 2\pi/T$, and the two interpretations will at present be indistinguishable. However, comparison of (8), (9), (14), and (15) shows that if the period of observation is extended to, say, $2T$, the two interpretations lead to quite different predictions.

If one is observing random pumping of a resonant mode, the power at the fixed frequency of the mode will remain constant, whereas if one is observing shot noise, one will see roughly twice (model 1) or 8 times (model 2) the old power $(\Delta\Omega)^2$ peaked, however, near the new frequency $\omega' \sim \pi/T$. In addition, the two shot noise models predict different power spectra, $\sim \omega^{-2}$ (model 1) and $\sim \omega^{-4}$ (model 2). Thus future observations can easily decide among these possibilities, either by extending the length of the observing period, or by providing more accurate and more frequent

Table 2

Inferred Shot Noise and Tkachenko Oscillation
Parameters for Her X-1 and Cen X-3

<u>Parameter</u>	<u>Her X-1</u>	<u>Cen X-3</u>
$(RT/\eta^2\beta^2)_{N1}$	~ 1	~ 3
$(\eta^2\gamma^2RT)_{N2}$	~ 50	~ 20
P_{Tk} (months)	$\sim 20(\lambda/10^6 \text{ cm})$	$\sim 40(\lambda/10^6 \text{ cm})$
$(I_c/I_n)^2(RT^2/\beta^2\tau)_{Tk1}$	~ 8	~ 20
$(I_n/I_c)^2(\gamma^2RT)_{Tk2}$	~ 10	~ 2

period determinations which would allow the data to be analyzed in segments of varying length. Should the resonant mode interpretation be confirmed, and the observing period extended to $T \gg \tau$, it would be possible to resolve the peak in the power spectrum due to the mode, and thus to measure τ directly.

IV. CONCLUDING REMARKS

Our calculations show that fluctuations in the accretion torque could account for the period variations in the pulsating X-ray sources, Her X-1 and Cen X-3. The values of the fluctuation parameters, R_{γ}^2 , inferred from either a shot noise or Tkachenko mode interpretation of the data are, moreover, consistent with values to be expected from processes at the magnetospheric boundary of an accreting neutron star.

Although present observations do not permit one to decide among the various interpretations of the period variations that have so far been proposed (shot noise, Tkachenko oscillation, slow but very large amplitude torque variations, or triple star system), this should become possible on the basis of future observations. If a period variation proves not to be genuinely periodic, this would be strong evidence against the Tkachenko oscillation or triple star interpretation. The shot noise model predicts that the amplitude of the period variation will increase steadily with the length of the observing period T , and that the residuals will show $P_{\text{var}} \sim T$. Slow but very large amplitude non-random torque variations would not be expected to show such a scaling.

On the other hand, a genuinely periodic variation would be strong evidence against the shot noise or changing torque interpretations. Both the Tkachenko oscillation and triple star models make definite predictions. The triple star model predicts a near-perfect periodicity, with power confined to a very narrow bandwidth characteristic of changes in the orbital motion, whereas the Tkachenko oscillation model predicts a bandwidth $\Delta\omega \sim 1/\tau$, or, if more than one mode is excited, somewhat larger. Thus a quasi-periodicity, characterized by a fixed period but an appreciable bandwidth, would be consistent with the Tkachenko model, but probably not with the triple star model. An independent determination of τ would further constrain the Tkachenko model, but given uncertainty as to whether overtones can be significantly excited, and the wide range of torque fluctuations which are consistent with current accretion theory, might not be decisive. If periodic variations are found in a number of regularly pulsating X-ray sources, and the periods all correspond to those expected for the fundamental Tkachenko mode, this would be indirect evidence favoring the Tkachenko oscillation model.

Should torque fluctuations be confirmed as the cause of the period variations in Cen X-3 and Her X-1, X-ray timing observations may yield valuable information about the flow of accreting matter into neutron star magnetospheres. The rate and size of fluctuations, and the relative contributions of torque and angular momentum jumps would provide important clues about instabilities at the Alfvén surface (Lamb 1975b) and the extent to which changes in the flow are preserved.

In conclusion, we note that fluctuating mass flow rates may be responsible for other phenomena observed in compact X-ray sources. For example, randomly fluctuating torques can start up wobble whose initial amplitude is zero, as noted by Lamb *et al.* (1975). As a second example, in close binary systems experiencing mass transfer, fluctuations in the mass flow rate may lead to binary period variations, such as those observed in the Krzeminski's star - Cen X-3 system. Finally,

we note that similar phenomena are to be expected in the case of accreting degenerate dwarfs: fluctuations in the mass transfer rate can cause variations in the orbital period, while fluctuations in the accretion torque acting on the dwarf can cause variations in the dwarf spin period.

We should like to thank D. Q. Lamb for many valuable discussions. We are also grateful to E. J. Groth and M. R. Nelson for helpful comments. One of us (JS) was a visitor in the Department of Physics, University of Illinois, while part of this work was carried out and expresses his thanks for its warm hospitality. This research has been supported in part by the United States-Israel Binational Science Foundation.

- F. K. Lamb: Department of Physics, University of Illinois at Urbana-Champaign, Urbana, Illinois, 61801.
- D. Pines: Department of Physics, University of Illinois at Urbana-Champaign, Urbana, Illinois, 61801.
- J. Shaham: Racah Institute of Physics, Hebrew University, Jerusalem, Israel.

REFERENCES

- Baym, G., Pethick, C. J., Pines, D., and Ruderman, M. 1969, *Nature* 224, 872.
- Boynton, P. E., Groth, E. J., Hutchinson, D. P., Nanos, G. P., Jr., Partridge, R. B., and Wilkinson, D. T. 1972, *Ap. J.* 175, 217.
- Brecher, K., and Wasserman, I. 1974, *Ap. J. (Letters)* 192, L125.
- Davidson, K., and Ostriker, J. P. 1973, *Ap. J.* 179, 585.
- Doxsey, R., Bradt, H. V., Levine, A., Murthy, G. T., Rappaport, S., and Spada, G. 1973, *Ap. J. (Letters)* 182, L25.
- Giacconi, R. 1974, in *Astrophysics and Gravitation*, Proc. 16th International Solvay Conference (L'Université de Bruxelles), p. 27.
- Giacconi, R. 1975, in Proc. 7th Texas Symposium on Relativistic Astrophysics, *Ann. N. Y. Acad. Sci.* 262, 312.
- Giacconi, R., Gursky, H., Kellogg, E., Levinson, R., Schreier, E., and Tananbaum, H. 1973, *Ap. J.* 184, 227.
- Groth, E. J. 1972, Ph.D. thesis, Princeton University.
- Groth, E. J. 1975, *Ap. J. Suppl.*, in press.
- Holt, S. S., Boldt, E. A., Rothschild, R. E., Saba, J. L. R., and Serlemitsos, P. J. 1974, *Ap. J. (Letters)* 190, L109.

- Lamb, D. Q., Lamb, F. K., Pines, D., and Shaham, J. 1975, Ap. J. (Letters) 198, L21.
- Lamb, F. K. 1975a, in Proc. International Conference on X-rays in Space, Calgary, 14-21 August, 1974, p. 613.
- Lamb, F. K. 1975b, in Proc. 7th Texas Symposium on Relativistic Astrophysics, Ann. N. Y. Acad. Sci. 262, 331.
- Lamb, F. K., and Pethick, C. J. 1974, in Astrophysics and Gravitation, Proc. 16th International Solvay Conference (L'Université de Bruxelles), p. 135.
- Lamb, F. K., Pethick, C. J., and Pines, D. 1973, Ap. J. 184, 271.
- Pines, D. 1974, in Astrophysics and Gravitation, Proc. 16th International Solvay Conference (L'Université de Bruxelles), p. 147.
- Pringle, J. E., and Rees, M. J. 1972, Astr. and Ap. 21, 1.
- Rees, M. 1974, in Astrophysics and Gravitation, Proc. 16th International Solvay Conference (L'Université de Bruxelles), p. 97.
- Ruderman, M. 1970, Nature 225, 619.
- Schrier, E. J., Swartz, K., Giacconi, R., Fabbiano, G., and Morin, J. 1975, preprint.
- Shaham, J. 1975, in preparation.
- Shapiro, S. L., and Lightman, A. P. 1975, preprint.
- Tkachenko, V. K. 1966, Zh. Eksp. Teor. Fiz. 50, 1573 [Sov. Phys.-JETP 23, 1049].
- Tsakadze, Dz. S., and Tsakadze, S. Dzh. 1973, ZhETF Pis. Red. 18, 605 (Sov. Phys.-JETP Letters 18, 355).



VARIABILITY OF HZ HERCULIS DURING THE
OPTICAL OFFS

WM. LILLER

Center for Astrophysics
Harvard College Observatory and
Smithsonian Astrophysical Observatory
Cambridge, MA

ABSTRACT

Additional material from the archival photograph collection at the Harvard Observatory has been used to derive an improved light curve for HZ Her during its optical OFFs. The full amplitude of the double sinusoidal variation, $\Delta B = 0.187 \pm 0.054$ mag.

From archival photographs stored at the Harvard College Observatory, Jones, Forman and Liller (1973) discovered that at 10-20 year intervals, the ~ 2 mag, 1.7 day variation in brightness of HZ Her ceases abruptly (within a 9-day interval), and for the next several years, the only variability that remains is a small-amplitude double sinusoidal fluctuation caused, presumably, by the rotating figure of the Roche lobe surrounding the normal star as it is seen first end-on and then broad-side. Jones et al. estimated that the full amplitude of HZ Her during optical OFFs was $\Delta m_{pg} = 0.28 \pm 0.06$ mag. This result was based entirely on 26 blue-sensitive plates taken with a 41-cm refractor.

Because the variability of HZ Her during optical OFFs gives us important information about the two components and the Roche lobe, it is desirable to determine as accurately as possible the nature of this variability. Presented here is a refined result based on these same 26 points (now given double weight) and 86 additional magnitude determinations made from patrol plates taken with 10- and 4-cm diameter lenses. Most plates were taken in the OFF periods of 1937-1942 and 1948-1957. Figure 1 shows the normal B magnitudes plotted against the phase, $\phi = (t-2441506.3921)/1.700165n$ where t is Julian days. $\phi = 0$ corresponds to center of X-ray eclipse; the curve is a least squares sine curve with full amplitude $\Delta B = 0.187 \pm 0.054$ mag and the phase at minimum light, $\phi_0 = 0.046$. Thus, to the accuracy of the result, the phase agrees with that predicted from the ephemerides given by the full ~ 2 mag fluctuation and by the X-ray eclipses.

The author would like to thank the National Science Foundation for supporting much of this research.

REFERENCES

- Jones, C. A., Forman, W. F., and Liller, W. 1973, Ap. J.
(Letters), 182, 109.

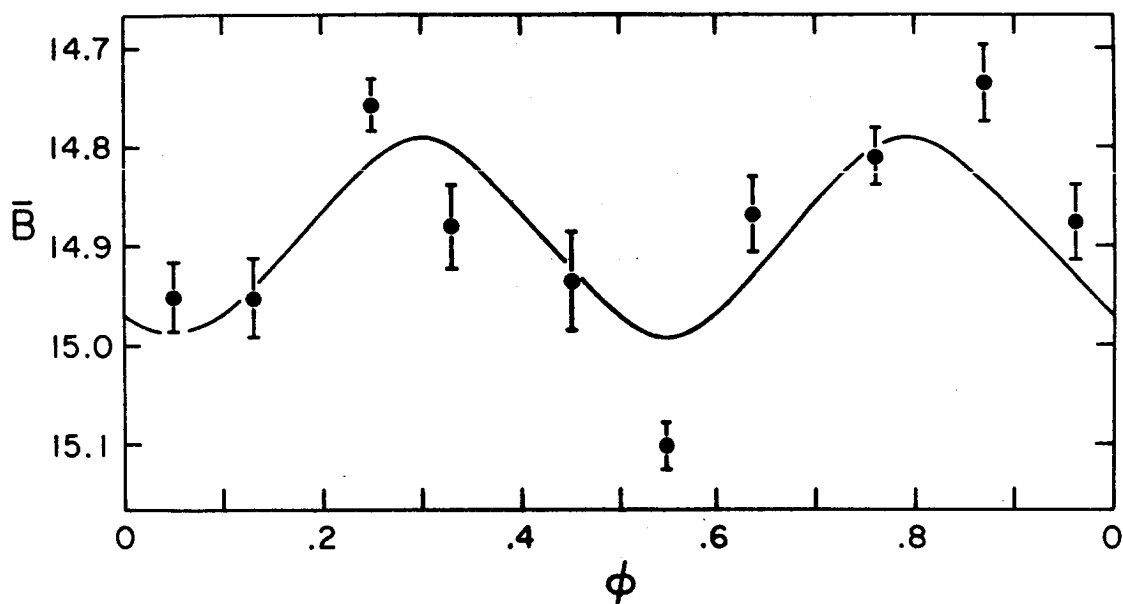


Fig. 1. - The B-magnitude light curve of HZ Her during optical OFFs as derived from 112 blue photographs in the collection of the Harvard College Observatory. The data are folded modulo 1.700165 days and averaged in phase bins of 0.1. The full length of the error bars is twice the mean error.

PRECESSIONS OF THE NORMAL STAR IN X-RAY BINARIES

Jacobus A. Petterson
Physics Department
Yale University
New Haven, CT. 06520

Is it possible that the rotation axis of the normal star in an X-ray binary system performs a non-negligible precession? Since the star is in an expanded state, we may not simply apply rigid body mechanics to answer this question; on the other hand fluid dynamics is not prepared at the moment to give us an accurate description of the behaviour of matter in such a star under the influence of a large external torque.

For a precession to occur it is needed that the rotation axis of the star is not aligned with the rotation axis of the binary system. However, the theory of tidal evolution of binary systems is not ready at present to predict how large a misalignment we may expect.

The existence of a 35 day period in Hercules X-1 has provoked the suggestion that the clock of this periodicity is the kind of precession we are looking for.

Therefore it is of some interest (and not only for those who want to explain Her X-1), to see whether direct evidence for this precession can be obtained.

We discuss observations that might lead to this direct evidence.

References

- Roberts, W.J. 1974, Ap. J. 187, 575.
Petterson, J.A. 1975, Ap. J. 201, L1.

OSO-8 OBSERVATIONS OF HERCULES X-1

S. H. Pravdo[†], R. H. Becker, E. A. Boldt, S. S. Holt,
R. E. Rothschild, P. J. Serlemitsos, and J. H. Swank
NASA/Goddard Space Flight Center
Greenbelt, Maryland 20771

ABSTRACT

The X-ray binary Her X-1 was observed by the GSFC cosmic x-ray detectors aboard OSO-8 between August 26 and September 3, 1975. Our data indicate that Her X-1 turned on in its ~ 35 -day cycle by 10^h UT August 28. The results reported here are based on "quick look" tapes which contain less than 10% of the total time spent on source. Spectra have been observed during different phases of the binary period including the anomalous low state (dip) in X-ray intensity. The normal high spectra is well represented by a power law with a short cutoff above ~ 25 keV. A significant and varying enhancement in the intensity around 6.7 keV is observed, suggesting the presence of an iron line. Absorption is seen in the spectrum immediately following eclipse. The dip spectrum is found to be considerably flattened. Also spectra are presented for different phases of the pulse period.

The GSFC Cosmic X-ray Spectroscopy experiment aboard OSO-8 observed Hercules X-1 for over a week during late August and September of this year. By monitoring real time satellite passes, we were able to determine that Her turned on its X-rays at about 10^h UT August 28, probably near phase .25 of the binary cycle. This time is within the limits of an extrapolation from previous cycles of a ~ 35 day period (Davison and Fabian, 1974). On the basis of "quick look" data which represent a small but significant fraction of the total time on source, we would like to share some spectral observations which perhaps yield clues to the nature of Her X-1

The first spectra (Fig. 1) were actually taken last, leaving Her. The binary eclipse ends at phase .068 so the transition spectrum shown below occurs during the rapid rise to the high state--about 5 minutes. The high state spectrum above shows the same general features as an earlier Goddard observation in a rocket flight (Holt et al., 1974)--a power law in photon intensity per unit energy versus energy with a sharp cutoff around 27 keV. There in addition appears an enhancement in intensity around 7 keV. The transition spectrum can be interpreted as a high state spectrum modified by absorption through cold matter. A better fit is obtained by increasing the iron abundance in the material by a factor of ~ 10 over solar abundance. The absorption is due to $4 - 40 \times 10^{22}$ equivalent hydrogen atoms per square centimeter. From known and estimated orbital parameters it is possible to determine the average path length through which the X-rays are absorbed. Using 5 minutes as the time between total eclipse and high state, this distance is 6×10^{10} cm. Assuming a uniform spherical shell of absorbing material yields an average density of 6×10^{11} atoms/cc. The shell thickness is $\sim 10^{10}$ cm which is larger than the scale height of the HZ Her atmosphere but is approximately equal to the

[†]Permanent address: University of Maryland, College Park, Maryland

difference between theoretical estimates of the stellar radius and the Roche lobe radius.

The second set of spectra (Fig. 2) are the earliest of this group. They were taken with an argon detector with response up to 24 keV so no cutoff is observed. The high state spectrum is similar to the previous high state spectrum from the Xenon detector except that the enhanced intensity around 7 keV has a much narrower width and greater statistical significance--about 7 sigma. This feature can be interpreted as an emission line from iron. This line contains about 6% of the continuum energy between 2 and 10 keV, and has an equivalent width of $\sim .5$ keV.

The lower spectrum was collected 30 minutes after the high state, during one of the intensity dips which occur once per uneclipsed portion of each binary cycle. The X-ray intensity has fallen by a factor of 10 during this dip. In contrast to the transition spectrum shown before, this dip cannot be explained by passage of the high state spectrum through cold matter. In fact the best fit is for a flat photon spectrum (spectral index = 0) with absorption. If ionized matter were the absorber we would not expect such a substantial depletion in the softer X-rays relative to those above 10 keV.

The origin of a varying iron emission line is not clear. Optical emission lines are observed from HZ Herc which vary in intensity relative to the continuum as a function of binary phase. According to one model (Basko and Sunyaev, 1973) the temperature in some areas of the stellar atmosphere heated by the X-rays can reach 10^6 K but even this is low for thermal emission of iron K lines. Fluorescence of iron from either the stellar atmosphere or the neutron star are other possibilities.

Figure 3 is a histogram of the Her light curve folded modulo the 1.24 second pulse period. The pulse shows the characteristic fast rise and slow decay observed before (Doxsey et al., 1973) with little or no interpulse. About 55% of the emission is pulsed--a constant fraction from 2 to 24 keV. Spectra from yet another time were obtained from the photons represented in the two shaded areas.

The upper pulsed spectrum in Figure 4 gives an acceptable fit for a simple power law which may be somewhat flatter than that obtained before. The lower minimum spectrum has the same general shape as the pulsed but also exhibits an enhancement around 6 keV. This is a broad feature and may relate to iron again. Finally, the average spectrum (Figure 5) of all photons in the light curve resembles closely the xenon detector high state.

In summary iron may have been detected in the Her X-1 spectrum both in an emission line (high state) and an absorption edge (transition). Also the region giving rise to the non-pulsed component could be responsible for this iron. Absorption by cold matter can explain the transition spectrum but not the dip spectrum which is considerably flattened.

REFERENCES

- Basko, M. M. and Sunyaev, R. A. 1973, *Astr. and Sp. Sci* 23, 117.
- Davison, P. N. and Fabian, A. C. 1974, *Mon. Not.* 169, 271.
- Doxsey, R., Bradt, H. V., Levine, A., Murthy, G. T., Rappaport, S., and Spada, G. 1973, *Ap. J. (Letters)* 182, L25.
- Holt, S. S., Boldt, E. A., Rothschild, R. E., Saba, J. L. R., and Serlemitsos, P. J. 1974, *Ap. J. (Letters)* 190, L109.

HERCULES X-1
XENON DETECTOR
SEPTEMBER 3, 1975

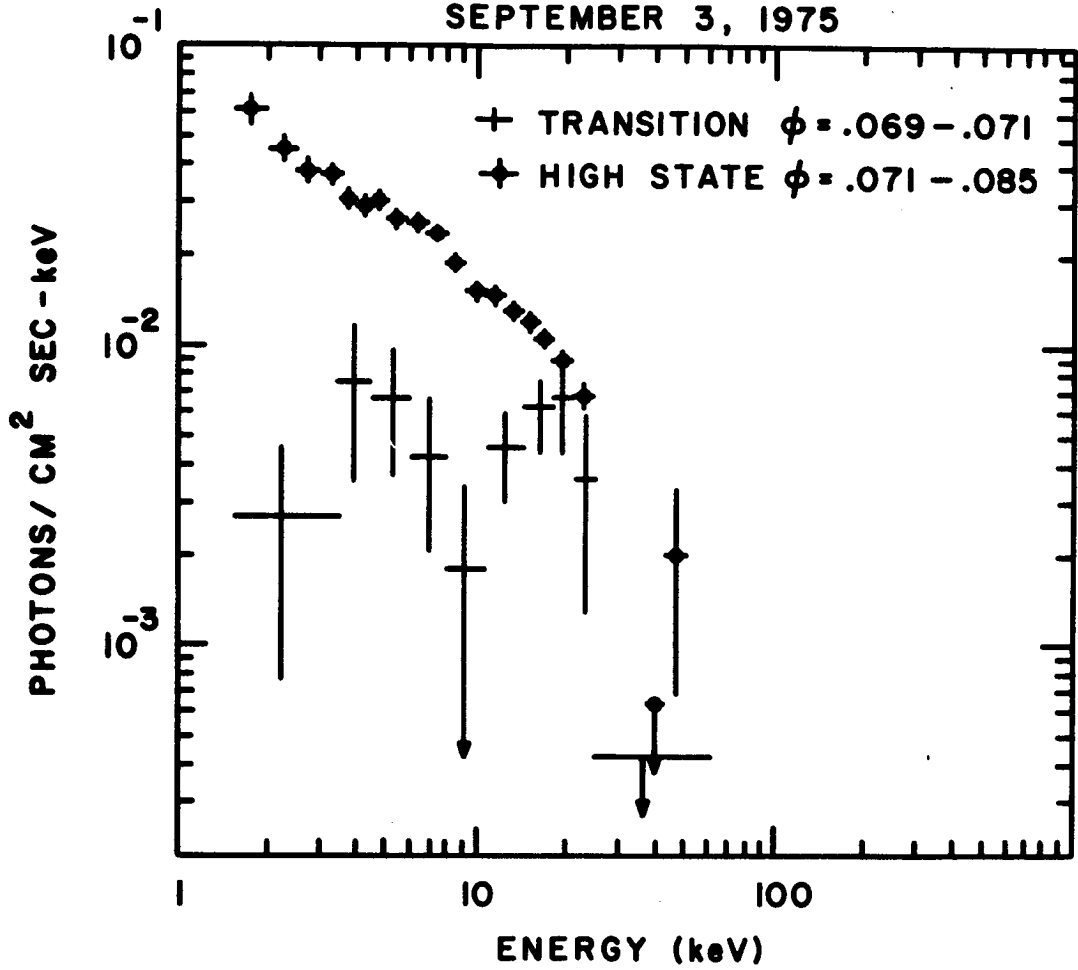


Figure 1. The lower spectrum is data taken from Hercules X-1 for five minutes between total eclipse and high state. The upper spectrum is the high state.

HERCULES X-1
ARGON DETECTOR
AUGUST 30, 1975

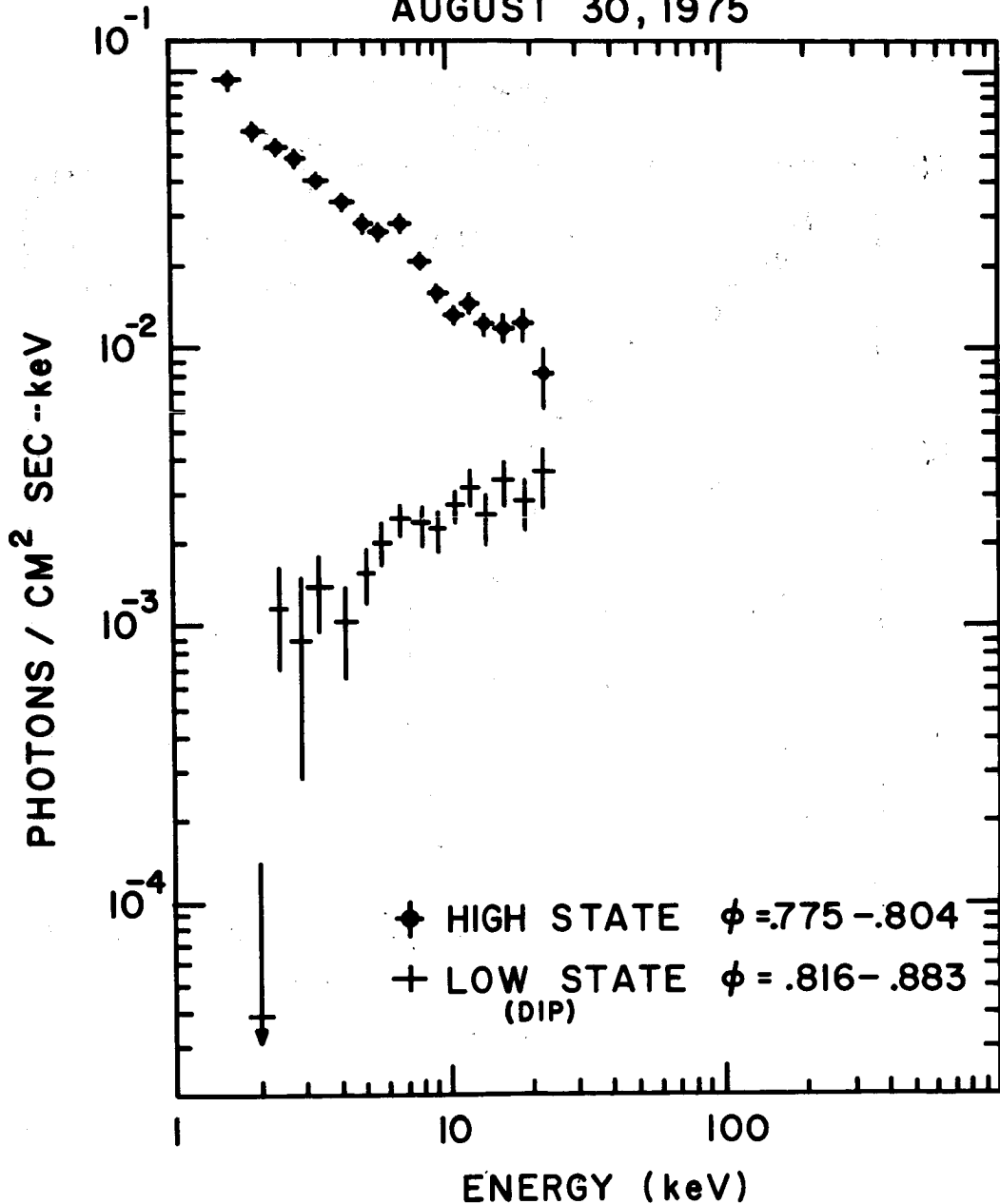


Figure 2. The lower spectrum is of the pre-eclipse dip in intensity. The upper spectrum is a high state which exhibits the strongest and narrowest feature at ~ 7 keV which could be iron line emission.

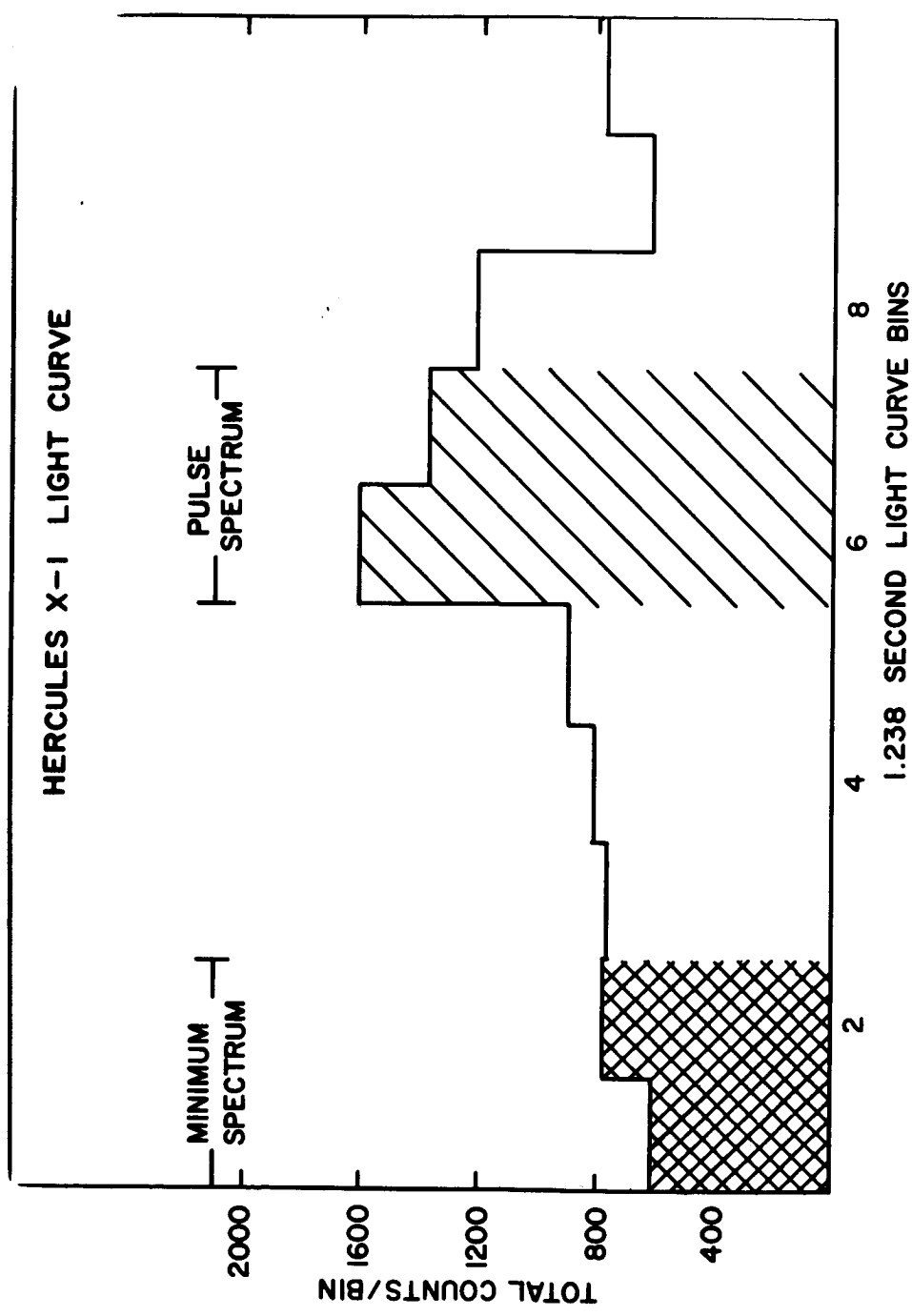


Figure 3. Hercules X-1 light curve folded over the pulse period. Shaded regions indicate photons used for "pulse" and "minimum" spectra.

HERCULES X-1
ARGON DETECTOR
SEPTEMBER 2, 1975

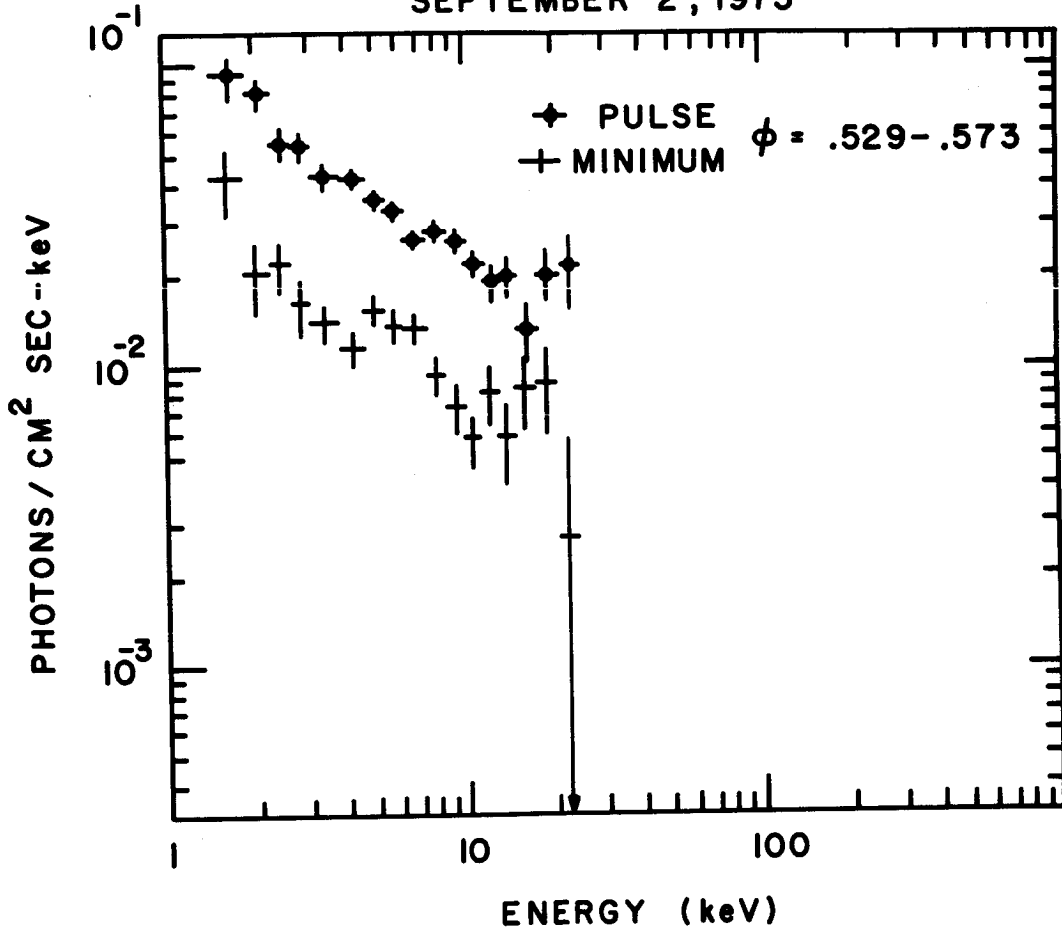


Figure 4. Pulse (upper) spectrum is taken from the peak of the light curve folded over pulse period. Minimum (lower) spectrum is taken from minimum of light curve.

HERCULES X-1
ARGON DETECTOR
SEPT. 2, 1975

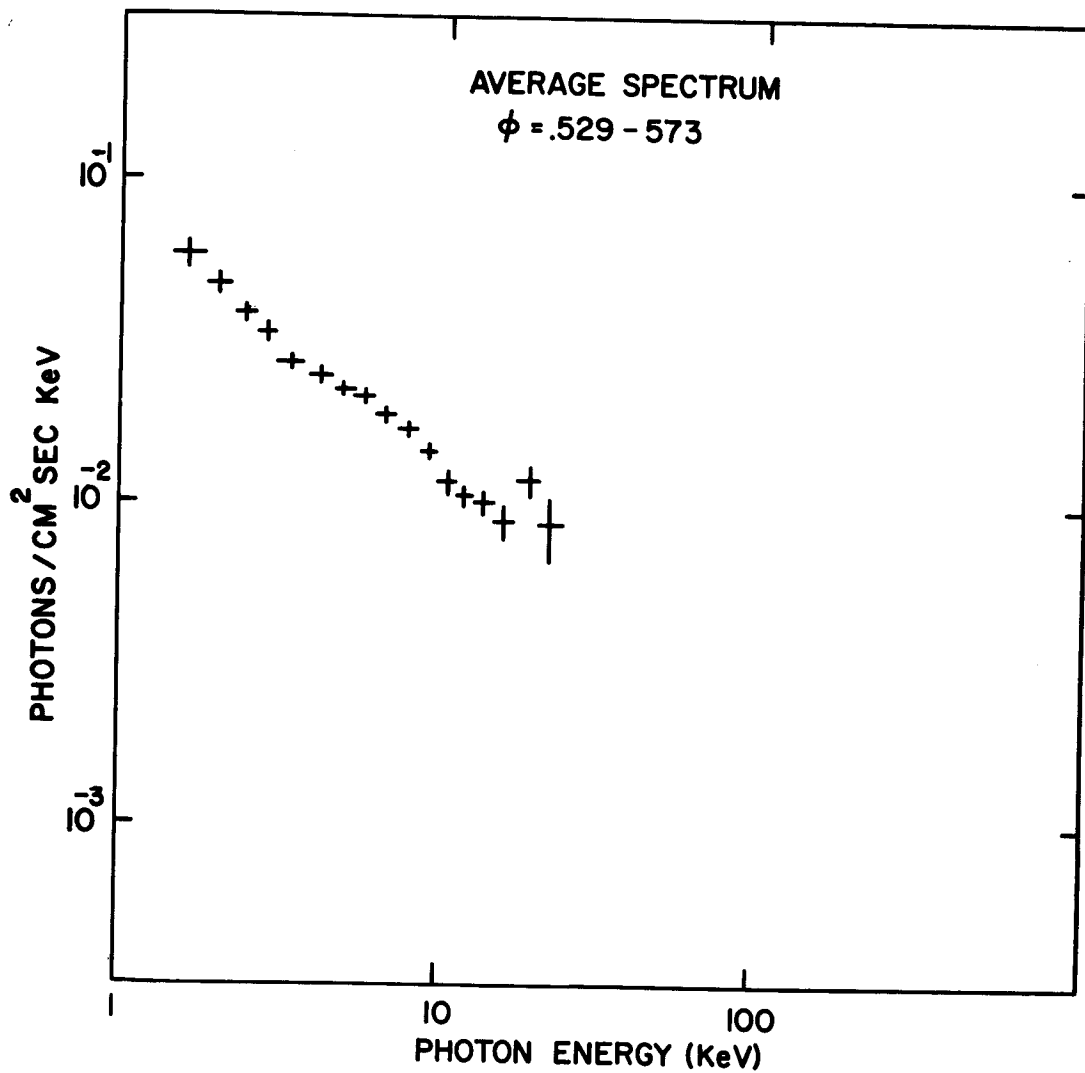


Figure 5. The average spectrum due to all the photons in the Hercules light curve.

OPTICAL FLICKERING IN HZ HERCULIS

Richard H. St. John
Department of Physics and Astronomy
University of New Mexico
Albuquerque, New Mexico 87131

ABSTRACT

Observations of HZ Herculis over two 35^d periods show the existence of nonperiodic optical flickering. The flickering peaks at phase 0.5 in the 1.7^d period. The difference of the flickering curves obtained during X-ray on and X-ray off shows no detectable 35^d dependence.

THE 35^d CYCLE DEPENDENCE OF THE 1.7^d B-V
LIGHT CURVE OF HZ HERCULIS

Richard H. St. John and Victor H. Regener
Department of Physics and Astronomy
University of New Mexico
Albuquerque, New Mexico 87131

ABSTRACT

The 1.7^d light curve obtained during two 35^d cycles of HZ Herculis shows a hot component during X-ray on that is not seen during X-ray off. The disappearance of this hot component near X-ray eclipse suggests that it is associated with the X-ray source.

HER X-1

Discussion

Comments following paper read by R. Henry (Soft X-Rays From Her X-1 During the "Off" Phase).

- H. Gursky - Since the pulsation is 50% at 1-2 keV, if you can detect the x-rays at all, you can detect the pulsation. Have you Fourier-analysed the 1-2 keV data?
- R. Henry - No, we have not. We only realized a few days ago that we were detecting Her X-1 in this energy range. This is certainly something that should be done, and we will do it.
- D. Eardley - The model of Thorne and Price is for Cygnus X-1, not for Hercules X-1, and will not be directly applicable to that object.
- R. Henry - This is certainly true. Thorne and Price are dealing with black holes in general, and Cygnus X-1 in particular, and we are dealing with the accretion disk of a neutron star, Hercules X-1. We are guided by Thorne and Price only because it seems to be the only thing available. It may be entirely inappropriate.
- P. Joss - The suggestion that the spectral shape is the same in the "off" phase as in the "on" phase, but reduced in intensity, is consistent with a picture wherein the 35-day cycle is due to variable grey obscuration. Such observation could be produced by electron scattering in very highly ionized matter that periodically intercepts the line of sight between the source and the earth.
- R. Henry - There is a most important point, which I simply forgot to mention. R. Giacconi and his colleagues (Ap. J. 184, 227, 1973; Ann. N. Y. Acad. Sci. 262, 312, 1975) have found that there is no detectable change in the spectrum of Her X-1 as the off-phase commences. Also, Joss and Fechner (Ann. N. Y. Acad. Sci. 262, 385, 1975) have found that the Her X-1 pulse shape varies little during most of the "on" phase, but that the pulsations disappear as the "off" phase commences. They suggested that both the variable obscuration of the pulses and the production of the unpulsed component are due mostly to electron scattering by very highly ionized matter.

CENTAURUS X-3: THE OBSERVATIONAL PICTURE

H. Mauder
 Astronomisches Institut
 Universität Tübingen
 D-7400 Tübingen Fed. Rep. of Germany

In their well known paper Schreier et al. (1972) were able to identify for the first time a stellar X-ray source with a binary star. The analysis of the 4.84 s pulsations yielded a sinusoidal variation of the pulsation period due to Doppler-effect. Variability in the X-ray intensity was interpreted as an eclipse of the X-ray emitting source by a large, massive companion. They derived the orbital period and the mass function which allowed for a first interpretation of the system. Besides of that they found a short transition stage between the high and the low level of the X-ray intensity, due to an atmospheric occultation of the X-ray emitter by the large companion. Their main results were

Time of Mid-eclipse	JD	(244 1132.081 \pm 0.001) +(2.08712 \pm 0.00004) x E
Mean pulsation period		4.842 s
Projected orbital velocity		415.1 \pm 0.4 km s ⁻¹
r sin i		(1.191 \pm 0.001) x 10 ¹² cm
Mass function		(3.074 \pm 0.008) x 10 ³⁴ g
Duration of total eclipse		(0.488 \pm 0.012) d
Duration of transition		(0.035 \pm 0.007) d

Based on these results several authors used the eclipse duration together with a limiting Roche configuration and the mass function to derive the individual masses of the two components, see e. g. Wilson (1972), Osaki (1972) and van den Heuvel and Heise (1972), and got astonishingly low values for the mass of the neutron star. It was pointed out by Weedman and Hall (1972) and by McCluskey

and Kondo (1972) that the derived results might be remarkably altered by the presence of obscuring material outside of the Roche limiting surface. A theoretical model for pulsating X-ray binaries was presented by Davidson and Ostriker (1973) who mentioned also the importance of departure from corotation for the massive primary star. In this case the Roche configuration must be replaced by a Tidal limiting surface, which in turn leads to remarkably different results for the limiting masses in the system.

Krzeminski (1974) succeeded in identifying the optical counterpart of Cen X-3 with a 13.4 mag, heavily reddened star just outside the UHURU error box of Giacconi et al. (1974), but inside the refined error box derived by Parkinson et al. (1974) from Copernicus observations. Spectroscopic observations by Rickard (1974), Vidal et al. (1974) and Osmer et al. (1975) show the primary star to be an early type giant or supergiant of spectral type O 6.5 (Osmer), O 9.5 - B 0.5 Ib (Rickard) or O 9 III - V (Vidal). P Cygni type profiles are seen in several lines indicating an expansion of the stellar atmosphere with a velocity of 800 km s^{-1} . Comparison of the spectra with the non-LTE model atmospheres of Auer and Mihalas (1972) shows that the spectra are consistent with values of $T_{\text{eff}} = 30\,000 - 32\,000 \text{ K}$ and $\log g = 3.5$. No spectral changes with the orbital phase were detected thus indicating that heating of the visible star by the X-rays plays no important role.

Optical light curves were obtained by Krzeminski (1974), Mauder (1975) and Petro (1975). The light curves show a double wave with an amplitude for the deeper minimum of 0.10 mag (Petro), 0.12 mag (Krzeminski) and 0.14 mag (Mauder). The light variations are interpreted as due to the orbital motion of the distorted primary star around the center of gravity. From the light curves it is possible to derive limiting values for the mass ratio thus yielding lower limits on the mass of the compact object, which is believed to be a neutron star. Petro and Mauder derived remarkably high lower limits for the mass of the neutron star, $2.5 M_{\odot}$ and $3.0 M_{\odot}$, respectively. A rediscussion of the system properties, including the duration of the X-ray eclipses, for instance by Avni and Bahcall (1975) and by Wickramasinghe (1975), give lower limiting masses. The problem of interpreting the optical light curves will be discussed later in this panel. Krzeminski (1974) and Mauder (1975) also derived UBV colours for Cen X-3, giving

	V	B-V	U-B
Krzeminski	13.35 mag	+1.065 mag	-0.04 mag
Mauder	13.38	+1.04 \pm 0.02	-0.08 \pm 0.02

The high amount of reddening of the early type star as well as the appearance of interstellar lines in the spectrum points to a large distance of Cen X-3. A reasonable estimate of a distance between 6 and 9 kpc was recently given by Humphreys and Whelan (1975) who also refer to earlier distance determinations.

The X-ray pulsations were observed in several energy bands over a longer time interval by Baity et al. (1974) and by Ulmer et al. (1974). Additional X-ray observations were obtained with the Copernicus satellite by Tuohy and Cruise (1975) and with the Ariel 5 satellite by Pounds et al. (1975). Pounds et al. were able to observe the transition of Cen X-3 from an extended low during several consecutive orbital cycles until to the normal high stage. The observations support the model of extended lows to be caused by enhanced activity of the stellar wind from the primary star. Several dips were observed in the X-ray intensity during the uneclipsed high state by Pounds et al. as well as by Tuohy and Cruise. The simultaneous hardening of the X-ray spectrum during the dips is consistent with the interpretation of the dips as absorption by circumstellar matter and probably due to the shock front of an accretion wake in the stellar wind. Pounds et al. derived from the Ariel 5 data the times of minima of Cen X-3 and concluded, that the orbital period of Cen X-3 remained constant between May 1972 and November 1974 within the range of uncertainty given for the UHURU data by Schreier et al. (1972). On the other hand, Tananbaum and Tucker (1974) give the variations of the orbital period of Cen X-3, based on UHURU data from 1971 and 1972. They also report variations in the 4.84 s pulse period, probably correlated with extended low states.

A search for optical 4.84 pulsations was done by Lasker (1974), Canizares and McClintock (1974) and Peterson et al. (1975) with negative result. However, as mentioned by Tuohy and Cruise (1975), this search was done during extended low stages of Cen X-3; the X-ray intensity of Cen X-3 was almost certainly weak and optical pulsations were hardly to be expected during this research.

Several theoretical investigations were also done on Cen X-3 but it is not the aim of this short review to discuss those papers.

REFERENCES

- Avni, Y., J. N. Bahcall, 1975, preprint
Auer, L. H., D. Mihalas, 1972, Ap. J. Suppl. 24, 193
Baity, W. A., M. P. Ulmer, W. A. Wheaton, L. E. Peterson, 1974, Ap. J. 187, 341
Canizares, C. R., J. E. McClintock, 1974, Ap. J. 193, L65
Davidson, K., J. P. Ostriker, 1973, Ap. J. 179, 585
Giacconi, R., S. Murray, H. Gursky, E. Kellogg, E. Schreier, T. Matilsky,
D. Koch, H. Tananbaum, 1974, Ap. J. Suppl. 27, 37
Humphreys, R. M., J. Whelan, 1975, preprint
Krzeminski, W., 1974, Ap. J. 192, L135
Lasker, B. M., 1974, Nature 250, 308
Mauder, H., 1975, Ap. J. 195, L27
McCluskey, G. E., Y. Kondo, 1972, Ap. Space Sci. 19, 279
Osaki, Y., 1972, Publ. Astr. Soc. Japan 24, 419
Osmer, P. S., W. A. Hiltner, J. A. J. Whelan, 1975, Ap. J. 195, 705
Parkinson, J. H., K. O. Mason, P. W. Sanford, 1974, Nature 249, 746
Peterson, B. A., J. Middleditch, J. Nelson, 1975, Ap. J. 195, L31
Petro, L. D., 1975, Ap. J. 195, 709
Pounds, K. A., B. A. Cooke, M. J. Ricketts, M. J. Zurner, M. Elvis, 1975,
Mon. Not. R. A. S. 172, 473
Rickard, J. J., 1974, Ap. J. 189, L113
Schreier, E., R. Levinson, H. Gursky, E. Kellogg, H. Tananbaum,
R. Giacconi, 1972, Ap. J. 172, L79
Tananbaum, H., W. H. Tucker, 1974, in X-ray Astronomy, eds. R. Giacconi, H.
H. Gursky, Dordrecht, p. 207
Tuohy, I. R., A. M. Cruise, 1975, Mon. Not. R. A. S. 171, 33P
Ulmer, M. P., W. A. Baity, W. A. Wheaton, L. E. Peterson, 1974, Ap. J. 191, 593
van den Heuvel, E. P. J., J. Heise, 1972, Nature Phys. Sci. 239, 67
Vidal, N. V., D. T. Wickramasinghe, B. A. Peterson, M. S. Bessell, 1974,
Ap. J. 191, L23
Weedman, D. W., D. S. Hall, 1972, Ap. J. 176, L19
Wickramasinghe, D. T., 1975, Mon. Not. R. A. S. 173, 21
Wilson, R. E., 1972, Ap. J. 174, 227

CENTAURUS X-3 PANEL SUMMARY

H. Mauder
Astronomisches Institut
Universität Tübingen
D-7400 Tübingen
Fed.Rep. of Germany

From the presentations and subsequent discussions it turned out, that we are still far from being able to present a model for Cen X-3, which explains all the observations and details, especially in the X-ray region. However, a general picture can be given which may serve at least as a preliminary model. To a first approximation Cen X-3 can be described in terms of the Roche model with the primary star filling or almost filling its critical surface. The spectrum of the primary star is not classified beyond any doubt; the spectral type is around O9 with an uncertainty of one or possibly even two subclasses. The luminosity class is most probably about III. It is difficult to find a solution for the mass ratio which is consistent with the X-ray eclipse duration as well as with the amplitude of the optical light variations. For an orbital inclination close to 90° it was shown, that the eclipse duration is not in conflict with a mass ratio less than 0.12; on the other hand, an explanation of the light curves requires a mass ratio at least equal to or larger than 0.12. No consistent solution is possible if the inclination is remarkably less than 90° . Therefore, the most probable values for Cen X-3 are

Orbital inclination	$80^\circ - 90^\circ$
Mass of Primary	$19.5 M_\odot$
Mass of Secondary	$2.3 M_\odot$

Consequently the compact object in Cen X-3 should be a neutron star.

Stellar wind activity is present and variable in time, as is clearly shown by the observations of UHURU, Copernicus and Ariel 5. The extended lows in Cen X-3 are due to enhanced stellar wind activity rather than to a fading out of the stellar wind. This was obviously seen in the time dependent behaviour during disappearance and reappearance of the X-ray source. In the X-ray inten-

sity between the eclipses pronounced dips are seen around orbital phase 0.7. The dips are correlated with a hardening of the spectrum indicating obscuration by circumstellar material. Very probably the dips are due to the shock front of an accretion wake in the stellar wind. The position of the dips gives a measure of the wind velocity in the system at the distance of the compact object from the primary star. Detailed studies of the spectral behaviour in the X-rays yielded a very complex structure. There is an indication of absorption by ionized and by cold matter, variable features may be due to absorption and emission by iron and other elements. In general, the interpretation of the X-ray spectra presents a very difficult problem.

A study of the times of mid-eclipse yielded no significant variations of the orbital period since 1972. Studies of the X-ray pulses gave a linear speeding up of the mean pulse period according to the accretion of mass on the compact object. The Doppler shift of the pulses due to the orbital motion allowed for the determination of an upper limit of the orbital eccentricity which must be less than $e = 0.003$. Estimates of the hydrogen column density gave some suggestion of the influence of the interstellar matter on the low-energy cut-off in Cen X-3; again the variable effects cannot be interpreted by a simple model.

THE INTERPRETATION OF OPTICAL LIGHT VARIATIONS OF CENTAURUS X-3

H. Mauder
Astronomisches Institut
Universität Tübingen
D-7400 Tübingen Fed.Rep. of Germany

ABSTRACT

The interpretation of optical light variations of X-ray binaries is discussed for the case of negligible reflection effect. The limiting cases of synchronous rotation of the visible star (Roche configuration) and of no rotation (pure tidal deformation) are considered. The theoretical results are compared with the available light curves of Cen X-3. X-ray data of the Copernicus satellite are used to get an impression of the atmospheric structure of the outer layers of the visible component. It is shown, that the X-ray eclipse duration is in good agreement with the mass ratio derived from the optical variations. The X-ray eclipse duration is discussed with respect to the extended low states and a possible correlation of the extended lows with the appearance of the optical light curves is considered.

INTRODUCTION

In binary systems, like Cen X-3, where only the mass function is available, it is necessary to get additional information on the mass ratio to derive limiting masses of the components. There are two informations which can be helpful: the duration of the X-ray eclipse and the amplitude of the light variations. However, both values are derived empirically and may be subject to observational errors as well as systematic ones. This is clearly demonstrated by the extreme solutions of Wilson (1972), who finds a maximum mass for the neutron star of $0.23 M_{\odot}$ using the eclipse duration, and that of Mauder (1975), which yielded a lower limit for the mass of the neutron star of $3.0 M_{\odot}$ from the light curve.

It is also especially necessary to allow for the possibility of no bound rotation of the primary star, as pointed out by Davidson and Ostriker (1973). Modeling the shape of the primary star for calculations of the eclipse duration and for obtaining synthetic light curves, the Roche limiting lobe as well as the Tidal lobe must be taken into account as extreme cases.

MODEL LIGHT CURVES

The program for generating synthetic light curves was set up by Ammann (1976). It is based on the papers of Hutchings and Hill (1973), but with different handling of the geometry and the integration grid and with a variable opacity coefficient for the stellar atmosphere. For a comparison of the results with the data of Wickramasinghe and Whelan (1975) some test cases were calculated. The amplitudes for orbital phase 0.0 (X-ray eclipse) are identical with the values of the grey atmosphere program of Wickramasinghe and Whelan within 0.001 mag and are on the average 0.005 mag lower for phase 0.5 (inner Lagrangian point towards observer). The same was done for the case of pure tidal distortion, the results were compared with Wickramasinghe (1975). Again there is excellent agreement for phase 0.0 but the amplitudes for phase 0.5 are on the average 0.005 mag lower than those of Wickramasinghe. This small difference is probably caused by the local variability of the opacity coefficient, the deviation from the mean opacity coefficient is largest in the vicinity of the inner Lagrangian point. For particulars see Mauder (1976).

According to the spectroscopic results model light curves for Cen X-3 were calculated for $T_{\text{eff}} = 30\,000\text{ K}$, an assumed orbital inclination $i = 90^\circ$ and the mass ratios $q = M_x/M_1 = 0.05$ (dotted line) and $q = 0.15$ (full line). The Roche geometry is used. In Figure 1 the observed light curves are shown together with the model light curves. The light curve on the top represents the observations of Mauder (1975), in the middle are the observations of Petro (1975) and at the bottom the values of Krzeminski (1974). It is evidently seen that a mass ratio as small as $q = 0.05$ is in conflict with the observations while $q = 0.15$ gives a satisfactory fit. Replacing the Roche geometry by a tidal lobe reduces the amplitudes of the theoretical curves by about

5 % for phase 0.0 and by 10 % for phase 0.5 for the same mass ratio; a reduction of an equal amount is introduced by changing the orbital inclination from $i = 90^\circ$ to $i = 75^\circ$. No definite values for i and q can be derived from the light curves available, but limiting cases are obviously given. An inclination i remarkably smaller than 90° forces the mass ratio to be larger than $q = 0.15$. On the other hand, if i is close to 90° , than a mass ratio in the range $0.10 < q \leq 0.15$ is necessary.

ECLIPSE DURATION

It was pointed out already by Schreier et al. (1972) that the duration of the X-ray eclipse in Cen X-3 seemed to be variable. It is clearly shown by Pounds et al. (1975) how the X-ray eclipse half angle ν_E^h is affected by the activity of the stellar wind. Pounds et al. find an eclipse half angle for the undisturbed X-ray light curve of $39^\circ \pm 2^\circ$. Avni and Bahcall (1975) derive the mass ratio especially from the eclipse half angle. However, in the mass ratio range under consideration q depends very sensitively on the right value of ν_E^h . In the case of Roche geometry $\nu_E^h = 39^\circ$ corresponds to $q = 0.07$ while $\nu_E^h = 36^\circ$ gives $q = 0.12$. On the other hand it seems questionable, whether in a star with an expanding atmosphere, which produces an observable stellar wind, the Roche limiting surface can be attributed to the atmospheric layer which causes the X-ray eclipses. To get an impression of the importance of the effect, the Copernicus data of Parkinson et al. (1974), who observed the atmospheric eclipse, were used to derive the structure of the outer atmosphere of the Cen X-3 optical star. An exponential atmosphere was assumed with

$$\kappa_g = \kappa_0 \exp(-\alpha r)$$

where r is the radial distance from the center of the star in units of the orbital diameter. In Figure 2 the respective optical depths are shown for $\alpha = 20$ and $\alpha = 25$, together with the optical depths of the 4 - 12 keV band observations. An extrapolation of the Copernicus data to an optical depth $\tau = 1$ gives $\nu_E^g = 40.5^\circ$. Taking the mean absorption cross section per proton from Cruddace et al. (1974) for the X-rays and assuming the mean opacity in the visible region to be due to Thompson scattering on

free electrons, yields an optical depth $\tau = 1$ in the visible light at $\nu_E^{\beta} = 36^{\circ}$. Therefore, the optical photosphere which is used for the light curve calculations and is normally identified with the Roche limiting lobe, maybe somewhat smaller than the lobe suggested by the X-ray eclipse duration.

The scale height derived for the atmosphere is 6×10^{10} cm and the number density $n_H = 4 \times 10^{12} \text{ cm}^{-3}$ above the optical photosphere at $r = 0.59$. This is in good agreement with Schreier et al. (1972) who estimated a scale height of 5×10^{10} cm and a number density in the order of 10^{12} cm^{-3} . If the optical photosphere is identified with the limiting lobe of the star, than the mass ratio from the X-ray eclipse duration would be $q = 0.12$ in the Roche case and $q = 0.17$ in the Tidal case. Since the mass ratio depends very sensitively on the eclipse angle it is at least dangerous, to take the mass ratio derived from this value as granted.

DISCUSSION

Trying to find a consistent model for Cen X-3 it seems to be most reasonable to accept a mass ratio $q = 0.12$ and an inclination i close to 90° . It would be very difficult to understand the eclipse duration with a larger mass ratio. On the other hand, a lower mass ratio or a lower inclination would be in conflict with the optical light curves. The most probable values for Cen X-3 are therefore $M_1 = 19.5 M_{\odot}$ and $M_X = 2.34 M_{\odot}$. As a consequence, the projected orbital velocity of the primary star would be $v_1 \sin i = 50 \text{ km s}^{-1}$. This is still a possible value according to the spectral investigation of Osmer et al. (1975).

It might be questionable whether the synthetic light curves are adequate to describe the light changes in X-ray binaries. However, the detection of pulsed X-rays in Vela X-1 offers the possibility of a test calculation. Particulars on Vela X-1 will be discussed later in this symposium, but from the mass ratio $q = 0.084$ the theoretical light amplitudes can be calculated to be 0.073 mag and 0.098 mag. The observed values are, according to Wickramasinghe and Whelan (1974), 0.08 mag and 0.10 mag. The agreement is satisfying. It should be noted that the three light curves of Cen X-3 are some-

what different, showing also different amplitudes. Of course, intrinsic variability of the optical star is superposed on the pure rotational light changes. However it should be noted that the light curves are taken at different stages of X-ray activity, and therefore also stellar wind activity, of the system. From Tuohy and Cruise (1975) it can be seen, that the observations of Krzeminski are taken partly during high stages and partly during extended lows of X-ray intensity. The light curve of Petro was taken mainly during an extended low and the light curve of Mauder during a high stage. It would be interesting to investigate further the influence of stellar wind activity on the light variations.

REFERENCES

- Ammann, M., 1976, *Mitt. Astron. Ges.* 38, in press
 Avni, Y., J. N. Bahcall, 1975, preprint
 Cruddace, R., F. Paresce, S. Bowyer, M. Lampton, 1974, *Ap. J.* 187, 497
 Davidson, K., J. P. Ostriker, 1973, *Ap. J.* 179, 585
 Hutchings, J. B., G. Hill, 1973, *Ap. J.* 179, 539 and references
 Krzeminski, W., 1974, *Ap. J.* 192, L136
 Mauder, H., 1975, *Ap. J.* 195, L27
 Mauder, H., 1976, *Mitt. Astron. Ges.* 38, in press
 Osmer, P. S., W. A. Hiltner, J. A. J. Whelan, 1975, *Ap. J.* 195, 705
 Parkinson, J. H., K. O. Mason, P. W. Sanford, 1974, *Nature* 149, 746
 Petro, L. D., 1975, *Ap. J.* 195, 709
 Pounds, K. A., B. A. Cooke, M. J. Ricketts, M. J. Turner, M. Elvis, 1975, *Mon. Not. R. A. S.* 172, 473
 Schreier, E., R. Levinson, H. Gursky, E. Kellogg, H. Tananbaum, R. Giacconi, 1972, *Ap. J.* 172, L79
 Tuohy, I. R., A. M. Cruise, 1975, *Mon. Not. R. A. S.* 171, 33P
 Wickramasinghe, D. T., J. Whelan, 1974, *Mon. Not. R. A. S.* 167, 21 P
 Wickramasinghe, D. T., J. Whelan, 1975, *Mon. Not. R. A. S.* 172, 175
 Wickramasinghe, D. T., 1975, *Mon. Not. R. A. S.* 173, 21
 Wilson, R. F., 1972, *Ap. J.* 174, L27

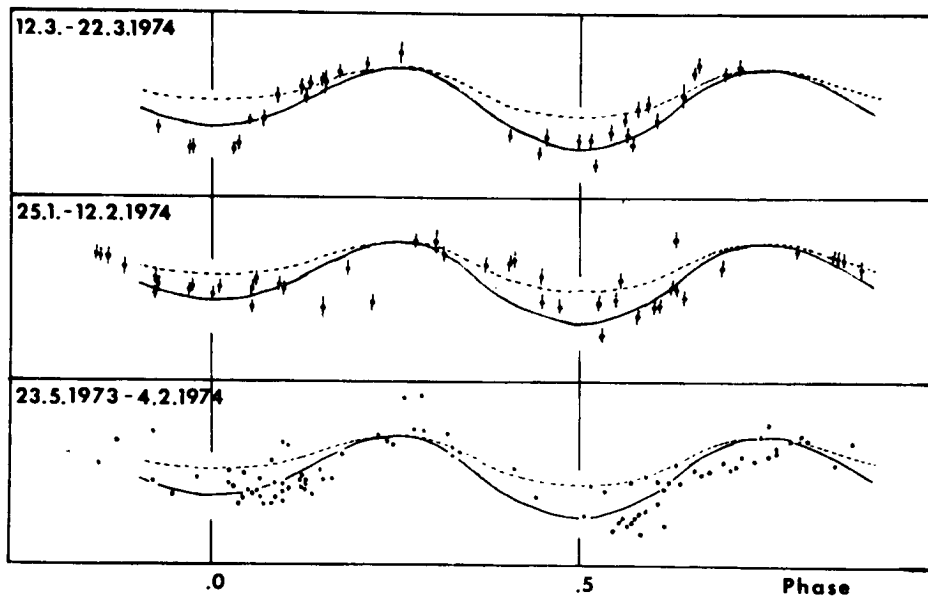


Figure 1: Observed light curves of Cen X-3 in the visual region. Theoretical light curves for $i = 90^\circ$ and Roche geometry are given for the mass ratios $q = 0.05$ (dotted) and $q = 0.15$ (full line).

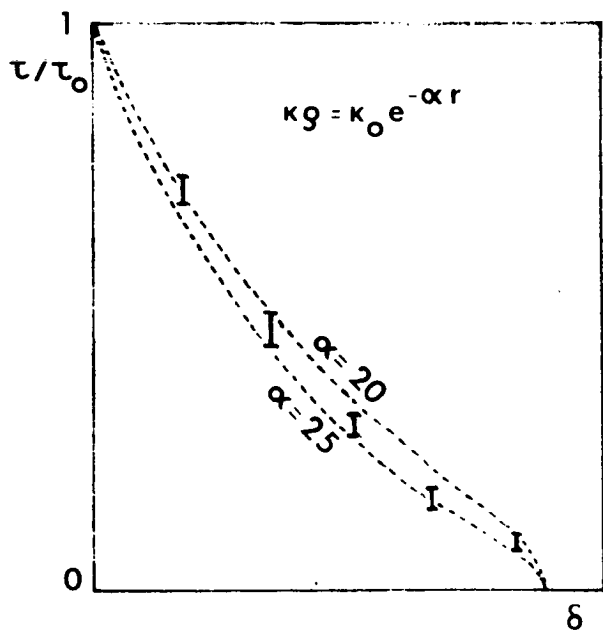


Figure 2: Normalized optical depths for two exponential atmospheres, together with the Copernicus X-ray optical depths derived from the data of Parkinson et al. (1974).

Wisconsin Soft X-Ray Observations of Cen X-3

A. N. Bunner and W. T. Sanders

Dept. of Physics, Univ. of Wisconsin

Abstract

A sounding rocket experiment on 12 November 1973 observed pulsed X-rays from the vicinity of Cen X-3 in the 0.6 to 10 keV range with a period of 4.84 sec while Cen X-3 was at binary phase 0.41. The intensity is roughly consistent with that reported by Bleeker et al. (Ap. J. 183, L1, 1973). The pulsed fraction in the 0.6 to 2 keV band is small, consistent only with the low energy tail of an absorbed ~ 15 keV bremsstrahlung spectrum. An additional non-pulsed component is required between 0.6 and 2 keV to fit the observations. Fast Fourier transform analysis of the $\sim 10^4$ counts recorded reveals no evidence for other periodicities in the range 0.2 to 260 Hz.

THE INTERSTELLAR MATTER COLUMN DENSITY TO CEN X-3.

C. Ryter*
NASA/Goddard Space Flight Center
Greenbelt, Maryland 20771

ABSTRACT

The usual gas-to-dust ratio has been shown to hold quite precisely for a sample of supernova remnants with available X-ray spectra and interstellar reddening observations. Supernova remnants are extended objects, tenuous enough to be optically thin in the X-ray range; it appears that the X-ray observations can readily be interpreted in terms of a main source component and of an interstellar perturbation affecting the lower part of the spectrum. The value

$$N_{\text{H}}/E_{\text{B-V}} = (6.8 \pm 1.5) \times 10^{21} \text{ H atoms cm}^{-2} \text{ mag}^{-1} \quad (1)$$

has been found to hold, without any sizeable systematic deviation up to $E_{\text{B-V}} \approx 1.7$. Here, N_{H} expresses the total hydrogen column density, including ionized, atomic, and molecular forms.

Cen X-3 is associated with an OB supergiant, and $E_{\text{B-V}} = 1.29$ mag; eq. 1 thus yields $N_{\text{H}} = 8.8 \times 10^{21}$ H atoms cm^{-2} . The effect of such a column density is easily detectable in the X-ray range. The spectrum exhibits a low energy cut-off, which, according to the usual practice, is parametrized by a column of cold matter, N_{X} . The cut-off is definitely observed to be variable, and values of N_{X} range from ~ 0 to 1.5×10^{23} H atoms cm^{-2} . There is a suggestion that sometimes $N_{\text{X}} < N_{\text{H}}$. It may be concluded that on those occasions a spurious soft X-ray component is present in the source, bearing close similarity with Cyg X-1. When N_{X} is large, self-absorption in an optically thick gas is very likely to take place.

INTRODUCTION

Absorption of x-rays emitted by cosmic sources is due to photoelectric effect, mainly taking place in medium Z-elements (C, N, O, Ne, Si---). Interstellar extinction is produced by dust grains which are mostly built from some of the same elements (C, O, Si---). Consequently, one may expect both attenuation effects to be correlated, and indeed it is observed to be the case in the galactic plane, for distances ranging from

*NAS/NRC Research Associate. On leave from the French Atomic Energy Commission.

some hundreds of parsecs to a few kiloparsecs of the sun.

Interstellar matter column density to an X-ray source can be evaluated whenever it is associated with a well-defined object for which a color excess can be assigned. Such a case is exhibited by Cen X-3, which is a compact X-ray source forming a binary system with an OB Ib supergiant star. The color excess, $E_{B-V} = 1.29$, is one of the largest observed in identified X-ray sources. The determination of the interstellar matter column density independently of X-ray observations allows an unambiguous assessment of the spectrum of the source to be made.

X-RAY ABSORPTION

Absorption of X-rays in interstellar space is due to photoelectric interaction. It is practically independent of the physical state of the matter (solid, gaseous, or ionized), provided the K-electrons are not stripped from the nuclei. The cross-section $\sigma_{\text{e}}(E)$ of a mixture of elements with universal, or cosmic, abundances is represented in figure 1. At photon energies $E \geq 0.5$ keV, elements with $Z \geq 16$ are obviously dominant, and the large contribution of oxygen is due to its large relative abundance, $A = 8.9 \times 10^{-4}$. It is usual practice in X-ray astronomy to parametrize the observed spectra using some simple function (free-free radiation, black body, power law), and to introduce a low frequency cut-off produced by a column of intervening cold matter, N_{X} . It must be clear that (i) N_{X} is expressed in H atoms cm^{-2} and explicitly relies on the assumption that universal abundances hold, and (ii), other mechanisms inherent to the source may contribute to the cut-off, as, for instance, a non-negligible optical thickness. The contribution of the true interstellar absorption to N_{X} will be expressed as N_{H} in the sequel, based on qualification (i).

INTERSTELLAR REDDENING

Some of the medium Z-elements which absorb X-rays in interstellar space are believed to be the constituents of the dust grain which scatter light, giving rise to interstellar extinction, A_{V} , or reddening, E_{B-V} . It is indeed found that X-ray absorption and interstellar reddening correlate surprisingly well in the case of extended sources which are optically thin throughout the X-ray range. In figure 2, the observed quantity N_{X} is plotted as a function of the color excess E_{B-V} for a sample of supernova remnants. The data are those used by Ryter et al. (1975) in a similar plot, complemented by more recent results from Moore and Garmire (1975) for Vela X, from Charles et al. (1975) for Cas A, and from Hill et al. (1975) for Cas A and Tycho's supernova. The spectra of the sources are believed to be relatively well understood and interpreted, and a strong case can be made that $N_{\text{X}} \equiv N_{\text{H}}$. The value

$$N_{\text{H}}/E_{B-V} = (6.8 \pm 1.5) \times 10^{21} \text{ H atoms cm}^{-2} \text{ mag}^{-1} \quad (1)$$

is found, where N_{H} includes any three forms of hydrogen, ionized, atomic, and molecular.

THE COLUMN DENSITY TO CEN X-3

The spectral type of the star associated with Cen X-3 has been studied in detail by several authors (see H. Mauder, this conference); the interstellar reddening is $E_{B-V} = 1.29$ to 1.30 mag (Rickard 1974; Mauder 1975). Thus

equation 1 yields for the column density of the object

$$N_H = 8.8 \times 10^{21} \text{ H atoms cm}^{-2} \quad (2)$$

Since Cen X-3 is located at 10 kpc of the sun, but at ~ 11 kpc of the galactic center and at a distance of ≈ 60 pc of the galactic plane, the line of sight to it crosses a region of the Galaxy which is large, but which should not have properties much different of those prevailing in the solar vicinity. For instance, the average density is $\langle n_H \rangle = 0.28 \text{ cm}^{-3}$. It is interesting to note that the column density of atomic hydrogen, N_{HI} , deduced from 21 cm observations is $N_{HI} = 4 \times 10^{21} \text{ H atoms cm}^{-2}$ (Hindman and Kerr 1970), i.e. only about half the total hydrogen column density. This result is in good agreement with the estimate that molecular hydrogen is as abundant as atomic hydrogen (Hollenbach et al. 1971).

DISCUSSION

The values of N_X which have been reported for Cen X-3 are listed in table 1. There are obvious time variations, which cover a wide range. However, there is no need to attribute them to variations of the density of intervening matter. To the accuracy of proportional detectors, self absorption in an optically thick source can easily mimic photoelectric absorption. For instance, Giacconi et al. (1971) obtained very similar spectra (and a good fit to their data), either assuming an optically thin source ($kT \sim 16 \text{ keV}$) with $N_X = 1.5 \times 10^{23} \text{ H atoms cm}^{-2}$, or assuming an optically thick source, i.e. a black body ($kT \sim 3 \text{ keV}$), with $N_X = 0$. In this case, the spectrum peaks at $kT \sim 6 \text{ keV}$, and the contribution of interstellar absorption to the low energy cut-off is very small and unobservable. At the other extreme, the value of N_X reported by Bleeker et al. (1973) is so small that a spurious low energy source is required to compensate for the effect of interstellar absorption, although Long et al. (1975) have argued that in that particular measurement, confusion with the local sky background might be important.⁽¹⁾ Nevertheless, a soft X-ray excess seems to have been present again lately during the OSO-8 observations, since the parameter N_X appears to be clearly smaller than N_H (Swank et al., this conference).

Strong variations of the temperature and intensity of the X-ray emission of compact sources are common, as are large changes in the optical thickness of the emitting region. The latter are evidenced by the variability of the low energy cut-off. However, there is growing evidence that a soft component with $kT \approx 0.5 \text{ keV}$ or so, seems to manifest itself sporadically. It has been proposed to be a specific feature of one of the possible equilibrium state of an accretion disk around a compact object (Thorne and Price 1975); it has almost certainly been observed in Cyg X-1 and in Sco X-1 (Garmire and Ryter 1975). There are now also indications that a similar phenomenon might occur in Cen X-3, even though the observed pulsation sets stringent limits on the size of the emitting region.

(1) A similar comment has been made by Dr. A. Bunner (private communication).

Table 1
 Some Values of the Parameter N_X Representing the Low
 Energy Cut-off of the X-ray Spectrum of Cen X-3

$10^{-21} N_X$ H atoms cm^{-2}	Date of Observation	References
6.3 ~ 8.9	May 12, 1970	Hill et al. 1972.
150	Jan-Apr 1971	Giacconi et al. 1971.
15 ~ 150		Gursky and Schreier 1974.
0.5 ~ 1	May 26, 1971	Bleeker et al. 1973.
30 ~ 40	Feb 13, 1973	Margon et al. 1975.
30 ~ 40	Nov 1, 1973	Long et al. 1975.
*	July 16-25, 1975	Swank et al., this conference
<hr/>		
$10^{-21} N_{\text{HI}} \geq 4$		Hindman and Kerr 1970.
$10^{-21} N_{\text{HI}+\text{H}_2} = 8.8$		this work.

*cannot be uniquely determined - low value for the pulsating component.

REFERENCES

- Bleeker, J., Deerenberg, A., Yamashita, K., Hayakawa, S., and Tanaka, Y. 1973, Ap. J. (Letters) 183, L1.
- Brown, R. L., and Gould, R. J. 1970, Phys. Rev. D1, 2252.
- Charles, P. A., Culhane, J. L., Zarnecki, J. C., and Fabian, A. C. 1975, Ap. J. (Letters) 197, L61.
- Fireman, E. L. 1974, Ap. J. 187, 57.
- Garmire, G. P., and Ryter, C. E. 1975, Astrophys. Letters 16, 121.
- Giacconi, R., Gursky, H., Kellogg, E., Schreier, E., and Tananbaum, H. 1971, Ap. J. (Letters) 167, L67.
- Gursky, H., and Schreier, E. 1976, IAU Symposium 67. "Variable Stars and Stellar Evolution", edited by Sherwood, V., and Plaut, L. in press.
- Hill, R. V., Burginyon, G., Grader, R. J., Palmieri, T. M., Seward, F. D., and Stoering, J. P. 1972, Ap. J. 171, 519.
- Hill, R. W., Burginyon, G. A., and Seward, F. D. 1975, Ap. J. 200, 158.
- Hindman, J. V., and Kerr, F. J. 1970, Australian J. Phys., Ap. Suppl. No. 18.
- Hollenback, D. J., Werner, M. W., and Salpeter, E. E. 1971, Ap. J. 163, 165.
- Long, K., Agrawal, P. C., and Garmire, G. 1975, Ap. J. (Letters) 197, L57.
- Mauder, H. 1975, Ap. J. (Letters) 195, L27.
- Moore, W. E., and Garmire, G. P. 1975, Ap. J. 199, 680.
- Rickard, J. J. 1974, Ap. J. (Letters) 189, L113.
- Ryter, C., Cesarsky, C., and Audouze, J. 1975, Ap. J. 198, 103.
- Thorne, K., and Price, R. 1975, Ap. J. (Letters) 195, L101.

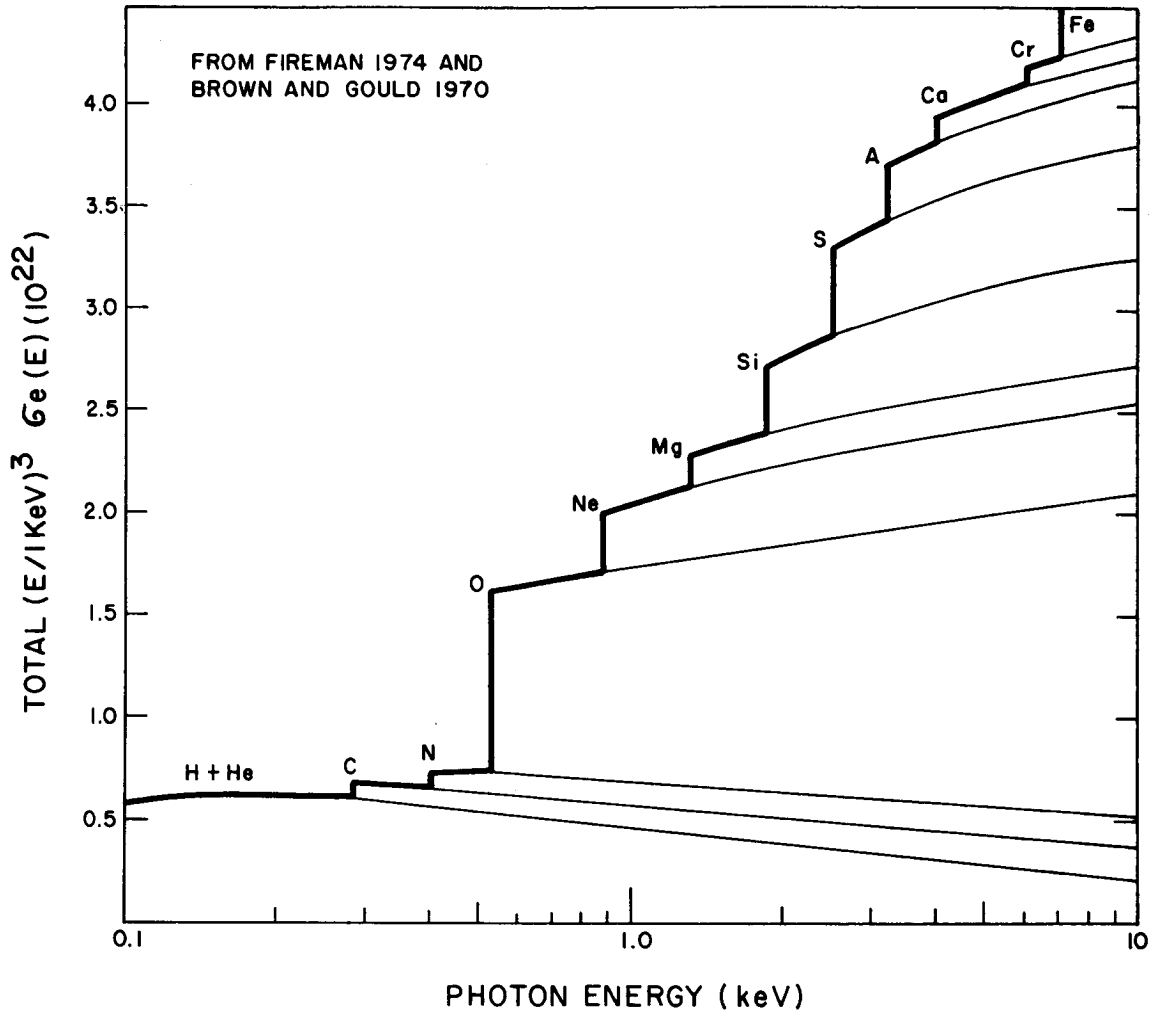


Figure 1. The photoelectric cross-section of a mixture of elements with cosmic abundances, multiplied by $(E/1\text{keV})^3$, and expressed in units of 10^{-22} cm^2 . The absorption edges are labeled by the chemical symbol of the relevant elements, Z_i . The solid line represents the total cross-section of the mixture, normalized per hydrogen atom. The light lines represent the contributions of elements with $Z \leq Z_i$.

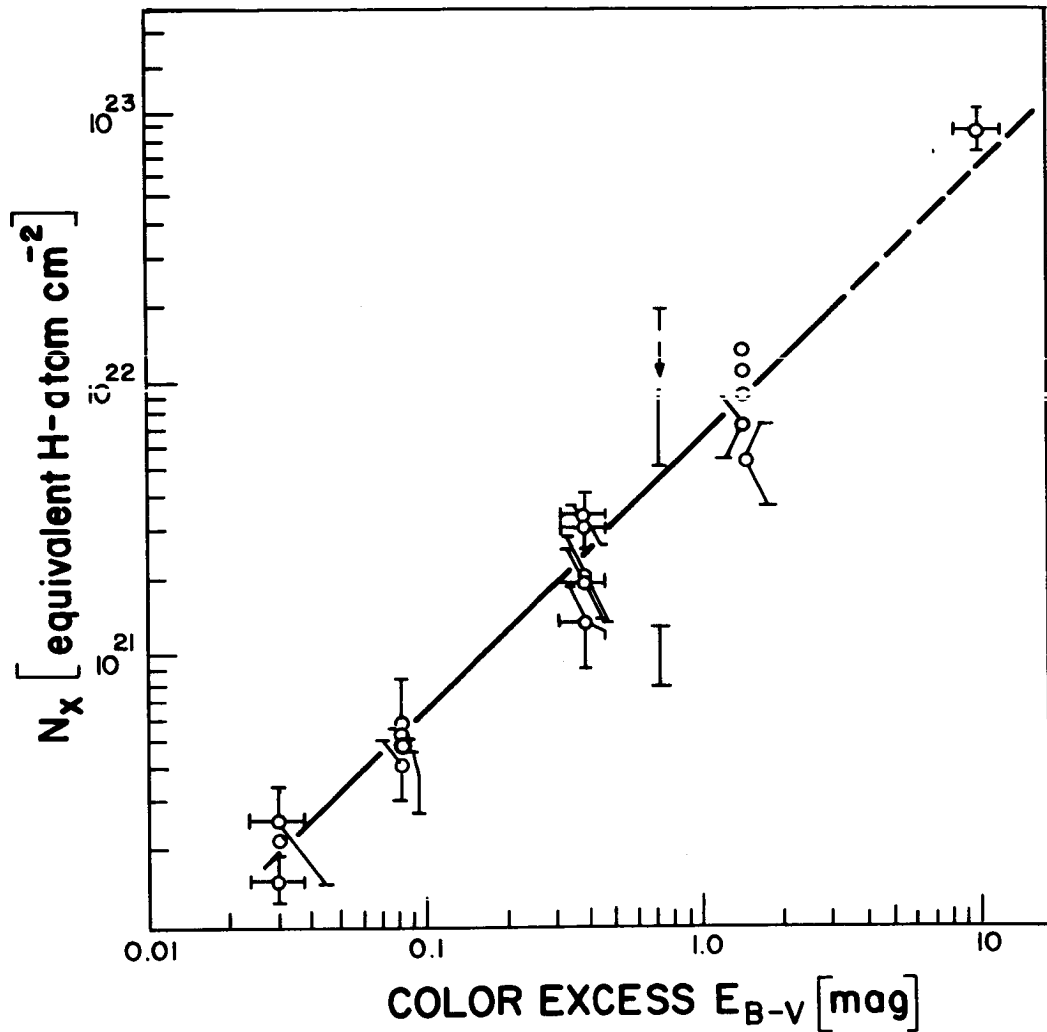


Figure 2. Relationship between the parameter N_X representing the absorption of X-rays by cold matter, and interstellar reddening, E_{B-V} . Upward, from left to right: Vel X, Cygnus Loop, Tau A, SN 1572 (Tycho), Cas A, galactic center. The heavy line represents the relation $N_X = 6.8 \times 10^{21} E_{B-V}$ H atoms cm^{-2} . Most of the references are to be found in Ryter et al. (1975). Newly published data are from Moore and Garmire (1975) for Vel X, from Charles et al. (1975) for Cas A, and from Hill et al. (1975) for Cas A and SN 1572.

RECENT UHURU RESULTS ON CENTAURUS X-3

E.J. Schreier and G. Fabbiano
Center for Astrophysics
Harvard College Observatory/
Smithsonian Astrophysical Observatory
Cambridge, Massachusetts 02138

ABSTRACT

The current status of the analysis of Cen X-3 data from UHURU concerning pulsations, orbital period and eccentricity, and extended lows, are reviewed. The pulse period decreases irregularly, with $\dot{p}/p \approx 2 \times 10^{-4} \text{ year}^{-1}$ over 1971-1972. The pulsed fraction (2-7 keV) is 70%-90% for single pulses but significantly less for superpositions of pulses, due to variability in shape. The pulses are narrower at higher energies with a correlated increase in fraction pulsed. The orbital period is found to both decrease and increase with \dot{p}/p on the order of a few times $10^{-5} \text{ year}^{-1}$. A three sigma upper limit on the eccentricity of .003 is obtained; if no significant periastron motion is allowed over two years, the upper limit becomes .0016. The orbital period is found to be detectable during some extended lows but with a significantly decreased ratio of eclipsed to non-eclipsed intensity. Two transitions between normal high states and extended lows are studied, and a consistent model is obtained in which extended lows are caused by both burying the source in an increased stellar wind from the companion, and starving the source by decreasing the stellar wind. Changes in fraction pulsed during transitions and systematic differences in the harmonic content of the pulses are also found.

INTRODUCTION

The X-ray source Centaurus X-3 occupies a central position in the study of the binary X-ray sources. It was both the first source showing X-ray eclipses and the first source (other than the Crab) with regular X-ray pulsations. Cen X-3 and Her X-1 have been studied for some time, and recently 3U0900 - 40 was found to be a pulsar as well. As is by now well known, the presence of a regularly pulsating object in a binary system allows remarkably precise determinations of many of the parameters of the system. Furthermore, the study of the binary X-ray light curves allows for increased understanding of the properties of the companion star and of the nature of the accretion mechanism.

In this talk, we will briefly review the current status of the analysis of Cen X-3 data from UHURU, indicating some directions for future work and the obvious extensions using current satellite experiments. In particular, we will summarize the UHURU data over an approximately two year baseline (1971-1972) concerning pulse period and shape, orbital period, eccentricity, extended lows and transitions between high and low states, and systematics of pulse fraction changes.

PULSATION PERIOD AND CHARACTERISTICS

The technique for determining pulsation period (and simultaneously, orbital phase, velocity and mass function) by fitting individual measurements of pulse phase to the binary Doppler curve is well known (see e. g. , Schreier et al, 1972). Nine independent observations of several day durations were each fitted, the results are shown in Figure 1. Two points are worthy of comment: first on the average over the two year baseline, there is a significant speedup, with $\dot{p}/p \approx -3 \times 10^{-4} \text{year}^{-1}$; and second, the speedup is neither uniform nor monotonic. On at least one occasion, in 1972 September-October, the pulsation period increased. (The errors on each point are a microsecond or less.) In comparison, Her X-1 shows a non-monotonic average speedup as well, but a hundred times less, with $\dot{p}/p \approx -4 \times 10^{-6} \text{year}^{-1}$. The important question of the continuity or discrete nature of the period changes is currently being studied. The average speedup is indicative of a significant transfer of angular momentum. Thus, even though Cen X-3 shows strong evidence for stellar wind accretion (see below), an accretion disk may exist.

The pulsed percentage is typically 70-90% for single pulses; however, when many pulses are superposed (~ 100 seconds), the value drops to 45-55%. This indicates the existence of variability of pulse shape on short time scales. This was apparent during some observations in the very early UHURU data (Giacconi et al, 1971; Schreier et al, 1972). Systematics of pulse variability will be discussed below. There is also a larger pulsed fraction at higher energies (10-20 keV) than at the lower energies (2-6 keV) (Ulmer, 1975); alternatively, the spectrum is harder at the pulsation maximum.

ORBITAL PERIOD AND ECCENTRICITY

Comparing successive eclipse times, as determined by the pulsation phase fitting, accurate determinations of the average orbital period can be obtained. Figure 2 shows the orbital period determinations during 1971-1972. In the course of the first year, the period shortened with $\dot{p}/p \sim -6 \times 10^{-5} \text{year}^{-1}$. There was then some evidence for a smaller slow down, $\dot{p}/p \approx 1 \times 10^{-5} \text{year}^{-1}$. Because of the discrete sampling and the small number of points, no more quantitative statement can be made.

The eccentricity can also be determined from the Doppler fit to the pulsation phases by looking for deviations from a sine curve. In the early UHURU analysis, it was obvious that no significant deviations existed. However, by fitting the residuals from the individual sinefits to the lowest order eccentricity term (twice the orbital frequency), a three sigma upper limit of 0.003 has been obtained. If no significant periastron motion is allowed, i. e. , if we require phase coherence of any eccentricity effect, the three sigma upper limit is a factor of two lower. (Her X-1 shows a three sigma upper limit of 0.002 for eccentricity.)

LONG TERM BEHAVIOR

The long term behavior of Cen X-3 concerning extended lows and transitions between states as studied with UHURU has recently been discussed (Schreier et al, 1975). We will just summarize the relevant points.

1) The orbital period persists (5 ± 1 cts/sec eclipsed vs. 11 ± 1 cts/sec non-eclipsed) through at least some of the extended lows, indicating that the source does not always "turn-off" during these periods. The fact that the low state eclipse intensity is less than the normal eclipse intensity indicates some correlation between eclipse and non-eclipse intensity; the eclipse flux is not just a constant nearby source.

2) A transition from extended low to high state which was observed in 1972 July (Figure 3) is consistent with a stellar wind accretion model (Davidson and Ostriker, 1973) with a variable wind density. The source first appears as a slight increase in intensity at phase 0.5; this spike gradually increases in intensity, with a small decrease in low energy absorption. There is significant absorption on the shoulders of the spike. The pulsed fraction also increases in the course of the transition.

3) An extension of the work by Pringle (1973), also discussed by McCray (1974) leads to a model where a cold dense wind "buries" the source to produce this kind of extended low (Figure 4). As the density decreases through a factor of 5, the X-rays start to ionize the wind, first at phase 0.5 and then for successively longer phase durations. The increase in intensity of the spike and increased pulse fraction is due primarily to decreased Thomson scattering, while the shoulders are due to photoelectric absorption.

4) A transition from high to low observed in 1973 February (Figure 5) is qualitatively different; the decrease is smooth, with no significant spectral changes. It is estimated that a decrease in stellar wind and thus accretion by a factor of about 20 could "starve" the source to produce a second kind of extended low.

5) The overall model then is one in which the density of the stellar wind from the primary can vary by close to two orders of magnitude. At the extremes, the source is in extended lows, either by starvation or by burying.

SYSTEMATIC PULSATION VARIABILITY

An extension of the work above consists in looking for systematic changes in the pulse shape at different times, as might be caused by changing density and Thomson scattering. In particular, during the several interesting observing periods discussed in Schreier et al, 1975, the harmonic content of the pulses were studied. Each individual 20 sec observation was fit with the fundamental sine period and several harmonics; the fractional power at each frequency, averaged over an orbital period, is shown in Figure 6. In the 1972 July turn-on, it is seen that the power in the fundamental increases much faster than the power in the first harmonic; at the beginning when the source is first emerging from the wind, it is mainly double pulsed. It is difficult to ascribe the effect to decreased Thomson scattering -- one would expect the faster components to be affected more. It is interesting to compare the relative pulsed fractions in 1971 December, a "normal" high state; it is seen that by the end of the transition in July, the relative fractions were consistent with this normal state.

The 1973 February turn-off does not show as significant a trend. However, it is seen that the first harmonic is strongest (i. e. "double-pulsed" or strong inter-pulse) and that there is some indication for increased fraction pulsed as the source is "starved". In 1972, March, where the source increased over two days, but not necessarily as part of a transition, no significant systematics were observed.

The primary point to emerge thus far is that the changes in pulse shape cannot be ascribed solely to scattering by the wind. There must be a correlated change in the emission mechanism at the compact object to cause the variations in pulsed fraction.

REFERENCES

- Davidson, K. and Ostriker, J. P., 1973, *Astrophys. Journ.* 179, 585.
- Giacconi, R., Gursky, H., Kellogg, E. M., Schreier, E., and Tananbaum, H., 1971, *Astrophys. Journ. (Lett.)* 167, L67.
- McCray, R., 1974, International Conference on X-rays in Space, Calgary, Alberta, Canada.
- Pringle, J. E., 1973, *Nature Phys. Sci.* 243, 90.
- Schreier, E., Levinson, R., Gursky, H., Kellogg, E. M., Tananbaum, H., and Giacconi, R., 1972, *Astrophys. Journ. (Lett.)* 172, L79.
- Schreier, E., Swartz, K., Giacconi, R., Fabbiano, G., and Morin, J., CFA Preprint No. 53, to be published in *The Astrophys. Journ.*, February, 1976.
- Ulmer, M., CFA Preprint No. 75-083, to be published in *The Astrophys. Journ.*, 1 March 1976.

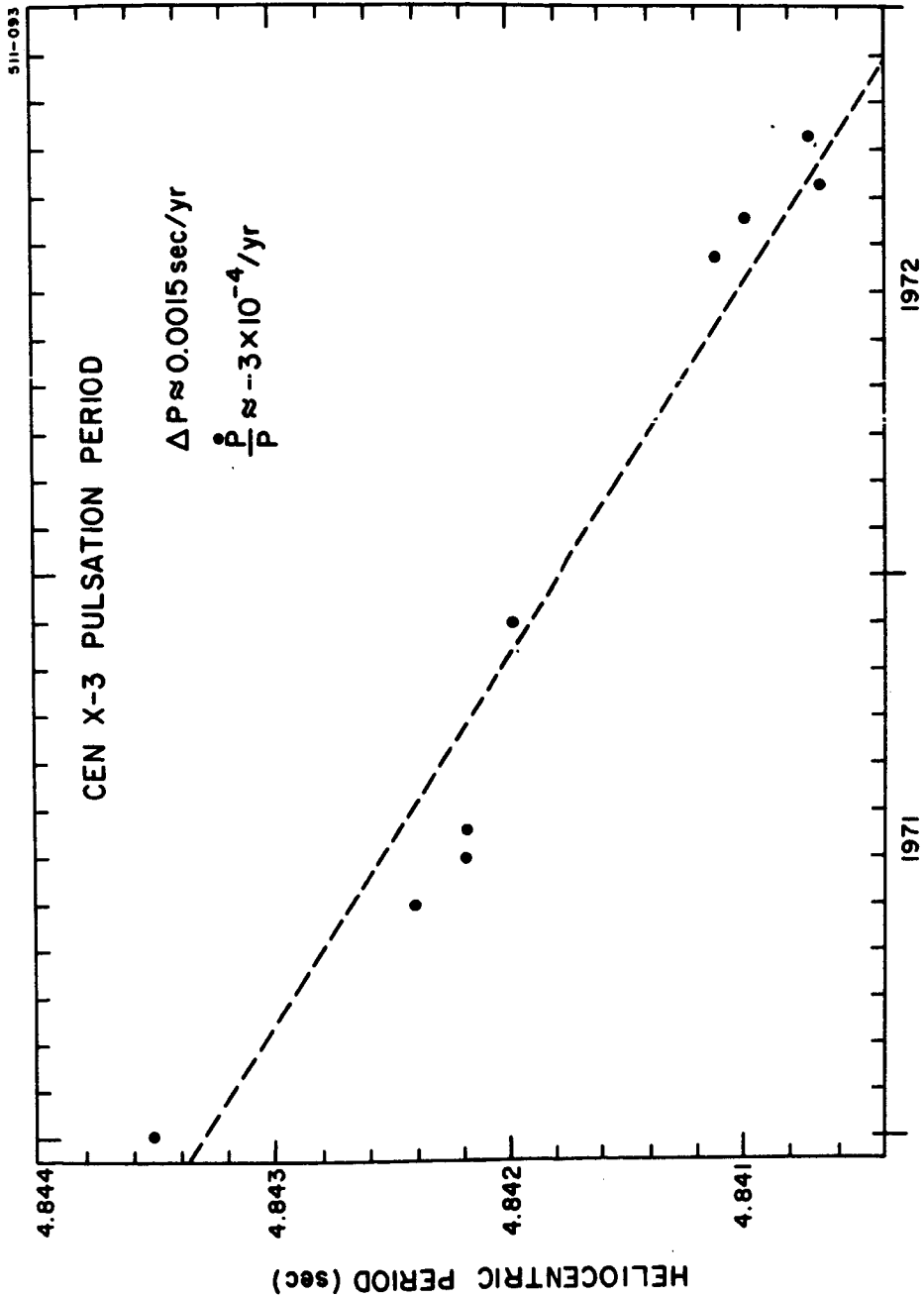


Figure 1. Centaurus X-3 heliocentric pulsation period as observed with UHURU during 1971 and 1972. Also shown is the approximate average rate of speed up. The 1σ errors are smaller than the data points, on the order of 1μ sec or less.

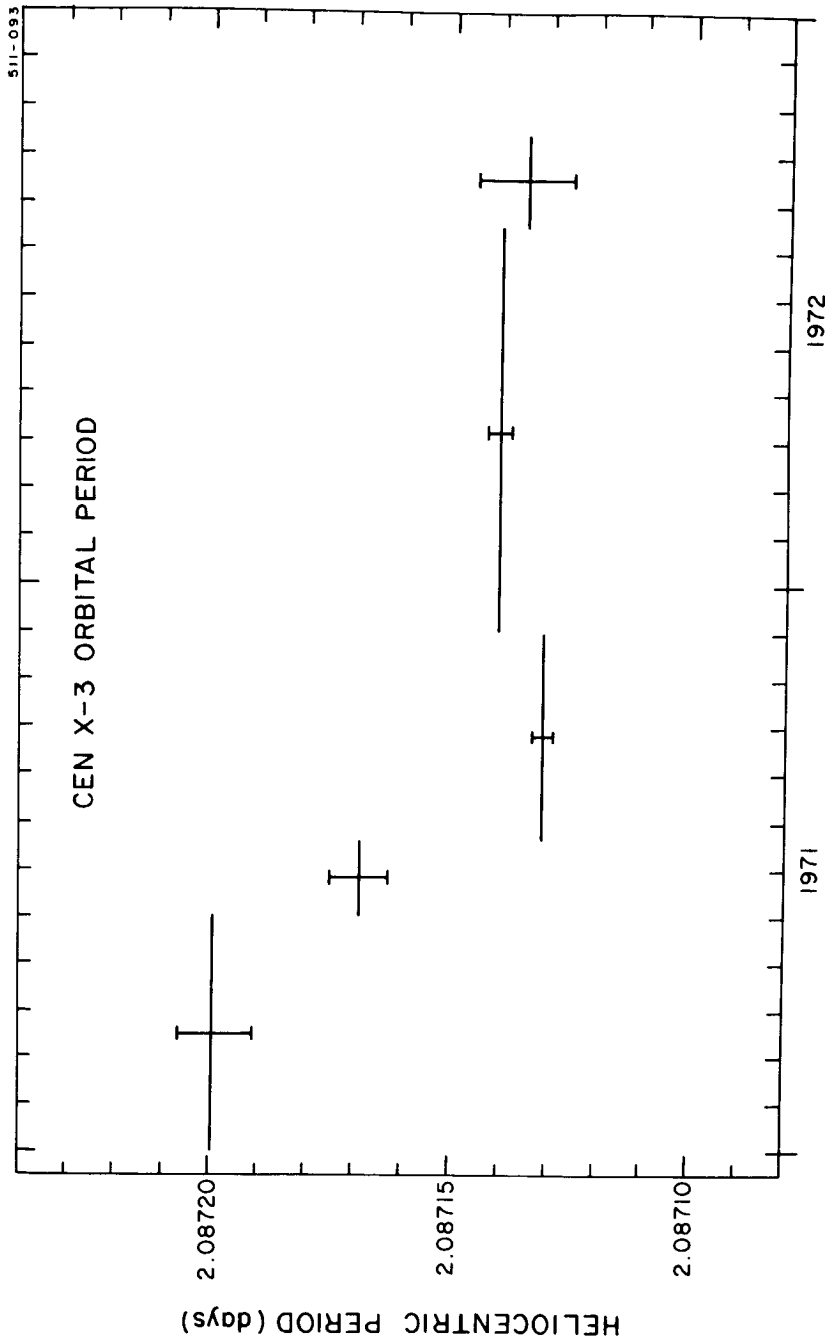


Figure 2. Centaurus X-3 heliocentric orbital period, measured over the same base lines as in Figure 1, with 1 σ errors.

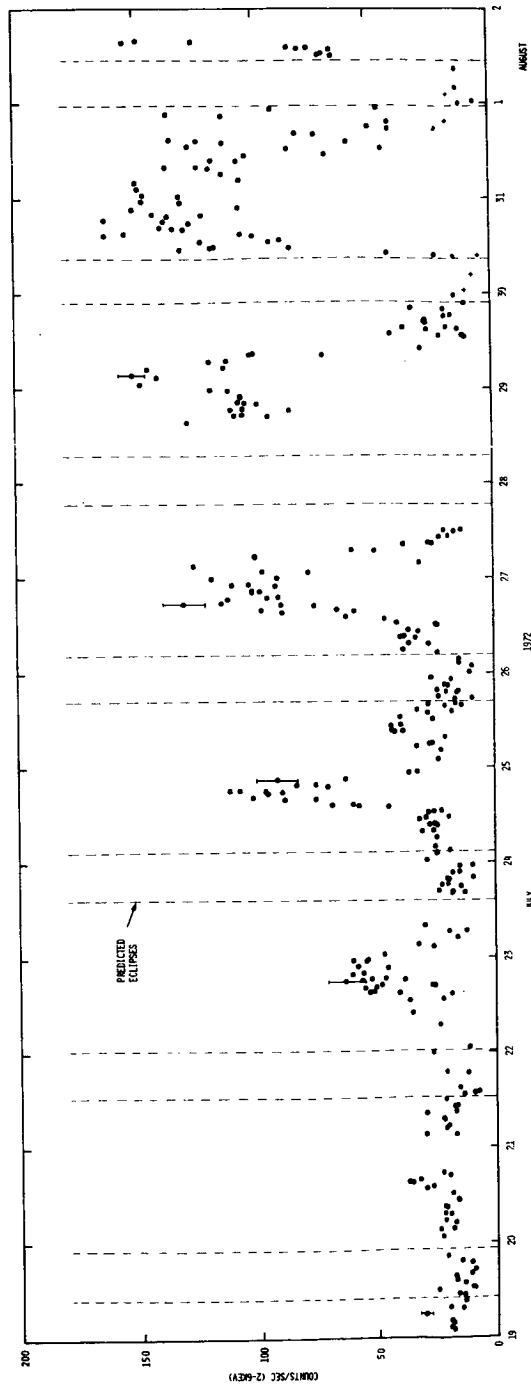


Figure 3. Centaurus X-3 light curve in 1972 July. Each point represents the average intensity (2-6 keV) over 20 seconds, with background subtracted, corrected for elevation in the field of view of the collimator. Typical 1σ error bars include counting statistics and aspect correction errors. The predicted eclipse phases are extrapolated from fits to the pulsation phase changes (Schreier et al, 1972). The gap in coverage during 27.5-28.5 July is due to loss of pointing. The points indicated by + signs are 20 upper limits.

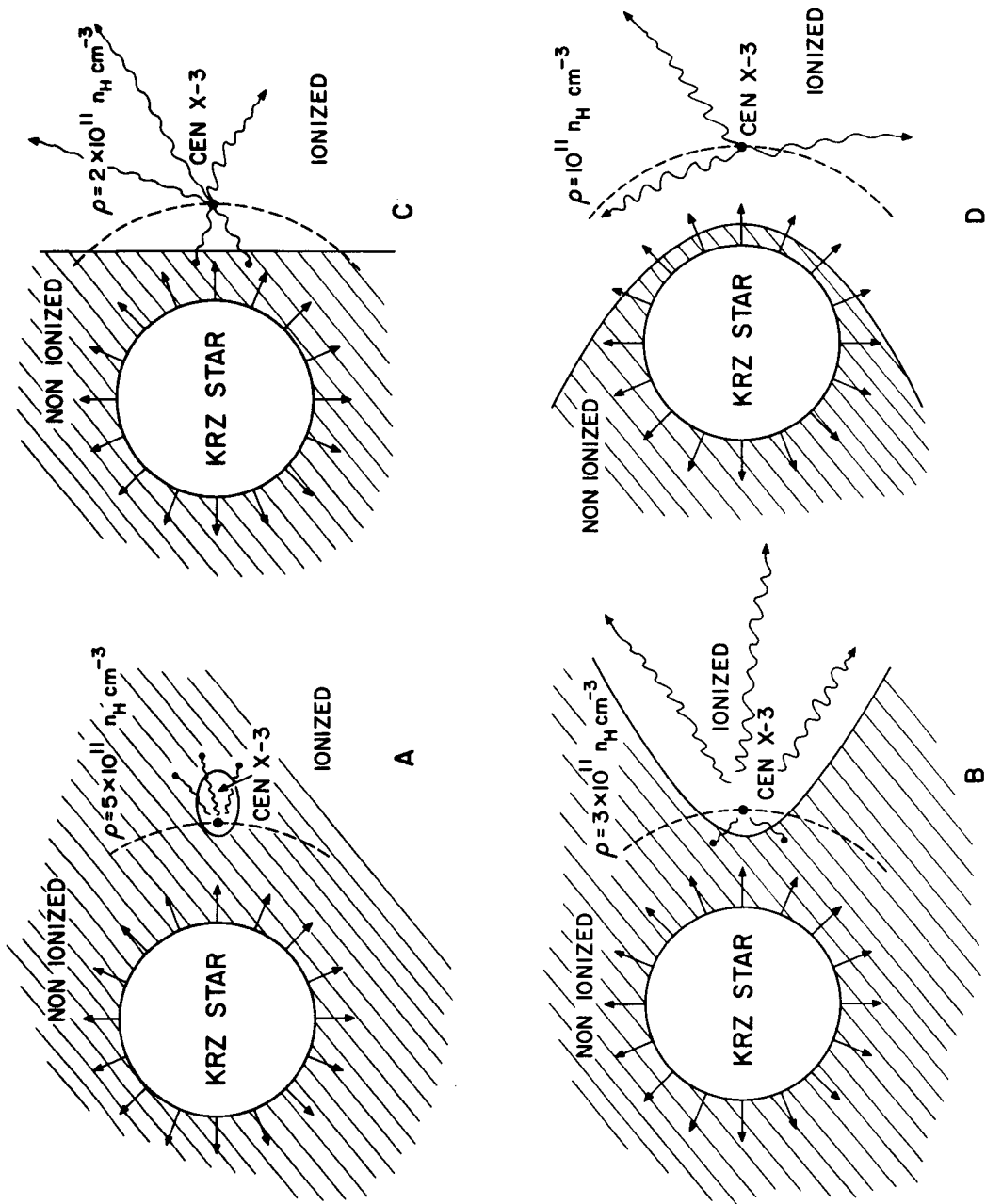


Figure 4. A representation of the 1972 turn-on of Centaurus X-3. Part A shows the extended low with the source "buried" in the stellar wind. Part B and C show the appearance and progressive widening of the "spike" near phase 0.5. Part D shows the normal high state, with a wind density at the neutron star of 10^{11} cm^{-3} .

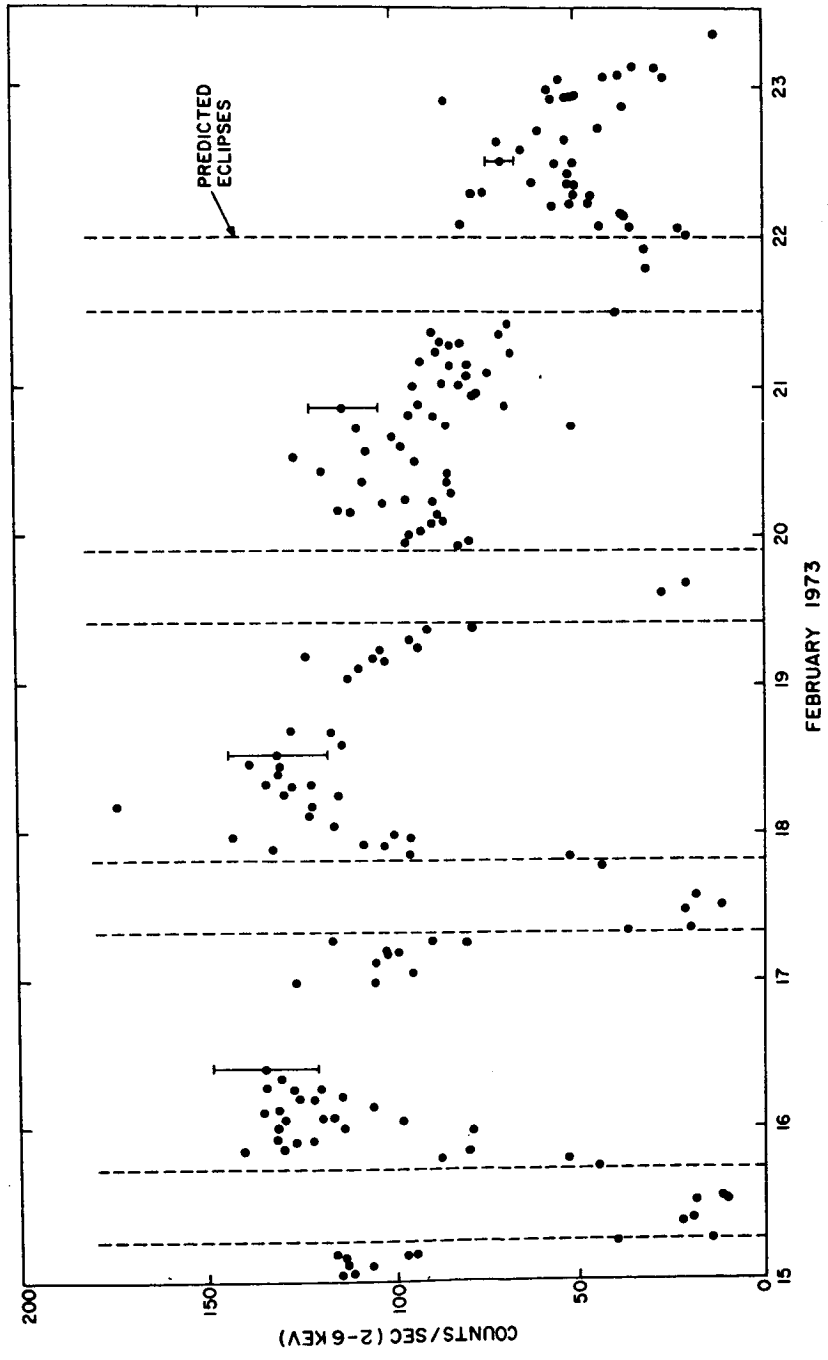


Figure 5. Centaurus X-3 light curve in 1973 February. See comments for Figure 3.

CENTAURUS X-3 PULSED FRACTION

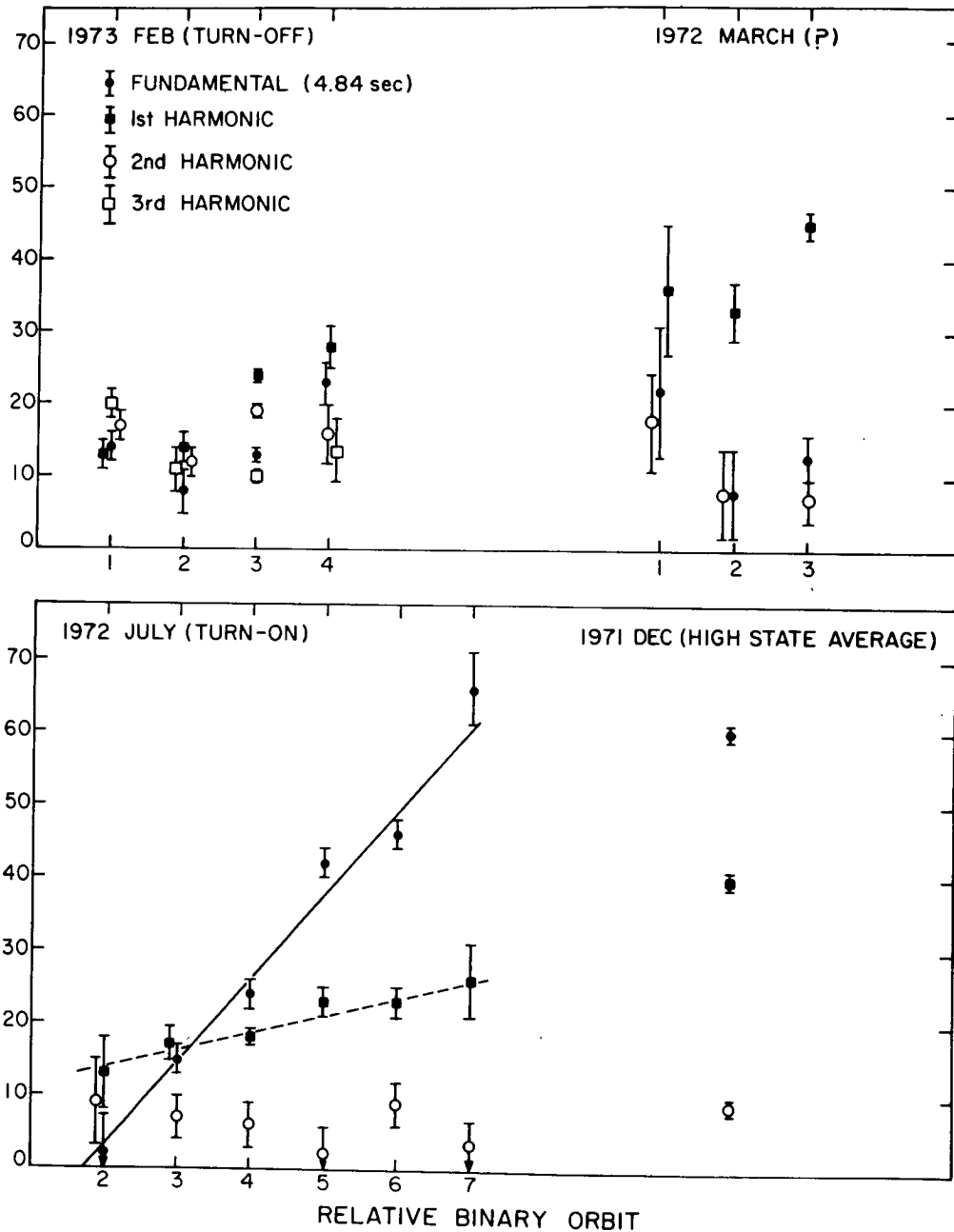


Figure 6. The pulsed fraction of Cen X-3 emission in the fundamental and several harmonics as averaged over orbital periods, during different intervals of time as indicated.

OSO-8 GSFC RESULTS ON CEN X-3

J. H. Swank, R. Becker, E. Boldt, S. Holt, S. Pravdo
R. Rothschild and P. J. Serlemitsos
NASA/Goddard Space Flight Center

ABSTRACT

Spectra of Cen X-3 during eclipse, in transition out of eclipse, and during several later phases of the binary orbit were obtained from quick look data of the July 16-25, 1975 observation by the Goddard X-ray spectroscopy experiment on OSO-8. In the high state there was no absorption turn over. Pulsations were present at least to 23 keV. The spectrum at the pulse minimum was flatter above 7 keV than that of the pulse peak. In transition out of eclipse Cen X-3 emerged above a small low energy flux seen during eclipse. The observations appear to indicate absorption by cold and ionized matter and the presence of iron in the companion's atmosphere. Decreased intensities were observed at late phases of some binary orbits in some cases corresponding to dips. Absorption appears although the low energy component remains. Variable features may be interpretable as absorption and emission by iron and possibly other trace elements.

INTRODUCTION

Cen X-3 was observed by the Goddard x-ray spectroscopy experiment for about 4 1/2 binary orbits in July 1975. The experiment has been described by P. Serlemitsos (1975). Data was obtained for about 3 1/2 orbits with the argon detector sensitive from 1 1/2 to 24 keV and for 1 orbit with the xenon detector sensitive up to 60 keV. Preliminary results have been obtained from the quick look data. Cen X-3 is known to exhibit a variety of behaviors. OSO-8 saw some of these and obtained detailed spectral information.

CEN X-3 AVERAGE SPECTRUM

For parts of all the binary orbits observed Cen X-3 had an average spectrum which was similar to the one shown in Fig. 1 observed with the argon detector on July 18 or the one shown by P. Serlemitsos observed with the xenon detector on July 16. The number spectrum is approximately described by the exponential function. The energy emission peaks at 6 keV. No fit to a thermal bremsstrahlung spectrum with absorption by cold matter was acceptable over the entire energy range. Good fits of that form are obtained for the energies over 7 keV and reasonable fits for the energies over 4 keV, but the kT and absorption cut off depend on the lower energy bound. For comparison the absorbed thermal bremsstrahlung spectra are indicated in the figure for typical parameters sometimes seen. The July 18 average spectrum included ~ 0.58 photons $\text{cm}^{-2} \text{s}^{-1}$ from 2-6 keV.

CEN X-3 PULSE SPECTRUM

Our quick look data shows a single pulse with a fast rise and slow fall similar to the one seen by Uhuru in 1972 (Schreier et al. 1975). Usually we see about 60% of the power pulsed from 1.4 to 24 keV. For one binary orbit we have real time data and can construct either spectra as a function of the pulse phase or pulse profiles for selected energy intervals. The flux is clearly pulsed up to 24 keV.

Fig. 2a shows the spectra of .6 sec at the pulse peak and .6 sec at the minimum. The peak spectrum is steep while for energies above 7 keV the minimum spectrum is relatively flat, falling like E^{-2} . If the minimum spectrum represents largely scattered radiation the spectrum has been modified.

If the minimum spectrum is an unpulsed component the contribution of just the pulse can be obtained by using the minimum spectrum as background. The results are shown in Fig. 2b for the peak and for .6 sec a half pulse period later on the shoulder of the peak. These results are free of any background contribution. If the peak spectrum for energies greater than 4 keV is fit to a thermal spectrum with absorption the best fit parameters are $kT = 15$ keV and $E_a = 3.5$ keV with $\chi^2 = 22$ for 10 degrees of freedom. The fit is not really good for energies above 15 keV and departs radically below 4 keV. The lowest energy points may be adjusted in a final analysis by perhaps 20%, but probably not enough to give a good fit of this form.

ECLIPSE

We have observations during 2 eclipses, all during the second half of the eclipse. The average of these is shown in Fig. 3a. The flux did not vary over these observations more than could be accounted for by our present uncertainty in aspect. This flux amounts to .022 photons $\text{cm}^{-2} \text{s}^{-1}$ from 2-6 keV. We cannot at present rule out contamination by 3U1134-61 which Uhuru saw as a 10 count s^{-1} source. At that level it could contribute $\sim 1/3$ of the flux we see during eclipse. However, the observed flux is near the lowest observed by Uhuru during eclipse (Schreier et al. 1972), so that the contamination cannot be large. The spectrum fits a power law of index 2 or a thermal bremsstrahlung spectrum of $kT \sim 6$ keV. In this average flux no line emission is observable.

TRANSITION FROM ECLIPSE

For the transition from one eclipse we have data for the first 20 minutes after a pulsed signal is observed. The observed flux is shown in Fig. 3b. The flux observed during eclipse is still present. If we use as background the observations from the eclipse immediately preceding this observation we have the contribution due to Cen X-3 shown in Fig. 3c.

The contribution due to Cen X-3 can be fit to the high state spectrum absorbed by $\sim 7 \times 10^{23} \text{cm}^{-2}$ equivalent hydrogen atoms of cold matter with the the abundances of medium elements taken from Brown and Gould (1970) and

the iron to hydrogen ratio $\sim 3 \times 10^{-5}$ (Cameron 1970). The column density of electrons required to bring the highest energy channels down from the level observed in the state of highest intensity is $\sim 1.7 \times 10^{-24} \text{ cm}^{-2}$, so that more than a half of the absorbing material is ionized.

For the transition from a different eclipse the pulse and minimum spectra were obtained for a sequence of later phases as shown in Fig. 4. The pulse and minimum spectra continue early in the transition to show the same low energy component at nearly the same level as seen during the eclipse. As the transition continues a pulsed low energy flux appears and the low energy contribution to the minimum flux increases. The latter could be either scattered radiation originating on the compact object or more of whatever appears during eclipse. The spectra of the minima seem to exhibit the same absorption cutoffs as do the peak spectra, indicating if it is scattered radiation that the scattering occurs closer to the compact object than the absorbing atmosphere.

If the observations during the minima are used as the backgrounds for these pulse peak observations, the spectra shown in Fig. 5 result. By comparing these with a pulse spectrum at the highest level of emission we can estimate the number of ionized and unionized atoms in the line of sight and trace these numbers the transition proceeds. Over the $\sim 1 \frac{3}{4}$ hr of the transition the column density of cold matter falls from near 10^{24} cm^{-2} to less than 10^{22} cm^{-2} . The column density of electrons falls more slowly early in the transition. It does not seem possible to choose the parameters in the model suggested by Pringle (1973) of a Stromgren surface to match the observed changes, if the density is inversely proportional to r^2 . The observations should provide an accurate picture of the companion's atmosphere. Some finer features in these spectra deserve but bare mention at this time. An iron edge may still be observable at $\sim 7 \text{ keV}$. Emission features may sometimes appear.

ABSORPTION DIPS

Whereas the absorption during transitions into and out of eclipse are expected to provide information about the companion's atmosphere, the intensity decreases at phases well away from eclipse carry clues about the environs of the compact object, whether a disk, a wake, or both exist. One quick look data include one observation with real time data of a 6% intensity decrease at phase near .7 and a sequence of observations during one binary orbit when absorption dips seem to have occurred.

In Fig. 6 are shown the pulse and minimum spectrum for the observation showing the small decrease in intensity from a high intensity level immediately preceding it. The pulse spectrum seems to show absorption by cold matter. This spectrum can be fit to a thermal bremsstrahlung spectrum with absorption by cold matter (although the high kT required would probably prevent the high energy points from falling fast enough at energies above 24 keV).

The accompanying minimum spectrum is for most energies of less intensity

than that of the immediately preceding observation, but there is relatively more emission in the regions near 8 keV and 2 keV, perhaps indicating a complex situation. We do not yet have data for any later phases of that binary orbit.

In an earlier binary orbit as sequence of observations about an hour apart, from phase $\sim .72$ to $\sim .83$ found low intensity levels of 31%, 38%, and 18% of the high state with intervening highs of 47% and 54%, suggesting the sort of dips which have been seen by Uhuru (Schreier 1975), Copernicus (Tuohy and Cruise 1975), and Ariel 5 (Pounds et al. 1975), for examples. The spectra of the levels at 47% and 54% were similar as were those of the 31% and 38% levels. Examples of these two as well as of the high state and the 18% level are shown in Fig. 7.

The spectrum of the highest of the reduced levels resembles the high state spectrum for that orbit. If it is assumed to be related to it by absorption, the optical depth is nearly independent of energy. The reduction would require $2-6 \times 10^{23} \text{ cm}^{-2}$ of electrons in the line of sight.

In the intermediate case the optical depth seems independent of energy over 16 keV, increases as the energy decreases from 16 to 11 keV and is flat down to 5 keV. For the lowest energies a steep flux similar to the one present when Cen X-3 was in eclipse is influencing the spectrum. But the observations above 5 keV do not seem describable as a simple combination of absorption by cold matter and scattering by ionized matter.

In the lowest case the optical depth more closely resembles the behavior of the cross section for cold matter (with a column density of a few $\times 10^{23} \text{ cm}^{-2}$) plus electrons (with the column density of electrons up to $\sim 2 \times 10^{24} \text{ cm}^{-2}$). The detector in this case has a 5° full width at half maximum and could pick up 3U1145-61 (at low efficiency). However the pulsed fraction during the observation of the lowest intensity was about 50% and the non-pulsed part can nearly be accounted for by the steep low energy flux. The latter is at a level only slightly greater than observed in the other detector during eclipse. We did observe an eclipse with this detector but as yet do not have the data.

SUMMARY

In summary these observations give some details to a view of the Cen X-3 system. We have a picture of the spectrum across the pulse. The variations in the column densities in transition out of eclipse show the ionized and unionized wind, with the companions atmosphere containing iron in a reasonable abundance. The dip spectra indicate that the beam sometimes traverses large column densities of ionized matter and probably sometimes large column densities of cooler matter. More precise information should be obtainable with further analysis and the remaining data from these observations.

REFERENCES

- Brown, R. L., and Gould, J. 1970, Phys. Rev. D, 1, 2252.
- Cameron, A. G. W., 1970, Space Sci. Rev. 15, 121.
- Pounds, K. A., Cooke, B. A., Ricketts, M. J., Turner, M. J., and Elvis, M., 1975, M.N.R.A.S., 172, 473.
- Pringle, J. E., 1973, Nature Phys. Sci. 243, 90.
- Schreier, E., Levinson, R., Gursky, H., Kellogg, E., Tananbaum, H., and Giacconi, R. 1972, Ap. J. (Letters), 172, L79.
- Schreier, E. J., Swartz, K., Giacconi, R., Fabbiano, G., and Morin, J. 1975, to be published in Ap. J.
- Serlemitsos, P. J., 1975, this conference.
- Tuohy, I. R., and Cruise, M., 1975, M.N.R.A.S., 171, 33P.

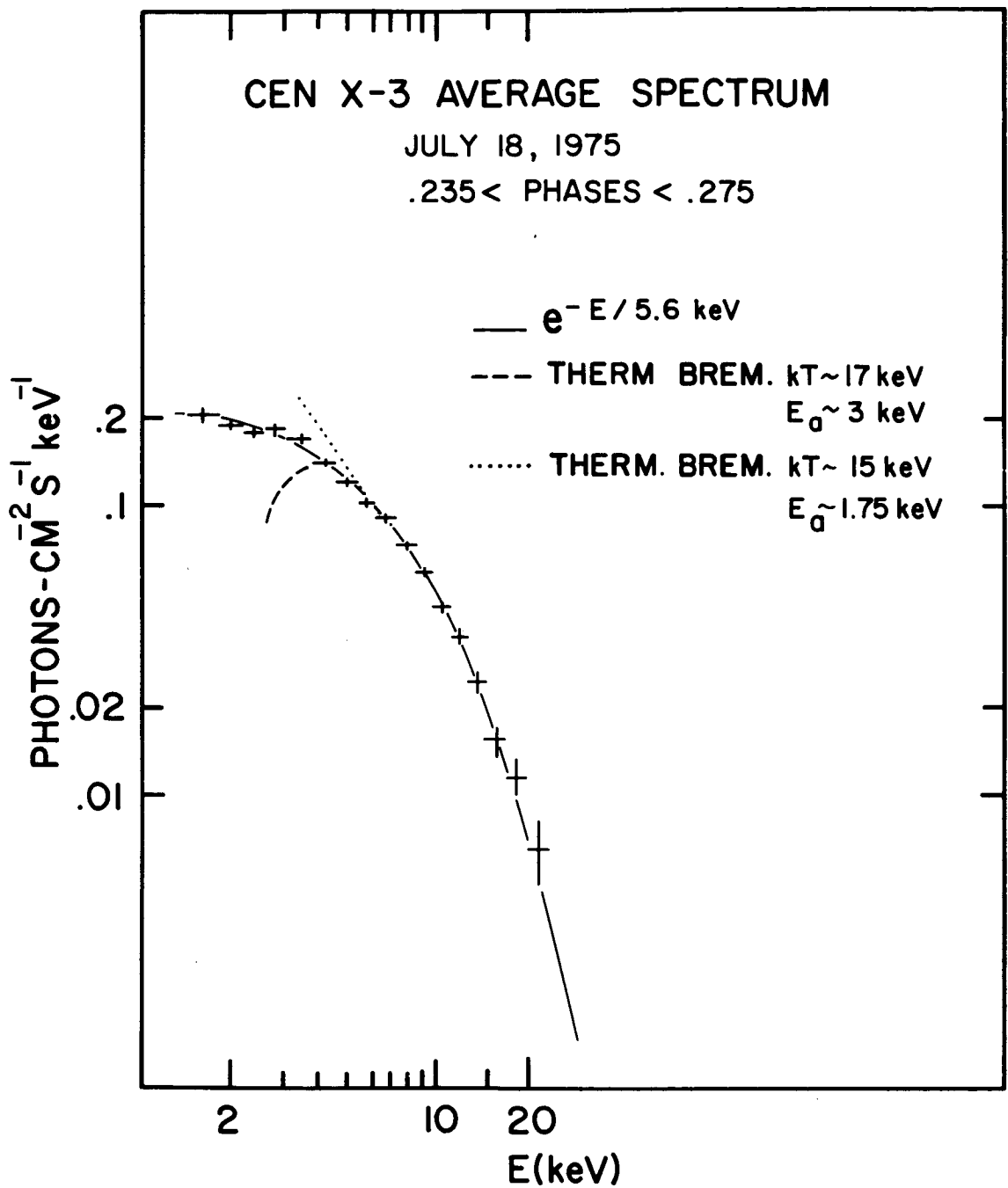


Figure 1. Cen X-3 Average Spectrum. This spectrum was the average of 40 minutes of data on July 18, 1975 in the argon detector. The background was accumulated from several days during the week prior to July 16 from galactic latitudes between -25° and 0° .

SPECTRA OF CEN X-3 PULSE

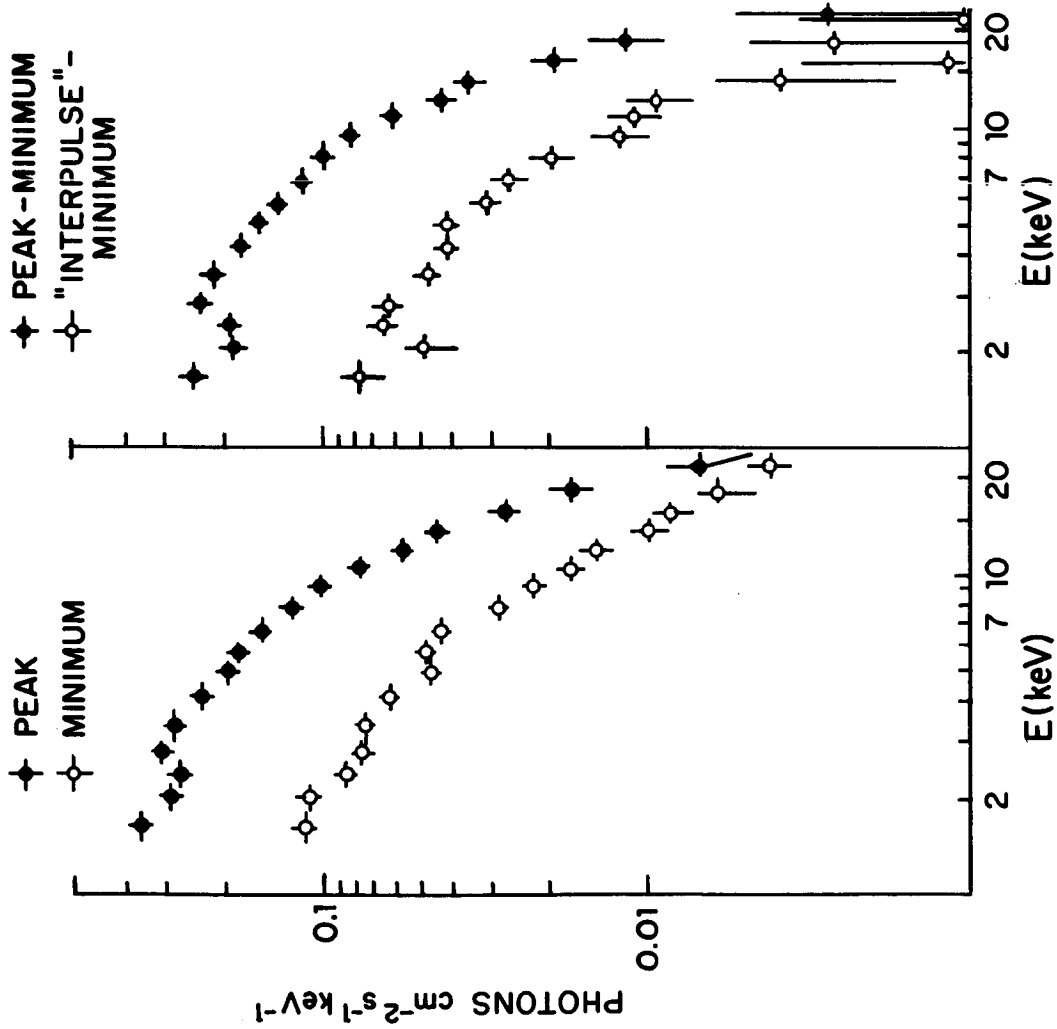


Figure 2. Spectra of Cen X-3 Pulse. The counts in 63 channels in the argon detector were folded on the pulse period into 8 bins. (a) The spectra for .6 sec at the pulse peak and .6 sec at the pulse minimum using the source free background described for Fig. 1. (b) The spectra for .6 sec at the peak and .6 sec a half pulse period later using the data from .6 sec at the minimum as background.

OBSERVATIONS DURING ECLIPSE AND ITS END

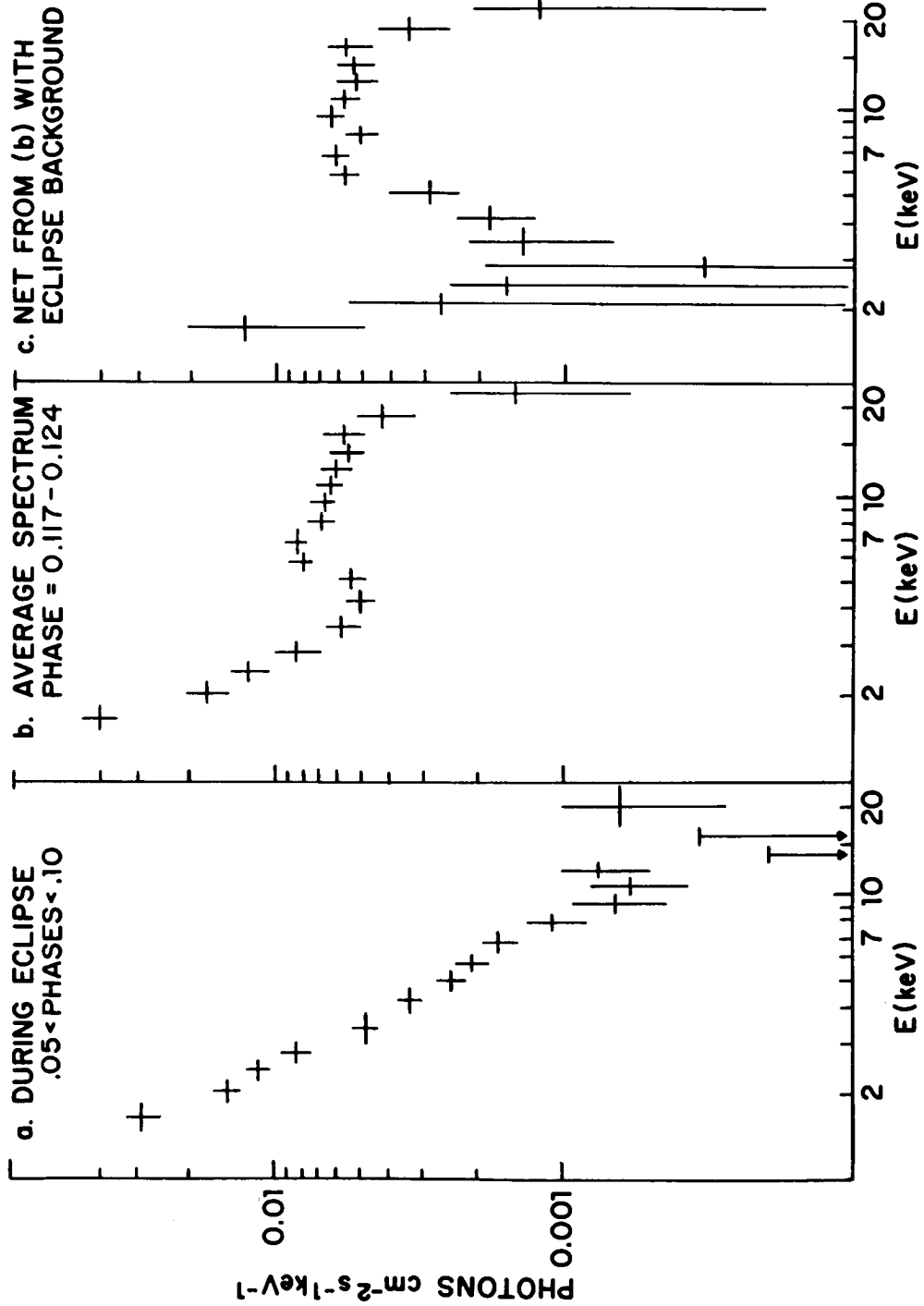


Figure 3. Observations During Eclipse and Its End. (a) The spectrum observed in the argon detector during 2 eclipses (July 22 and July 24). (b) The spectrum observed during the first interval obtained on July 22 which showed pulsed power. (c) The same as (b) using data accumulated from .5-2.75 hr before, during the eclipse.

CEN X-3 EMERGING FROM ECLIPSE

—◆— PULSE PEAK ◆ PULSE MINIMUM

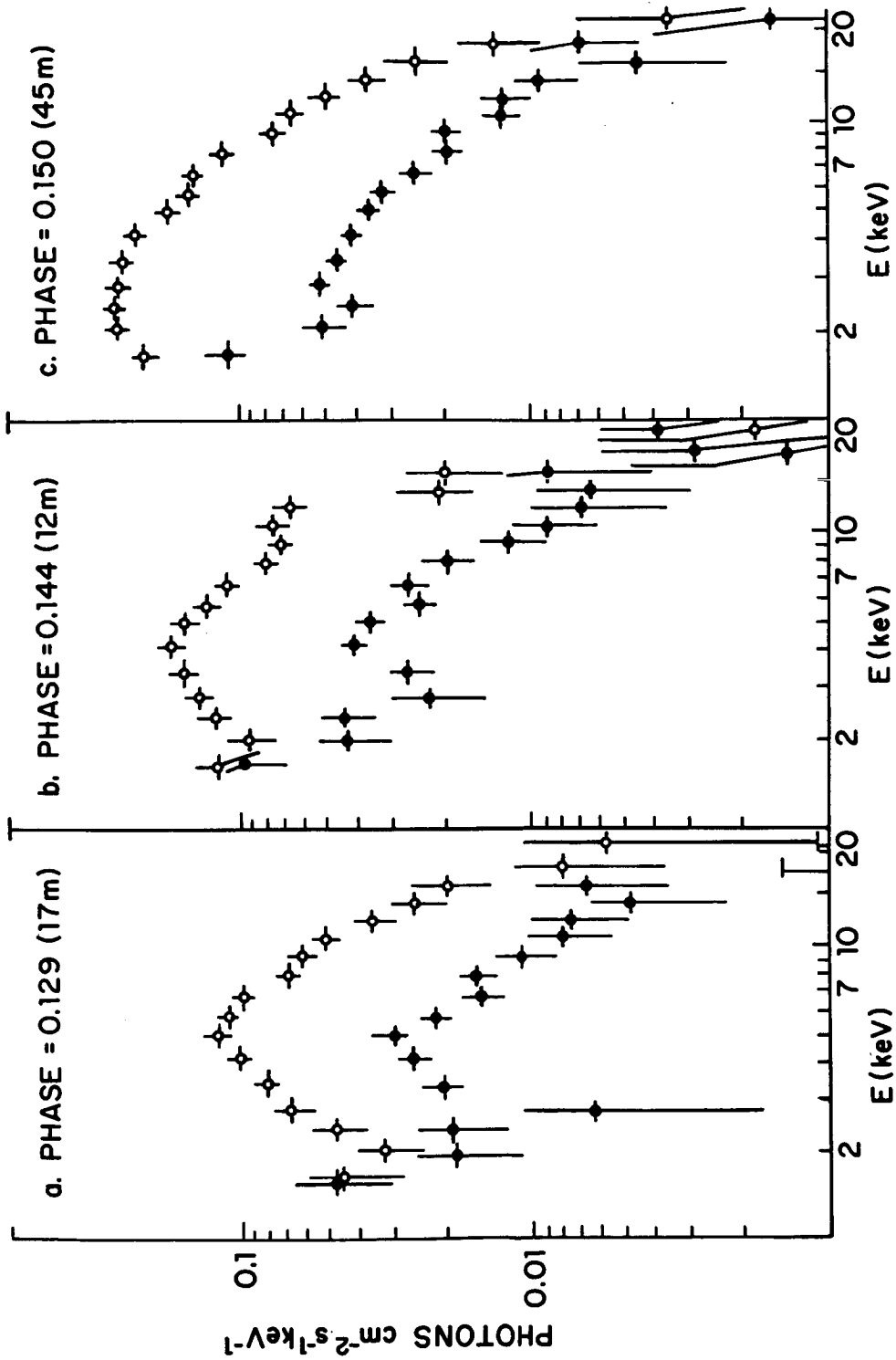


Figure 4. Cen X-3 Emerging from Eclipse. Background is from a source free region as described for Fig. 1.

CEN X-3 EMERGING FROM ECLIPSE

PULSE PEAK - MINIMUM

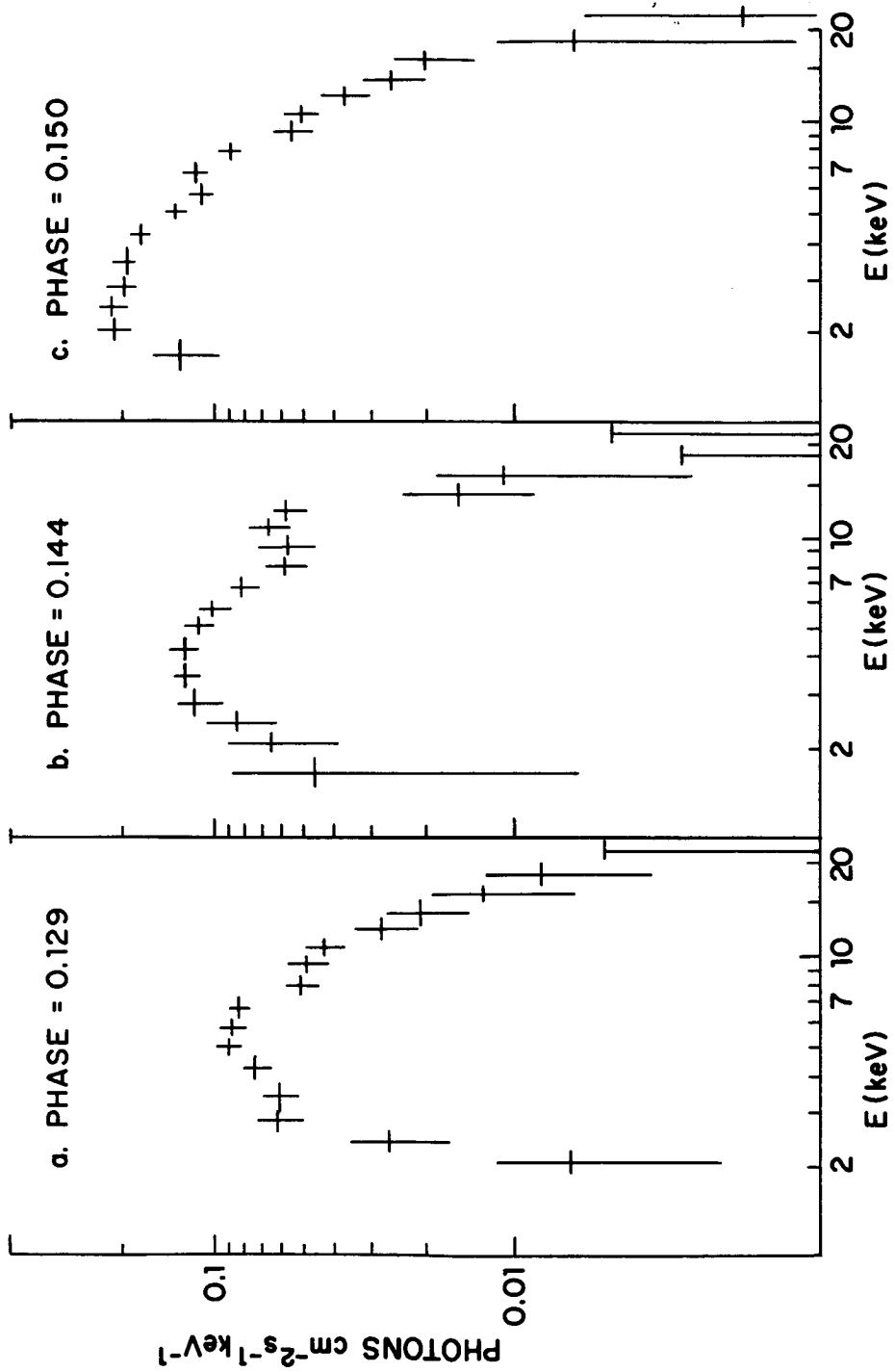


Figure 5. Cen X-3 Emerging from Eclipse. The data from .6 sec at the minimum is used as background.

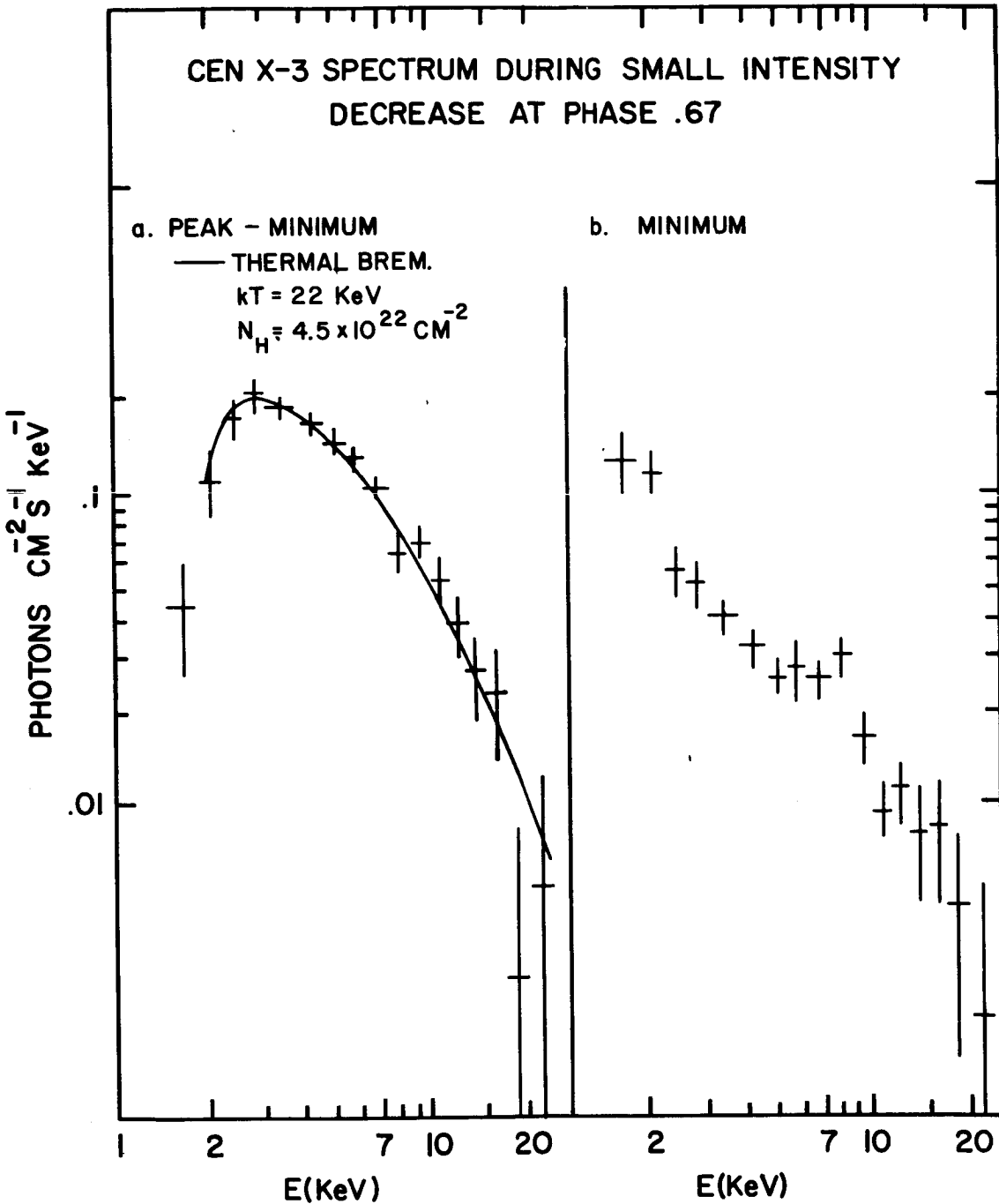


Figure 6. Cen X-3 Spectrum During Small Intensity Decrease at Phase .67. (a) .6 at peak using .6 at minimum as background. The best fit function to thermal bremsstrahlung and absorption by cold matter with Brown and Gould abundances is shown. (b) .6 at the minimum.

AVERAGE CEN X-3 HIGH STATE AND DIP SPECTRA

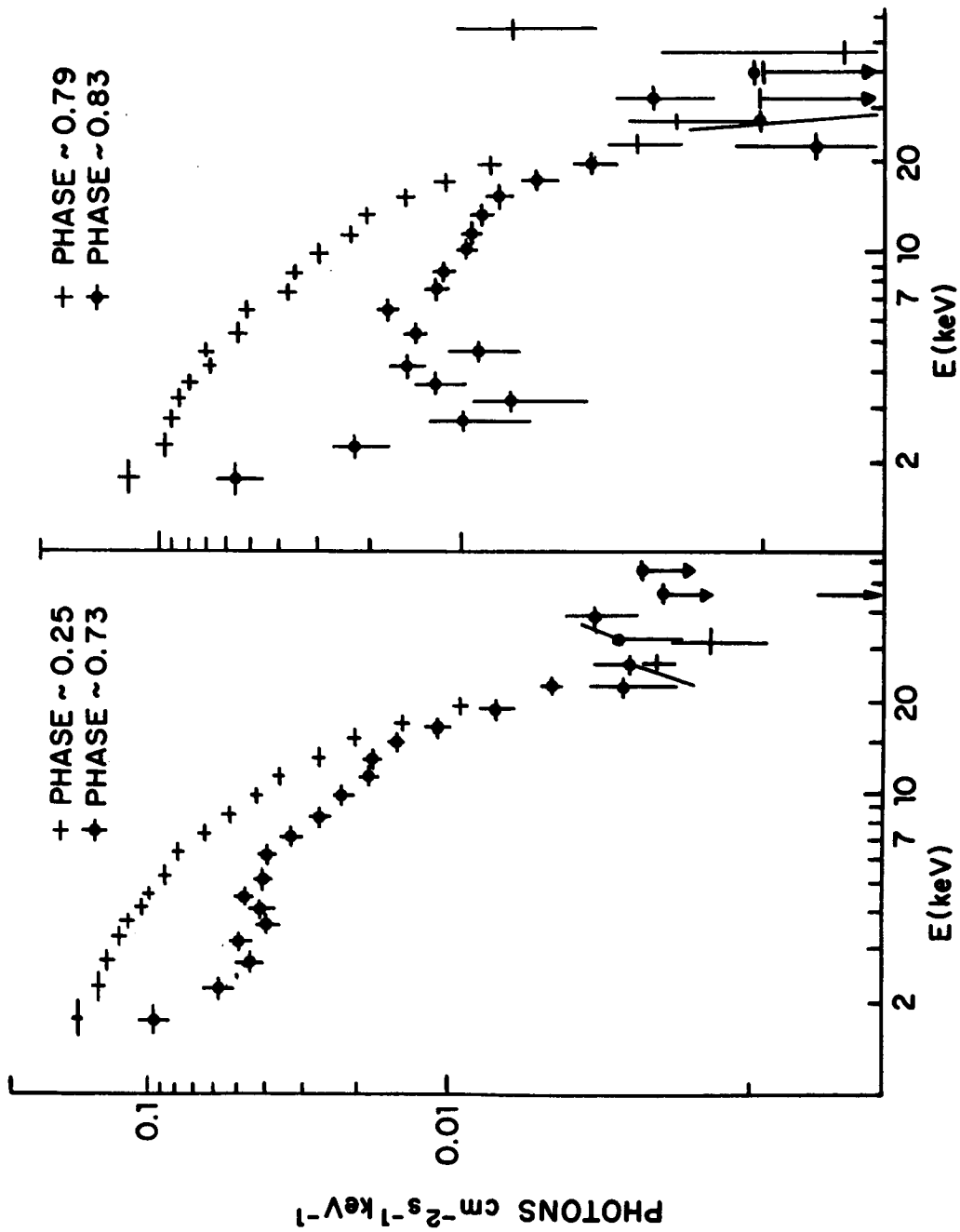


Figure 7. Average Cen X-3 High State and Dip Spectra. These were taken with the xenon detector. Phase .25 corresponded to a high state. At phases .73, .79, and .83 the average intensities were 31%, 54% and 18% of the high state intensity.

PULSED X-RAY OBSERVATIONS OF CEN X-3 FROM ARIEL-5

I. R. Tuohy*
University College London
Mullard Space Science Laboratory
Holmbury St. Mary, Dorking, Surrey,
England

ABSTRACT

The 4.8 second X-ray pulsations from Centaurus X-3 were monitored by the MSSL collimated proportional counter on board Ariel-5 between 18-27 January 1975. Analysis of the source Doppler effect shows that the pulsation period of Cen X-3 decreased by 3.70 ± 0.04 milliseconds during the preceding 2.3 years. The Doppler analysis also yields updated values for the binary phase and period of Cen X-3. Phase zero occurred at JD 2442438.628 \pm 0.003 and the average heliocentric binary period between October 1972 and January 1975 was 2.087129 \pm 0.000007 days. Light curves of the 4.8 second pulsations in the 3-9 keV band are characterized by two pronounced peaks, in contrast with the single peak profiles observed by Uhuru.

INTRODUCTION

A large fraction of the X-ray emission from the binary source Centaurus X-3 is known to be emitted in the form of 4.8 second pulsations (Giacconi *et al.* 1971, Schreier *et al.* 1972). The pulsations are believed to result from accretion of material onto the two magnetic poles of a rotating neutron star (Pringle and Rees 1972, Davidson and Ostriker 1973). Recent X-ray measurements indicate that the accreting material is derived from the stellar wind of the supergiant companion to Cen X-3 (Tuohy and Cruise 1975, Pounds *et al.* 1975, Schreier *et al.* 1975). This paper presents new observations of the Cen X-3 pulsed emission by the MSSL collimated proportional counter on board the Ariel-5 satellite. Updated values for the pulsation period, binary phase and binary period are derived, together with 4.8 second light curves in the 3-9 keV range.

* New Address: Downs Laboratory of Physics 320-47
California Institute of Technology
Pasadena, California 91125

EXPERIMENT DESCRIPTION

The MSSSL collimated proportional counter has an effective area of 90 cm^2 and a field of view of 3.5° FWHM which is offset by 1.75° from the satellite spin axis. In the spacecraft pulsar mode, counts from the detector are folded at a specified period into 16 phase bins for a pre-selected integration time. The integration time is chosen to keep any phase change during the measurement to a small part of one phase bin. At the end of an integration period, storage of the pulses continues without interruption at the corresponding phase in the next set of 16 bins. A total of 128 separate light curves can be accumulated during one satellite orbit, but phasing information is normally lost between successive orbits. The folding period is controlled by a 2.1 MHz crystal clock and is known to a precision of a few microseconds. Due to the large storage requirements of the pulsar mode, no direct determination of the counter background is possible, nor is any spectral information available. However, the energy region of interest can be selected from 8 bands within the region 2-30 keV.

OBSERVATIONS AND RESULTS

Centaurus X-3 was observed in the pulsar mode frequently between 18-27 January 1975. A satellite folding period of 4.841768 seconds was used and the integration time was set to 48.000 seconds (i.e., 9.9 pulsation periods per individual light curve). Cen X-3 was typically visible for 30 minutes during each orbit but the data often spanned a period of up to 60 minutes, depending on the source-Earth occultation pattern. The double pulse structure from Cen X-3 was detected strongly on ~ 30 orbits, and due to the source Doppler effect (± 6.7 milliseconds change in pulsation period per binary period), the phase of the pulsations drifted by different rates during each set of orbital light curves. The magnitude of the drift for each orbit was determined by introducing a linear time displacement of Δt between the individual light curves and summing all the counts into 16 bins for different values of Δt . A value of χ^2 was derived for each Δt by testing the summed data against the mean number of counts per bin. The best value of Δt and the associated uncertainty were determined from the resulting χ^2 peak. Chi-squared maxima ranging up to 650 were obtained, but only distributions exceeding $\chi^2 \approx 50$ were useful in deriving a well defined value of Δt . The data for each orbit were also subjected to a power spectral analysis by treating the light curves as a sequential data set, but this approach was not as sensitive as the χ^2 technique in determining the best value of Δt .

The best-fit Δt values yield the source Doppler curve directly when expressed as the change in period per pulsation period. A phasing analysis similar to that of Schreier et al. (1972) was applied to the data by fitting a 4-parameter function of the form:

$$\Delta t = \Delta p - A \sin \frac{2\pi}{T} \left[(t - t_0) \right],$$

where t is the mean observation time, A is the half-amplitude of the Doppler curve, T is the binary period of Cen X-3, t_0 is the time corresponding to binary phase zero, and Δp is the correction between the intrinsic geocentric period of the source and the satellite folding period. It was not necessary to allow for the small change in the pulsation period during the measurements or the orbital velocity of the satellite. The quality of the fit is illustrated in Figure 1, together with the four best-fit parameters and a representation of the Cen X-3 binary intensity. The data points span 4.2 binary cycles and contain several gaps due to different experiment operating modes, Cen X-3 eclipse or low source intensity. The residuals of the fit were less than the error bars for nearly all data points and this resulted in a low value for the reduced chi-squared ($\chi^2_r = 0.4$).

The values of the binary period and Doppler amplitude (Fig. 1) are in good agreement with the more precise results of Schreier *et al.* (1972). The intrinsic heliocentric pulsation period of Cen X-3 at the time of the Ariel-5 observation was 4.83704 ± 0.00004 seconds which is 3.70 ± 0.04 milliseconds less than the value of 4.840736 ± 0.000001 seconds measured by Schreier (1975) in October 1972. The average decrease in the pulsation period over the 2.3 year interval is therefore -1.6 milliseconds/year. This rate is comparable with the figure of -1.5 milliseconds/year during the previous 1.8 years (Gursky and Schreier 1974), and therefore indicates a relatively uniform decrease in the pulsation period with time (see Figure 2). Significant positive and negative deviations from this linear trend do occur however (Gursky and Schreier 1974), and possible explanations for this behavior have been discussed recently by Lamb *et al.* (1975a).

The Doppler analysis also yields a new binary phase for Cen X-3 corresponding to the center of the eclipsed state. Phase zero occurred at 1975 January 26.128 \pm 0.003 or JD 2442438.628 \pm 0.003. This updated phase reduces the accumulated uncertainty in the original Uhuru ephemeris from 36 minutes to 4 minutes. Furthermore, the new phase can be used to derive a recent binary period for Cen X-3 over the interval following the last Uhuru phase zero datum of JD 2441599.60209 \pm 0.00014 (Schreier 1975). The average heliocentric period between October 1972 and January 1975 was 2.087129 \pm 0.000007 days. Inclusion of this value on the plot of Gursky and Schreier (1974) indicates an erratic, but net long term decrease in the binary period of Cen X-3 (see Figure 3). Various mechanisms to explain the fluctuations in the binary period have been considered by Sparks (1975).

An integrated 4.8 second light curve was generated for each satellite orbit by using the measured Doppler curve to produce precise values of Δt . Figure 4 shows three examples of the double pulse profile in the 3-9 keV range, averaged over a time-scale of ~ 60 minutes. The first pulse is distinguished by a fast rise and slow fall, whereas the second pulse is wider and more symmetric. The two peaks are equally spaced (2.4 ± 0.2 seconds) and have average half-widths of 1.0 and 1.2 seconds. The ratio of power in the first pulse to the second is typically 0.90 ± 0.05 . It is not possible at present to derive accurate values

for the total pulsed fraction from Cen X-3 due to the limited knowledge of the detector background in the pulsar mode and the presence of a transient source in the field of view (Ives et al. 1975). However, the data are consistent with a pulsed fraction in the range 30-60% between 3-9 keV. Schreier et al. (1975) point out that the true pulsed fraction tends to be reduced when the data are folded over long intervals.

A few 4.8 second light curves were also obtained in the 9-16 keV region. The double peak profile is clearly present in this energy range, but detailed assessment of the pulse shape is precluded by insufficient statistics. The data do suggest however that there is a greater difference between the intensities of the two peaks in the 9-16 keV band than in the 3-9 keV band. If confirmed, this would imply that the two peaks have different energy spectra.

The shape of the pulse profile remained relatively stable on a time-scale of ~ 60 minutes for the duration of the Ariel-5 observations, although small but significant differences can be seen in Figure 4 (in the pulse shapes and in the level between the two peaks). As noted by Schreier et al. (1975), the pulse profile exhibits considerable short term variability. Successive 96 second light curves show pronounced changes in the pulse shape, and on occasions, one or both peaks virtually disappear.

The Ariel-5 pulse profiles agree well with the double peak structure observed during a Caltech rocket flight (Long et al. 1975). However, both the Ariel-5 and Caltech results are very different from the single peak light curves depicted by Ulmer et al. (1974) and Schreier et al. (1975), although the latter authors state that the emission from Cen X-3 was mainly double pulsed during 3 binary cycles in March, 1972. As emphasized earlier, the integrated Ariel-5 pulse profile remained double pulsed throughout the 10-day observing period. The observations therefore indicate that the variability in the average light curve is a relatively long term effect. In this case, the pulse shape variability may be related to stellar wobble of the neutron star and the extended low behavior of Cen X-3 (Lamb et al. 1975b).

ACKNOWLEDGEMENTS

I am grateful to Professor R. L. F. Boyd, C.B.E., F.R.S. for his support and am indebted to John Ives who is Project Scientist for the MSSL experiment. I thank Drs. J. Bell-Burnell, A. M. Cruise, P. J. N. Davison and G. P. Garmire for their assistance and advice.

REFERENCES

Davidson, K. and Ostriker, J. P. 1973, Ap. J. (Letters), 179, L585.

- Giacconi, R., Gursky, H., Kellogg, E., Schreier, E., and Tananbaum, H. 1971, Ap. J. (Letters), 167, L67.
- Gursky, H. and Schreier, E. 1974, IAU Symposium No. 67, 'Variable Stars'.
- Ives, J. C., Sanford, P. W., and Bell-Burnell, S. J. 1975, Nature, 254, 578.
- Lamb, F. K., Pines, D., and Shaham, J. 1975a, Preprint.
- Lamb, D. Q., Lamb, F. K., Pines, D., and Shaham, J. 1975b, Ap. J. (Letters), 198, L21.
- Long, K., Agrawal, P. C., and Garmire, G. 1975, Ap. J. (Letters), 197, L57.
- Pounds, K. A., Cooke, B. A., Ricketts, M. J., Turner, M. J., and Elvis, M. 1975, M.N.R.A.S., 172, 473.
- Pringle, J. E. and Rees, M. J. 1972, Astron. and Astrophys., 21, 1.
- Schreier, E., Levinson, R., Gursky, H., Kellogg, E., Tananbaum, H., and Giacconi, R. 1972, Ap. J. (Letters), 172, L79.
- Schreier, E. J., Swartz, K., Giacconi, R., Fabbiano, G., and Morin, J. 1975, submitted to Ap. J.
- Schreier, E. J. 1975, Private Communication.
- Sparks, W. M. 1975, Ap. J., 199, 462.
- Tuohy, I. R. and Cruise, A. M. 1975, M.N.R.A.S., 171, 33P.
- Ulmer, M. P., Baity, W. A., Wheaton, W. A., and Peterson, L. E. 1974, Ap. J., 191, 593.

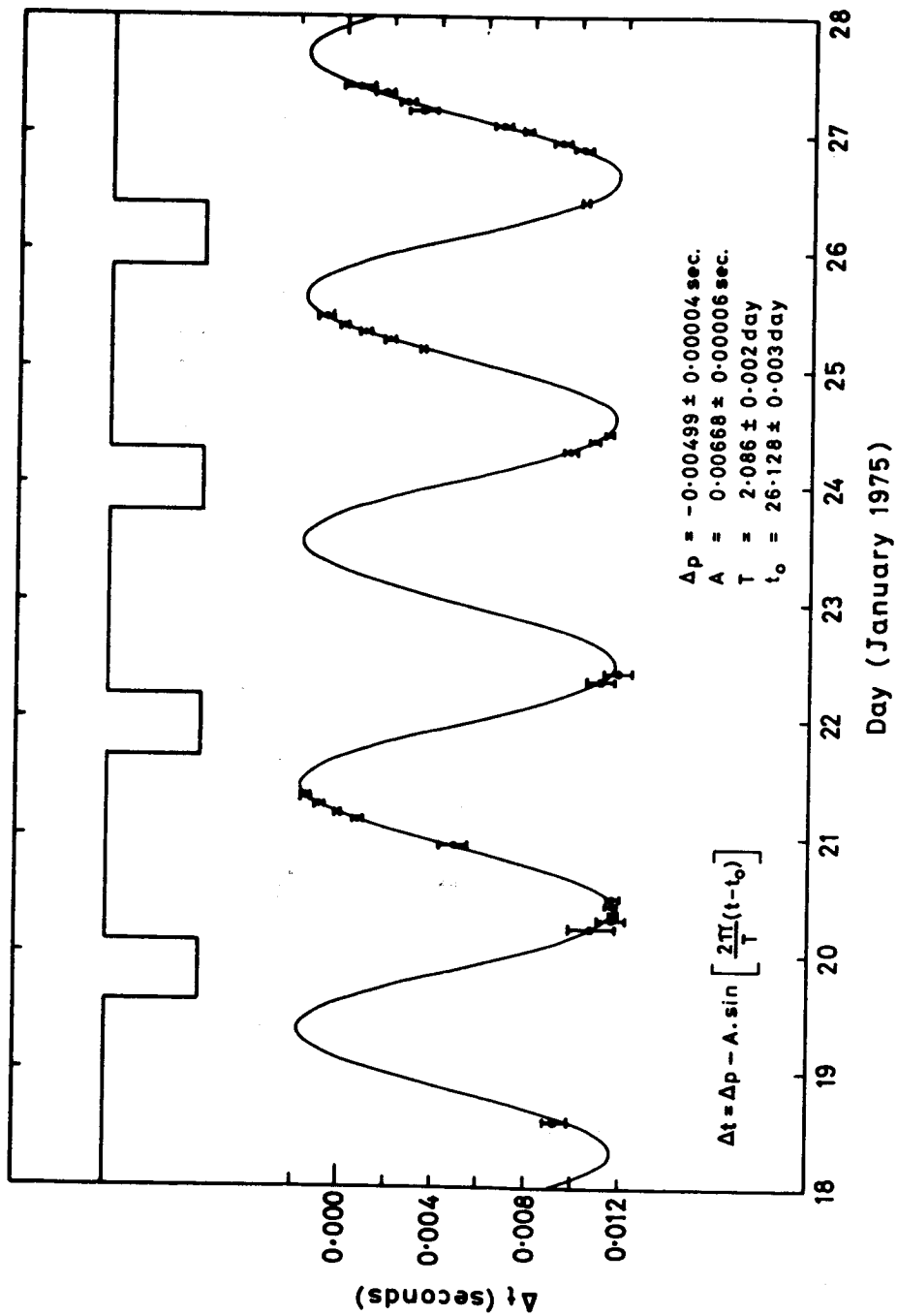


Figure 1. Doppler curve and best-fit parameters for Cen X-3 between 18-27 January 1975. A schematic representation of the Cen X-3 binary intensity is also shown.

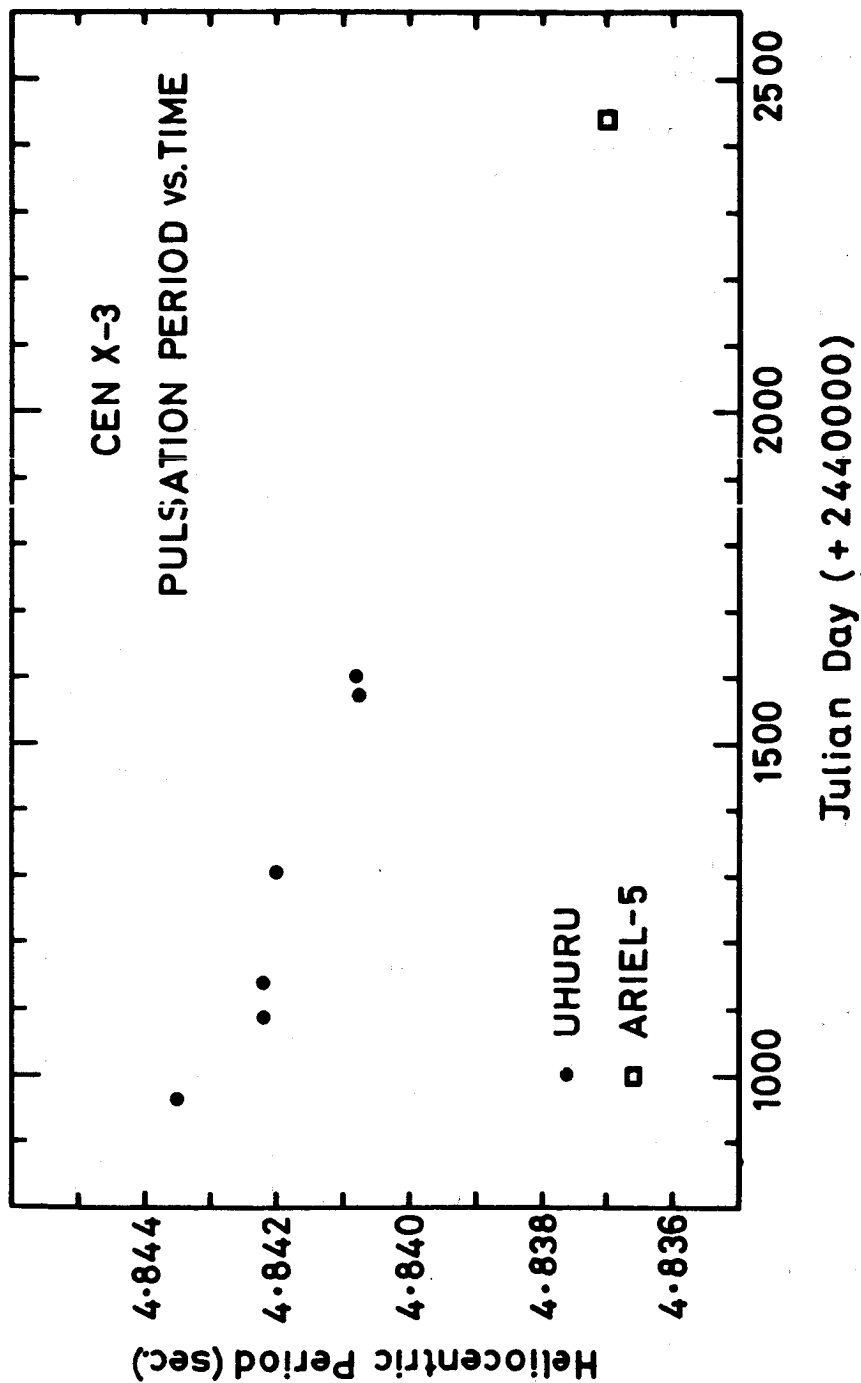


Figure 2. Change in the pulsation period of Cen X-3 with time. Uhuru data points are from Gursky and Schreier (1974).

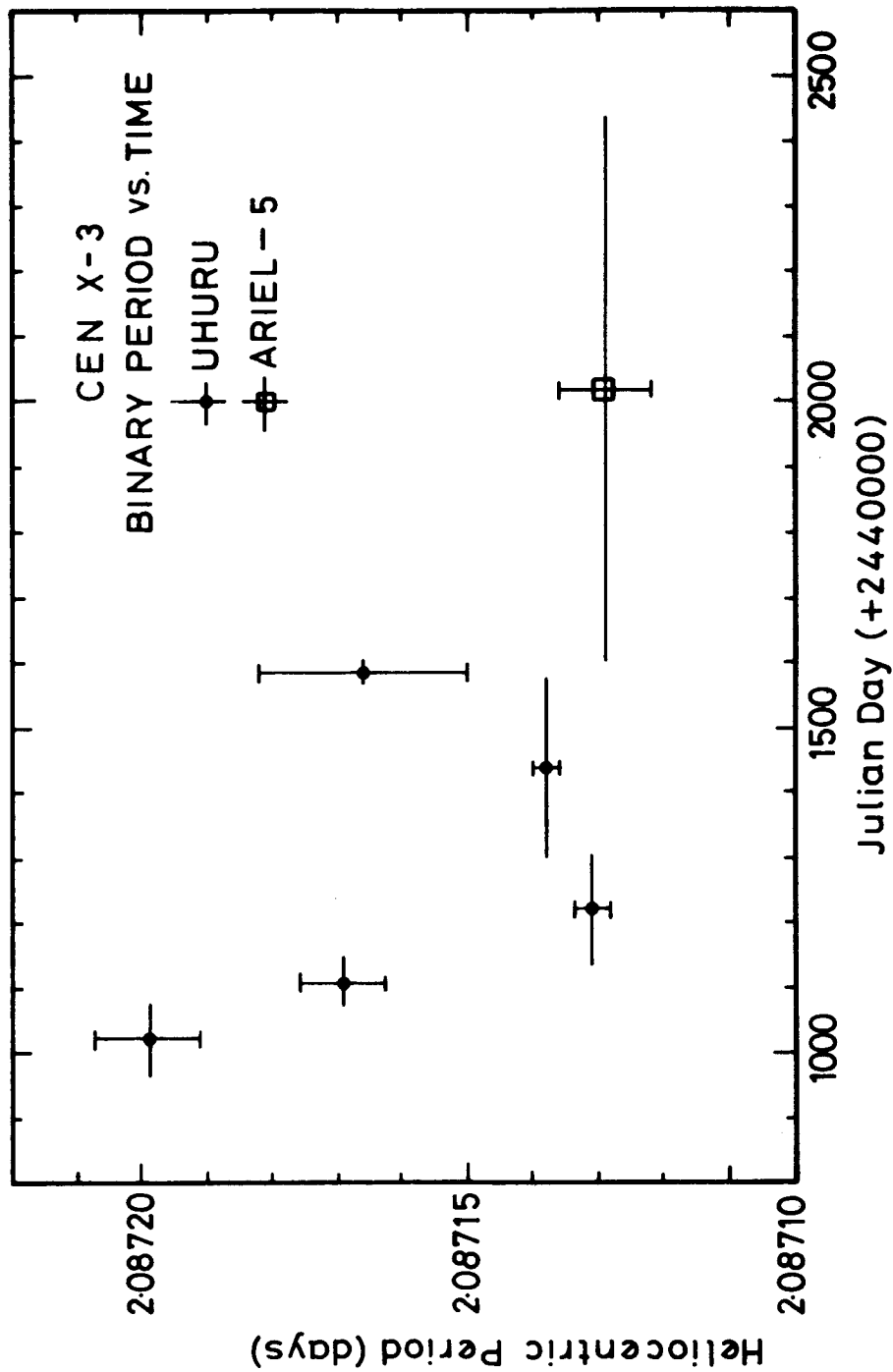


Figure 3. Change in the binary period of Cen X-3 with time. Uhuru data points are from Gursky and Schreier (1974).

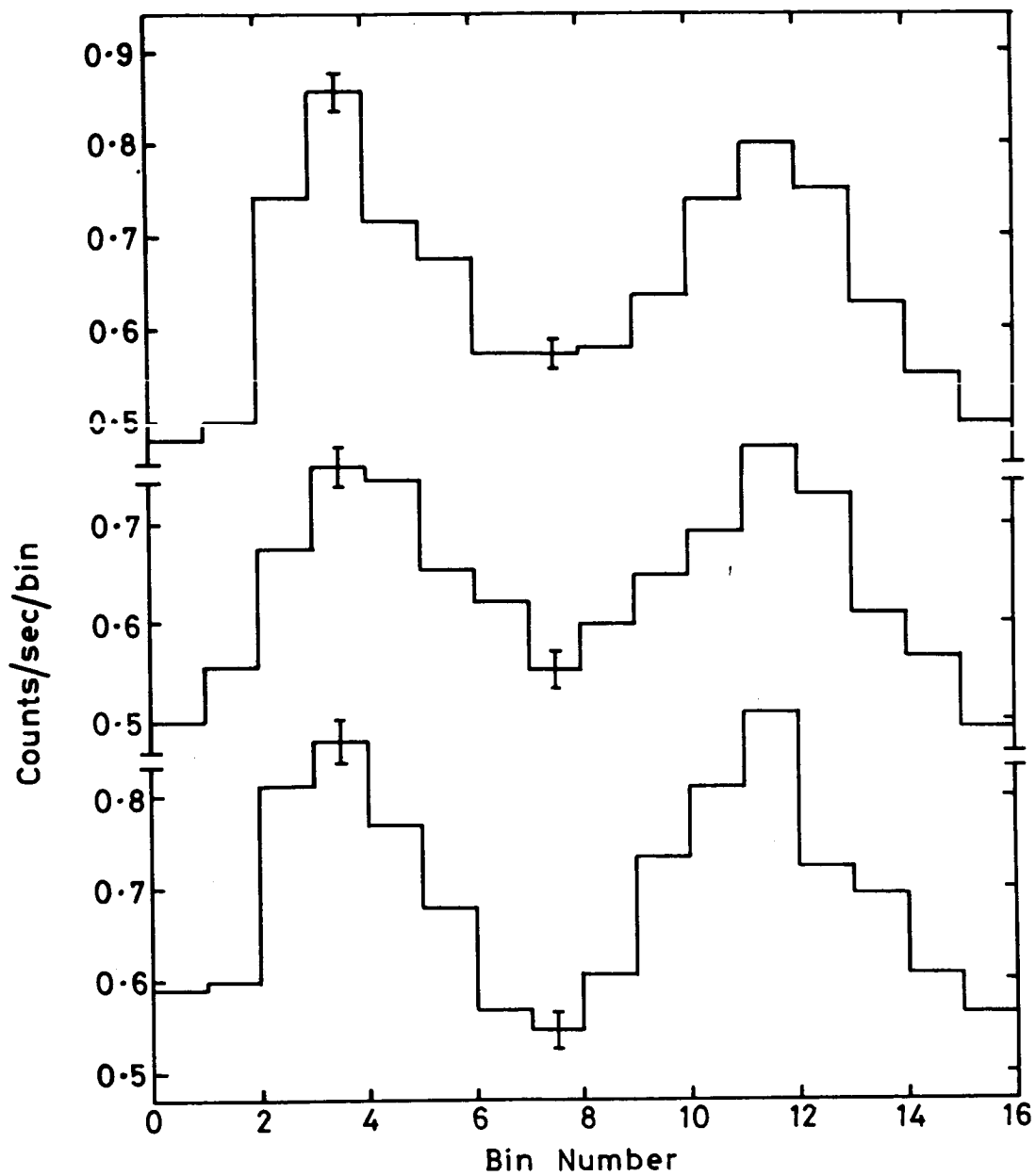


Figure 4. Three 4.8 second light curves of Cen X-3 in the range 3-9 keV, averaged over a time-scale of ~ 60 minutes.

CEN X-3

Discussion

N. V. Vidal:

I would like to draw attention to the paper by Osmer, Hiltner and Whelan (Ap.J. 195, 705, 1975) concerning the radial velocity and the spectral type of Krzeminsky's star. These authors claim an upper limit of ~ 50 km/sec in the radial velocity from absorption lines. This value should be taken with great caution. Our experience shows that (due to weak emissions) the line profiles change and that radial velocity measurements reflect the shape of a particular line profile rather than true orbital motion. As to the spectral type, image tube spectra are as good as direct spectra for spectral classification as long as the differences in spectral and luminosity classes can be detected on the spectra of standard stars. This was the procedure used by us (Vidal et al., Ap. J. L191, L23, 1974). Unfortunately Osmer et al. did not notice that the He II lines $\lambda 4200$ and $\lambda 4541$ did show in our reproduced spectra and they disregarded the related remarks in the text as well. Still, with these lines present it was impossible to determine a spectral class earlier than O8 from our spectra, as against O6 determined by Osmer et al.

H. Gursky:

I have a question and a comment to Schreier or Pounds. My impression is that there is the following inconsistency in the Cen X-3 model. On the one hand there is the large rate of spin-up of the rotation of the X-ray source which requires a large transfer of angular momentum by the accreting material. As I understood the situation this is consistent with the matter originating from Roche lobe overflow, but not from a stellar wind where the outflowing matter does not have appreciable angular momentum. On the other hand, the model Schreier and Dr. Pounds presented to describe absorption phenomena was a stellar wind model. My question is then is there a real inconsistency here?

Y. Avni:

There is no real inconsistency since mass loss by a stellar wind and corotation are not mutually exclusive. There are two separate things that should not be confused: (1) the shape of the geometry, as dictated by the rotational angular velocity, and (2) whether the star overfills the critical radius. The primary could be both corotating with an effective radius close to the critical radius and transferring mass via a stellar wind. This also answers another question raised earlier in this session by Liller. As you may remember, Liller asked whether the stellar wind mechanism requires the very large values of M_x claimed by Mauder using the tidal lobe approximation. Mauder's positive answer was incorrect. Even with a stellar wind, the Roche geometry may be applied, so that from the existence of the wind alone there is no need for large masses. I will explain the situation with the masses in my talk at the 3U0900-40 session.

SUMMARY OF SESSION ON CYG X-3

R. M. Hjellming
National Radio Astronomy Observatory *
Charlottesville, Virginia 22901

INTRODUCTION

This summary of the workshop session on Cyg X-3 will obviously be a non-X-ray astronomer's impression of what we have learned about this object. Since it was only after the Cyg X-3 session was finished that I learned that a summary from each session chairman would be required, I was not taking the notes that would have been useful. Therefore my summary will consist solely of the main points that stand out in my mind. In doing so, I am sure that I will inadvertently be unfair to the work presented by some speakers. For this reason I would like to discuss eight major aspects of our knowledge of Cyg X-3 without attempting to give specific credit to particular individuals or groups.

THE PARTICLE ACCELERATOR

Although it is probably not the most important, the first point that I would like to emphasize derives mainly from the radio data on Cyg X-3.

We know from empirical evidence that much of the radio flaring of Cyg X-3 on time scales of hours to days is due to synchrotron radiation from relativistic electrons. This then has the immediate consequence that one of the major things to be explained by any model of Cyg X-3 is the mechanism by which 10^{42} - 10^{44} relativistic electrons containing 10^{37} - 10^{39} ergs of energy are accelerated in the Cyg X-3 environment in a very variable manner to radiate in regions of high plasma and magnetic field density at distances greater than 10^{14} cm from the central system.

UNIQUE XR-IR RELATIONSHIP

Cyg X-3 has a unique relationship between the observed X-ray and infra-red emission. This is the only object yet known which exhibits synchronized modulation of XR and IR emission, and it occurs with a rigid 4.8 hour periodicity. This synchronization is and will continue to be one of the principal problems for models of the source. This unique relationship between XR and IR also provides great potential for IR investigation of effects first seen at X-ray wavelengths. A case in point is the possible 17 day periodicity discussed for some of the X-ray data presented at this workshop.

* The National Radio Astronomy Observatory is operated by Associated Universities, Inc., under contract with the National Science Foundation.

STABLE MODULATION CYCLE

Many of the papers presented on Cyg X-3 make it clear that we now know that the 4.8 hour modulation cycle has a surprisingly stable, asymmetric shape. This is an important advance from the times when a simple sinusoid was sufficient to fit the data. The work on the Cyg X-3 at a wide range of energies has also shown that, to first order, the modulation cycle is the same at all energies, that is, the X-ray spectral distribution is roughly independent of the modulation cycle. This again plays a remarkable constraint on models for the source.

TWO TYPES OF FLUCTUATIONS

It now seems to be fairly well established that at least two types of fluctuations in mean level do occur in the X-ray emission from Cyg X-3. The first type involves variations frequently seen in the high portion of the 4.8 hour modulation cycle; and the second involves major changes in mean level seen at least during the time of the major radio outbursts in September 1972. The occurrence of a higher level of X-ray intensity at the time of the radio outbursts is vaguely reminiscent of the transitions in level seen in Cyg X-1.

POSSIBLE 17 DAY PERIODICITY

One of the more interesting developments reported at this workshop is the evidence from two independent groups that there may be a 17 day periodicity in the Cyg X-3 X-ray emission. From the data shown, the chances appear to be good that the periodicity is real; however, there are some questions remaining. One obvious question is whether it is a modulation in mean level or perhaps a modulation of the fluctuations seen at the high portion of the 4.8 hour cycle. In any case, the data to prove or disprove the reality of the 17 day cycle will be in hand soon with all the X-ray satellites currently in orbit. As mentioned above, there is also the obvious interest in seeking signs of a 17 day cycle in the infra-red emission of Cyg X-3.

SIGNS OF Fe LINE EMISSION

There is tantalizing evidence for an emission line feature at 6.5 keV from the Ariel 5 satellite data. Other data show no clear sign of this feature, presumably due to Fe. It should be one of the most important goals of current and future X-ray observations of Cyg X-3 to establish the reality and nature of this spectral feature. With so many cycles popping up in the X-ray data, one of the more obvious questions is whether this feature is variable in time.

CORRELATION BETWEEN kT and INTENSITY

Another major development discussed in this session is the evidence for correlations between kT and I, that is, between the parameter of a bremsstrahlung fit to the Cyg X-3 spectra and the X-ray intensity. This

has now been seen in at least two ways. First in the UHURU data showing a rise and fall in kT during the September 1972 radio outbursts, and secondly in more recent detailed studies of the spectrum of the source. Clarification of what lies behind this apparent correlation will be critical to our understanding of Cyg X-3. Explanation of this correlation should be a major objective in models of Cyg X-3.

FUTURE OF COORDINATED OBSERVATIONS OF CYG X-3

Lastly, it seems well worth reminding ourselves of the uniqueness of the existence of radio-XR-IR correlations in Cyg X-3, and the potential this implies for future coordinated observations. Because of this, and because of the variety of phenomena found in the source, it is one of the few objects where massive efforts at coordinated XR-IR-radio observations are likely to bear fruit.

THE RADIO SOURCES ASSOCIATED WITH CYG X-3

R. M. Hjellming
National Radio Astronomy Observatory*
Charlottesville, Virginia 22901

ABSTRACT

Some of the conclusions derived from the data on the radio flaring of Cyg X-3 are summarized. In addition, recent data showing that Cyg X-3 has both active and "quiet" radio behavior are presented.

INTRODUCTION

The radio source associated with Cyg X-3 is one of the most interesting and most spectacular variables in the radio sky. It can fairly be described as a nano-quasar, both because of qualitative behavior which is similar to a quasar, though shorter in time scale by factors of 10-100, and because of the energetics involved in the synchrotron radiating particles that dominate the radio behavior of both Cyg X-3 and the quasars. In this paper some of the information derived from the data on the flaring Cyg X-3 radio source is reviewed, and new studies of low level, "quiet" Cyg X-3 behavior are summarized.

RADIO ACTIVE CYG X-3

Since the initial observations of Cyg X-3 radio flaring events in September-October 1972, for which multi-frequency data (Hjellming 1973) are shown plotted as a function of time in Figure 1, this object has shown many periods of wildly variable radio emission. The event of September 2-14, 1972 and the highly polarized event of May 1974 (Seaquist et. al. 1974) have been subjected to the most extensive and useful interpretation. The papers by Davidsen and Ostriker (1974), Gregory and Seaquist (1974), and Marscher and Brown (1975) have expanded upon and supported the early conclusion (Gregory et. al. 1972, Hjellming and Balick 1972) that an expanding, synchrotron radiating cloud of relativistic particles is basically responsible for individual Cyg X-3 radio flaring events. The gross energetics of an event are roughly the following.

Something of the order of 10^{42} - 10^{44} relativistic electrons with energies of 10^{37} - 10^{39} ergs are supplied by the central object and radiate at radio wavelengths at radii in excess of 10^{14} cm where, at least initially, there are magnetic fields of 0.1-10's gauss and electron concentrations (N_e) from

*The National Radio Astronomy Observatory is operated by Associated Universities, Inc. under contract with the National Science Foundation.

10^3 - 10^7 per cc. For events with large N_e the radio emission is de-polarized, and most events seem to be of this type; however, when N_e is at the lower end of the density range, the radio emission is highly linearly polarized with a surprisingly stable position angle during the evolution of an event. Most Cyg X-3 flaring events start out with a compact, optically thick radio source, and, according to Marscher and Brown (1975), free-free absorption and synchrotron self-absorption are competitive at all frequencies. The cloud or clouds of relativistic particles then expand with velocities of 0.01-.1 the speed of light, and the radio source evolves rapidly in time. The early portions of the optically thin decay of an event show an exponential-like decrease which is due to the effects of synchrotron energy losses in the radiating particles. However, as the source expands, a power law decay takes over as adiabatic energy losses become dominant.

The need for 0.1-10's gauss magnetic fields at radii greater than 10^{14} cm from the center of the Cyg X-3 system is one of the main reasons for needing some version of a strong stellar wind in the system, as first discussed by Davidsen and Ostriker (1974), to carry fields originating in the central system out to the radio-emitting regions. The only other option would be to postulate a dynamo mechanism for the magnetic fields; however, no models of this type have been suggested.

RADIO QUIET CYG X-3

Less understood is the low level, quiet behavior of Cyg X-3 radio emission. The most extensive body of data on this was obtained in September 1974 (Mason et. al. 1976) when a coordinated campaign of radio, X-ray, and infrared observations was rewarded not with extensive data on Cyg X-3 flaring behavior, but rather with a roughly three week period of low level behavior at radio, XR and IR wavelengths. The contrast between this and the normal flaring behavior is most striking in the radio region. Figure 2 shows a plot of the radio data at 2695 and 8085 MHz as a function of time from September 7 through September 29, 1974. Noting the different ordinate scales in Figures 1 and 2, the contrast different ordinate scales in Figures 1 and 2, the contrast between the radio active Cyg X-3 and the radio quiet Cyg-3 is obvious. The data in Figure 2 show both slow variations in the mean level for each day and modulations about that mean on each and every day. The slow variation in the mean radio flux levels is best shown in Figure 3, where the averages for each day, and the associate spectral index, $\alpha = \log(S(8085)/S(2695))/\log(8085/2695)$, are plotted as a function of time. There is no doubt about a slow evolution of the mean spectral index from roughly 0.3 to roughly 0.4 over a three week period, and the mean radio fluxes on each day are not entirely independent of each other. Thus some major parameter of the environment of the radio source evolves on times scales of a few days to weeks.

The unusual stability of the Cyg X-3 radio source during September 1974 is further emphasized by the data on the radio spectrum taken during this period, as shown in Figure 4. In Figure 4 the sparse data at 1.4 and 80 GHz are shown together with matching data (Mason et. al. 1976) at 2.7 and

and 8.1 GHz - with the total range of variation at the latter two frequencies during September 1974 indicated by arrows.

The data on the radio quiet has not yet been subjected to extensive interpretation. Although it would be simplest to assume that the low level Cyg X-3 radio emission is just the superposition of large numbers of miniature versions of the large Cyg X-3 flares, different models should be considered seriously. This is largely because of the much longer time scales for the evolution of the "mean" radio source as discussed above.

REFERENCES

- Braes, L.L.E., Miley, G.K., Baars, J.W.M., and Hin, A.C. 1974, private communication
- Davidson, A., and Ostriker, J.P. 1974, Ap. J., 189, 331.
- Gregory, P.C., and Seaquist, E.R. 1974, Ap. J., 194, 715.
- Gregory, P.C., Kronberg, P.P., Seaquist, E.R., Hughes, V.A., Woodsworth, A., Viner, M.R., and Retallack, D. 1972, Nature, 239, 440.
- Hjellming, R.M. 1973, Science, 182, 1089.
- Hjellming, R.M., and Balick, B. 1973, Nature, 239, 443.
- Marscher, A.P., and Brown, R.L. 1975, Ap. J., 200, 719.
- Mason, K.O., Becklin, E.E., Blankenship, L., Brown, R.L., Elias, E., Hjellming, R.M., Matthews, K., Murdin, P.G., Neugebauer, G., Sanford, P.W., and Willner, S. 1976 (submitted to Ap. J.)
- Seaquist, E.R., Gregory, P.C., Perley, R.A., Becker, R.H., Carlson, J.B., Kundu, M.R., Bignell, R.C., and Dickel, J.R. 1974, Nature, 251, 394.

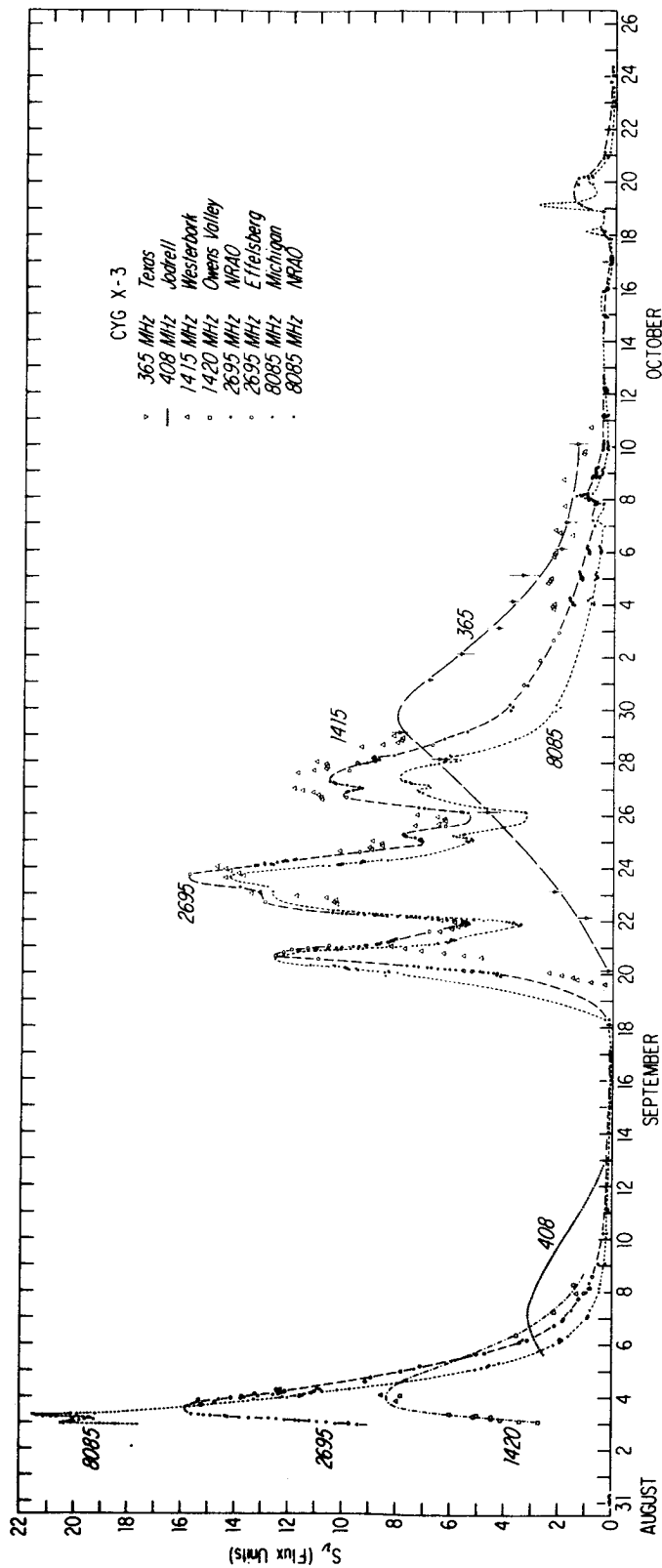


Figure 1. — The radio flux densities of Cyg X-3 are plotted as a function of time for several frequencies for measurements taken during the period August-October 1972 (adapted from Hjellming 1973).

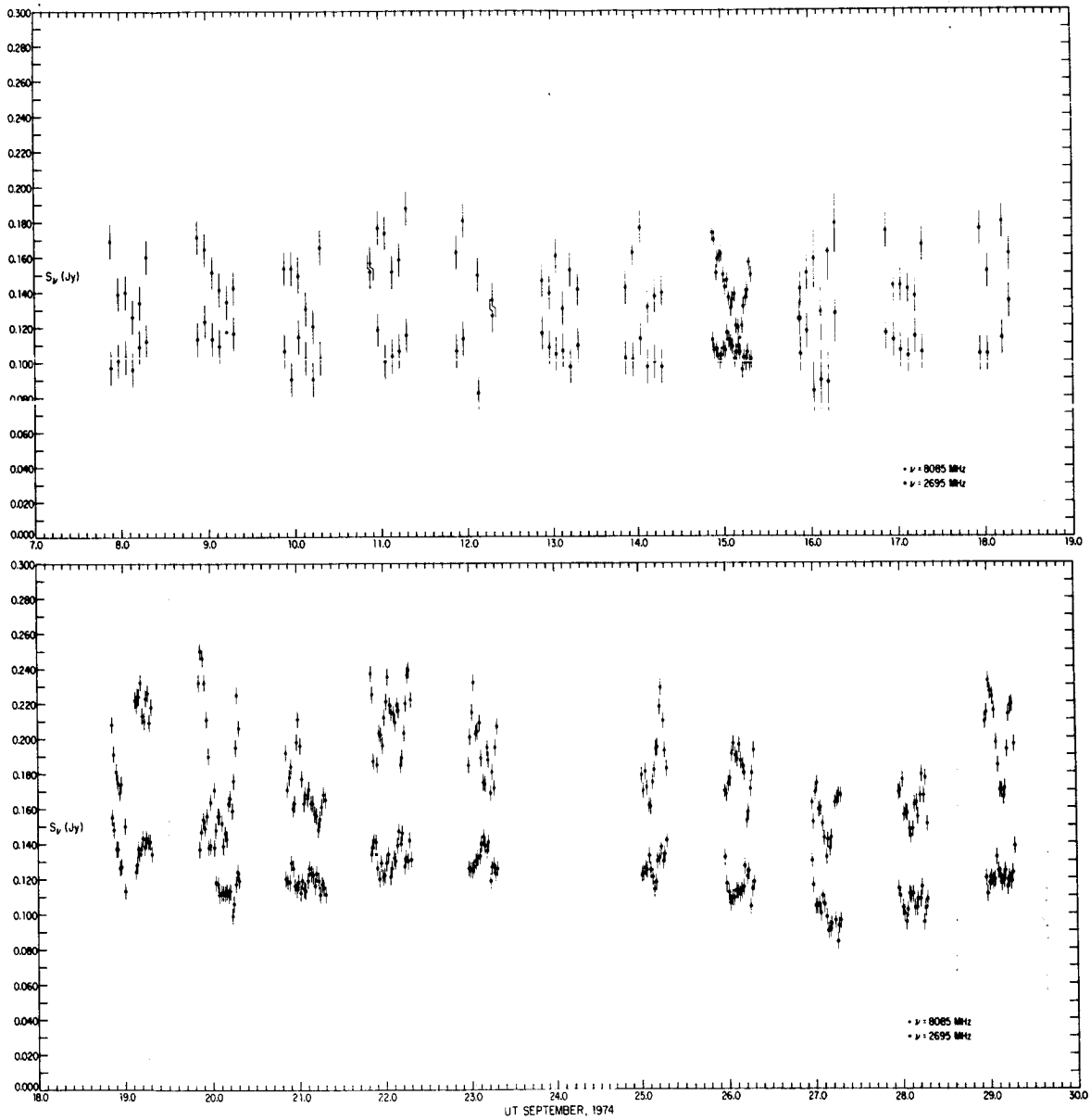


Figure 2. - The radio flux densities of Cyg X-3 at frequencies of 2695 and 8085 MHz are plotted as a function of time for the period September 7-29, 1974.

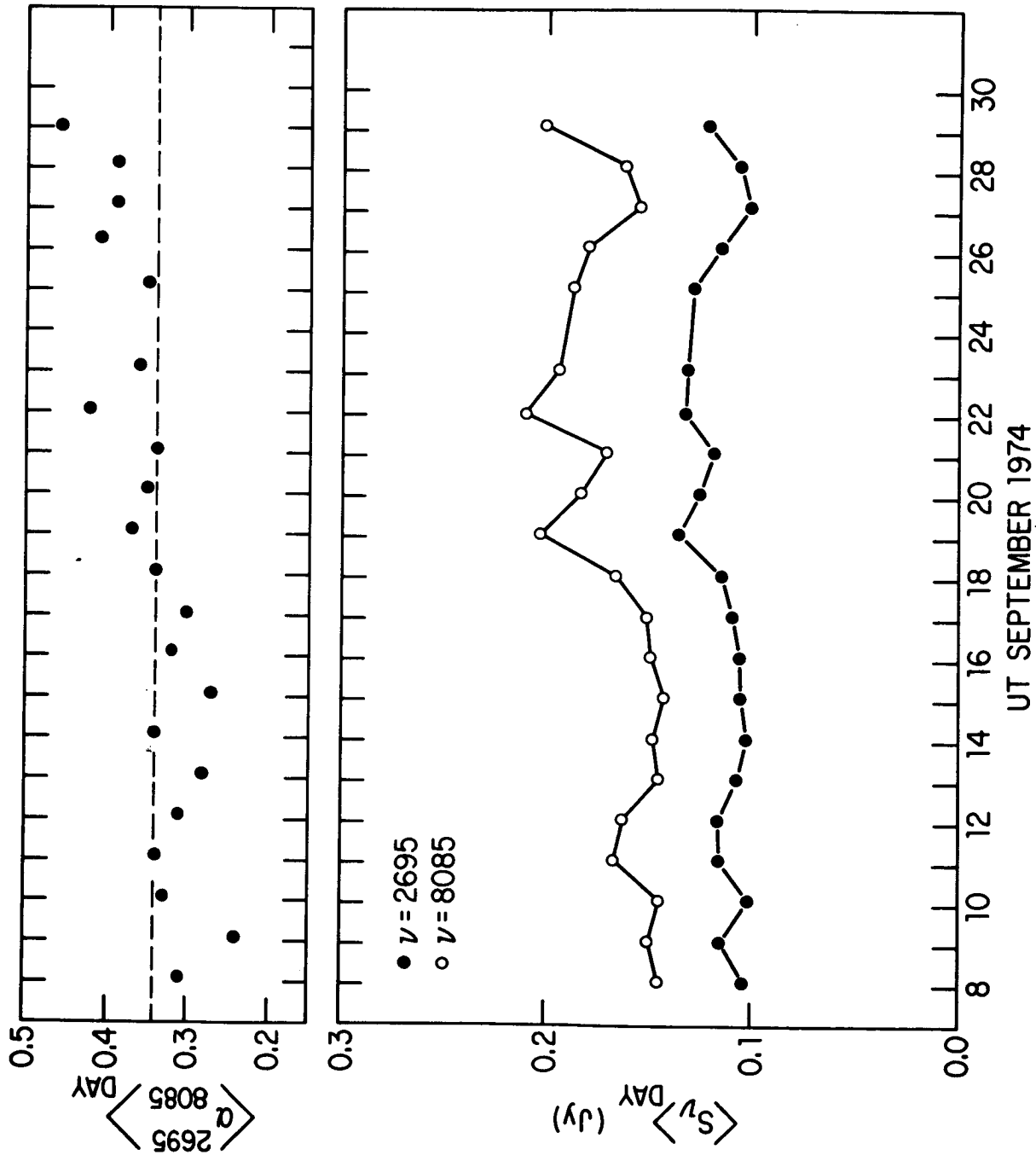


Figure 3. — The mean daily flux densities at 2695 and 8085 MHz and the spectral index derived from these data are plotted as a function of time for the period September 7-29, 1974.

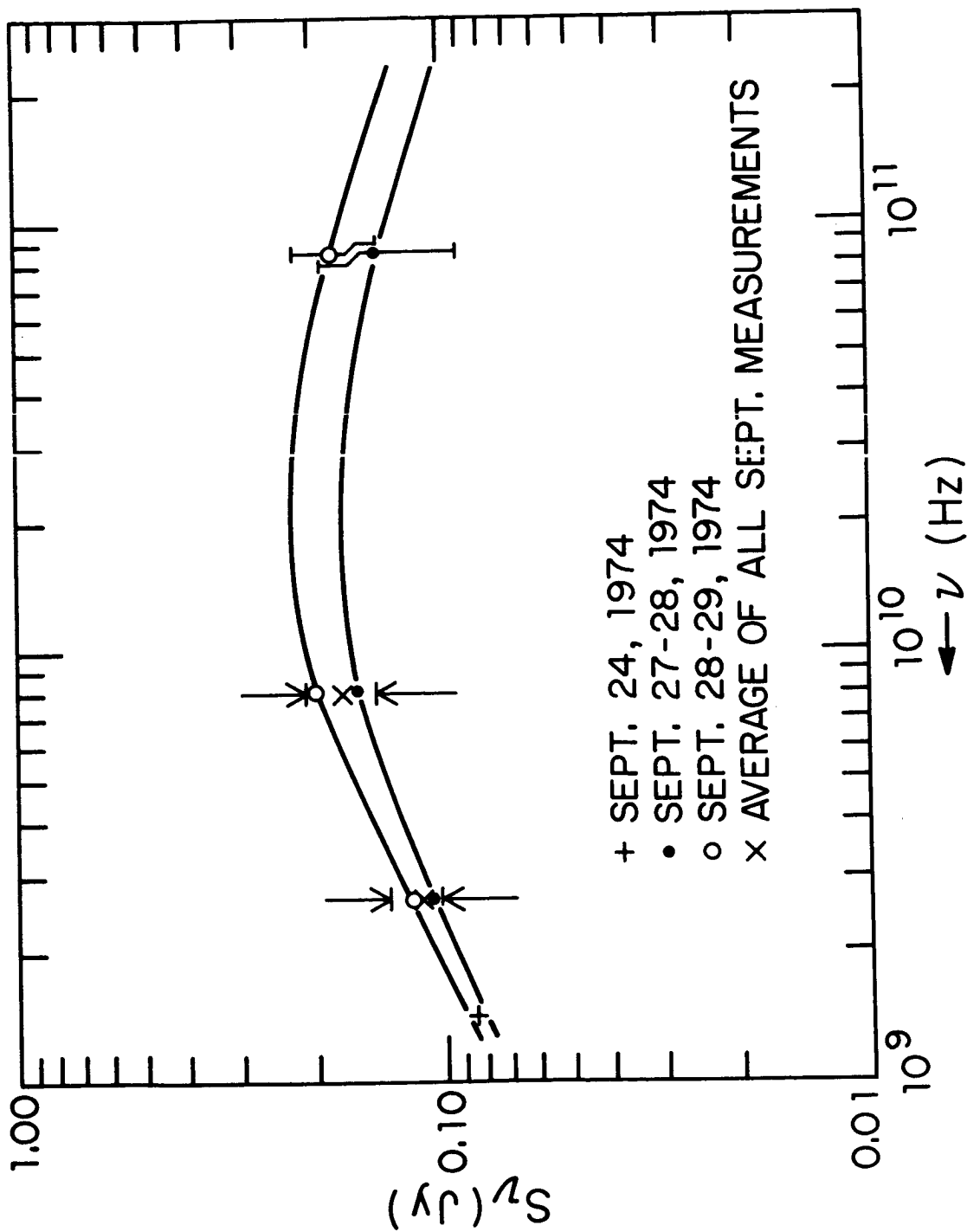


Figure 4. — The radio spectrum of Cyg X-3 during September 1974 is shown as obtained from the average daily fluxes at 80, 8.1, and 2.7 GHz. The point at 1.4 GHz was obtained by Braes et. al. (1974).

OBSERVATIONS OF CYGNUS X-3 BY ANS

A.C. Brinkman, J. Heise, A.J.F. den Boggende
R. Mewe, E. Gronenschild, H. Schrijver
Space Research Laboratory
Utrecht, Holland

ABSTRACT

The medium energy detector (1-8 keV) on board the ANS has observed Cygnus X-3 twice so far, in November 1974, May 1975. The average intensity during the first observing period was very high (about 375 UHURU-counts), during the second observing period the count-rate was more usual (195 UHURU-counts). Spectral parameters have been determined by fitting the count histograms to theoretical photon number spectra. The established 4.8 hour period appears to be stable over the total observed period of 4 years.

INTRODUCTION

The medium energy (1-8 keV) detector on-board ANS has observed Cyg X-3 in 1974 from November 18 until November 22 and in 1975 from May 19 until May 23. The data of the Cambridge instrument (1.5 - 28 keV) on-board ANS, will be discussed separately by D.E. Parsignault.

INTENSITY AND SPECTRAL MEASUREMENTS

During the November period of observation the intensity of Cyg X-3 appeared to be unusually high. In order to study the well-known 4.8 hour period and to determine the average intensity, all data points with low errors were folded modulo the 4.8 hour period. The formula used in folding is $I = a + b \sin [\omega(t-T) - \frac{\pi}{2}]$. The period, $P = 0d.1996811$ was taken from Leach et al. 1975. The result of the folding is given in figure 1. Also drawn in are the data points with large errors which did not take part in the folding. The average intensity is 16 counts sec^{-1} (about 375 UHURU-counts), one of the highest intensities of Cyg X-3 observed so far. The relative amplitude $\frac{b}{a}$ is 54%. A sudden drop in intensity was observed on November 19 between 12h20^m and 12h26^m. The countrate in the 1.5 - 8 keV energy range changed from 14.42 ± 0.88 c/s to 10.2 ± 0.82 c/s within 5 minutes of time. This is indicated in Fig. 1, as a long vertical bar around 2.8 hours. The decrease was not seen in the 1 - 28 keV detector of the Cambridge group, which was measuring simultaneously. This may be explained by the different spectral sensitivity.

If we look at the light curve, it appears that there are a number of measurements, prior to this intensity change, which do not fit the folded light curve well. The intensity of all these points seems about one value of σ too low. Due to unfavourable observing conditions such as high particle background and large off-set from the source, all of these measurements have large errors.

The data has been fitted to theoretical photon number spectra. The best fit was obtained with a black-body spectrum. The parameters are $kT = 1.15 \pm .05$ and $N_H = (3 \pm .5) \times 10^{22}$ atoms cm^{-2} . All data used to derive the parameters were taken after the sudden intensity change described above. Unfortunately no spectral data is available before the intensity change, to look for a possible spectral change associated with the intensity change.

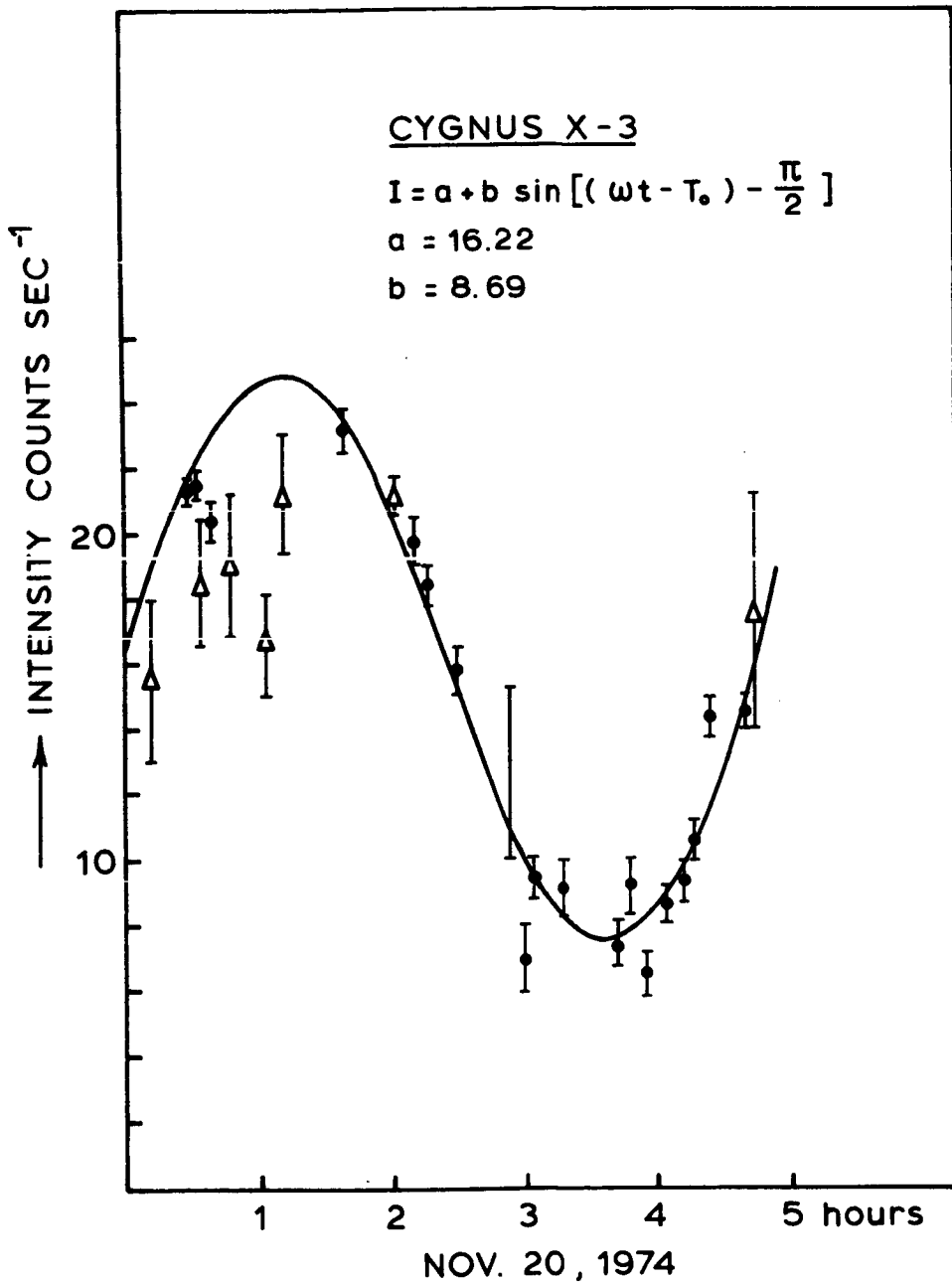
A number of measurements were taken in the high time resolution mode (time resolution .125 seconds) in order to search for periodicities. Power spectral density analysis was carried out for ten measurements of typically 300 seconds each. No periodicities in the range from .250 sec up to about 75 seconds were found.

During the May period, the intensity was equal to the UHURU intensity. Again the data points were folded modulo the known period, see figure 2. The average countrate is 8.5 counts sec^{-1} . Due to the much higher density of data points in May, the time of minimum epoch, T_0 , could be established rather accurately. By combining our T_0 , with the earlier data of Leach et al., it is possible to slightly improve the accuracy of the period. If one assumes no sudden change in the period, which is reasonable in view of the rather good long term coverage of the source, see e.g. paper of K. Mason this conference, the period and error becomes $.1996811 \pm 10 \times 10^{-7}$ instead of $.1996811 \pm 16 \times 10^{-7}$.

In order to look for possible spectral changes associated with the 4.8 hour cycle, we divided the data into 3 sets according to intensity. There is no indication of a variation in spectral parameters with the 4.8 hour cycle. The best fit for each set as well as for the total data together, yields $kT = 1.45 \pm .05$ and $N_H = (3 \pm .4) \times 10^{22}$ atoms cm^{-2} . The sensitivity of our highest energy channel is too low to make a significant statement about possible F_e -line emission.

REFERENCES

- Leach, R.W., Murray, S.S., Schreier, E.J., Tananbaum, H.D.,
Ulmer, M.P., Parsignault, D.R. 1975, Ap. J. 199, 184.



Light curve folded modulo UHURU period.

Figure 1, the Cyg X-3 intensity as observed in November 1974 folded modulo the 4.8 hour period.

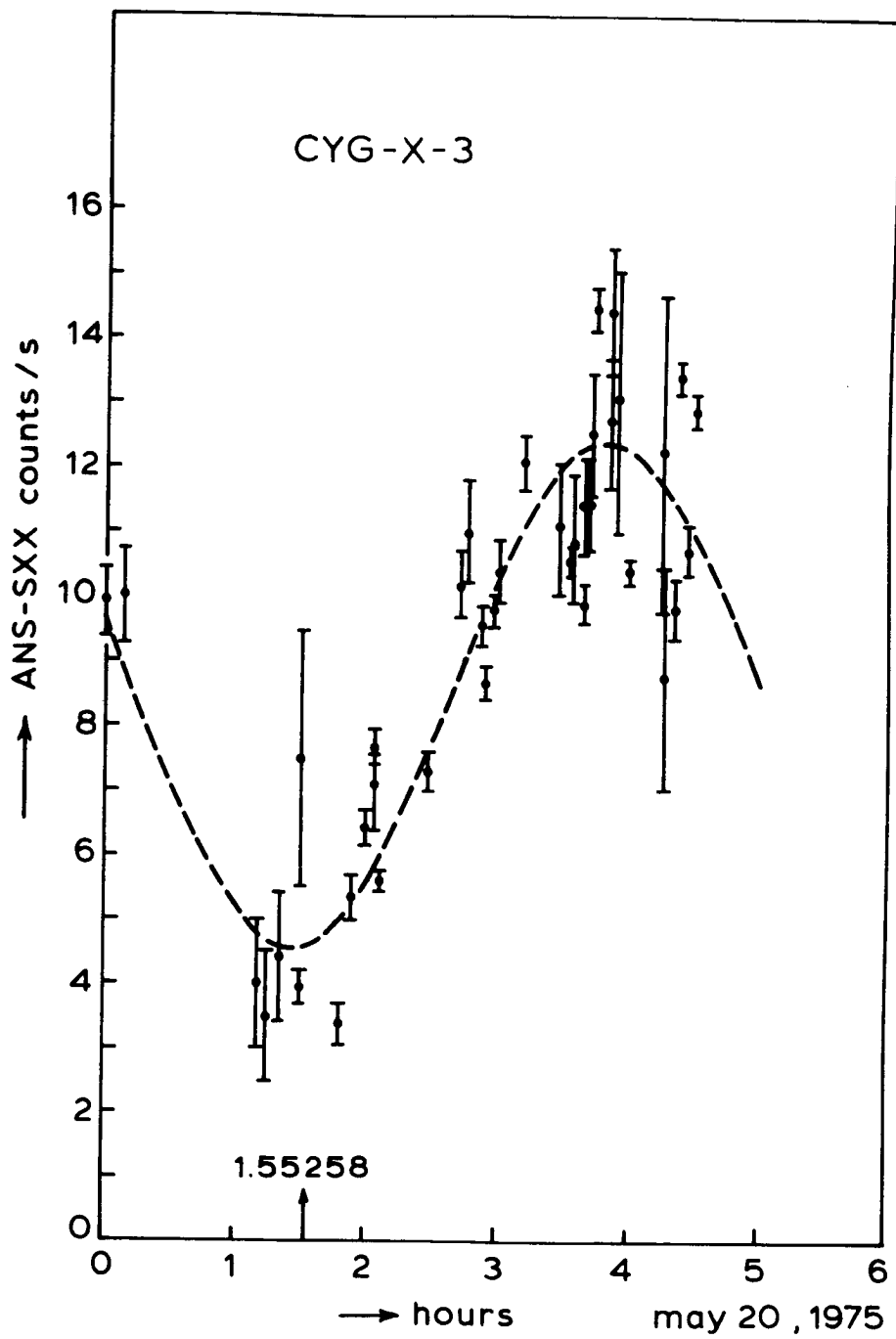


Figure 2, the Cyg X-3 intensity as observed in May 1975 folded modulo the 4.8 hour period.

EVIDENCE FOR A 17d PERIODICITY FROM Cyg X-3

S. S. Holt, E. A. Boldt and P. J. Serlemitsos
Laboratory for High Energy Astrophysics
Goddard Space Flight Center, Greenbelt, Maryland 20771

L. J. Kaluziński and S. H. Pravdo
Department of Physics and Astronomy
University of Maryland, College Park, Maryland 20783

A. Peacock, M. Elvis, M. G. Watson and K. A. Pounds
Department of Physics
University of Leicester LE1 7RH

Cyg X-3 (3U 2030+40) has exhibited phenomena which are observationally unique among identified x-ray sources. The giant radio flare of 1972 is, perhaps, the most spectacular such anomaly, but there are others no less unusual. A wide variation in x-ray spectra has been observed, including the identification of x-ray emission lines at some times, and consistency with a black-body at others.¹ The \sim sinusoidal 4.8h variation² is at a period far in excess of any rotation period which has been ascribed to the compact members of other binary sources, and at least four times shorter than any comparable orbital period. Models have been constructed which identify the 4.8h variation with orbital period^{3,4,5}, acknowledging the peculiar geometries which could give rise to a smooth 4.8h effect in observed x-rays. The present data indicate that a much longer periodicity of \sim 17d is also characteristic of Cyg X-3.

The Ariel-5 All-Sky Monitor, from which most of the present data are taken, has been described in detail elsewhere⁶. The important parameters are an effective pinhole area of 0.6cm² in the energy band

3-6 keV, an average duty cycle for source observation of ~1%, and no temporal resolution finer than 100 min. Typically, ~10 Cyg X-3 counts are accumulated each 100 min. orbit in a resolution element of spatial dimensions $\sim 10^\circ \times 10^\circ$, with a background of ~2 counts.

Figure 1 is a useful verification of experiment performance on Cyg X-3. Single-orbit data from ~100 days are plotted modulo 4.8h from Cyg X-3 and, as a control, Cyg X-1 (with which it might conceivably be confused with resolution elements centered $\sim 10^\circ$ apart). Data points are accepted only if they represent an unambiguous determination of source intensity (i.e. there is less than a 10% possible contribution from other sources, and the intensity is at least twice the estimated one-sigma error after all corrections have been applied). In folding, the data from each 100 min. accumulation are tagged with the orbit midtime. Each bin in Figure 1 is statistically independent from the others, as an orbit contributes to only the bin that contains its midtime (even though the data are accumulated over the equivalent of 3-4 bins). The smooth light curve obtained for Cyg X-3 is not, therefore, an artifact of the folding procedure. Both the shape (and phase) are in excellent agreement with the results of ref. 7, indicating that the present measurements are consistent with their period (and error) of $0.1996811 \pm .0000016d$.

Additionally, there is considerable variability in the day-to-day intensity of Cyg X-3, as evidenced by Figure 2. This behavior is in marked contrast to the constant (within the relatively poor statistics) day-to-day nature of Cyg X-1 measured simultaneously with the same experiment^B. There is, however, some indication of regularity in the Cyg X-3 variations, as illustrated in Figure 3. As the Cyg X-3 data

from individual orbits do not always satisfy the 2σ condition, the All-Sky Monitor data used in both Figures 2 and 3 are derived from $\sim \frac{1}{2}$ -day accumulations which are then analyzed in exactly the same way as are the individual orbits. It is not possible to unambiguously compensate completely for the 4.8h variation in the construction of these Figures, so that no attempt has been made to do so. This variation, as well as gaps in the finite data string and an apparently erratic source behavior, result in many periods in excess of a few days which give relative χ^2 maxima (9.5d, 14.5d and the 15.7d exhibited in Figure 3 are among the more pronounced maxima). The 17d effect is not only the most significant statistically, but also exhibits a roughly symmetrical χ^2 distribution which has a width commensurate with the length of the data sample. On the basis of Figure 3 alone, we would estimate a period of $16.9 \pm .3d$ and a phase at maximum of JD 2,442,387.5 \pm 2 near the most pronounced peak of Figure 2, where this phase is estimated from the peak in the total data string folded at 16.9d.

Figure 2 also contains data from the Ariel-5 Sky Survey Experiment against which the 17d hypothesis may be tested. It is important to note that the latter measurements are obtained in the gaps of the All-Sky Monitor coverage, as the two experiments possess mutually exclusive fields-of-view. All the data are generally consistent with the displayed grid of 16.9d, but it is clear that the effect is not completely reproducible. Almost all of the apparent maxima fall relatively close to the grid, but they are not always clearly defined (and are sometimes absent).

We have attempted to test the 17d hypothesis with older data in the literature, with inconclusive results. Ref. 1 contains a point measurement of high intensity (JD 2,441,959.65) and one of low intensity (JD 2,442,323.71) just prior to the commencement of Ariel-5 operation. Older relatively high intensity measurements from UHURU⁷ are JD 2,440,988.5 and JD 2,441,450.0. A period of 17.05d, at the phase determined by the All-Sky Monitor folding, results in all three historical "maxima" falling at a phase within $\pm .05$ of the expected maximum centroids, while the "minimum" falls more than 0.3 away. In view of the fact that the present maxima are not as precisely locatable (the times of the older measurements are determined by the reported midtimes of the observations only), we expect that this agreement is fortuitous. It would appear that the reality of the 17d effect can be tested only by continuous observation over another year or so.

In Ref. 1, the authors point out that the "high intensity state" of Cyg X-3 is relatively well-fit by a structureless black-body, in contrast to the considerably more complex spectra observed in lower intensity states. They further suggest that the total source luminosity is close to Eddington-limited, and approximately constant regardless of spectral form. This interpretation of "high intensity state" is, therefore, a manifestation of the relatively better efficiency of contemporary experiments near the black-body peak than at higher energies. We are assuming here that this interpretation is correct, and that the times of Cyg X-3 maximum correspond to increased electron scattering in the source.

One possible explanation would arise naturally if the 17d effect was the orbital period of the binary system containing Cyg X-3. In

this case, however, the stability of the 4.8h variation (which would now be interpreted as a slow source rotation) would seem to severely constrain this hypothesis. No apparent 17d Doppler variation in the 4.8h modulation is detectable in the present data ($v_x \sin i < 300$ km/sec), and it is difficult to account for the long-term stability of this period unless the surface field is much lower than that expected if the observed 4.8h modulation arises from rotation.

A less drastic suggestion (i.e. one which does not alter the identification of 4.8h with the orbital period) is that the 17d effect is analogous to the 35d variation in Her X-1 (c.f. ref 9). The consistency of both Cyg X-3 and Her X-1 with contact-binary models (in contrast to the supergiant-stellar-wind models reconcilable with the mass source in other identified x-ray binaries) makes this conjecture attractive. It is interesting to note that the interpretation of this effect in terms of free precession^{10,11} does not necessarily require a neutron-star source for Cyg X-3 just because the 17d and 35d time-scales are comparable. A precession period of 17d is entirely consistent with either a neutron star with rotation period ~ 1 sec, or a white dwarf having a rotation period of the order of minutes. Its interpretation in terms of the precession of the primary member of the binary system (c.f. ref. 12) is likewise insensitive to the nature of the secondary. While it does not appear that the 17d effect can unambiguously distinguish between a white dwarf and a neutron star, the inferred high luminosity and relatively hard spectrum out to ~ 40 keV would seem to favor the latter.

References

1. Serlemitsos, P. A., Boldt, E. A., Holt, S. S., Rothschild, R. E., and Saba, J. L. R., Astrophys. J. Letts., 201, L9 (1975)
2. Parsignault, D. R., Gursky, H., Kellogg, E. M., Matilsky, T., Murray, S., Schreier, E., Tananbaum, H., Giacconi, R., and Brinkman, A. C., Nature (Phys. Sci.), 239, 123 (1972)
3. Davidsen, A. and Ostriker, J. P., Astrophys. J., 189, 331 (1974)
4. Basko, M. M., Sunyaev, R. A., and Titarchuk, L. G., Astron. and Astrophys., 31, 249 (1974)
5. Pringle, J. E., Nature, 247, 21 (1974)
6. Holt, S. S., Proc. COSPAR Symp. Fast Transients X- and Gamma-Ray Astron., Astrophys. Space Sci., (in the press)
7. Leach, R. W., Murray, S. S., Schreier, E. J., Tananbaum, H. D., Ulmer, M. P., and Parsignault, D. R., Astrophys. J., 199, 184
8. Holt, S.S., Boldt, E. A., Serlemitsos, P. J. and Kaluzienski, L. J., Astrophys. J. Letts. (in the press)
9. Giacconi, R., Gursky, H., Kellogg, E., Levinson, R., Schreier, E., and Tananbaum, H., Astrophys. J., 184, 227 (1973)
10. Brecher, K., Nature, 239, 325 (1972)
11. Brecher, K., Nature, 257, 203 (1975)
12. Petterson, J., Astrophys. J. Letts., 201, L61 (1975)

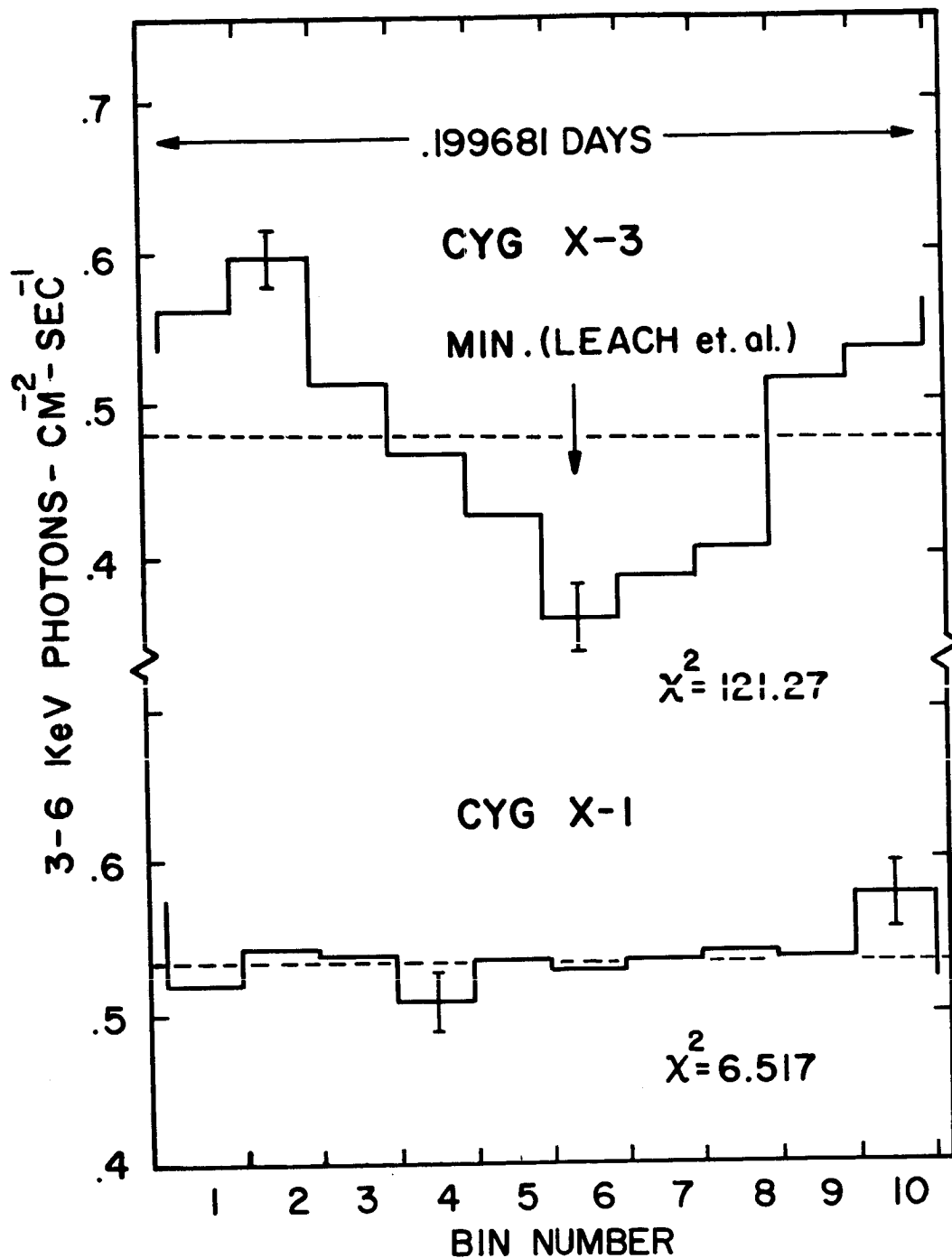


Figure 1. Approximately 100 days of single-orbit Cyg X-3 and Cyg X-1 All-Sky Monitor data obtained between December 1974 and March 1975 folded at the Cyg X-3 period (with indicated phase) of ref. 7. The indicated χ^2 values are for 10-bin folds (9 degrees of freedom) against the hypothesis of a constant source intensity.

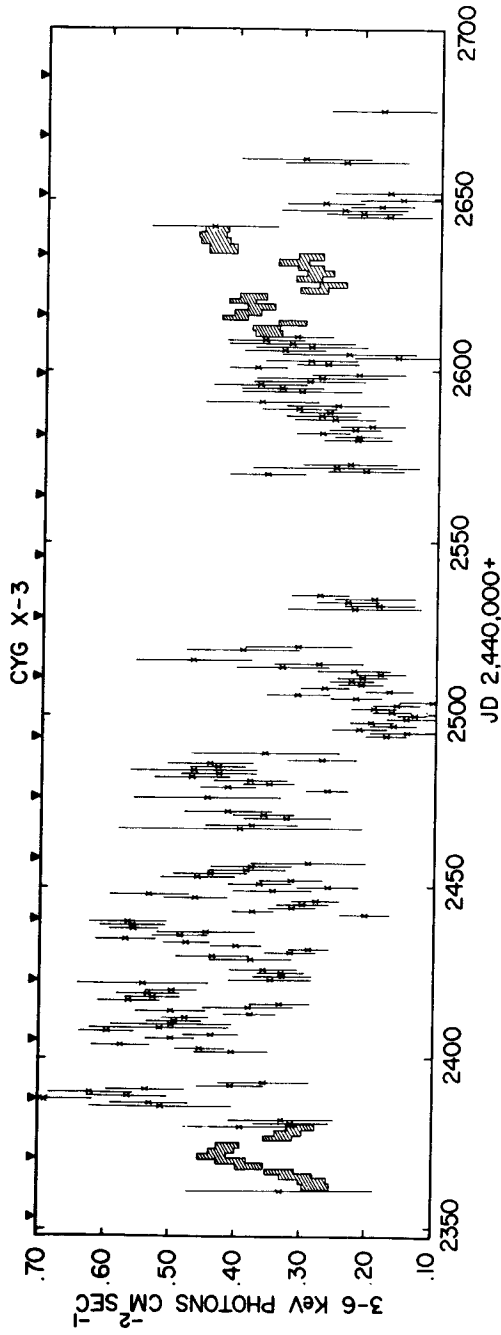


Figure 2. Continuous record of Cyg X-3. The data points are daily averages of All-Sky Monitor data, with $\pm 1\sigma$ error bars. The shaded bars are $\pm 1\sigma$ thick, 1.6d averages of Sky Survey Experiment data. These latter are 2-18 keV measurements which are normalized to the natural All-Sky Monitor ordinate with the response of both instruments to the Crab Nebula. The grid above the data indicates the positions of expected maxima with the best fold values of period (16.9d) and maximum (JD 2,442,387.5).

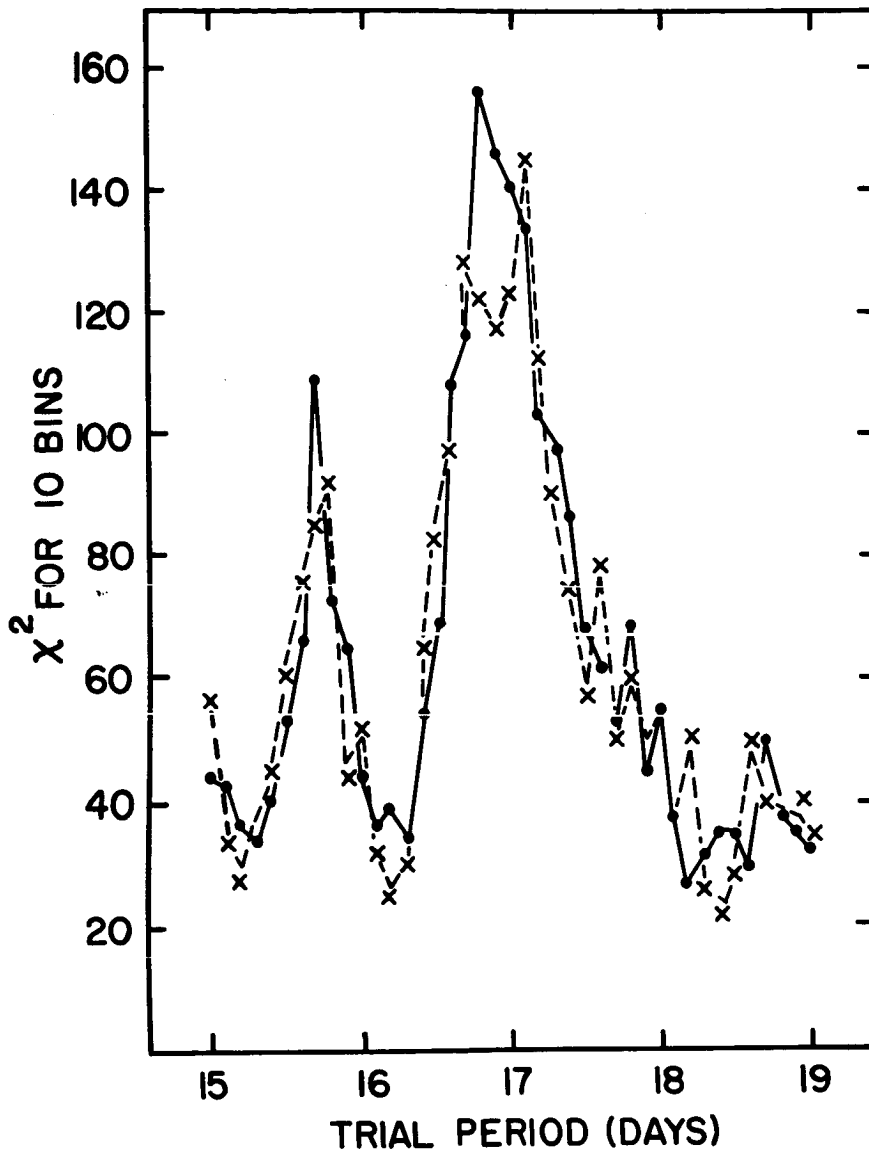


Figure 3. χ^2 obtained by folding the All-Sky Monitor data at 0.1-d intervals between 15 and 19 days in 10 bins, against the hypothesis of a constant source intensity. The two traces correspond to the same data folded at two different binning phases (i.e. $\frac{1}{2}$ -bin out of phase at 16.9d). As in Figure 1, Cyg X-1 data similarly folded did not yield any significant values of χ^2 near the Cyg X-3 maximum.

SOME FEATURES OF THE X-RAY SOURCE CYG X-3

Keith O. Mason, Peter Sanford and John Ives
Mullard Space Science Laboratory,
University College, London,
Holmbury St. Mary, Dorking, Surrey, U.K.

ABSTRACT

Data from the Copernicus satellite are presented which show that the 4.8 hour light curve of Cyg X-3 has been relatively stable in period, shape and amplitude since the observation of the first giant radio outburst in 1972 September. A pulse height spectrum of the source obtained by the Ariel 5 satellite in the 1.5 to 26 keV energy band shows convincing evidence for line emission at about 6.5 keV. The strength of this feature varies in phase with the 4.8 hour continuum modulation, but there is no simple long term relation with the mean continuum intensity per 4.8 hour cycle. Evidence will be presented which indicates that the average 2-6 keV intensity of Cyg X-3 has been higher by a factor of ~ 3 since the onset of the radio flares.

Cyg X-3 is a powerful and complex source at X-ray, infra red and radio frequencies. In this paper we would like to draw attention to three particular aspects of its X-ray behaviour: 1. The relative stability of the 4.8 hour light curve; 2. the presence, on occasion, of an emission feature in the X-ray spectrum; and 3. the existence of a correlation between the level of radio activity and the 2-6 keV X-ray intensity.

To illustrate the first point, figure 1 shows Cyg X-3 data collected with the M.S.S.L. X-ray telescope onboard Copernicus between September 1972 and May 1974. The 4.8 hour modulation is obviously

present during each observation, but with long term changes in the source output superimposed. The best fit parameters of the modulation as derived from four years of Copernicus observations are

$$\begin{aligned} \text{Epoch} &= \text{JD } 2,442,147.995 \pm 0.002 \\ \text{Period, } P &= 0^{\text{d}}.1996846 \pm 0^{\text{d}}.0000008 \end{aligned}$$

$$\frac{1}{P} \frac{dP}{dt} < 3 \cdot 10^{-13} \text{ s}^{-1}$$

and we have folded the data of figure 1 on this best fit period. The result is shown in figure 2 (histogram) and reveals that the mean light curve is asymmetrical, with a sharp fall to minimum, a slower rise, and a relatively broad maximum. There are no large scale fluctuations in the curve on a timescale shorter than the modulation period. The filled circles in figure 2 show a similar mean light curve for a period (September 1974) when the overall 2.5-7.5 keV flux of Cyg X-3 was low. These curves have been normalized to the same flux level so that they might be compared, but the intrinsic difference in source strength between them is almost a factor of 3. Of the order of twenty-five 4.8 hour cycles of data have gone into each. The two curves are remarkably similar; in particular they have the same degree of asymmetry and the same depth of modulation. We would assert, therefore, that over the ~ 4 years that Copernicus has been observing Cyg X-3, the mean X-ray light curve has not changed significantly in period or shape, nor is it affected by changes in the overall source output. This is not to say that individual cycles are all typical of the mean light curve. Indeed this is not the case, as is illustrated in figure 3, where selected portions of data are compared with the mean curve. There are significant variations, both in the depth of modulation and in the form of the curve; in particular, the X-ray flux sometimes undergoes fluctuations of up to $\sim 30\%$ on a timescale of ~ 30 minutes which are most noticeable in the rising part of the 4.8 hour modulation. The fact that fluctuations on this timescale do not appear in the time averaged light curve suggests that these features do not persist at the same phase for long periods.

Turning now to the X-ray spectrum, Cyg X-3 was observed in May 1975 with the M.S.S.L. experiment C instrumentation onboard the Ariel 5

satellite. Experiment C is designed to provide detailed energy spectra of X-ray sources in the 1.5 to 26 keV range, and the results of two days of observation of Cyg X-3 are shown in figure 4. An analysis of these data has recently been published (Sanford, Mason and Ives 1975) so we shall only dwell on the main features of the data here. The filled circles in figure 4 are measurements made in high gain mode, the open circles low gain, and the error bars represent ± 1 sigma statistical uncertainties. The most striking feature of the spectrum is the excess of counts above a black body continuum in the region centered on ~ 6.5 keV; at maximum, the data lies ~ 11 standard deviations off the continuum. In addition, above 10 keV there is an excess of energy above an extrapolation of the 2-10 keV spectrum.

The most likely interpretation of the count excess near 6.5 keV is that it is an iron emission feature. The energy contained in the feature above the best fit continuum would then be 0.18 ± 0.03 keV $\text{cm}^{-2} \text{s}^{-1}$ and its equivalent continuum width 0.33 ± 0.06 keV. The observed FWHM of the feature is consistent with that expected for a monochromatic line broadened by the counter resolution, and we can set an upper limit of about 1 keV on the intrinsic line width.

To determine the behaviour of the emission feature with phase in the 4.8 hour intensity modulation, we divided our data according to whether it was taken in the high or low intensity part of the cycle. Plotted in figure 5 are the residual photon fluxes above the best fitting 2-10 keV continua for each of the two intensity bins. The mean Copernicus light curve is drawn below and indicates to which part of the cycle the bins refer. It is evident from this diagram that the line is most intense at the maximum of the 4.8 hour modulation, and this conclusion is quantified in table 1 from which it can be seen that the equivalent continuum width is the same, within the uncertainties, in both the high and low intensity bin - i.e. the strength of the line is proportional to that of the continuum.

The emission feature seen in the Ariel 5 data is almost certainly the same as that observed by Serlemitsos et al (1975). However, the Ariel 5 observation was made at a time when the 2-10 keV flux from Cyg X-3 was relatively high, and this rules out a correlation suggested by

Serlemitsos et al, between the presence of a line feature and the occurrence of the low 2-10 keV intensity state.

Finally, figure 6 shows a compilation of Cyg X-3 data taken by several different observers between 1970 and 1975. Plotted as a function of time is the average 2-6 keV flux per 4.8 hour cycle, and where the original data do not refer to the 2-6 keV range, a correction has been applied. The diagram indicates that the 2-6 keV flux from Cyg X-3 has been systematically higher since the onset of the giant radio flares, in September 1972, than it was during the ~ 2 years previous to this. Note that it is very unlikely the effect could be caused by systematic differences between the various instruments used to obtain the data, since in several cases simultaneous or near simultaneous observations have been made with two different instruments, and in each case there is good agreement.

This result does not necessarily imply that the total X-ray flux from Cyg X-3 increased. It is now well established (Leach et al 1975; Serlemitsos et al 1975) that variations in the average 2-10 keV source strength are accompanied by changes in the spectral slope; for instance comparison of the two spectra obtained by Serlemitsos et al (1975) indicates that, while the 2-10 keV flux level differed by a factor of ~ 3 (corrected for 4.8 hour phase), the total emission from the source integrated to higher energies was about the same in each case.

However, whatever the nature of the X-ray variability, we must conclude that there is now substantial evidence (cf. also Leach et al 1975) that the Cyg X-3 radio flares are related to a change in the behaviour of the X-ray source.

REFERENCES

- Canizares, C.R., McClintock, J.E., Clark, G.W., Lewin, W.H.G., Schnopper, H.W. and Sprott, G.F., 1973 *Nature Phys. Sci.*, 241, 28
- Leach, R.W., Murray, S.S., Schreier, E.J., Tananbaum, H.D., Ulmer, M.P. and Parsignault, D.R. 1975 *Ap.J.* 199, 184
- Sanford, P., Mason, K.O., and Ives, J. 1975 *Mon. Not. R. astr. Soc.* 173, 9P
- Serlemitsos, P.J., Boldt, E.A., Holt, S.S., Rothschild, R.E., and Saba, J.L.R. 1975 *Ap.J.* 201, 19

T A B L E 1

Phase (measured from Minimum)	Best Fit 2-10 keV Black Body Continuum kT(keV)	N_H	1.5 - 13 keV Incident photon flux ($\text{ph cm}^{-2} \text{s}^{-1}$)	Strength of Emission Feature ($\text{ph cm}^{-2} \text{s}^{-1}$)	Equivalent Continuum Width (keV)
0.8 to 0.3	1.41 ± 0.04	$(5.3 \pm 0.5) \cdot 10^{22}$	0.65	0.019 ± 0.003	0.30 ± 0.05
0.3 to 0.8	1.40 ± 0.04	$(5.2 \pm 0.4) \cdot 10^{22}$	1.2	0.042 ± 0.005	0.37 ± 0.05

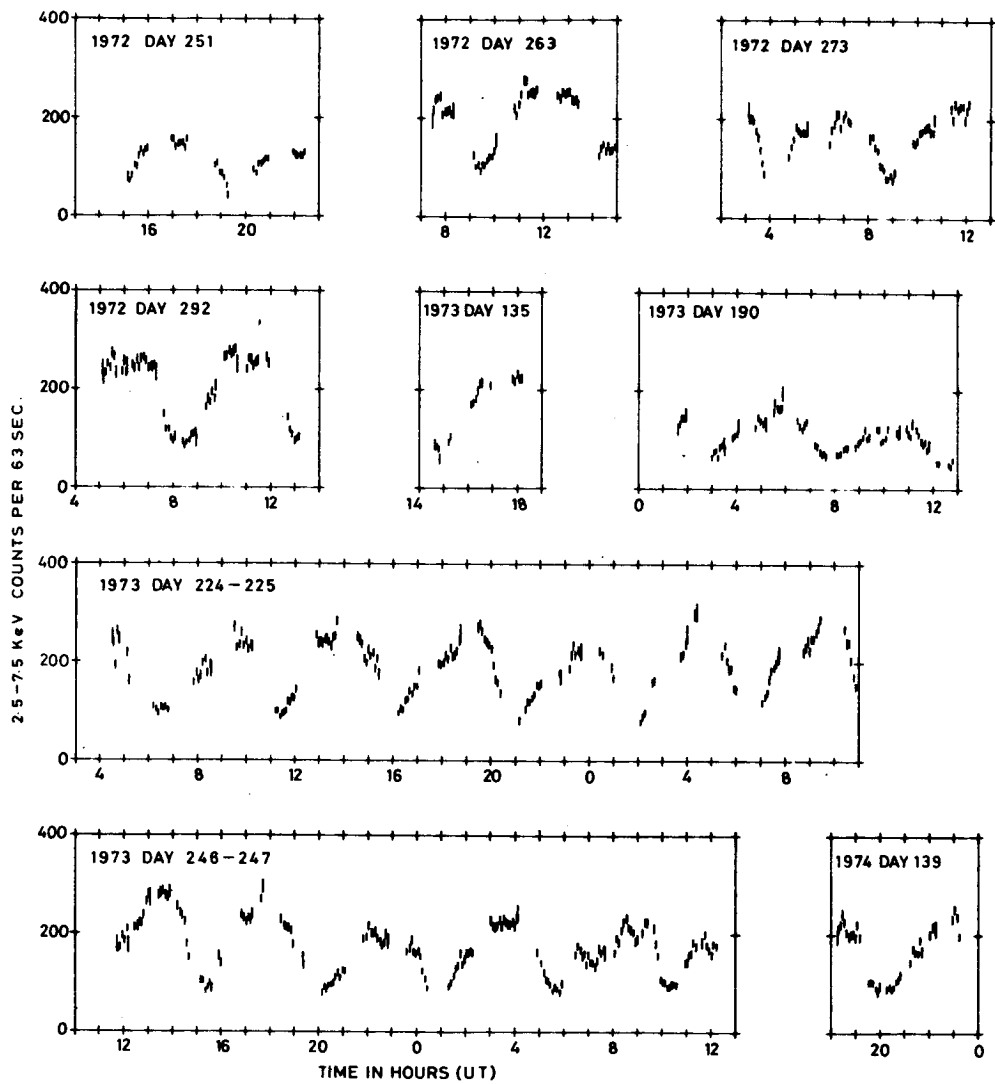


Figure 1 - Data from observations of Cyg X-3 made by the Copernicus X-ray experiment in the 2.5 to 7.5 keV energy range. The data is integrated in blocks of 4.5 minutes duration.

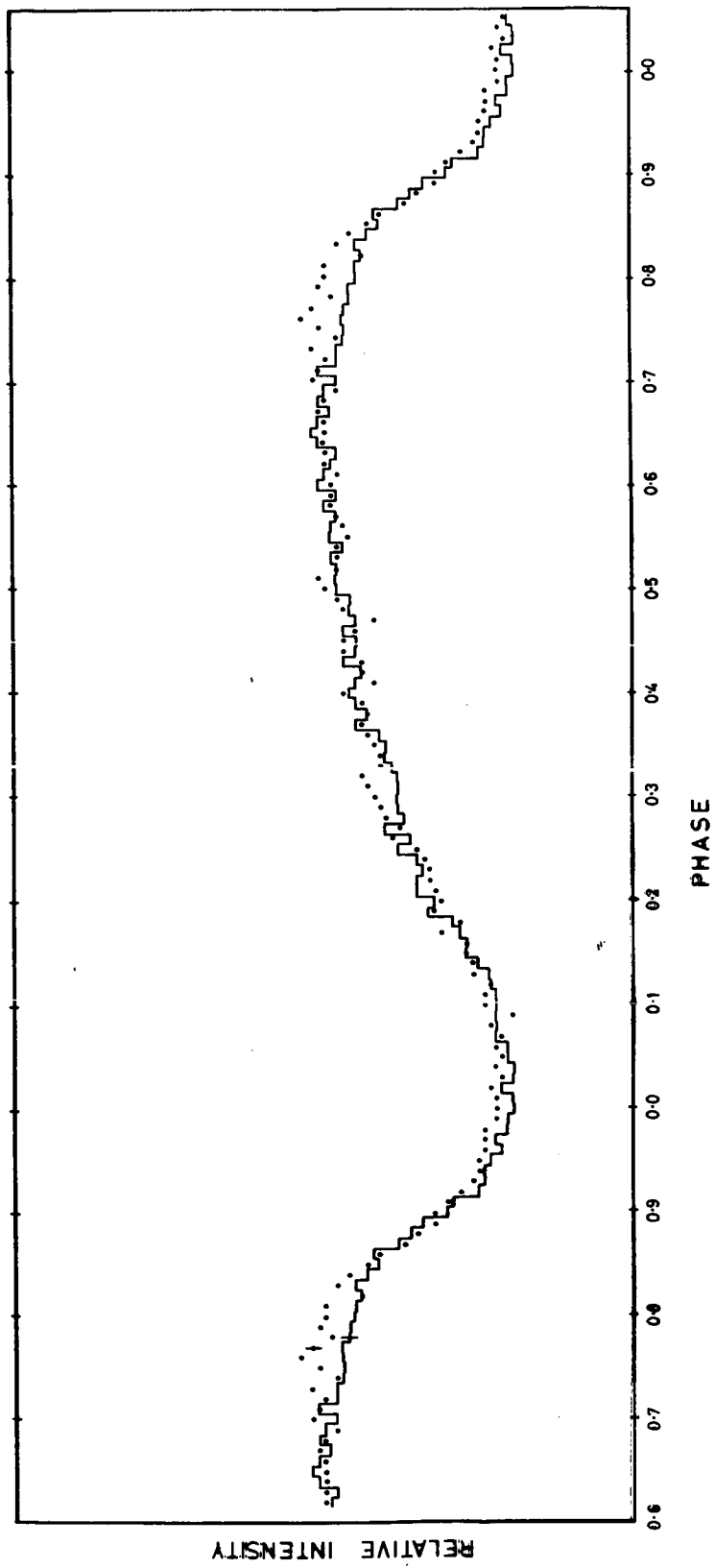


Figure 2 -- Time averaged light curve of Cyg X-3 obtained by folding together high intensity (□) and low intensity (•) data modulo the best fit period given in the text. Slightly more than one cycle is shown in each case for clarity.

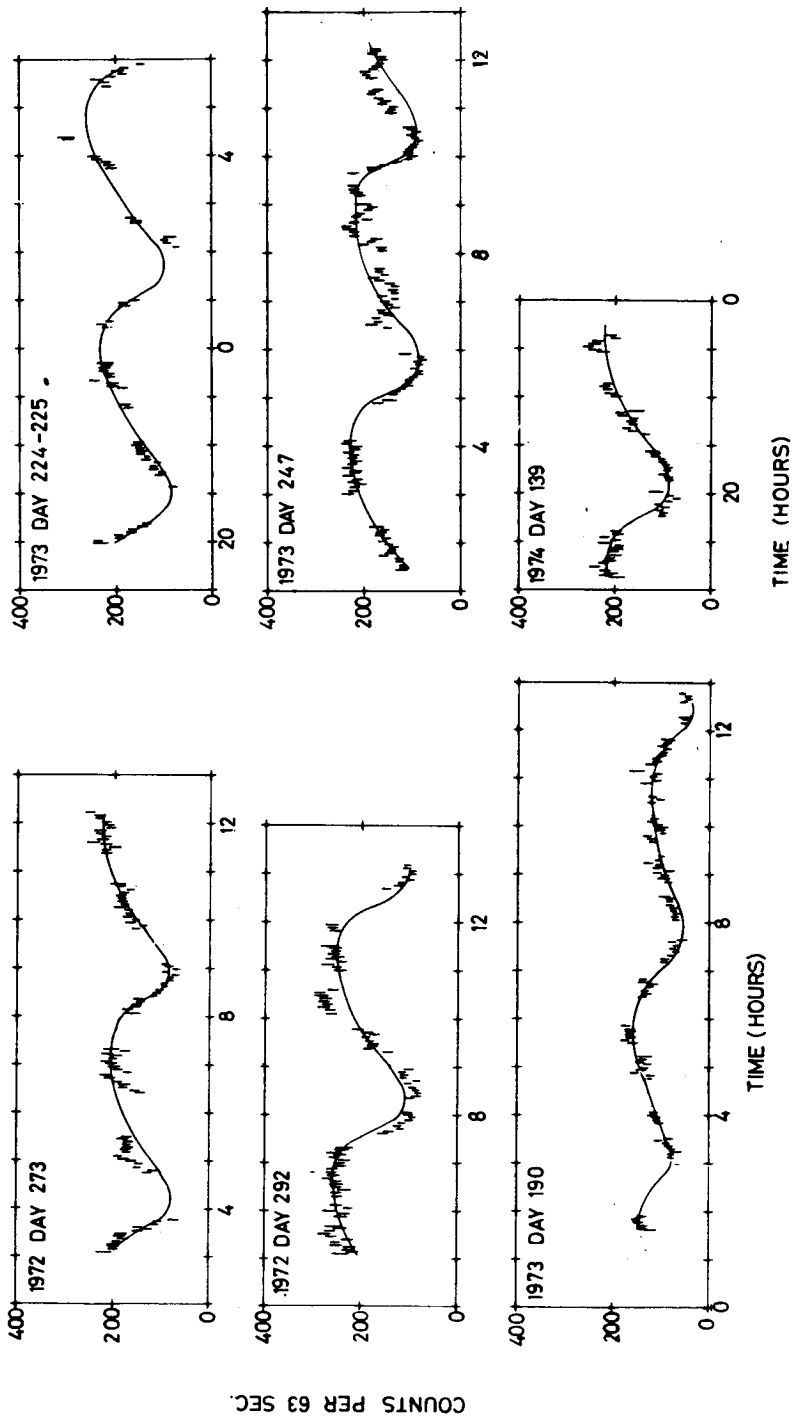


Figure 3 - Selected data from figure 1 compared with the mean X-ray light curve. The integration time is here 3 minutes.

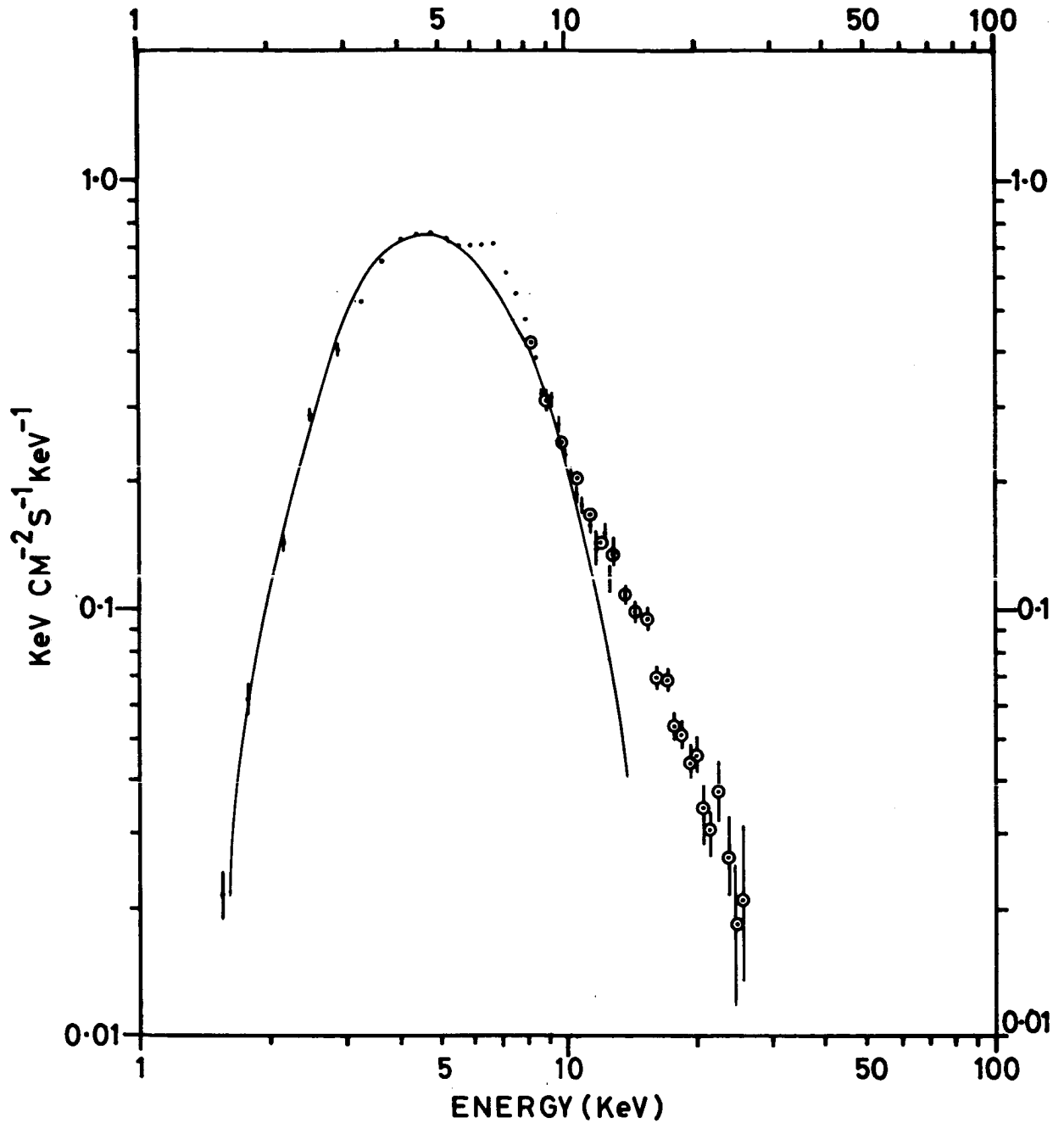


Figure 4 - Spectrum of Cyg X-3 in high gain (•) and low gain modes during 1975 May. The solid curve represents a blackbody spectrum of temperature $1.6 \cdot 10^7$ °K with a low energy cut-off equivalent to absorption by $5.2 \cdot 10^{22}$ H atoms cm^{-2} of cold interstellar material.

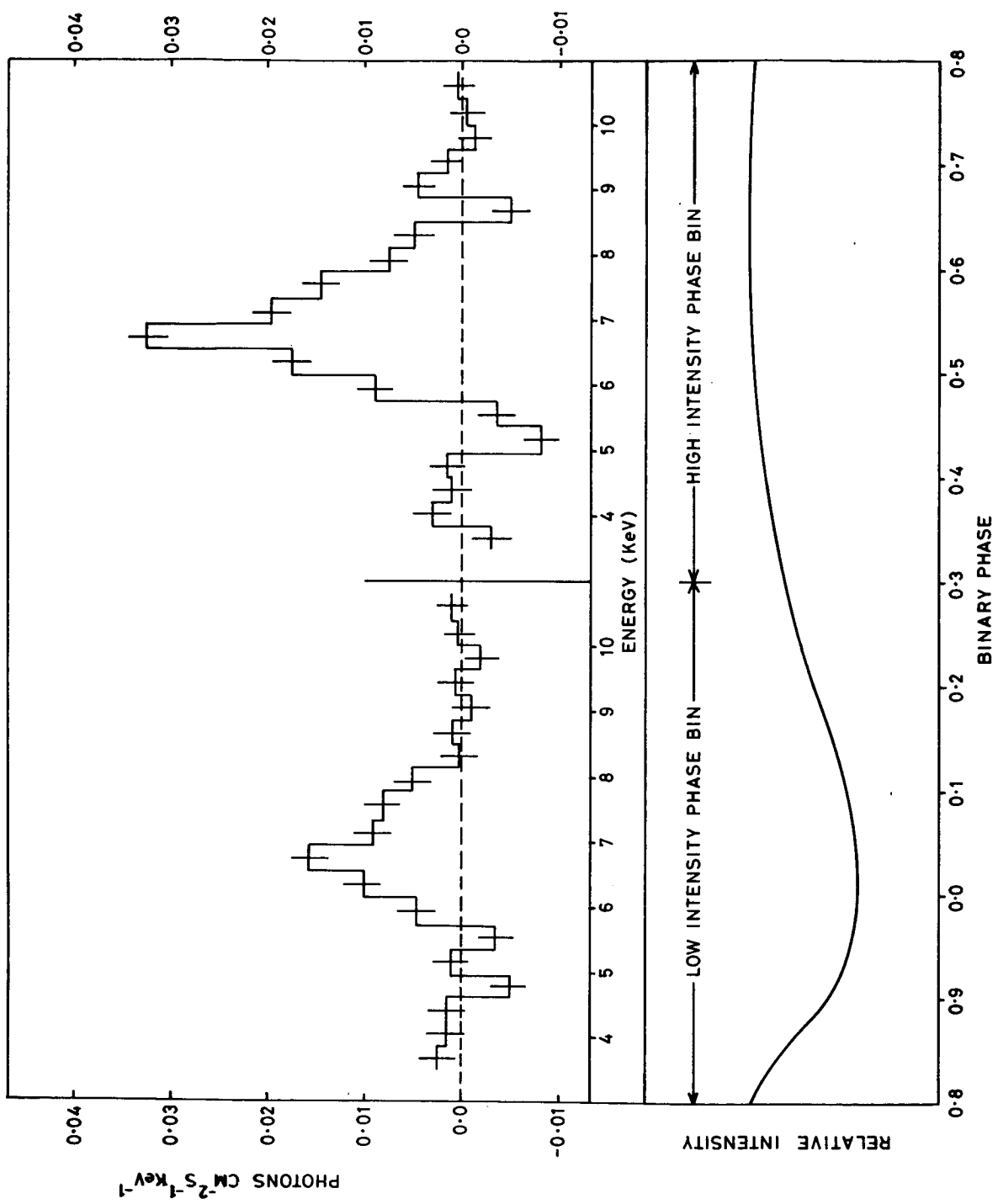


Figure 5 - Residual photon flux in the vicinity of the emission feature after subtraction of the best fitting 2-10 keV continuum. The data have been binned according to whether they refer to the low or high intensity phase of the 4.8 hour cycle (see text). The lower part of the diagram shows the average light curve for Cyg X-3 derived from observations with Copernicus.

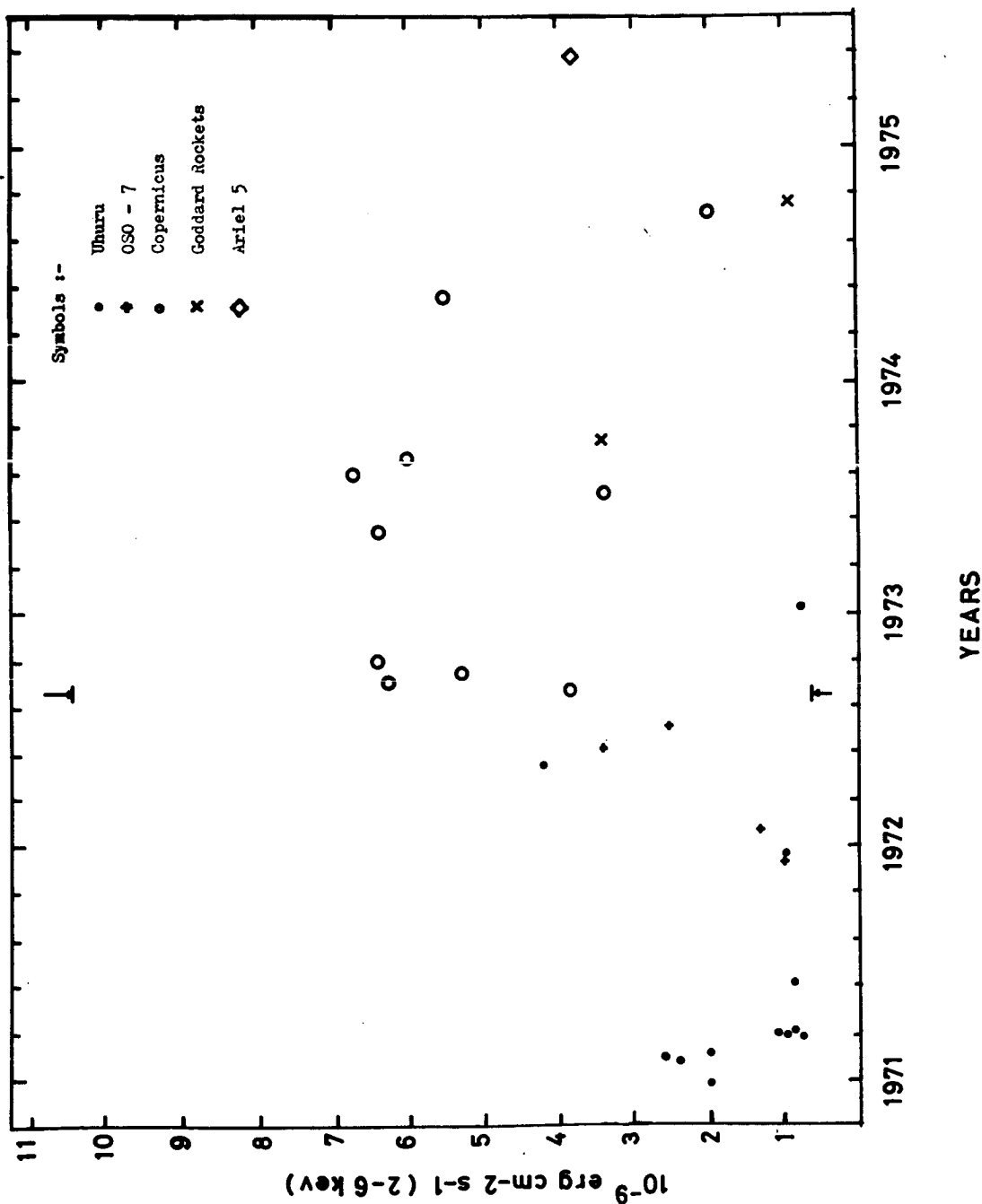


Figure 6 — Compilation of Cyg X-3 flux measurements from several sources. Uhuru data are taken from Leach et al (1975), OSO-7 from Canizares et al (1973), Goddard rocket flights from Serlemitsos et al (1975) and Ariel 5 from Sanford et al (1975). The 2-6 keV flux per 4.8 hour intensity cycle is plotted and the Goddard rocket data have been corrected for phase using the mean Copernicus light curve. The upper and lower limits marked in August-September 1972 represent the flux limits seen by Leach et al during that time.

OBSERVATIONS OF CYGNUS X-3 BY ANS

D. R. Parsignault
Space Division
American Science and Engineering
Cambridge, Massachusetts 02139

and

E. Schreier, J. Grindlay, H. Schnopper and H. Gursky
Center for Astrophysics
Harvard College Observatory/
Smithsonian Astrophysical Observatory
Cambridge, Massachusetts 02138

ABSTRACT

The hard X-ray experiment (1 - 28 keV) on ANS observed Cygnus X-3 in November 1974, and in May 1975. The average flux intensities for these time periods were found to be 22.4 ± 0.5 cts/sec and 12.8 ± 0.3 cts/sec (1.3 - 7.1 keV), the former being the highest average value ever observed. The spectrum studies have shown an excess in the flux above the fitted continuum which can be interpreted as a line emission of FeXXIV and/or FeXXV, at ≈ 6.5 keV. The strength of this feature varied in phase with the 4.8 hr X-ray modulation, and remained at a constant relative intensity. We have refined the period of the X-ray modulation to 0.1996813 ± 0.0000006 day and obtained at a 2σ upper limit to a continuous change in the period of 5×10^{-13} sec⁻¹. This new limit places serious constraints on several models for this object which have been proposed up to now.

INTRODUCTION

Cygnus X-3 has characteristics not found in any other of the galactic X-ray sources. Its X-ray flux has been shown to vary almost sinusoidally with a unique period of ~ 4.8 hours, possibly the shortest of the X-ray binary stars, in the energy range from 2 to about 70 keV (Parsignault et al, 1972; Sanford and Hawkins, 1972; Canizares et al, 1973; Ulmer, 1975; Leach et al, 1975; Pietsch et al, 1975). This object flares in the radio band from time to time, becoming on these occasions one of the brightest radio source in the galaxy. As with other X-ray sources, it exhibits a wide, but not extreme, range of variability.

With the Hard X-ray Experiment (HXX) instrumentation on board the Astronomical Netherlands Satellite (ANS) we have observed Cygnus X-3 in November, 1974, and later in May, 1975. Described here are the following investigations of the data:

1) We have refined the period of the X-ray intensity modulation and found a new limit to any change in the period.

2) We have found evidences in the X-ray spectrum for a significant excess in the energy range 4.6 - 7.2 keV which is consistent with FeXXIV or FeXXV line emissions. Such a feature in the X-ray spectrum had recently been reported by Serlemitsos et al (1975) and Sanford et al (1975).

3) We have found significant variability near the maximum of the 4.8 hours, intensity variation which is not present near the minimum. This result may have an important bearing on the geometry of the X-ray emitting region.

THE EXPERIMENT

The ANS was programmed to observe Cygnus X-3 from November 16 until November 22, 1974, and at a later time, from May 14 until May 23, 1975. During these time periods, monitoring of the X-ray flux from this stellar object was done using the Hard X-ray Experiment (HXX), Large Area Detectors (LAD), to obtain an X-ray light curve and spectrum information in the energy range of 1.0 to 28 keV. For a description of the HXX instrumentation and of its in-flight calibration, the reader is referred to another publication (Gursky, Schnopper and Parsignault, 1975).

RESULTS AND ANALYSIS

The 4.8 Hour Period

Figure 1 shows the X-ray light curves folded module 0.1996811 day (Leach et al, 1975), for our November 1974 and May 1975 observations. Each point represents an integration time of between 256 sec to 512 sec. The error bars represent 1σ statistical and aspect uncertainties. As seen in this figure, significant variability is evident between 0.0 and 0.6 of the phase, whereas no such variability is seen between 0.6 and 1.0 of the phase. For example, on November 16, around phase 0.05 - 0.2, the observations revealed an intensity at about 20 cts/sec, whereas a few days later and at the same phase, the count rates were between 26 and 30 cts/sec. Furthermore, the intensity peaked at about phase 0.13 in that particular cycle of the 4.8 hrs variation. We found similar examples in the May data: at phase ~ 0.4 , several observations showed a flux intensity of about 12 cts/sec, while two days later the count rates were around 22 cts/sec at the phase. The variability is such that we do not see the "sinusoidal" shape during individual cycles; rather only when the data are folded modula 4.8 hours does the envelope of the intensity variations define the sinusoid. This excess variability can actually be seen in the first reported observations of the 4.8 hours periodicity (Parsignault et al, 1972).

We have tried to further refine the period of Cygnus X-3 using the technique of analysis described in an earlier paper (Leach et al, 1975). We first fitted the data to a function $I = A_0 + A_1 \sin \left(\frac{2\pi}{P} (t - t_0) - \frac{\pi}{2} \right)$, with $P = 0.1996811$ days, the best period found by Uhuru. The results of these fits are shown in Table 1.

TABLE 1

Observation	A_0 (cts/sec)	A_1 (cts/sec)	t_0 JD2, 440,000+	A_1/A_0
November	22.4 ± 0.5	10.3 ± 1.0	$2370.447 \pm .005$	0.46 ± 0.05
May	12.8 ± 0.3	4.9 ± 0.6	$2551.366 \pm .005$	0.38 ± 0.05

The errors shown are 1σ statistical errors, except in the case of the phase of minimum intensity t_0 where the uncertainty includes systematic errors for varying the shape of the 4.8 hour X-ray modulation using the different shapes of the modulation found in the Uhuru data analysis. We then refit each observation, varying the period P , and considering the total χ^2 , we obtained for the period $P = 0.1999 \pm 0.0002$ days.

Finally, we divided the separation of the two minima by integer numbers of periods, and obtained 3 possible periods within the overall range determined above; namely, 0.199690, 0.199910 and 0.200132 (± 0.00008) days. Assuming the true period to be close to the period found by Uhuru, i. e., 0.199690 day, we divided each time interval in the Uhuru data and our data by this period, and plotted the results, i. e., number of periods n versus time. We then fitted these data points to $t_{\min} = t_0 + \tau \cdot n$. The results of this phasing analysis are presented in Figure 2, together with the residuals. The period thus obtained is equal to

$$P = 0.199,681, 3 \pm 0.000,000, 6 \text{ day.}$$

The other 2 possible values for the period found in our observations could not fit the Uhuru data at all, and could only have given a good fit after 1972, provided the period of Cygnus X-3 had increased to one of these values in a step manner. Our data cannot rule out the possibility of a change before 1974, but observations made after 1972 by Mason et al (1975) showed that there was no such change in the period.

To investigate our data for evidence of a continuous change in the 4.8 hours period, we assumed a linear variation of the period $P = P_0 + d(t - t_0)$ and we fitted the form $t = t_0 + P_0 n + 1/2 d P_0 n^2$, to the values of t_0 , the times of the X-ray minima from the Uhuru observations (see Table 1, Leach et al, 1975) together with the t_0 of the present ANS observations (Table 1). This fit gave a 2σ upper limit for \dot{P}/P of $5 \times 10^{-13} \text{ sec}^{-1}$.

The X-Ray Spectrum

Using the data from our 15 channel logarithmic PHA (1 - 28 keV), we investigated spectrum variations as function of the 4.8 hour intensity variation. We divided the phase into 10 bins, and our preliminary results show no systematic phase dependence of the spectrum of the X-ray continuum. Some 30 individual spectra were summed up to obtain an average spectrum. In both the November and May data, we fitted the data to a thermal bremsstrahlung plus a low energy cutoff, using the abundances of the elements as published by Brown and Gould (1970). Table 2 shows the results for such a fit.

TABLE 2

Observation	E_a (keV)	Temperature k T	$^{\circ}\text{K}$	I(cts/sec)
November	2.46 ± 0.11	2.84 ± 0.29	3.3×10^7	22.4
May	2.89 ± 0.10	3.35 ± 0.25	3.9×10^7	12.8

The errors in the parameters are 1σ deviations, corresponding to $\chi^2_{\min} + 3.5$ (10 degrees of freedom).

Both in the November and May spectra, we found a statistically significant excess above the fitted continuum in two of the energy channels, i. e., between 4.6 - 7.2 keV. We then divided the data into two parts: 0.0-0.65 and 0.65 - 1.0 (the "high" and "low" part respectively). We fitted the spectra leaving out the two channels containing the excess. For the "low" part of May, we found the following parameters: $E_a = 2.95 \pm 0.17$ keV, $k T = 3.16 \pm 0.41$, $\chi^2 = 14$ (for 10 degrees of freedom), and I (the intensity of the feature) = $33 \pm 10\%$ of the continuum, or an equivalent width of 0.87 ± 0.28 keV. Figure 3 shows the experimental data and the best fit. Similarly, in the "high" part of the light curve, we found the excess to be $26 \pm 7\%$ in the energy interval, i. e., an equivalent width 0.68 ± 0.17 keV. In November, for the "low" and "high" parts, we found an excess of $38 \pm 11\%$ ($\chi^2 = 15$) and $14 \pm 9\%$ ($\chi^2 = 16$) respectively, i. e., 1.00 ± 0.29 keV and 0.37 ± 0.23 keV equivalent widths.

Observations made few days apart of Cygnus X-1 and Cygnus X-2 didn't show such an excess in this energy range, thus ruling out that this feature was an artifact of the instrument.

DISCUSSION AND CONCLUSIONS

During our November observations the average X-ray intensity of Cygnus X-3 in the energy range of 1.3 to 7.1 keV was the highest ever recorded: 22.4 ± 0.5 cts/sec ANS = 340 cts/sec Uhuru. This flux intensity is to be compared to the 245 ± 11 cts/sec recorded by Uhuru during the September 1972 radio flare. Unfortunately, there was no radio coverage of this object during our period of observation; however, a few weeks later a giant radio flare from this object was reported (Osawa, 1974). The May data put again in evidence a rather high intensity state for Cygnus X-3: ≈ 200 cts/sec Uhuru. The average spectra for November and May are characterized by temperatures of 3.3 and 3.9×10^7 K for counting rates equivalent to 340 and 200 cts/sec Uhuru. These temperatures are consistent with the temperature of 4.3×10^7 K found for a 245 cts/sec intensity in September 1972, and in agreement with the relation found up to now, by different observers which relates the temperature inversely to the average intensity.

The 0.2 day X-ray modulation of Cygnus X-3 may be explained as the partial eclipse or the changing aspect of an X-ray emitting cloud, or wind which has "buried" the primary X-ray source. Pringle (1974) discussed such a model and ascribed the modulation to a stellar wind in which the optical depth varied from τ to $\tau + 1$. Davidsen and Ostriker (1974) described the system as containing an X-ray emitting white dwarf enveloped in a thick stellar wind. The data presented here place certain constraints on these models.

Davidson and Ostriker assumed a massive white dwarf and derived an accretion rate of $\sim 10^{-6} M_{\odot}/\text{year}$ to obtain the observed power. However, they estimated the mass loss from the system via the stellar wind, to be ~ 500 times this value or about $5 \times 10^{-4} M_{\odot}/\text{year}$. On the basis of this number, we would predict a $\dot{P}/P \approx 2 \times 10^{-4}/\text{year}$, for an isotropic mass loss, (Batten, 1973) compared to our 2σ upper limit of $\approx 10^{-6} M_{\odot}/\text{year}$. Thus, our data are not compatible with the stellar wind described by Davidson and Ostriker. Pringle's model, which make use of a neutron star or black hole, requires a much smaller loss rate of $\sim 10^{-6} M_{\odot}/\text{year}$ which is just compatible with our limit on \dot{P}/P . However, the observation of excess variability at the maximum of the X-ray modulation places serious doubt on any model which invokes scattering to modulate the X-rays. This includes reflection models such as those proposed by Basko et al (1974). These models invoke a scattering region of about $1 R_{\odot}$ in which the light travel time is only seconds; in such a region opacity differences of hundreds and not near unity would be required to smooth out the observed variability which is on a time scale of minutes to hours.

Thus Cygnus X-3 must be more complex than first imagined. It would appear that a dual source is required - one is a compact X-ray emitting star which like many other X-ray sources, displays significant time variability on a time scale of minutes. This source must be eclipsed during the observed minima, leaving behind a larger X-ray emitting region which is either very opaque or which has a long cooling time in order to wash out the intensity variations.

ACKNOWLEDGEMENT

This work was supported in part by NASA contracts NAS5-11350 and NAS5-23282.

REFERENCES

- Basko, M. M., Sunyaev, R. A., and Titarchuk, L. G., 1974, *Astron. and Astrophys.* **31**, 249.
- Batten, A., 1973, *Binary and Multiple Systems of Stars*, Pergamon Press, Oxford, England.
- Brown, R. M. and Gould, R. J., 1970, *Phys. Rev. D*, **1**, 2252.
- Canizares, C. R., McClintock, J. E., Clark, G. W., Lewin, W. M. G., Schnopper, M. W., and Sprott, G. F., 1973, *Nature Phys. Sci.* **241**, 28.
- , A. and Ostriker, J. P., 1974, *Astrophys. Journ.* **189**, 331.
- Gursky, H., Schnopper, H., and Parsignault, D. R., 1975, *Astrophys. Journ. (Lett.)* **201**, L127.
- Leach, R. W., Murray, S. S., Schreier, E. J., Tananbaum, H. D., Ulmer, M. P. and Parsignault, D. R., 1975, *Astrophys. Journ.* **199**, 184.
- Mason, K. and Sanford, P., 1975, *Symposium on X-ray Binaries*, NASA/GSFC, October.

- Osawa, K., 1974, IAU Circular #2734, December 24.
- Parsignault, D.R., Gursky, H., Kellogg, E.M., Matilsky, T., Murray, S., Schreier, E., Tananbaum, H., and Giacconi, R., 1972, Nature Phys Sci. 239, 123.
- Pietsch, W., Kendziorra, E., Staubert, R., and Trumper, J., 1975, Astrophys. Journ. (Lett.) to be published.
- Sanford, P.W. and Hawkins, F.M., 1972, Nature Phys. Sci. 239, 135.
- Sanford, P.W., Mason, K.O., and Ives, J., 1975, Mon. Not. R. astr. Soc. 173, 9P.
- Serlemitsos, P.J., Boldt, E.A., Holt, S.S., Rothschild, R.E., and Saba, J.L.R., 1975, Astrophys. Journ. (Lett.) 201, L9.
- Ulmer, M.P., 1975, Astrophys. Journ. 196, 827.

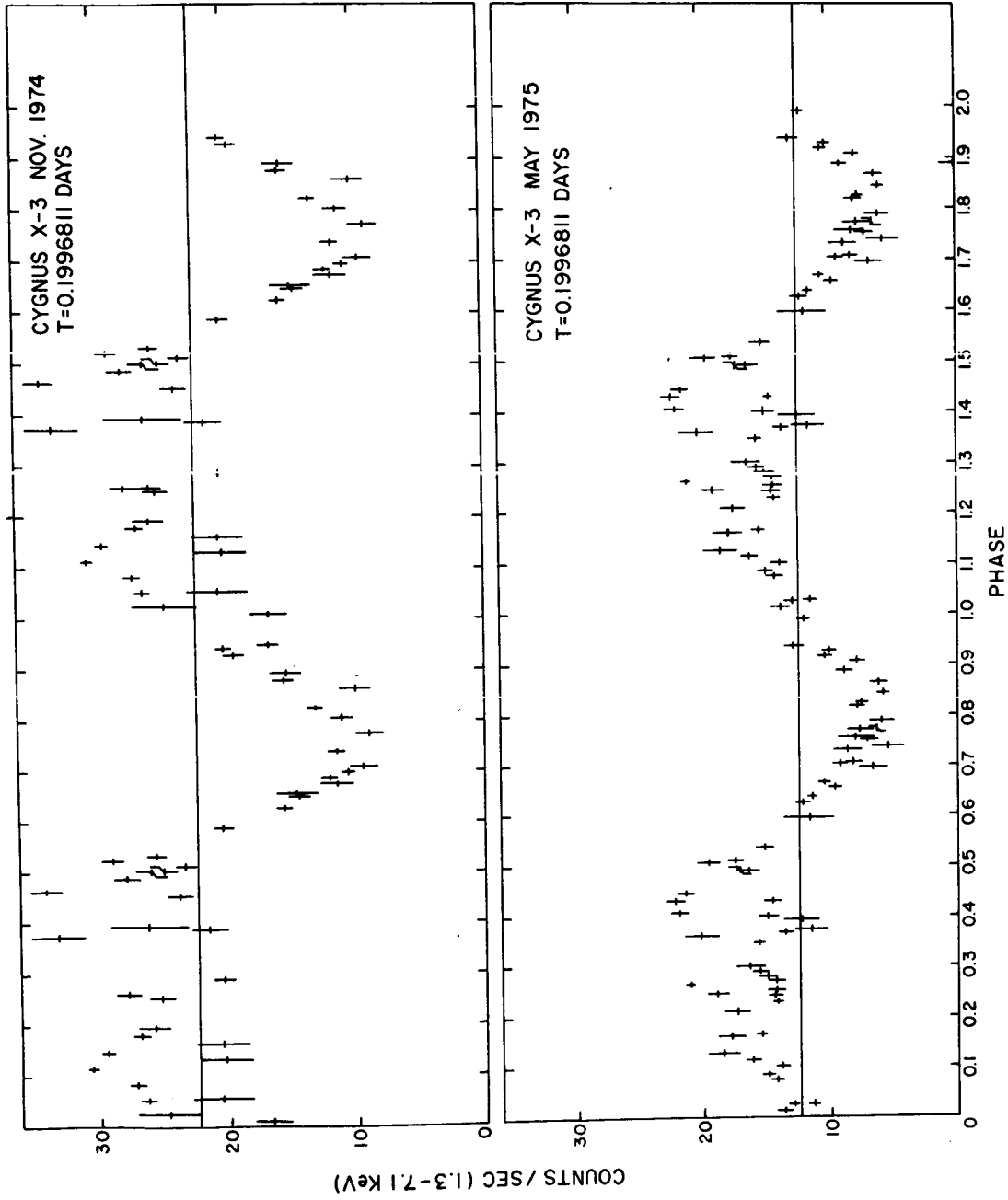


Figure 1. X-ray light curves (1.3 - 7.1 keV) for our observations of November 1974 and May 1975, folded modulo 0.1996811 day. The error bar on end point equals $\pm 1\sigma$.

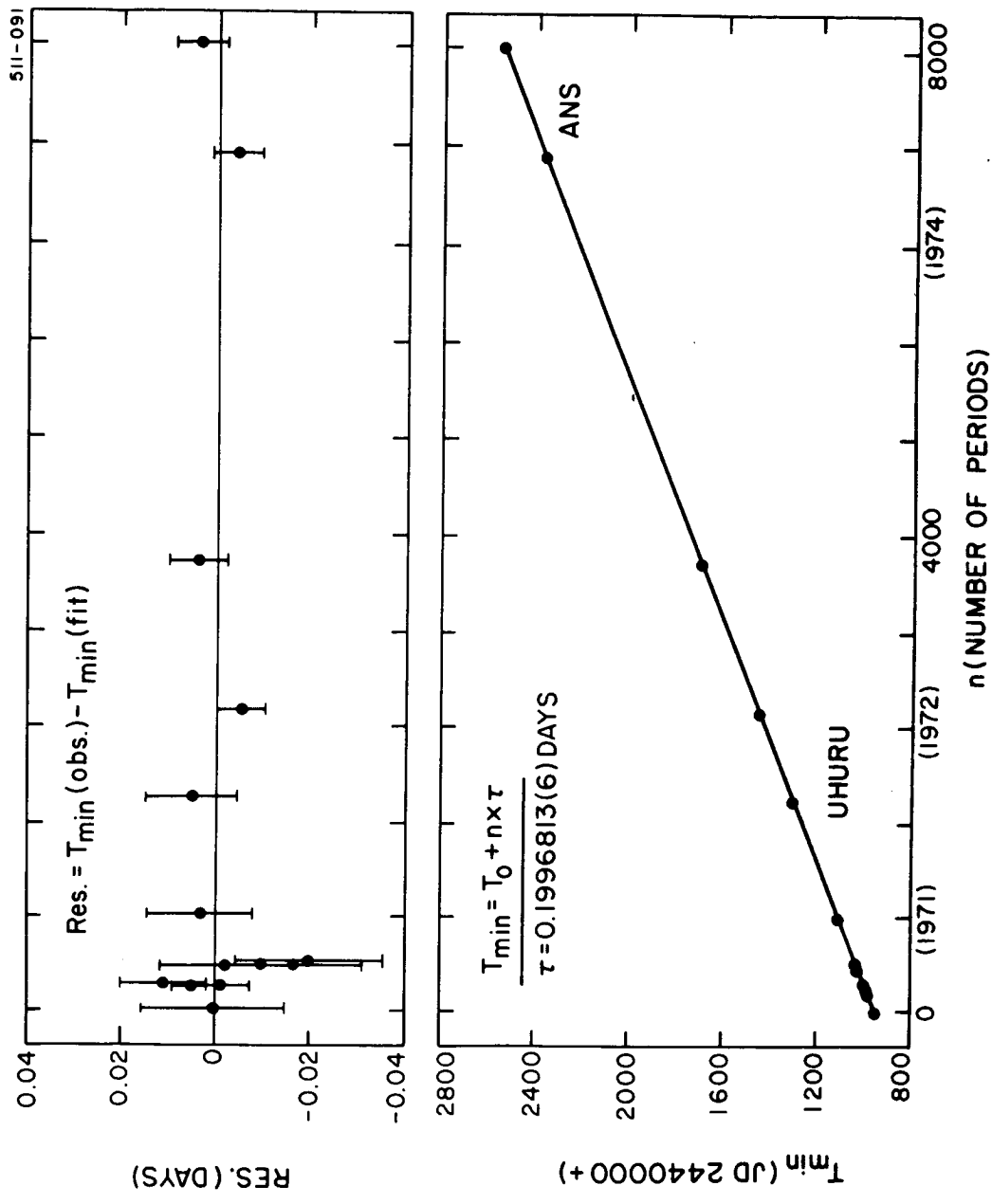


Figure 2. Plots of n, the number of periods (P = 0.199690) versus T_0 , the time of the X-ray minima of the 4.8 hr variation, and of the residuals of the fit.

CYGNUS X-3, MAY 1975
SUMMATION OF SPECTRA
"LOW PART" OF 4.8 HRS CYCLE

$E_0 = 2.95 \pm 0.17$ KeV
 $KT = 3.7 \times 10^7$ °K (± 0.3)
 $\chi^2 = 14$

I LINE = $33 \pm 10\%$ OF CONTINUUM

◆ EXPERIMENT
▲ FITTED SPECTRUM

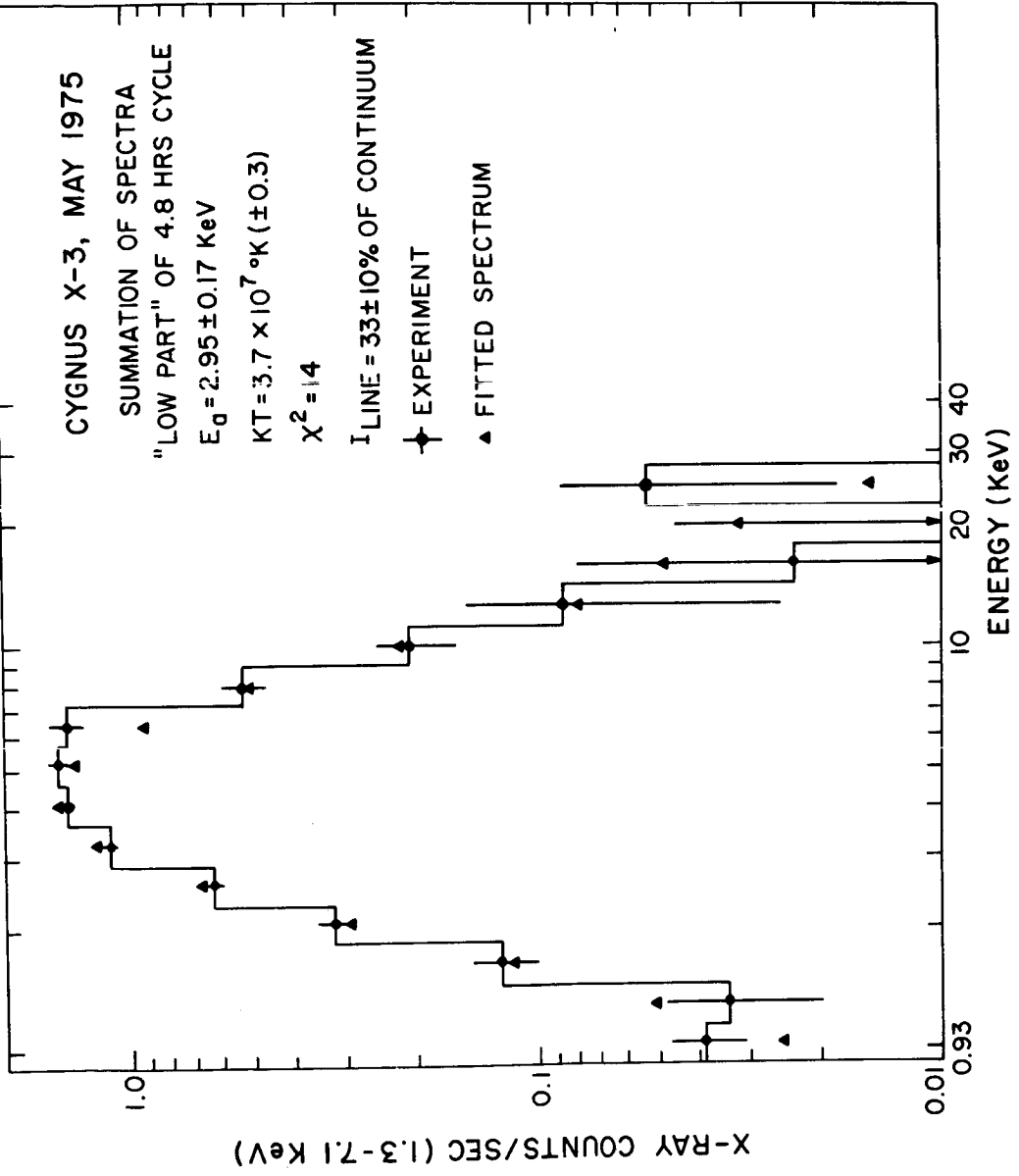


Figure 3. Cygnus X-3 energy spectrum.

THE 4.8 H VARIATION OF CYGNUS X-3 AT HIGH X-RAY ENERGIES*

W. Pietsch, E. Kendziorra, R. Staubert and J. Truemper**
Astronomisches Institut Der Universitaet Tuebingen
74 Tuebingen, Waldhaeuserstr. 64, Germany

ABSTRACT

On 1975 February 20, 14-19 H UT, the Cygnus region was observed in the X-ray range 32-150 keV. The balloon payload was launched from Palestine, Texas and floated in an average atmospheric depth of $2,4 \text{ g/cm}^2$. The instrument was a NaI scintillation detector with 87 cm^2 effective area and a 2 degree by 10 degree slat collimator in heavy anticoincidence shielding. For 3.5 hours an "on-off" observation was performed on Cygnus X-3 yielding a source spectrum between 32 and 150 keV. Also an intensity variation has been found which is in phase with the low energy X-ray 4.8 hour sinusoidal light curve. The relative amplitude found in the energy range 32-64 keV is $0.37 (+0.31, -0.29)$ (Chisquare ± 1 errors). Compared to results at lower energies there is no indication for an energy dependence of the relative amplitude up to 64 keV.

*Published in Astrophysical Journal Letters 1976, 203.

**Now at Max-Planck-Institut Fuer Extraterrestrische Physik,
8046 Garching, Germany

OBSERVATIONS OF CYGNUS X-3 FROM
A BALLOON-BORNE X-RAY TELESCOPE

G. R. Ricker, A. Scheepmaker[†], J. E. Ballantine,
J. P. Doty, G. A. Kriss, S. G. Ryckman, and W. H. G. Lewin

Department of Physics and Center for Space Research
Massachusetts Institute of Technology
Cambridge, Massachusetts 02139

ABSTRACT

X-ray measurements in the energy range 20-150 keV were made from a balloon-borne telescope on 1975 June 1. Three scans, centered at phases 0.45, 0.60, and 0.70, respectively, of the 4.8 hr cycle, were conducted. Each scan was ~ 20 to 30 minutes in duration. The observed relative intensity as a function of phase differs significantly from previously reported X-ray measurements. Variations in source intensity on times scales of minutes were also observed.

I. Introduction

The 4.8 hour periodicity in the intensity of the X-ray emission from Cyg X-3 is well-established at energies less than 20 keV. A very comprehensive set of low energy X-ray measurements spanning two years of observations has recently been compiled by Mason *et al* (1975), based primarily on Copernicus data. At higher X-ray energies (>20 keV), the observational picture is less clear cut. Ulmer *et al* (1974) established an upper limit on a possible 4.8 hour variation based on OSO-7 data for energies greater than 22 keV. Recently, Pietsch *et al* (1975) have claimed that the 4.8 hour period in Cyg X-3 is detectable in the 29-70 keV range, based on positive detections of rather low statistical significance (~ 2 to 4σ data points). Using an instrument of large effective area (~ 575 cm²) and low background counting rate ($\lesssim 4 \times 10^{-4}$ photons cm⁻²s⁻¹keV⁻¹), we have recently measured the hard X-ray emission from Cyg X-3 with improved statistical precision. In this paper, preliminary results on the relative intensity as a function of phase in the 4.8 hour period will be given. Analysis of our spectral data within the 20-150 keV range is not yet complete, and will be published later.

[†]Present address: Cosmic Ray Working Group
Leiden, The Netherlands

* Supported in part by National Science Foundation Grant MPS 75-02963 and National Aeronautics and Space Administration Grant NGL 22-009-015.

II. Observations

On June 1, 1975, we observed Cygnus X-3 in the energy range 20-150 keV for ~ 80 minutes during a balloon flight from Palestine, Texas. The X-ray telescope consisted of phoswich detectors con- signed to two independent banks which viewed the sky through $3^\circ \times 3^\circ$ FWHM and $1.5^\circ \times 6^\circ$ FWHM slat collimators, respectively. The telescope was mounted in an altazimuth configuration. A 52.6 million ft ($1.49 \times 10^6 \text{ m}^3$) balloon, manufactured by Winzen Research, Incorporated, carried the gondola to an altitude of 144,000 ft (43.9 km; $\sim 2.0 \text{ gm cm}^{-2}$). The data were both recorded on board and transmitted to a ground-based station. X-rays were recorded in eight energy channels covering the energy range from ~ 20 to 150 keV.

We used the drift scan technique in conducting our measurements; viz., we aimed the telescope ahead of a source (in Right Ascension) and the gondola was stabilized so that a source drifted through the collimator fields-of-view at the sidereal rate, resulting in charac- teristic triangle-like counting-rate plots. Figure 1 shows the raw data from three drift scans over Cyg X-3 for one of our two de- tector banks ($\sim 300 \text{ cm}^2$ effective area; $3^\circ \times 3^\circ$ FWHM collimator). A scan over Cyg X-1 was conducted between the first and second Cyg X-3 scans. The Cyg X-3 scans were centered about phases 0.45, 0.60, and 0.70 of the calculated (low energy X-ray) light curve. The reference epoch and period used for our phase calculations were $\text{JD}_{\phi=0} = 2442147.995 \pm 0.002$ and $P = 0.1996846 \pm 0.0000008$, respectively. This information was kindly provided by K. Mason, based on the 2.5-7.5 keV measurements from Copernicus.

The detection of Cyg X-3 is statistically significant at levels of 6σ , 14σ , and 12σ , respectively, for the three scans shown in Figure 1. Independent detections of comparable significance were achieved in the other detector bank ($1.5^\circ \times 6^\circ$ FWHM collimator; data not shown). Variations in the source intensity on time scales of \sim minutes are evident; a complete analysis of these variations is presently under way.

In Table 1, we have compared the results derived from our $3^\circ \times 3^\circ$ detector bank (corrected for aspect and atmospheric depth effects) with those from 2 other observations of Cyg X-3. For each of the three sets of data, the reported intensities have all been divided by the intensity at $\phi = 0.7$ for the particular data set. Thus, the tabulated intensities are all relative to $\phi = 0.7$. The differences in the three measurements is most striking at $\phi = 0.45$, with the relative intensity determined in this experiment being significantly lower than that reported in previous work.

III. Discussion

We find, contrary to the conclusions of Pietsch *et al*, that, at least at the time of our observations, the high energy light curve (20-150 keV) of Cyg X-3 differed significantly from the ac- cepted, time-averaged low energy X-ray light curve (Mason *et al*

1975). Our findings would seem to support those models for Cyg X-3 which predict an energy-dependent light curve (Basko et al, 1974). However, Canizares et al (1973) have found that there can be significant variations in the shape of the light curve from one cycle to the next at low energies (1-10 keV). If this is also true at higher energies, then further measurements with good statistical precision, taken over a number of different cycles of the 4.8 hr period, will be required to definitively answer the question: Is the X-ray light curve of Cygnus X-3 different at high energies (>20 keV) compared to low energies (<20 keV)?

IV. Acknowledgements

The assistance of J. Bokor, P. Downey, and D. Strauss in the preparation of the gondola, and of P. Missel and S. Roby in the data analysis, was essential. We wish to thank the personnel of the National Center for Atmospheric Research Scientific Balloon Facility for a flawless launch of the record-breaking balloon (the largest ever flown), and for whole-hearted and effective support during all phases of the expedition culminating in this successful flight.

Table 1: Relative Intensity of Cyg X-3 at three phase points in the 4.8 h period.

Energy (keV)	Relative Intensities			Time of Observation	Reference
	$\phi=.45$	$\phi=.60$	$\phi=.70^*$		
2.5-7.5	$0.86 \pm .05^\dagger$	$0.94 \pm .05^\dagger$	1	Sept 1974	Mason <u>et al</u> 1975
29 - 70	$1.21^{\dagger\dagger}$	$1.15^{\dagger\dagger}$	1	20 Feb 1975	Pietsch <u>et al</u> 1975
29 - 150	$0.50 \pm .10$	1.17 ± 0.09	1	1 June 1975	Present Work

* Intensity normalized to unity for all observations.

† Table entry and its 1σ statistical error estimated from data given in Figure 9 of Mason et al, 1975.

†† Table entry estimated from fitted curve in Figure 1 of Pietsch et al, 1975, with the epoch and period corrected to the improved value of Mason (private communication; see text).

References

- Basko, M. M., Sunyaev, R. A., and Titarchuk, L. G., 1974, *Astron. & Astrophys.*, 31, 249.
- Canizares, C. R., McClintock, J. E., Clark, G. W., Lewin, W. H. G., Schnopper, H. W., and Sprott, G. F., 1973, *Nature Physical Science*, 241, 28.
- Mason, K. O., Becklin, E. E., Blankenship, L., Brown, R. L., Elias, J., Hjellming, R. M., Matthews, K., Murdin, P. G., Neugebauer, G., Sanford, P. W., and Willner, S., 1975, to be submitted to *Ap. J.*
- Pietsch, W., Kendziorra, E., Staubert, R., and Trümper, J., 1975, *Ap. J.* (in the press).
- Ulmer, M. P., Baity, W. A., Wheaton, W. M. A., and Peterson, L. E., 1974, *Ap. J.*, 192, 691.

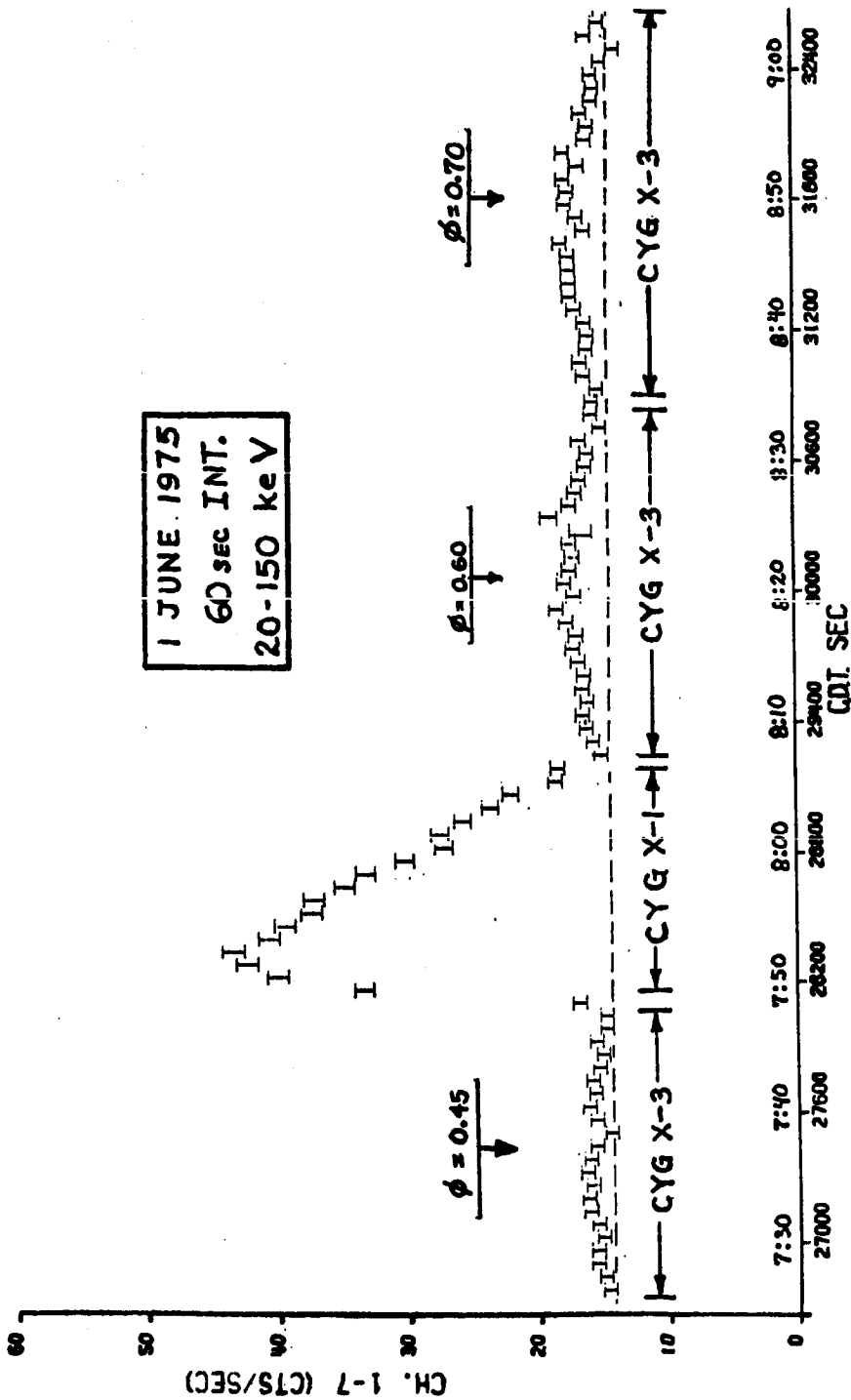
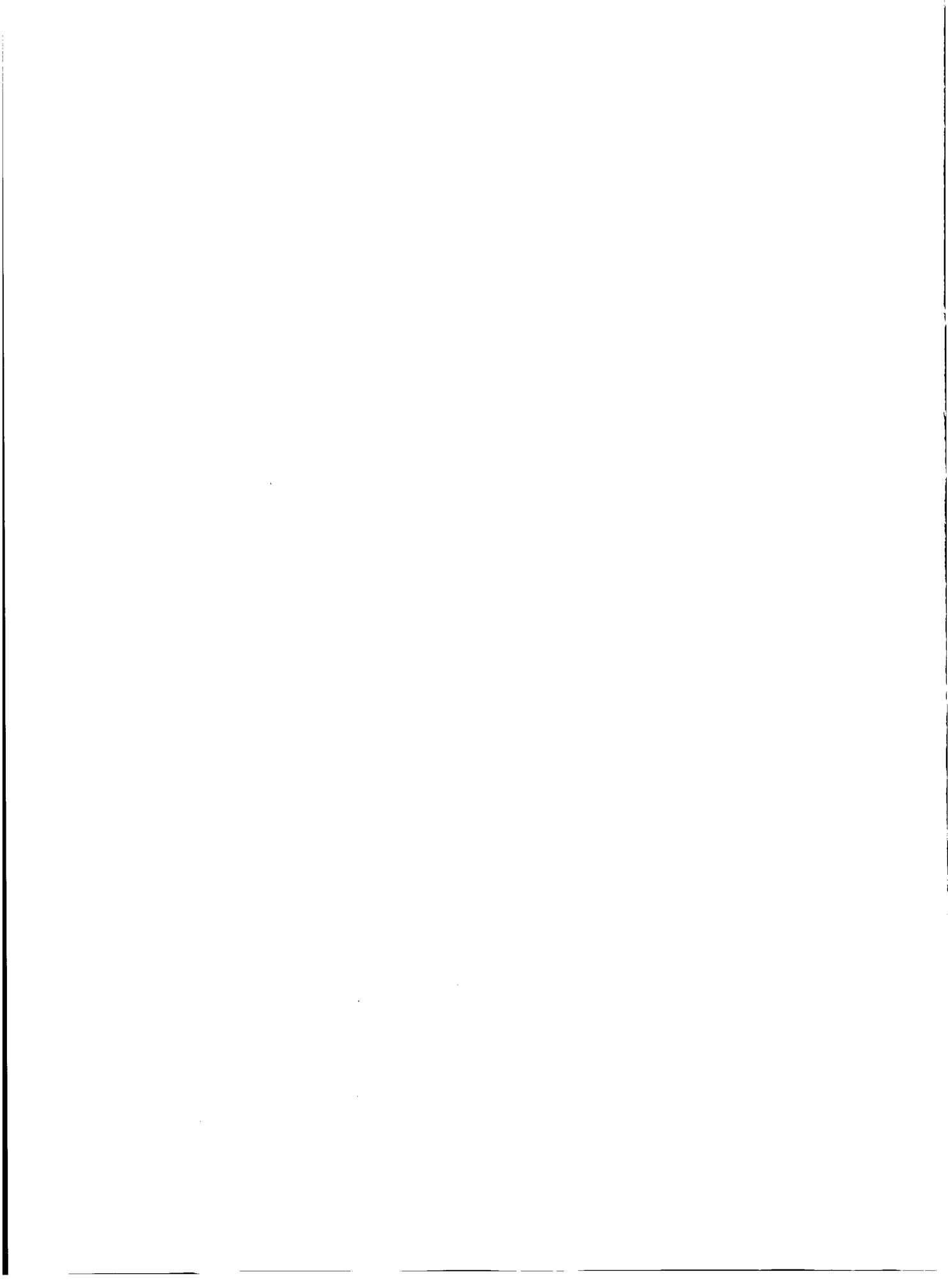


Figure 1. Drift Scans of Cygnus X-3. Counting rate versus time for a portion of our data (i.e. detector bank with ~ 300 cm² effective area; $3^\circ \times 3^\circ$ FWHM collimator) is shown. Central Daylight Times are given, in both seconds after midnight and hours: minutes (CDT = UT-5 hr). Before each of the scans shown, we pointed our telescope ahead of the source (in Right Ascension) and then allowed the source to drift through the field of view at the sidereal rate. The telescope was being repointed in the three gaps between the four scans (one scan of Cyg X-1 is shown). For the first Cyg X-3 scan, the source approached within $\sim 0.3^\circ$ of the collimator center during its drift through the field of view. For the second and third scans, the angular distance of closest approach was ~ 0.1 degrees. The three phase points marked by vertical arrows are derived by extrapolation from the epoch and period measurements of Mason (see text), as are the associated error bars. The dotted line denotes the background counting rate. Error bars on individual data points are $\pm 1\sigma$.



ABSENCE OF IRON LINE EMISSION IN CYG X-3

S. Shulman, H. Friedman, G. Fritz and D. Yentis
E. O. Hulburt Center for Space Research
Naval Research Laboratory
Washington, D. C. 20375

and

W. A. Snyder, A. F. Davidsen and R. C. Henry
Department of Physics
Johns Hopkins University
Baltimore, Maryland 21218

ABSTRACT

An observation of Cygnus X-3 was made with soft X-ray detectors launched on an Aerobee rocket at 0500 U.T. on 7 September 1974. A blackbody spectrum with $T = 2.2 \times 10^7 \text{K}$ ($kT = 1.9 \text{ keV}$) and a hydrogen column density of $2.3 \times 10^{22} \text{ cm}^{-2}$ fits the data reasonably well. The iron line emission observed one month later (Serlemitsos *et al.* 1975) and in May 1975 (Sanford, Mason and Ives 1975) was not found. A 3σ upper limit for this feature in our data is $0.006 \text{ ph cm}^{-2} \text{ s}^{-1}$.

INTRODUCTION

Recently, Serlemitsos *et al.* (1975) have reported two rocket observations of Cyg X-3 separated by about one year in which they found significant spectral differences. In their October 1973 data, at binary phase 0.81, the spectrum was best fit by a blackbody with a temperature of $1.4 \times 10^7 \text{K}$ and a hydrogen column density of $2.7 \times 10^{22} \text{ cm}^{-2}$. Their October 1974 observation, at binary phase 0.01, was significantly different. The intensity in the 2-6 keV band was reduced by a factor of ten from their earlier observation, and the spectrum was best fit by thermal bremsstrahlung with a temperature greater than $2.0 \times 10^8 \text{K}$ and a hydrogen column density of $7.0 \times 10^{22} \text{ cm}^{-2}$. They also detected iron line emission at 6.7 keV with a line strength of 0.018 photons $\text{cm}^{-2} \text{ s}^{-1}$. May 1975 observations of iron line emission together with a blackbody spectrum have been obtained with Ariel 5 (Sanford, Mason and Ives 1975). These authors find

a high average flux from Cyg X-3 and a line strength of $0.027 \text{ photons cm}^{-2} \text{ s}^{-1}$.

OBSERVATIONS

An NRL Aerobee payload launched at 0500 U.T. on 7 September 1974 observed Cyg X-3 for 44 seconds. The payload consisted of two proportional counters; one with a 3° (FWHM) field of view, the other with a 5° (FWHM) field of view. Each had an effective area of 1200 cm^2 , a 2-micron Kimfol (polycarbonate) window, and used P10 gas (90% Argon, 10% Methane) at 15.5 p.s.i.a. Figure 1 shows the count-rate as a function of time throughout the flight for the 3° detector over the energy range from 1.0-10 keV. Cyg X-3 was in the field of view from 101 to 145 seconds. An Fe-55 calibration source was placed in the field-of-view from 85-100 s and from 286-302 s. Figure 2 shows the spectral data for the Cyg X-3 observation with the 3° detector. The background data subtracted are from a region 15° north of Cyg X-3. It was impossible to obtain background data nearer the source because of the large field-of-view and source confusion near Cyg X-3. The background data used are from the time interval 161-187 s. The slightly negative values in Figure 2 below 0.4 keV are due to an increase in the soft X-ray background at the higher galactic latitude of the background region.

The spectrum that best fits our data (solid line in Figure 2) in the energy range 1.5-8 keV is a blackbody distribution with a temperature $T = 2.2 \times 10^7 \text{ K}$ and a hydrogen column density $N_{\text{H}} = 2.3 \times 10^{22} \text{ cm}^{-2}$. χ^2 per degree of freedom for this fit is 1.9. Other simple spectra (thermal bremsstrahlung, power law) gave worse fits with χ^2 per degree of freedom exceeding 3.5. The data were not fit below 1.5 keV because we believe that another source is contributing at these energies. To demonstrate the source confusion below 1.5 keV, Figure 3 shows the spectral data from the 5° detector plotted together with the previously determined blackbody spectrum. A large excess peaking at 1 keV is readily apparent. To produce this difference between the two detectors, another soft X-ray source must be present near the edge of the field of view of the 3° detector. This source will be discussed elsewhere.

An iron emission line feature at about 6.5 keV has been searched for in our data. We can place a 3σ upper limit on such a feature of $0.006 \text{ photons cm}^{-2} \text{ s}^{-1}$.

DISCUSSION

There are currently two reports in the literature of iron line emission in the spectrum of Cyg X-3 (Sanford,

Mason and Ives 1975, Serlemitsos et al. 1975). Our observation and one observation by the second group of authors above found no such line emission. From the compilation of all these observations, there is as yet no apparent correlation of line emission with spectral shape, 2-10 keV intensity, or binary phase. Table 1 shows the range of conditions observed in the source.

One can use the fact that a blackbody spectrum is observed to deduce a minimum radius for the X-ray emitting region. From their October 1975 data, Serlemitsos et al. (1975) deduced a radius of 15 km and used this estimate to argue that the compact object is smaller than a white dwarf, which is the compact object in the model proposed by Davidsen and Ostriker (1974). A similar estimate from our observation yields a radius of only 5 km. However, an approximately blackbody spectral form can be obtained with a source which is optically thin to true absorption and optically thick to electron scattering (Felten and Rees 1972), but the intensity in this case is far below that of a true blackbody. If such a model is applicable to Cyg X-3, the emission region may be substantially larger than the 5-15 km obtained above. Thus it is probably too early to rule out models involving white dwarfs based on these spectral data. Of course, the occurrence of a blackbody spectral form and an emission line together (Sanford et al. 1975) may be difficult to understand in any single-component X-ray source model.

Table 1.

<u>Cyg X-3 Spectral Results</u>						
Date	Spectrum	T (°K x10 ⁻⁷)	N _H (cm ⁻² x10 ⁻²²)	Flux (2-10 keV) (ergs cm ⁻² s ⁻¹ x 10 ⁹)	Phase	Line Strength (cm ⁻² s ⁻¹)
Oct 1973 ^a	Blackbody	1.4	2.7	6.2	.81	not seen
Sept 1974 ^b	Blackbody	2.2	2.3	2.1	.80	≤ 0.006
Oct 1974 ^a	Bremsstrahlung	≥ 20	7-8	1.2	.01	0.018±0.004
May 1975 ^c	Blackbody	1.6	5.3	6.8	.3-.8	0.042±0.005
	-	-	-	3.8	.8-.3	0.019±0.003

^aSerlemitsos et al. 1975.

^bThis paper.

^cSanford, Mason and Ives 1975.

REFERENCES

- Davidson, A., and Ostriker, J. P. 1974, Ap. J., 189, 331.
Felten, J. E., and Rees, M. J. 1972, Astron. and Astrophys.,
17, 226.
Sanford, P., Mason, K. O. and Ives, J. 1975, M.N.R.A.S.,
173, 9P.
Serlemitsos, P. J., Boldt, E. A., Holt, S. S., Rothschild,
R. E., and Saba, J. L.R. 1975, Ap. J. (Letters), 201, L9.

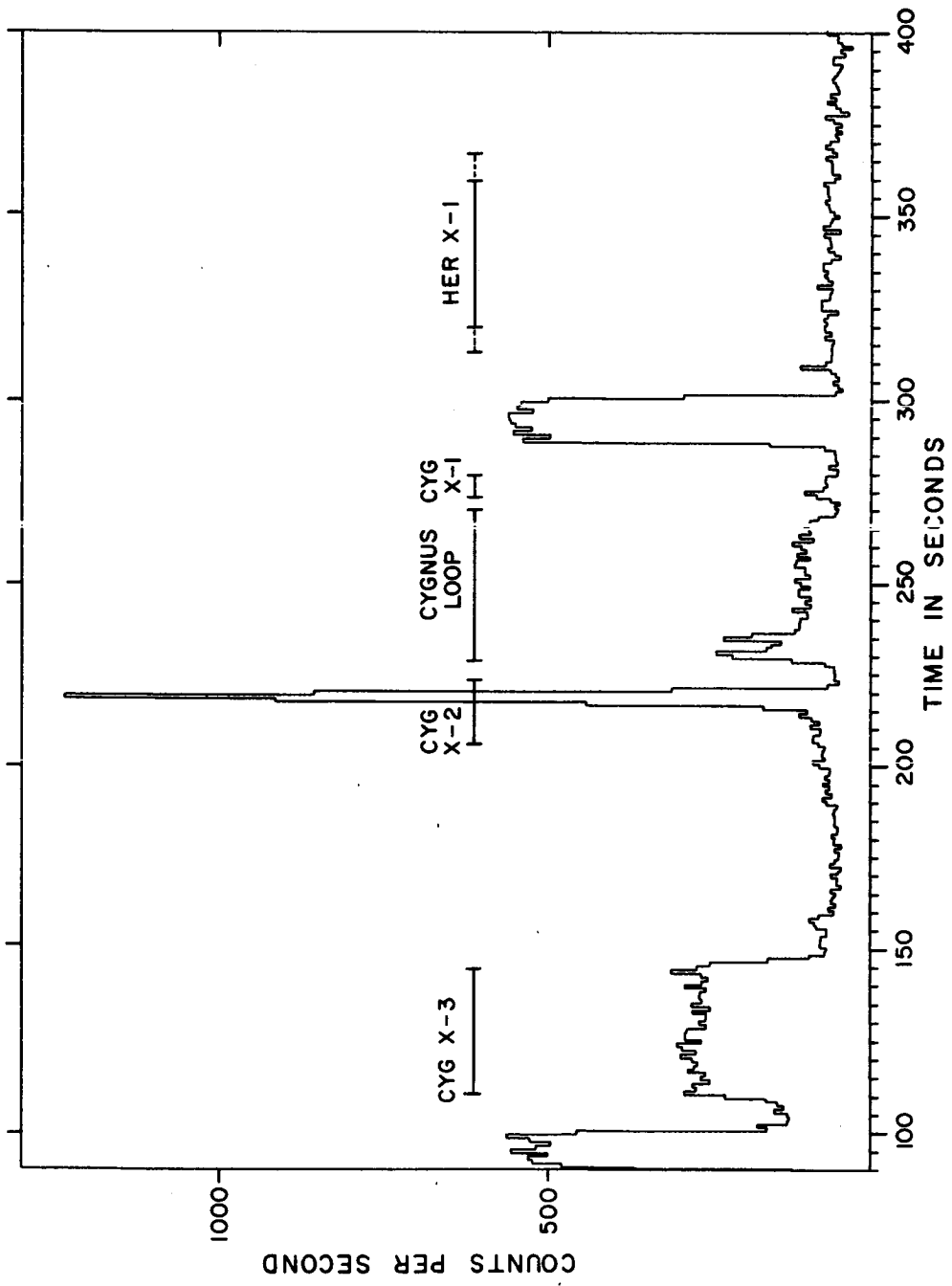


Figure 1. The count-rate (1.0 - 10 keV) throughout the flight in the 3° (FWHM) detector.

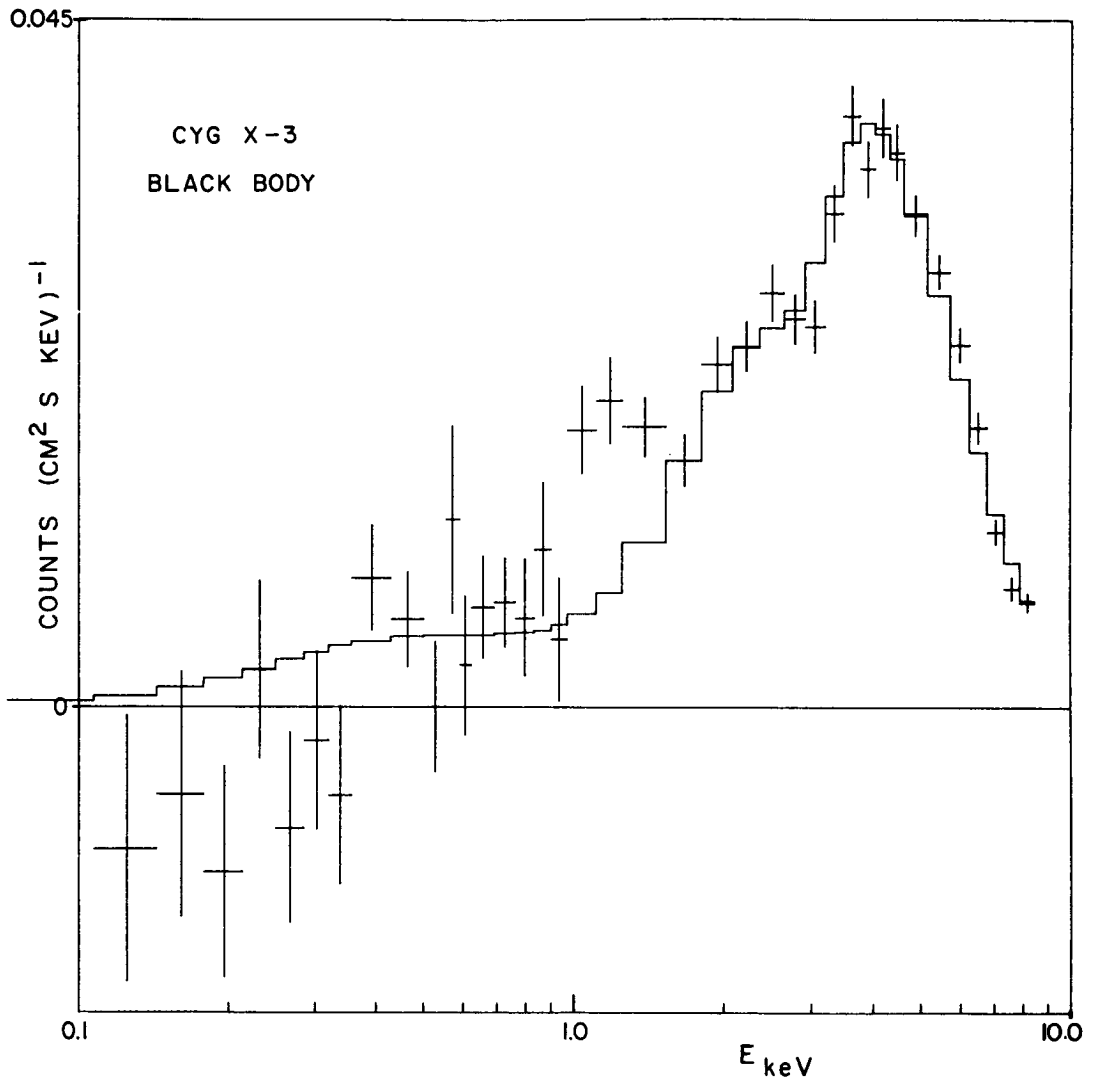


Figure 2. Spectral data (3° detector) from Cyg X-3 with background subtracted. The solid line is the best fit blackbody spectrum with $T = 2.2 \times 10^7$ °K and $N_H = 2.3 \times 10^{22}$ cm⁻².

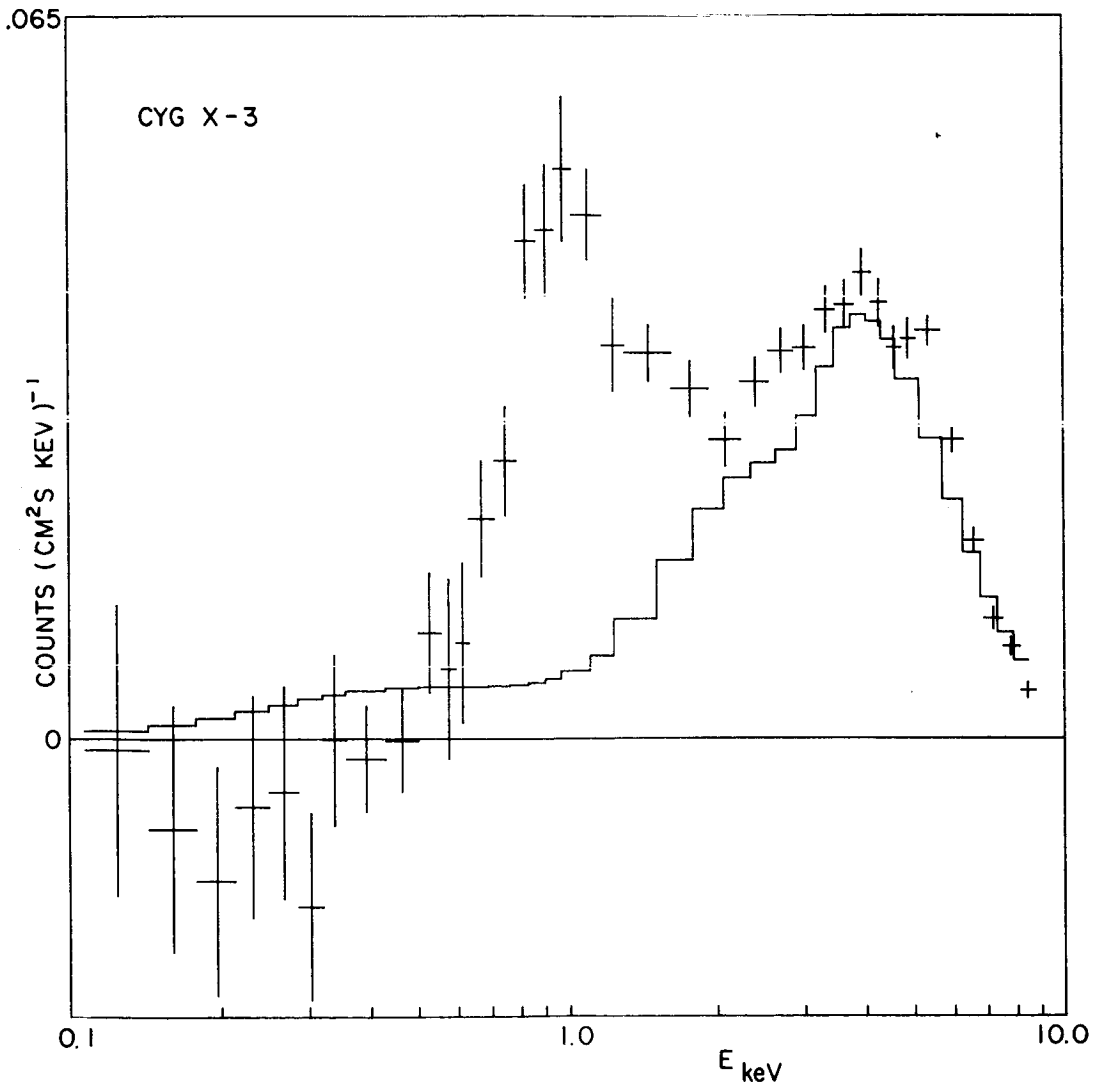


Figure 3. Spectral data for Cyg X-3 obtained with 5° (FWHM) detector. The solid line is the same spectrum as in Figure 2. The large excess peaking at 1 keV is due to another (uncatalogued) source within the field of view.

Cyg X-3

Discussion

N. V. Vidal to R. M. Hjellming:

Do you have any idea what is the source of relativistic particles in the system?

R. M. Hjellming:

A series of consecutive shock waves may accelerate particles

THE TRANSIENT X-RAY SOURCE A0620-00

(NOVA MONOCEROTIS 1975)

Stephen P. Maran
Laboratory for Solar Physics and Astrophysics
NASA-Goddard Space Flight Center
Greenbelt, Maryland 20771

ABSTRACT

A0620-00 is the first of the so-called "X-ray novae" to be identified with an optical object. Emission in the ultraviolet, infrared and radio wavelength regions has also been observed from this source. From the observed properties of the optical radiation, it has been suggested that the source is a recurrent nova and indeed the IAU Circulars now refer to it as Nova Monocerotis 1975, but there are other possible interpretations. This paper includes both the "Introductory" and "Summary" remarks that were separately presented at the session on A0620-00 during the Symposium on X-Ray Binaries and some additional material.

INTRODUCTION

During the eight years since the first transient X-ray source (Centaurus X-2) was observed, there has been only modest progress in determining the physical nature of these objects. Now, however, thanks to the optical identification of the recent transient source A0620-00, it should be feasible to formulate and test detailed models for at least this one object. In fact, there are also ultraviolet, infrared and radio measurements of A0620-00 and so we have indeed almost an embarrassment of riches and it will be probably at least a year or two before it becomes possible to critically evaluate the bulk of the observational material. Indeed, present satellite instrumentation can probably continue

to monitor the declining X-ray emission of the source for several years to come.

As many authors have noted recently, it has become clear that there are at least two distinct types of transient X-ray source. A0620-00 belongs to the type (called Class II by Brecher and Morrison) whose outbursts are longer-lived, unpulsed, characterized by softer spectra, and also perhaps (according to Kaluzienski et al. 1975) intrinsically both less common and more luminous.

In the past few months, as reports of several new transient sources, including A0620-00, have appeared, it has become increasingly clear that they represent not only an important and numerous category of object, but also that they very plausibly can be considered as candidate binary systems. We therefore added this special session on A0620-00 to the program of the Symposium on X-Ray Binaries.

Looking through the many IAU Circulars that report results on A0620-00, one is struck by the fact that this object has been successively described as A0601-00, as A0621-00, as the transient source "in Orion," as A0620-00, and (most recently) as Nova Monocerotis 1975. For the record, we might note that the first designation simply resulted from an erroneous position, while the more recent shift from "A0621-00" to "A0620-00" just reflects a refinement in the position measurements. The source is about one half of a degree east of the Orion border in

Monoceros, so that its description as a transient object "in Orion" is less excusable than that of the briefly famous "Nova Cephei," which we now remember as Nova CP Lacertae, and which erupted only arc seconds outside the Cepheus border. (On the other hand, one has to admit that the nearby star "78 Orionis" is much further into Monoceros than is A0620-00. Has ever a physicist, high-energy or otherwise, ventured into astronomy and not run afoul of the mysterious conventions and units?)

A slightly more interesting question is posed by the designation of A0620-00 as "Nova Monocerotis 1975." This action was taken by the IAU Central Bureau for Astronomical Telegrams on the basis of optical properties of the source, just as has been done in the past in the case of every "nova". But, in retrospect, the X-ray astronomers who searched in vain this summer for a signal from the bright optical object Nova Cygni 1975 while at the same time A0620-00 (optically, 10,000 times fainter) was the brightest X-ray source in the sky, might well question the propriety of "Nova" Monocerotis. In the radio wavelengths as well, A0620-00 seems to be very different from the classical novae in that its radio emission was already present when first searched for only two days after the source attained maximum luminosity.

If we then admit that Nova Monocerotis 1975 is not a classical nova, one might well ask whether among the extensive literature on the classical novae and related stars (very few of which, of course, have been studied by non-optical techniques) there might be perhaps other interlopers similar to A0620-00 that, thanks to the lack of X-ray satellites in the past, went unrecognized? A good summary of the optical light curve and spectral development of A0620-00, when it becomes available, might form the basis for a reconnaissance of the literature in search of such an object. (Take a contrary position for a moment, and assume that A0620-00 is indeed a recurrent nova as proposed by Eachus, Wright and Liller: then perhaps we now have a basic diagnostic, namely the occurrence of prompt X-ray and radio emission, to distinguish a recurrent nova from an ordinary one. In that case we might disprove a dictum of my late Professor and an authority on novae, D. B. McLaughlin: "It is not possible to list criteria whereby a recurrent object might be recognized at its first recorded outburst.")

THE OBSERVATIONS

The X-ray emission of A0620-00 has been observed by at least four automated satellites and from a manned space station. Satellite measurements have also been made in the ultraviolet. A great many radio and optical observations and some infrared measurements have been obtained from the

ground. A preliminary and almost surely incomplete chronology, given in Table 1, will give you the flavor of this exciting recent history. If you will grant the chairman the usual privilege of a few moments of pontification and I-told-you-so's, I think a few points are worth making. The tremendous job that has been done on the investigation of this transient source has not rested alone on the traditional fine international cooperation and communications among all astronomers. It has also been enabled by the availability in space this summer of a satellite with excellent capabilities for monitoring and surveying large areas of the sky (Ariel-5) and of another satellite (SAS-3) with, among its many virtues, the ability to point various instruments as needed at a selected location on fairly short notice. We have also benefited from the ANS satellite, which has given us the first extensive ultraviolet photometry of this and other stellar X-ray sources. The optical identification of A0620-00 is among the first results of a new facility (McGraw-Hill Observatory) that fulfills the long-felt need for a substantial telescope dedicated to full-time support of the high-energy investigations underway with spacecraft. Finally, surely among the most important results is the discovery of the prior eruption, half a century ago, in the Harvard plate stacks. Are we doing enough nowadays to ensure that a similar collection, representing our own era, will be available to future astronomers (and indeed for ourselves)?

TABLE 1

Chronology of A0620-00 Investigations

(1975)

August 3	Source discovered by Ariel-5 Sky Survey Experiment (2 - 18 keV).
6	Intensity reaches 2 - 18 keV "precursor" peak. For thermal bremsstrahlung fit, $kT \approx 30$. Already stronger than the Crab, source brightens in ensuing days, spectrum softens and in fact flux above 10 keV actually decreases. Low energy cutoff becomes evident.
7	Discovery is telexed to IAU Central Bureau.
8	SAS-3 observations commence.
13	Maximum intensity in 2 - 18 keV band. For 1 - 10 keV, $kT = 1.7$ keV.
14	SAS-3 measures position with modulation collimators.
15	SAS-3 group provides accurate position to ground-based observers. Radio source is detected at NRAO (1400 MHz) and Arecibo (2380 MHz).
16	Optical source is detected at McGraw-Hill Observatory. Radio source detected at Jodrell Bank (962 MHz). Intensity decreases by factor e in about five days. 2695 MHz observations commence at NRAO.
17	High dispersion spectrograms with KPNO 4-meter telescope show no stellar lines.
20	Radio source observed at Nancay (1408 MHz)
22	Radio source measured at Mullard Observatory (5000 MHz). Optical fluctuations of 10% on 30 - 60 minute time scale are reported from South Africa.

TABLE 1, Continued: Chronology of A0620-00 Observations

August 23	UBV photometry commenced at European Southern Observatory.
26	Infrared emission (1.25 - 3.45 microns) measured at Kitt Peak.
27	Prior eruption in 1917 reported after search of Harvard plate collection. SAS-3 low energy instrument detects strong 0.4 - 0.8 keV emission with spectrum characterized by prominent cutoff due to interstellar absorption. $kT = 1.3$ keV.
28	Four-day modulation of UBV light appears in ESO light curves; total amplitude about 0.2 magnitude. Photographed at Herstmonceux to derive astrometric position.
31	Multichannel photometry with 200-inch Hale reflector shows flat continuum.
September	
1	Ariel-5 All Sky Monitor (3 - 6 keV) observes source declining continuously throughout September.
8	Optical emission lines detected and measured with Anglo-Australian 4-meter telescope.
10	Salyut-4 cosmonauts observe source in six X-ray bands.
12	UBV linear polarization (apparently interstellar), measured at Kitt Peak, is reported.
22	Amplitude of 4-day UBV modulation found at ESO has decreased to about 0.1 magnitude.
24	Infrared photometry (2.2 microns) commences at Tenerife 152-cm telescope.
27	ANS X-ray and ultraviolet observations begin. $kT = 1.0$ keV at 1 - 8 keV. Light curves obtained at five wavelengths from 1550 to 3300 angstroms.

TABLE 1, Continued: Chronology of A0620-00 Observations

October	1	OSO-8 X-ray observations commence.
	5	Source about 15% brighter (3 - 6 keV) than in late September; decline resumes. At present rate, source should remain above threshold for Ariel-5 All Sky Monitor for another year or more.
	10	Discussion at Royal Astronomical Society meeting; negative results of search for ionized silicon and sulphur X-ray emission lines are reported. Ariel-5 data also yield report of less than 3 % linear polarization at 6 keV. High-speed photometry at McDonald Observatory shows no random or periodic variations on time scales of 2 - 200 sec.
	20	Symposium at NASA-Goddard Space Flight Center.
	23	First papers on the source appear in <u>Nature</u> .

In Table 2, I summarize the highlights of the observations of A0620-00 that have been reported (in many cases at this symposium) by many groups. Some results clearly require confirmation. For numerical data, consult the related papers in these Proceedings and the other references listed in the bibliography.

One surely would like to have more optical spectra than those reported thus far. They can be used to examine the hypothesis that we are dealing with a nova or recurrent nova and (as the star returns to minimum light) they may possibly reveal the physical nature of the (non-eruptive) companion. Do the emission lines recently detected with the Anglo-Australian telescope show any indication of orbital motion or of expansion of an ejected envelope? These are among the immediate and vital questions that are as yet unanswered.

A variety of interstellar absorptions have been observed against the respective optical, ultraviolet, and X-ray continua of A0620-00. These include the Na D lines, a diffuse feature at 5780 \AA , the extinction feature near 2200 \AA and the low-energy cut-off in the X-rays. Evidence for any time changes in these quantities should be carefully examined as it would indicate changes in the distribution of circumstellar material. (Like the conventional X-ray binaries, the transient sources probably have accretion disks. In the case of the transient sources, the disks may evolve on rather short time scales, so that the investigation of changes in

TABLE 2

Highlights of A0620-00 Observations

Outbursts in 1917 and 1975.

From interstellar diagnostics, $1 \lesssim D < 3$ kpc.

From optical light curve and recurrent nova analogy,
 $D = 11$ kpc.

For $D \gtrsim 1$ kpc, X-ray luminosity $> 10^{38}$ erg sec, near
Eddington limit for one solar mass.

At maximum, X-ray and radio emission are observed,
contrary to the properties of classical novae.

Enormous X-ray amplitude of the outburst, $> 10^4$.

No periodic X-ray or optical pulsations on time scales
of fractions of a millisecond to two days.

Precursor peak occurred one week before X-ray maximum.

X-ray spectrum hard in early stage of outburst, softened
dramatically toward and after maximum intensity.

No X-ray lines detected.

Polarization less than a few per cent at 6 keV.

Visible light fades more slowly than X-rays after maximum.

Optical emission lines detected well after maximum.

Four day oscillation emerges in UBV light curves two weeks
after maximum.

Flat radio spectrum is probably nonthermal.

Optical, UV continua individually suggest $T \approx 30,000$ K.

Visible light is red at minimum; blue during outburst.

Optical polarization is probably interstellar.

Amplitude of optical outburst is 8 magnitudes in B.

the "interstellar" diagnostics may shed light on the dynamics of these processes.) Further spectral work to verify the conclusion of Snow et al., that the source is closer than 3 kpc, is especially important, since this result is in gross contradiction with the 11 kpc distance of Eachus, Wright and Liller, and hence with the recurrent nova model. The other interstellar absorption results in general just tell us that A0620-00 is at least 1 kpc away.

The detection of a 4-day modulation in \bar{U} , B, and \bar{V} , while still subject to independent confirmation, looks quite real in the data of Duerbeck and Walter (1975). It is obviously important to search the data in the other wavelength ranges for evidence of this periodicity, which might well be that of the binary orbit.

The optical counterpart of A0620-00 is very red at minimum light on the Palomar survey plates; Ward et al. estimate $B - R \approx 3.6$ and discuss various possibilities for the companion star of the eruptive object, assuming that it is the companion that was photographed at minimum. If the companion is a red giant, this would place the source at a distance of at least 15 kpc. The amplitude and hence the distance estimated by Eachus, Wright and Liller on the assumption that the object is a recurrent nova would each be larger on the assumption that the object on the Palomar plates is actually the companion. (See Cowley 1975.) Multiband photometry or spectra at minimum light might resolve this question.

THE THEORIES

Conventional nova outbursts are thought to be stimulated by the accretion on a white dwarf of matter lost from its cool and larger companion star through the inner Lagrangian point of the binary system (cf. Starrfield, Sparks and Truran 1975). Models proposed for A0620-00 include the suggestion that it is in fact a recurrent nova (Eachus, Wright and Liller 1975). An alternate and quite attractive possibility is that we have here a nova-like system, but one in which the compact star is a neutron star or a black hole (Elvis et al. 1975). Ricketts, Pounds and Turner (1975) and Doxsey et al. (1975) describe brief scenarios for the evolution of the outburst in such a binary.

Doxsey et al. consider the case when the outburst arises from the sudden onset of massive accretion, perhaps at periastron. In this case, the 58-year recurrence time is the orbital period. Assuming that the X-ray luminosity is near the Eddington limit, they require a mass of four suns for the compact object, which is therefore a black hole, providing that the distance exceeds 1.5 kpc.

Arguing from the appearance of the star at minimum on the same Palomar survey plates, Ward et al. conclude that the nondegenerate companion may be a red dwarf, Cowley proposes that it is a giant, and Endal et al. call it subgiant.

In Cowley's nova-like model, the 4-day apparent periodicity found in U,B,V is identified with the orbital period. Endal, Devinney and Sofia (1975) argue that the system is not nova-like, since many of the observed properties are so different from classical novae, and they propose an Algol-type system. In their model, the compact star is a white dwarf.

Brecher and Morrison (1975) make the ingenious suggestion that the X-rays arise when a shock collides with the local stellar wind or other pre-existing gas within a binary system.

Most of the theories advanced thus far are qualitative and based on only a particular subset of the data. Since most of the material discussed here remains to be published, this is hardly unreasonable! We do not yet have a compelling case to accept any of the models, but surely the results summarized in Table 2 are trying to tell us something and perhaps a clearer picture will emerge in a year's time.

CONCLUDING REMARKS

At peak intensity, A0620-00 was much stronger than Sco X-1 and indeed was the brightest known extrasolar X-ray source. The researchers who have on occasion searched for ionospheric influences of Sco X-1 would thus do well to look for the signature of A0620-00's outburst in August, 1975. Transient sources of this magnitude may occur relatively frequently, but have been overlooked in large part previously thanks to the lack of appropriate all sky X-ray monitors. Now that we know that fairly bright optical emission can accompany the X-ray eruptions, it is to be hoped that observers with Schmidt and other appropriate telescopes will respond more vigorously and promptly to announcements of new satellite discoveries, even when the initial position measurements are very crude. Even should the optical counterpart escape immediate notice on the plates when the positional uncertainty of the X-ray source is quite large, later refinement of the X-ray position may enable both a retrospective identification and the possibility of constructing a light curve in the optical starting from as soon as possible after the X-ray discovery.

It is a pleasure to thank the organizers of this symposium, Drs. Y. Kondo and E. Boldt, for their courtesy in adding the session on this source to the program at almost the final minute. I am indebted for very interesting discussions to Drs. L.G. Jacchia, W. Liller, B.G. Marsden and K. Pounds, and I thank Dr. S. Kleinmann for communicating the infrared data in advance of publication.

The following bibliography cites a fair number of references that were consulted in the preparation of these remarks but which are not directly cited in the text. As one final confusing note, it should be mentioned that recently the SAS-3 group has discovered another transient source, MX0656-07, which has been called the "X-ray nova in Monoceros" (IAU Circular, No. 2843).

REFERENCES

- Boley, F., Wolfson, R., Bradt, H., Doxsey, R., Jernigan, G., and Hiltner, W.A. 1975, "Optical Identification of A0620-00," preprint, Dartmouth College.
- Bradt, H., and Matilsky, T. 1975, Symposium on X-Ray Binaries, NASA-GSFC.
- Brecher, K., and Morrison, P. 1975, Symposium on X-Ray Binaries, NASA-GSFC.
- Brinkman, A.C. 1975, Symposium on X-Ray Binaries, NASA-GSFC.
- Cowley, A.P. 1975, Symposium on X-Ray Binaries, NASA-GSFC.
- Davis, R.J., Edwards, M.R., Morrison, I., and Spencer, R.E. 1975, Nature, 257, 659.
- Dolan, J.F. 1975, Symposium on X-Ray Binaries, NASA-GSFC.
- Doxsey, R., Jernigan, G., Hearn, D., Bradt, H., Buff, J., Clark, G.W., Delvaile, J., Epstein, A., Joss, P.C., Matilsky, T., Mayer, W., McClintock, J., Rappaport, S., Richardson, J., and Schnopper, H. 1975, "X-Ray Nova A0620-00: Celestial Position and Low Energy Flux," preprint CSR-P-75-28, Massachusetts Institute of Technology.

- Duerbeck, H., and Walter, K. 1975, Symposium on X-Ray Binaries, NASA_GSFC.
- Eachus, L.J., Wright, E.L., and Liller, W. 1975, Symposium on X-Ray Binaries, NASA-GSFC.
- Elvis, M., Page, C.G., Pounds, K.A., Ricketts, M.J., and Turner, M.J.L. 1975, Nature, 257, 656.
- Endal, A.S., Devinney, E.J., and Sofia, S. 1975, "A Model for the X-Ray Nova A0620-00," preprint, NASA-GSFC.
- Kaluzienski, L.J., Holt, S.S., Boldt, E.A., and Serlemitsos, P.J. 1975, Symposium on X-Ray Binaries, NASA-GSFC.
- Kleinmann, S., Joyce, R.R., and Capps, R.W. 1975, Symposium on X-Ray Binaries, NASA-GSFC.
- McLaughlin, D.B. 1960, in Stellar Atmospheres, ed. J.L. Greenstein, Chicago: Univ. of Chicago Press, p.585.
- Owen, F. 1975, Symposium on X-Ray Binaries, NASA-GSFC.
- Ricketts, M.J., Pounds, K.A., and Turner, M.J.L. 1975, Nature, 257, 657.
- Serlemitsos, P.J. 1975, Symposium on X-Ray Binaries, NASA-GSFC.
- Snow, T.P., Jr., York, D.G., Gull, T.R., and Henize, K.G. 1975, Symposium on X-Ray Binaries, NASA-GSFC.
- Starrfield, S., Sparks, W.M., and Truran, J.W. 1975, IAU Symposium No. 75, Evolution and Structure of Close Binary Systems, in press.
- Ward, M.J., Penston, M.V., Murray, C.A., and Clements, E.D. 1975, Nature, 257, 659.
- Willmore, A.P. 1975, Symposium on X-Ray Binaries, NASA-GSFC.

Wolfson, R., and Boley, F. 1975, Symposium on X-Ray Binaries,
NASA-GSFC.

Wu, C.-C. 1975, Symposium on X-Ray Binaries, NASA-GSFC..

Also see information in IAU Circulars, No. 2814, 2817,
2819, 2822, 2823, 2830, 2835, 2837, 2840, 2846, 2854,
and 2864.

THE EARLY LIGHT CURVE OF A0620-00

L. J. Kaluziński*, S. S. Holt, E. A. Boldt and P. J. Serlemitsos
NASA/Goddard Space Flight Center
Greenbelt, Maryland 20771

The Ariel-5 All-Sky Monitor measured the 3-6 keV x-ray intensity of 0620-00 for two days shortly after peak emission in August 1975, and continuously throughout September 1975. The effective exposure each day for this source (and every other source in the ~80% of the celestial sphere covered by the monitor) is ~250 cm²sec.

Figure 1 illustrates the 512 elements (in spacecraft coordinates) into which the monitor data is stored for readout each orbit. A complete description of the experiment is given in Holt (1975). At the time of source appearance, the spacecraft spin axis was in an extended (~1 month) hold at the north galactic pole, so that the galactic plane $\pm 10^\circ$ was inaccessible to the experiment. Shortly after maximum, the satellite reoriented to place the spin axis in the direction of A0620-00, so that approximately two days of data were obtained before the source moved into the "polar dead spot".

The light curve obtained through October 1 (when the spin axis was again pointed to A0620-00) is shown in Figure 2. Shown for purposes of crude comparison are the data reported from other Ariel-5 experiments in IAU telegrams (where we have normalized the quoted intensities in UHURU counts to the Crab Nebula). The intensity difference at maximum is obviously a manifestation of the very soft spectrum of the source. Clearly, A0620-00 was approximately four times as bright as Sco X-1 at maximum in the band 3-6 keV. The decay is quite smooth, but cannot be fit with a single e-folding time. The interval between the early All-Sky Monitor points and the onset of continuous coverage has an inferred e-folding time of ~22 days, but it is continually increasing throughout September. When next observed on 5 October (not shown in the figure), the intensity is actually ~15% higher than at the end of September, but it has since resumed its decline.

A0620-00 is apparently similar in its x-ray character to the very strong, long-lasting transient x-ray sources which presently number six in the data catalog. In contrast, only three can be sensibly reconciled with the lower-intensity, shorter-duration hard-spectrum transients which have been found to "pulse" on a time scale of minutes. Table I lists these "unqualified" transients.

*Working at GSFC under U. of Md. contract 21-002-316.

TABLE I		
Spectrum:	$\alpha > \text{Crab}$	$\alpha < \text{Crab}$
Timescale:	$t_{\text{on}} > 1 \text{ month}$	$t_{\text{on}} < 1 \text{ month}$
Intensity at max:	$> \text{Crab}$	$< \text{Crab}$
Pre-Ariel-5	Gen X-2 Gen X-4 1543-47	1735-28
Ariel-5	1524-61 1742-28 0620-00	1118-61 0535+26

It is important to note that the All-Sky Monitor has a sensitivity of ~ 0.1 Crab for sources which have a duration of ~ 1 week for $/b/ > 10^\circ$, and somewhat worse (~ 0.3 Crab on the average, depending on source confusion) for comparable on-times in the galactic plane. All of the Ariel-5 transients listed in Table I were close to the plane, and the obvious lack of long-duration sources with intensities below that of the Crab is a bit surprising. If we assume that such sources may occur anywhere in the galactic plane with roughly equal probability and with roughly comparable absolute luminosity, the assumption of an effective experimental threshold at the intensity of the Crab Nebula yields, after Silk (1973):

$$N(>S, t) = \frac{t}{\tau} \frac{L}{4\pi SR^2}$$

$$\frac{L}{\tau \text{ yr}} \text{ ergs}^{-1} = 3.6 \times 10^{38} \frac{N(>S, t)}{t \text{ yr}} \left(\frac{R}{15 \text{ kpc}} \right)^2 \frac{S}{S_{\text{Crab}}}$$

where $N(>S, t)$ is the number observed above an intensity S in a time t , assuming a mean time τ between source appearances at peak luminosity L in the galaxy (of radius R). As there were three sources of the long-duration variety (left side of Table I) during the first year of Ariel-5 operation, it is safe to say that $\tau > .1$ (on the average), and that $L > 10^{38} \text{ erg s}^{-1}$. The lack of lower intensity sources above the All-Sky Monitor threshold similarly is indicative of a peak luminosity in transients similar to 0620-00 which is at least this high. If these sources are fueled by the conversion of gravitational potential energy from accreted mass, such high peak luminosities may be indicative of an Eddington-limited mass flow.

In contrast, the harder-spectral, shorter-duration sources on the right side of Table I are not as luminous at peak. All18-61 was out of the field of view of the All-Sky Monitor for its entire lifetime, but would have been below the experimental sensitivity of the monitor anyway. The short lifetime of these sources allows τ to be as low as $\sim 10^{-3}$ without conflicting with any measurements of which we are aware (the most restrictive being the upper limit for a galactic "ridge"). There certainly can be ~ 100 sources of this kind in the galaxy each year, with peak luminosity $\leq 10^{37} \text{ erg s}^{-1}$. The characteristics which this type of transient have in common with Vela X-1 (3U0900-40) are important in suggesting that the latter represents a "stable" counterpart for these objects.

It is not at all clear that a similar counterpart exists for the long-duration transients. Perhaps the best candidate is Aql X-1 (3U1908+00), which "flared" in 1975. As shown in Figure 3, the general light curve characteristics are quite similar to those of A1524-61 (c.f. Kaluziński, et al. 1975), but on a shorter timescale. Copernicus measurements placed Aql X-1 at a level \sim two orders of magnitude below its maximum intensity in Figure 3 for the two years prior to outburst (the Crab Nebula has an intensity of 1.4 in the units of Figure 3), so that Aql X-1 would have easily satisfied the conditions for being labelled a "transient" had it not been catalogued previously.

The optical identification of A0620-00 has enabled a more detailed study of this transient than any other, but the x-ray phenomenology has not yet been exhausted. As the present intensity of A0620-00 is two orders of magnitude above the All-Sky Monitor sensitivity, we expect that its light curve will be continuously recorded for at least another year.

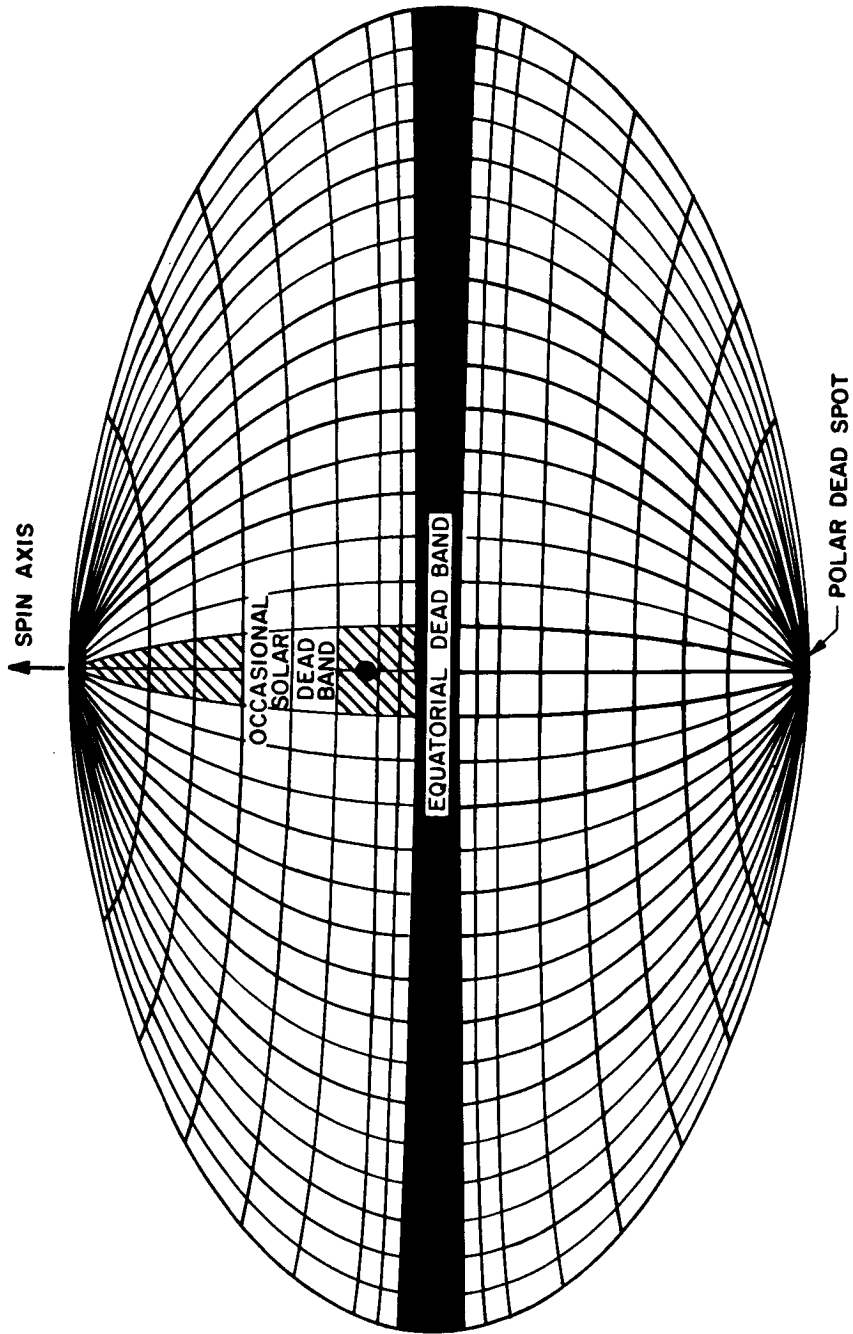


Figure 1 The 512 elements, in spacecraft coordinates, into which the All-Sky Monitor data is accumulated for readout once per orbit. The solar "image" is the image size of a point source ($\sim 4^\circ$), compared to a typical resolution element size of $\sim 10^\circ \times 10^\circ$. At the time of A0620-00 appearance, the galactic plane was coincident with the "equatorial dead band".

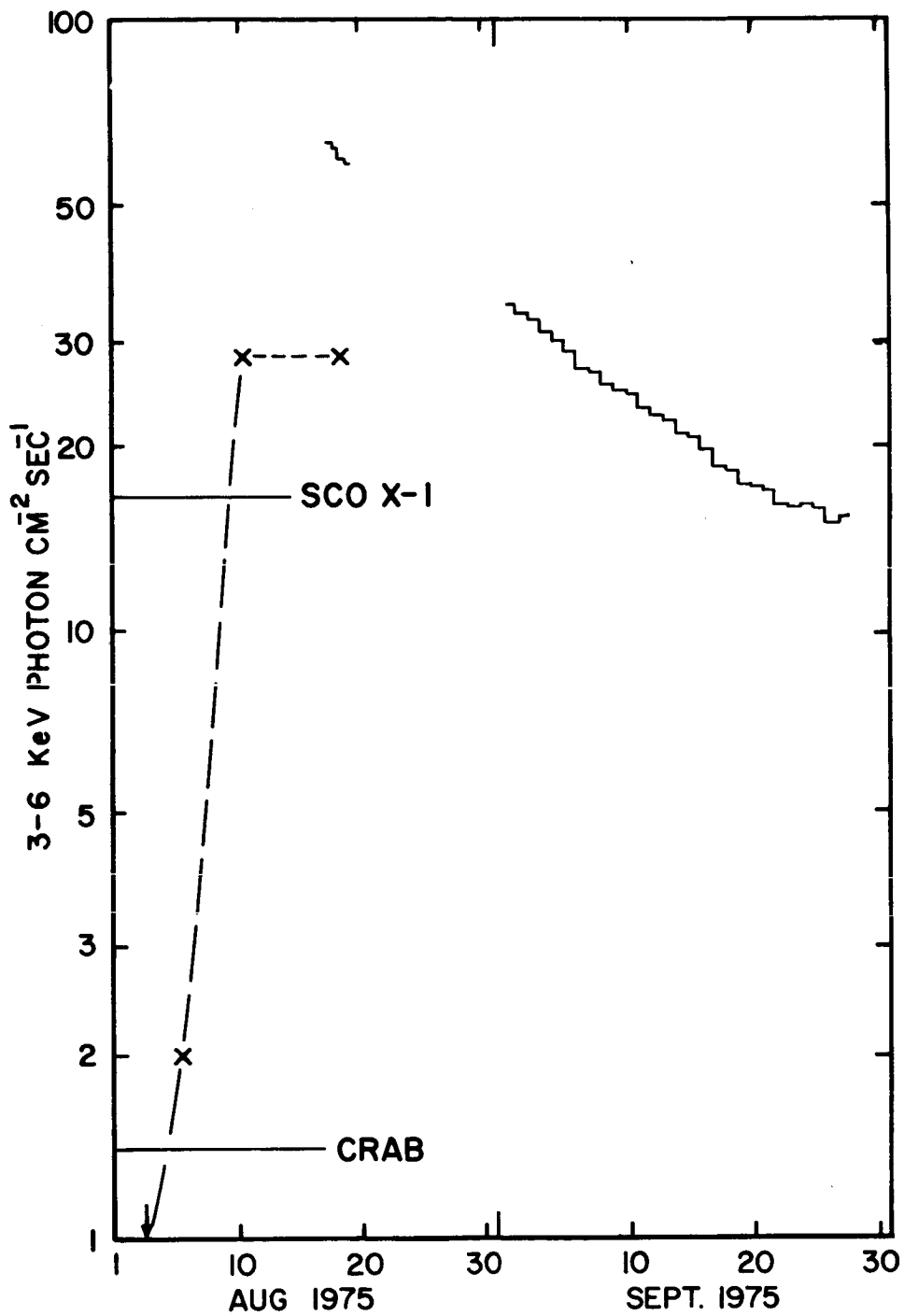


Figure 2 The early light curve of A0620-00. The typical statistical error is $<2\%$. The dashed trace is a reproduction of other Ariel-5 data reported in IAU telegrams, normalizing to the present experiment with the Crab Nebula.

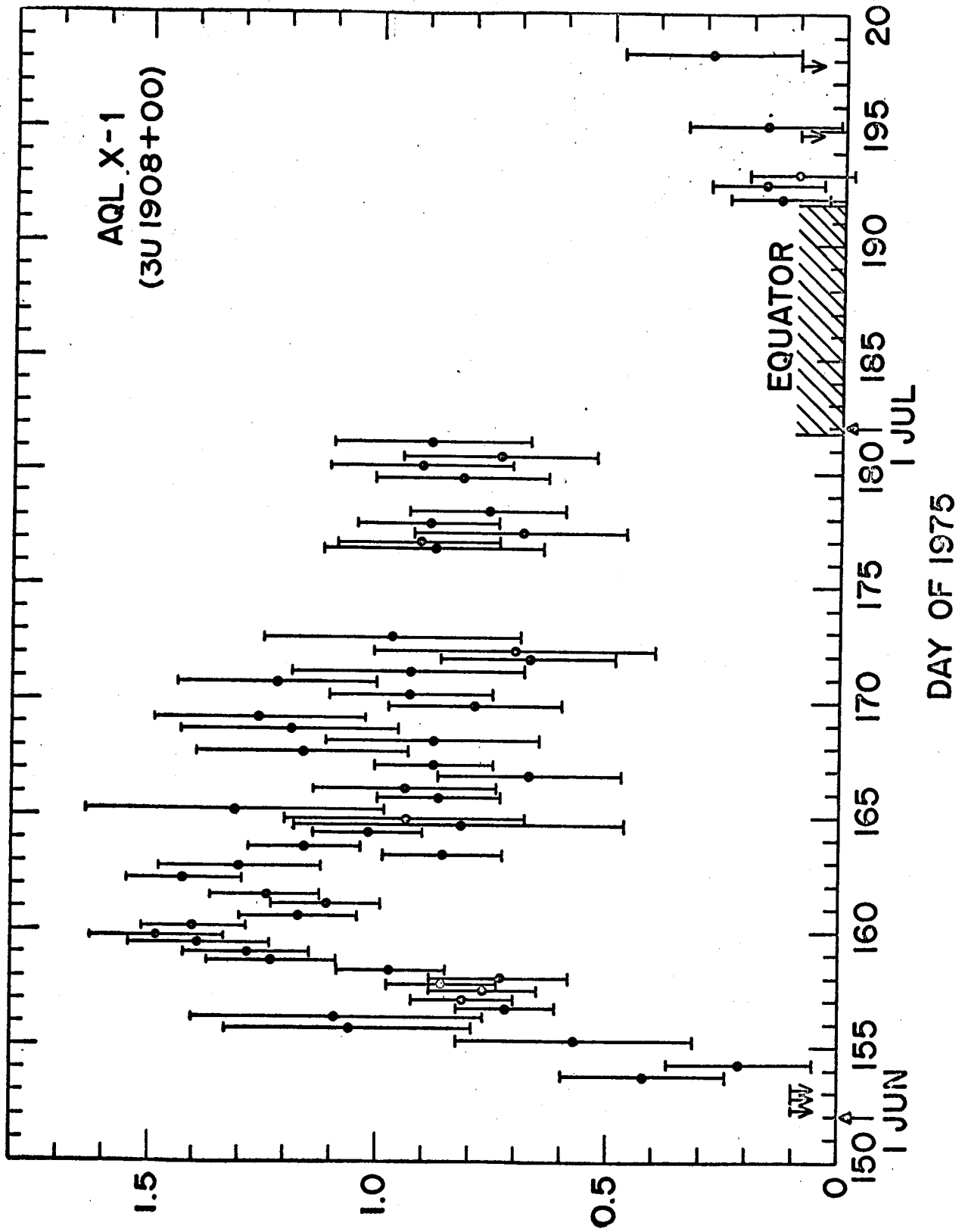


Figure 3 The light curve of the flare in Aql X-1.

OBSERVATIONS OF A0620-00 BY SAS-3*

H. Bradt and T. Matilsky
Department of Physics and Center for Space Research
Massachusetts Institute of Technology

ABSTRACT

The transient X-ray source A0620-00 has been observed by the SAS-3 group with the SAS-3 X-ray observatory since Aug. 3. At maximum X-ray luminosity, \sim Aug. 13, and thereafter, we have placed limits of $< 2\%$ on periodic variations from 0.2 ms - 2000 sec. On Aug. 15, a precise position was obtained with the rotating modulation collimator. This led directly to radio and optical identification by groups at the NRAO, Arecibo, and McGraw Hill Observatories. On Aug. 27, the low energy (0.15-0.9 keV) system was pointed at the source, and we derived a spectrum: $kT \sim 1.3$ keV and $F = 1.0 \times 10^{-6}$ ergs cm^{-2} s^{-1} (0.3-10 keV) with $N_H = (3.5 \pm 0.3) \times 10^{21} / \text{cm}^2$. (See table I) Hardness ratios are presented, as well as detailed light curves, from Aug. 8 to Oct. 14. Of particular interest is a dramatic initial softening of the source on Aug. 8 (previously reported by the Ariel-5 group), a gradual hardening from Aug. 9 - Aug. 14, and a softening from Aug. 20 - Sept. 17. (See figures 2,3,4)

* This work was supported in part by the National Aeronautics and Space Administration under contract NAS 5-11450.

TABLE I
HISTORY AND PRINCIPAL RESULTS

JD	
633 8/8	<u>FIRST SAS-3 SIGHTINGS - SPINNING MODE</u> VERY SOFT SPECTRUM. (BUFF, JOSS, LAUFER)
637-8 8/12-13	<u>POINTED OBSERVATIONS 1.5 - 50 KEV</u> <0.4% PULSED 0.8-430 s <2% PULSED 0.2 MS - 0.3 s $kT \approx 1.7$ KEV $F = 1.7 \times 10^{-6}$ ERGS $CM^{-2} S^{-1}$ (1-10 KEV) (MATILSKY, MAYER, PRIMINI, LI)
640 8/15	<u>POSITION MEASUREMENT - RMC</u> $6^H 20^M 9^S.5$ (1950) $-0^{\circ} 19' 1''.5$ ERROR RADIUS 60" (DOXSEY, JERNIGAN)
640	RADIO IDENTIFICATION (NRAO/ARECIBO)
641 8/16	<u>OPTICAL IDENTIFICATION (MCGRAW HILL)</u>

TABLE I (Continued)

JD

652
8/27

POINTED OBSERVATIONS 0.15 - 50 KEV

INTENSE FLUX, 0.4 - 0.9 KEV

$kT = 1.3$ KEV

$F = 1.0 \times 10^{-6}$ ERGS $\text{CM}^{-2} \text{S}^{-1}$
(0.3 - 10KEV)

$N_H = (3.5 \pm 0.3) \times 10^{21}$ H CM^{-2} (X-RAY)

$N_H \approx 3.5 \times 10^{21}$ (21 CM)

(HEARN, RICHARDSON, DOXSEY)

653-98

8/28 -
10/13

SPINNING OBSERVATIONS

LIGHT CURVES

HARDNESS RATIOS (See Following Figures)

(MATILSKY, BUFF, ZUBROD)

699

10/14

POINTED OBSERVATIONS 1.5 - 50 KEV

$\sim 2 \times 10^7$ COUNTS/ORBIT

NO PULSING ($\leq 1\%$)

0.2 MS - 2000 S

$kT \approx 1.1$ KEV

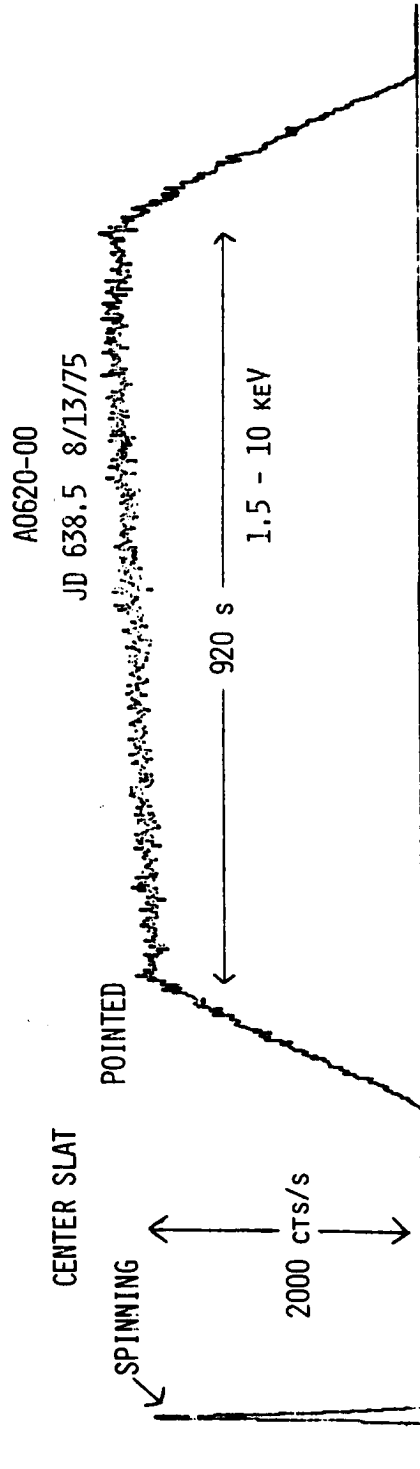


Fig. 1. Slit collimator (1° FWHM) observation of A0620-00. The slow increase in rate is due to a slow drift of the satellite orientation. Note the absence of apparent pulsations.

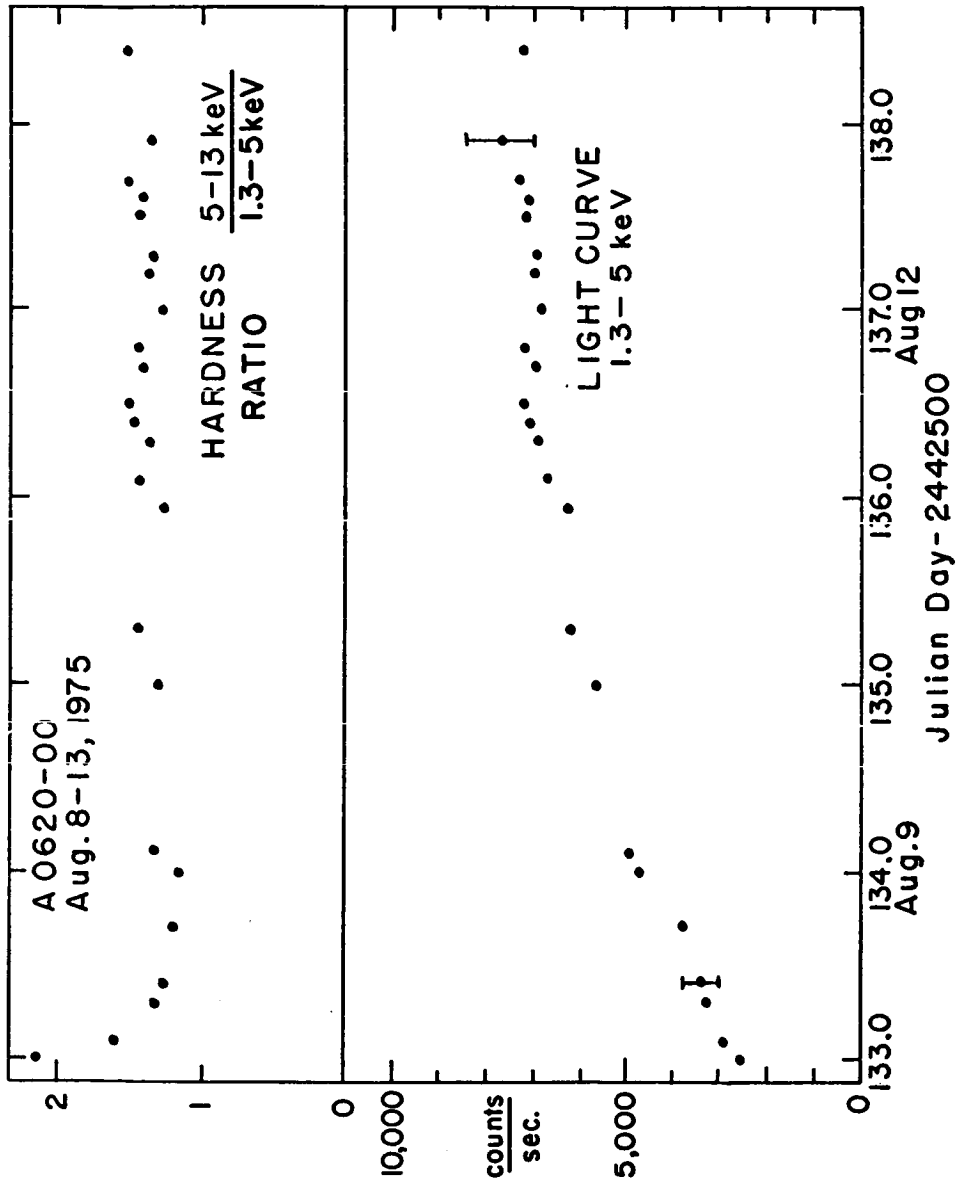


Fig. 2. Light curve and hardness ratios for 1975 Aug. 8-13. Note pronounced softening, JD 133.0-134.0, (see Ricketts, et al. Nature in press) and gradual hardening thereafter. The error bars represent estimated uncertainty in effective detector area.

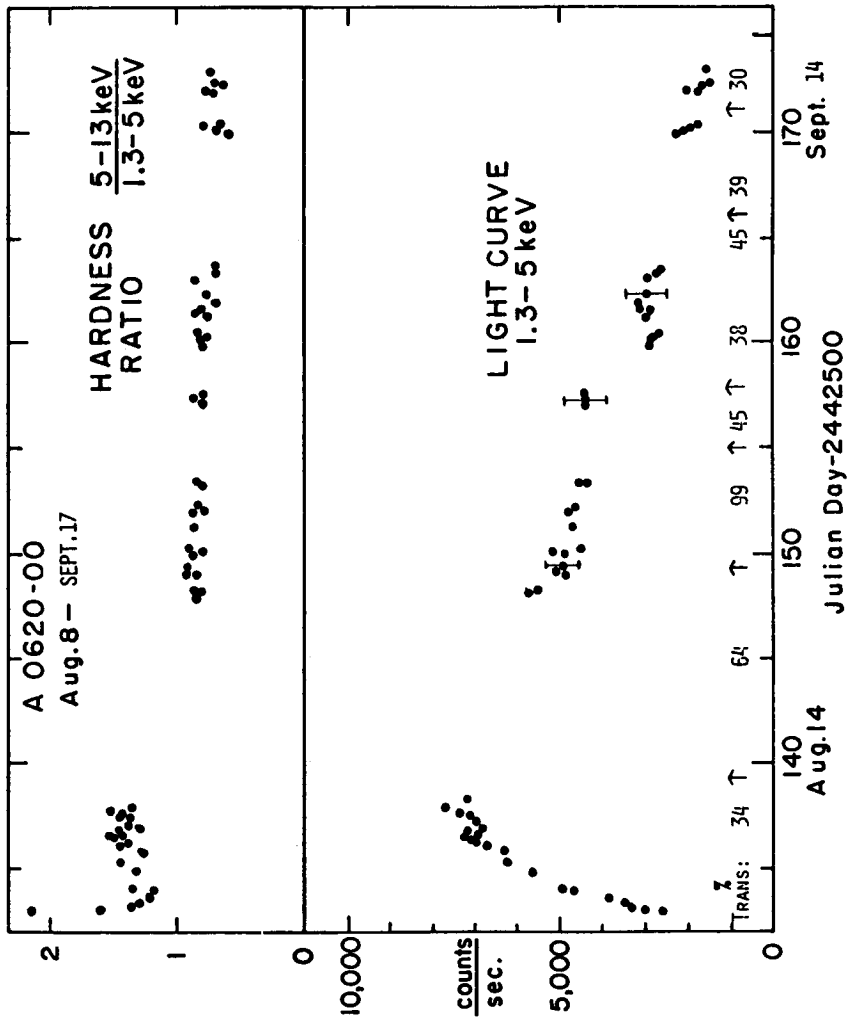


Fig. 3. Preliminary light curve and hardness ratios for Aug. 8 - Sept. 17. Note gradual softening after JD = 146. The arrows indicate the times of maneuvers. The approximate percentage transmissions are also indicated. The error bars represent the estimated uncertainty in the effective detector area. In-flight calibrations of the slit collimator effective areas as a function of source elevation have not yet been analyzed. Therefore discontinuities in the light curve at times of maneuvers should be viewed with caution. The drift in the hardness ratio is independent of spacecraft attitude.

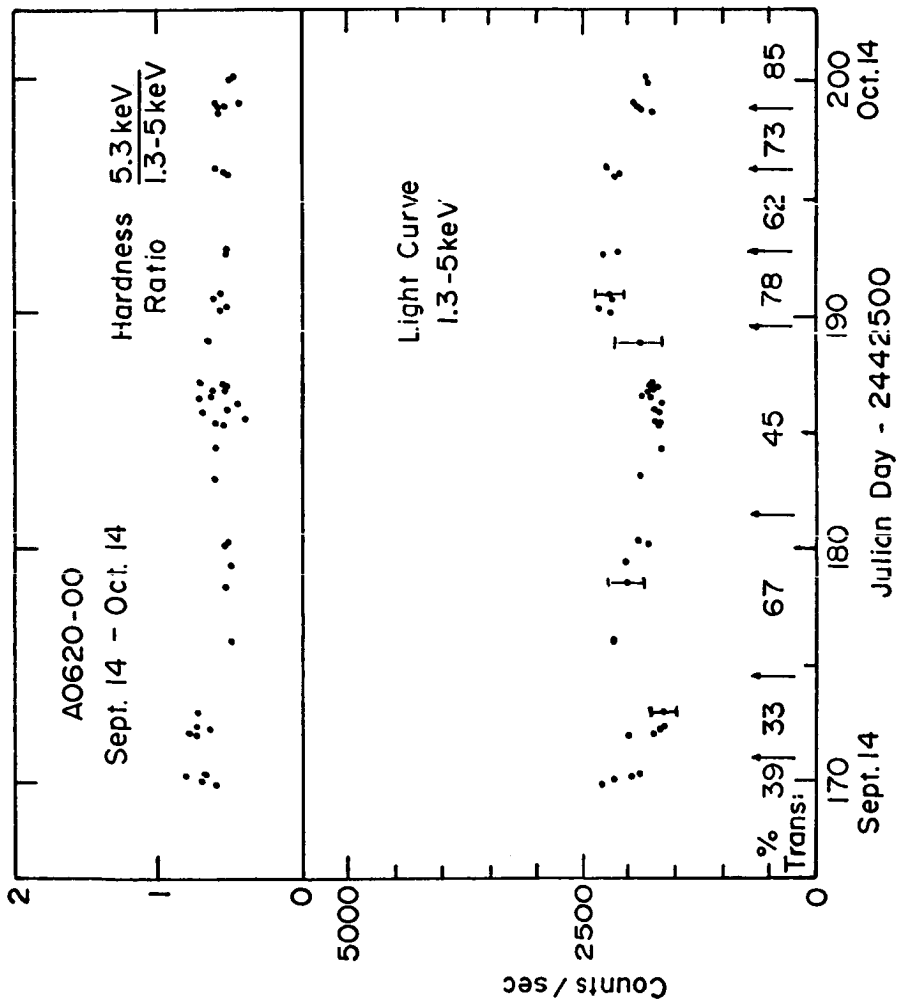


Fig. 4. Preliminary light curve and hardness ratios for Sept. 14 - Oct. 14. Note the constancy of the hardness ratio after J.D. 176 and the possibility of an enhancement of the 1.3-5 keV flux beginning at J.D. = 190. See caption to figure 3.

A0620-00

JD699.9 10/14/75

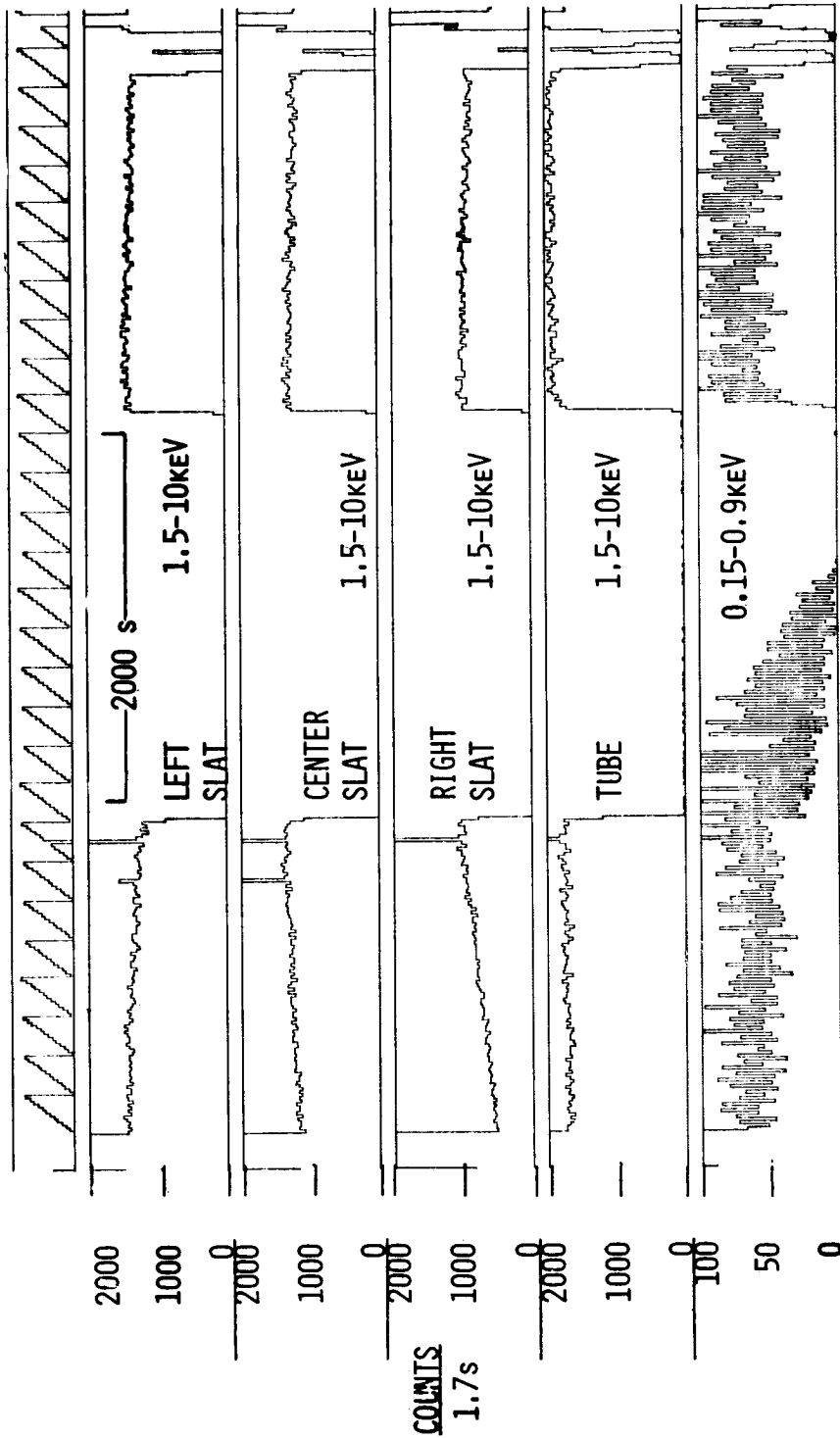


Fig. 5. Counting rates for 4 SAS-C data channels, during pointed observation of A0620-00. The gap in the data is due to Earth occultation.

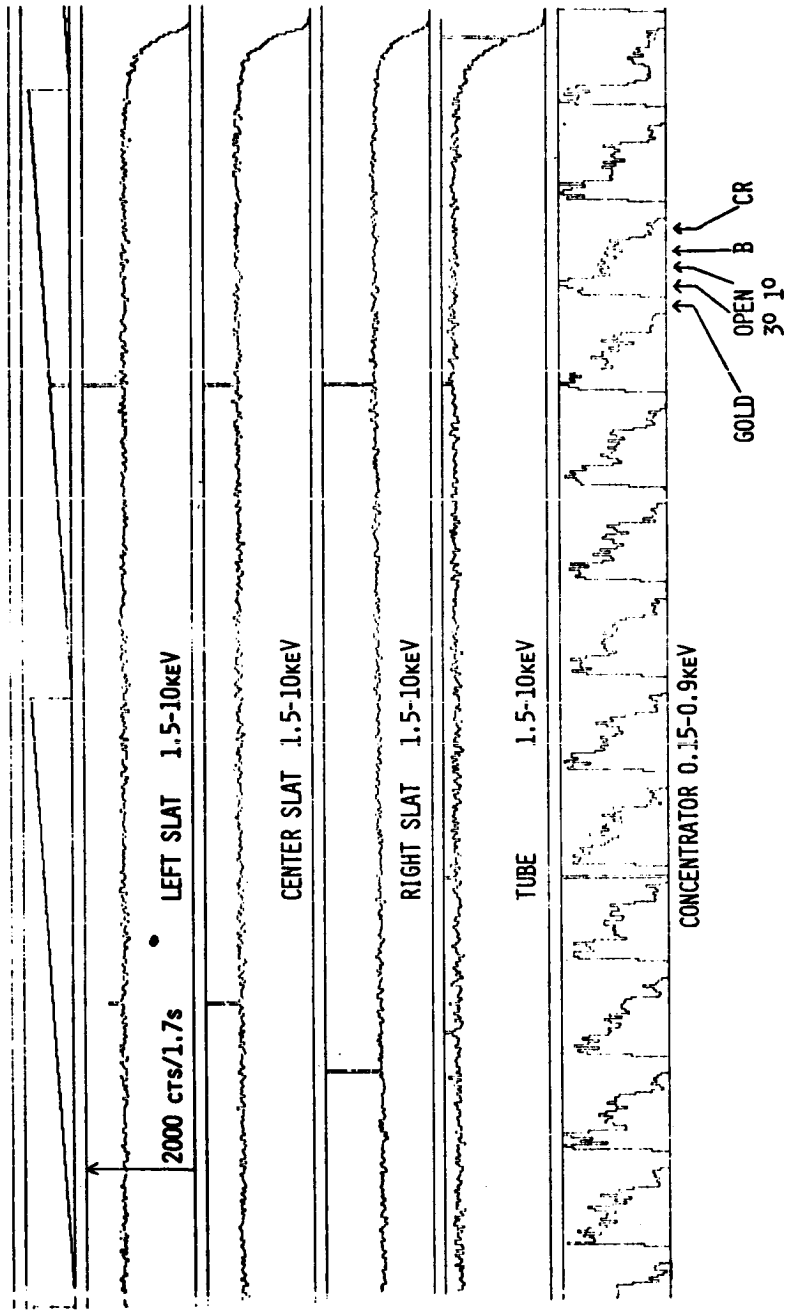


Fig. 6. Expanded portion of figure 5, also showing low energy concentrator counting rates which are modulated by the five filter wheel positions as indicated. Most of the low energy flux was in the range 0.4 - 0.9 keV, which yielded $N_H = (3.5 \pm 0.3) \times 10^{21}/\text{cm}^2$. Note the absence of periodic or aperiodic fluctuations in the slat data.

OPTICAL IDENTIFICATION QF A0620-00

R. Wolfson and F. Boley
Department of Physics and Astronomy
Dartmouth College
Hanover, New Hampshire 03755

ABSTRACT

Identification of the optical counterpart to the transient x-ray source A0620-00 was made on 16 August, 1975, using image tube photography at the McGraw-Hill Observatory on Kitt Peak, Arizona. Spectra taken subsequent to the identification showed no stellar absorption or emission features. Photometric data gave a V magnitude of $11.2 \pm .1$. This is about 8 magnitudes brighter than the object appears on the Palomar Sky Survey.

INTRODUCTION

The optical counterpart to the transient x-ray source A0620-00 (Elvis et al. 1975) was identified and studied spectroscopically and photometrically about two weeks after the first x-ray detection. Observations were made with the 1.3 meter telescope at the McGraw-Hill Observatory on Kitt Peak. This observatory was opened in the spring of 1975 with the primary purpose of studying optical counterparts to x-ray sources. Optical identification of A0620-00 was made possible through close coordination between the observatory and the MIT SAS-3 satellite group.

OBSERVATIONS

The x-ray source was first detected on Aug. 3 by the Ariel-5 satellite (Elvis *et al.* 1975), but it was not until Aug. 15 that a precise position ($\pm 2'$) was determined by SAS-3 (Matilsky 1975). On Aug. 16 we obtained eight two minute image tube exposures of a region centered on the SAS-3 position. Figure 1 shows a portion of one of these plates, along with the corresponding portion of the red Palomar Sky Survey plate. The object marked on the McGraw-Hill plate lies about one arc minute from the Aug. 15 SAS-3 position, and about 25" from a subsequent refined x-ray position (Doxsey *et al.* 1975). The object is within 2" of a faint star on the Palomar plate, whose position (epoch 1950) is:

$$\alpha = 6^{\text{h}} 20^{\text{m}} 11.2^{\text{s}}$$

$$\delta = -0^{\circ} 19' 10''$$

(Boley and Wolfson 1975). We estimate the 1975 object to be at least six magnitudes brighter than the corresponding Palomar star.

Subsequent to the optical identification, we obtained three image tube spectra at a dispersion of 120 Å/mm. These spectra show no absorption or emission features. High dispersion spectra obtained by Gull and York (1975) are similarly lacking in stellar lines. Observations made about three weeks later (Peterson, Jauncey, and Wright 1975) showed N III $\lambda\lambda 4634-4640$ and He II $\lambda 4686$ appearing in

emission.

Four nights of photometric data were obtained beginning on Aug. 22. Photometric observations were severely hampered by the proximity of the sun, which allowed as little as half an hour of observing time at the start of the optical work. Figure 2 shows the reduced V band photometric data. The data also yield a B-V color index of $.2 \pm .1$. High and rapidly changing sky counts, as well as cloud contamination, resulted in substantial uncertainties in the magnitude and color index. We searched the data for variations on time-scales from .1 second to 2 seconds, but found none statistically significant.

Our visual magnitude estimate of 11.2 is consistent with that reported by French (1975) on Aug. 26, and differs by more than the uncertainty from the value 11.4 reported on Sept. 14-15 (Bortle 1975). A decline in the optical light curve is thus evident.

DISCUSSION

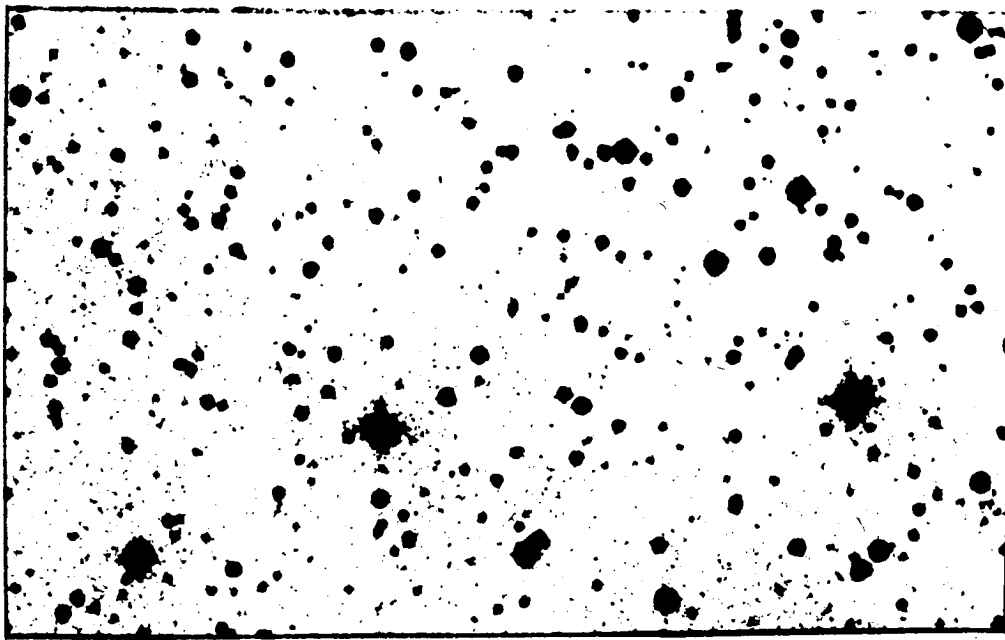
Photometric behavior of the object resembles that of a nova. Both the brightness increase and subsequent decline are consistent with observations of recurrent novae (Payne-Gaposchkin 1964; Liller 1975). If optical maximum is assumed to have occurred in August, however, the spectroscopic behavior is in contrast to that of most novae, which show absorption and often emission lines near maximum light (Payne-Gaposchkin 1964). It is intriguing to note that

the ratio of optical to x-ray emission for A0620-00 is the same as for Sco X-1, neglecting possible differences in interstellar absorption (Boley et al. 1975).

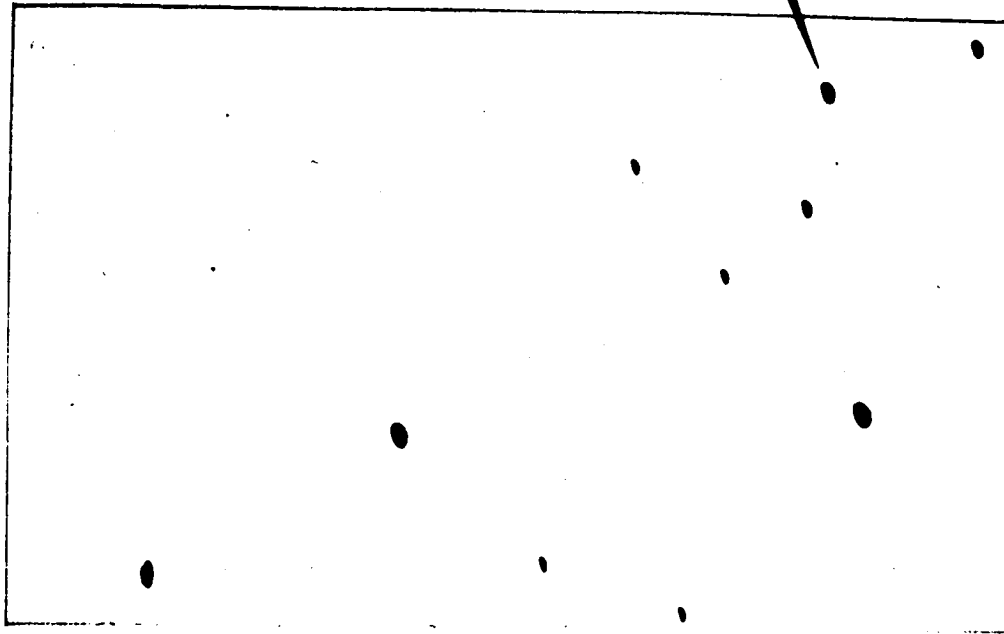
We are grateful to the MIT SAS-3 group for their cooperation throughout the observations, and to W.A. Hiltner for providing much valuable advice. R.W. acknowledges support from the Danforth Foundation.

REFERENCES

- Boley, F., Wolfson, R., Bradt, H., Doxsey, R., Jernigan, G.,
and Hiltner, W.A. 1975, submitted to Ap. J. Letters.
- Boley, F. and Wolfson, R. 1975, IAU Circ., #2819.
- Bortle, J. 1975, IAU Circ., #2837.
- Doxsey, R., Jernigan, G., Hearn, D., Bradt, H., Buff, J.,
Clark, G.W., Delvaile, J., Epstein, A., Joss, P.,
Matilsky, T., Mayer, W., McClintock, J., Rappaport, S.,
Richardson, J., and Schnopper, H. 1975, submitted
to Ap. J. Letters.
- Elvis, M., Griffiths, C.G., Turner, M.H.L., and Page, C.G.
1975, IAU Circ., #2814.
- French, H. 1975, IAU Circ., #2835.
- Gull, T., and York, D. 1975, IAU Circ., #2819.
- Liller, W. 1975, IAU Circ., #2823.
- Matilsky, T. 1975, IAU Circ., #2819.
- Payne-Gaposchkin, C. 1964. The Galactic Novae (New York:
Dover).
- Peterson, B., Jauncey, D., and Wright, A.E. 1975,
IAU Circ., #2837.



PALOMAR SKY ATLAS



McGRAW-HILL PLATE 8/16/75

Figure 1 - (Left) A portion of the red Palomar Sky Survey plate (© National Geographic Society) taken in 1955. (Right) (Right) McGraw-Hill plate of the same region, taken Aug. 16, 1975.

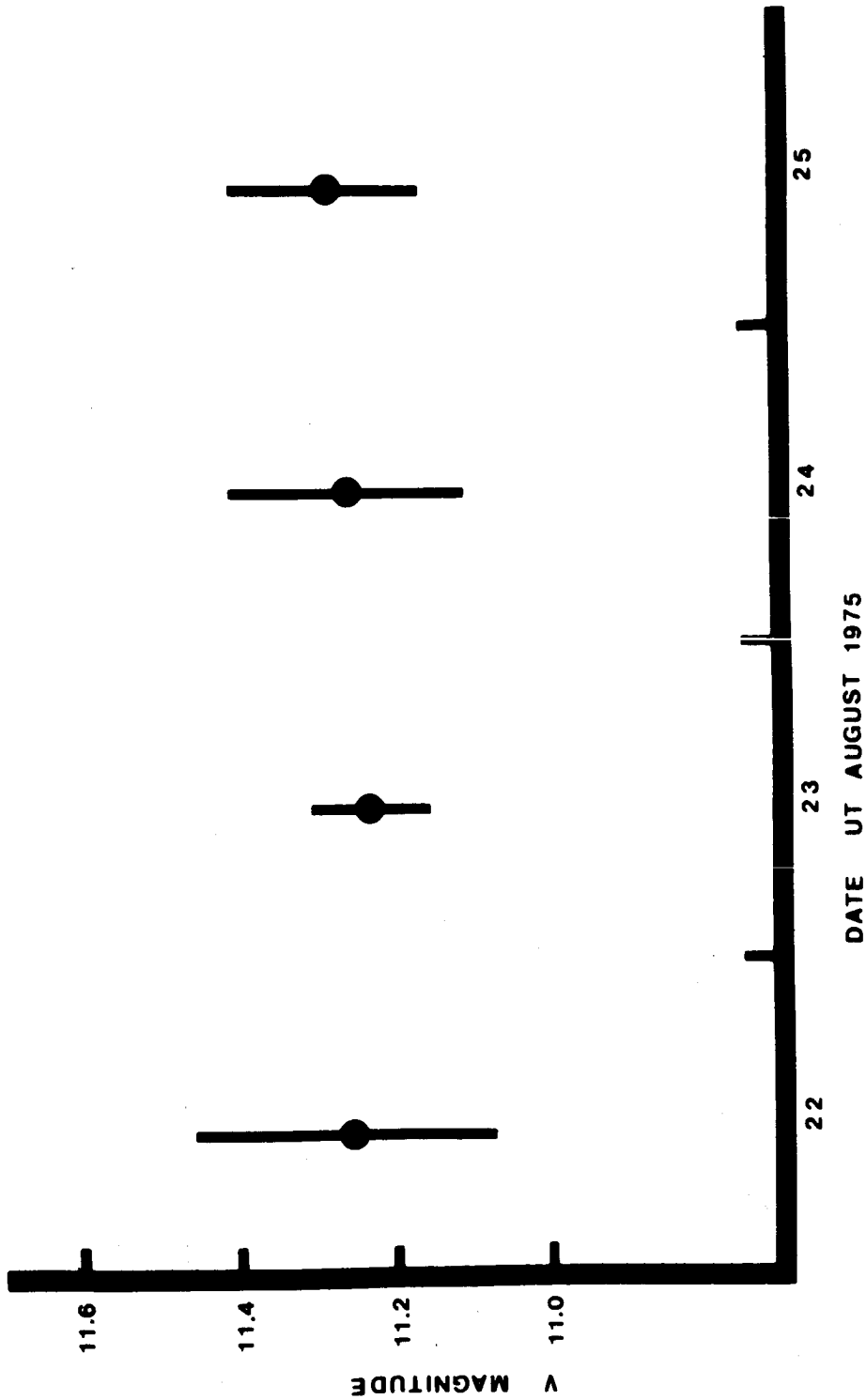


Figure 2 - Reduced V band photometric data for the A0620-00 optical counterpart.

A0620-00 AS A RECURRENT NOVA

WILLIAM LILLER

Center for Astrophysics

Harvard College Observatory and

Smithsonian Astrophysical Observatory

Cambridge, MA

ABSTRACT

Evidence for and against the star associated with A0620-00 being a nova is presented. The conclusion is that this star closely resembles other recurrent novae with the only unusual characteristic being the apparent high temperature at maximum brightness.

Following the discovery by Boley and Wolfson (1975) of an optical source which was coincident in position with the X-ray transient source A0620-00 and which had risen in brightness from $B \sim 20$ to $B = 11.5$, Lola J. Eachus, working with a finding chart kindly provided by S. Rappaport, searched through the archival sky photographs in the collection at the Harvard College Observatory and discovered (Eachus 1975) that in late October or early November, 1917, the star underwent a similar outburst. The 1917 light curve, which has been published elsewhere (Eachus, Wright and Liller 1976, hereinafter referred to as EWL), shows a rapid rise (>0.14 mag/day) to a maximum brightness of $B = 12.0$ followed by a decline, $d \approx 0.011$ mag/day. The current outburst appears to exhibit a similar rate of fading.

I should like to review the characteristics of these outbursts and critically compare them to those of recurrent novae in order to evaluate the evidence for and against A0620-00 being a typical member of that sub-group of cataclysmic stars. For ease of comparison, I list in Table 1 the properties of the 6 recognized recurrent novae, with the Boley-Wolfson star added at the bottom with the data claimed by EWL.

It should be noted in Table 1 that it has long been recognized (see, e.g., Payne-Gaposchkin 1963) that the quantities in the second and third columns are related and probably likewise the fourth and fifth columns. In the case of rate of fading, d , and M_{\max} , a least squares straight line fit to the

data of Table 1 gives

$$M_{\max} = -8.42 - 1.297 \log d,$$

The average deviation of the values from this fit is only 0.27 mag.

A similar relationship holds for ordinary (non-recurrent) novae. Certainly the most unbiased survey was that made by Arp (1956) who patrolled our sister galaxy, M 31, for a year and discovered 30 novae. His results show that approximately

$$M_{\max} = -8.6 - 1.43 \log d$$

Because all these novae were at sensibly the same distance, the coefficient of $\log d$ is well-determined. The constant depends, of course, on a knowledge of the distance to M 31.

Concluding that A0620-00 is a typical re-current nova, EWL derived that $M_{\max} = -5.9$ with an uncertainty of a few tenths of a magnitude. However, it should be pointed out that A0620-00 has a slower rate of decline than the other recurrent novae and is slightly "slower" than the slowest nova observed by Arp (viz. 0.017 mag/day). There do exist a number of recognized galactic novae which are slower: for example, AR Cir, V999 Sgr, DO Aql and Nova Centauri 1947, recently described by Henize and Liller (1975).

According to Kukarkin and Parenago (1934), the recurrent novae and the U Geminorum stars, such as SS Cygni, fit a single

relation between the amplitude in magnitudes, A , and the interval between maxima in days, P . Payne-Gaposchkin (1964), using photographic magnitudes corrected for the presence of companion stars, gives for this relation

$$A = 2.00 + 1.78 \log P$$

For the 7 recurrent novae in Table 1, this formula predicts a relatively small range in A , going from 8.7 to 9.9, and for A0620-00, $A_{\text{pred}} = 9.7$. A comparison of the pre-outburst images of A0620-00 on the Palomar Sky Survey prints shows that the system was conspicuously red with the (B-R) color ~ 2.5 , suggesting that we were seeing the light primarily from a red companion and not the blue dwarf usually associated with the nova phenomenon. Therefore, it is not surprising that the predicted amplitude is 1.2 mag larger than observed.

Because of the preponderance of X-rays coming from A0620-00, one might now conclude that the system is composed of a more or less normal red main sequence star with a highly degenerate and hence invisible companion. However, as EWL point out, if A0620-00 is a normal recurrent nova, its distance must be ~ 10 kpc and its X-ray flux exceeds 10^{40} ergs/sec, too large to be explained by a normal accretion mechanism.

The one optical characteristic of A0620-00 which puts it into the category of "unusual" is the purely continuous spectrum exhibited by the star shortly after maximum (Gull 1975). According to McLaughlin (1960), the spectrum of a nova at

maximum light typically resembles that of an A or F supergiant, although just before peak brightness, it usually is of earlier spectral type. Nine days before maximum the slow nova DQ Herculis 1934 was classified as B5, changing to F0 at maximum and then to F5 shortly afterwards. Allen (1973) gives $T_{\text{eff}} = 15,500^\circ$ for spectral type B5, and for O5, $T_{\text{eff}} = 40,000^\circ$, which is probably near the minimum expected temperature for a continuous spectrum object.

According to Brecher (1975), the maximum distance which A0620-00 could have and still be radiating X-rays by accretion is ~ 3 kpc and if the interstellar absorption amounts to 2.0 mag (EWL), then the absolute B magnitude at maximum brightness must have been fainter than or equal to -3.0 . Thus, A0620-00 would have been sub-luminous by at least 3 magnitudes, if classified as a typical recurrent nova.

In conclusion, we find that save for a much higher temperature at peak brightness than is usually found, A0620-00 is quite typical of that sub-class of cataclysmic variables known as recurrent novae. If its luminosity at maximum brightness is also typical, then the distance of 11.0 ± 2.5 kpc derived by EWL must be correct, and the X-ray radiation must be produced by a mechanism other than simple accretion onto a degenerate star. If simple accretion is responsible for the observed X-ray flux, then the distance is ≤ 3 kpc and the absolute magnitude is at least 3 magnitudes fainter than expected on the basis of A0620-00 being a typical recurrent nova. Hopefully this conflict of characteristics can soon be resolved.

I should like to thank the National Science Foundation for supporting this research. Lola J. Eachus, E. L. Wright and K. Brecher all contributed to the content of this presentation, and I am grateful to them.

REFERENCES

- Allen, C. W. 1973, Astrophysical Quantities, 3rd ed. (London: Athlone).
- Arp, H. C. 1956, Astron. J., 61, 15.
- Boley, F. and Wolfson, R. 1975, IAU Circ., No. 2819.
- Brecher, K. 1975, private communication.
- Eachus, L. J. 1975, IAU Circ., No. 2819.
- Eachus, L. J., Wright, E. L. and Liller, W. 1975, Ap. J. (Letters), January 1976.
- Gull, T. 1975, IAU Circ., No. 2819.
- Henize, K. G. and Liller, W. 1975, Ap. J., 200, 694.
- Kukarkin, B. V. and Parenago, P. P. 1934, Peremennye Zvesdy, 4, 251.
- McLaughlin, D. B. 1960, Stellar Atmospheres, ed. J. L. Greenstein (Chicago: Univ. of Chicago), p. 605.
- Payne-Gaposchkin, C. 1964, The Galactic Novae (New York: Dover).

TABLE 1

PROPERTIES OF RECURRENT NOVAE

Name	Rate of Fading	M_{\max}	Δ_m	Period
U Sco	0.67 mag/day	-7.6	8.7	37 yr
T Cor B	0.52	-8.1	8.5	79
RS Oph	0.30	-9.5	7.3	35
WZ Sco	0.10	-7.1	8.6	32
V1017 Sgr	0.034	-6.4	7.0	17
T Pyx	0.032	-6.4	6.8	18

A0620-00	0.011	-5.9	8.5	58

A PERIODIC BRIGHTNESS VARIATION OF THE OPTICAL
COUNTERPART OF AO620-00

H.W.Duerbeck

Universitäts-Sternwarte Bonn, F.R.G., and
European Southern Observatory, La Silla, Chile

K.Walter

Astronomisches Institut der Universität Tübingen, F.R.G.,
and European Southern Observatory, La Silla, Chile

(presented by H.Mauder)

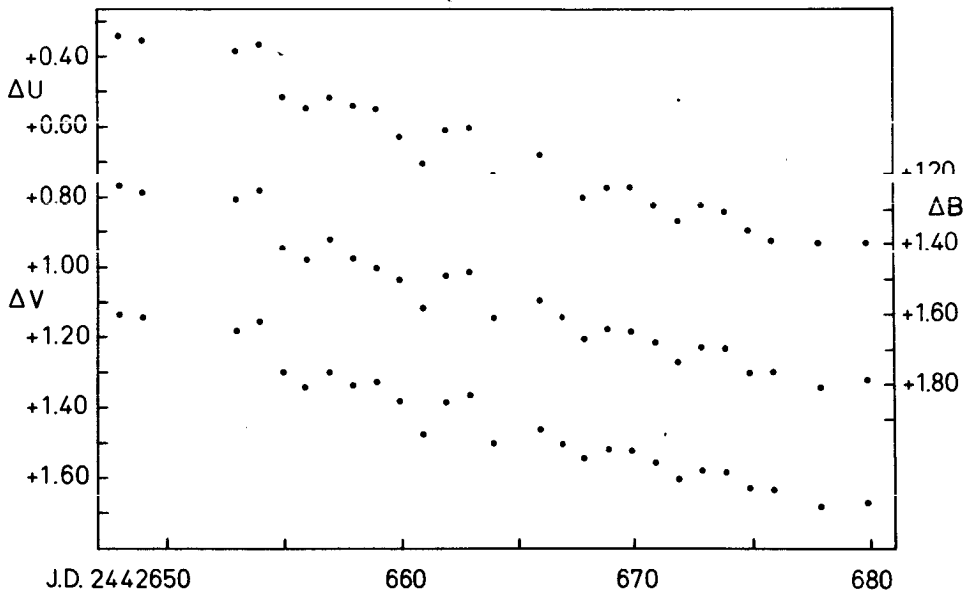
Immediately after Boley and Wolfson's discovery of an 11 magnitude star near the position of the transient X-ray source AO620-00, we started observations with the 50 cm telescope equipped with a single channel UBV photometer of the European Southern Observatory in Chile.

During an observing run of 33 nights, 27 nights were suitable for photometric observations. The 27 data points in figure 1 represent means of 2 to 6 individual measurements of the magnitude differences between the variable and the comparison star BD -O⁰1275. The brightness of this star was found to be $V = 10^m.00$, $B-V = + 0^m.13$, $U-B = + 0^m.03$.

The most striking feature of the light curves is the fairly rapid decline of approximately $0^m.5$ in 1 month, superimposed by semi-periodic brightness variations with a mean period of 4.0 ± 0.3 days, and amplitudes decreasing from $0^m.10$ to $0^m.05$. This phenomenon closely resembles the behavior of some novae during the transition stage. (A $4/3$ day period cannot be excluded, because the daily observations were obtained at about the same hour of the night).

Equally remarkable is the strong U brightness, apparent from $U-B = - 0^m.74$ as compared to $B-V = + 0^m.25$. The colour indices remained fairly constant with an increase of only $0^m.01 / 10$ days.

A spectrogram of the star was obtained on September 24, 1975 with the 1 m telescope and a Cassegrain spectrograph of ESO. The dispersion is 86 \AA mm^{-1} . The most noticeable features are two very broad weak emissions identified with He II 4686 and C III 4650, N III 4640. These and the appearance of the continuum suggest a very hot star.



Spectroscopic Observations of the Candidate Star Coincident

with A0620-00.

Theodore P. Snow, Jr.
and
Donald G. York
Princeton University Observatory

Theodore R. Gull
Lockheed Electronics Co., Inc.

and
Lyndon B. Johnson Space Center

Several spectra of the optical object identified with the X-ray flare source A0620-00 were obtained at 5 \AA min^{-1} with the cassegrain echelle spectrograph on the 4 m Mayall telescope at Kitt Peak National Observatory. The energy distribution of the source between 4250 and 7400 \AA was derived by comparison with spectra of ι Ori obtained with the same instrumentation, and was dereddened for $E(B-V) = 0^m.9$, derived on the basis of the strength of the diffuse interstellar band at 5780 \AA . The flux distribution resembles that of an O-star, with a possible ultraviolet excess. The luminosity of the object between 4250 and 7400 \AA is roughly $5 \times 10^{35} \text{ erg s}^{-1}$, if its distance is 2 kpc which is the value roughly estimated from the velocities and strengths of the interstellar Na I D lines. No stellar lines are seen in the spectra, and the upper limits on the Balmer and He II lines are quite inconsistent with the strengths expected for O-stars. The data are generally consistent with an interpretation that the object is a slow nova, although its absolute magnitude is probably fainter than is usually found for objects in this class, and the apparent high temperature and lack of absorption spectrum are somewhat unusual as well.

MEASUREMENTS OF A0620-00 WITH ANS

A.C. Brinkman, J. Heise, A.J.F. den Boggende,
R. Mewe, E. Gronenschild, H. Schrijver
Space Research Laboratory
Utrecht, Holland

ABSTRACT

The Astronomical Netherlands Satellite (ANS) observed A0620-00 from September 27 until October 3. About fifty measurements were taken in spectral and high time resolution mode. A preliminary light curve has been made and the spectral parameters have been determined.

INTRODUCTION

The medium energy (1-8 keV) X-ray detector (Brinkman et al., 1974, Boggende et al., 1975) on board ANS, has observed A0620-00 from September 27 until October 3, 1975. Only real-time data has been available to us so far. Most measurements were taken in the spectral mode (7 energy channels between 1 and 8 keV), some in the high time resolution mode (time resolution of .125 seconds); no data from the pulsar mode (1 milli-second resolution) is available yet.

INTENSITY AND SPECTRAL MEASUREMENTS

The intensity curve as a function of time is given in figure 1. The units along the vertical axis are ANS-counts per second. The statistical one sigma error bars are far smaller than the size of the dots. The uncertainties are dominated by systematic effects. Each data point represents a measurement of typically five minutes. A countrate of 1000 ANS-counts per second is about 1.5 times the intensity of SCO X-1. (SCO X-1 was measured with this detector on August 30, 1975, the countrate observed was 645 c/s).

Although these measurements were taken when the intensity on a long term time-scale was decaying, see review by Dr. Willmore, it is interesting to note that on October 1 the intensity increased. The daily averages are given in table 1. On a time-scale of hours, the intensity varies as much as 20%. Power density spectra have been made to search for periodicities. Five stretches of data about 550 seconds each were used. No indication of periods between .25 and 100 seconds were found. The data has been fitted to photon number spectra of exponential, thermal bremsstrahlung (exponential with energy dependant gaunt factor), power law and black-body. The simple exponential

gives the best fit to the data, the reduced χ^2 is 2 to 4. Thermal bremsstrahlung is nearly equally acceptable. The parameters are

exponential	$kT = 1.0 \pm .05$	$N_H = (5 \pm 1) \times 10^{21}$
bremsstrahlung	$kT = 1.2 \pm .05$	$N_H = (5 \pm 1) \times 10^{21}$
power	$\alpha = 4.2$	$N_H = (1 \pm .5) \times 10^{22}$

The fit to the power law is quite bad, reduced $\chi^2 = 10$, the parameter values have been given only for purpose of comparison with other observations. The fit to a black-body spectrum gave no acceptable solution. No spectral changes were seen over the five day observing period.

REFERENCES

- Brinkman, A.C., Heise, J., de Jager, C. 1974, Philips Tech. Rev. 34, 43.
- Den Boggende, A.J.F., Lafleur, H.T.J.A. 1975, I.E.E.E. Trans. on Nucl. Sci. 22, 555.

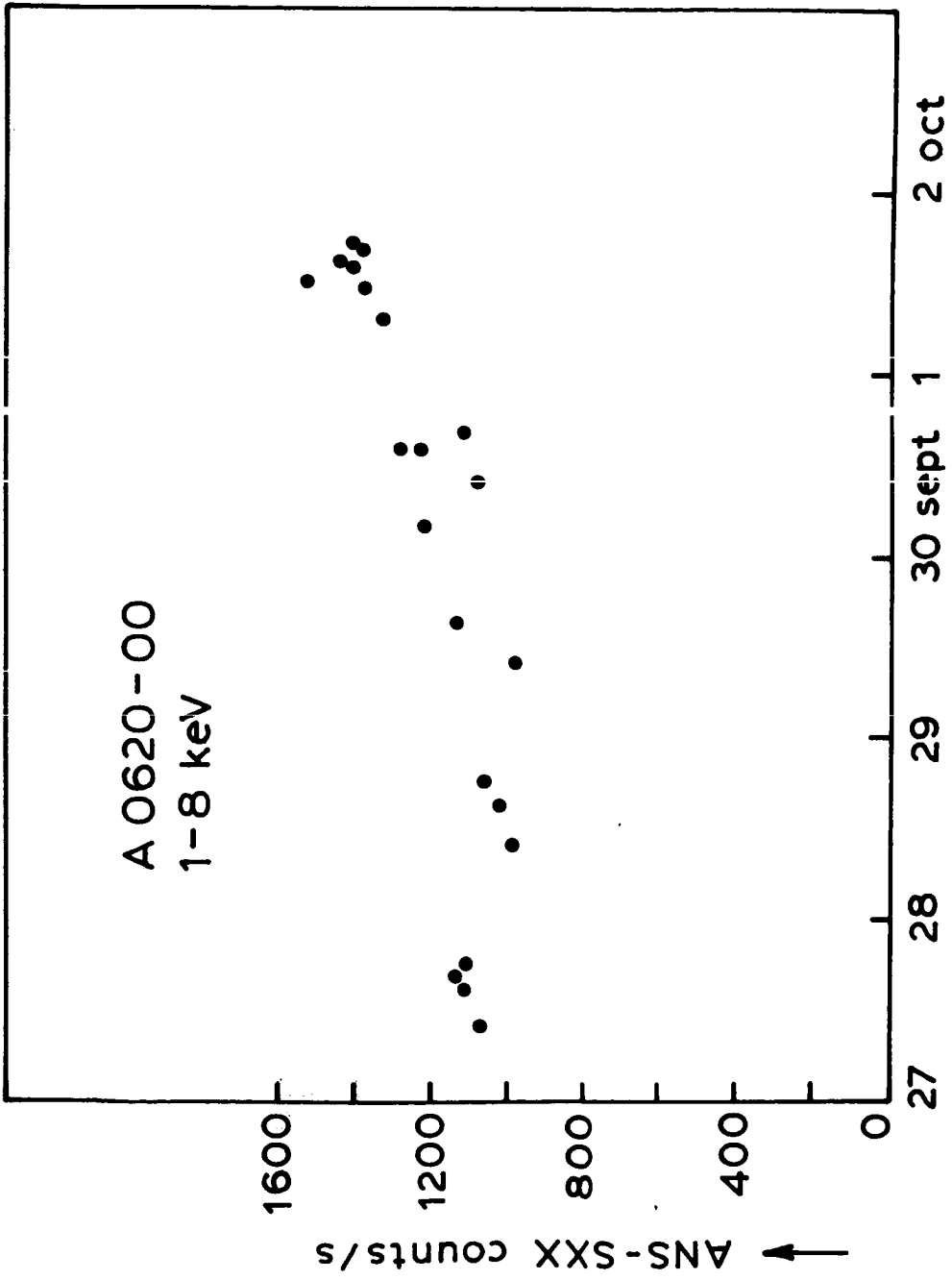


Figure 1 - Intensity of A0620-00 as a function of time.

Table 1
Daily A0620 Measurement Averages

SUMMARY A0620 - 00		1 - 8 KEV		PRELIMINARY ANS - DATA	
DATE	27/09	28/09	29/09	30/09	01/10
INTENSITY C/S	1113 ± 10	1004 ± 10	1053 ± 10	1188 ± 10	1410 ± 10
SPECTRUM : BEST FIT WITH EXPONENTIAL					
$N(E) \propto e^{-\frac{E}{KT}} N_H$ $\text{PHOTONS CM}^{-2} \text{ SEC}^{-1} \text{ KEV}^{-1}$					
$KT = 1.0 \pm .05$ $N_H = (5 \pm 1) \times 10^{21}$					

A STUDY OF A0620-00 IN THE ULTRAVIOLET

Chi-Chao Wu, J. W. G. Aalders, R. J. van Duinen, D. Kester and P. R. Wesselius
Kapteyn Astronomical Institute, Dept. of Space Research
University of Groningen

ABSTRACT

A0620-00 was observed 7 times with the ultraviolet instrument on board the ANS in the period 1975 September 28.91-30.52 UT. Variations of semi-amplitude 0.2 mag are present in all five wavelength bands. These variations seem to be correlated at different wavelengths, and the amplitude at 3300, 2500 and 2200 angstroms seems to be slightly larger than that at 1800 and 1550 angstroms. The observed spectrum is de-reddened until a smooth energy distribution is obtained between 1800 and 2500 angstroms, the amount of reddening correction required is $E(B-V) = 0.39 \pm 0.02$ (for more detail concerning the ANS instrument and the procedure for estimating the amount of interstellar reddening, see the discussion of Cygnus X-1 by Wu et al. in this proceeding). This de-reddened spectrum matches perfectly with a blackbody curve of 28000 degree Kelvin temperature. Furthermore, this energy distribution of A0620-00 agrees very well with those of three dwarf novae (U Geminorum, VW Hydri and SU Ursae Majoris) at minimum. Probably, A0620-00 is a thermal source with the flux between 1550 and 3300 angstroms comes primarily from an optically thick accretion disk.

INFRARED MEASUREMENTS OF NOVA MONOCEROTIS 1975 (A0620-00)

S. G. Kleinmann*
 Massachusetts Institute of Technology
 Cambridge, Mass.

R. R. Joyce and R. W. Capps
 Kitt Peak National Observatory
 Tucson, Arizona

ABSTRACT

An infrared source at the location of the transient X-ray source A0620-00 was detected and measured on 26.5 and 29.5 August 1975 with the 50-inch reflector at Kitt Peak National Observatory. A preliminary summary of the results is presented here.

We observed infrared emission from A0620-00 in the J, H, K, and L bands, which correspond respectively to wavelengths of 1.25, 1.65, 2.2 and 3.45 microns. In addition, an upper limit was set at 4.6 microns. The results are presented in Table 1.

TABLE 1

<u>Date (U.T.)</u>	<u>Wavelength</u>	<u>Magnitude</u>	<u>Average</u>
26.5 Aug	1.25 μ	10.68	10.72 \pm 0.04
29.5	1.25 μ	10.75	
26.5	1.65 μ	10.49	10.53 \pm 0.06
29.5	1.65 μ	10.53	
29.5	1.65 μ	10.56	
26.5	2.2 μ	10.18	10.24 \pm 0.07
29.5	2.2 μ	10.30	
26.5	3.45 μ	9.79	9.90 $^{+0.28}$ $^{-0.19}$
29.5	3.45 μ	10.00	
26.5	4.6 μ	>6.70	(3 σ upper limit)
29.5	4.6 μ	>6.49	(3 σ upper limit)

The tabulated uncertainties in magnitude are one-sigma statistical values. We have averaged the measurements taken on the two dates as the decay of the infrared light curve is not very strong.

* Visiting Astronomer, Kitt Peak National Observatory.

It should be noted that the total uncertainty (which includes up to fifteen percent uncertainty in absolute calibration) in any measurement may be as large as four times the tabulated standard deviation.

In Figure 1, the curve drawn through these infrared measurements assumes that

$$(F_{\nu})_{\text{intrinsic}} \propto \nu^2$$

and

$$A_{\nu} = 4.2 \text{ magnitudes.}$$

The latter quantity is the maximum visual extinction that is consistent with the assumed character of the intrinsic F and the one-standard deviation error in the J and K data. A better estimate of the extinction can be obtained by combining the infrared data with optical data.

NOTE: The authors of the above paper were unable to attend the symposium. The paper is based on rough notes that they kindly sent to the session chairman who prepared this manuscript for the proceedings and accepts responsibility for any errors that may have inadvertently been introduced. Some of the tabulated quantities have been rounded off during this preparation.

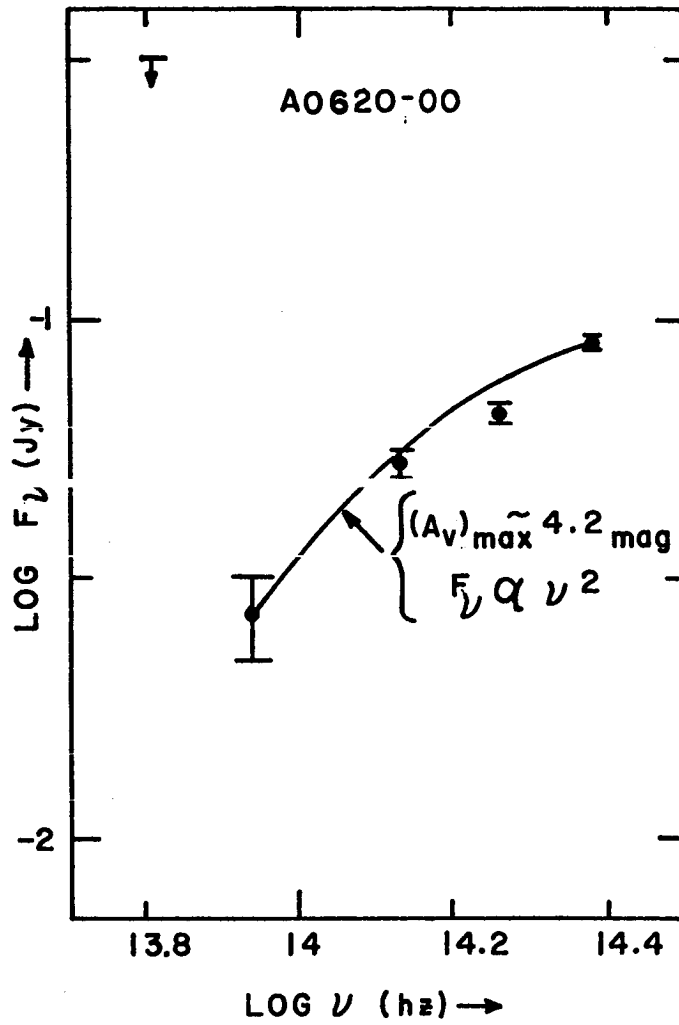


Figure 1. Infrared Measurements

COLLIDING SHELLS MODEL

K. Brecher and P. Morrison

Department of Physics and Center for Space Research
Massachusetts Institute of Technology, Cambridge, Mass. 02139

Abstract

We suggest that there are two distinct classes of transient x-ray sources: (I) pulsating x-ray sources showing hard x-ray spectra such as A1118-61 and A0535+26, probably powered by sporadic infall of matter onto rapidly-rotating magnetized collapsed objects similar to those underlying the non-transient sources Her X-1 and Cen X-3, and (II) unpulsed soft-spectrum sources, such as A0620-00 (Nova Monocerotis 1975), Cen X-2, Cen X-4 and the Lupus transient source, whose radiation probably arises from thermal bremsstrahlung by gas previously ejected from the system, resembling rather the continuously emitting source Sco X-1. We suggest that Class II transient x-ray sources are the result of the shock-heating of pre-existing optically thin circumstellar gas which surrounds mass exchanging binary systems. In this picture, only rapid mass exchange binaries ($dM/dt \gtrsim 10^{-6} M_{\odot} \text{ yr}^{-1}$) should produce Class II transient x-ray sources at currently detectable levels. Recurrent novae, such as WZ Sge, or wind-driven rather than Roche-overflow binary systems containing white dwarfs, are likely candidate sources. Such a model for Class II sources accounts in a natural way for the great difference in the x-ray to optical luminosity ratio of the 1975 Cygnus and Monoceros novae; the relative radio, optical and x-ray fluxes, and the absence of conspicuous absorption features in the optical spectrum of the Monoceros nova; the time course of the x-ray source intensity; the total radiated flux; and the yearly rate of such events. Other properties of both Class I and Class II transient x-ray sources are considered.

THE NATURE OF THE X-RAY NOVA A0620-00

A. S. Endal* and E. J. Devinney †
Laboratory for Optical Astronomy
NASA/Goddard Space Flight Center
Greenbelt, Maryland 20771

and
S. Sofia ‡
NASA Headquarters
Washington, D. C.

ABSTRACT

We present a model for the X-ray nova A0620-00. Identification with a nova can be ruled out on two counts. A binary consisting of a late-type subgiant near the Roche lobe, irradiated by an accreting compact companion is shown, however, to be in agreement with all known observations, including new data presented at this Symposium. Photometry of the optical object should be pursued since variability on an approximately eight hour period is expected.

THE OBSERVATIONS AND SOME IMPLICATIONS

The transient X-ray source A0620-00 was discovered on 3 August 1975 by the Ariel 5 detectors. Subsequently, transient optical and radio radiation was detected at the X-ray position. Even before the Symposium, the observations seemed adequate to determine a viable model (Endal, Devinney and Sofia 1975). New data presented at the Symposium supports the proposed model and makes possible further elaboration. We first find it useful to give a summary of the relevant observational facts.

X-ray

Abrupt rise to 20,000 UHURU counts and decay with e-folding time $\sim 27^d$. Initially hard, then softening spectrum.

* NAS-NRC Postdoctoral Research Associate

† NAS-NRC Senior Research Associate

‡ On leave from the Department of Astronomy, University of South Florida

Optical

Abrupt rise to $\sim 11^m.2$, decay with e-folding time $\sim 69^d$.
Recurrent: in 1917, $m > 13$ for 75 to 150 days.
No intrinsic polarization.
Spectrum featureless but for interstellar lines.
Pre-outburst object red and $m_B \lesssim 18$.

Radio

Rapidly decaying early radio source with flat spectrum.

In the data presented one can find photometric behavior resembling that of the classical recurrent nova. The optical amplitude and time interval between outbursts does fit the Kukarkin-Parenago relation. The typical recurrent nova has $M_v \sim -7.5$ at maximum and this would then imply a distance of 5.7 kpc (with absorption at 1 mag/kpc). The pre-outburst absolute magnitude would then be near zero. Liller has fit the 1917 outburst to the absolute magnitude-decay rate data for novae (McLaughlin 1960). (However, the conversion from mag/day decay rate quoted by Liller to time for a three magnitude decay does not seem correct. t_3 should have been 300^d leading again to a distance of 4-5 kpc, rather than 11 kpc.) The X-ray luminosity at these distances would have the corresponding large value of $L_x \sim 1.5 \times 10^{39}$ ergs/second.

We believe, however, that the nature of the optical spectrum rules out identifying A0620-00 as a classical recurrent nova. According to McLaughlin (1960) dean of nova experts, "All novae near maximum have strong, shortward displaced absorption spectra---". (Of course, in the quiescent state novae do show a continuous, and more or less featureless spectrum). Later on, broad emission appears as well, leading to the classical signature of an expanding shell. Such a shell, thick enough to produce the observed broad features ought to be quite absorptive for soft X-rays (as was well demonstrated by Nova Cygni). Copious emission of X-rays is further incompatible with the current theoretical picture of the nova mechanism (Starrfield, et al. 1974). Spectra taken by Oke and Greenstein (1975) and by Peterson, et al. (1975) are not nova-like in character. An image-tube spectrogram taken as recently as UT0700 Nov. 12, by one of us (EJD) shows no evidence of nova-like features. Line identifications for the few observed features are given for the 4-meter Anglo-Australian spectra of Peterson, et al. That the lines are not mentioned as being highly displaced from their rest positions is noteworthy. We conclude that the optical radiation does not arise in an expanding shell.

THE PROPOSED MODEL

We are led to consideration of accretion as the mechanism for X-ray production. The Eddington limit will then regulate the flux of X-rays. For reasons noted below, we consider the mass of the compact member to be $M_x \lesssim 1.4M_\odot$. The corresponding Eddington limited flux is $L_x \lesssim 10^{38}$ ergs/second, and with the observed flux giving $L_x = 4.5 \times 10^{37} R^2$ (R in kpc), we must have $R \lesssim 1.5$ kpc. This limit is confirmed, since the A0620-00 UV flux observed by ANS (Netherlands Astronomical Satellite) appears properly dereddened at ~ 1 kpc (Wu 1975). At this distance the objects' flux distribution has neither a bump nor a dip in the spectral region of anomalous interstellar absorption, located at 2200Å. At a distance of 1.5 kpc, the pre-outburst apparent magnitude $m_B \sim 18$ on the Palomar Sky Survey Plates immediately requires it to have $M_B \geq 5.6$, for 1 mag/kpc absorption. The PSS O and E plates further indicate an intrinsic color not earlier than that corresponding to about K3. Thus, the companion is a late type star of sub-giant or lower luminosity. The ability to rule out a giant companion, in particular, has interesting consequences, for Warner (1975) considers it very likely that recurrent novae all have giant companions.

The low mass inferred for the companion red star suggests to us that the compact star is a white dwarf, since formation of a neutron star would have disrupted the system by the Blaauw mechanism. Furthermore, it seems other than coincidental that the X-ray flux observed is that appropriate to white dwarf accretion, Eddington limited. (Note that the distance estimate from ANS is independent of mechanisms or assumptions regarding X-ray production.)

The red companion must trigger the repetitive outbursts, requiring that it be very close to its inner critical Roche surface. The behavior required here, in fact, is reminiscent of the late-type sub-giant secondaries of Algol-like close binaries. These stars lose mass due to some instability of their convective envelopes, providing accreting material to the companion. Not only is the time interval (58 yrs) between outburst easily accommodated in this picture, but the mass lost by the sub-giant is large enough to power the X-rays for the needed time. For example, in Biermann and Hall's study of μ Cephei (Biermann and Hall, 1973) there were two period changes in a 50 year interval for which the implied mass loss rates were $10^{-4} M_\odot/\text{yr}$. On the other hand, a $1M_\odot$ white dwarf requires only $10^{-5} M_\odot/\text{yr}$ to reach the Eddington limit; i.e., Algol-type mass transfer is sufficient. Transfer of material from the companion would form a disk about the compact member. Accretion of material by it from this disk would power the X-rays. The model leads to the

obvious speculation that the X-ray-precursor (Willmore, 1975) might be due to an initial infall of low angular momentum material directly onto the compact companion. Again, it is a curious fact that radio emission noted early in the history of the outburst had a flat spectrum, like that noted for the binary star radio sources, which are well represented with sub-giant active members. Is the seat of radio emission in A0620-00 then the late-type star itself?

COMPUTATIONS AND PREDICTIONS

We will now show that consideration of the X-ray irradiation of the K-star will yield results in accord with the temperature and spectrum of the optical radiation, and with the X-ray and optical e-folding decay times.

The total power available to the K-sub-giant depends only on the fraction of 4π steradians subtended from the x-source, or $L_A = (\Omega/4\pi) L_x$. We also have, for $0.1 \leq M_{SG}/M_x \leq 1.0$, $0.12 \leq \Omega \leq 0.44$. Since $L_x = 4.5 \times 10^{37} R^2$ erg/second, we have for the available power:

$$L_A = 3.6 \times 10^{36} \Omega R^2 \text{ erg/second.}$$

The X-radiation will be absorbed by the K-star, thermalized and re-radiated. The effective temperature of the re-radiated energy will be given by

$$T_e = 3.2 \times 10^4 (R/r)^{1/2} (\Omega/f)^{1/4} \text{ } ^\circ\text{K.}$$

Here r is the radius, in solar units, of the K star and f is the fraction of the total surface area heated by the X-ray source. If we take $R = 1.5 \text{ kpc}$, $r_{SG} = 1.5 R_\odot$ and $\Omega = 0.44$, we have for $f = 0.5$, $T_e \approx 30,000 \text{ } ^\circ\text{K}$. Since the visual magnitude during the outburst reached $11^m.2$, the above temperature with a typical O-star bolometric correction yields $M_{BOL} = -8.3$ with corresponding luminosity

$$L_{OPT} = 1.47 \times 10^{36} R^2 \text{ erg/second.}$$

Thus the X-rays can power the observed radiation. As was noted in our paper referred to earlier, the line-free nature of the optical spectrum is that expected for a stellar atmosphere heated by a strong soft X-ray flux. The ionization balance is then dominated by the X-ray flux yielding a very high ionization temperature and an emission dominated by continuous mechanisms (free-free and recombination) as is consistent with the featureless optical spectrum. The fourth power of the effective temperature, T_e^4 , of the emitting region of the late-type star is directly proportional to the irradiating X-ray flux, while the optical flux, say at 4330\AA (B effective wavelength for O-stars) is assumed given by a Planck function. We know that the e-folding time for the X-rays (total flux) is ~ 27 days and for the $\sim \lambda 4330$ flux it is ~ 69 days. Within our single temperature

parametrization of the optical radiation (which could be regarded as an average temperature) there can be only one initial temperature T_0 which yields such decay times. At $\lambda 4330$ we have,

$$B_{4330} = B_0 e^{-t/69},$$

while for the total flux we have

$$L_x = L_{x0} e^{-t/27}, \text{ or } T_e = T_{e0} e^{-t/4 \times 27} \\ T_{e0} e^{-t/108}.$$

With

$$\partial \ln T_e / \partial t = -1/108; \partial \ln B_{4330} / \partial t = -1/69,$$

then

$$\partial \ln B_{4330} / \partial \ln T_e = 1.57.$$

From Planck's law

$$f(T_4) = \frac{\partial \ln B_{4330}}{\partial \ln T_e} = \frac{3.33}{T_4} [1 - e^{-3.33/T_4}]^{-1} = 1.57$$

$$(T_4 = 10^{-4} T_e)$$

We thus obtain the following table:

T_4	$f(T_4)$
3.2	1.61
3.4	1.57
3.5	1.55
4.0	1.47

An average initial temperature for the emitting region of about 34,000 is inferred consistent with our earlier derived temperature. According to Wu (1975) the dereddened UV flux was that of a 28,000 K black body. We should not, however, place too much confidence in the agreement of these figures, due to the unsophisticated treatment of the irradiated region. Furthermore, the actual optical thickness of the radiating region is unknown, so that the emergent spectrum, while continuous, may not be Planckian.

We expect that A0620-00 is a low mass ($\sim 2M_\odot$) close binary system, so that orbital period of a fraction of a day would be expected. The orbital inclination is expected to be low, for the observed soft X-ray spectrum suggests little absorption by the accretion disk. In optical data then,

expected periodic light changes due to the heated region of the sub-giant may be small. The optical observations reported by Duerbeck and Walter (1975) are noted as showing evidence of variation of a possibly periodic nature.

REFERENCES

- Bierman, P. and Hall, D. S. 1973, Astr. and Ap., 27, 249.
- Duerbeck, H. and Walter, K. 1975, preprint in Workshop Papers for a Symposium on X-ray Binaries, ed. Y. Kondo and E. Boldt. (Goddard SFC Doc. #-660-75-285).
- Endal, A., Devinney, E., and Sofia, S. 1975, Submitted to Ap. J. (Letters).
- Liller, W. 1975, A0620-00 Session Communication, this Symposium.
- McLaughlin, D. B. 1960, in Stellar Atmospheres, ed. J. L. Greenstein (Chicago: University of Chicago Press), p. 585.
- Oke, J. B. and Greenstein, J. L. 1975, private communication.
- Peterson, B., Jauncey, D., and Wright, A. E. 1975, IAU Circ. #2837.
- Warner, B. 1975, paper at IAU Symposium #73 on Structure and Evolution of Close Binary Systems, Cambridge, UK, 27-31 July.
- Wu, C.-C. 1975, A0620-00 Session Communication, this Symposium.

A0620-00

Discussion

A. P. Cowley:

An alternate model to that discussed during this meeting (i.e., white dwarf + low-mass main sequence star) is one in which the binary system contains a red giant as its non-degenerate member.

The fact that the observed B-V color (about +2 mag) of A0620-00 at minimum light is so red suggests that one might primarily be observing the non-degenerate star at that time. If that is the case, then the amplitude of the nova outburst (observed as about 8 magnitudes) can only be considered as a lower limit on the full range, and thus one should be cautious about using this amplitude to obtain other parameters of the system.

At this meeting, we heard reported the photometric observations of Duerbeck and Walter who find a possible 4 day modulation. We know of several novae which have late-type giants as companions of their degenerate members. GK Persei, for example, contains a K-giant and has an orbital period of about 1.9 days. T CrB has an M-giant companion and its orbital period is near 225 days. Thus one expects periods of several days or more, as opposed to fractions of a day.

This hypothesis predicts that the late-type giant should be observable spectroscopically when the brightness of the source has dropped by about three magnitudes from maximum. Finally, even now, some of the infrared luminosity might arise from this proposed cool giant.

N. V. Vidal to S. Holt:

Since at some stage the shell is developing (emission lines in the optical region) it would be interesting to follow the position of the low energy cut off in the X-ray spectrum.

INTRODUCTION TO CYG X-1 X-RAY PANEL

Elihu Boldt
NASA/Goddard Space Flight Center
Greenbelt, Maryland 20771

STATUS OF X-RAY OBSERVATIONS:

SPECTRAL STATES

- 1) Stable (years)
 $dL/d(h\nu) \approx 10^{36} (h\nu)^{-0.6} \text{ ergs cm}^{-2} \text{ s}^{-1} \text{ keV}^{-1}$ Added soft component?
 $L \approx 10^{37} \text{ ergs/s}$ (2-40 keV; 2.5 kpc) High energy cut-off?
- 2) Unstable (months) One component?

TRANSITIONS

Anti-correlation: soft and hard intensities Two Components?
Radio association Correlation to radio (phase, intensity, spectrum)?

PERIODIC BEHAVIOR

Absorption dips (5.6 days) Phase stability?
 Multiplicity?
 Preludes to transition?
 Smooth periodicities?

FLUCTUATIONS

Shot-noise behavior: Entire emission shot-noise?
 ~20 events/s (stable state)
 >100 events/s (unstable state)
Basic underlying event: Characteristics invariant?
 Energy $\approx 10^{36}$ ergs. Duration ≤ 0.5 s Duration independent of (h ν)?

BURSTS

Duration $\approx 10^{-3}$ s Rate $\approx 10^{-1} \text{ s}^{-1}$ Absence of substructure?
 Random?
Energy emitted $\approx 10^{35}$ ergs/burst Spectral difference?

CYG X-1 X-RAY PANEL SUMMARY

Elihu Boldt
NASA/Goddard Space Flight Center
Greenbelt, Maryland 20771

INTRODUCTION

In the introduction to this panel I briefly summarized, in tabular form, my own evaluation of the status of X-ray observations. Along with several general aspects of the X-ray emission that appear to be quite well established, I indicated some rather specific questions that present themselves when we try to piece together all the observed phenomena into a coherent phenomenological picture. In many instances this involved more data and/or analysis than was available in the published literature prior to this meeting, and the purpose of listing such questions as an introduction to this panel was to provide a framework for extracting some of the answers I expected from the more recent work to be reported here. Following the format of the introduction, I have outlined an updated status of X-ray observations based upon the discussions in this panel. References to panel members by name are to their papers in this proceedings.

SPECTRAL STATES

Although Cyg X-1 is notorious for spectral variability, largely due to the pioneering UHURU satellite monitoring of the unstable behavior during the few months preceding the transition of March - April 1971, we have now heard of the increasing evidence for regularity. Two detailed broadband (2 - 40 keV) rocket-borne experiments (Rothschild et al., this symposium) separated by a year (October 1973 - October 1974) obtained identical power-law spectra (energy spectral index $\alpha = 0.55$). Further long-term monitoring over a narrow band (3 - 6 keV) since October 1974 with Ariel 5 (Holt et al., this symposium) shows that, until the transient event of April-May 1975, Cyg X-1 was one of the most stable strong sources in the sky, exceeded in stability only by the Crab Nebula. However, balloon-borne experiments (Matteson et al., this symposium) prior to 1973 show that the hard X-ray behavior (well above 20 keV) varies considerably, even as regards high energy cut-off, during times when the lower energy spectrum was likely to have been stable.

An examination of data prior to the transition of March-April 1971 reveals a relatively stationary spectral intensity at about 8 keV (Matteson et al., this symposium) over wide variations of energy spectral index (i.e. $\alpha = 1/2 - 3$). When the overall spectrum (2 - 200 keV) was steep, such as in September 1970, no high energy cut-off was detected. The suggestion by Matteson (this symposium) that a single power-law component of variable index may be sufficient for describing most spectral changes has important theoretical implications for the emission model involving soft photon Comptonization in a hot accretion disk (Eardley, this symposium). The anticipated spectral component representing the soft photon reservoir may only rarely, if ever, exhibit itself above about 2 keV.

TRANSITIONS

It has become apparent from this panel that there are distinctions to be made between transitions and transient events. The event of March-April 1971, when the 2-20 keV spectrum stabilized and the radio source intensity increased to observability, was the clearest example to date of a transition and may have been the only one. While the event of April-May 1975 may have signaled the onset of increased transient behavior (Holt et al., this symposium), such as the subsequent "flare" of September 1975 (Canizares et al., this symposium), the radio intensity exhibited activity at an increased level rather than the decrease to be expected for a real transition back to the state that existed immediately prior to March-April 1971.

PERIODIC BEHAVIOR

Earlier indications of X-ray variations associated with the 5.6 day binary period have been clarified and considerably extended. The classical absorption dips seen with the OAO-Copernicus and OSO-7 satellites do occur preferentially near to superior conjunction, but with considerable scatter involving no obvious systematic trend (Murdin, this symposium). Observations with the APO satellite (Raisigault et al., this symposium) suggest that the phenomenon of absorption dips may be a rather permanent aspect of the Cyg X-1 emission, possibly occurring during every cycle of the binary during some epochs and with a variable complex profile (e.g. multiplicity). The Ariel 5 monitor (Holt et al., this symposium) shows a pronounced decrement of intensity in the vicinity of superior conjunction by an amount that greatly exceeds that which may be accounted for by the classical absorption dips, even if the complication of multiplicity is introduced. That this modulation increased prior to the large event of April-May 1975 and then possibly disappeared afterwards suggests that further tracking of this effect could provide us with direct evidence for conditions that lead to transient behavior.

Discussions of possible periodicities other than at 5.6 days showed that there was no positive evidence for such, where the periods searched for ranged from a few hours to about a month.

FLUCTUATIONS

On time scales from a fraction of a second to hours, the fluctuations in the intensity for the stable spectral state (at $\sim 2-20$ keV) may be described by shot-noise arising from events of fixed decay time ($\tau \approx 0.5$ s) occurring at an average rate $\lambda \approx 20$ s⁻¹ (Weisskopf, this symposium). Measurements prior to the transition of March-April 1971 indicate that, although λ may vary considerably, the decay time τ to be associated with the basic underlying events remains remarkably invariant and is thereby providing us with a fundamental time constant for the emission process. During the stable state much if not most of the emission arises from such events, independent of photon energy (at least within the band $\sim 2-20$ keV).

Tracking the shot-noise parameters λ and τ on time scales of days has turned up a possible correlation with binary phase (Weisskopf, this symposium) which needs to be pursued further. Direct fluctuations of intensity on such time scales indicate that there may be some pronounced stochastic behavior in addition to the shot-noise discussed for shorter times.

If the bulk of the X-ray emission is shot-noise due to random events at the rate $\lambda \approx 20 \text{ s}^{-1}$, then the energy per event is about 10^{36} ergs. However, this value for the energy depends critically on the fraction of the emission that is shot-noise and could be an order of magnitude less if the shot-noise fraction were as low as 50%.

BURSTS

The millisecond bursts identified in the emission of Cyg X-1 are characterized by an enhanced luminosity that is an order of magnitude greater than average. Of the 13 clearly discernible bursts so far detected in 230 s of observation (Rothschild et al., this symposium), only one indicated submillisecond structure and a spectrum definitely harder than average. The remaining 12 bursts were consistent with an emission process that is homogeneous in time during the millisecond duration and a spectrum somewhat softer than the overall emission, but at a level of statistical significance corresponding to less than 3σ .

It appears that the phenomenon of millisecond bursts might well represent the most precise and telling aspect of the X-ray emission from Cyg X-1. By comparing individually measured events, we are led to consider that, for the most part, they represent a process with sharp characteristics. Each burst carries: 1) a spectrum close to that of the overall Cyg X-1 emission, 2) an energy of about 10^{35} ergs which is likely to be comparable to that of the basic shot-noise event defining the bulk of the fluctuations in emission and 3) a millisecond time constant that might represent an effective "free-fall" for disturbances in the accretion disk. Are these bursts random events? We need more data to decide on potential correlations.

SAS-3 OBSERVATIONS OF AN X-RAY FLARE FROM CYGNUS X-1*

C. R. Canizares, H. Bradt, J. Buff and B. Laufer
Center for Space Research and Department of Physics
Massachusetts Institute of Technology
Cambridge, Massachusetts 02139

ABSTRACT

Preliminary results are presented for the SAS-3 observation of an X-ray flare from Cygnus X-1 in 1975 September. The 1.5-6 keV intensity rose by a factor of four and exhibited variability on several time scales from seconds to hours. The 6-15 keV intensity showed less activity. The event is similar to that observed in May by ANS and Ariel-5, but lasted less than two weeks.

We present preliminary results from a SAS-3 observation of an enhancement in the X-ray flux from Cygnus X-1 which occurred in 1975 September (Primini 1975). The results are based on quick-look data from the long slat collimator experiment collected both while the satellite was spinning and when it was stopped and pointed at Cyg X-1.

Figure 1 shows a history of the 1.5-6 keV X-ray activity of Cyg X-1 from 1975 May to September. The first observations were made shortly after the launch of SAS-3, when the source had just resumed its "low state" following the May enhancement studied by ANS and Ariel-5 (Heise *et al.* 1975, Holt *et al.* 1975, Sanford *et al.* 1975). The X-ray intensity remains roughly constant through the summer months until Sept 6.5 when it begins to rise, eventually reaching a value four times its previous level. The 6-15 keV intensity was more nearly constant throughout the whole period with some indication of variability of about a factor of two.

The data obtained during the enhancement are shown in Figure 2 on an expanded scale. The onset of the event in the 1.5-6 keV band occurs over about one day, as it did during the May enhancement (Holt *et al.* 1975). There is evidence for very large variability during the event with time-scales of hours.

*Supported in part by the National Aeronautics and Space Administration under contract NAS-5-11450. (CSR-P-75-31)

The event is mainly evident in the softer channel, representing an increase in the photon spectral index from ~ 1.8 to ~ 2.6 , but there is also considerable variability in the 6-15 keV channel apparently not directly correlated to the fluctuations at lower energies. The decay of the event is more rapid than the previous one--later SAS-3 observations indicate an overall duration of less than two weeks, whereas the May event lasted a month.

Short time variability was also observed during some of the pointed observations made with the source near maximum intensity. Figure 3 shows raw quick-look plots for two observations separated by about three hours. The first has clear indications of intensity fluctuations with time-scales of 10-100 sec, while the second does not.

The event observed by SAS-3 and reported here is clearly similar to the May event in spectrum and intensity. However, its short duration makes it appear much more like a "flare" caused by some unstable, transient phenomenon than like a metastable "high state" as was suggested by the Uhuru observations (e.g., Boldt 1974). The indication of short-term variability at maximum intensity may bear on the size scale of the region responsible for the enhanced emission (Thorn 1975). Detailed analysis of the data now in hand and of the production data when they are available may help bring new insight into the detailed character of the source.

REFERENCES

- Boldt, E., Holt, S., Rothschild, R., Serlemitsos, P., 1974, presented at International Conference on X-Rays in Space, Calgary, Canada.
- Heise, J., Brinkman, A. C., Schrijver, J., Mewe, R., Den Boggende, A., Gronenschild, E., Parsignault, D., Grindlay, J., Schnopper, H., Schreier, E., Gursky, H., 1975, Nature, 256, 107.
- Holt, S. S., Boldt, E. A., Kaluziński, L. J., Serlemitsos, P. J., 1975, Nature, 256, 108.
- Primini, F., 1975, I.A.U. Cir. No. 2833.
- Sanford, P. W., Ives, J. C., Bell Burnell, S. J., Mason, K. O., 1975, Nature, 256, 110.
- Thorn, K., 1975, private communication.

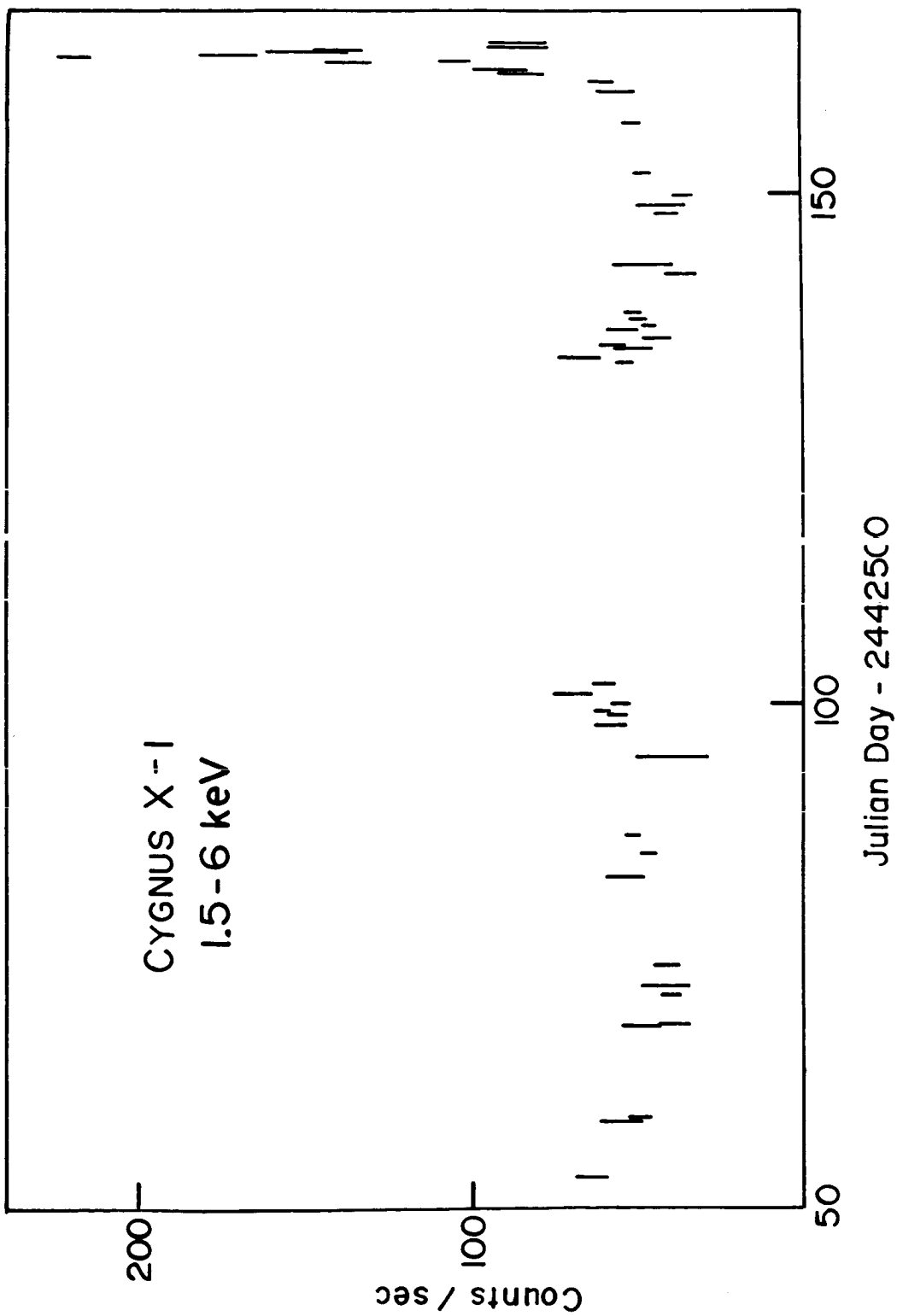


Figure 1. X-ray intensity of Cygnus X-1 vs. time showing the outburst of September 1975. Data were obtained from the slat collimator experiment on SAS-3. The error bars are statistical only. Additional point-to-point systematic uncertainties of ~10-15% may be present.

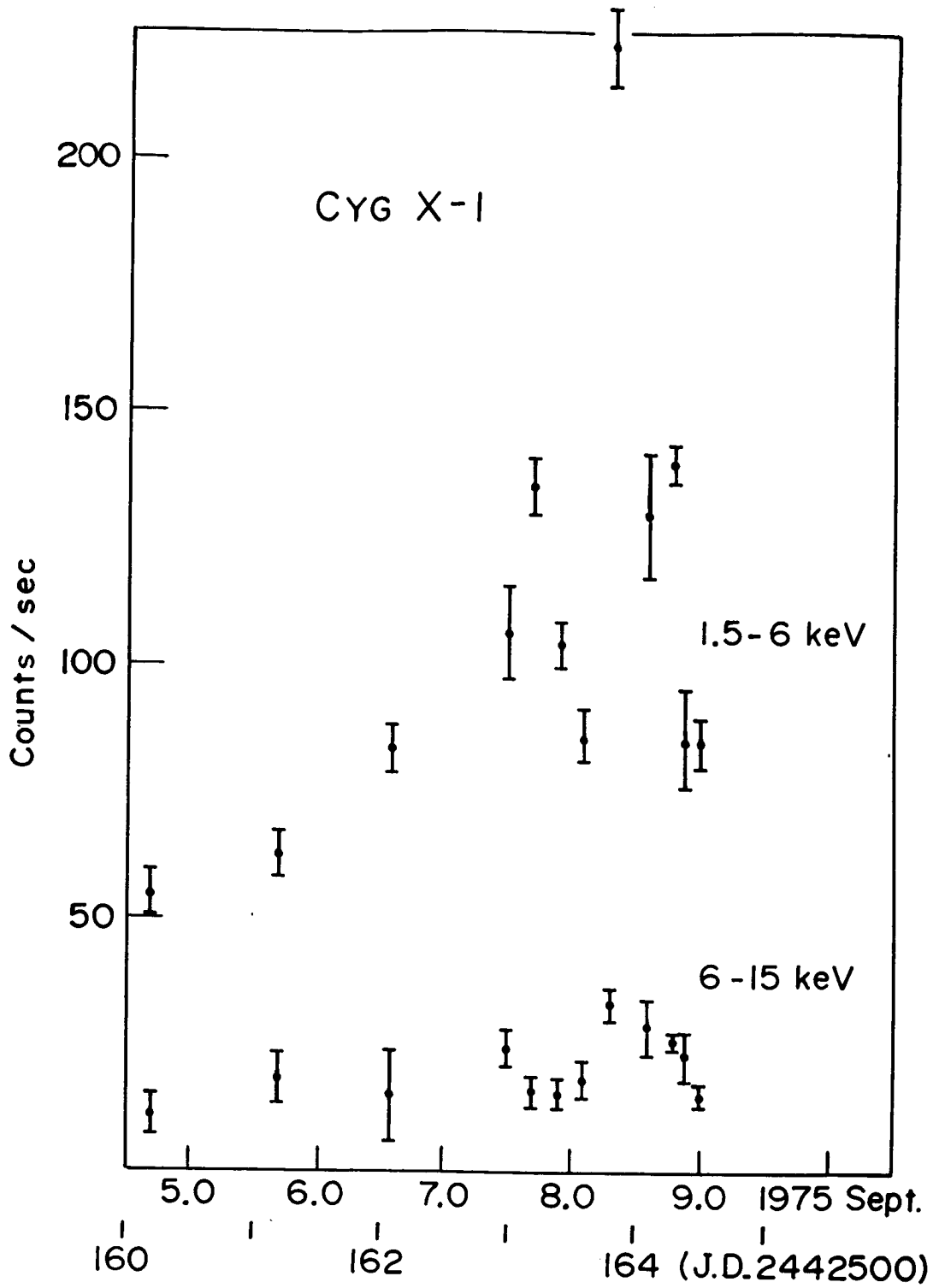


Figure 2. X-ray intensity of Cygnus X-1 during the September outburst for two broad energy channels.

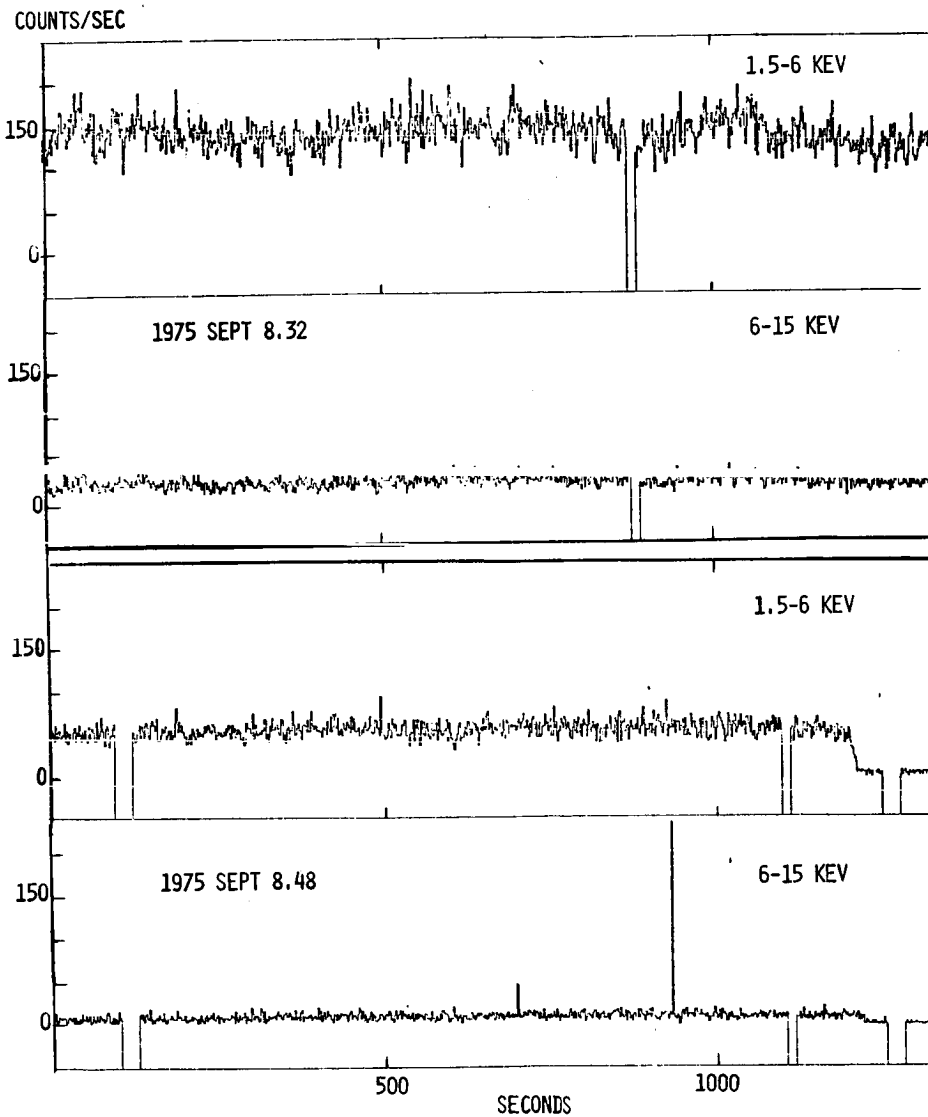


Figure 3. Background subtracted quick-look data from Cygnus X-1 collected during the September outburst. The satellite was pointed steadily at the source during these observations. Data are shown for two broad energy bands and are binned in 1.6 sec intervals. Sudden gaps are due to data dropouts. The decrease at the end of the Sept 8.48 observation is due to Earth occultation of the source.

FORMATION OF HARD X-RAY TAILS

Douglas M. Eardley
Department of Physics
Yale University
New Haven, CT. 06520

ABSTRACT

X-ray observations of Cygnus X-1 have shown a power-law spectrum. I discuss a natural way that this spectrum might arise: Inverse Compton scattering of a soft photon flux in a very hot accretion disk, $kT_e \sim 100$ keV. The slope of the spectrum may vary if source conditions vary.

INTRODUCTION

An optically thick accretion disk around a $10M_\odot$ black hole ought to emit a very soft X-ray spectrum at luminosities of a few times 10^{37} erg s^{-1} , because of the huge emitting area, $\geq 10^5$ km². This difficulty has bedeviled attempts to interpret the remarkably hard observed spectrum of Cyg X-1 (Thorne and Price 1975, Lightman and Shapiro 1975). Recently Lightman, Shapiro and I (Eardley et al. 1975, Shapiro et al. 1975) found a way around this difficulty. We showed that there exists a second, quite different solution to the structural equations for an accretion disk, subject to the same boundary conditions, which can fit at least the "non-flaring" or "low-state" data fairly well (see, e.g., Agrawal et al. 1972, Haymes and Harnden 1970, Frontera and Fuligni 1975). The old, "standard" solution (Pringle and Rees 1972, Shakura and Sunyaev 1973, Novikov and Thorne 1973) tends to be optically thick, geometrically thin in the vertical direction, and cool ($kT_{\text{surface}} \sim 1$ keV); I'll call it the "cool disk". Our new solution consists of a very optically thin, very hot, two-temperature plasma ($kT_e \sim 100$ keV; 300 keV $\leq kT_1 \leq 300$ MeV), and tends to be so geometrically thick that it may be more

of a cloud than a disk; I'll call it the "hot disk". The hot disk cools by inverse Compton scattering of soft photons off the hot electron gas, and gives a much harder spectrum; see Fig. 1.

INVERSE COMPTON SPECTRA

My main purpose is to describe, in a more or less model-independent way, the shape of an inverse-Compton spectrum, based partially on new results reported this year by Shapiro, Lightman and myself (Shapiro et al. 1975), and independently by Katz (1975). A hard, inverse-Compton "tail" forms when a soft X-ray source, of characteristic photon energy E_{Soft} , shines out through a hot cloud, of electron temperature $kT_e \gg E_{\text{Soft}}$. (I assume $kT_e \leq m_e c^2 = 511 \text{ keV}$ in what follows.) The total number of photons is not changed in the formation of the tail, because Compton scattering conserves photons; but the total luminosity can increase enormously, because the mean photon energy increases. In Sco X-1 the observers may possibly be seeing a fairly weak inverse Compton tail as the hard excess (Peterson et al. 1966, Riegler et al. 1970, Zel'dovich and Shakura 1969). In Cyg X-1, most theorists believe that the observers are seeing a very strong tail formed from a weak photon source, a source perhaps so soft as to be unobservable behind the interstellar absorption ($E_{\text{Soft}} \leq 1 \text{ keV}$?).

The shape of the tail is fairly simple, and seems to be independent of source geometry, shape of soft input spectrum, and other mundane aspects (although further theoretical work is needed on this question). In terms of spectral energy intensity $I(E) \equiv dL/dE$, it is a power law between E_{Soft} and kT_e ,

$$I(E) \propto E^{-m}, \quad E_{\text{Soft}} \leq E \leq kT_e, \quad (1a)$$

where

$$m = -\frac{3}{2} + \left[\frac{9}{4} + \left(\frac{kT_e}{m_e c^2} N_{\text{scat}} \right)^{-1} \right]^{1/2} \quad (1b)$$

(the last term in the square root needs, strictly speaking, a relativistic correction; see Shapiro et al. 1975). Here N_{scat} is the mean number of scatterings suffered by an outgoing photon, which is related to Thomson optical depth τ of the hot cloud in a somewhat geometry-dependent way: roughly,

$$N_{\text{scat}} \sim \tau, \quad \tau \lesssim 1; \quad (2a)$$

$$N_{\text{scat}} \sim \tau^2, \quad \tau \gtrsim 1. \quad (2b)$$

Above $E = kT_e$, the spectrum cuts off very roughly like an exponential,

$$I(E) \propto \exp(-E/kT_e), \quad E \gtrsim kT_e; \quad (3)$$

See Fig. 2. The observer, if he or she should be so lucky or persistent as to see the whole spectrum, can infer the electron temperature of the hot cloud from the location of the knee at $E = kT_e$, and then infer N_{scat} , and then τ , from the fitted spectral index m , through Eqs. (1) and (2).

[The shape is more complicated if $(kT_e/m_e c^2) N_{\text{scat}}$ becomes greater than 2 or so; the simple knee at $E = kT_e$ is replaced by a hump above the power law, followed by a cutoff above $\sim 3kT_e$. There seem to be no sources that look like this in the hard X-ray, so I'll ignore this "saturated" case. The "unsaturated" case I'm discussing lies in the range $1/20 \lesssim (kT_e/m_e c^2) N_{\text{scat}} \lesssim 2$.]

Why an X-ray source picks a certain value of spectral index m is largely determined by the internal energy budget. If the luminosity L_{Hard} that the hot cloud wants to deliver is much greater than the luminosity L_{Soft} of the soft source, then m cannot be steeper than about 1, and in fact m will stay close to 1 (say $0.5 \lesssim m \lesssim 1$) for a fairly wide range of $L_{\text{Hard}}/L_{\text{Soft}}$ (say a factor of 6). In our hot-disk model, we interpret the "low-state", or "non-flaring", data as an inverse Compton spectrum with a knee a little above 100 keV

and a spectral index $m \sim 0.5$ to 1.0. Changes in m should occur if the ratio $L_{\text{Hard}}/L_{\text{Soft}}$ changes in the source. We cannot predict such changes in detail, because we presently are unable to model the soft photon source in detail. However, our model definitely predicts (a) a knee somewhere near 100 keV, and (b) at any one instant, a simple power-law spectrum from the knee down to E_{Soft} , which for several reasons we expect to be below 1 keV. The spectral index m could conceivably change in ~ 1 sec. (timescale for inner part of disk to fill or dump); on the other hand, m might remain constant for very long periods if the mass flow is steady. The balloon observations reported here by Matteson et al. (1975) seem consistent with these predictions.

Sunyaev, Shakura, and Illarionov (unpublished) have recently found that an inverse-Compton spectrum has a knee at ~ 150 keV, even if kT_e substantially exceeds 150 keV, because of the decreasing Klein-Nishina cross-section.

TRANSITIONS OF CYG X-1

The "flares" or "transitions to a high state" in Cyg X-1 (Tananbaum et al. 1972, Boldt et al. 1974, Heise et al. 1975, Holt et al. 1975, Sanford et al. 1975, Boldt 1975) seem to require a further complication of the model; I believe the data to be good enough to support such a complication. One possible source of the increased soft flux ($E \lesssim 10$ keV) is some gas distant from the hole, heated by the hard flux, as suggested by Thorne (1975). Another possible source is an annulus of cool disk, surrounding a core of hot disk around the hole (Fig. 3a); this picture is plausible, but the predicted soft flux is too soft to match the observations (Thorne and Price 1975, Shapiro et al. 1975). A third possibility, which I'll concentrate on here, is that the excess soft flux is an inverse Compton spectrum formed in a hot disk, just as in the low state, except that the soft photon source has now become extremely luminous for some reason, $L_{\text{Soft}} \gg L_{\text{Hard}}$, which forces the slope to become

very steep. (For instance, some vestige of a cool disk might exist occasionally in the equatorial plane of the hot disk; this situation has been examined by Price and Liang (1975). See Fig. 3b.) Let me illustrate the spectral changes that might be expected for this third possibility. If L_{Soft} were to remain constant while L_{Hard} varied, one would see a direct correlation between observable luminosity and spectral hardness (Fig. 4). This doesn't look much like the observations. On the other hand, if L_{Hard} remains constant (at, say, 2 or 3×10^{37} erg s $^{-1}$) while L_{Soft} varies wildly, one sees a striking anticorrelation between luminosity and hardness (Fig. 5). The spectrum at any one instant is always a fairly accurate power law, but the spectral index varies widely ($m = 0.5$ to $m = 4$ in one example); and the spectrum always pierces the same "pivot point" (at $E \sim 10$ keV in the example). This model behavior is consistent with these actually observed effects: (a) Greatly increased number flux below ~ 10 keV; (b) Accurate representation by a power law at any one time, at least below 10 keV; (c) Anticorrelation of intensity above 10 keV with that below. There is one possible inconsistency: The model predicts that the whole spectrum below ~ 100 keV is an accurate power law at any one instant, while Tananbaum et al. (1972), Heise et al. (1975), and Sanford et al. (1975) report an excess at $E \gtrsim 10$ keV over the extrapolation of the steep, low-E power law, an excess which perhaps represents a nearly unchanged version of the low-state, flat power law. As the theoretically simplest resolution of this inconsistency, let me suggest that the reported spectra might be time-averages of a single power-law with a strongly time-dependent slope, i.e. time-averages over many spectra as in Fig. 5. As a minimum timescale for major changes, ~ 1 min. seems likely. If this idea of a time-dependent, simple power-law is wrong (and several groups may already possess the data to shoot it down), that is, if the source really has two intrinsic spectral components in "high state", then I would alternatively suggest that each separate component ($E < 10$ keV, $E > 10$ keV) might be an independent inverse-Compton spectrum, i.e. a separate power-law, as seems likely if both originate

near the hole in different regions of the disk.

I emphasize that Fig. 5 does not result from a complete model calculation; the hot disk is modeled with some care, but the soft source is stuck in ad hoc. The shapes of the spectra above ~ 1 keV should be taken seriously, but not their precise relative normalization.

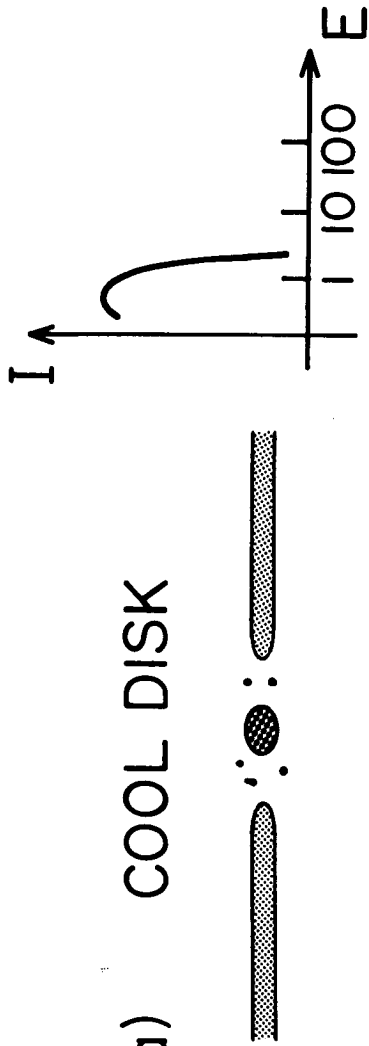
I am grateful to numerous participants of this symposium for helpful conversations, and to K.S. Thorne for helpful communications. This work was partly supported by the National Science Foundation (Grant No. GP-36317).

REFERENCES

- Agrawal, P.C., Gokhale, G.S., Iyengar, V.S., Kunte, P.K., Manchanda, R.K., Sreekantan, B.V. 1972, Astrophys. Space Sci. 18, 408.
- Boldt, E. 1975, this symposium.
- Boldt, E., Holt, S., Rothschild, R., Serlemitsos, P. 1974, presented at "International Conference on X-Rays in Space", University of Calgary (Canada).
- Eardley, D.M., Lightman, A.P., Shapiro, S.L. 1975, Astrophys. J. (Letters), 199, L153.
- Frontera, F. and Fuligni, F. 1975, Astrophys. J. 196, 597.
- Haymes, R.C. and Harnden, F.R., Jr. 1970, Astrophys. J., 159, 1111.
- Heise, J., Brinkman, A.C., Schrijver, J., Mewe, R., den Boggende, A., Gronenschild, E., Parsignault, D., Grindlay, J., Schnopper, H., Schreier, E., Gursky, H. 1975, Nature, 256, 107.
- Holt, S.S., Boldt, E.A., Kaluziński, L.J., Serlemitsos, P.J. 1975, Nature, 256, 108.
- Katz, J. 1975, Astrophys. J. (in press).
- Lightman, A.P. and Shapiro, S.L. 1975, Astrophys. J. (Letters), 198, L73.

- Matteson, J.L., Mushotzky, R.F., Paciesas, W.S., Laros, J.G.
1975, this symposium.
- Novikov, I.D. and Thorne, K.S. 1973, in Black Holes, eds.
C. DeWitt and B. DeWitt (New York: Gordon and Breach).
- Peterson, L.E. and Jacobson, A.S. 1966, Astrophys. J.,
145, 962.
- Price, R.H. and Liang, E.P. 1975, "Accretion Disk Coronas
and Cygnus X-1", preprint (University of Utah).
- Pringle, J.E. and Rees, M.J. 1972, Astron. and Astrophys.,
21, 1.
- Riegler, G.R., Boldt, E., Serlemitsos, P. 1970, Nature,
226, 1041.
- Sanford, P.W., Ives, J.C., Bell Burnell, S.J., Mason, K.O.,
Murdin, P. 1975, Nature, 256, 200.
- Shakura, N.I. and Sunyaev, R.A. 1973, Astron. and Astrophys.
24, 337.
- Shapiro, S.L., Lightman, A.P. and Eardley, D.M. 1975,
Astrophys. J. (in press).
- Tananbaum, H., Gursky, H., Kellogg, E., Giacconi, R.,
Jones, C. 1972, Astrophys. J. (Letters), 177, L5.
- Thorne, K.S. 1975, "Cygnus X-1: A Two-Source Source?",
preprint (Caltech).
- Thorne, K.S. and Price, R.H. 1975, Astrophys. J. (Letters),
195, L101.
- Zel'dovich, Ya.B. and Shakura, N.I. 1969, Astron. Zh.
46, 225 [Sov. Astron.-AJ 13, 175].

(a) COOL DISK



(b) HOT DISK

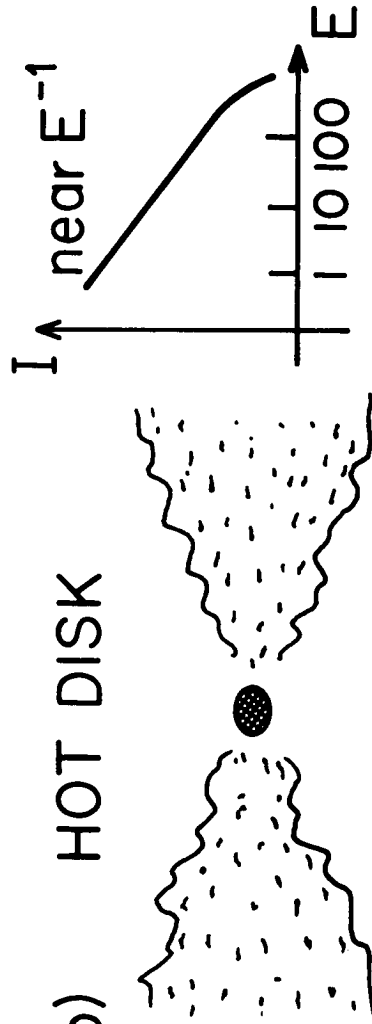


Fig. 1. Two possible equilibrium configurations of an accretion disk around a black hole, with representative energy spectra (E in keV). (a) "Cool disk" prefers to emit at a few keV, although it can be pushed higher. (b) "Hot disk" emits a power law near E^{-1} , extending to beyond 100 keV.

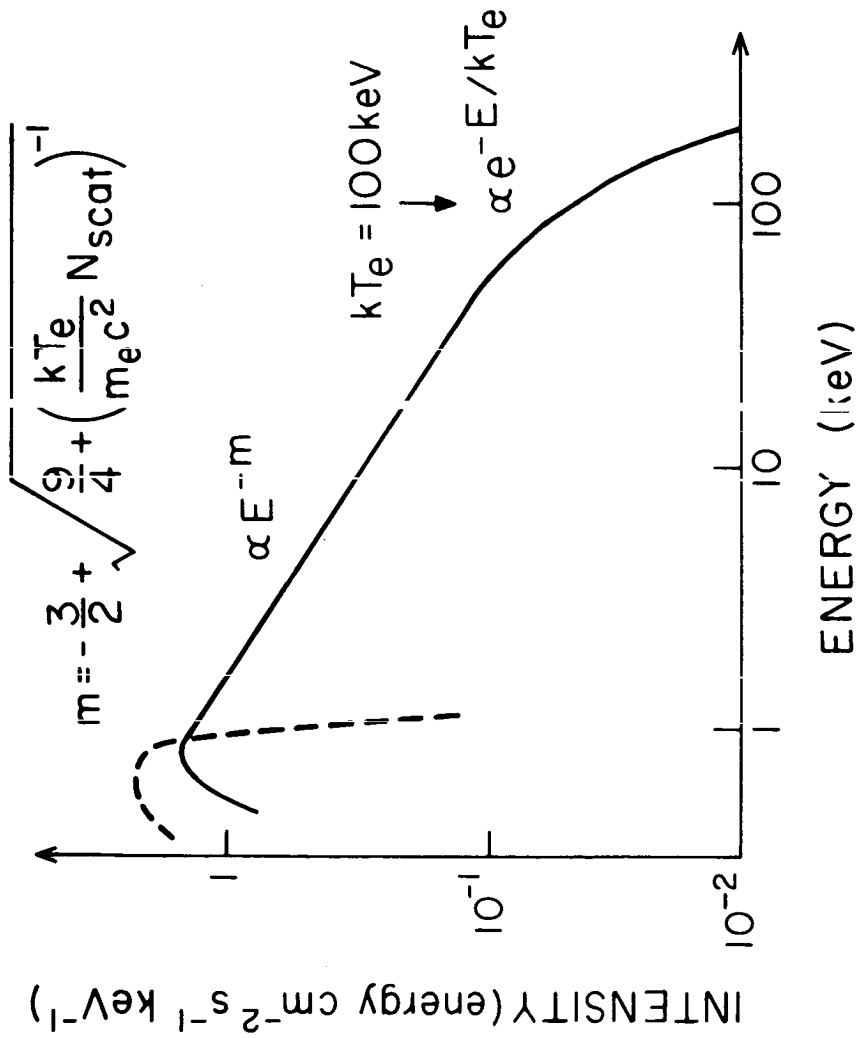
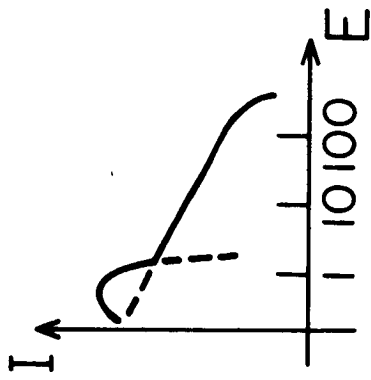
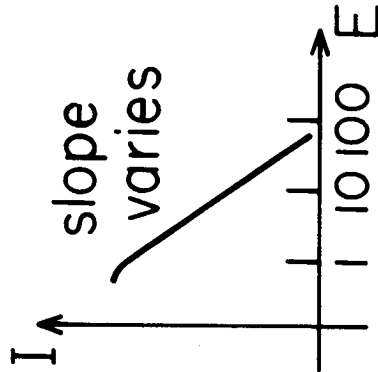
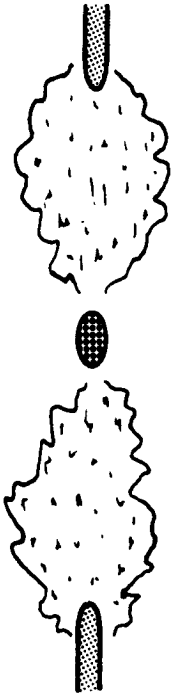


Fig. 2. Typical inverse Compton spectrum, for adopted values $kT_e = 100$ keV and $m = 0.67$. Input, "soft" spectrum is dotted curve. Output, "Comptonized" spectrum is full curve. Symbols are defined in text. In real life, some portion of the soft spectrum might be directly visible in the output.



(a) COOL + HOT



(b) COOL INSIDE HOT

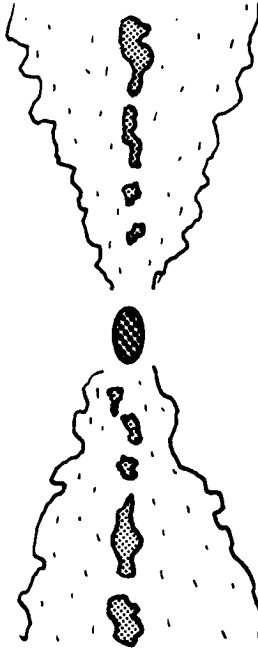


Fig. 3. Complicated disk models to explain "flaring" or "high" state of Cyg X-1. (a) "Cool + Hot" model has both configurations present in tandem; spectra just superpose. This model predicts too soft a soft component. (b) "Cool Inside Hot" model postulates a variable amount of cool matter (or other soft source) inside hot disk. Soft spectrum is processed through the hot cloud to yield an inverse Compton spectrum of variable slope.

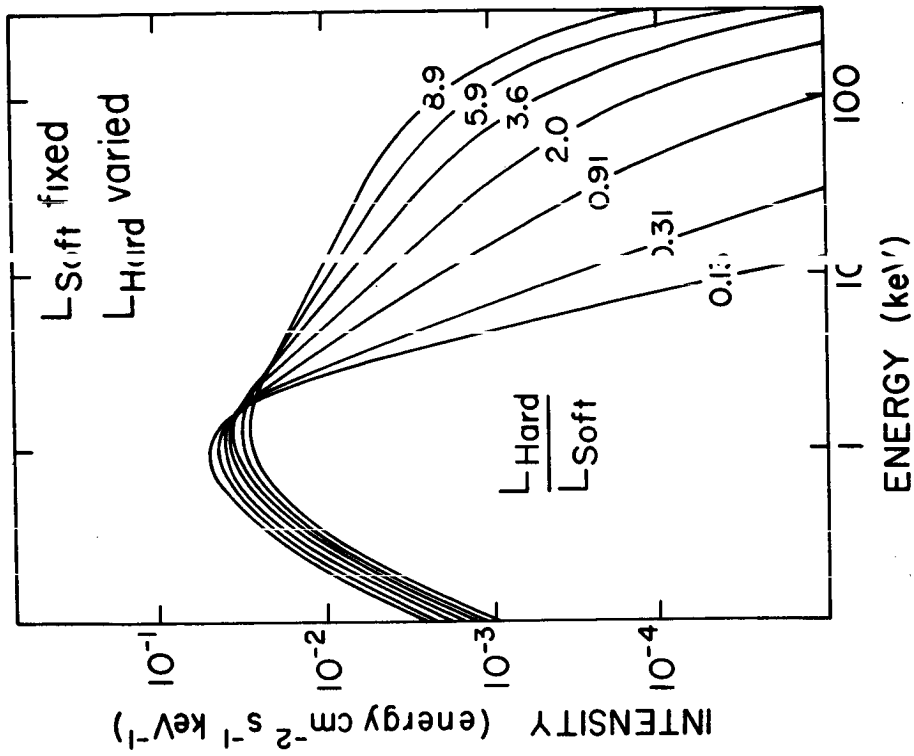


Fig. 4. Variable spectrum of "Cool Inside Hot" model if soft luminosity L_{Soft} stays constant, luminosity L_{Hard} of hot cloud varies. Shape of soft source is a black body at a temperature of 0.3 keV. Label on curves is ratio $L_{\text{Hard}}/L_{\text{Soft}}$.

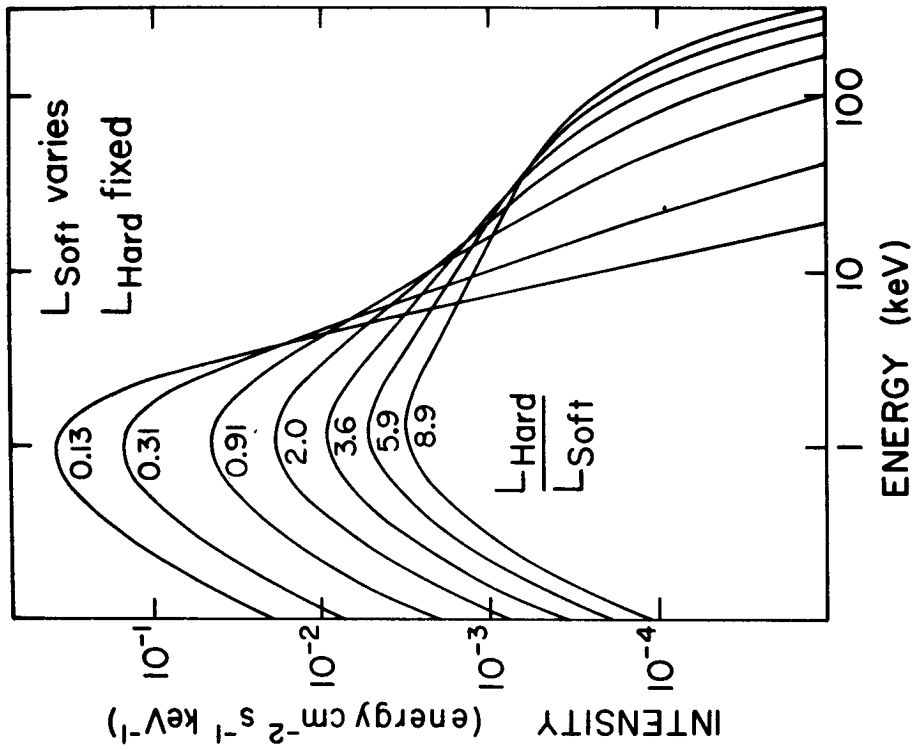


Fig. 5. Same as Fig. 4, except that L_{Hard} stays constant, L_{Soft} varies. Note "pivot-point" near 10 keV.

New Results from Long-Term Observations of Cyg X-1

S. S. Holt, E. A. Boldt and
P. J. Serlemitsos
Laboratory for High Energy Astrophysics
Goddard Space Flight Center
Greenbelt, Maryland 20771

L. J. Kaluzienski
University of Maryland
College Park, Maryland 20742

Received: 1975 August 22

ABSTRACT

Observations of Cyg X-1 between October 1974 and July 1975 reveal a persistent 5.6 day modulation of the 3-6 keV x-ray intensity, having a minimum in phase with superior conjunction of the HDE 226868 binary system. The modulation is found to be most pronounced just prior to the April-May 1975 increase of Cyg X-1, after which both the modulation and intensity are at their lowest values for the entire duration of the observations. These data imply that the x-ray emission from Cyg X-1 arises from the compact member of HDE 226868, and that the increase of April-May 1975 may have represented the depletion of accreting material which had not yet been mixed into a cylindrically symmetric accretion disk about the compact member.

Subject headings: x-ray sources—black holes

Accepted for publication in Ap. J. Letters

I. INTRODUCTION

Cyg X-1 has consistently been associated with x-ray intensity variability on virtually all time scales (c.f. Boldt, et al. 1975). In contrast to its chaotic behavior on timescales ≤ 1 sec (c.f. Rothschild, et al. 1974), however, the presently reported data indicate that variations from one day to the next are typically within the $\sim 10\%$ statistical uncertainty of the data. The relative constancy on this timescale is perturbed only by a persistent 5.6 day modulation in phase with the binary period of HDE 226868. The effect is too large to be sensibly associated with "absorption dips" previously reported, but the coincidence in phase over >30 cycles would appear to dispel any doubts which may remain about the association of Cyg X-1 with HDE 226868.

On longer timescales, the present data yield an apparently monotonic slow increase until the sudden factor-of-three increase of April-May 1975, after which the Cyg X-1 intensity is lower than before. Apparently tracking the Cyg X-1 intensity is the magnitude of the 5.6d modulation. Both of these results can be interpreted as arising from an elevated amount of matter between the binary components prior to the April-May outburst which manifests itself in both an increasing level of emission as the material is accreted onto the secondary, and increased absorption at HDE 226868 superior conjunction.

II. EXPERIMENTAL RESULTS

All of the data reported here are obtained from the Ariel-V All-Sky X-Ray Monitor, a complete description of which may be found in Holt (1975). The experiment is a scanning x-ray pinhole camera which observes most

of the celestial sphere each orbit. The important parameters are a pinhole area of 1 cm^2 , an average duty cycle for source observation of $\sim 1\%$, and an efficiency of $\sim 60\%$ in the energy range 3-6 keV. The finest temporal resolution of the experiment is one orbit (~ 100 minutes), and there is no energy resolution available in the data within the 3-6 keV acceptance window.

Figure 1 displays the Cyg X-1 data reported here in daily averages (the gaps are times when the source was out of the useful field of view of the experiment). The increase in the spring of 1975, first reported by Gursky, et al. (1975), commenced on 22 April (Holt, et al., 1975), apparently reached maximum in early May (Heise, et al. 1975), and was well on the way to recovery to the pre-flare state by mid-May (Sanford, et al. 1975). It was out of the field-of-view of this experiment during the decay phase of the flare-up, and when next unambiguously observed in early June 1975 it had apparently returned to its pre-flare low-intensity level.

The same data which were used in the construction of Figure 1 (excluding only the flare-up) were searched for the binary period of HDE 226868 by direct folding of individual measurements taken over no more than $1/2$ day. As shown in Figure 2, there is a significant χ^2 deviation from the assumption of source constancy at the HDE 226868 period of 5.60089 days. Important, also, is the observation that the largest contribution to this χ^2 is from the bin centered at superior conjunction of the binary system; the period and phase of HD 226868 used here are from the Copernicus ephemeris (Mason, private communication, 1974).

As a check on the stability of the effect, the data were broken into

~ 56 day intervals which were each folded at the same period and phase as in Figure 2. These results are displayed in Figure 3, where the bin centered at superior conjunction is always a minimum prior to the increase of April-May 1975, but may not be afterwards. Similarly, the average intensity' of the source after May 1975 appears to be less than before. It should be noted that the error bars in all three figures are statistical only, and there are systematic effects (mostly arising from pointing inaccuracies) which are not recoverable. These appear to play no significant role in the 5.6d folds (as evidenced by the lack of a 5.6d component in the Crab Nebula), but could conceivably be important in the interpretation of the gross intensity variation of Figure 3. We estimate that the true error on the four average values in Figure 3 is no larger than the statistical error displayed for each individual bin, as the Crab Nebula is found to be consistent with constancy over the entire interval with a smaller systematic contribution to the error. Figure 3 demonstrates, therefore, that Cyg X-1 exhibited a slowly increasing intensity and 5.6d modulation until the April-May 1975 increase, after which both were significantly lowered. We note that a linear extrapolation of the trend indicated for the data over the interval October 1974 to April 1975 backward in time to October 1973 would imply that the average intensity one year prior to the launch of Ariel 5 could have been lower by a factor of about two, whereas rocket-borne observations (Rothschild et al. 1975) on 4 Oct. 73 and 3 Oct 74 indicate that the 2-40 keV absolute spectrum (averaged over about a minute at a binary phase of 0.17) was invariant to within a limit of about 10% for any likely error in normalization. This suggests that the timescale for the build-up to the April-May 1975 flare is no more than ~ 1/2 year.

III. DISCUSSION

The 5.6 day modulation of the Cyg X-1 intensity cannot be solely attributed to "absorption dips". Such maxima have been reported by Mason, et al. (1974) and Li and Clark (1974) with the following "typical" characteristics:

- 1) a spectral hardening attributable to absorption by cold matter in the line of sight which would amount to no more than 50% decrease in the 3-6 keV acceptance window of this experiment
- 2) a binary phase within $\sim 10\%$ of superior conjunction
- 3) a duration of ~ 1 hour
- 4) a probability of occurrence of $< 50\%$ at each superior conjunction.

These characteristics imply a overall light curve decrement arising from absorption dips of .002, compared with the $.027 \pm .004$ actually observed in the data displayed in Figure 2 (and $.020 \pm .005$ if only the data prior to the April-June 1975 outburst are used). A recent observation from ANS in November 1974 (Brinkman, et al. 1975) indicates a considerably more complex absorption dip situation around that superior conjunction (including three absorption dips). This does not substantially alter the "typical" situation inferred from the previous observations (based on >10 superior conjunction measurements), but does indicate a larger fraction of the presently reported decrement may be assignable to a more generalized absorption phenomenology which characterized Cyg X-1 between October 1974 and April 1975.

Sanford, et al. (1974) have reported a 5.6d modulation of the Cyg X-1 intensity over a single cycle which may be relatable to the present measurements. Although the predominant feature of their light curve is a relative maximum at inferior conjunction, the magnitude of the effect is similar. Utilizing the present prescription of calculating the decrement in the 20% of the binary phase centered at superior conjunction relative to an average for the whole cycle calculated from the remaining 80%, we estimate that the Copernicus "decrement" amounted to ~ 0.05 . These authors remarked that this magnitude was not in conflict with the lack of detectable 5.6d modulation in 35 continuous

days of UHURU observation (Tananbaum et al., 1972). It may be important to note, however, that the UHURU search was performed less than a year after the spring 1971 transition to its low-intensity state, while the Copernicus observation was performed two years after the UHURU study. If the trends in the present data are an indication of what might have happened after the 1971 transition, the Copernicus data may have been taken during the build-up phase to another flare while the UHURU data were not.

Mason et al., (1974) have interpreted the absorption dip phenomenon as arising from the core of a stream of cold matter between the two components of the HDE 226868 system which occasionally intercepts the line of sight to Cyg X-1. It is tempting to postulate that the presently reported 5.6d modulation is a lower-level absorption effect. The simplifying assumption of a cosine line-of-sight circumstellar matter distribution centered at superior conjunction yields an average column density in the central bin of Figure 2 of 94% of maximum, while the adjacent bins have a column density of less than 1/3 maximum (there is no absorption contribution to the two outermost bins). Assuming universal abundances in cold matter, Brown and Gould (1970) cross-sections yield a column density of $\sim 2 \times 10^{22}$ H-atoms cm^{-2} in the line-of-sight at superior conjunction. This amount of cold material should have caused a severe reduction in the intensity of x-rays of lower energy than can be measured by this experiment (at least during the time of our observations), but such an effect has not been reported by other investigators. There are several possible resolutions of this apparent inconsistency. Either a high circumstellar temperature ($> 10^6$ K) or an overabundance of heavy -Z material (sulfur and heavier) may be invoked to reduce the relative absorption

of soft x-rays to hard, but an accretion disk model for Cyg X-1 (c.f. Pringle and Rees, 1972; Shakura and Sunyaev, 1973; Thorne and Price, 1975) may offer a natural explanation. Here the soft x-rays are predominantly produced in the outer, optically thick region of the accretion disk, while the hard component is produced much closer to the accreting black hole (Thorne and Price, 1975, estimate the transition between "soft" and "hard" to be at ~ 2 keV). An increase in the density of the stellar wind to the accretion disk would then have the effect of shadowing the hard emission more efficiently than the soft, and could also yield an increased soft emission owing to a higher accretion rate. Both of these effects would tend to mask any absorption in soft x-rays relative to hard x-rays. Similarly consistent with this qualitative explanation is the slow increase in hard x-ray emission, as the characteristic gas drift time into the hard x-ray-emitting region of the disk is ≥ 1 month (Thorne and Price, 1975).

IV. SUMMARY

The present data yield an unmistakable association with HDE 226868 which is independent of the interpretation which we have ascribed to the overall variation in intensity and modulation. The χ^2 distribution of Figure 2 does not allow a period which differs by more than 4×10^{-3} of the HDE226868 period of 5.60089d, and the minimum at superior conjunction prior to the April-May 1975 flare-up is similarly suggestive of a firm association.

The interpretation we have given the intensity and modulation variation may not be unique, but is consistent with this and other observations. We suggest that stellar wind pile-up from the HDE 226868 primary, in loading the Cyg X-1 accretion disk, is directly responsible for the two

new effects we are reporting here: the gradually increasing hard x-ray luminosity, and the low-level line-of-sight absorption around superior conjunction.

The increasing x-ray emission may, in turn, increase the radiation pressure to the point where the Lightman and Eardley (1974) instability may trigger the flare-up of April-May 1975. This "high-intensity" state was considerably shorter in duration than that prior to the March-April 1971 "transition", but was typified by the same high degree of variability on time scales ~ 1 day (c.f. Sanford et al., 1975), in marked contrast to the regular behavior of the source we report here in its low intensity state. The April-May 1975 increase was the only such flare-up observed between October 1974 and July 1975, but may not have been the first since the 1971 transition.

We are grateful to John Bahcall for suggesting that we also include whatever limits our data may allow on Cyg X-1 modulation at periods consistent with a three-body system. We cannot place a sensible limit on any 30-40d periodicity owing to the sample length being < 10 cycles, but we can place a firm upper limit of 10% "pulsed fraction" (5% amplitude sinusoid) on any variation at a period near the ~ 8 hours expected from a close 3-body model.

We also note that the increase of April-May 1975 was characterized by x-ray variation on a timescale of a few days. Figures 4 and 5 (from Holt, et al., 1975) illustrate this behavior in All-Sky Monitor data with a temporal resolution of 1 day and $\sim 1/2$ day, respectively, and the effect persisted throughout the decay (c.f. Sanford, et al., 1975). The dynamics of the flare phenomenon are clearly reflected in this characteristic behavior, and any model of the phenomenon should predict such a few-day timescale for factor-of-two variations.

Lastly we note two effects in the All-Sky Monitor in data taken after that included in the paper. A short-duration increase (first noted by SAS-C) was detected at a peak amplitude of $> \frac{1}{2}$ Crab Nebula on 8 September, but it returned to its pre-flare level by 18 September so that it was neither as intense nor as long-lasting as the April-May increase. The second remark is that data taken through mid-October still show no statistically significant modulation at 5.6 days.

References

- Boldt, E., Holt, S., Rothschild, R., and Serlemitsos, P. 1975, Proc. Int. Conf. X-Rays in Space, D. Venkatesan, ed., University of Calgary.
- Brinkman, A. C., Heise, J., Mewe, R., den Boggende, A. J. F., Schrijver, J., Gronenschild, E., Tanaka, Y., Parsignault, D. R., Grindlay, J., Schreier, E., Schnopper, H., Gursky, H. 1975, Proc. COSPAR Symp. Fast Transients X- and Gamma-Ray Astron., Astrophys. Space Sci., in press.
- Brown, R. L. and Gould, R. J. 1970, Phys. Rev., D1, 2252.
- Gursky, H., Grindlay, J., Schnopper, H., Schreier, E., Parsignault, D., Brinkman, A., Heise, J., Schrijver, J., Mewe, R., Gronenschild, E., and den Boggende, A. 1975, IAU Circular No. 2778.
- Heise, J., Mewe, R., Brinkman, A. C., den Boggende, A., Schrijver, J., Gronenschild, E., Parsignault, D., Grindlay, J., Schreier, E., Schnopper, H., and Gursky, H. 1975, Nature, 256, 106.
- Holt, S. S. 1975, Proc. COSPAR Symp. Fast Transients X- and Gamma-Ray Astron., Astrophys. Space Sci., in press.
- Holt, S. S., Boldt, E. A., Kaluzienski, L. J., and Serlemitsos, P. J. 1975, Nature, 256, 108.
- Li, F. K. and Clark, G. W. 1974, Ap. J. (Letters), 191, L27.
- Mason, K. O. 1974, private communication.
- Mason, K. O., Hawkins, F. J., Sanford, P. W., Murdin, P., and Savage, A. 1974, Ap. J. (Letters), 192, L65.
- Pringle, J. E. and Rees, M. J. 1972, Astr. and Ap., 21, 1.
- Rothschild, R. E., Boldt, E. A., Holt, S.S. and Serlemitsos, P. J. 1974, Ap. J. (Letters), 189, L13.
- Rothschild, R. E., Boldt, E. A., Holt, S. S., and Serlemitsos, P. J. 1975, Bull. Am. Phys. Soc., 20, 604.
- Sanford, P. W., Ives, J. C., Bell Burnell, S. J., Mason, K. O., and Murdin, P. 1975, Nature, 256, 109.
- Sanford, P. W., Mason, K. O., Hawkins, F. J., Murdin, P., and Savage, A. 1974, Ap. J. (Letters), 190, L55.
- Shakura, N. I. and Sunyaev, R. A. 1973, Astr. and Ap., 24, 337.
- Tananbaum, H., Gursky, H., Kellogg, E., Giacconi, R., and Jones, C. 1972, Ap. J. (Letters), 177, L5.
- Thorne, K. S. and Price, R. H. 1975, Ap. J. (Letters), 195, L101.

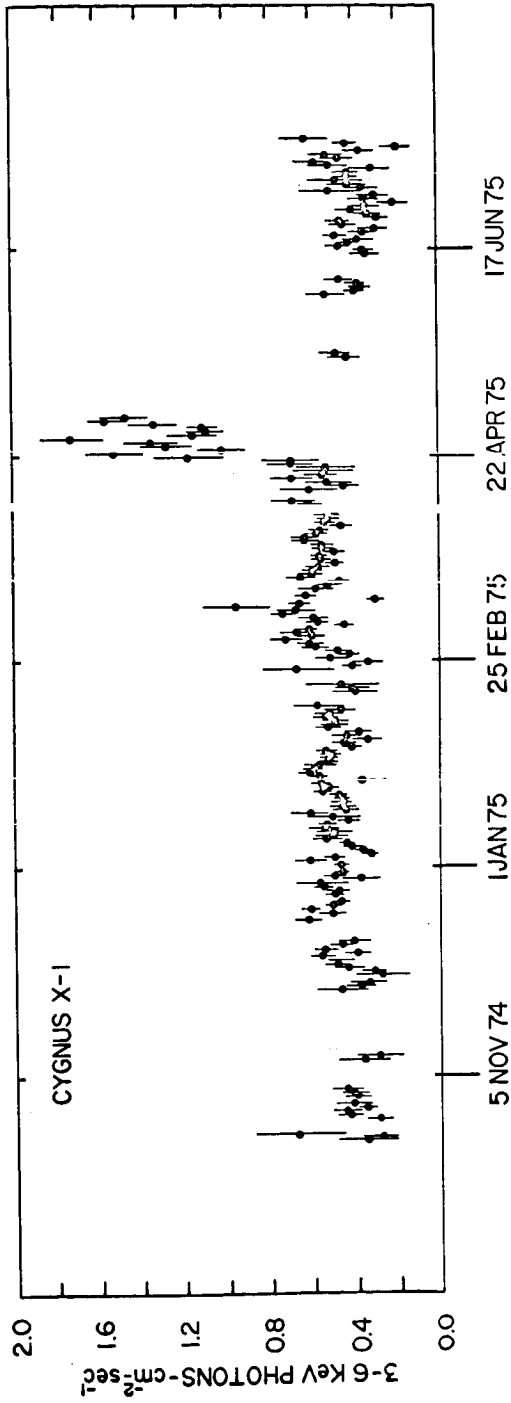


Figure 1. Daily average intensities for Cyg X-1 with $\pm 1\sigma$ statistical error³. As described in the text, unrecoverable systematic errors are estimated to be no larger than statistical. The gaps in coverage are times when Cyg X-1 is out of the usable field-of-view of the experiment.

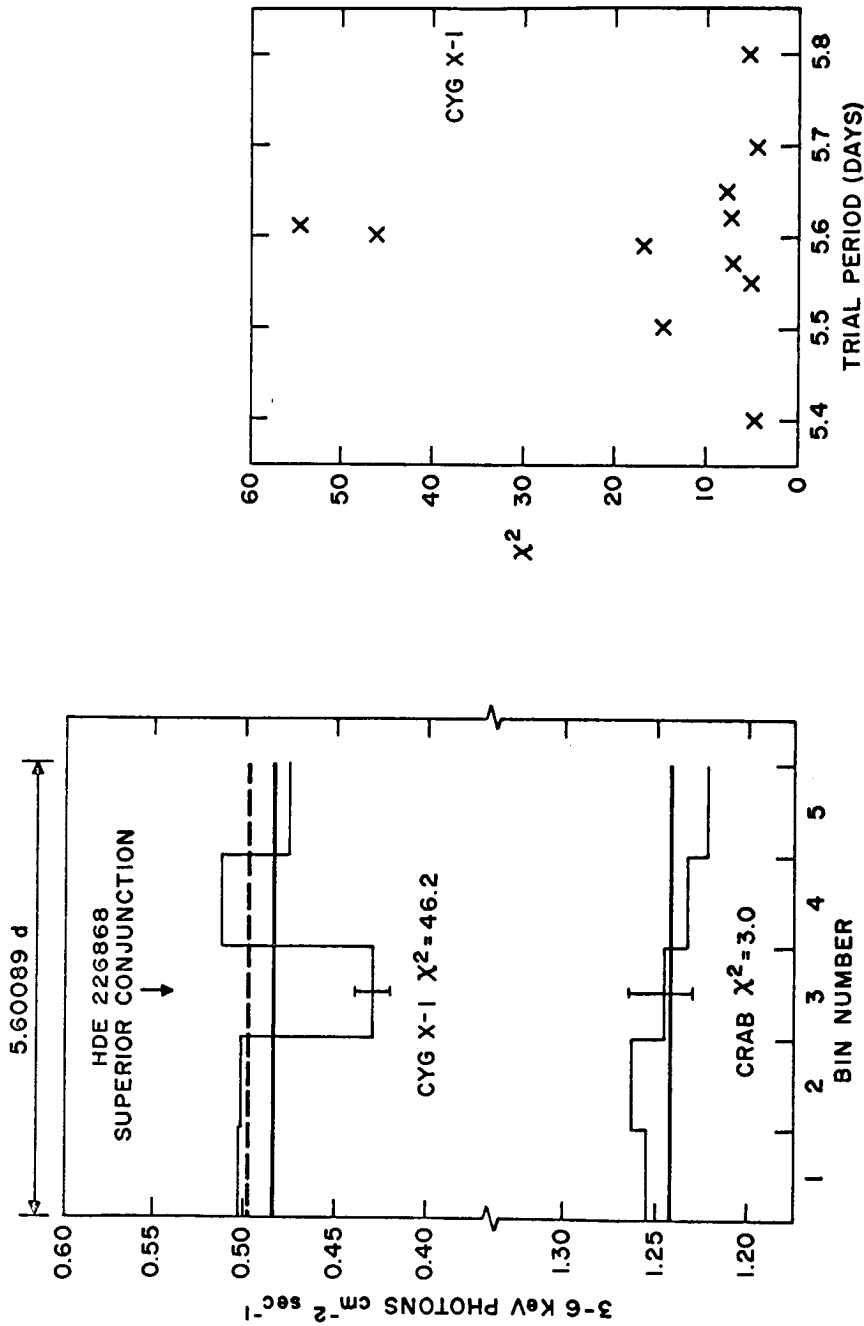


Figure 2. (a) Cyg X-1 and the Crab Nebula folded in 5 bins at the binary period of HDE 226868 with superior conjunction centered in the middle bin. The heavy solid lines are the average source intensities over the whole time interval (which excludes only the flare-up interval from 22 April 1975 to 5 July 1975), and the heavy dashed line in the Cyg X-1 trace is the average of the four bins not including HDE 226868 superior conjunction. (b) Values of χ^2 in 5-bin folds for the hypothesis of a constant source at the overall average value of Cyg X-1 for representative trial periods. In 60 trial folds at .05d intervals between 4.0d and 7.0d (excluding 5.60d), both the mean and median values of χ^2 were approximately 10. Using the FWHM of a triangular fit to the peak near 5.6d as a measure of the period uncertainty, we obtain $5.605 \pm .008d$.

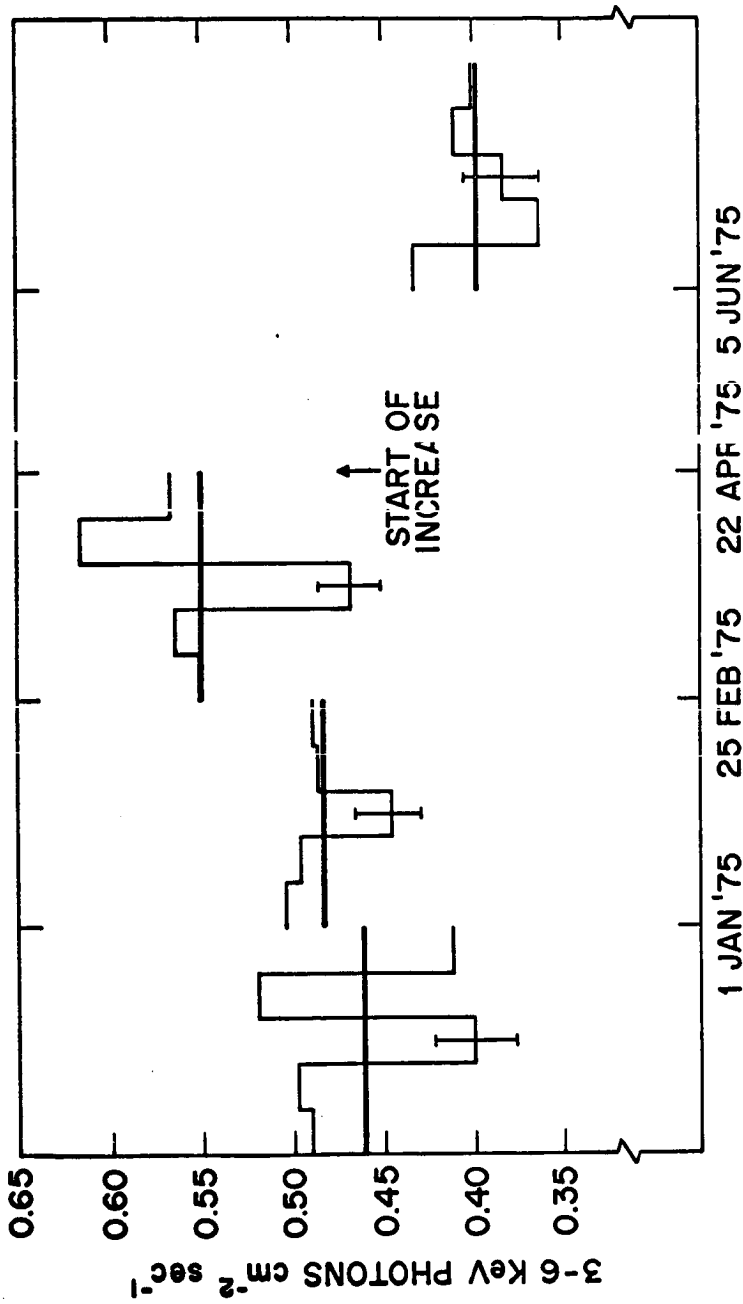


Figure 3. Cyg X-1 folded with the same period and phase as in Figure 2 in four intervals of ~ 56 days each. The solid heavy lines are average values in each interval, and the total uncertainty in these averages (including aspect as well as statistics) is approximately the same as the statistical error displayed for the individual central bin during the same interval.

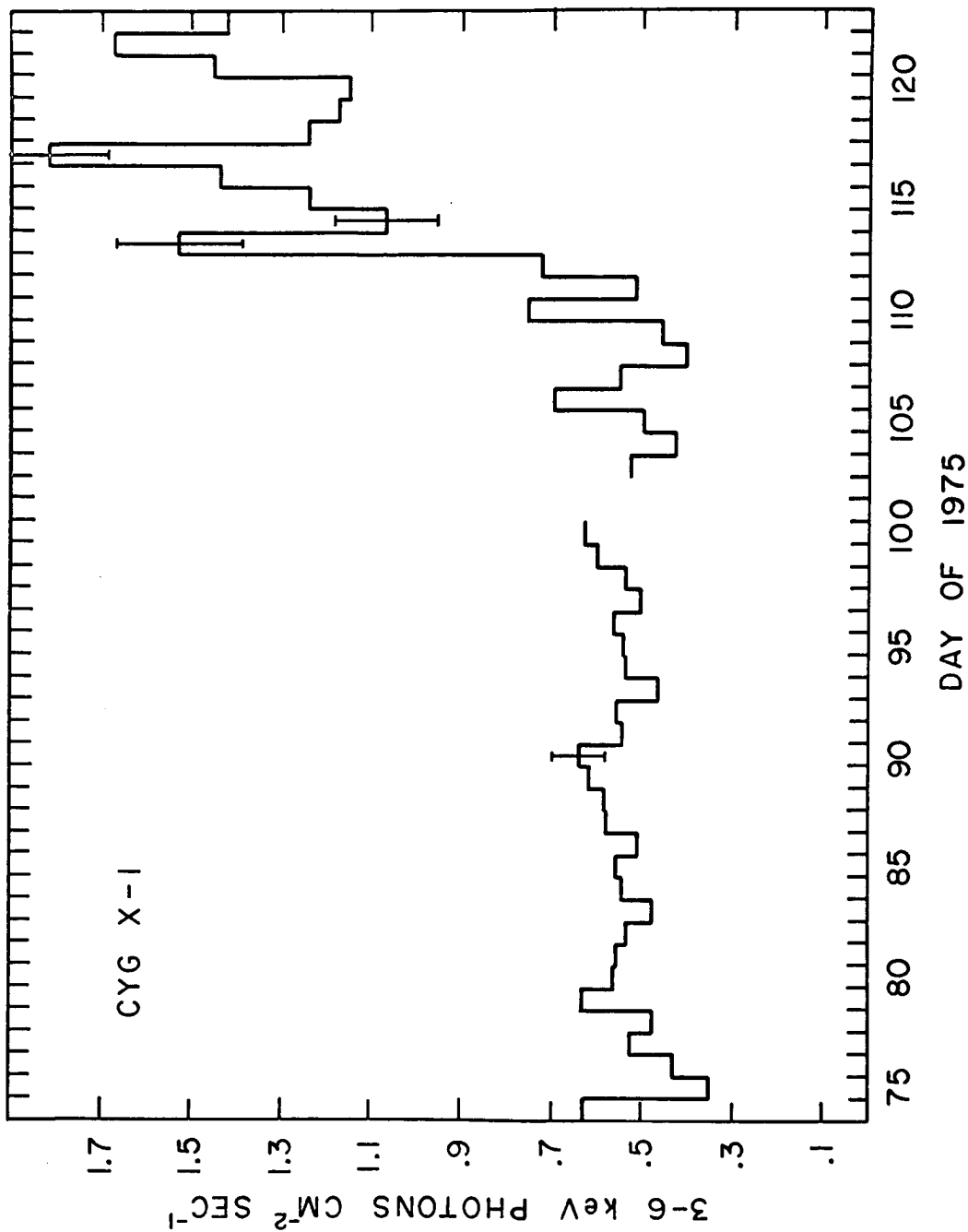


Figure 4. X-ray Variation in All-Sky Monitor Data with Temporal Resolution of One Day

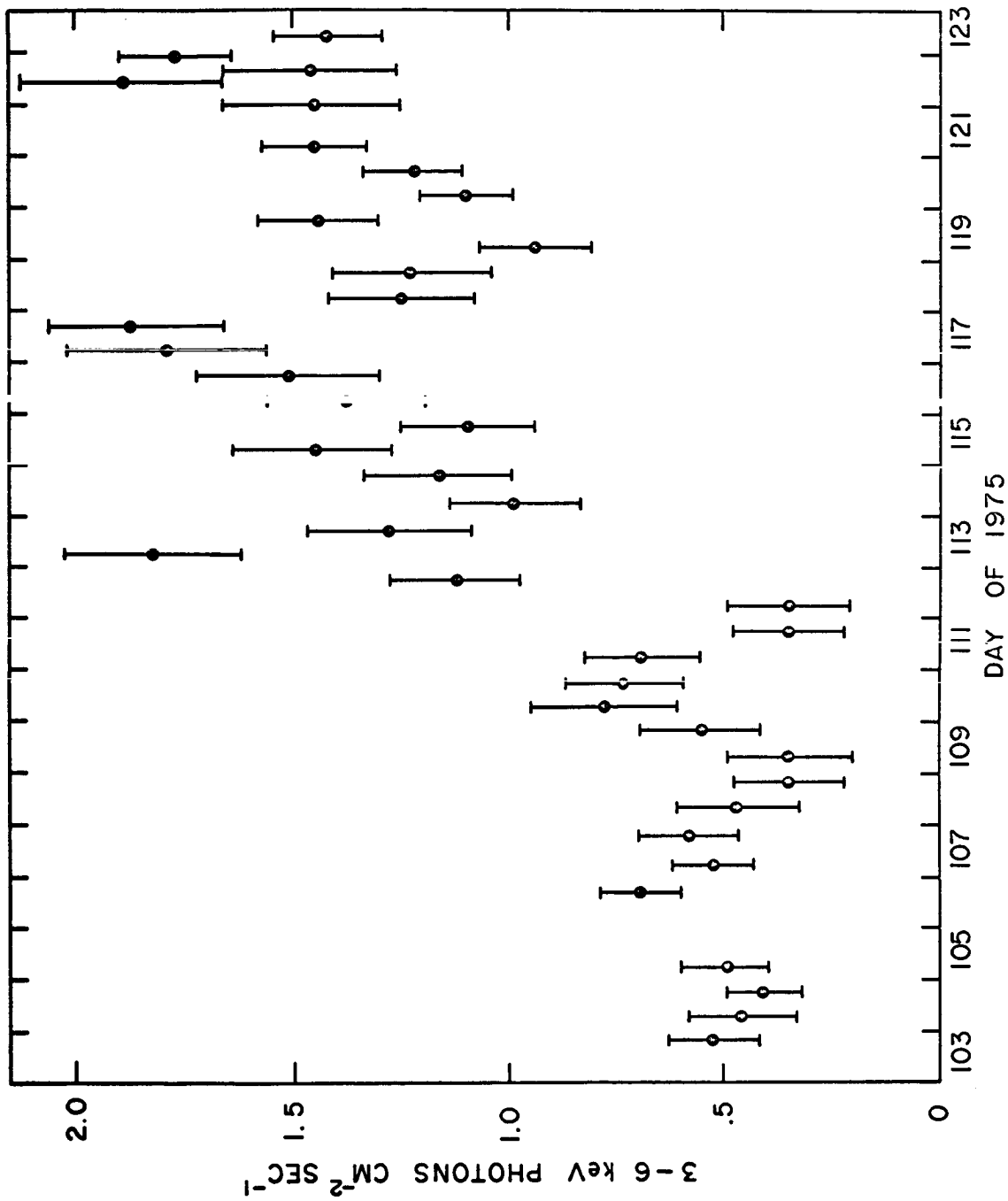


Figure 5. X-ray Variation in All-Sky Monitor Data with Temporal Resolution of One-Half Day

INTENSITY AND SPECTRAL VARIATIONS OF CYG X-1
OBSERVED FROM BALLOONS

J. L. Matteson, R. F. Mushotzky and W. S. Paciasas
Department of Physics, C-011
University of California, San Diego
La Jolla, California 92093

and

J. G. Laros
University of California
Los Alamos Scientific Laboratory
Los Alamos, New Mexico 87544

ABSTRACT

Observations of Cyg X-1 with a 20 to 200 keV balloon carried X-ray telescope in 1969, 1970, and 1972 are presented. These results reveal the following characteristics of Cyg X-1: The steep spectrum observed at $E < 10$ keV during the "radio quiet" phase can extend to 200 keV. This phase may have lasted 21 months (July 1969 to March 1971). The flux at 30 keV can vary from 1.1×10^{-2} to 1.4×10^{-3} ph (cm²-sec-keV)⁻¹ and that at 100 keV from 1.4×10^{-3} to 10^{-4} . The low flux values are factors of 3 and 8 below the "normal" values at 30 and 100 keV respectively, are rarely observed, and may be associated with the early phase of the 1971 April X-ray transition. During some one hour periods the intensity remained constant to $\sim 20\%$ and during other periods it varied a factor 2 in 5 minutes and a factor 10 in 1 hour. Complex spectral variations accompanied the intensity changes.

I. INTRODUCTION

The X-ray spectrum of Cyg X-1 has been measured in numerous balloon, rocket and satellite observations. However, the energy coverage of the instruments used have not allowed the total spectrum, from ~ 0.1 to ~ 500 keV, to be determined at any one time. Furthermore, the observed variability at most energies make formation of reliable composite spectra from different observations difficult. Nevertheless, most observations lie near what we term the "normal" spectrum and which we will use for comparison purposes. This is a power law, $dN/dE \sim E^{-\alpha}$, with $\alpha \sim 1.6$ at energies below some spectrum break energy E_b . Above E_b the spectrum becomes a steeper power law or perhaps an exponential, $dN/dE \sim e^{-E/E_0/E}$. The "normal" flux at 10 keV is then $\sim 3 \times 10^{-2}$ ph/cm²-sec-keV. E_b has been observed to range from 32 keV (Baity et al. 1973) to ~ 120 keV (Haymes and Harnden 1970). A single power law fit through the break energy will indicate $\alpha > 1.6$. The "pre-transition" spectra measured by Uhuru (Schreier et al. 1971; Tananbaum et al. 1972) and the recent increase in low energy flux seen by Ariel V (Holt et al. 1975) are not associated with the "normal" spectrum.

To study variations of the normal spectrum, search for departures from it and determine the relation of > 20 keV variations to those at lower energy, we conducted a series of balloon flight observations from 1969 to 1972. We emphasized control of systematic effects in order to measure the statistics limited spectra required by theoretical models of Cyg X-1.

II. INSTRUMENTATION, TECHNIQUE AND ANALYSIS

All observations reported here were conducted with the same X-ray telescope (Peterson, Pelling, and Matteson 1972) which will be briefly described. The NaI(Tl) detector had 34.2 cm^2 of effective area with a circular aperture of 5.9° FWHM. It had a $1 \frac{1}{2}$ " thick CsI(Na) shield operated in anticoincidence. The 20 to 100 keV background was $\sim 3 \text{ sec}^{-1}$ in the 1969 flights and was reduced to $\sim 1.2 \text{ sec}^{-1}$ for the later flights. X-ray counts were pulse height analyzed into 256 channels and telemetered to a ground station. Data were tape recorded and later analyzed at UCSD. The telescope was carried in a servo controlled balloon gondola which provided absolute pointing accuracy of $\sim 0.5^\circ$ and aspect accuracy of $\sim 0.1^\circ$. Observations were conducted by holding the telescope's axis fixed relative to the earth and allowing the earth's rotation and balloon drift to sweep the aperture over the X-ray source. Cyg X-1 and Cyg X-3 were always resolved. Background was usually measured before and after the source exposure. Periodic inflight calibrations using radioactive X-ray sources were performed.

Determination of the photon spectrum required three basic steps: First, the background and source counting rate spectra were separated by finding the counting rate component proportional to the detector area exposed to the source. Second, model photon spectra at the top of the atmosphere had their corresponding detector counting rate spectra calculated and the best fit model parameters and standard deviations were determined. Third, the counts to photons correction factors of the best fit model were applied to the source counting rate spectrum to give the photon spectrum. Minimum χ^2 defined best fit model parameters and their standard deviations were obtained using the $\chi^2 + 1$ method for the case of independent errors.

Laboratory measurements verified computer simulation of the instrument response which included photoelectric absorption, K X-ray emission and Compton scattering to all orders in the detector, energy dependence of the aperture, absorption and scattering by an undesired passive material behind the detector window, and non-vetoed Compton scattering in the collimator by high energy X-rays giving lower energy X-ray counts in the detector. The latter two effects gave a 30% decrease in count rate at ~ 25 keV in Flights 46 and 47 only, and a $\sim 20\%$ increase in the rate at ~ 100 keV for an $E^{-1.8}$ power law spectrum. Residual atmospheric depth was measured to an accuracy of 0.1 gm/cm^2 . Remaining systematic errors in our spectra are estimated to be $< 10\%$ in the 25 to 150 keV range and $< 20\%$ in the 20 to 200 keV range.

III. BALLOON FLIGHTS

Table I summarizes the balloon flights. The periods of observation are indicated or, in the case of Flight 47, the center of 40 minute intervals of one sighting each 14 minutes. All observations were conducted at $\sim 3 \text{ gm/cm}^2$ residual atmosphere after balloon launch from Palestine, Texas.

IV RESULTS

Also presented in Table I are the measured 20 to 200 keV intensities. In 1969 June the intensity was comparable to that obtained in earlier observations by many workers, 15 to 30 keV/cm²-sec, characteristic of the normal spectrum. A month later, during Flight 47, the average intensity was a factor six lower. During all eight Cyg X-1 sightings of this flight the intensity was low, indicating that the low state lasted at least 6 hours. Fourteen months later, during Flight 50, the flux was again low. We are unaware of observations of Cyg X-1 above 20 keV during the Flights 47 to 50 interval and therefore conclude that the low intensity state may have lasted more than 14 months. Flights 60 and 61, in June 1972, showed that the average flux was normal. An earlier observation by Agrawal et al. (1972) in 1971 April also showed the normal state, so the low state lasted less than 21 months.

The X-ray spectra measured in this work are presented in Figure 1 and their model spectrum parameters in Table I. Although the power law fit to the Flight 46 spectrum is allowed, the spectrum clearly has a break at ~ 85 keV, steepening from $\alpha \approx 1.4$ to $\alpha \approx 2.6$ with increasing energy. This spectrum is normal and is in substantial agreement with that observed 5 days earlier by Haymes and Harnden (1970). [It also agrees with an earlier rocket observation at low energies by LRL (Macgregor et al. 1970).]

The spectra of Flights 47 and 50 are, within the errors, the same. α for Flight 60 is uncertain due to instrument background problems. During Flight 61 large intensity changes which varied with energy resulted in power law spectra which took on extreme values indicated by the boundaries of the boxed region.

Figure 2 shows the result of a search for short time scale variations during Flight 46. On a one-minute scale the intensity is constant to $\sim 20\%$.

Other energy bands also show a constant intensity. A similar result was obtained during Flight 50 with a limit of $\sim 40\%$ on five-minute variations (Figure 3). During Flight 61, however, the intensity was extremely variable as the three-minute integrations in Figure 4 indicate. In the 0520 to 0620 period the 20 to 200 keV intensity decreased from $\sim 30 \text{ keV/cm}^2$ to $\sim 8 \text{ keV/cm}^2$ -sec as α changed from ~ 1.8 to ~ 2.5 . The intensity decrease was approximately exponential in time with a characteristic time of ~ 25 minutes. During the 0815 to 0915 period the intensity increased from $\sim 8 \text{ keV/cm}^2$ -sec to $\sim 20 \text{ keV/cm}^2$ -sec while α changed from ~ 1.2 to ~ 2 . The variations are not as smooth as in the earlier interval. In particular, the average 22-83 keV intensity is approximately a factor of two higher during 0850 to 0910 than during 0830 to 0850 while the higher energy intensity remains relatively constant. In both observation periods the high intensity phases have $\alpha \approx 2.0$. However, in the low intensity state α ranges from ~ 1.2 to ~ 1.8 .

V. DISCUSSION

The establishment of the relative constancy, to within a factor ~ 2 , of the low energy spectrum over a period of days, first by Uhuru (Tananbaum et al. 1972) and more recently by Ariel V (Holt et al. 1975), ANS (Heise et al. 1975) and Copernicus (Sanford et al. 1975) allow spectra taken within approximately a month to be combined with some confidence. Of course, one must avoid X-ray transitions such as seen in April 1971 (Tananbaum et al. 1972) or April 1975 (Holt et al. 1975).

Therefore, we combine the spectrum of GSFC (Bleach et al. 1972) obtained on 1970 September 21, shown in Figure 1, with ours obtained 12 days earlier. The result is a single power law with $\alpha \approx 2.5$ which fits the spectrum from 2 to 200 keV. Its shape is between the normal spectrum and the $< 9 \text{ keV}$ "pre-transition" spectrum observed by Uhuru in 1970

December 21 (Schreier et al. 1971) which had $\alpha = 3.8$. We associate the September spectrum with the pre-transition state. However, the Uhuru spectrum had $\alpha = 1.6$ for $9 \text{ keV} < E < 20 \text{ keV}$ indicating that the $E > 9 \text{ keV}$ spectrum underwent an increase in intensity and decrease in α in the 1970 September to December period. Thus a complete picture of the variations near the transition of 1971 April appears to involve at least three phases, A, B, and C in Figure 5, and summarized in Table II.

The transition from phase B to C has been explained by Thorne and Price (1975) as due to an increase in the "thinning radius". This caused the 2 to 10 keV spectrum to cease being produced in the optically thick outer accretion disk and begin being produced in the optically thin inner region. For phase A to fit this model, it must be due to a decrease in the thinning radius to a value such that contribution of the inner region is negligible below $\sim 100 \text{ keV}$. Although I and α varied greatly in the phases, the flux at 8 keV remained within 30% of $5 \times 10^{-2} \text{ ph/cm}^2 \text{-sec-keV}$.

The intensity decrease during the first observation period of Flight 61 has the same basic characteristic as the long time scale variations: That is, low intensity is associated with large α , the extrapolated flux at 8 keV remaining approximately constant. However, during the second observation period the opposite occurred. In particular, from 0826 to 0831 (binary phase 0.60) the 22 to 43 keV flux is only $(6 \pm 15) \times 10^{-4} \text{ ph/cm}^2 \text{-sec-keV}$, making determination of α uncertain, but requiring $\alpha < 1.45$ and a flux at $20 \text{ keV} < 5 \times 10^{-3} \text{ ph/cm}^2 \text{-sec-keV}$, at 95% confidence. Extrapolation of this upper limit spectrum to lower energies requires the 2 to 10 keV flux to be < 0.3 of the normal value. Long term monitoring by Uhuru and Ariel V have not indicated such large decreases. Absorption events have been seen by Copernicus (Mason et al. 1974) and OSO-7 (Li and Clark 1974). These cause $\sim 50\%$ reduction in the flux at a few keV with a negligible effect at higher energy. If the low flux we measured at 22 to 43 keV was

due to attenuation by Compton scattering in some region, the minimum column density in the line of sight is 2×10^{24} H atoms/cm². This becomes optically thick against absorption at 10 keV, requiring a total eclipse at lower energy. Such a phenomenon has not been reported. In any case, the low flux and hard spectrum seen at ~ 0828 represent a distinct spectral state of Cyg X-1. The corresponding low energy state has not been determined.

The sudden intensity increase at 0848 is similar to the 20 to 200 keV variations observed by Agrawal et al. (1972) in 1971 April. They also observed an X-ray flare in which the intensity doubled for a few minutes with α remaining constant. We have seen no such flares in 6 hours of observation and conclude that they are rare events.

VI. SUMMARY

We have performed a systematically consistent set of observations of Cygnus X-1 in the energy range 20-200 keV during the period 1969 June to 1972 June. The results may be summarized as follows:

- 1) If lower energy data are carefully included, the "time-averaged" (after the fashion of Thorne and Price 1975) wideband spectrum shows evidence for at least three distinct phases, differing significantly in almost all parameters considered. The inferred flux at 8 keV, however, remains relatively constant; this may be fortuitous.
- 2) During most of the observations variations above 20 keV are small on time scales of a few minutes. On 23 June 1972, however, considerable activity was observed, with variations in spectral shape and intensity being, at best, only partially correlated. Whether such variability relates to a particular "time-averaged" state is not known.

3) No significant flares were observed on time scales of a few minutes. A relatively low probability of occurrence is inferred.

4) A possible "absorption" feature was observed on 23 June 1972. If at this epoch high energy and low energy X-ray emission had a common origin the effect below ~ 10 keV would have been dramatic, but no such data are available. Coordinated wideband observations of Cygnus X-1 have obvious advantages and we recommend them.

VII. ACKNOWLEDGEMENTS

We thank Professor L. E. Peterson for his patient support. Also, thanks to everyone who aided in the UCSD balloon program over the years, especially F. Duttweiler, R. Jerde, H. Klaser, and Dr. M. Pelling.

REFERENCES

- Agrawal, P. C., Gokhale, G. S., Iyengar, V. S., Kunte, P. K.,
 Manchanda, R. K., and Sreekantan, B. V. 1972, Astrophys. and
 Space Sci., 18, 408.
- Baity, W. A., Ulmer, M. P., Wheaton, W. A., and Peterson, L. E. 1973,
Nature Phys. Sci., 245, 90.
- Bleach, R. D., Boldt, E. A., Holt, S. S., Schwartz, D. A., and
 Serlemitsos, P. J. 1972, Ap.J., 171, 51.
- Haymes, R. C., and Harnden, F. R., Jr. 1970, Ap.J., 159, 1111.
- Heise, J., Brinkman, A, Schrijver, J., Mewe, R., den Boggende, A.,
 Gronenschild, E., Parsignault, D., Grindlay, J., Schnopper, H.,
 Schreier, E., and Gursky, H. 1975, Nature, 256, 107.
- Holt, S. S., Boldt, E. A., Kaluzienski, L. J., and Serlemitsos, P. J.
 1975, Nature, 256, 108.
- Li, F. K., and Clark, G. W. 1974, Ap.J. (Letters), 191, L27.
- MacGregor, A., Seward, F., and Turiel, I. 1970, Ap.J., 161, 979.
- Mason, K. O., Hawkins, F. J., Sanford, P. W., Murdin, P., and
 Savage, A. 1974, Ap.J. (Letters), 192, L65.
- Peterson, L. E., Pelling, R. M., and Matteson, J. L. 1972, Space Sci.
 Rev., 13, 320.
- Sanford, P. W., Ives, J. C., Bell Burnell, S.J., Mason, K. O., and
 Murdin, P. 1975, Nature, 256, 109.
- Schreier, E., Gursky, H., Kellogg, E., Tananbaum, H., and Giacconi, R.
 1971, Ap.J. (Letters), 170, L21.

Tananbaum, H., Gursky, H., Kellogg, E., Giacconi, R., and Jones, C.
1972, Ap. J. (Letters), 177, L5.

Thorne, K. S., and Price, R. H. 1975, Ap. J. (Letters), 195, L101.

TABLE I

UCSD Observations of Cyg X-1
from Balloons
(20 to 200 keV)

FLIGHT	DATE	TIME (U. T.)	ORBITAL PHASE	INTENSITY (keV/cm ² -sec)	SPECTRAL PARAMETERS
46	10 June 1969	0900-1000	0.676	16.7 ± 0.7	$\alpha^* = 1.88 \pm .07$ or $E_0^\dagger = 90 \pm 8$ keV
47	17 July 1969	0400, 0720, 0930	0.239-0.279	2.7 ± 0.6	$\alpha = 1.6 \pm .5$
50	9 Sept. 1970	0445-0545	0.033	2.5 ± 0.2	$\alpha = 2.31 \pm .23$
60	11 June 1972	0930-1000	0.483	20.5 ± 1.3	$\alpha \sim 2.1$
61	23 June 1972	0516-0616 0818-0918	0.595	{ 8 to 30 } { (variable) }	$1.8 < \alpha < 2.5$ ($\alpha_{avg} = 2.04 \pm .08$) $1.2 < \alpha < 2.0$ ($\alpha_{avg} = 1.9 \pm .15$)

* $dN/dE \sim E^{-\alpha}$

† $dN/dE \sim e^{-E/E_0}/E$

TABLE II
Cyg X-1 Variations

PHASE*	DATE	α^\dagger		Intensity (keV/cm ² - sec)		
		1-10 keV	10-200 keV	1-10 keV	10-200 keV	1-200 keV
A	? - 9/70 - ?	2.6	2.4	10	3	13
B	12/21/70	3.8	1.6	50	20	70
C	4/71. (12/71-1/72)	1.5	1.5	5	30	35

* The corresponding spectra are shown in Figure 5.

† α = spectrum index; $dN/dE \sim E^{-\alpha}$.

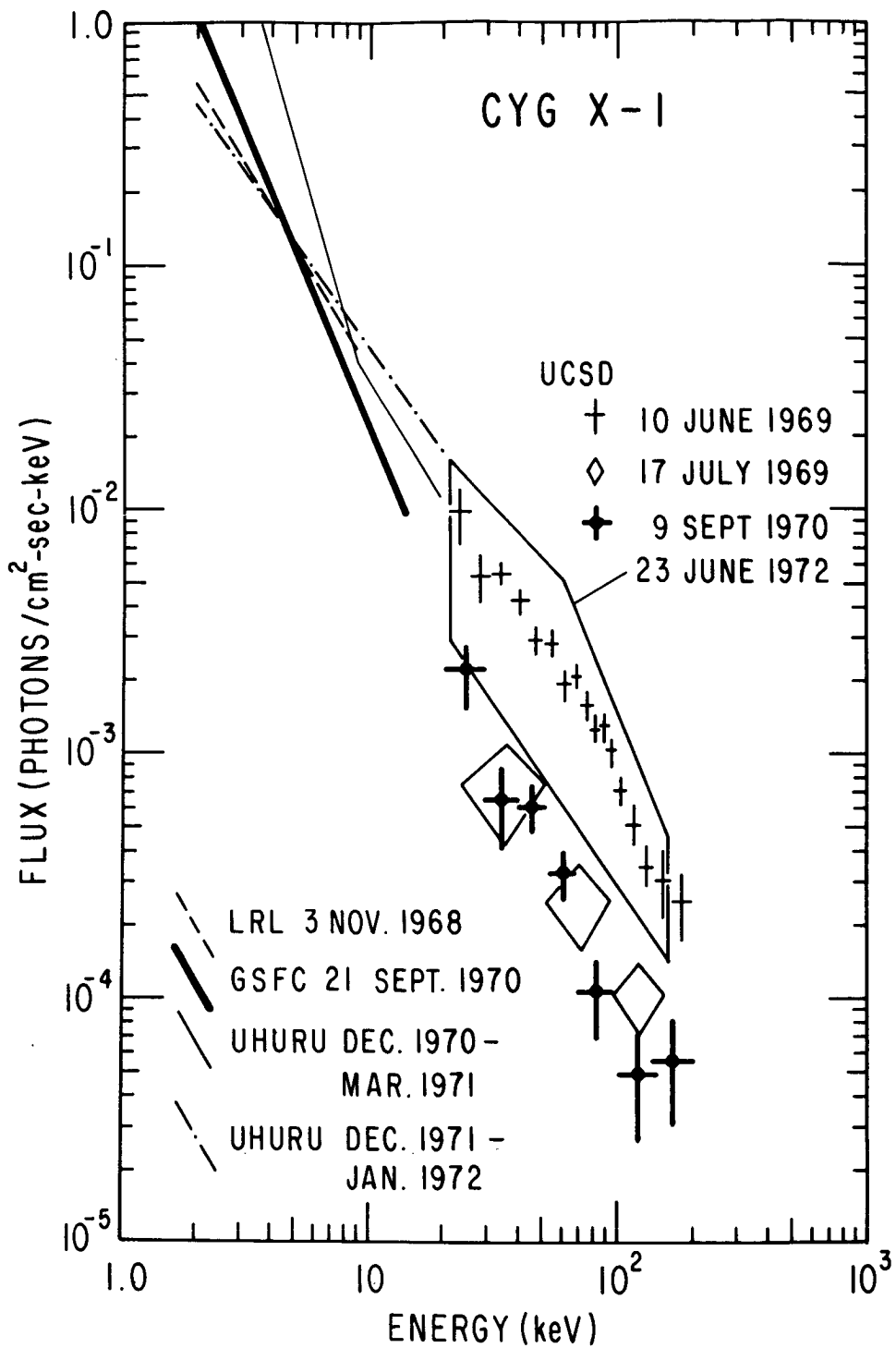


Figure 1. Photon spectra of Cygnus X-1 as measured with the UCSD balloon-borne X-ray telescope between 1969 and 1972. Also shown are relevant low energy spectra obtained by other experimenters. During the 23 June 1972 flight the source spectra varied within the limits of the boxed region.

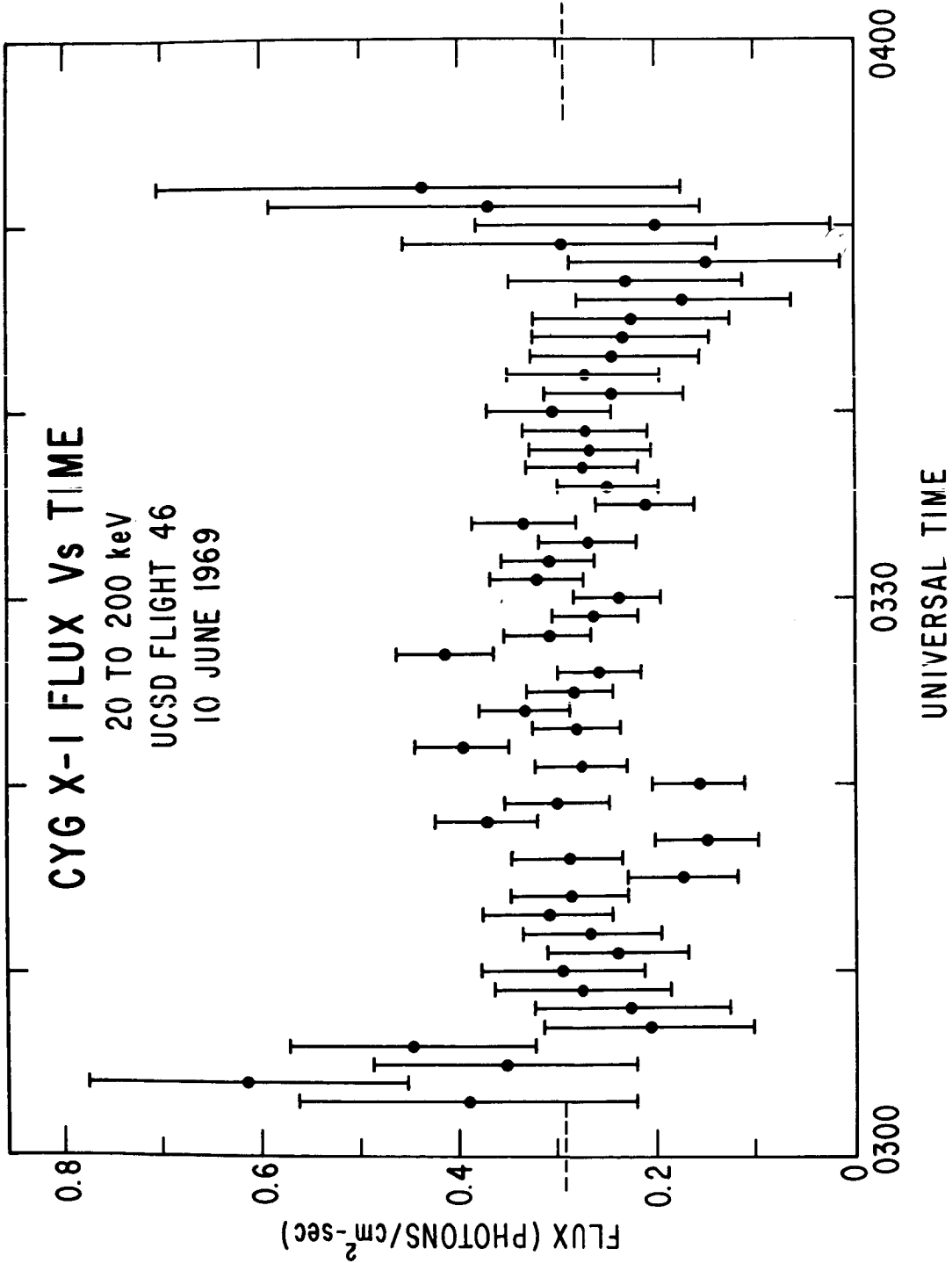


Figure 2. Cygnus X-1 data from flight 46 divided into one-minute intervals. Dotted lines indicate the flux obtained by averaging over the entire observation time.

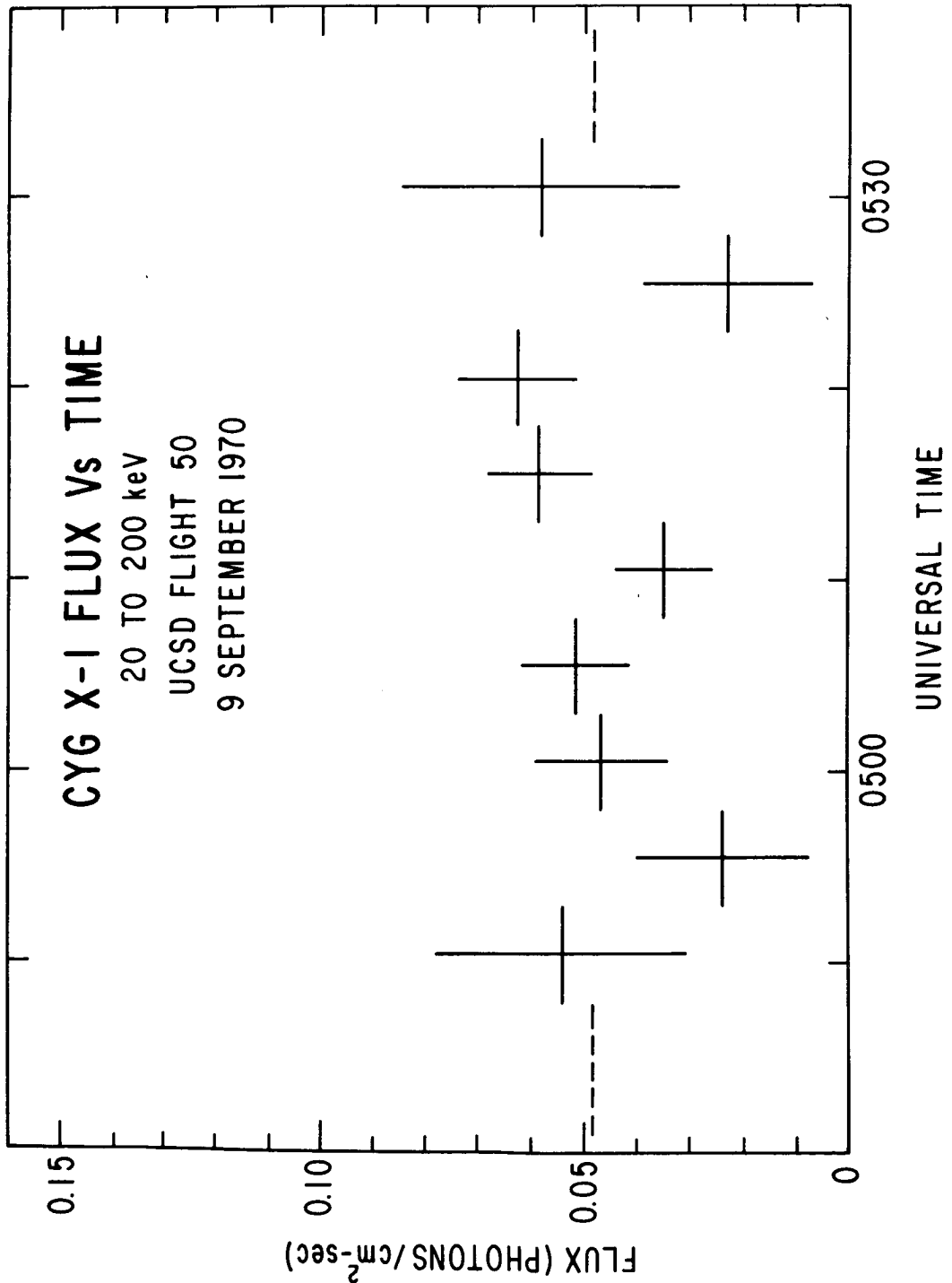


Figure 3. Cygnus X-1 data from flight 50 divided into five-minute intervals. Dotted lines indicate the flux obtained by averaging over the entire observation time.

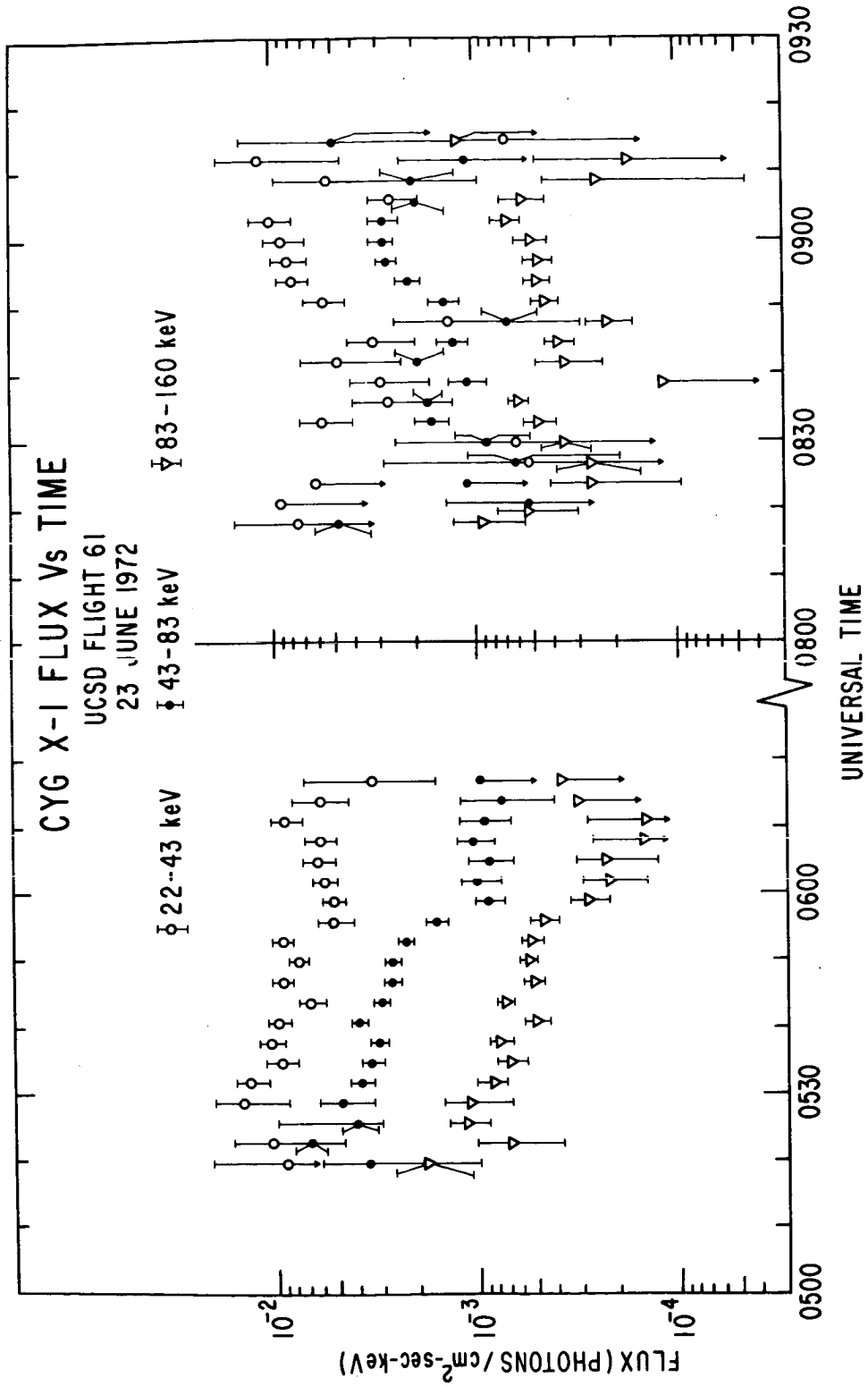


Figure 4. Cygnus X-1 data from flight 61 divided into three-minute intervals for three separate energy ranges.

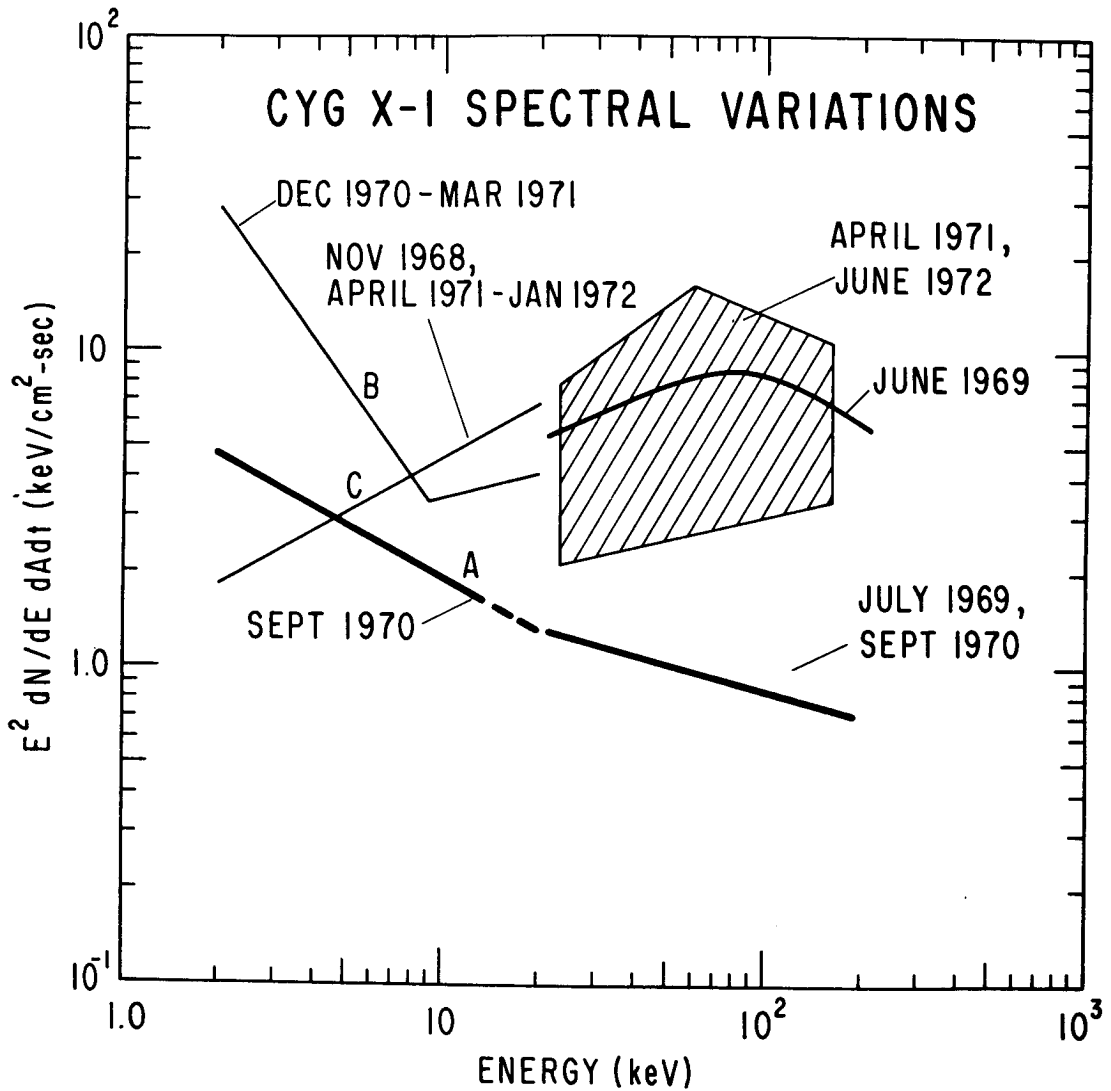


Figure 5. A summary of the observed spectral states of Cygnus X-1. The letters A, B and C refer to separate states as discussed in the text. The ordinate is $E^2 dN/dE dA dt$, the advantages of which were noted by Thorne and Price (1975).

ABSORPTION DIPS AT LOW X-RAY ENERGIES IN CYGNUS X-1

Paul Murdin

Royal Greenwich Observatory, Hailsham, Sussex, UK.*

ABSTRACT

Absorbing material in Cygnus X-1 jitters about near the line joining the two stars, out of the orbital plane.

I. THE ABSORPTION DIPS

Three more looks with the Copernicus satellite at Cygnus X-1 have produced four more examples of absorption dips - decreases in the 2 to 7 keV flux from Cygnus X-1 with an increase of spectral hardness consistent with photoelectric absorption (Mason et al 1974). The nine now seen, including one by OSO-7 (Li and Clark 1974), are listed in Table 1. Their phase in the spectroscopic binary HD 226868 is also listed, calculated from a newer ephemeris than that in Mason et al (1974), adding the radial velocities by Bolton (1975) and unpublished RGO radial velocities from the 1975 season. (These elements do not differ significantly from Bolton's (1975).)

Table 1

Nine Absorption Dips

Date (JD - 2440000)	Phase with respect to superior conjunction	Duration (phase units)	Log Column density N_H (atoms cm^{-2})
1628.4	0.00	(end seen only)	22
1684.5	+0.03	0.005	22
1818.6	-0.03	(end seen only)	22
1930.5	-0.05	0.023	24
1986.5	-0.06	0.013	23
2187.6	+0.02	0.037	22
2322.1	-0.12	0.004	23
2322.8	0.00	0.089	23
2586.5	+0.09	0.004	22

The table shows that: (i) The dips occur preferentially near to superior conjunction, when the B supergiant (B) lies between Earth and the unseen companion (X). (ii) There is significant scatter about the line joining the two stars (± 0.10 of an orbit, i.e. $\pm 35^\circ$). (iii) The angle subtended by the absorbing material at X varies from 1° to 32° . (iv) The column density varies by at least two powers of ten.

* Present address: Anglo-Australian Observatory, PO Box 296, Epping NSW 2121, Australia.

II. WHAT IS THE CAUSE OF THE DIPS?

(A) Is it the B supergiant?

A(i) Its atmosphere? (Like Cen X-3 eclipse shoulders; Pounds et al (1975).) The dips are not regular enough, can last too brief a time and the line of sight passes too high above the B star's surface (4 stellar radii).

A(ii) Prominences on B or blobs in a stellar wind ejected from B?

The prominences or blobs have the right kind of irregularities in phase angle and column density, and are distributed about the correct axis. Based on an inclination angle of 30° for the orbital plane with respect to the plane of the sky (Hutchings et al 1973), however, the prominences or blobs reach 4 stellar radii above the B star's surface in the direction perpendicular to the plane, whereas they reach less than 1 stellar radius from the B star's surface in the direction in the orbital plane. If they are part of a spherical distribution about B and the orbit were tilted by only 4 more degrees we would not be able to see them. This seems a bit arbitrary. Perhaps they could be ejected from the polar regions of B. The prominences would, however, have to be of enormous size, the largest dip subtending an angle at X almost twice as large as the B supergiant.

The two longest dips show more absorption in intensity than the increase in spectral hardness would indicate (Mason 1975, private communication), indicating that they also contain neutral electron scattering because of greater ionisation. The larger angle which they subtend at X and the greater ionisation together suggest proximity to X. At the same time the concentration of the dips to the line joining the two stars does indicate that the absorbing material knows about the B star, either because it feels its gravitational field or because it came from B and remembers this. This suggests the origin of the absorption is in:

B The gas stream? (Mason et al 1974, Bolton 1975)

B(i) Extension of the gas stream perpendicular to the orbital plane?

Because the inclination of the orbital plane to the sky is 30° (Hutchings et al 1973) and the width of the stream is not large, the absorption must take place near to X. The closest approach of the gas stream to X is $3 R_\odot$ (calculations by Lubow and Shu 1975) and at

this point the z-extension of the gas stream is $\sim 0.1 R_{\odot}$. Even given blobbiness in the gas stream it seems unlikely that a higher pressure could drive the stream to a z-extension as high as the $5R_{\odot}$ required to intersect the line of sight. The stream is, moreover, very rigidly bound to the binary star system, and is unlikely to jitter by the $\pm 30^{\circ}$ observed, unless the stream is fed by material ejected from the Lagrangian point at orbital speeds (10^3 km/s).

B(ii) Splashes of the gas stream into the z-direction as it plays onto the accretion disk at the hot spot?(Shu 1975, private communication).

If the splashes are deflected elastically by the rigid edge of the accretion disk, they could certainly reach $5 R_{\odot}$ in the z-direction, so they could intersect the line of sight. They would also splash with motion in the orbital plane. One would therefore expect a broad distribution in phase angle for the dips, upwards of 60° (c.f. the 70° observed). However the hot spot is located at 70° to the line joining the centers of the stars as seen from X, whereas the dips are distributed about the line itself.

There seem to be difficulties whichever solution is proposed, but I feel the answer to the problem of the origin of the dips is important since the dips represent a different mode of mass transfer in this binary star to the mode evidenced by the wake seen in Cen X-3 (Pounds et al 1975). The way in which the X-ray observations provide a challenge to the optical spectroscopists to continue to give phases of HD 226868 accurate to a thousandth of a revolution illustrates well the importance of the coordination of observations of these stars to which this Conference is dedicated.

REFERENCES

- Bolton, C.T., 1975. Ap.J., 200, 269.
Hutchings, J.B., Crampton, D., Glaspey, J. and Walker, G.A.H., 1973. Ap.J., 182, 549.
Li, F.K. and Clark, G.W., 1974. Ap.J. (Letters), 191, L27.
Lubow, S.H. and Shu, F., 1975. Ap.J., 198, 383.
Mason, K.O., Hawkins, F., Sanford, P.W., Murdin, P., and Savage, A. 1974. Ap.J. (Letters), 192, L65.
Pounds, K., Cooke, B.A., Ricketts, M.J., Turner, M.J., Elvis, M., 1975. M.N.R.A.S., 172, 473.

OBSERVATIONS OF CYGNUS X-1 IN ITS TWO INTENSITY STATES BY ANS

D. R. Parsignault
Space Division
American Science and Engineering
Cambridge, Massachusetts 02139

and

J. E. Grindlay, H. Schnopper, E. J. Schreier and H. Gursky
Center for Astrophysics
Harvard College Observatory and Smithsonian
Astrophysical Observatory
Cambridge, Massachusetts 02138

ABSTRACT

The hard X-ray experiment (1 - 28 keV) on ANS, observed Cygnus X-1 in November 1974, and in May 1975, putting in evidence the two dramatically different states of this object. The average intensity in November was 15 cts/sec, and the observations showed remarkable features in the X-ray light curve and in the spectrum, which were correlated with the 5.6 days period of HDE226868. The May observations showed a count rate of ~ 80-100 cts/sec, with fluctuations up to ~ 130 cts/sec, uncorrelated with the spectroscopic binary. The May X-ray spectrum was much softer than the November one, and possibly was made up of two components.

INTRODUCTION

Cygnus X-1 was observed by the hard X-ray experiment on ANS in November 1974, and later in May 1975. These two sets of observations revealed dramatically different behaviors of this object. In our November observations, we found that around the time of superior conjunction of the spectroscopic binary HDE226868, significant changes, both in the X-ray flux intensity and its energy spectrum were observed. In our May data, the average intensity had increased by about a factor 6 with respect to its November value. The intensity exhibited large fluctuations on a time scale of several hundred seconds, but the observations around the time of superior conjunction did not show the features observed in the

November data. The X-ray spectrum in May, which was much softer than in November, was found to be remarkably constant during our 8 days of observation.

THE EXPERIMENT

Cygnus X-1 was observed by ANS from 3h 36min UT, November 3, 1974, until 2h 40min, November 9, and six months later from 1h 09min UT May 1, 1975, until 17h 16min, May 8. The data presented here were obtained with the Large Area Detectors (LAD) of HXX. The instrument package has been described in detail elsewhere (Gursky, Schnopper and Parsignault, 1975).

RESULTS AND ANALYSIS

The source was observed on the average of 14 times/day, each observation lasting between a few hundred to as long as 1500 seconds.

1. The November Observations

Figure 1 shows the light curve as seen by the HXX LAD differential discriminators (1.3-7.1 keV). Most points correspond to a 256 second integration time. However, if during a given extended observation no statistical significant intensity variations were found, then the average intensity for the entire observation is shown regardless of its duration, and about 15 percent of the points in our light curve represent an integration time of over 500 seconds.

The average intensity over the six days observation was 15.6 counts/sec (corresponding to about 240 c/sec UHURU). The count rates varied between 7.2 c/sec and 24 c/sec. During that time, 3 dips in the X-ray intensity were recorded on November 4, at ~18:00 UT and on November 5 at ~8:00 UT and 17:00 UT. Figure 2 shows the intensity as a function of time during the first 2 events. Each point represents the average count rate over 64 seconds. The November 4 event lasted from about 18:30 UT to 23:40 UT at the latest when the intensity was back at 18 c/sec. The time coverage of the second dip started at ~6:00 UT on November 5 when the average intensity was about 15 c/sec. At 7:47, the X-ray intensity was at 11.4 c/sec, and it further decreased to 7.2 c/sec by 8:02. Thus, the intensity in the 1.3 - 7 keV decreased by 50 percent in about 100 minutes (Figure 2). Statistically significant intensity fluctuations were seen during that decrease. The third dip was observed primarily by the soft X-ray experiment (SXX) on board ANS. It occurred at about 17:40 UT that same day when the flux intensity was 17.8 c/sec and it decreased to 7.1 c/sec by 17:45. The count rate returned to 18.2 c/sec at 17:52.

Between November 6 and November 9 the observations showed a rather quiet period during which the maximum amplitude of the fluctuations were within ± 2.3 c/sec from the average intensity, except for one data point

on November 7 at 14:28 UT, when the intensity reached 24 c/sec.

In order to further study the intensity dips observed in the present data, we calculated the times for the inferior and superior conjunctions, starting with the orbital parameters of the spectroscopic binary HDE226868, as presented by Mason et al. (1974): phase zero equal to JD2, 441, 163.351 ± 0.100 , and the period of the system equal to 5.60096 ± 0.00038 days. As such, we found the superior conjunction ($\phi = 0$), i. e., the X-ray source behind the BO star to have occurred on 4 November 1974 at 20.54 ± 3.10 UT. This time coincided with one of the three large decreases in intensity observed by our instruments. More precisely, these minima occurred successively at $\phi = 0.00$, $+0.085$, and 0.16 (± 0.023).

We have studied the energy spectrum of the X-ray emission during these three dips. The data from the 15-channel PHA of HXX were fitted to a power law spectrum, with an absorption cutoff. A fit to a thermal bremsstrahlung spectrum gave systematically larger χ^2 . First, an "average" energy spectrum was obtained by fitting the data of 16 different observations when the intensity in the LAD discriminators were between 14.0 - 17.0 c/sec. The resulting fit gave an $\alpha = 0.58 \pm 0.04$ (keV/keV-cm²-sec), and an energy cutoff $E_a = 1.01 \pm 0.11$ keV, corresponding to an hydrogen column density of $0.5 \pm 0.2 \times 10^{22}$ atoms/cm². ($\chi^2 = 17$, for 12 degrees of freedom.) The errors quoted correspond to $\chi^2 + 3.5$ which is equal to 1 σ deviation, for 12 degrees of freedom and 3 adjustable parameters (Margon et al., 1975). Subsequently, the different spectra were compared to this "normal" spectrum.

We found that during these dips in intensity the spectrum became very hard ($\alpha = 0.0 \pm 0.2$, $E_a = 0.8 \pm 0.7$ keV) as compared to a normal spectrum. Most of the observed decrease in the X-ray flux occurred below ~ 5 keV. Figure 3 shows two typical X-ray spectra of 64 second integration time each, taken just before and in the middle of the second dip.

We further analyzed the dips in intensity in the following way: using our spectrum program which fits a given type of spectrum to the PHA data, and whose output are a spectral index and a cutoff energy, we first fixed the equivalent hydrogen column density at 7×10^{21} atoms/cm², which is the amount of interstellar matter from here to the object using Brown and Gould abundancies (1970) (Gorenstein, 1975). Then, the spectrum program's only output was the spectral index which we plotted as a function of intensity. Figure 4 shows that there definitely exists a relation between these two quantities. Conversely, if we held the energy index of the spectrum fixed at its value for a "normal" spectrum, i. e., $\alpha = 0.6$, we found a definite correlation between the intensity and the energy cutoff of the spectrum (Figure 5).

Finally, observations made near the time of inferior conjunctions showed that the X-ray spectrum was characterized by the parameters of a "normal" spectrum. In the case of the high intensity point when $I = 24.0 \pm 2.0$ (see Figure 1), $\alpha = 0.5 \pm 0.20$ and $E_a = 1.0$ keV.

2. The May Observations

Figure 6 shows the X-ray light curve obtained during our 8 days of observations, with the LAD. The data points correspond to between 256 and 640 seconds integration times. On May 1, we observed a count rate of 58 cts/sec, or about 4 times the average recorded in November, 1974. With time, we found that the intensity increased further, to about 80 cts/sec. From the same figure, we can devine some kind of an envelop which indicates that the flux had reached its maximum around May 6-7. This deduction is born out by ARIEL 5 observations (Sanford et al., 1975). During our observations, we saw large intensity fluctuations of about 30%, on a time scale of 80 sec. For example, the intensity varied on May 4, from 138 ± 4 to 107 ± 1 cts/sec. No particular features around the time of inferior or superior conjunctions were observed.

The X-ray continuum was well fitted by a power law spectrum, and the characteristic parameters E_a and α were rather independent of the intensity. An average spectrum obtained by summing up observations when $70 \lesssim I \lesssim 120$ cts/sec yielded $E_a = 0.63 \pm 0.17$, corresponding to 1.5×10^{21} atom of hydrogen/cm², using Brown and Gould abundancies, (1970), and a slope of $\alpha = 2.12 \pm 0.09$ keV. In Figure 7, a May observation of the X-ray continuum is presented together with an observation made in November, 1974, for comparison. As can be seen from this figure, the intensity increases occure below 11 keV; namely a factor of about 20, for $E \lesssim 2$ keV; $\sim \times 12$ for $2 \lesssim E \lesssim 3$ keV; $\sim \times 7$ for $3 \lesssim E \lesssim 5$ keV; and $\sim \times 3.5$ for $5 \lesssim E \lesssim 11$ keV.

DISCUSSION AND CONCLUSIONS

The average intensity 15.6 c/sec of Cygnus X-1 in the 1.3 - 7 keV energy band, as seen by ANS during 1974 November, was consistent with the low intensity state of Cygnus X-1, as seen by UHURU, i.e., 240 c/sec (Tananbaum et al., 1972).

Abrupt decreases in X-ray flux intensity, in the 1 - 7 keV energy band, as observed in our November data, had previously been reported by other authors (Li and Clark, 1974; Mason et al., 1974). The first authors reported one such event (within 0.02 of the zero phase) out of three independent observations made near the zero phase of the binary. Mason et al. made a total of seven such observations and observed four such decreases in intensity which occurred between +0.031 and -0.060 of the zero phase of the spectroscopic binary. However, one of these events was not accompanied by any spectral hardening and therefore was not considered

to be similar to the other three events. They also concluded from their data that this type of intensity fluctuation was not random across the whole phase, but was definitely correlated to the time of superior conjunction. Thus, based on all the observations reported up to now, there would seem that there is a 45 percent chance that such a dip will occur and that it will occur near the time of zero phase of HDE226868. However, this does not take into account the coverage of each of the experiments: at least, Cygnus X-1 is occulted by the Earth for about 40 minutes each 90-minute orbit. Thus, since a number of the recorded events are shorter than 30 minutes, the present data are compatible with these dips occurring during every orbital period of Cygnus X-1. Furthermore, we see dips at superior conjunction and at about 0.5 and 0.9 days following this conjunction. Because of their limited observing time in six of seven observing periods, COPERNICUS was not observing at such long times following superior conjunction (Mason et al., 1974). Thus, they could not have seen the multiplicity of dips we report here. In one other extended observation of Cygnus X-1 (Li and Clark, 1974), there was actually a 30 percent decrease in intensity observed at about 0.4 days following superior conjunction which is consistent with our second dip, although these authors did not claim this event as significant.

Our conclusion therefore is that the absorption dip phenomenon in Cygnus X-1 is a more permanent and complex phenomenon than first believed. Based on our data, it extends at least from about $\sim 0^\circ$ to 60° in the orbital phase of the binary. The cause of these events is not apparent. Since we see 3 such events within a single period, a partial eclipse by the companion star can be ruled out. A gas stream, such as would be formed by material flowing through the inner Lagrange point can also be ruled out since its effects would appear prior to the time of superior conjunction, such as is seen in Hercules X-1 (Giacconi, 1975). It is possible that we are seeing the effect of a bow shock formed by the compact object, which is the X-ray source, moving through the stellar wind of the primary.

As we have noted, and also as reported by Mason et al., Li and Clark, the straight forward analysis of the X-ray spectrum during the "dips" reveals a hardening of the spectrum as well as a deficiency of low energy photons. Thus, even though we and others call these "absorption dips," they appear to be more complex than what would be expected simply by absorption of the X-ray flux in cold gas. In actuality our data only marginally support the possibility of a spectral hardening since when we fix the spectrum index α , the minimum χ^2 do not appreciably change. In the case of a fixed $\alpha = 0.6$, we find that the maximum equivalent hydrogen column density, using Brown and Gould abundances (1970), would have been about $5^{+2}_{-3} \times 10^{22}$ atoms-cm⁻².

Alternatively, we could think of these decreases in intensity as due not to absorption effects but to changes to the source spectrum. More specifically, if we thought in terms of a 2 independent component X-ray spectrum, then the observed changes in the X-ray spectrum could be due to a change in the intensity of the soft component whose maximum is well below the threshold

of sensitivity of our instrument. In such a case, only the "tail end" of this spectrum would be visible in our detectors, and as its intensity increased so would the power index of our composite spectrum (see Figure 5).

Finally, turning our attention to the time of inferior conjunction ($\phi = 0.5$), we found no excess in the X-ray flux about its average value of 15.6 ± 0.4 c/sec. Previously, Sanford et al. (1974) had reported a cusp-shaped distribution in their light curve of six days of observation of Cyg X-1, with a maximum coinciding with the time of inferior conjunction. Their peak to peak variation in the observed intensity corresponded to ~ 30 percent change in the X-ray flux. Our upper limit to a change in average intensity, during the one day interval centered on the time of inferior conjunction is about 5 percent. Earlier extended measurements made by the UHURU satellite (Tananbaum et al., 1972) did not find such a flux maximum at $\phi = 0.5$. Thus, based on our present data and on the previous UHURU results, we feel certain that the phenomenon observed by Sanford et al. is not a regular one.

The remarkable increase in the intensity of this source observed in our May data had been first thought of as the mirror image of the April, 1971, downward transition (Tananbaum et al., 1972). This event had been characterized by (1) a decrease in intensity from ~ 1000 cts/sec to ~ 250 cts/sec (Uhuru); (2) an average X-ray spectrum whose index below 8 keV went from 3.1 to 0.45; and (3) most importantly it was accompanied by the appearance of a radio source identified with the binary system (Braes and Miley, 1971). Since that time, several observations both in the X-ray and radio bands have shown the source to be remarkably stable. That the May 1975 event is not reciprocal of the April 1971 event is evident from the fact that, although the intensity reverted to about 1200-2000 cts/sec (Uhuru), and the X-ray spectrum became much softer, the radio source flux intensity increased, and showed large fluctuations (Hjellming et al., 1975). Furthermore, observations by COPERNICUS and ARIEL 5 satellites (Sanford et al., 1975) have since shown that this high intensity state was comparatively short lived; by the end of May, the X-ray flux had more or less reverted to its pre-flare value. Based on these brief arguments, it seems that one should think of the May event as a transient event, rather than the observation of the second "quantum" state for this object.

A preliminary detail analysis of the spectra in May seems to indicate that there is a hard component present at certain times together with the low energy soft component. This component is characterized by $\alpha \lesssim 0.5$. Quantitatively, it is seen from Figure 7, for example, that the X-ray spectrum about ~ 11 keV is essentially the same as for the November observations. At present, we hope to refine this analysis, after our PHA has been recalibrated, using our observations on the Crab Nebula of this past September.

ACKNOWLEDGMENTS

This work was supported in part by NASA contracts NAS5-11350 and NAS5-23282.

REFERENCES

- Braes, L. L. E., and Miley, G. K., Nature, 232, 246, 1971.
- Brinkman, A. C., J. Heise, and C. deJager, Philips Tech. Rev. 34, 43, 1974.
- Brown, R. H., and R. J. Gould, Phys. Rev. D 1, 2252, 1970.
- Giacconi, R., 7th Texas Symposium on Relativistic Astrophysics, December 1974 (to be published).
- Gorenstein, P., private communication, 1975.
- Gursky, H., H. Schnopper, and D. Parsignault, Astrophys. J. (Letters), 201, L127, 1975.
- Hjellming, R. M., D. M. Gibson, and F. N. Owen, Nature, 256, 112, 1975.
- Li, F. K., and G. Clark, Astrophys. J. (Letters) 191, L27, 1974.
- Magon, B., M. Lampton, S. Bowyer, and R. Cruddace, Astrophys. J. 197, 25, 1975.
- Mason, K. O., F. J. Hawkins, P. Sanford, P. Murdin, and A. Savage, Astrophys. J. (Letters) 192, L65, 1974.
- Sanford, P. W., K. O. Mason, F. J. Hawkins, P. Murdin, and A. Savage, Astrophys. J. (Letters) 190, L55, 1974.
- Sanford, P. W., J. C. Ives, S. J. Bell Burnell, K. O. Mason, and P. Murdin, Nature, 256, 109, 1975.
- Tananbaum, H., H. Gursky, E. M. Kellogg, and R. Giacconi, Astrophys. J. (Letters) 177, L5, 1972.

CYGNUS X-1, X-RAY LIGHT CURVE
SEEN BY ANS, NOV. 1974

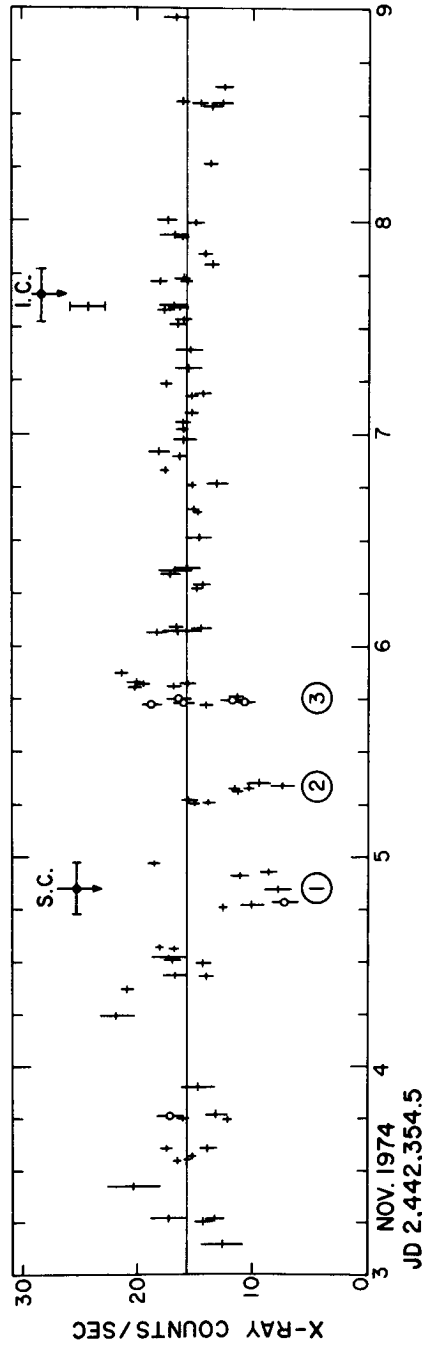


Figure 1. Cygnus X-1 ray light curve (1.3 - 7.1 keV) as observed by the HXX (+) from November 3 until November 9, 1974. The average count rate shown by the solid line is 15.6 ± 0.4 c/sec. The error bar on each point equals $\pm 1\sigma$. The points mark (ϕ) were observed by the soft X-ray Detector, of Utrecht University.

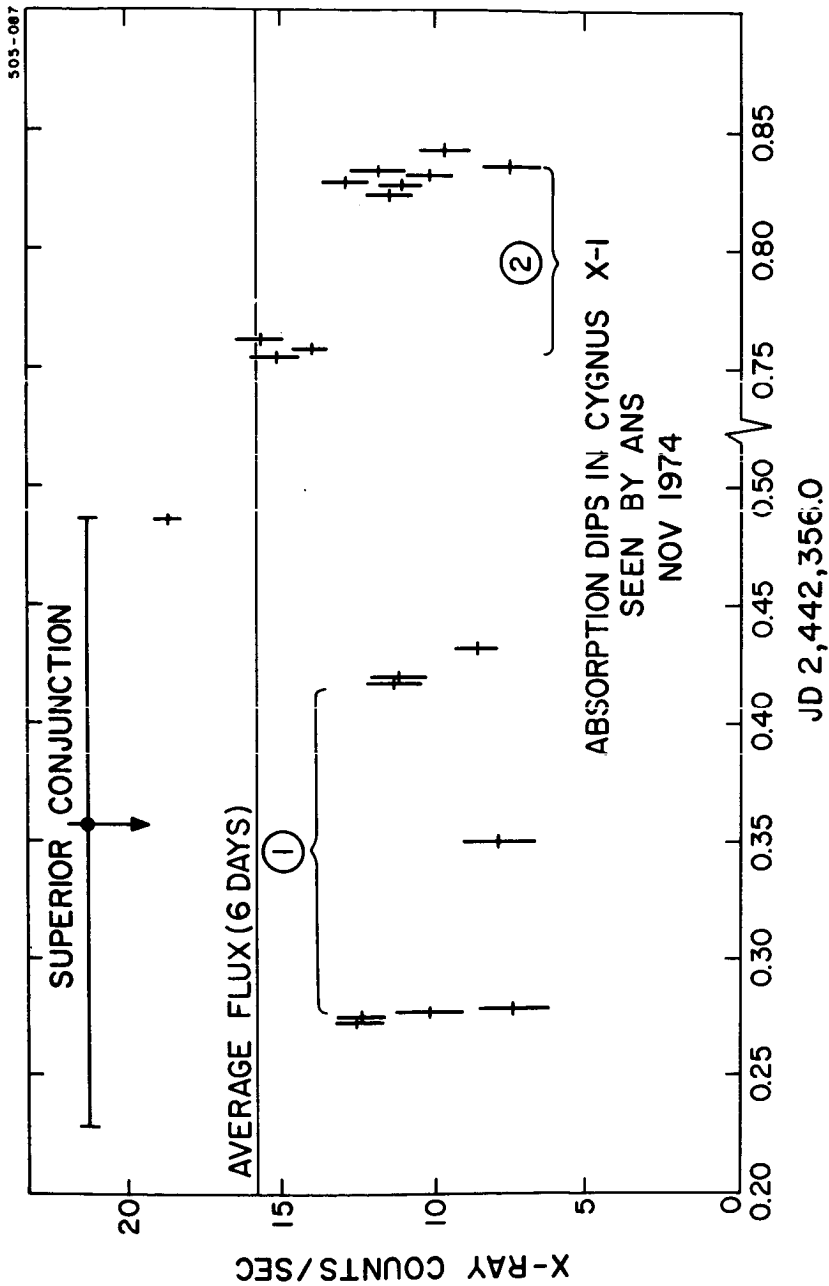


Figure 2. Details of the X-ray light curve around the time of superior conjunction of the spectroscopic binary HDE226868. Each point corresponds to the count rate averaged over a 64-second period, and the error bars = $\pm 1\sigma$.

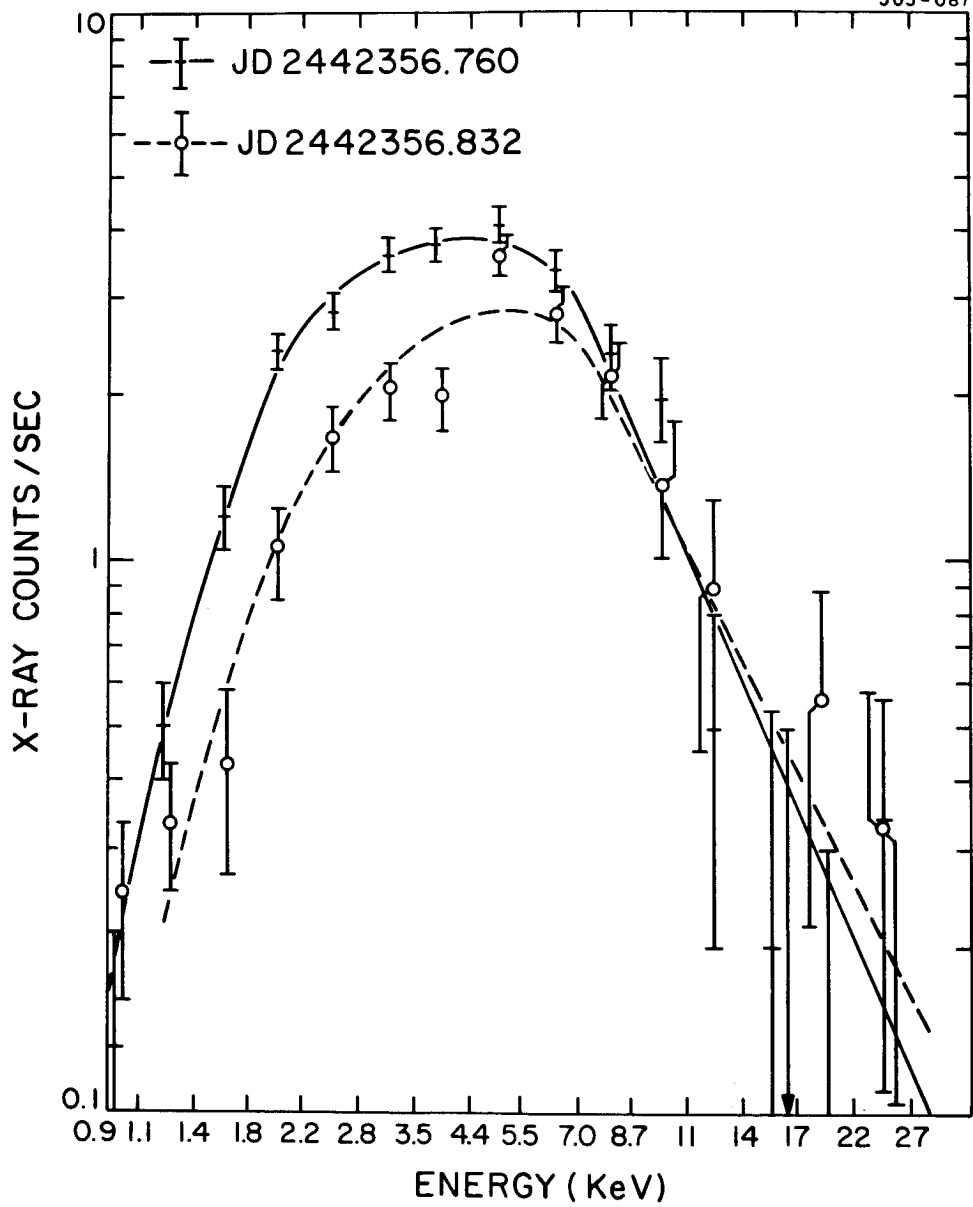


Figure 3. Two X-ray spectra taken before and during the dip in intensity on November 5, 1974, around 8:00 UT.

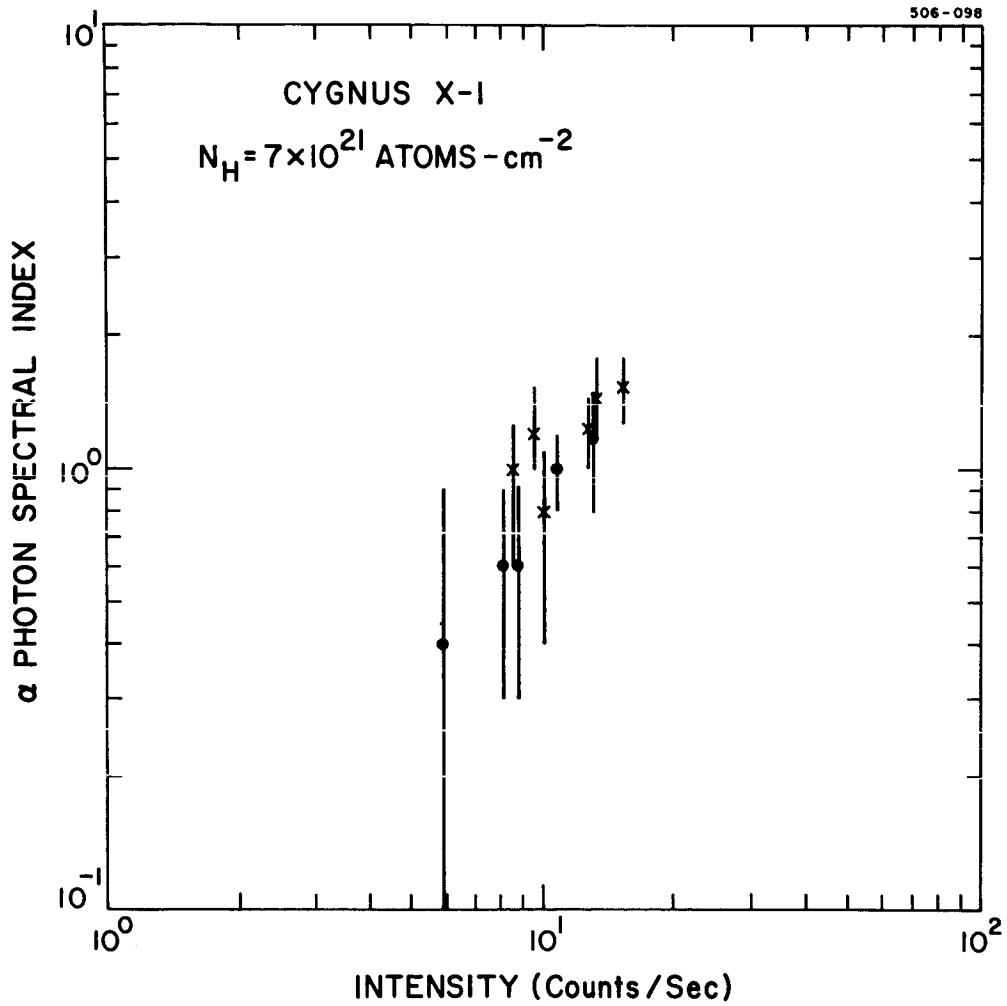


Figure 4.

Photon spectral index versus X-ray intensity at $\phi = 0.0$ (\circ) and $+0.16$ (\times). The column density is held fixed at $n = 7 \times 10^{21}$ atoms/cm². The error bars represent a 90 percent confidence level in the χ^2 fits.

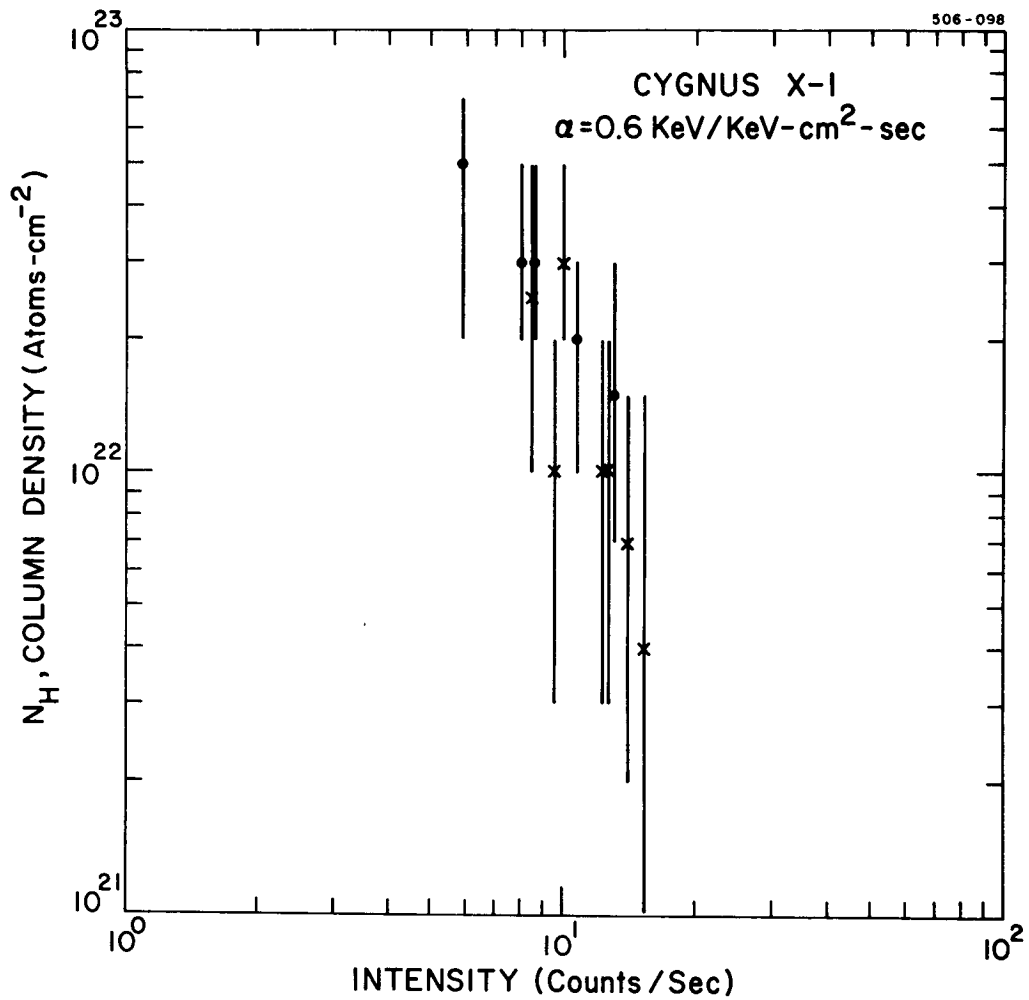


Figure 5. Column density versus intensity at $\phi = 0.0$ (ϕ) and $+0.16$ (x). The energy spectral index was held fixed at 0.6. The error bars represent a 90 percent confidence level in the χ^2 fits.

CYGNUS X-1, X-RAY LIGHT CURVE
 SEEN BY HXX, ON ANS, MAY 1975

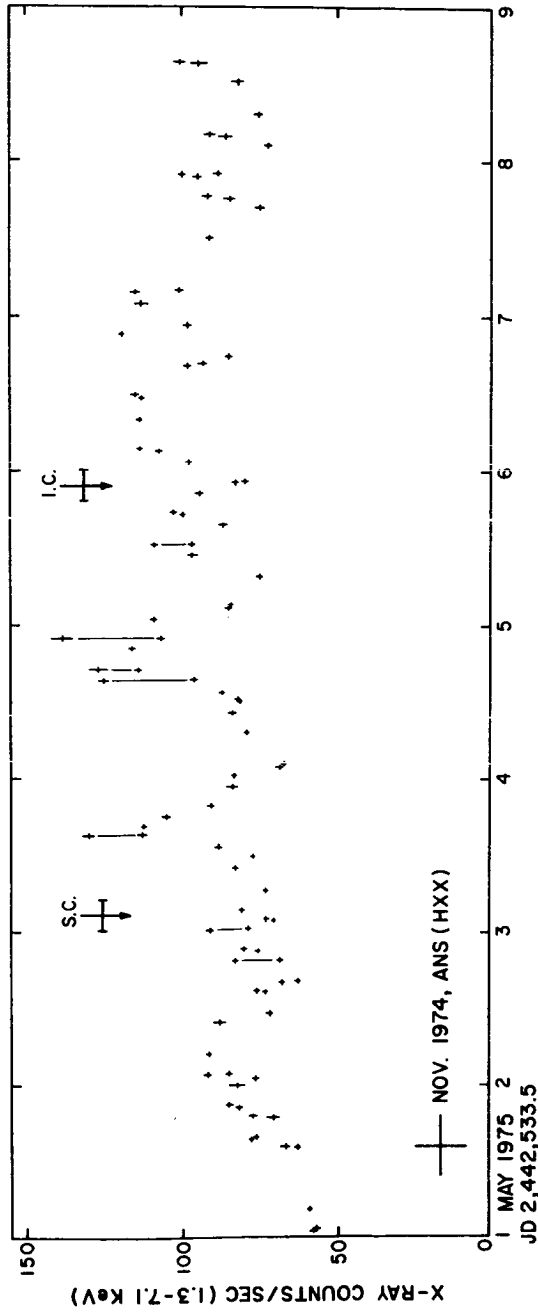


Figure 6. Cygnus X-1 X-ray light curve (1.3 - 7.1 keV) as observed by the HXX from May 1 until May 8, 1975. The error bar on each point equals $\pm 1\sigma$. The thin lines connecting two data points indicate sequential observations.

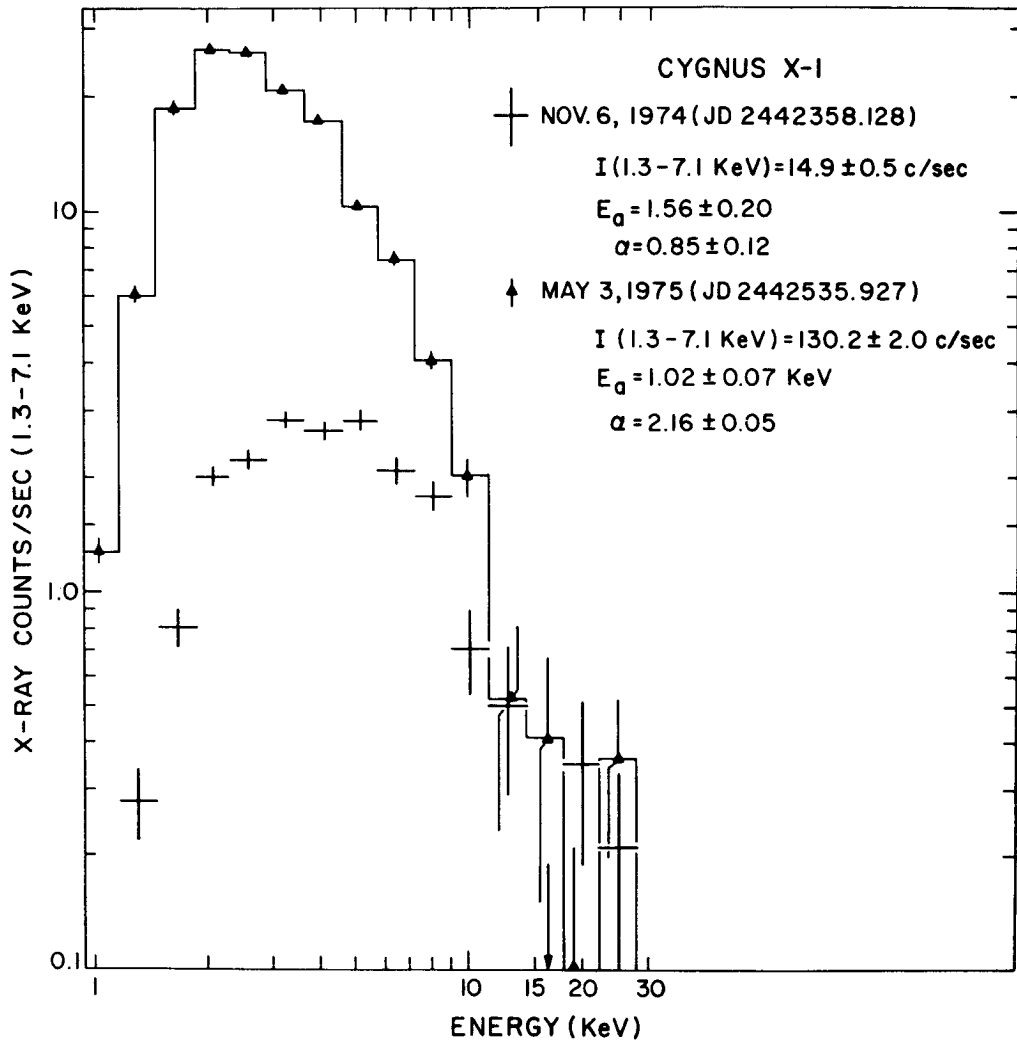


Figure 7. X-ray spectra as observed by HXX on November 6, 1974, and May 3, 1975.

HIGH RESOLUTION MEASUREMENTS OF CYG X-1 FROM ROCKETS

R. E. Rothschild, E. A. Boldt, S. S. Holt, and
P. J. Serlemitsos
NASA/Goddard Space Flight Center
Greenbelt, Maryland 20771

ABSTRACT

Cyg X-1 was observed on two occasions (Oct. 4, 1973 and Oct. 3, 1974) by the Goddard X-ray rocket payload. This payload consisted of two gas proportional counters (xenon-methane with 710 cm² and argon-methane with 610 cm²) using the same 128 channel pulse height analyzer and having 320 μ s temporal resolution on the 1973 flight and 160 μ s resolution on the 1974 flight. During both flights bursts of 1 ms duration were observed with very high statistical certainty. To date all 13 of these bursts have been analyzed for spectral and temporal character, and the results of this analysis will be presented. The spectra of overall x-ray emission from both flights will also be presented. In a source known for its variability it is remarkable that the spectra taken one year apart are virtually identical.

The Goddard x-ray group has observed Cyg X-1 on two occasions (Oct. 4, 1973 and Oct. 3, 1974) with our high resolution rocket payload. This payload consists of two multilayer, multiwire gas proportional counters - one containing xenon-methane and the other argon-methane giving an energy range of 1.5 - 35 keV with 128 channel pulse height analysis. Our basic temporal resolution was 320 μ seconds on the 1973 flight and 160 μ seconds on the 1974 flight with some information on even finer resolution that I'll speak of later. The Figure 1 shows the counting rate versus time for the 1973 flight. We pointed at Her X-1 for about a minute then scanned over to Cyg X-3 and pointed for about forty seconds. Finally we scanned over to Cyg X-1 and held until the doors closed exposing a calibration source a minute later. The count rate profile is quite chaotic. It resembles neither the regular pulsar profile of Her X-1 nor the constant rate profile of Cyg X-3. The mean rate of Cyg X-1 varies on most any time scale you wish to pick - be it milliseconds or months. It is just this chaos when Fourier analyzed over the short duration rocket observations that yielded a different periodicity for each exposure. This mystery was explained by Terrell who showed that randomly occurring overlapping pulses of a fraction of a second duration could replicate this chaos. This "shot-noise" picture of the variable mean intensity seems to work well in explaining the variability in the fraction of a second to tens of seconds time scale. Before I get into the high resolution temporal results, I would like to show the spectra of Cyg X-1 from these two exposures. The Figure 2 shows the photons per square centimeter second keV for the 1973 exposure (Flight 13.010) and the 1974 exposure (26.037) as a function of energy in keV. As you can see these two spectra, taken a year apart yet at the same orbital phase (.17), are remarkably similar.

They are identical except that the 1974 spectra has slightly harder spectrum beyond 10 keV. The fit to these spectra yields a power law of $E^{-1.55}$ with an upper limit of 3×10^{21} H atoms/cm² of cold interstellar absorption in the line of sight. We are not very sensitive to such low amounts of absorption - hence we can only give an upper limit. It is quite extraordinary for a source with such wild temporal behavior to exhibit such stability in spectral shape over a year's time.

Now I would like to turn to the millisecond temporal behavior of this source. During one of the periods of enhanced activity of the 1973 exposure three bursts of about one millisecond duration occurred within 20 mseconds. They are shown in Figure 3. This shows the count rate binned every 640 μ seconds for 80 mseconds. The three bursts are shaded. After seeing these we searched the entire exposure to Cyg X-1 for others. Five more were found for a total of eight where a Poisson distribution of counts would have predicted less than one. In order to confirm their existence our 1974 exposure looked at Cyg X-1 for 180 seconds. Five more bursts were discovered where random statistics would have predicted less than one. In a combined 230 seconds of exposure we have seen 13 bursts where slightly more than one would have been expected based on the count rate. We also searched for counts beyond expectation in time bins down to 160 μ s and up to 5 mseconds and nothing was found beyond prediction that hadn't been seen at one millisecond. Since burst determination depends on the local mean rate, we are less sensitive to a given height burst during times of enhanced activity.

One of the first questions that needs to be answered is whether or not there is any structure within a burst. Scrutinizing individual bursts for structure is useless due to the statistical uncertainties associated with so few counts. Instead we created a mean burst profile by aligning the centroids of each burst - this being the only reference available. Figure 4 shows $3\frac{1}{2}$ ms of this composite profile centered on the bursts for the 1974 flight that had 160 μ s resolution. The bins are 160 μ s wide. No significant structure is obvious. The dotted line shows the expected profile for a one millisecond rectangular burst containing the same number of counts as the composite. When twelve of the thirteen bursts are combined by aligning the centroids with 320 μ second resolution the result is shown in Figure 5. Once again the dotted line is a one millisecond rectangle containing the same number of counts as the 12 bursts here. Once again, no hint of any internal structure.

The 1974 flight also contained data that could provide information on internal structure of bursts. This data was related to bunching of counts as close together as 3 to 5 μ seconds and 5 to 50 μ seconds. Such bunching might then be indicative of substructure within a burst, which in turn could in theory yield values for the angular momentum of the collapsed object. This data was compared with data taken using radioactive sources to simulate the burst intensities. In all but one case the bursts showed no significant internal structure down to 3-5 μ s. But there was an exception. One burst, the most intense of the 13, and in fact the hardest one spectrally, had structure. There was definite evidence for bunching on the 3-5 μ second scale and a deficiency of counts in the 5 to 50 μ s range. Due to the anomalous nature of this burst, it was not included in the centroid-aligned burst profile on the screen.

We would like to know something of the energy spectrum of these bursts, but as with the temporal data, statistics are quite poor. There are only 53 pulse height values or counts in the 13 bursts. Building a spectra from this would be plagued by statistical uncertainties to say the least. We have calculated instead the mean observed energy of each burst along with its formal uncertainty. We have also done this for the overall emission. The result is that the observed mean energy of the bursts is less than that of the overall emission when the anomalous burst is not included in the sample, by $2\frac{1}{2}\sigma$. The mean observed energy of the 8 bursts from the 1973 flight agrees with that of the 1974 flight within experimental uncertainty. The anomalous event is harder than the overall emission, but its uncertainty is quite large and is consistent with both the overall emission mean energy and that of the other 12 bursts. Perhaps the bursts are appreciably softer than the overall emission. It would be difficult for us to say since our detector response tends to flatten the response of the mean energy observed to various spectral indices.

Finally we can plot the mean burst energy versus burst intensity. This is shown in Figure 6. The point at 18 counts with the asterick is our anomalous event. It seems to be in another class from the others. Hence, ignoring that point, we see no drastic variation in mean energy with burst intensity.

In conclusion we have again shown that Cyg X-1 is a source for everyone. It exhibits much temporal structure, yet its spectrum did not from 1973 to 1974. It has millisecond bursts that show no internal structure, yet its largest one did. If one uses the accretion disk calculations of Shakura and Sunyaev and if one assumes a non-rotating compact object (Schwarzschild metric) a mass of $10 M_{\odot}$ fits well. The emission region for the bursts is less than 100 km, thus ruling out white dwarfs. This evidence, combined with recent mass determinations points toward the black hole nature of Cyg X-1.

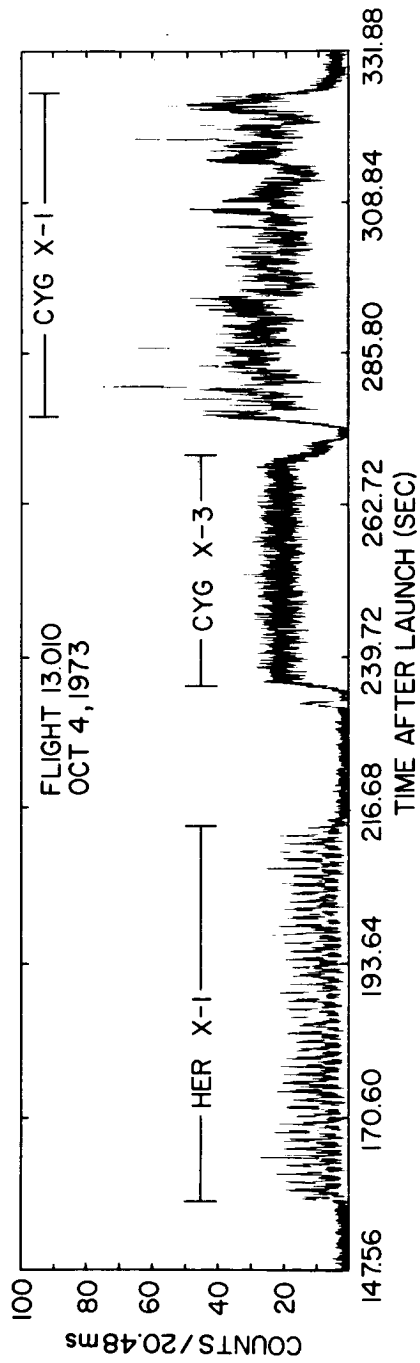


Figure 1: Temporal profile of Oct. 4, '73 flight, with the vertical axis being counts per 20.48 ms and the horizontal axis being time after launch in seconds.

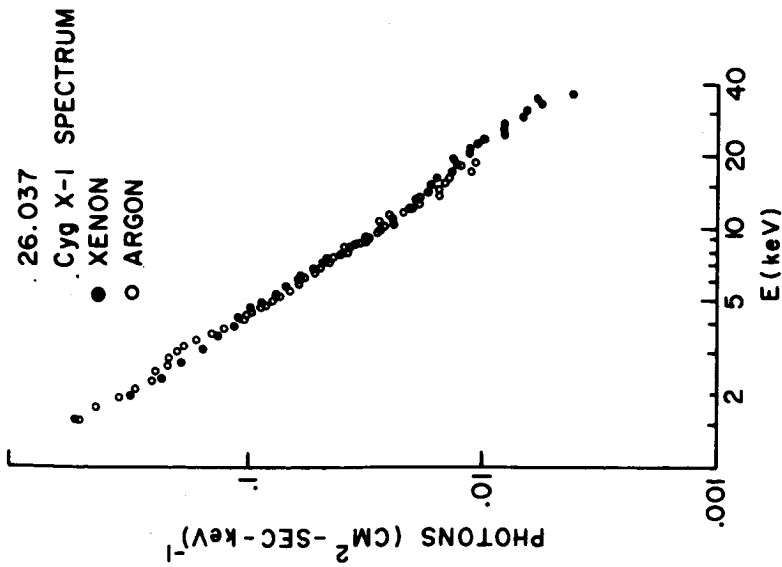
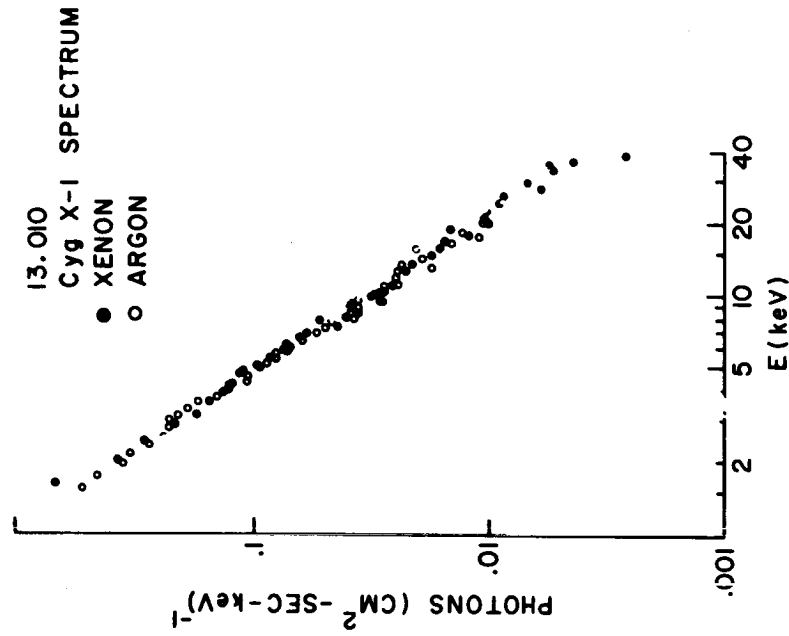


Figure 2. Spectra of both flights given in photons per cm²sec-keV versus energy for both the argon and xenon detectors. The Oct. 3, '74 spectra are on the left and Oct. 4, '75 spectra are on the right.

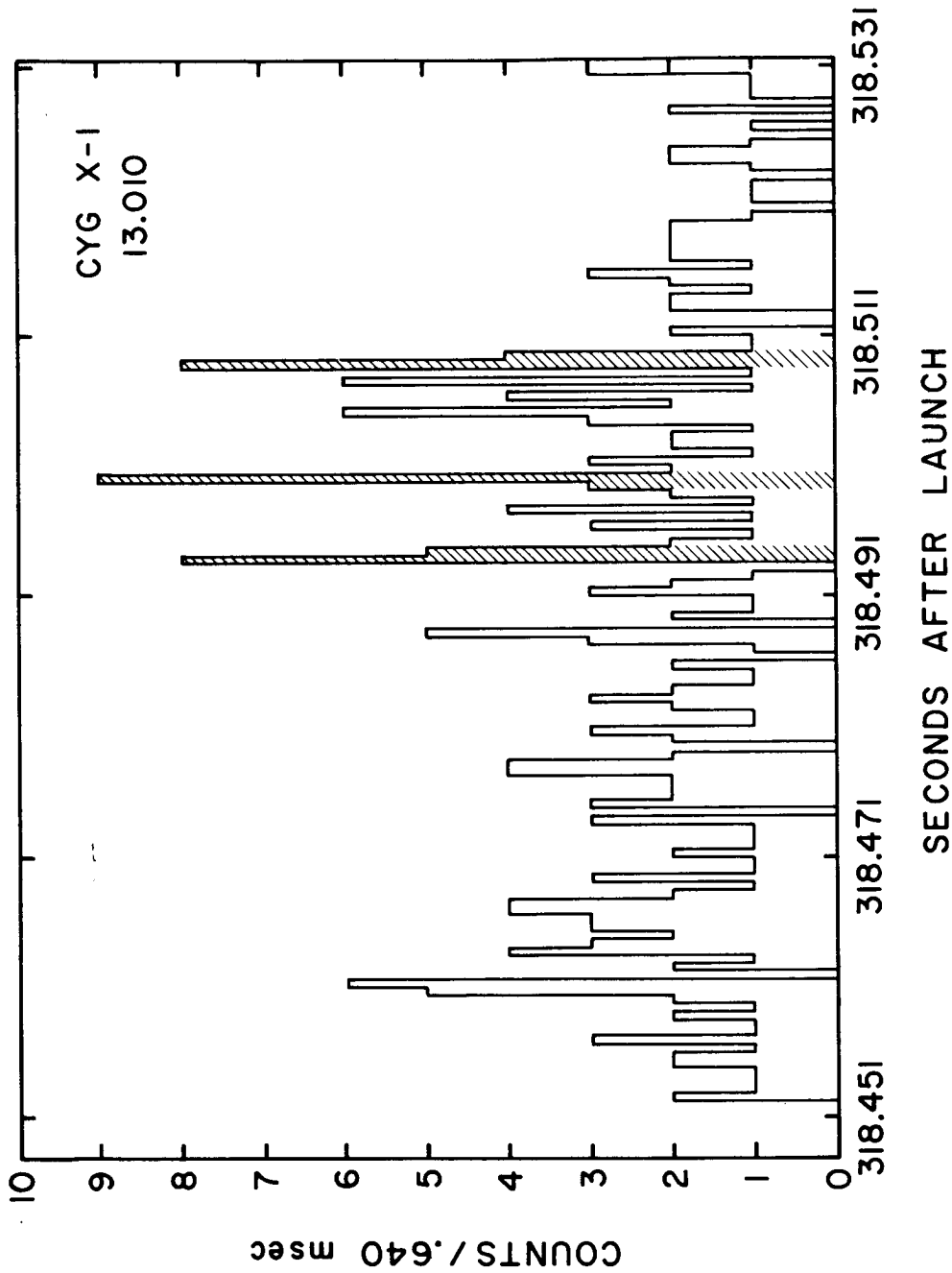


Figure 3. Eighty-two milliseconds of raw temporal data containing three one millisecond bursts (shaded) from the Oct. 4, '73 flight.

CENTROID-ALIGNED BURST PROFILE
26.037, CYG X-1

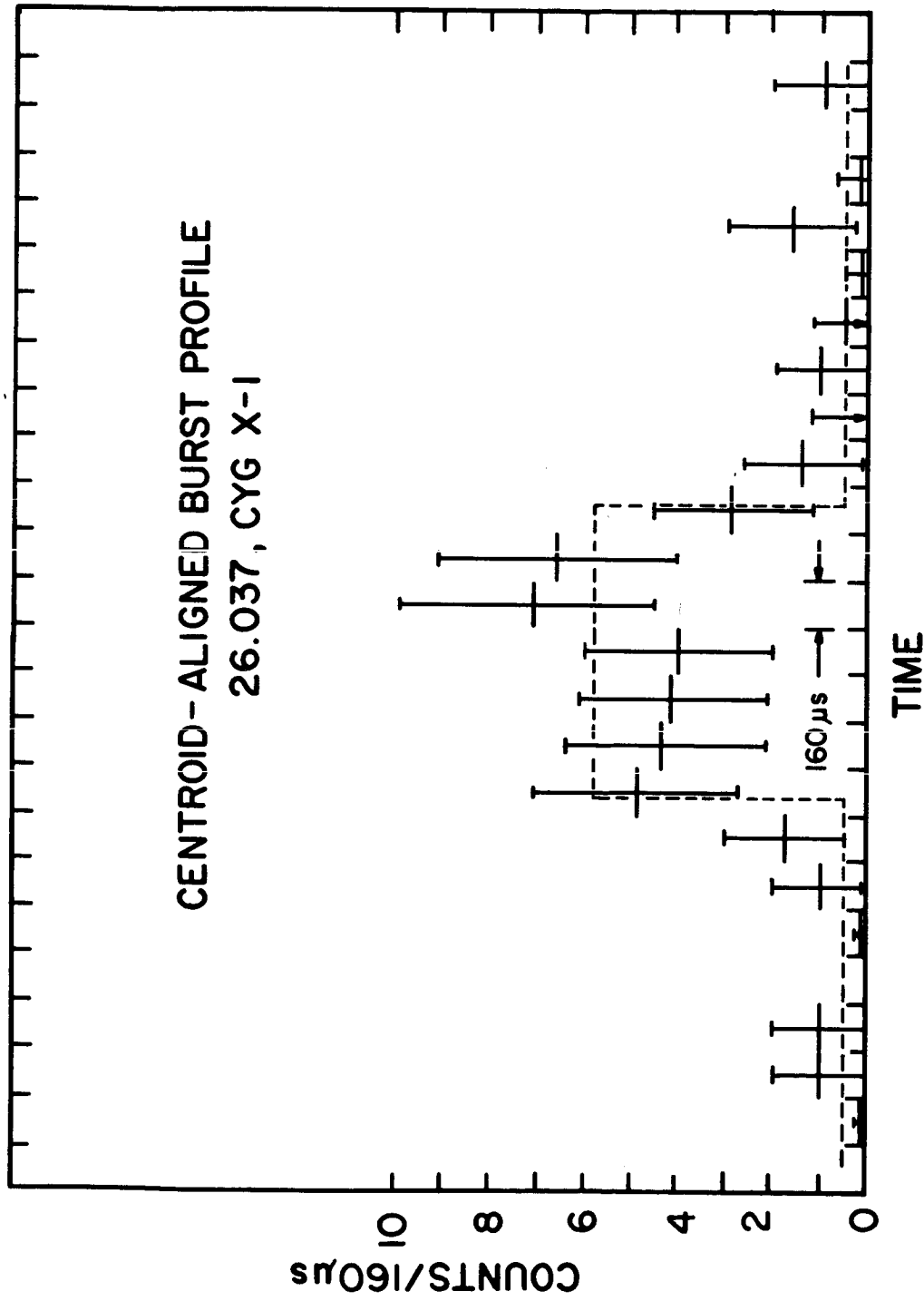


Figure 4. Centroid-aligned burst profile for the Oct. 3, '74 flight. The temporal bins are 160 μ s wide and represent 4 superimposed bursts. The dotted line represents the expected burst profile from a 1ms wide rectangular burst containing the same number of counts as the four observed bursts.

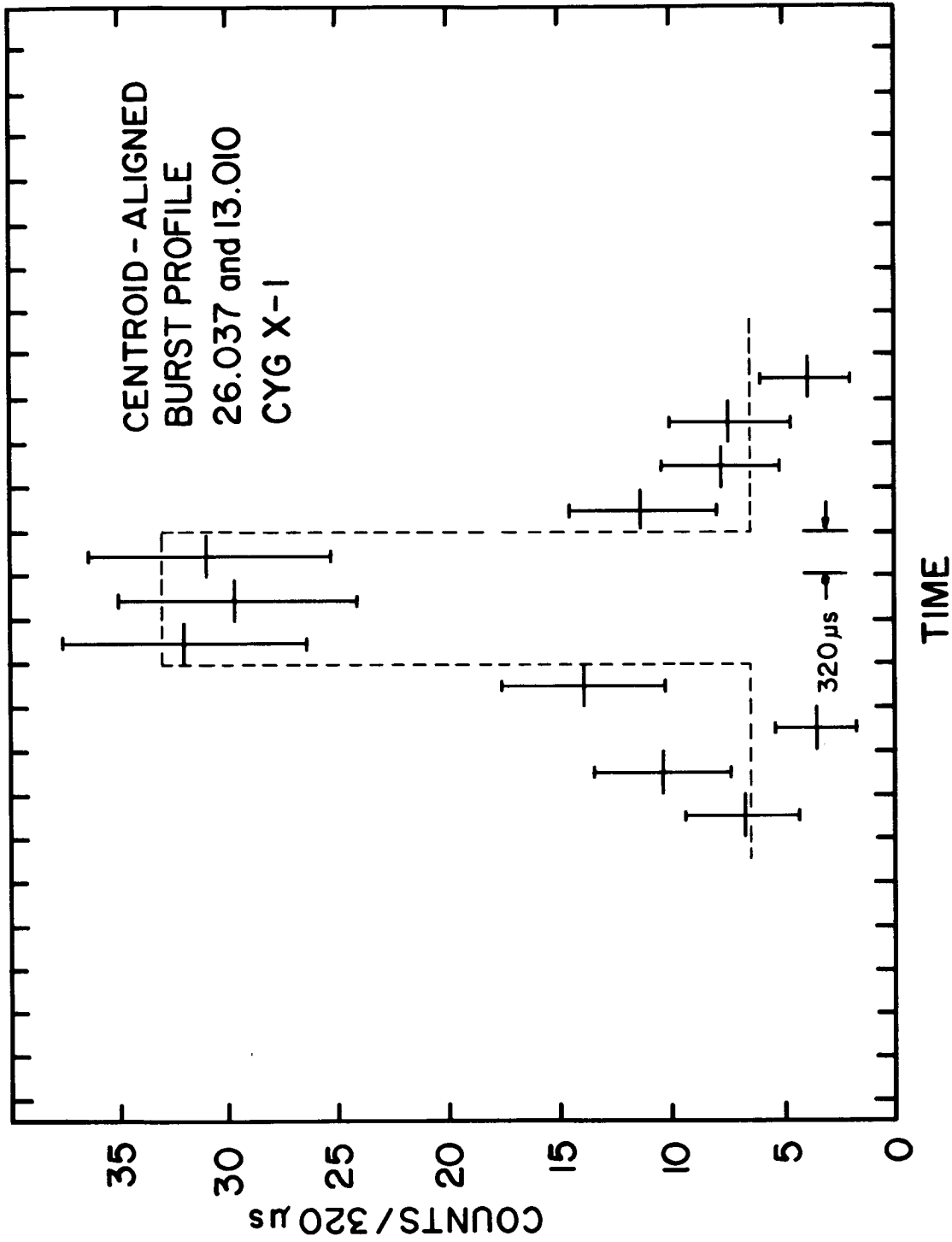


Figure 5. Centroid-aligned burst profile for the 12 bursts seen in both flights. The temporal bins are 320 μ s wide. The dotted line represents the expected burst profile from a 1 ms wide rectangular burst containing the same number of counts as the 12 observed bursts.

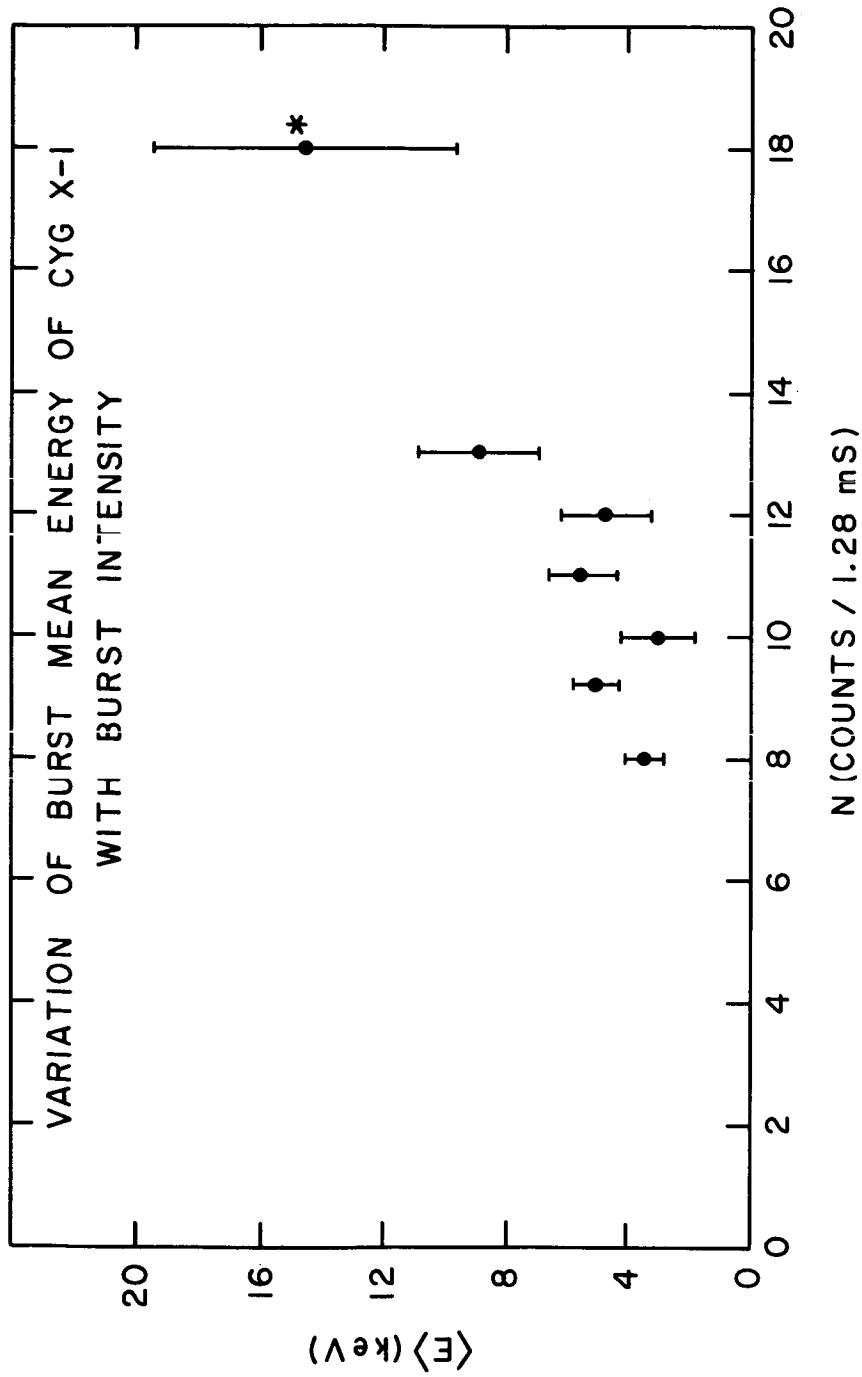
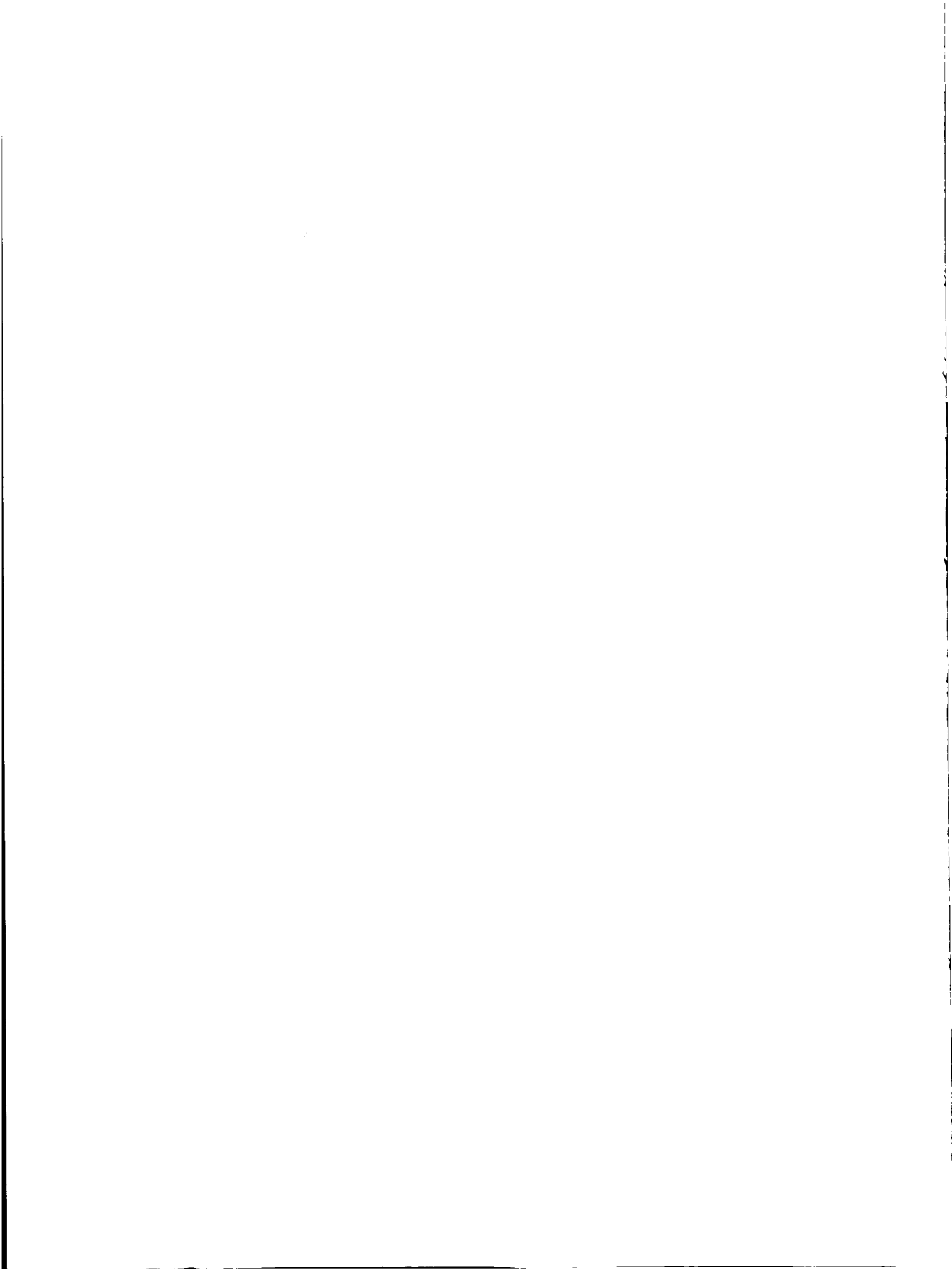


Figure 6. Variation of Burst Mean Energy with burst intensity. Mean energy in keV is plotted versus counts per 1.28 ms. The asterisk denotes the anomalous burst referred to in the text.



THE TIME VARIABILITY OF CYGNUS X-1

M. C. Weisskopf
Columbia Astrophysics Laboratory
Departments of Astronomy and Physics
Columbia University
New York, New York 10027

ABSTRACT

The shot-noise character of the short-term time variations of Cyg X-1 is reviewed. Evidence for the systematic variation of these parameters with the binary period is presented.

INTRODUCTION

In this paper we shall present a tentative result concerning the long-term variations of certain characteristics of the X-ray flux from Cyg X-1. Before we do this, however, it will be useful to review the work we have done concerning the short-term time variations of the flux from this object.

SHORT-TERM TIME VARIABILITY

In Figure 1 we show the mean autocorrelation function and corresponding power density spectrum obtained from 71 *Uhuru* observations of the source with the wide-field detector in 1972 January. These results have already appeared in the literature (Weisskopf, Kahn, and Sutherland 1975) and will only be reviewed here. The dashed lines in Figure 1 indicate the measured values of the functions shown, and the solid curves are the results corrected for the bias introduced by the photon counting statistics as described in our paper. The solid curves thus describe the time variability of the source itself.

Briefly, our results are as follows: (1) The average autocorrelation function and its corresponding power density spectrum, shown in Figure 1, are clearly not consistent with a white-noise or periodically pulsed source. (2) Furthermore, the shape of the autocorrelation function, essentially a simple exponential with an e folding time of 0.45 sec, is a classic example of what would be produced by a randomly pulsed or "shot-noise" source with exponentially decaying shots. This apparent behavior would be a natural consequence of the formation of local "hot" spots in an accretion disk or volume. (3) We find *no* evidence for any energy dependence in the autocorrelation function or power density spectrum. (4) We find a 100-percent correlation in time on the scale of the time resolution of the experiment (0.2 sec) between events in different energy bandwidths. This result would indicate that the hot spots or flares that give rise to the low- and high-energy photons have a common source. (5) When we compare our results with other similar analyses of data

obtained since the spectral transition of 1971 March (and previous to the recent variations reported this year), we find (once the effects of counting statistics are taken into account) that the results are in agreement and indicate that the seemingly *random* time variability is in fact a *steady* feature of this source.

The numerical parameters, i.e., the rate of occurrence of the shots (20 sec^{-1}) and their decay time (0.5 sec), are constant over time scales of the order of months. This fact would indicate that they are candidates for physical time constants intrinsic to the source emission mechanisms. We note further that these results are consistent with the qualitative features of most of the accretion disk models which invoke X-ray emission from two distinct regions: an optically thin, inner region from which the high-energy flux emanates, and an optically thick, outer region from which the lower-energy flux is emitted. The time-variable component of the X-ray flux in the 2–16 keV bandwidth that we have examined is clearly from a single region as the 100-percent cross correlation indicates. This result is consistent with the hypothesis that the relative intensities from the two regions shifted dramatically during the spectral transition of 1971 March. The spectral slope of the post-transition spectrum and the high-energy component of the pre-transition spectrum are identical, which would further indicate that we are observing the flux from the optically thin, inner region.

LONG-TERM TIME VARIABILITY

In addition to examining the short-term time variations of Cyg X-1, we have also examined the long-term (~days) time variations of several parameters over the 12 days spanned by the 71 observations. Of especial interest, of course, are variations occurring at the 5.6-day binary period detected from the optical counterpart. It is difficult to draw any definite conclusions because the data span is limited to 12 days and fluctuations due to counting statistics dominate each individual observation. Nevertheless, we have examined the long-term time variations of the following variables.

1. *The Background*

The sample spectrum of the background for each observation is shown in Figure 2. This spectrum is perfectly consistent with white noise and indicated to us that, despite the nonuniform data sampling, the data were not subject to gross systematic effects in the resulting power spectrum. This conclusion was also confirmed by means of the Monte Carlo simulations with white-noise sources.

2. *The Mean Count Rate per Observation*

The mean count rate per observation for these observations, corrected for the spacecraft attitude, is shown in Figure 3. Even in this rather limited data set, we see variations in flux by as much as a factor of four. The three error bars shown in the figure represent, respectively, the typical statistical

uncertainty based on the flux variations in each observation (σ_1), the typical uncertainty in the intensity resulting from the uncertainty in the aspect correction (σ_2), and finally, the uncertainty based on the scatter of the data about the mean (σ_3). The fact that the latter is almost three times larger than the former two indicates of course that these intensity variations are not consistent with those expected from a Poisson distribution.

This can be seen more clearly from the resulting power spectrum in Figure 4 where there are three peaks, each of probability of chance occurrence of 5×10^{-3} or less. In fact, these results make extremely unlikely that the long-term variations follow a white-noise process (with variance σ_3^2) as the probability of obtaining such peaks by chance is inordinately small. We are then faced with the following possible conclusions: (a) the long-term variations are consistent with those due to a white-noise source, and we happened to have observed the highly improbable chance occurrence of three statistically significant peaks in the power spectrum, or (b) in general, the source is a white-noise source, and two or even all three of the peaks in the power spectrum are indicative of a periodic process. Unfortunately, we have no *a priori* reason for singling out any of the periods of 3.6, 2.8, and 1.6 days for any special significance. We do find it interesting, however, that the 2.8-day variation, shown superimposed on the data in Figure 5, is *in phase* with the 2.8-day variations observed in the intermediate band *b*-magnitude of the visible companion HDE 226868 (as reported, e.g., by Lester, Noit, and Radostitz 1973). (c) The most reasonable interpretation, however, is that the long-term variations are describable by some unidentified stochastic process. In fact, one could speculate about a "superflare" process as indicated by the high power at low frequencies.

3. The Shot Parameters

Clearly a very interesting set of variables is the rate of occurrence of the shots (λ) and their decay time (τ). Unfortunately, the contribution of the photon counting statistics to the fluctuations is quite large in these data so that it is effectively impossible to make a meaningful measurement of these quantities from a single observation of the source. Furthermore, in order to remove the biasing effects due to counting statistics (as discussed in Weisskopf, Kahn, and Sutherland 1975), we are forced to lump observations together which, of course, implies a reduced sensitivity to long-term variations.

The resulting mean shot-model parameters as a function of phase for four phase bins are shown in Figure 6. There is clearly a correlation between the value of the parameters and binary phase outside the statistical variations, but there are not enough data to warrant an unambiguous selection of this period other than on *a priori* grounds. This result is very tentative, and we are concerned that the statistical biasing of counting statistics may not have been removed because of the limited number of observations. Furthermore, it is difficult to understand on physical grounds how the flaring process, if it is indeed the explanation for the short-term variations, is so strongly affected by the binary motion.

We thank Professor R. Giacconi, the Principal Investigator of the *Uhuru* Observatory, and the National Aeronautics and Space Administration for making the data available to us. In this regard, we also thank Dr. D. Koch, at American Science & Engineering, Inc., and Drs. E. Schreier, M. Ulmer, C. Jones, and W. Forman, at the Smithsonian Astrophysical Observatory. Professor R. Novick's constructive comments concerning this work are appreciated. This work was supported by NASA under grant NGR 33-008-194. This paper is Columbia Astrophysics Laboratory Contribution No. 119.

REFERENCES

- Lester, D. F., Nolt, I. G., and Radostitz, J. V. 1973, *Nature Phys. Sci.*, 241, 125.
- Weisskopf, M. C., Kahn, S. M., and Sutherland, P. G. 1975, *Astrophys. J. (Letters)*, 199, L147.

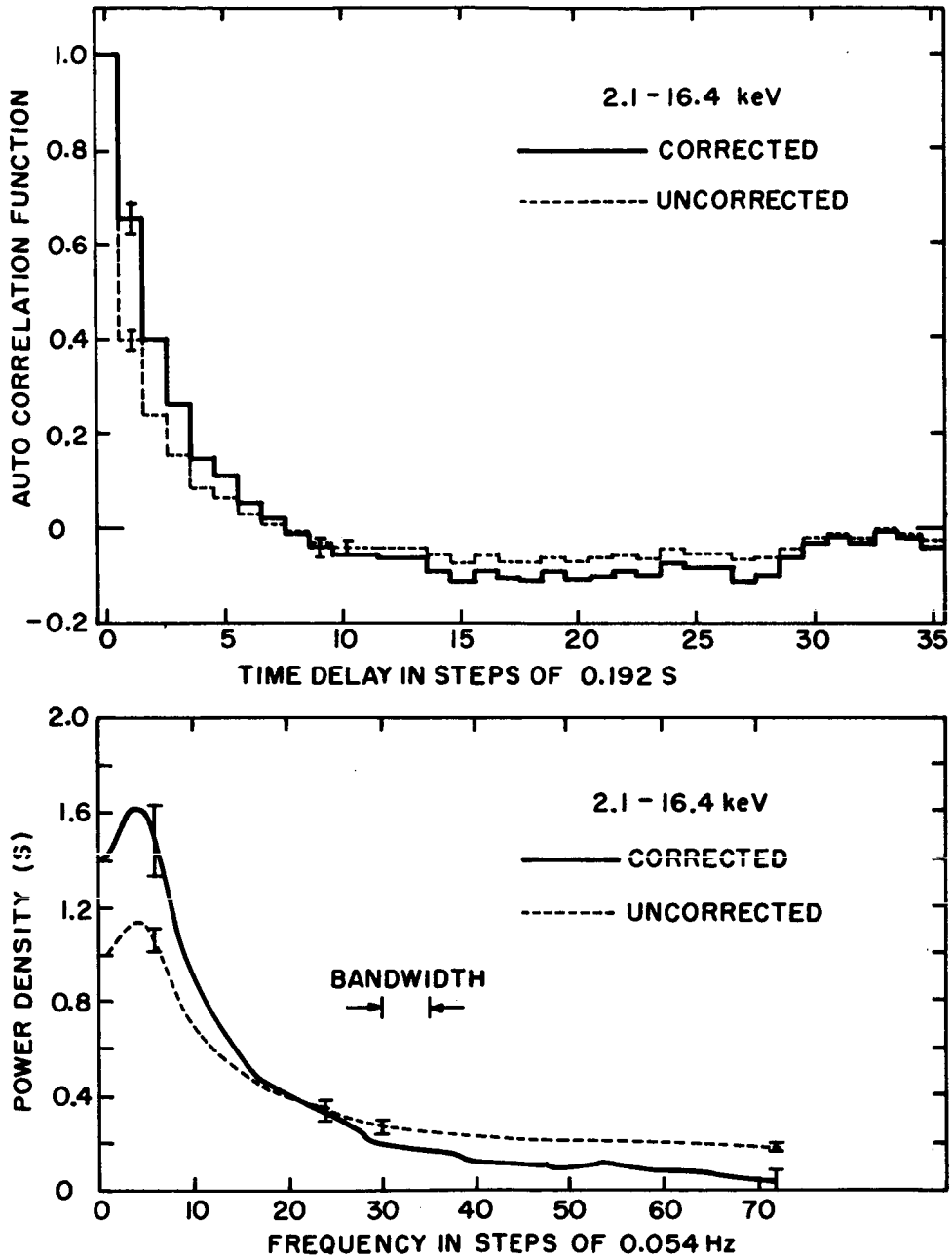


Figure 1. The average of 71 autocorrelation functions and power density spectra obtained from the wide-field *Uhuru* detector in 1972 January. Only the first 36 values of the autocorrelation function are shown. The error bars are based on the scatter of each data point about the mean for the results uncorrected for the bias produced by counting statistics. The error bars shown for the corrected functions also include the uncertainty in the correction factor. (Reproduced from Weisskopf *et al.* 1975.)

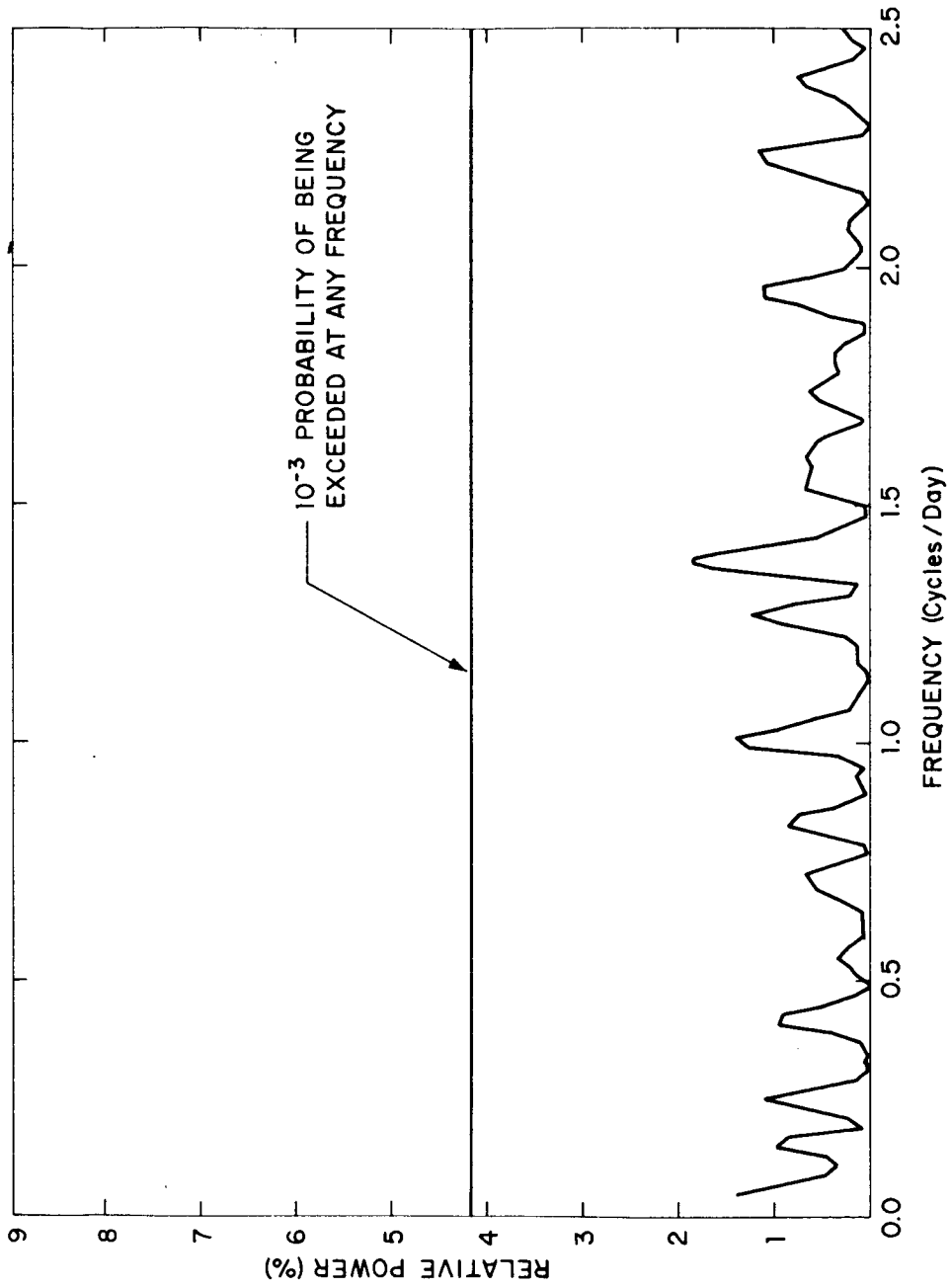


Figure 2. Power spectrum of the background for 71 observations of Cyg X-1 in the time interval from 1972 January 9 to 22.

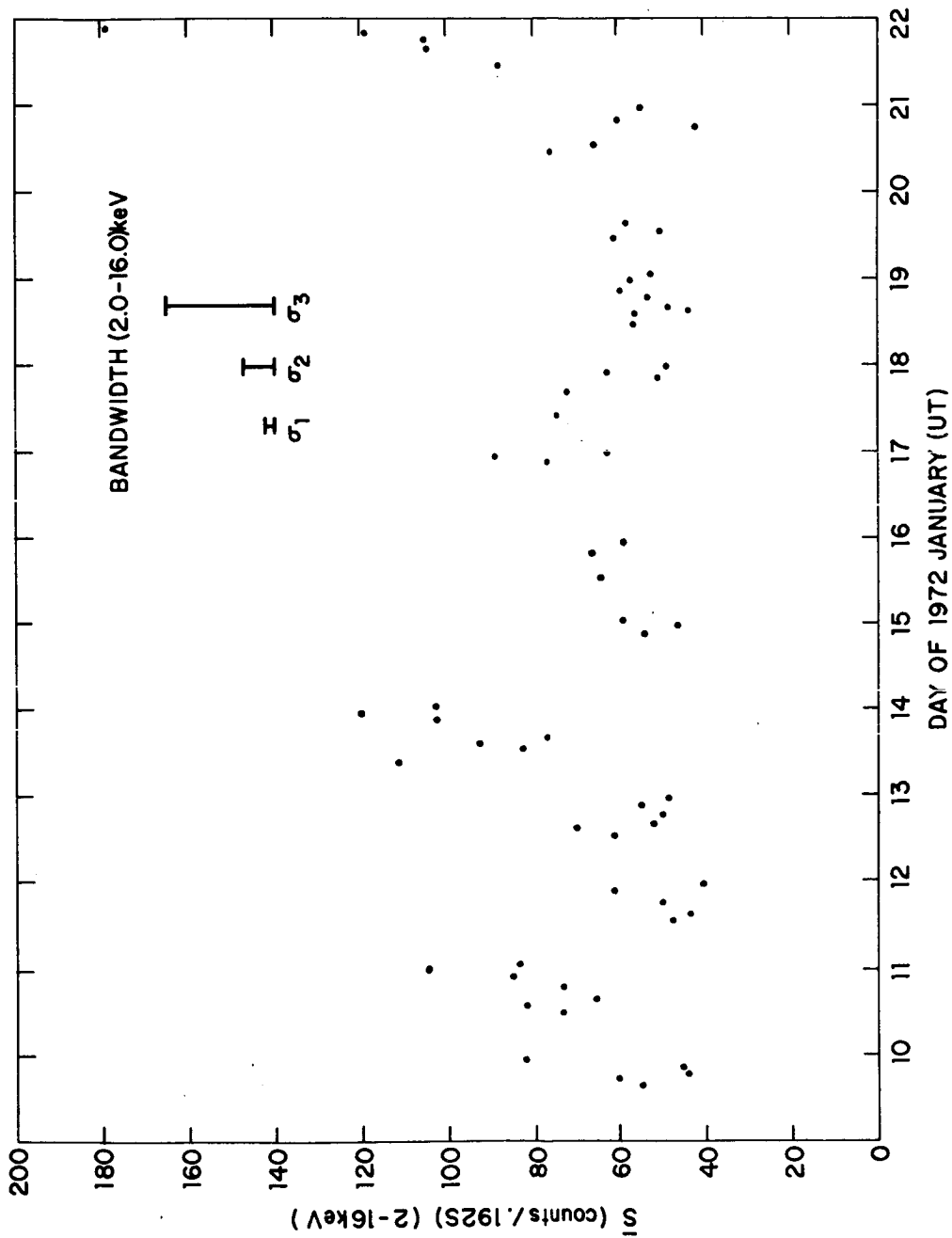


Figure 3. Intensity of Cyg X-1 as a function of time.

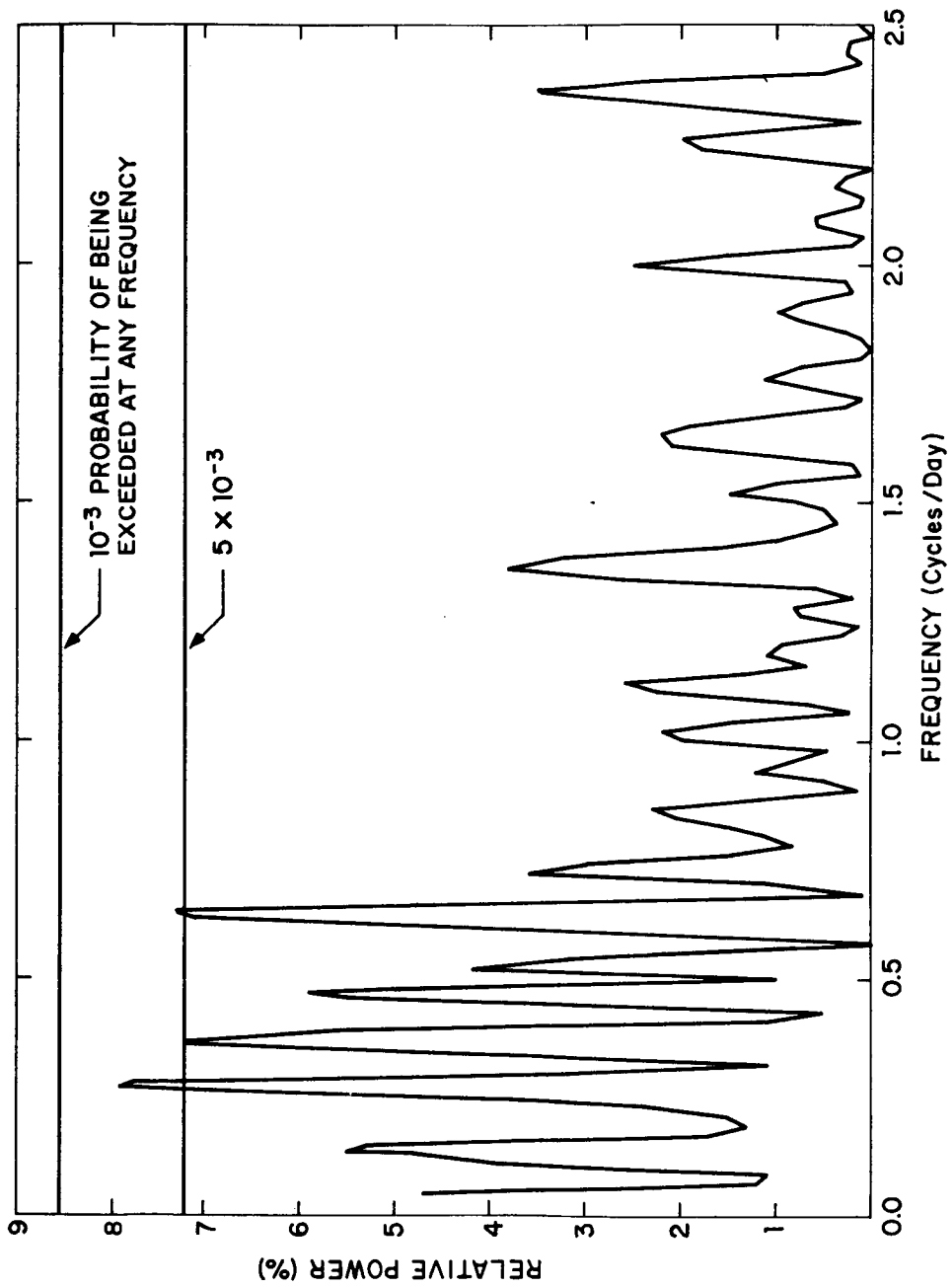


Figure 4. Power spectrum of the mean count rate.

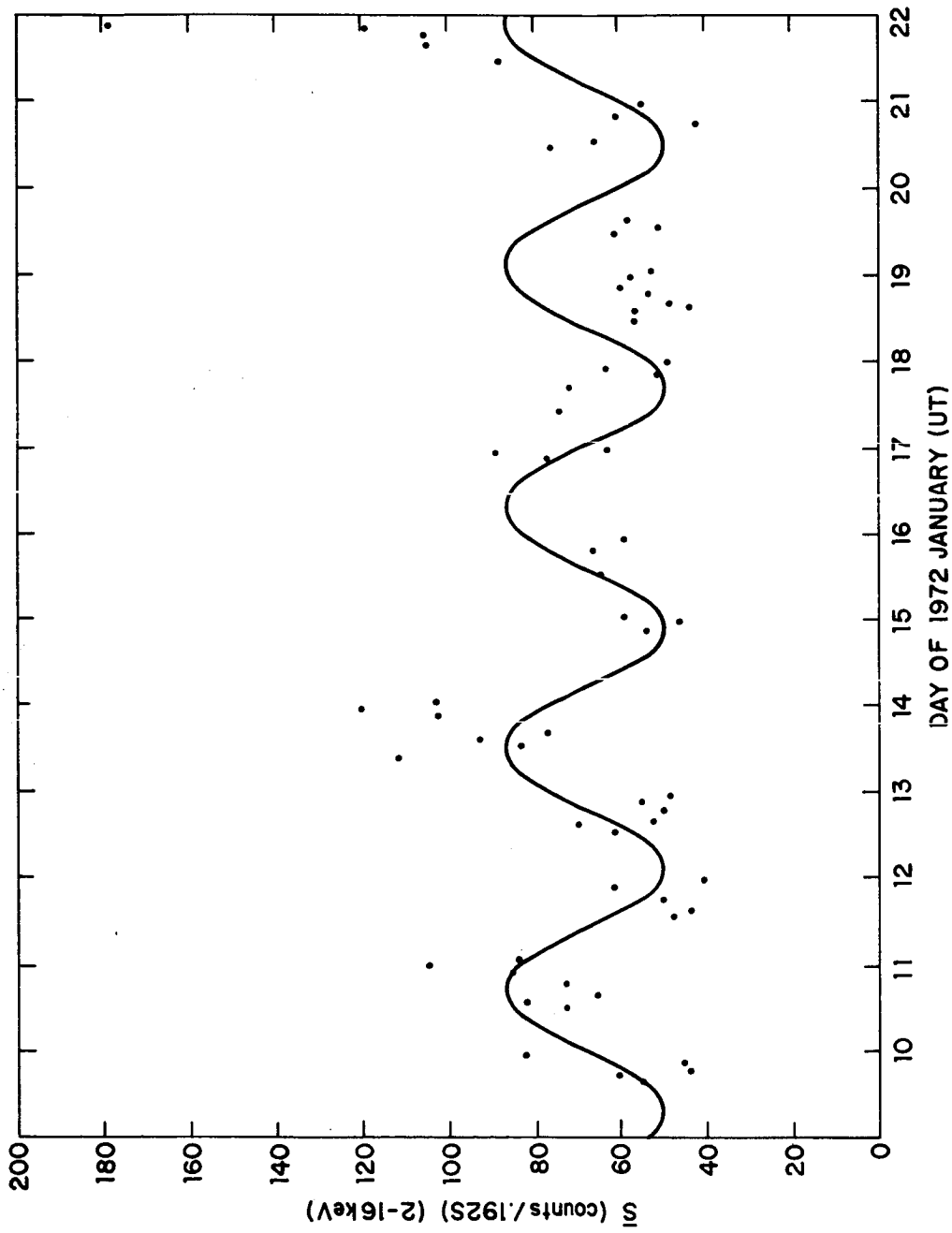


Figure 5. Intensity as a function of time. The 2.8-day variability is shown in a solid line.

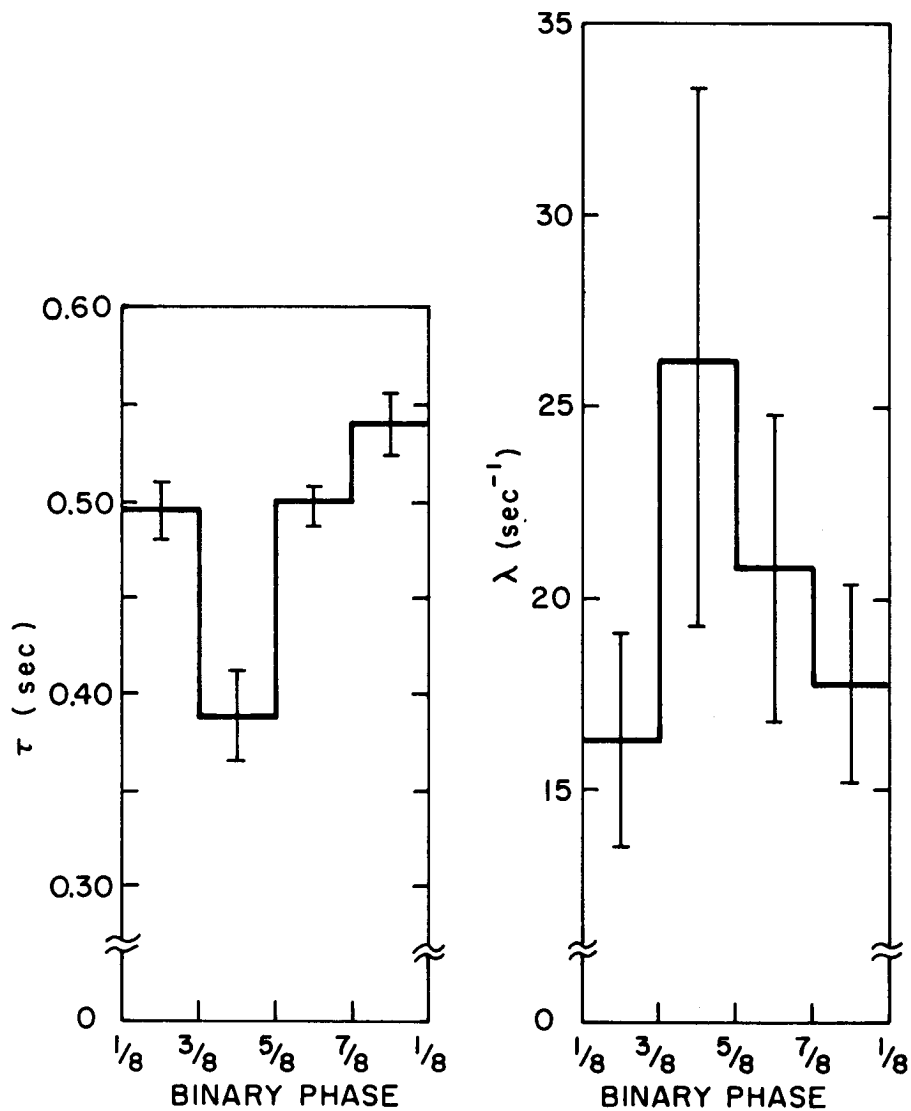


Figure 6. The shot decay (flare cooling) time and shot (flare) rate as a function of binary phase for an assumed 5.6-day period.

CYG X-1

Discussion

A. Bunner to R. Rothschild:

Do these rectangular one millisecond bursts have anything to do with the shot noise bursts?

R. Rothschild:

We have been unable to find any direct evidence linking the millisecond bursts to the shot pulses.

OPTICAL OBSERVATIONS OF HDE226868 = CYGNUS X-1:

A REVIEW

C.T. BOLTON

David Dunlap Observatory
University of Toronto
Richmond Hill, Ontario
CANADA

I. INTRODUCTION

Because of the nature of this conference I have set two tasks for myself. First, I want to summarize our present state of knowledge of the binary system HDE226868 = Cygnus X-1. Second, I wish to point out some deficiencies in the optical observations that make interpretation of the system difficult but which can be corrected. Because of the brief time allotted for this review, it is necessarily little more than an annotated bibliography. The listener (reader) should remember that I am making no effort to be comprehensive, and thus both the choice of papers and the annotations reflect my personal prejudices on the subject.

I wish to address myself to three problems in this review:

1. Dimensions of the system
2. Nature of the secondary (x-ray source)
3. Properties of the mass transfer

The investigation of 1. is almost solely dependent on optical observations in this system. The study of the remaining points depends on observations throughout the electromagnetic spectrum.

Since I shall only discuss the optical observations, I will try to indicate where the usefulness of these are limited and the x-ray observations (in particular) provide useful data. Some of my remarks are made with a fourth problem, the evolutionary history of the binary system, in mind, but our understanding of this is so poor at the present time that I do not wish to treat it explicitly here.

II. DIMENSIONS OF THE SYSTEM

Dimensions in this discussion are taken to be the semi-major axis and inclination of the relative orbit and the masses, radii, luminosities, and effective temperatures of the individual components.

Walborn (1973) has classified HDE226868 as O9.7Iab p var. (cf. Figure 1), where the p var. refers to the variable $\lambda 4686$ HeII emission. Smith, Margon, and Conti (1973) have confirmed this spectral type although they report small variations. I am inclined to doubt the statistical significance of these after tracing some of my plates. It should be noted that the blue absorption spectrum of HDE226868 is completely normal (Walborn 1973). In particular, the carbon and nitrogen line strength anomalies that are often found in other OB stars (Walborn 1975) are not present. This probably tells us something about the evolutionary status of the star, but we cannot interpret this information until we understand the OBCN stars.

The spectral type implies an effective temperature of 30,000 K, $\log g = 3.3$, and a bolometric correction of 2.9 mag.

(Conti 1973, Code 1974) with uncertainties of at least 10% in each. The best available dynamical masses for OB binaries imply a mass of 25-30 M_{\odot} for HDE226868 (Stothers 1972) if it is "normal" and a mass as large as 45 M_{\odot} is possible (Conti and Burnichon 1975).

The "normalcy" of the primary mass has been a controversial question. Numerous investigators have pointed out the difficulties involved in estimating masses from spectral types. These difficulties can be overcome to some extent if a distance (luminosity) estimate can be made independent of the spectral type. Bolton (1972) summarized the available evidence on this point, and Margon, Bowyer, and Stone (1973) and Bregman *et al.* (1973) have improved the reddening distance determination. All of the evidence, including interstellar reddening, polarization, interstellar absorption lines, and the spectral type are consistent with a distance of at least 2 kpc. This argues for a "normal" mass, but the uncertainties are such that, even at 2 kpc, a mass as low as 10 M_{\odot} is possible (van den Heuvel and Ostriker 1973).

HDE226868 = Cygnus X-1 is a binary system with a 5.^d6 period, and the remainder of our information comes from an analysis of the velocity and light curves of the tidally distorted primary star. Bolton (1975) has obtained a velocity curve and derived orbital elements from measurements of numerous high-dispersion spectrograms well-distributed in phase (Fig. 2). There is evidence that a few absorption lines, such as H β and HeI $\lambda\lambda$ 6678 and 5875, give spurious velocities because of mass motion in the system, but the velocity curve based on the other available lines seems undisturbed. Both the velocity curve and the light curve (Hutchings 1974) indicate that the orbit is slightly elliptical.

The emission line velocity curves are much more poorly defined, but they indicate that the emission velocities vary approximately in antiphase to the absorption line velocities. Bolton (1975) has summarized the existing measurements of the HeII $\lambda 4686$ emission line (cf. Figure 3), and Hutchings et al. (1973) have shown that the emission velocities are 120° out of phase with the absorption velocities after the emission profile is corrected for the presence of the $\lambda 4686$ absorption line from HDE226868. They find that the emission probably arises from a gas stream or hot spot near the secondary and derive a mass ratio $M_1/M_2 \leq 2$. Bisiacchi et al. (1974) have obtained similar results from the same data. Only a handful of velocities are available for the H α emission line, whose profile also has to be corrected for the intrinsic absorption line from HDE226868. The H α emission is very wide (Hutchings et al. 1974) and appears to arise in a disk around the unseen secondary. The corrected lines give velocities approximately in antiphase to the absorption velocities and indicate that $M_1/M_2 < 2$ (perhaps $M_1/M_2 \approx 1.6$).

Complete or nearly complete light curves by Lester, Nolt, and Radostitz (1973), Walker and Quintanilla (1974), Hilditch and Hill (1974), and Lyutyi, Sunyaev, and Cherepashchuk (1975) show that HDE226868 is an ellipsoidal variable with a color independent amplitude $\Delta m = 0.06$ magnitudes (Fig. 4). Walker and Quintanilla find that $\Delta m = 0.04$ mag., but their observations are questionable because they were obtained with a small (30 cm) telescope and an unrefrigerated photomultiplier. The scatter in all of the light curves is larger than the photon statistics, thereby indicating

some intrinsic variability other than that due to the tidal distortion. Nothing is known about this intrinsic variability other than its existence, and I know of no investigations of correlations between it and other phenomena in the system. Figure 5 shows that in spite of these intrinsic variations, the mean light curve is quite stable. Archival photographs show that the behavior in 1949 was the same as at present (Herczeg and Sutton 1975).

The analyses of the optical data for dimensions are far too numerous for me to give a complete listing. A subjective list of the most important includes those by Avni and Bahcall (1975), Bolton (1975), Hutchings (1974), and Lyutyi, Sunyaev, and Cherepashchuk (1975). Although each investigation has made somewhat different assumptions and adopted slightly different approaches, their final results are remarkably similar. Indeed, the insensitivity of the results to the crudity or sophistication of the analysis is one of the remarkable features of this system. Figure 5 from Bolton (1975) is representative of results obtained by others for M_1 , M_2 , i , and R_1/R_{ROCHE} . These results were obtained using the Russell-Merrill rotating limb and gravity darkened ellipsoid model. Calculations with a full Roche model tend to give larger inclinations, but there is not universal agreement on this point. Kondo (1974) has questioned whether the assumptions of the Roche model are valid in x-ray binaries. Bolton (1975) has argued that they may be used without significant error to analyze the HDE226868 system. In particular, radiation pressure and non-synchronous rotation probably have no effect on the mass determinations. However, the former may be very important in determining the properties of the mass transfer.

III. NATURE OF THE SECONDARY

Numerous models have been suggested for the binary system (cf. Bolton 1975 for a full discussion). The optical observations are relevant only to those models in which the secondary is a "normal" star. There are two classes of these: i) a single OB main-sequence star secondary in which the x-rays are produced by processes involving magnetic field connections between the primary and secondary (Bahcall, Rosenbluth, and Kulsrud 1973), ii) a binary secondary star (ternary system) in which the secondary consists of an OB main-sequence star with a neutron star in close orbit about it (Bahcall et al. 1974, Fabian, Pringle and Whelan 1974). There is a second class of triple star models in which the neutron star is in a wide orbit about the OB pair (Bahcall et al. 1974). This class is ruled out by the x-ray observations and is not considered here.

Bolton (1975) has argued that models of class ii) are ruled out by the "small" scatter in the HeII $\lambda 4686$ velocities. Both he and Avni and Bahcall (1975) agree that the ellipsoidal light curve is not inconsistent with the presence of a normal B main-sequence star in the system. The light and velocity curves permit secondaries between approximately B0V and B4V, but Avni and Bahcall have shown that at least some of this range could be excluded by spectrophotometry with a high signal to noise ratio. Figure 6 shows an attempt to do this by adding photographic spectra at the same phase. The noise is about 1%, and there is no indication of

a normal secondary down to at least 3 magnitudes fainter than HDE226868. This limits normal secondaries to spectral types of B3V - B4V.

Zeeman measures of the HeI $\lambda 6678$ line (Borra 1975) appear to rule out models of type i) with dipole fields, but more complicated magnetic geometries are not excluded.

IV. MASS EXCHANGE

Our knowledge of the mass exchange rests on the behavior of the optical emission lines and the x-ray absorption events (Mason et al. 1974, Li and Clark 1974). In the previous section I indicated the source regions for the emission features. Very little is known about these features. Hutchings et al. (1973) have shown that the equivalent width of the $\lambda 4686$ HeII line is phase dependent, and Bolton has argued in support of this with additional data. However, the data used is scattered over many cycles; Hutchings et al. have 10 observations from 4 different cycles in a 16 cycle span. Therefore it is impossible to differentiate random or non-random long-term variations from phase dependent variations. Similar remarks apply to the H α observations of Hutchings et al. (1974) and Brucato and Zappala (1974). An additional complication in the latter case is that no line profiles are given, only photographic reproductions of the plates. Evidence will be presented later in this meeting that there are long-term changes in the strength of H α and other lines. Because of these we must regard all models for the mass ex-

change that depend on this data with caution.

The x-ray absorption events give us information about the size, density, and location of absorbing clouds in the system. The question of location is key in differentiating different models for the mass transfer. The location is determined from the timing of the event relative to phases in the optical light or velocity curves. This requires good values for both the epoch (of inferior conjunction, say) and the period. The former is no special problem, but there has been considerable confusion with regard to the latter. Most of the recent spectroscopic (Mason et al. 1975, Brucato and Zappala 1974) and photometric (Lyutyi, Sunyaev, and Cherepashchuk 1975) period determinations have clustered near $5.^d601$. However, Bolton (1975) has shown that periods near 5.6000 ± 0.0002 give a better fit to the spectroscopic data, and when archival data is included, the best period is 5.59982 ± 0.00004 . Nevertheless, several other periods in the range $5.^d597$ to $5.^d603$ are possible. Herczeg and Sutton have derived a light curve for HDE226868 from photographic plates taken in 1949. When these are compared with recent observations, a number of possible periods are found. The only one of these in agreement with the possible spectroscopic periods is $5.^d6000$. It is interesting that if this period is used nearly all of the published absorption events occurred before superior conjunction of the x-ray source at a time when the line of sight would be expected to pass through any gas stream. Presumably the absorbing

material is very close to the x-ray source. Otherwise, the low inclination of the system requires that the material lie far out of the orbital plane.

The above discussion assumes that the period is constant. This is quite reasonable as it is easy to show using standard formulae for conservative mass exchange that a mass exchange rate of $10^{-7} M_{\odot}/\text{yr.}$ will lead to a period change $\Delta P/P \approx 10^{-10}$. This is several orders of magnitude lower than could conceivably be detected from either the velocity or light curves in a time interval of 100 years. Put another way, the period change due to a mass loss rate of $2 \times 10^{-2} M_{\odot}/\text{yr.}$ might be detectable in the data obtained since 1971.

V. POLARIZATION

I have placed the polarization observations in a separate section because it was not clear to me how these observations fit into any picture of the system. Nolt et al. (1975) have reported variations in the amount and position angle of the polarization in the U band that are significant at the $3-4\sigma$ level. The variations are synchronous with the 5.6^d period. Nolt et al. argue that the phasing of the variations is consistent with expectations for a binary system seen at low inclination, but they offer no model for the source (or sources) of the intrinsic polarization. Two groups (Michalsky, Swedlund, and Stokes 1975, Severny and Kuvshinov 1975)

have reported variable circular polarization from HDE226868. Michalsky, Swedlund, and Stokes show that the variability mimics the B light curve. The wavelength variation of the polarization is consistent with that produced by interstellar dust. They have suggested that the circular polarization could arise from the conversion of linear polarization to circular polarization in the interstellar medium or from polarized light produced in regions of high magnetic field, but there appears to be severe difficulties with either suggestion.

VI. DESIDERATA

There is no question that the most urgent need is for an all out campaign on HDE226868 = Cygnus X-1 to get full coverage of the various phenomena in the system over several orbital cycles. At present, essentially nothing can be said about the orbital variations of various phenomena because the density of observations is not high enough to separate these variations from longer or shorter time scale variations. Because of these problems it is impossible to say how variations of one type (e.g. emission lines) relate to variations of another type (e.g. x-ray intensity). It will be impossible to progress any further unless a coordinated campaign to monitor the spectrum and light variability and the x-ray intensity over at least two orbital cycles is carried out. This will require the dedication of as many large optical telescopes as possible at

all longitudes for the spectroscopic work. The HeII $\lambda 4686$, H α , and HeI $\lambda\lambda 6678, 5875$ lines should be monitored at resolutions of 1Å or better with the highest possible time resolution. At the same time uvby photometry and polarization measures should also be obtained, and the x-ray intensity monitored. It would be extremely useful to obtain vacuum UV observations, especially spectroscopic ones, but this may be difficult because of the strong interstellar absorption towards HDE226868. The UV is perhaps the one area other than x-ray where useful isolated observations can be obtained. Isolated optical observations may eventually become more useful when (and if) a good picture of the phase dependent behavior of the system at one epoch is available. Simultaneous infrared and radio observations are desirable, but they are probably not essential to obtain an understanding of the system.

REFERENCES

- Avni, Y., and Bahcall, J.N. 1975, Ap.J., 197, 675.
- Bahcall, J.N., Rosenbluth, M.N., and Kulsrud, R.M. 1973, Nature Phys. Sci., 243, 27.
- Bahcall, J.N., Dyson, F.J., Katz, J.I., and Paczynski, B. 1974, Ap.J. (Letters), 189, L17.
- Bisiacchi, G.F., Dultzin, D., Firmani, C., and Hacyan, S. 1974, Ap.J. (Letters), 190, L59.
- Bolton, C.T. 1972, Nature Phys. Sci., 240, 124.
 _____ . 1975, Ap.J., 200, 269.
- Borra, E.F. 1975, Ap.J. (Letters), 196, L109.
- Bregman, J., Butler, D., Kemper, E., Koski, A., Kraft, R.P., and Stone, R.P.S. 1973, Ap.J. (Letters), 185, L117.
- Brucato, R.J., and Kristian, J. 1973, Ap.J. (Letters), 179, L129.
- Brucato, R.J., and Zappala, R.R. 1974, Ap.J. (Letters), 189, L71.
- Code, A.D. 1974, in Multicolor Photometry and the Theoretical HR Diagram, ed. by Philip, A.G. Davis, and Hayes, D.S., (Albany: Dudley Obs.), p.221.
- Conti, P.S. 1973, Ap.J., 179, 181.
- Conti, P.S., and Burnichon, M.-L. 1975, Astr. and Ap., 38, 467.
- Fabian, A.C., Pringle, J.E., and Whelan, J.A.J. 1974, Nature, 247, 351.
- Herczeg, T.J., and Sutton, J.K. 1975, Ap. Letters, 16, 17.
- Hilditch, R.W., and Hill, G. 1974, M.N.R.A.S., 168, 543.

- Hutchings, J.B. 1974, Ap.J. (Letters), 193, L61.
- Hutchings, J.B., Crampton, D., Glaspey, J., and Walker, G.A.H.
1973, Ap.J., 182, 549.
- Hutchings, J.B., Cowley, A.P., Crampton, D., Fahlmann, G.,
Glaspey, J.W., and Walker, G.A.H. 1974, Ap.J., 191, 743.
- Kondo, Y. 1974, Ap. and Space Sci., 27, 293.
- Lester, D.F., Nolt, I.G., and Radostitz, J.V. 1973, Nature
Phys. Sci., 241, 125.
- Li, F.K., and Clark, G.W. 1974, Ap.J. (Letters), 191, L27.
- Lyutyi, V.M., Sunyaev, R.A., and Cherepashchuk, A.M. 1975,
Sov. Astron., 18, 684.
- Margon, B., Bowyer, S., and Stone, R.P.S. 1973, Ap.J. (Letters),
185, L113.
- Mason, K.O., Hawkins, F.J., Sanford, P.W., Murdin, P., and
Savage, A. 1974, Ap.J. (Letters), 192, L65.
- Michalsky, J.J., Swedlund, J.B., and Stokes, R.A. 1975, Ap.J.
(Letters), 198, L101.
- Nolt, I.G., Kemp, J.C., Rudy, R.J., Southwick, R.G., Radostitz, J.V.,
and Caroff, L.J. 1975, Ap.J. (Letters), 199, L27.
- Severny, A.B., and Kuvshinov, V.M. 1975 Ap.J. (Letters), 200, L13.
- Smith, H.E., Margon, B., and Conti, P.S. 1973, Ap.J. (Letters),
179, L125.
- Stothers, R. 1972, Ap.J., 175, 431.
- van den Heuvel, E.P.J., and Ostriker, J.P. 1973, Nature Phys. Sci.,
245, 99.

Walborn, N.R. 1973, Ap.J. (Letters), 179, L123.

Walborn, N.R. 1975, Ap.J., in press.

Walker, E.N., and Quintanilla, A.R. 1974, M.N.R.A.S., 169, 247.

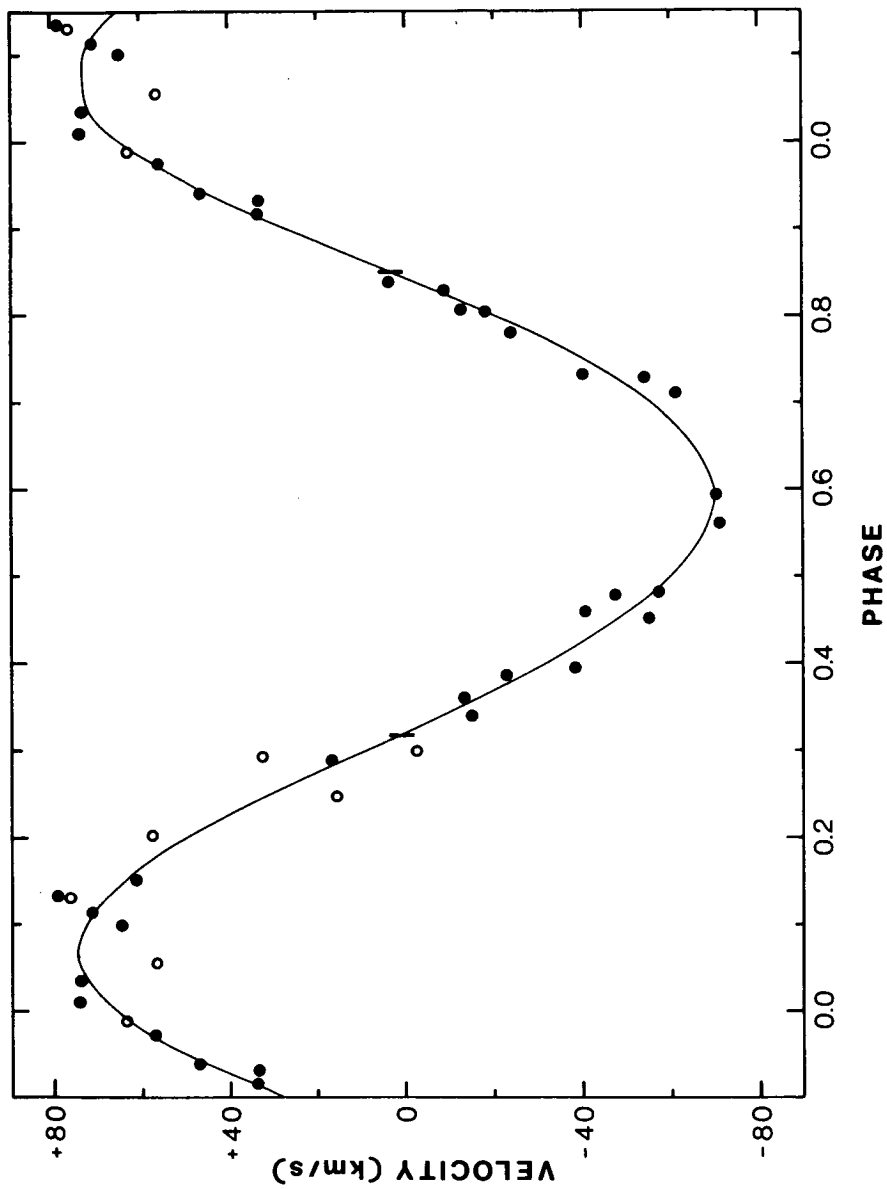


Figure 2. Absorption line velocity curve for HDE226868. Only the David Dunlap Observatory data are plotted. Vertical tick marks indicate phases of inferior and superior conjunction of the secondary star. (Bolton 1975).

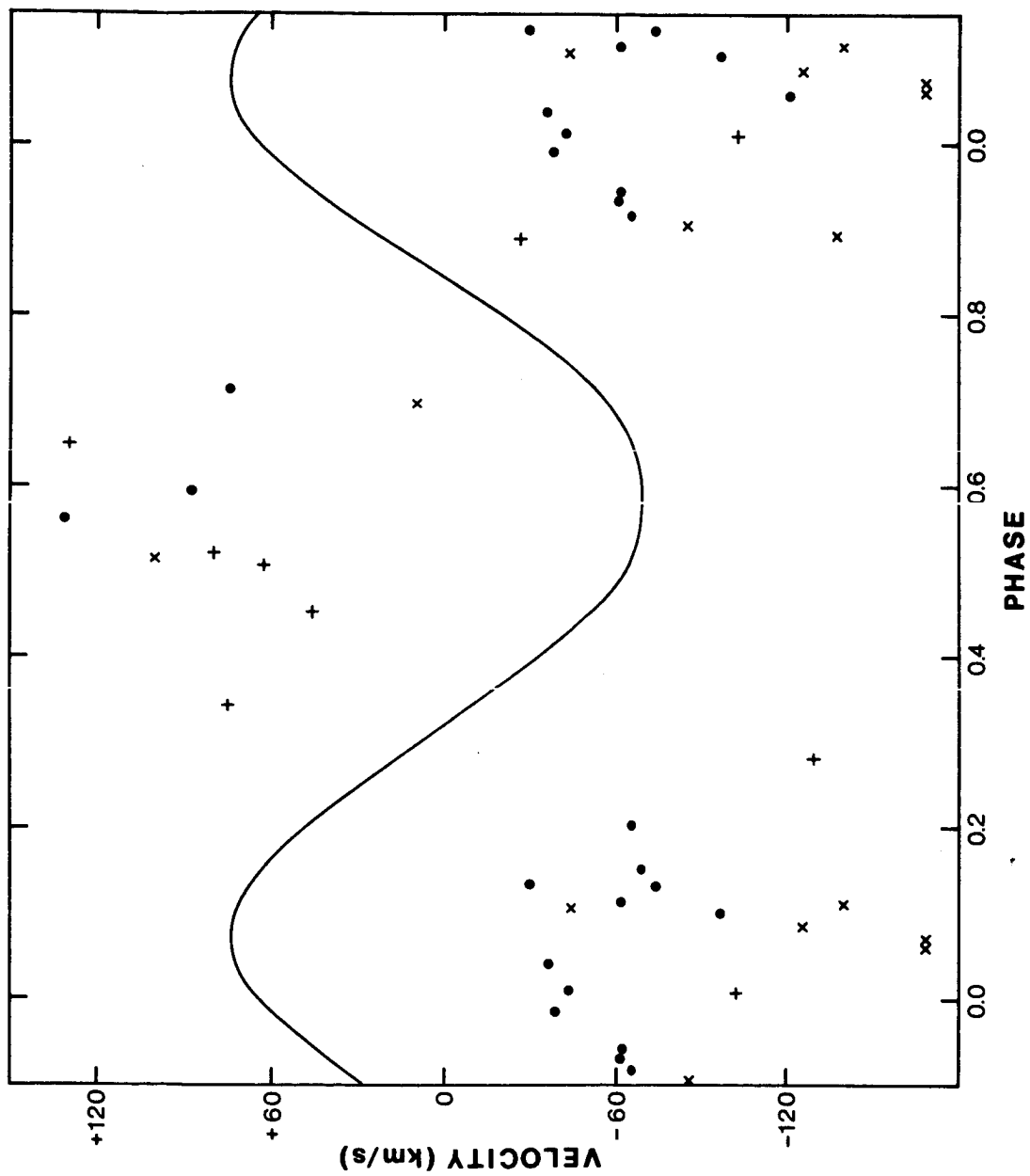


Figure 3. The HeII $\lambda 4686$ emission line velocity "curve". The calculated absorption line orbit is shown for reference. Dots, DDO measures; x's and +'s are from Brucato and Kristian (1973) and Hutchings et al. (1973). (Bolton 1975).

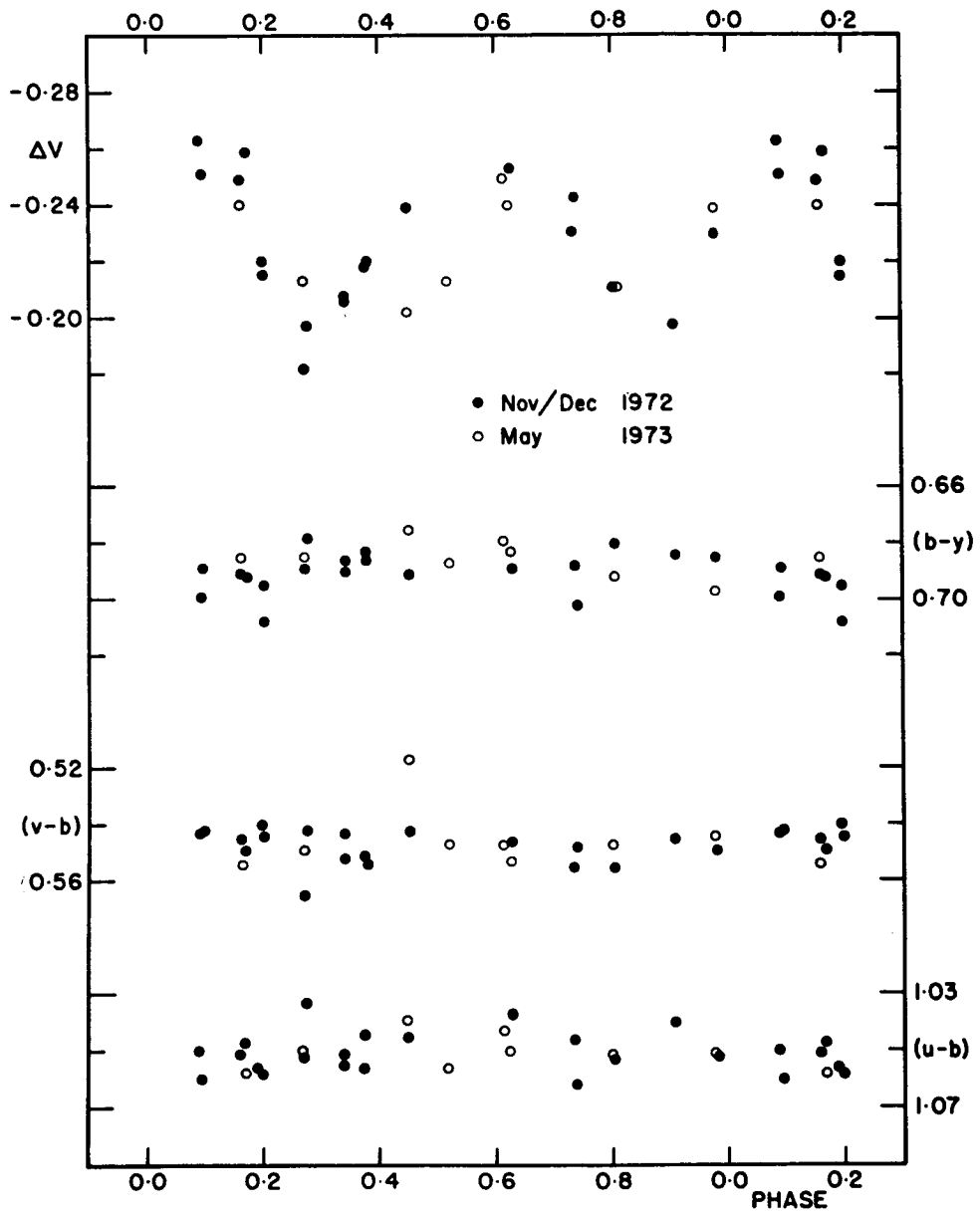


Figure 4. Four color light curve of HDE226868 from Hilditch and Hill (1974). The phases are referred to periastron passage.

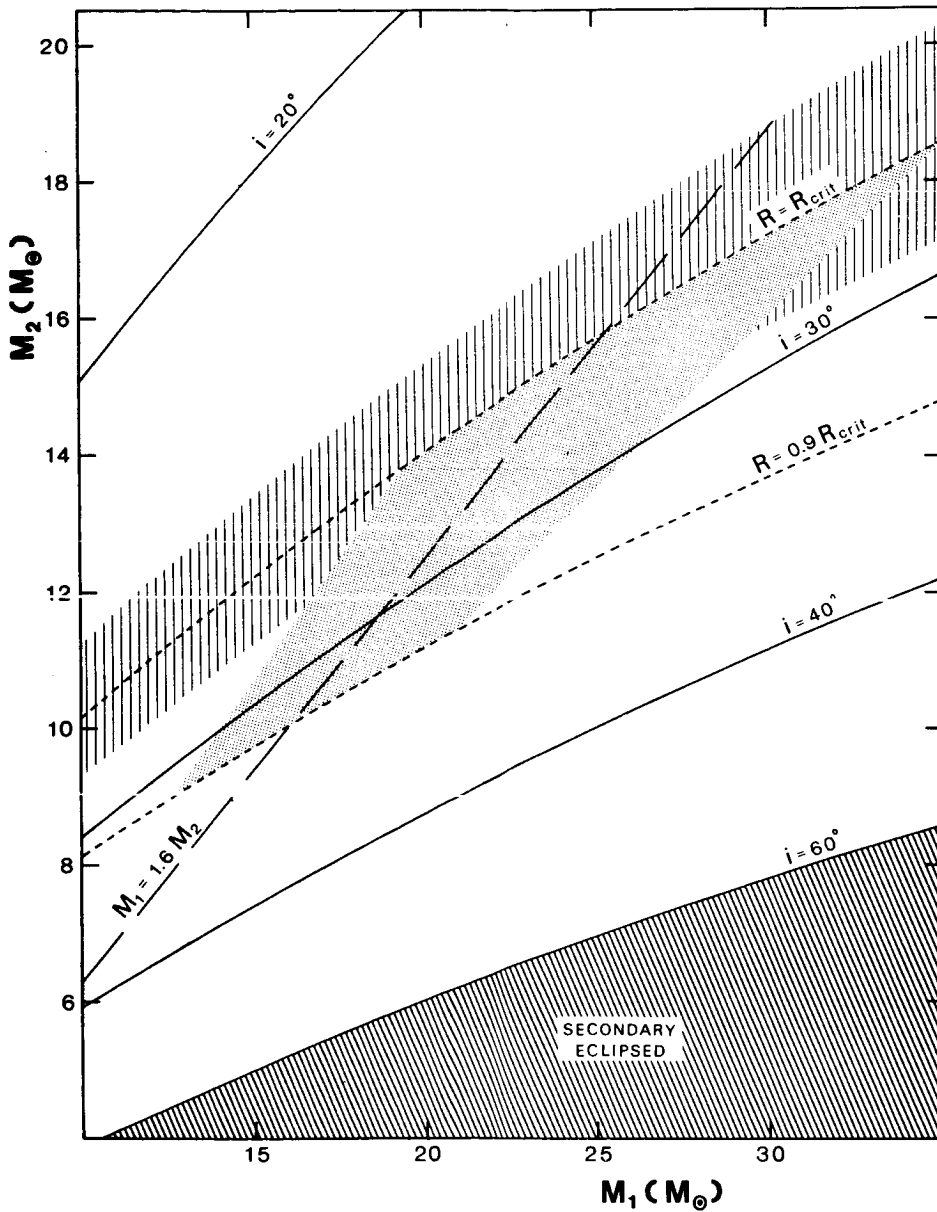


Figure 5. The $(M_2 - M_1)$ - plane for the HDE226868 = Cygnus X-1 system according to Bolton (1975). Solid lines are lines of constant orbital inclination. Short-dashed lines are lines of constant fractional radius for the primary. The vertical shading indicates the observational uncertainty in the positioning of the $R = R_{\text{CRIT}}$ line. The stippled area is the most probable location of the HDE226868 system.

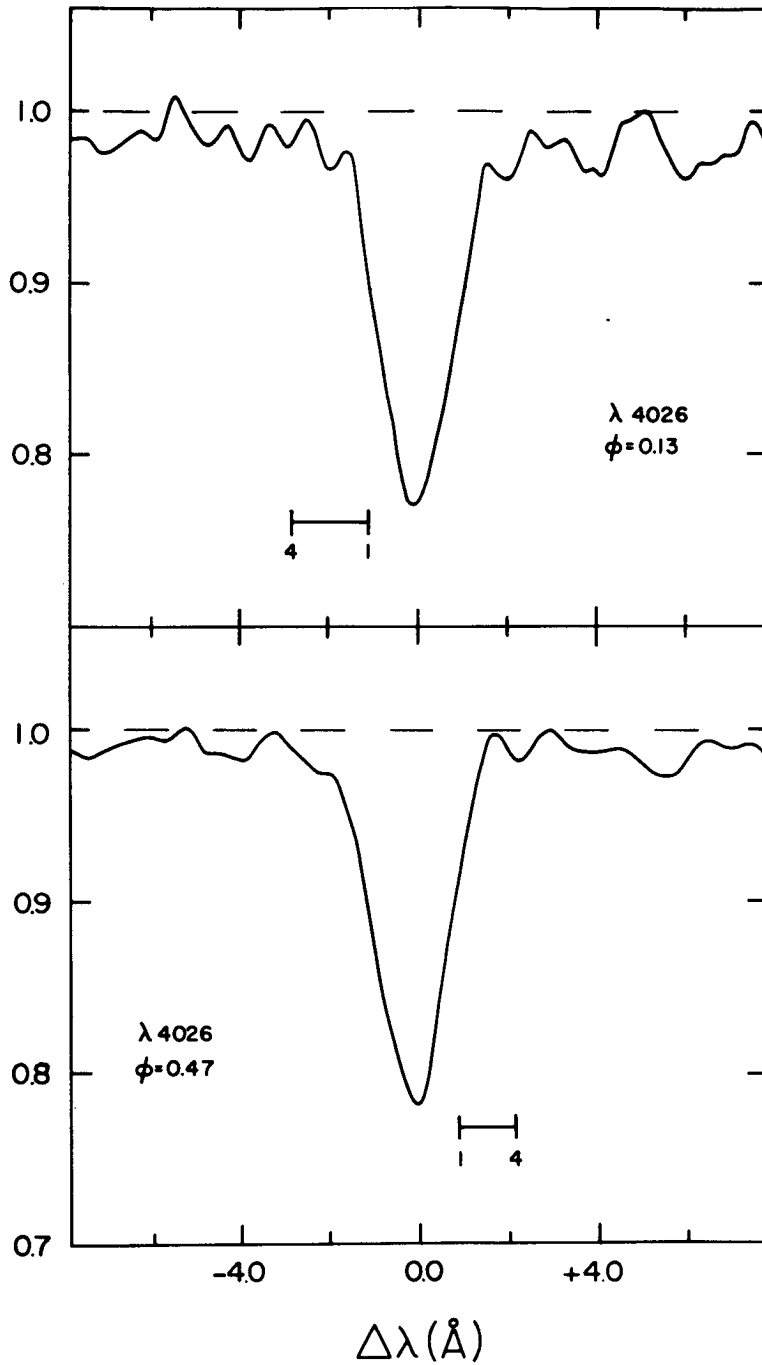


Figure 6. Normalized line profiles of HeI 4026 at two phases (from periastron). Four spectra have been co-added to obtain each profile. The expected positions of a line from a hypothetical normal secondary are indicated for $1 \leq M_1/M_2 \leq 4$.

SHORT TIME TRANSIENT PERIODICITIES FROM CYG X1.

G. Auriemma, D. Cardini, E. Costa, F. Giovannelli, M. Ranieri
Laboratorio Di Astrofisica Spaziale, Cnr. Frascati (Italy).

SUMMARY

The temporal behavior of three new events of modulated optical emission from Cyg X1, detected in July this year, is presented.

TEXT

The first detection of a strong modulated optical emission with a period near 83 ms from Cyg X1 was reported previously by our group ¹⁾.

In this paper we present the analysis of three more events of transient emission from the same source detected about one month later.

Short time periodicities in the optical band are investigated with the experimental set up shown in Fig.1. Single photon pulses from the photomultiplier are recorded on magnetic tape together with a very accurate 1 KHz reference frequency.

During playback of the tape the reference signal gives a 1 ms timing to a scaler interfaced with a small processor and the number of photon per millisecond is recorded on a digital tape.

Comparison with the BIH time standard received at 5 MHz allows a control of time base accuracy and stability which result better than 10^{-8} .

Periodicities are searched using stretches of data with a Fast Fourier Transform computer program based on Cooley Tuckey algorithm. At the moment the length of each data set is fixed to 458.752 s because of computer time limitations. In fact FFT analysis time increases faster than the length of the data set.

From a careful discussion of the various noise sources, reported elsewhere ²⁾, we deduce that this technique of data scan gives in the case of Cyg X1 (with 91 cm telescope), a threshold of .15% modulation for the detection

ction of an event with 99% statistical confidence.

During July we carried out observations of Cyg X1 with a total duration of about two hours spreaded over two nights with good weather conditions. The scan of these observations revealed the presence of three events of modulated emission occurring in a time span of less than one hour.

In Tab.I relevant parameter of the event (period of the modulation, variation of the period during each event, duration and modulated fraction) are compared with the same quantities observed in the event of June.

The "light curve" and the evolution shown in Figures 2, 3 and 4 for these events is qualitatively very similar to that of June, exception made for the duty cycle of the dips, which approaches to 50%.

These new observations of modulated emission from Cyg X1 confirm the first detection and stress the peculiarity of this phenomenon.

First of all the shape of the light curve, that is probably distinctive of a new mechanism of modulated emission, is entirely different from the pulse production mechanism in pulsars. The variability of the period both during each events (of the order of 10^{-4}) and between single events (of the order of 10^{-3}) strongly suggests that the observed periodicity does not come from a system governed only by celestial mechanics.

In the quiet state of the source, the upper limit of the periodic components in the optical emission is a factor ten below the level of the periodic emission during an event, as confirmed by other surveys ³⁾. This states probably that we observed really exceptional events, with a typical luminosity of the order of 10^{35} - 10^{36} erg/s, not being the extreme members of a more frequent, less powerfull, population of events.

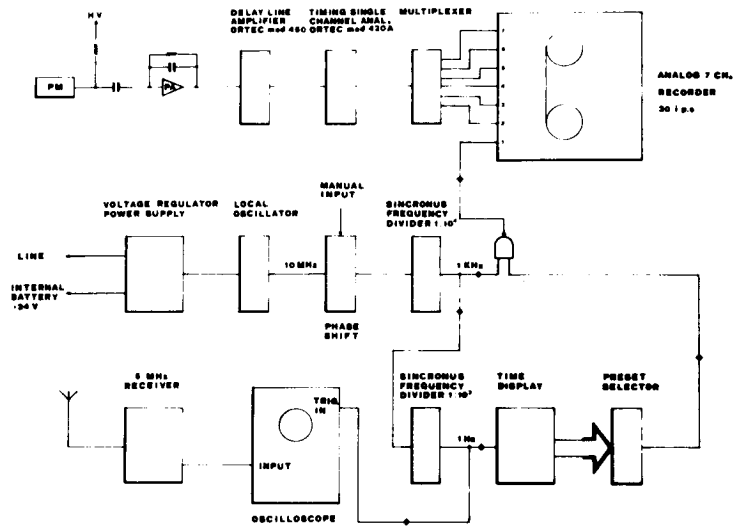
A reanalysis of the settling of the event observed in June shows (Fig.5) that the beginning of the modulated emission coincides very precisely with the brightening of the source. Time scale for this setting up is of the order of few seconds.

REFERENCES

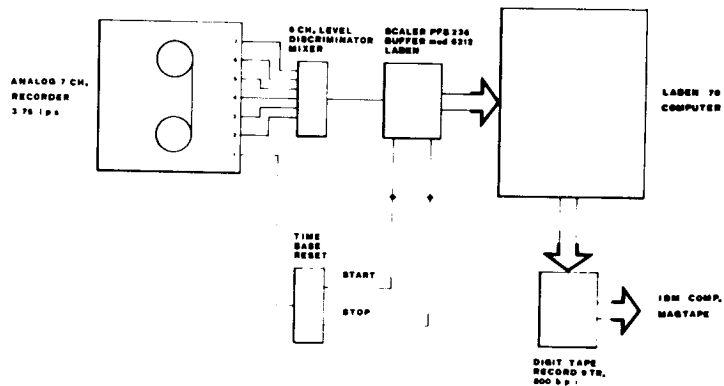
- 1) G. AURIEMMA, D. CARDINI, E. COSTA, F. GIOVANNELLI, M. ORCIUOLO and M. RANIERI. Nature (1975) in press.
- 2) G. AURIEMMA, D. CARDINI, E. COSTA, F. GIOVANNELLI and M. RANIERI
An upper limit to optical pulsations from Cyg X2. (in preparation).
- 3) CANIZARES, C.R., and Mc CLINTOCK, J.E., 1973, Bull. AAS, 5, 394.
CANIZARES, C.R., and Mc CLINTOCK, J.E., 1975, Ap.J. 200, 177.

TABLE I

TIME	PERIOD P (ms)	$\Delta P/P$	FILTER	DURATION (minutes)	$\Delta L/L$
June 11.06111 UT	83.531 ± 0.008	10^{-4}	Gray (x10)	10	3.5%
July 18.00410 UT	83.714 ± 0.008	$2 \cdot 10^{-4}$	R	> 10	2.5%
July 18.03674 UT	83.592 ± 0.008	$\approx 2 \cdot 10^{-4}$	B	> 6	3.7%
July 18.04854 UT	83.592 ± 0.008	$\approx 2 \cdot 10^{-4}$	Gray (x10)	> 8.5	4.2%

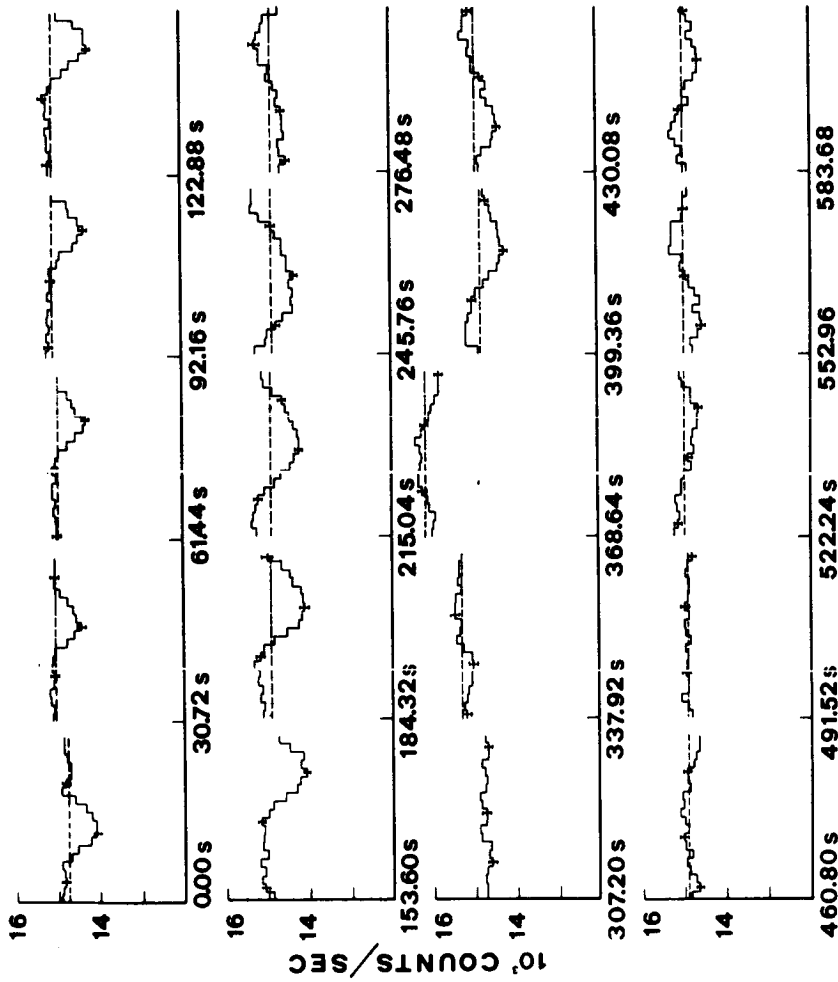


DATA RECORDING



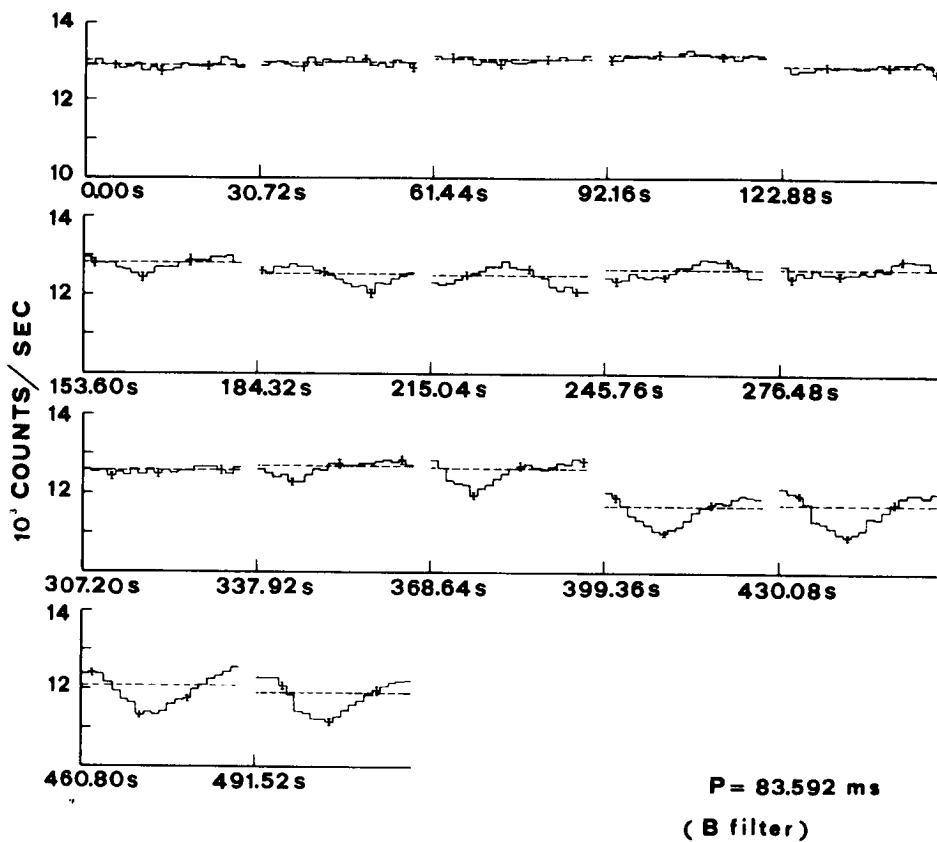
PLAYBACK

Fig.1. - The data acquisition system. Upper block diagram refers to the phase in which the data is recorded on analog tape; the lower block diagram shows the playback and conversion to the digital form.



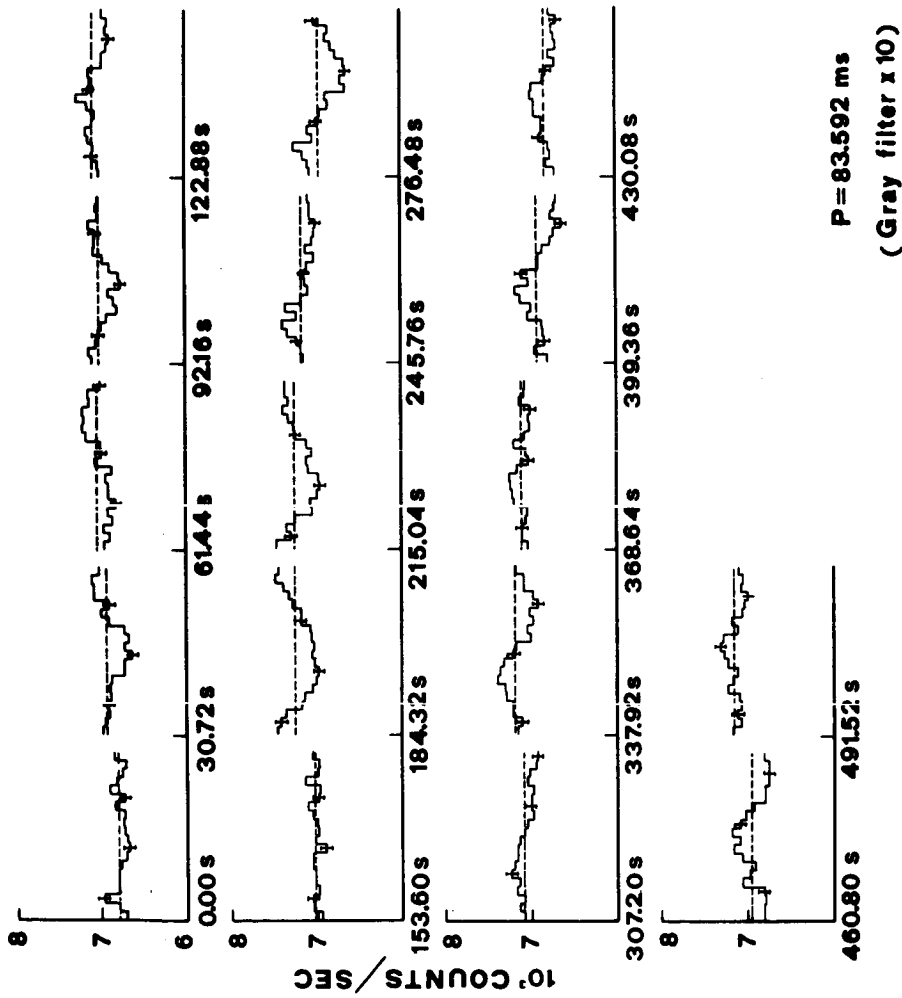
July 18, 1975
 P = 83.714 ms
 (R filter)

Fig.2. - Time evolution of the event of July 18.00410 UT. Plots are the foldings over about 30 seconds of subsequent stretches of data.



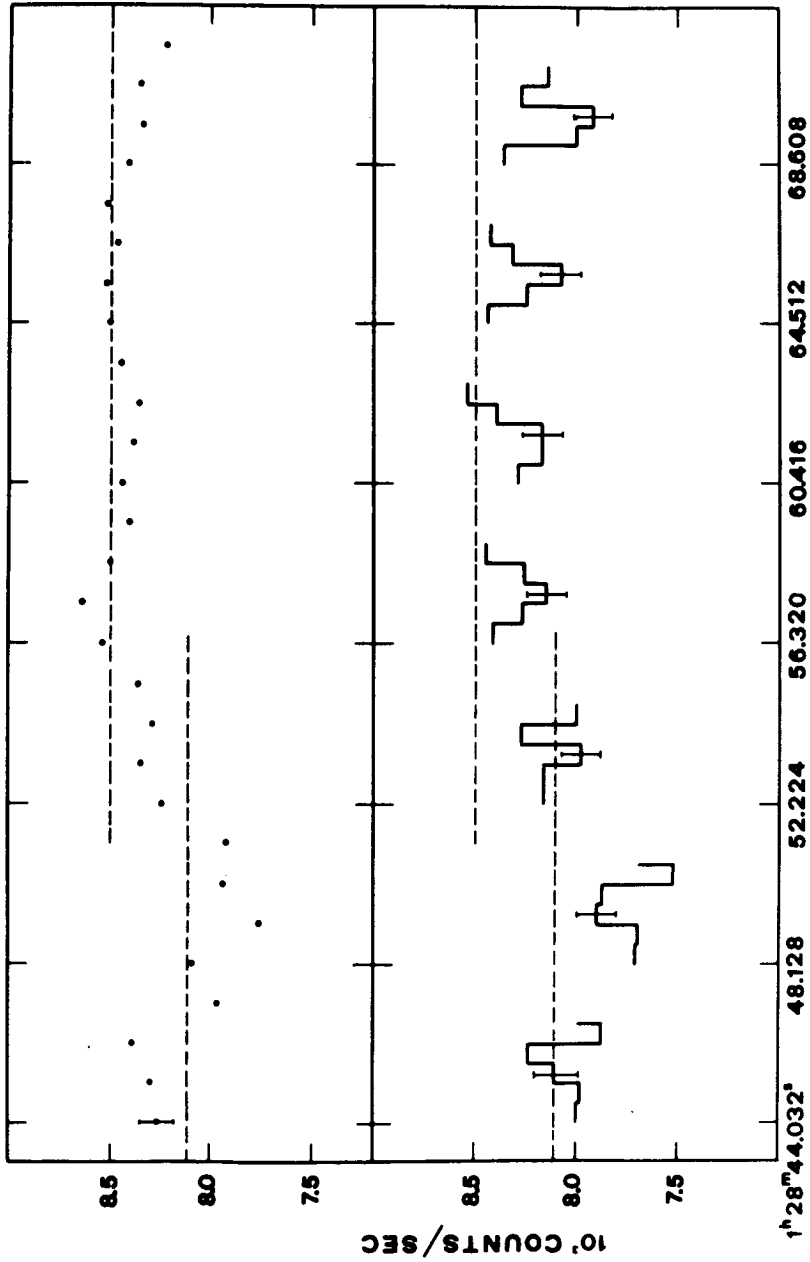
July 18, 1975

Fig.3. - Time evolution of the event of July 18.03674 UT. Plots are the foldings over about 30 seconds of subsequent stretches of data.



July 18, 1975

Fig.4. - Time evolution of the event of July 18.04854 UT. Plots are the foldings over about 30 seconds of subsequent stretches of data.



June 11, 1975

Fig.5. - Dots in the upper part are the countings averaged over 1.024 seconds. Dashed lines indicate the averages over one minute before and after the onset of the modulation. This latter is shown to appear in coincidence (in the lower part of the figure) with the rise in the countings. The rise time is about 4 seconds. Foldings are performed over 4 seconds intervals.

The Optical Polarization of HDE 226868 (= Cyg XR-1)

J. F. Dolan, Warner & Swasey Observatory, E. Cleveland, Ohio

Polarimetric observations of close binaries with orbit planes close to the line of sight and early type primaries may reveal the presence of a black hole secondary. The Einstein photometric effect (caused by the black hole acting as a gravitational lens) will introduce a characteristic, time varying signature upon the observed (interstellar) polarization of the primary by destroying the quasi-circular symmetry of the light distribution around the line of sight. Since Thomson scattering and the gravitational deflection of light are both wavelength independent, the effect is expected to be the same in all wavelength regions.

Observations of HDE 226868, the optical counterpart of Cygnus XR-1, reveal polarization variations in both magnitude and position angle which are correlated with spectroscopic phase. The magnitude of the variations is strongly wavelength dependent, however, being greatest in the U, less in the B, and smallest in the V wavelength band. Further, variability is present over much (if not all) of the orbit, and, in the U band, the polarization shows significant changes over periods of minutes (a fact which vitiates attempts to study this particular type of variability by taking nightly averages of observations). The variability may also not be strictly periodic with spectroscopic phase. For all these reasons, the variability is probably caused by Rayleigh scattering of the primary's light from recombining clumps of gas in the streams known to exist in the system.

Observations of X Persei show wavelength independent variability, but not enough observations have yet been made to allow further analysis.

THE MAY 1975 TRANSIENT RADIO EVENT IN CYG X-1

R. M. Hjellming *
National Radio Astronomy Observatory
Charlottesville, Virginia 22901

ABSTRACT

Radio observations of Cyg X-1 (HDE 226868) taken during the period May-June 1975 at 2695 and 8085 MHz are presented and discussed in the context of both the previous four years of data at these frequencies and subsequent data for September-October 1975. The data show that the radio event was a transient one with a time scale of the order of a few to several weeks, and that the observed radio decay was qualitatively similar to the observed decay of the enhanced X-ray state during this period.

INTRODUCTION

The X-ray and radio source Cyg X-1 (HDE 226868) has now shown two unique types of correlation between its X-ray and radio behavior. The first type was the sudden appearance (Hjellming and Wade 1971, Braes and Miley 1971) of a faint radio source on the position of the X-ray star HDE 226868 at the time of a major change in state in the X-ray source (Tanenbaum et. al. 1972) in March 1971. The second type of correlation occurred in May 1975 when both radio and X-ray source underwent a transient event with a time scale of roughly a month. The purpose of this paper is to discuss this transient radio event in the context of the data available both before and after this period May-June 1975.

RADIO DATA AT 2695 AND 8085 MHZ

Portions of the 2695 and 8085 MHz data obtained with the NRAO interferometer on the May 1975 radio event in Cyg X-1 have been published by Hjellming et. al. 1975; however, subsequent data obtained through October 1975 more clearly indicate the nature of the event to be a transient occurrence both preceded and followed by the "normal" radio behavior of Cyg X-1 (HDE 226868) seen since March 1971.

The radio history of Cyg X-1 between February 1971 and October 1975 at frequencies of 2695 and 8085 MHz is shown in Figure 1. The data up to and including May 1975 has been previously discussed by Hjellming (1973) and

*The National Radio Astronomy Observatory is operated by Associated Universities, Inc., under contract with the National Science Foundation.

Hjellming et. al. 1975. This includes a plot of the X-ray data in the 2-6 keV range during the March 1971 transition (Tanenbaum et. al. 1972).

We see from Figure 1 that, after the initial appearance of the radio source above detection limits between March 22 and March 31, 1971, the dominant characteristic of the radio source has been the continuous presence of a flat spectrum with both fluxes at, on the average, the 0.015 Jy level ($1 \text{ Jy} = 1.0 \times 10^{-26} \text{ W/cm}^2/\text{Hz}$). Except for occasional fluctuations about the mean level, which usually were minor enhancements of the radio flux, this mean level was not significantly exceeded until May 1975. The May 1975 radio observations of Cyg X-1 were initiated after being informed by H. Gursky that Cyg X-1 had been caught in an enhanced X-ray state. Observation on May 9, 1975 showed that the radio source associated with Cyg X-1 was at levels of 0.035 Jy at 8085 MHz and 0.024 Jy at 2695 MHz. As shown in Figure 1, this was followed by a rapid decay to only slightly above normal levels at 8085 MHz and a slower decay at 2695 MHz. Following a summer period when the dual-frequency system was not available on the NRAO interferometer, subsequent data were obtained in September-October 1975, as shown in Figure 1; these data showed the continued presence of the radio source at normal or only slightly above normal flux levels.

CONCLUSIONS

Although a detailed comparison has not yet been made, it is clear that the decay of the Cyg X-1 radio source during May-June 1975 was qualitatively similar to the decay seen at X-ray wavelengths during this period, particularly in the Ariel V data in the 2-6 keV and 1.5-15 keV energy ranges (Sanford et. al. 1975) following the initial rise of the X-ray source beginning on roughly April 22, 1975 (Holt et. al. 1975). Therefore both radio and X-ray data during this period show the enhancements in source emission to be transient in nature, in contrast to the relatively long-lived state transition that occurred in March 1971.

REFERENCES

- Braes, L.L.E., and Miley, G.K. 1971, Nature, 232, 246.
- Hjellming, R.M., and Wade, C.M. 1971, Ap.J. (Letters), 168, L21.
- Hjellming, R.M. 1973, Ap.J. (Letters), 182, L29.
- Hjellming, R.M., Gibson, D.M., and Owen, F.N. 1975, Nature, 256, 111.
- Holt, S.S., Boldt, E.A., Kaluzienski, L.J., and Serlemitsos, P.J. 1975, Nature, 256, 108.
- Sanford, P.W., Ives, J.C., Bell Burnell, S.J., and Mason, K.O. 1975, Nature, 256, 109.
- Tanenbaum, H., Gursky, H., Kellog, E., Giacconi, R., and Jones, C. 1972, Ap.J. (Letters), 168, L21.

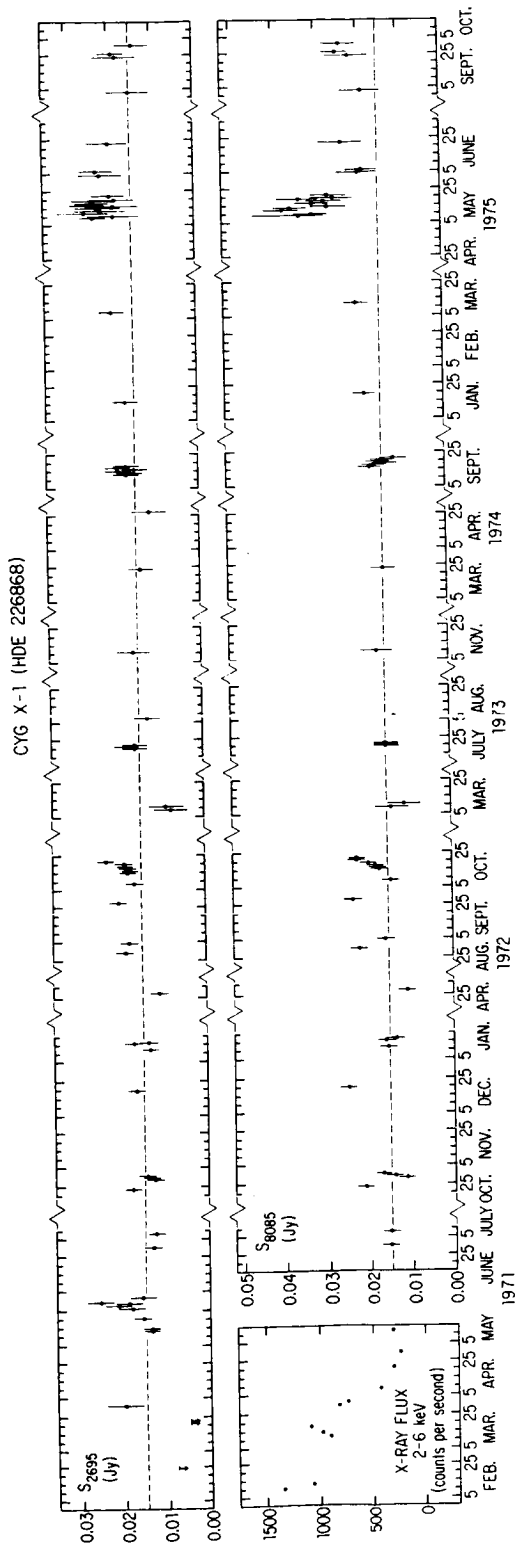


Figure 1. - The radio flux densities of Cyg X-1 (HDE 226868) at 2695 MHz are plotted as a function of time for the period 1971 through October 1975, together with the X-ray data in the 2-6 keV range during the March 1971 transition.

EFFECTS OF RADIATION PRESSURE ON THE
EQUIPOTENTIAL SURFACES IN X-RAY BINARIES

Yoji Kondo
NASA Johnson Space Center
Houston, Texas 77058

George E. McCluskey, Jr.
and
Samuel L. Gulden
Department of Mathematics
Lehigh University
Bethlehem, Pennsylvania 18015

ABSTRACT

Equipotential surfaces incorporating the effect of radiation pressure have been computed for the X-ray binaries Cen X-3, Cyg X-1 = HDE 226868, Vela XR-1 = 3U 0900-40 = HD 77581, and 3U 1700-37 = HD 153919. The topology of the equipotential surfaces is significantly affected by radiation pressure. In particular, the so-called critical Roche (Jacobian) lobes, the traditional figure 8's, do not exist. The effects of these results on modeling X-ray binaries is discussed.

INTRODUCTION

The optical component in most X-ray binaries is found to be an O-or early B-type giant or supergiant. As discussed below, it is well known that such stars are generally losing mass at a significant rate and that it is probably radiation pressure which plays the dominant role in causing this mass loss. An important factor in the theoretical and observational study of close binaries is the existence of the so-called critical Roche (or Jacobian) lobe which arises in the restricted three-body problem. It is usually assumed a priori that when the more massive star expands as it evolves and reaches its critical Roche lobe, it begins to transfer mass thru the inner Lagrangian point, L_1 , to the companion star. The duration and rate of mass flow are assumed to be governed by the size and shape of the critical Roche lobe as well as by the evolutionary expansion of the star. However, radiation pressure can change the size and even the shape of the Roche lobe. Consequently, when radiation pressure becomes significant, as it does for early-type stars, its effects on the Roche equipotentials must be taken into account.

We have computed the equipotential surfaces for four X-ray binaries both with and without radiation pressure. The calculations were performed for Cen X-3, Cyg X-1, 3U 0900-40, and 3U 1700-37. These binaries were chosen as the early spectral types of the optical components indicated that the effects of radiation pressure would be significant.

DISCUSSION

In this analysis, the effect of radiation pressure was computed following the work by Schuerman (1972) in which electron scattering is the principal mechanism for creating it.

Figures 1 through 8 demonstrate the differences in the equipotential surfaces with and without radiation pressure. The parameter μ is the relative mass of the X-ray star. The physical parameters adopted for these calculations are tabulated in Table 1. We assume that electron scattering dominates in hot stars and thus take $\kappa = 0.2(1-X) \approx 0.35$, where X is the fractional hydrogen abundance by number. Then:

$$\delta = 2.68 \times 10^{-5} \frac{L/L_{\odot}}{M/M_{\odot}}$$

where L is the luminosity and M the mass of the hot star.

Table 2 lists the radiation pressure parameter, δ , which is the ratio of the radiation pressure force to the gravitational force, and both the coordinate of the internal Lagrangian (L_1) point and the radius of the primary's Roche lobe with and without radiation pressure for each system.

The equipotentials incorporating the effects of radiation pressure (Figures 2, 4, 6, and 8) show that the critical Roche surface, figure "8", no longer closes behind the X-ray component. Matter escaping through the L_1 point will have access to regions surrounding the whole system rather than being limited to the neighborhood of the X-ray star. This may alleviate some of the difficulty in explaining why self-absorption or quenching of X-rays does not occur in some X-ray binaries where the rate of mass loss by the optical component is relatively high. Radiation pressure will decrease the fraction of mass accreted by the X-ray star. It should be noted that the gas streams found by Bessell, Vidal and Wickramasinghe (1975) in the Vela XR-1 system fit innicely with the topology of the Roche equipotentials when radiation pressure is present. As Table 1 indicates, for the systems Cyg X-1 and 3U 1700-37 where radiation pressure is relatively large, the radius of the critical Roche lobe surrounding the optical component is decreased by 15-20%. Our results

agree with Bolton (1975) that the shape of the primary's critical lobe is not significantly changed unless $\delta \gtrsim 0.9$. Consequently, use of the size of the Roche lobe is hazardous if radiation pressure is not accounted for while use of its shape is not unreasonable if $\delta \lesssim 0.9$.

Lucy and Solomon (1970) suggested that radiation pressure in the resonance lines of abundant ions might give rise to a stellar wind sufficient to explain ultraviolet observations of mass loss from OB supergiants. They predicted mass loss rates of $10^{-8} - 10^{-9}$ solar mass per year with outflow velocities of 1000 - 2000 km s⁻¹. The observed mass loss rates are at least 100 times higher in many cases. Recently, Castor, Abbott and Klein (1975) have found that by taking subordinate lines into account, the effect of radiation pressure could give rise to mass loss rates of 6×10^{-6} solar mass per year for an O5 star with a terminal outward velocity of 1500 km s⁻¹. This is in excellent agreement with values found by Morton (1967) from rocket spectra of OB stars and from a Copernicus far-ultraviolet study of the O7f primary in the system UW CMa (McCluskey, Kondo and Morton, 1975). Castor et al. (1975) found that the apparent size of the hot star would be increased by 10-30% due to electron scattering in the envelope of the star. They found that the material is accelerated rapidly by radiation pressure. The velocity is essentially zero at the photosphere and increases to the escape velocity at a distance of 0.1-0.2 stellar radius above the photosphere.

These results imply that at a small distance above the photosphere, δ may be equal to unity or even somewhat larger. Thus, the effective gravity of the primary, in regard to its gravitational attraction on gas particles, becomes zero or even negative. The critical Roche lobe surrounding the primary must in fact coincide essentially with the photosphere where δ becomes small. No closed lobes exist above the photosphere and no closed lobes surround the system. Only in the neighborhood of the X-ray component do closed lobes exist: these surround this component.

Consequently, the Roche equipotentials tell us nothing about the size of the optical component if it is of early spectral type and high luminosity. These surfaces also tell us nothing about the shape of the hot star. The critical Roche lobe surrounding this star is determined by the way in which the radiation pressure determines its effective gravity at each point. We would have to know δ as a function of position in order to calculate equipotentials. In short, as δ approaches or exceeds unity, the usual concept and usefulness of the Roche equipotentials vanish.

Observational work on several X-ray binaries agrees qualitatively with the theoretical stellar wind calculations. The optical component, HD 153919, in the X-ray binary 3U 1700-37 is an O7f star. Conti and Cowley (1975) discussed the emission line spectrum of this system and found an outwardly accelerating envelope surrounding the O7f star,

expanding at $300\text{--}1600 \text{ km s}^{-1}$. Hensberge (1974) estimates the mass loss rate as 2×10^{-6} solar mass per year.

Vidal et al. (1974) found P Cyg profiles for H β and He II $\lambda 4686$ in the spectrum of the optical component in Cen X-3. Expansion velocities of 800 km s^{-1} were found.

One must conclude that for any close binary in which one (or both) component is an early-type giant, supergiant or Of star, the radiation pressure is the dominant effect in causing mass loss and the Roche lobe probably plays a limited role at best. For stars not quite so luminous and with weaker stellar winds, the role of the Roche lobe becomes more important and for stars later than B0 or B1, with the possible exception of the most luminous supergiants, radiation pressure becomes negligible, and if the requirements of the restricted three-body problem are met (Kondo 1974), the Roche surfaces may yield important information about the system.

In order to investigate quantitatively the effects of radiation pressure, calculations of particle trajectories are currently being carried out both with and without radiation pressure. The computations were performed and figures plotted using a program written in Pascal 6000 on the CDC 6400 at the Lehigh University Computing Center.

REFERENCES

- Bessell, M. S., Vidal, N. V., and Wickramasinghe, D. T. 1975, Ap. J. (Letters), 195, L 117.
Bolton, C. T., 1975, Ap. J., 200, 269.
Castor, J. T., Abbott, D. C., and Klein, R. T. 1975, Ap. J., 195, 157.
Conti, P., and Cowley, A. 1975, Ap. J., 200, 133.
Hensberge, G. 1974, Astr. and Ap., 36, 295.
Kondo, Y. 1974, Ap. and Space Sci., 27, 293.
Lucy, L. B., and Solomon, P. 1970, Ap. J., 159, 879.
McCluskey, G. E., Kondo, Y., and Morton, D. C. 1975, Ap. J., 201, 607.
Morton, D. C. 1967, Ap. J., 150, 535.
Schuerman, D. W. 1972, Ap. and Space Sci., 19, 351.
Vidal, N. V., Wickramasinghe, D. T., Peterson, B. A., and Bessell, M. S. 1974, Ap. J., 191, L 23

Table 1

Adopted Parameters

Binary	SpT _{opt}	$\text{Log} \frac{L_{\text{opt}}}{L_{\odot}}$	$\frac{M_{\text{opt}}}{M_{\odot}}$	$\frac{M_X}{M_{\odot}}$
Cen X-3	08 III-V	5.25	20	2.7
Cyg X-1	09.7 Iab	5.70	22	12.8
3U 0900-40	B0.5 Ib	5.16	23	2.0
3U 1700-37	07 f	5.78	30	3.0

Table 2

Radiation Pressure, Coordinates of the
Internal Lagrangian (L₁) Point and
Radius of Primary's Roche Lobe

Binary	μ	δ	$x_1(0)$	$x_1(\delta)$	$r_1(0)$	$r_1(\delta)$
Cen X-3	0.11	0.24	-0.590	-0.554	0.583	0.533
Cyg X-1	0.39	0.61	-0.156	-0.044	0.417	0.317
3U 0900-40	0.08	0.17	-0.648	-0.624	0.600	0.590
3U 1700-37	0.09	0.54	-0.628	-0.522	0.592	0.500

Cen X-3

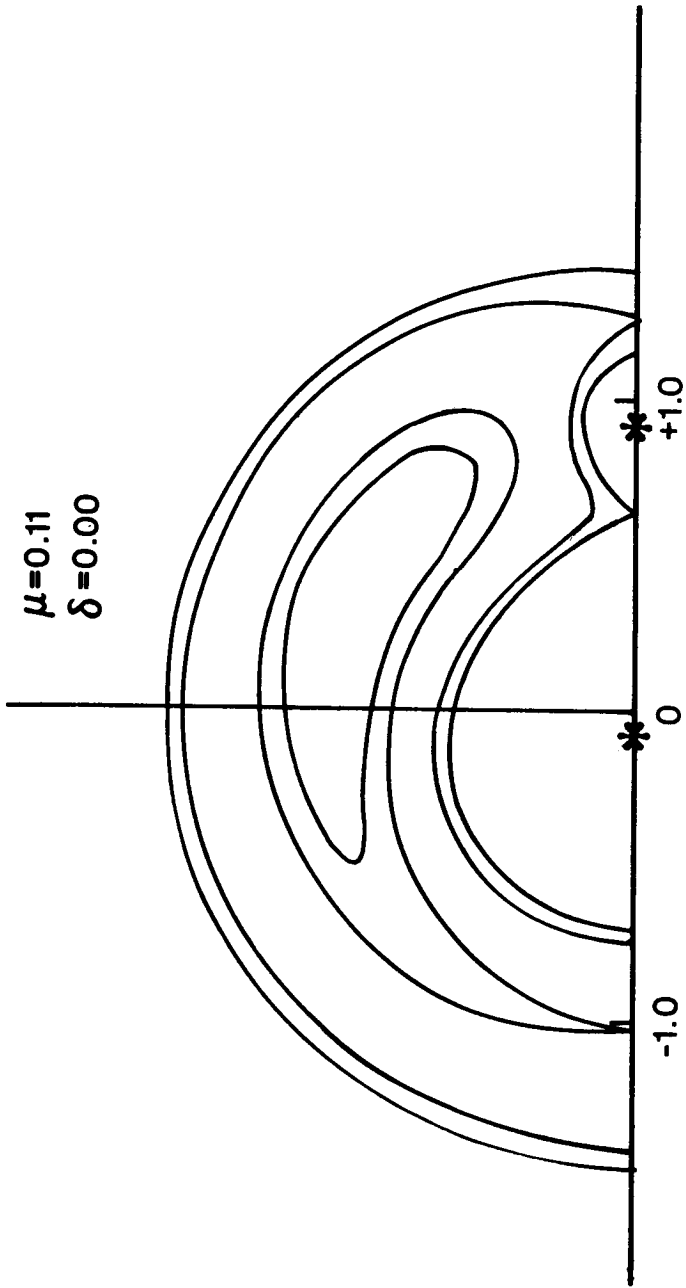


Figure 1 - Equipotential surfaces for Cen X-3. The parameter δ is the ratio of the radiation pressure force to the gravitational force for the optical component. The parameter μ is the ratio of the mass of the less massive component to the total mass of the system. The optical component is to the left of the Y-axis and the distance between the stars is defined to be unity.

Cen X-3

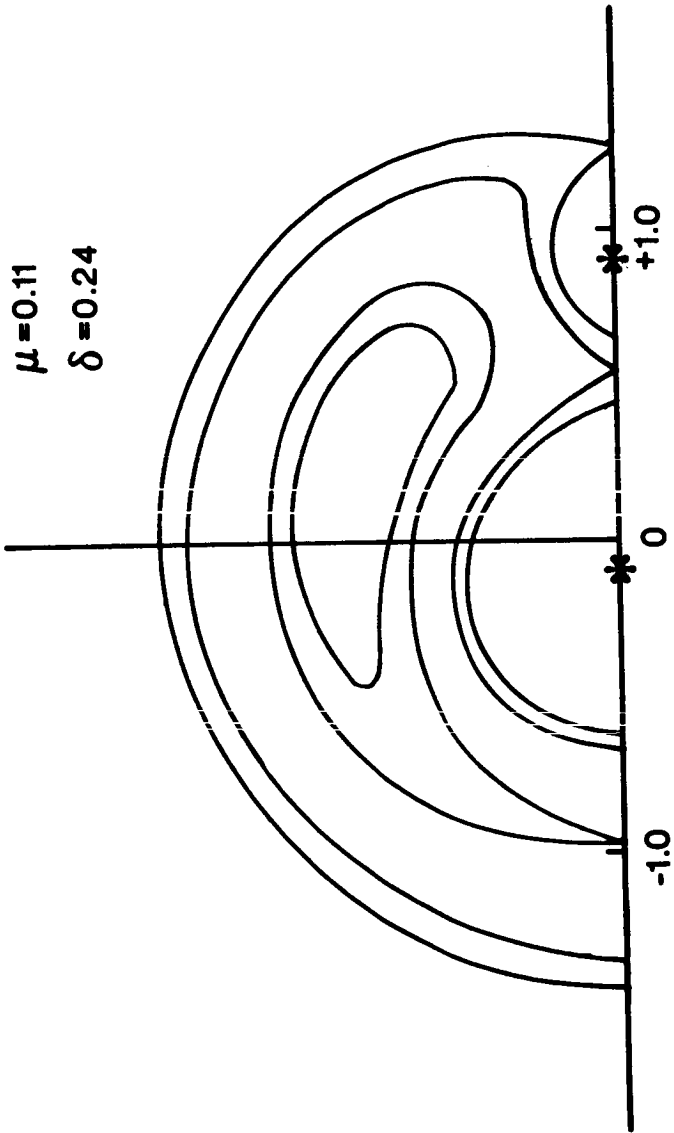


Figure 2 - Same as Figure 1. Note the effect of radiation pressure on critical Roche lobe as compared with Figure 1.

Cyg X-1 = HDE 226868

$\mu=0.39$
 $\delta=0.00$

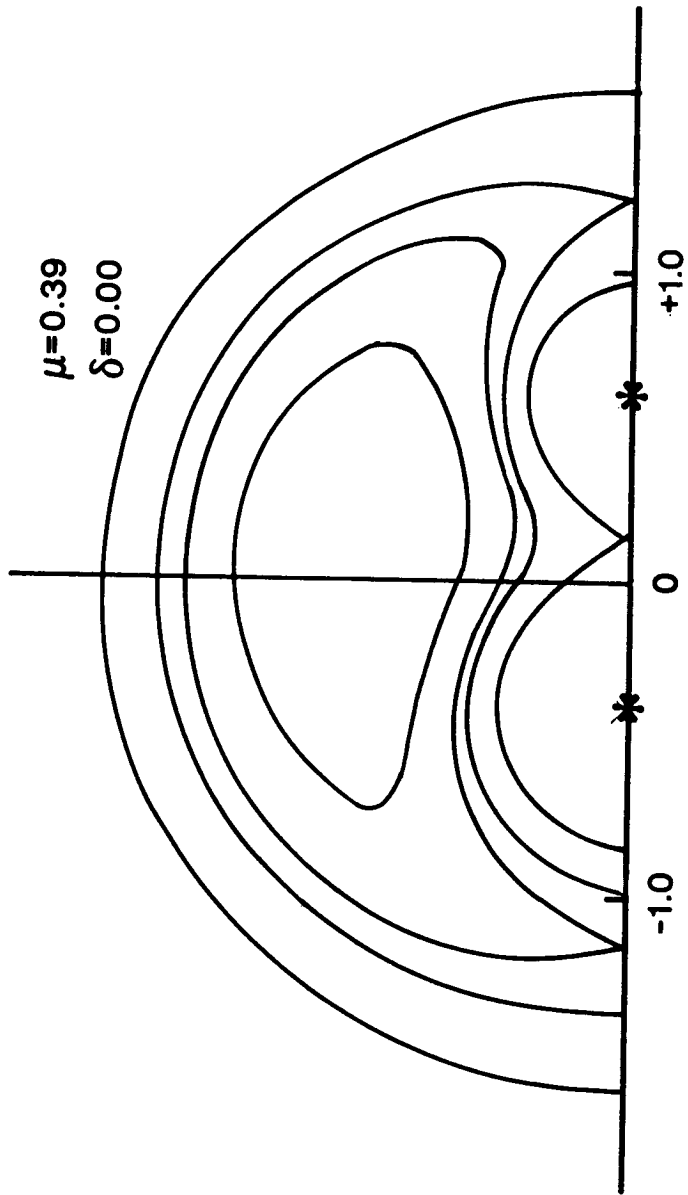


Figure 3 - Cyg X-1. Same as Figure 1.

Cyg X-1 = HDE 226868

$\mu=0.39$
 $\delta=0.61$

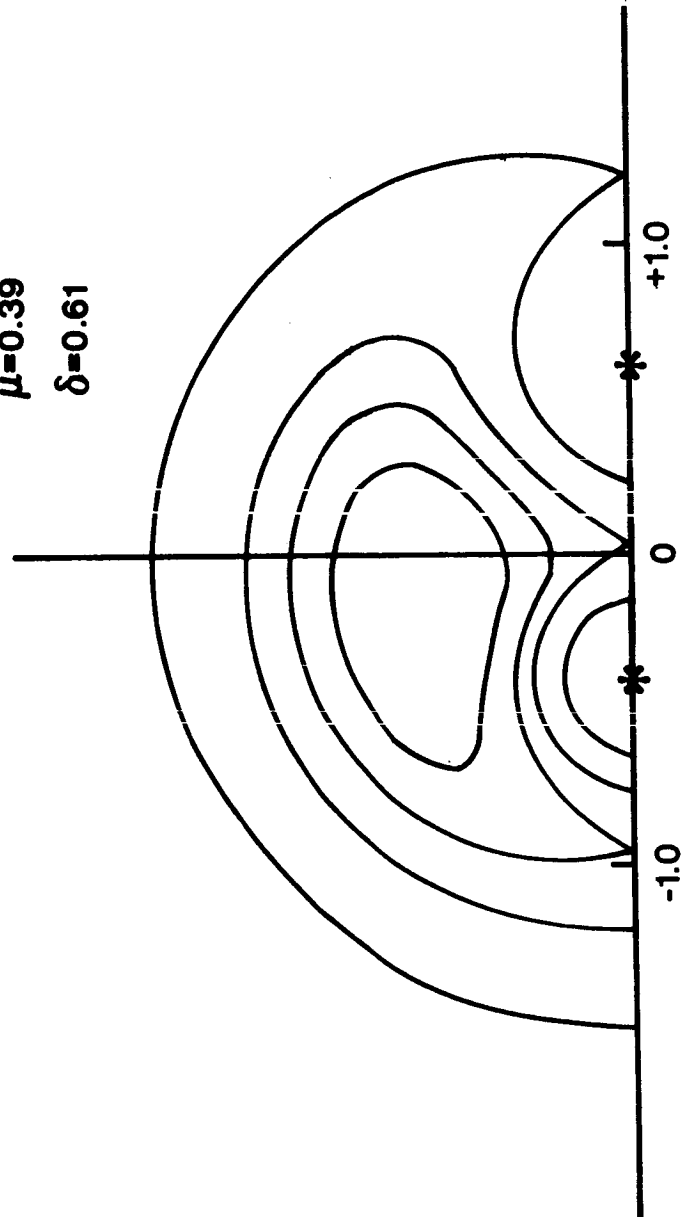


Figure 4 - Cyg X-1. Same as Figure 1.

3U0900-40 = HD 77851

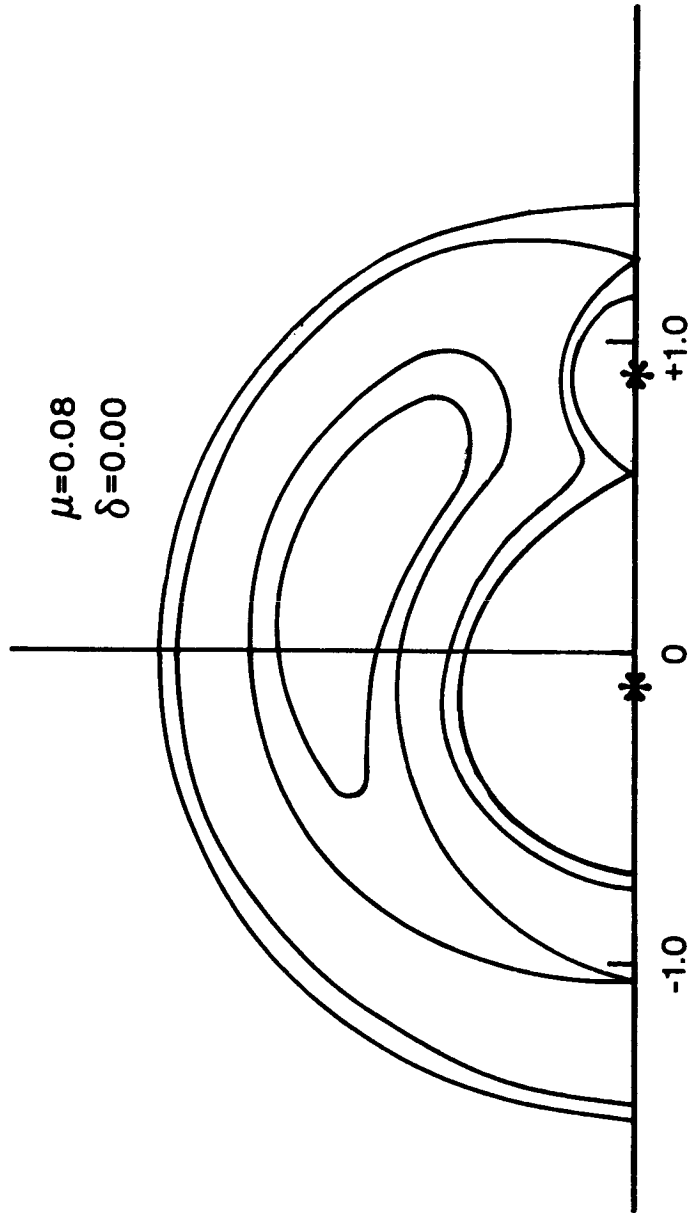


Figure 5 - 3U 0900-40 = HD 77851. Same as Figure 1.

3U0900-40 = HD 77851

$\mu=0.08$
 $\delta=0.17$

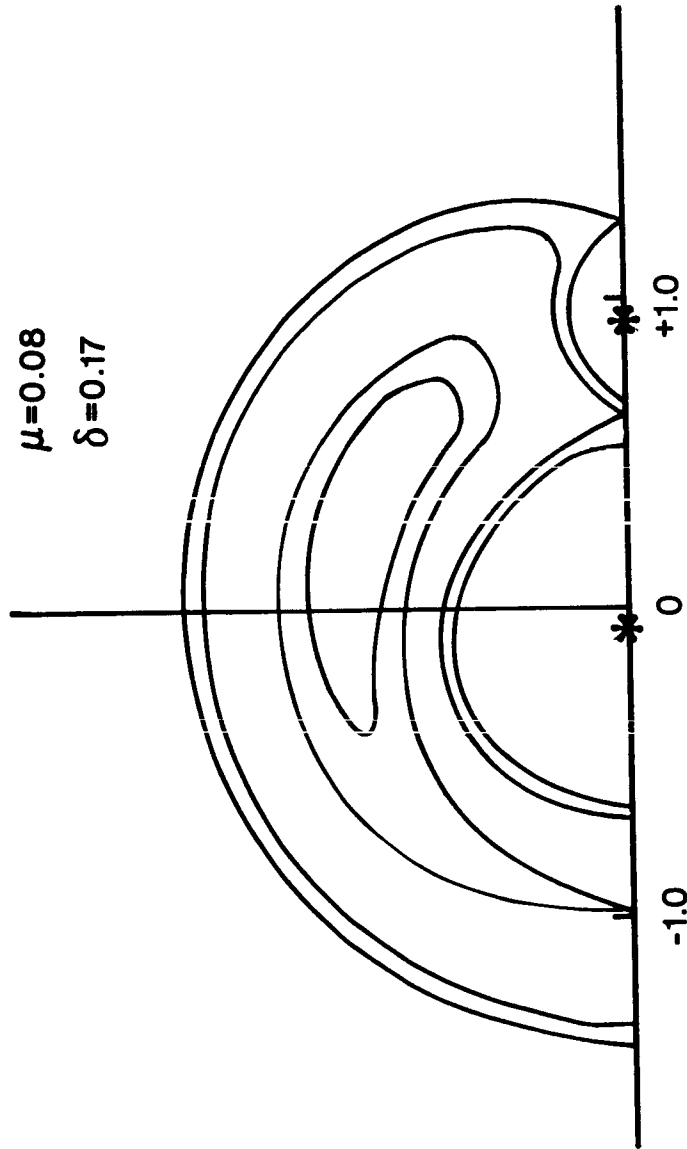


Figure 6 - 3U 0900-40 = HD 77851. Same as Figure 1.

3U1700-37 = HD153919

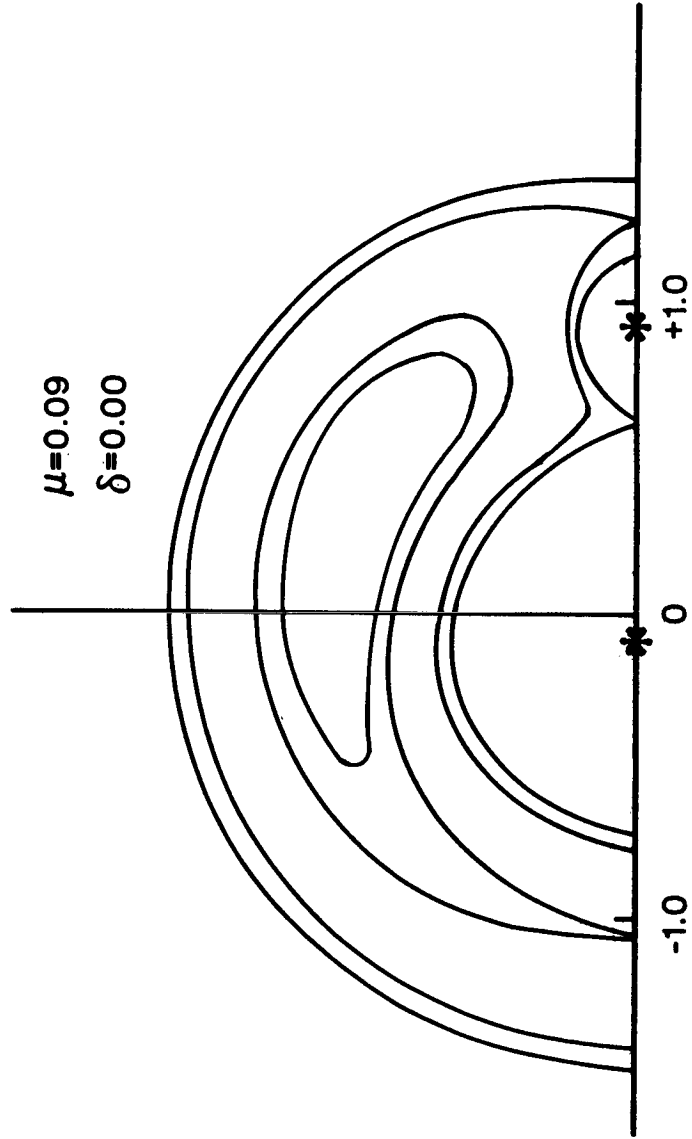


Figure 7 - 3U 1700-37 - HD 153919. Same as Figure 1.

3U1700-37 = HD153919

$\mu = 0.09$
 $\delta = 0.54$

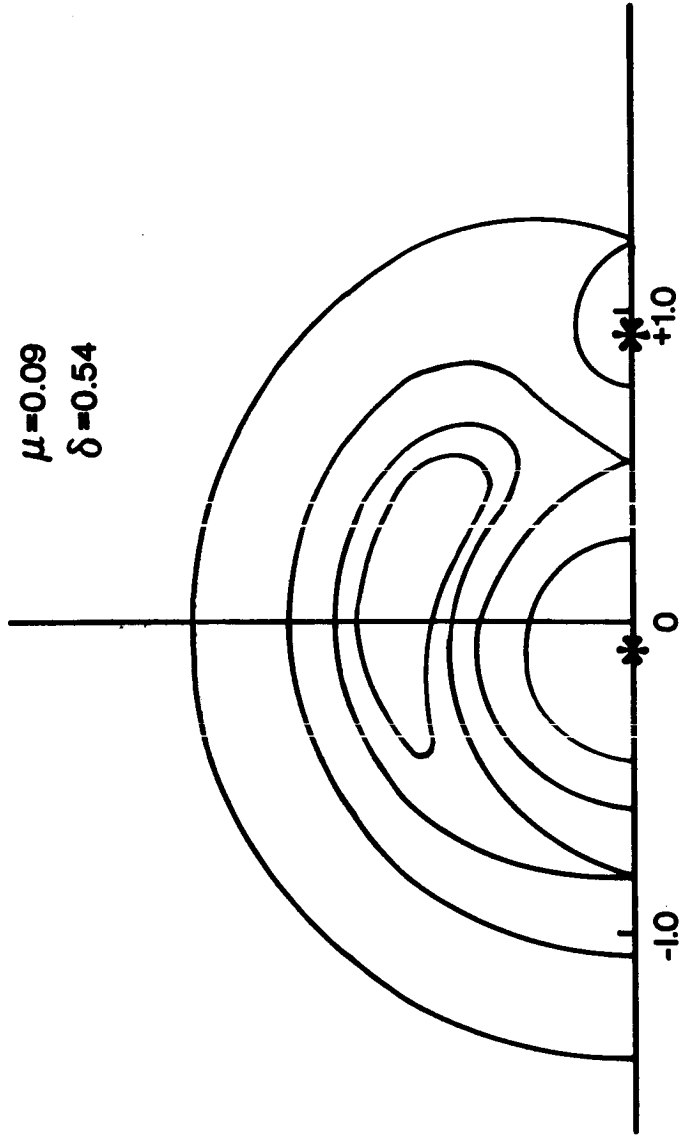


Figure 8 - 3U 1700-37 = HD 153919. Same as Figure 1.

THE LONG TERM VARIABILITY OF HDE 226868 = CYGNUS X-1

WM. LILLER

Center for Astrophysics
Harvard College Observatory and
Smithsonian Astrophysical Observatory
Cambridge, MA

ABSTRACT

Investigation of blue-sensitive photographs of HDE 226868 = Cygnus X-1 reveal no (± 0.06 mag) long-term changes in brightness since the beginning of the century nor any abrupt intensity changes similar to what has been observed at X-ray and radio frequencies. From the double sinusoidal fluctuation with 5.6 day period, an attempt is made to derive a more precise value for the orbital period, but problems are encountered and discussed. There exists evidence that the amplitude of the orbital fluctuations is increasing slowly with time.

While Cygnus X-1 has undergone a number of rapid changes in X-ray and radio brightness, no well-substantiated variations have occurred at optical frequencies except for the doubly-sinusoidal fluctuation of ~ 0.07 mag with a 5.6 day period due to the ellipsoidal figure of the supergiant primary.

We have made a photometric study of the blue sensitive photographs dating back to 1890 in the collection of the Harvard Observatory in order to investigate the possibility of long-term changes or occasional abrupt changes in the brightness of the optical source, HDE 226868. Dr. Arlo Landolt, who had found some evidence for a brightness change since 1960 (Landolt 1975), kindly supplied us with UBV magnitudes determined photoelectrically for a number of nearby stars. All of our measurements were made from Harvard plates with a digitized variable iris photometer.

No detectable long-term change in brightness (± 0.04 mag) occurred during the interval 1928 to 1952. Over this period of time, Harvard operated several sky patrol cameras, the one producing plates of the highest quality having an f/5.6 Ross lens with a diameter of 10 cm. Figure 1 shows the annual means of the B magnitudes of HDE 226868 derived from plates taken with this camera. The full length of the vertical error bars are twice the calculated mean error of the mean values. As can be seen, the unweighted average of the annual means, $\bar{B} = 9.746 \pm 0.011$ (standard error) falls within the error bars of 17 of the 22 yearly means indicating no long-term changes. We calculate that

the standard deviation of a single year's value is ± 0.04 mag and suggest this value as the upper limit of variability.

Around the beginning of the century, two series of blue plates were taken of the region with a 20-cm refractor. Thirty nine plates were exposed in 1903 yielding an average B magnitude of 9.808 ± 0.004 (standard error) and 8 plates in 1890 gave $\bar{B} = 9.801 \pm 0.010$. Therefore, we conclude that the optical counterpart of Cygnus X-1 has shown no evidence of variability since 1890 to a precision of ± 0.06 mag.

The brightest and faintest magnitudes recorded for HDE 226868 were $B = 9.49$ in July 1938 and 10.14 in October 1929. Both values fall within the expected spread of magnitudes derived from old plates. Hence, we have no evidence for any abrupt changes in brightness.

The 5.6 day double sine curve fluctuation in brightness, which in 1974 showed a full amplitude in B of 0.07 mag (Lester, et al., 1975), can be seen clearly in the 1903 data but only marginally in 148 magnitudes accumulated in 1944 and 1945. (See Figure 2.) The primary reason for this difference in visibility is presumably the quality of the plates: The early photographs were taken with slow, fine grain emulsions and a 20-cm refractor; the 1944-1945 plates were from the patrol series made with a 10-cm camera and coarser grain emulsions.

From a comparison of the 1903 and 1944-1945 light curves with that published by Lester et al. (1975), one should be able to derive unambiguously the orbital period of the Cyg X-1

system, assuming that there has been no change of period in the last 72 years nor abrupt phase shift as suggested tentatively by Walker (1975). Figure 3, which displays the possible periods derived from our data together with periods published by others, shows that our data indicate most strongly that $P = 5.60305 \pm 0.00015$ days with a second preference for $P = 5.59992 \pm 0.00020$ days. Possibly the 1944-1945 data are misleading and should be ignored; possibly a period change or phase shift has occurred. As soon as other investigators can come to better agreement on the best period, the 1974-1903 baseline should yield a precise period or else make us look for the other effects suggested.

An interesting preliminary result which we hope to investigate more thoroughly is the variation of the full amplitude of the 5.6 day light variations. As Table 1 shows, there appears to be a small increase in amplitude from 1903 to the present.

TABLE 1
Full Amplitudes of the 5.6 day Light Fluctuations
of HDE 226868 = Cyg X-1

Year	ΔB	m.e.
1903	0.035	0.010
1944-45	0.052	0.025
1974	0.067	0.008 (est)

The explanation for this increase might be that the X-ray heating of the luminous primary is decreasing due to decreased mass-accretion rates. Thus, the side of the supergiant facing the collapsed star is less luminous, and in 1974, more of the light fluctuations were due to the tidal distortion of the primary. Any heating of the front face of the supergiant would tend to decrease the fluctuations.

The author thanks the National Science Foundation who supported this research, Lola J. Eachus, William Forman and Christine Jones Forman, who made many of the measurements, and Drs. Arlo Landolt and C. T. Bolton for suggesting that this investigation be undertaken.

REFERENCES

- Bolton, C. T. 1975. This conference.
- Herczeg, T. J. and Sutton, J. K. 1975, Ap. Letters, 16, 17.
- Landolt, A. 1975. Private communication.
- Lester, D. F., Nolt, I. G., Stearns, S. A., Stratton, P., and Radostitz, J. V. 1975, preprint.
- Lyuti, V. M. 1972, Peremennye Zvesdi, 18, 417.
- Lyuti, V. M., Sunyaev, R. A., and Cherepashchuk, A. M. 1974, preprint.
- Murdin, P. 1975. This conference.
- Walker, E. N.-1975. This conference.

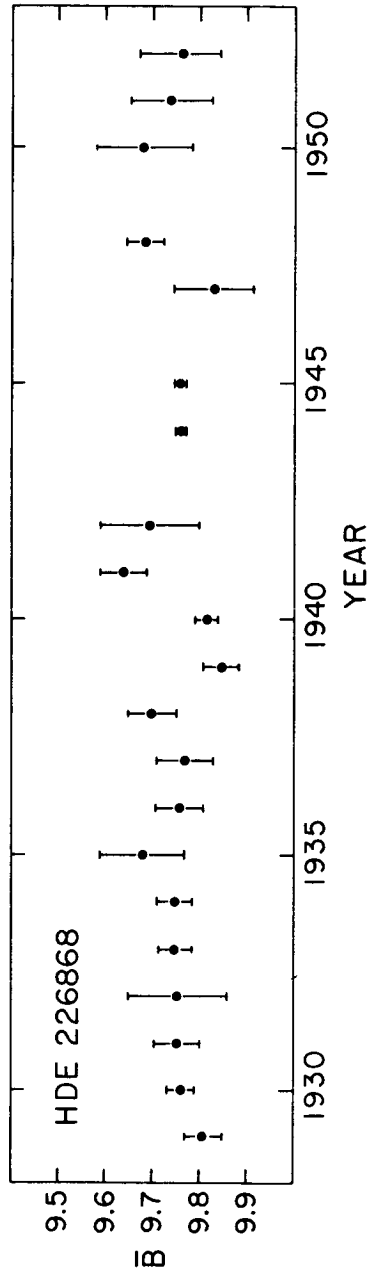


Fig. 1. - Annual mean values of the B magnitude of HDE 226868.

The lengths of the vertical bars are twice the standard error of the means. The mean brightness of HDE 226868 during this period was $\bar{B} = 9.746 \pm 0.011$ (standard error).

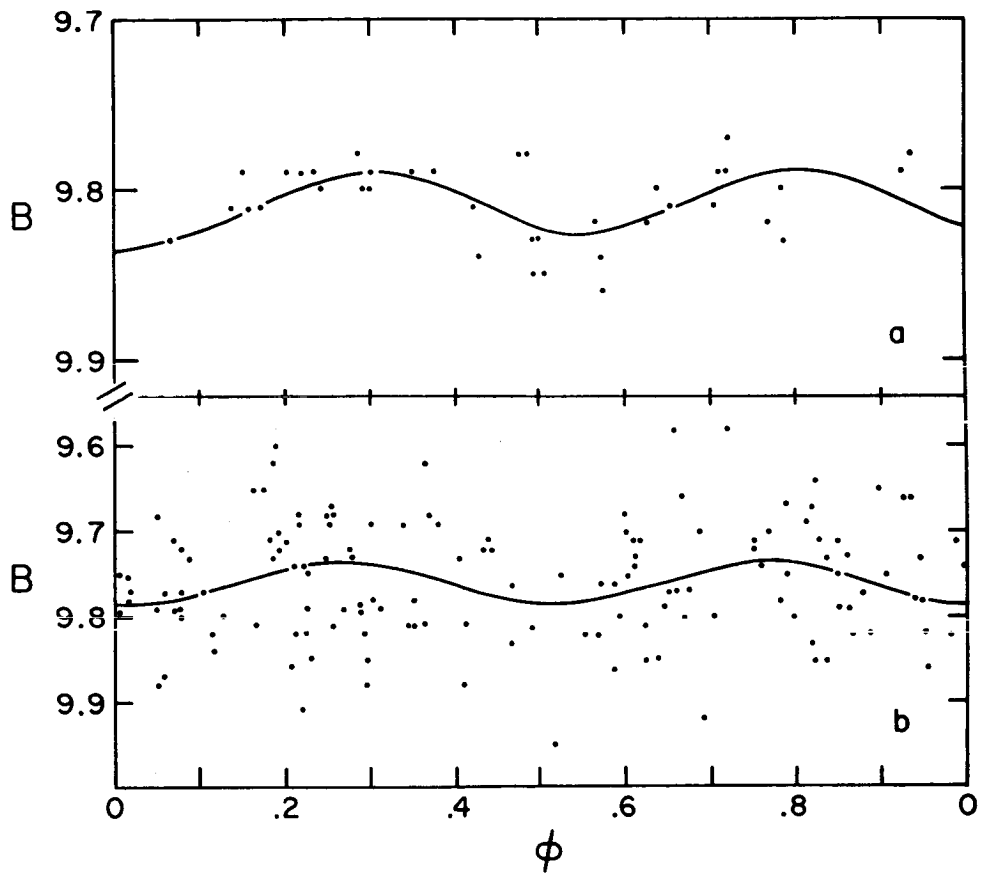


Fig. 2. - Mean light curves of HDE 226868 for the years (a) 1903 and (b) 1944-1945 mased on 39 and 148 magnitudes respectively. The better quality of the 1903 data is attributed to the larger telescope and the finer photographic grain (= slow emulsion).

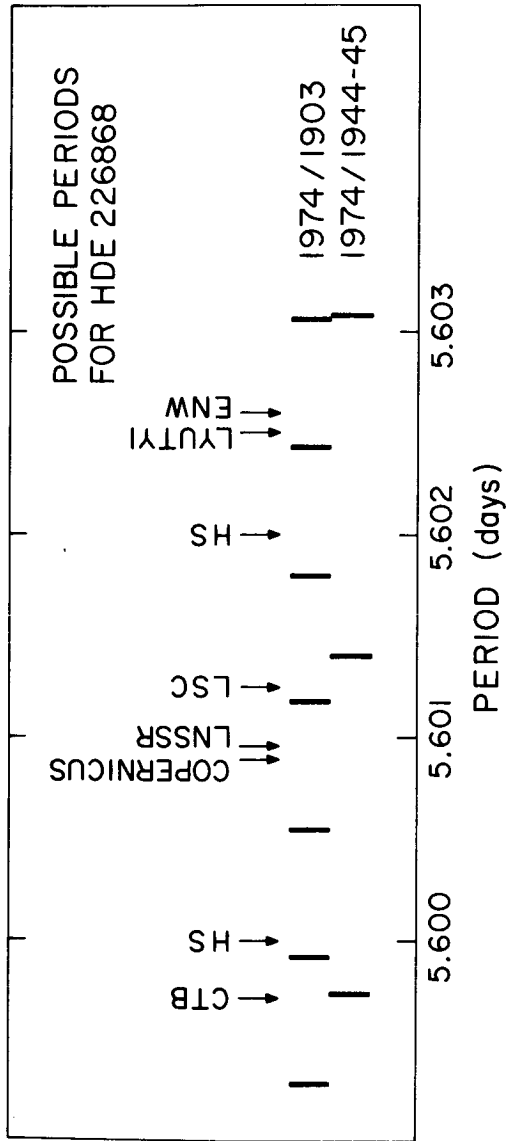


Fig. 3. - Reported orbital periods for HDE 226868 compared with periods derived from the data of Fig. 2 and modern photoelectric light curves (Lester et al., 1975). The abbreviation code is as follows: CTB = Bolton (1975); HS = Herczeg and Sutton (1975); Copernicus = Murdin (1975); LNSR = Lester, et al. (1975); LSC = Lyuti, Sunyaev and Cherepashchuk (1974); Lyuti (1972); ENW = Walker (1975).

Blue Band Photometry of Cygnus X-I

E. N. Walker

Royal Greenwich Observatory,
Herstmonceux Castle,
Hailsham,
Sussex,
England.

Abstract

The results of blue band photometry of HDE 226868 in the years 1972-3-4 and provisional results for 1975 are presented. A mean light curve is obtained from the first three years observations which is based on 192 nights observations. Intercomparison of the results from the different years shows that the light curve is not constant.

Introduction

In a series of papers Walker (1972), Walker and Rolland (1974), Walker, Rolland and Buck (submitted to MNRAS) we have presented the results of monitoring the star HDE 226868 for 29 nights in 1972, 55 nights in 1973 and 108 nights in 1974. We have obtained 72 nights observations at the time of writing in 1975 and expect to obtain approximately 30 more before the end of the 1975 season. Our results for 1975 should therefore be regarded as provisional. The general features of our light curves, which show two maxima and minima per orbital period, are in general agreement with those produced by other authors, Cherepashchuk et. al. (1972), Lester et. al. (1973) and Lyutyi et. al. (1974). However, as pointed out by Avni and Bahcall (1975), the present quality of the light curve is inadequate to differentiate between various models of the binary system. We present here the most detailed light curve yet obtained together with some conclusions to be drawn from the results. The reader is referred to the series of papers either published or submitted to Monthly Notices of the Royal Astronomical Society for detailed listing of the observations and for a more detailed description and discussion of the results.

The Period and Mean Light Curve

The best fit period to our 1972-3 and 4 observations is 5.6026 days. However using this period leads to a phase shift of $\sim 6\%$ for the 1975 observations. Following the results presented by Bolton and Liller at the conference who respectively have obtained periods of 5.59972 days and 5.60118 days we have reexamined our results. A period as short as Bolton's will remove the phase discrepancy between the 1975 results and the mean light curve but will cause the 1972 results, which are based on the smallest number of nights and hence the least well determined, to be very discrepant. Pending completion of the 1975 observations and reanalysis of all the data

we will present here results based on the period which fits our earlier results best. We would note that of the 192 nights results used to obtain this mean light curve 108 ($\sim 56\%$) were obtained in one year only while another 55 ($\sim 29\%$) were obtained only one year earlier. If the period 5.59972 days is correct, rather than 5.6026 days, this will lead to a phase discrepancy of only 3.7% between these two sets of data which should have a very small effect upon the mean light curve obtained.

Figure 1 shows the 192 nights results. The mean line drawn through these was obtained by taking a running median value for each 0.1 of the total period. The formal error of this curve as estimated from the scatter of points is everywhere better than $0.002 m_b$. Points to note particularly are the very different shapes of the minima, with that at $\phi \sim 0.5$ showing a standstill for 0.12P prior to the final drop to the minimum. Following this minimum the rise to maximum light occurs in only 0.08P. Both the standstill in the light curve and the rapid recovery of brightness are reminiscent of eclipse phenomena.

Intercomparison of the mean light curves from different years

In Figure 2 we show the mean light curves for 1972, 3 and 4 where the solid lines were obtained as described above for the three-year mean curve. In Figure 3 we show these three light curves superimposed, while in the lower part of Figure 3 we show the differences between the different light curves. The basic features of the light curve, i.e. the different minima and the rapid rise to maximum light, seem to have been present for the three years. However there has been a progressive brightening of the star which has occurred at about phase 0.5 and not at phase 0. This could be explained by increased heating of the primary by the secondary having taken place over the three years. A detailed analysis of the data shows that this effect occurred until mid 1974 after which there has been a progressive decline in this excess luminosity about phase 0.5.

In Figure 4 we show a provisional mean light curve for 1975 (based on the first 64 nights results) superimposed on top of the three year mean curve. Even ignoring the phase shift, which might be a product of an incorrect period, it can be seen that there has been a major change in the light curve from previous years. The minimum near phase 0 now has a completely different character from that seen previously while the rapid rise in light near $\phi = 0.6$ now has much more the character of that near $\phi = 0.1$. Pending completion of the 1975 observations no conclusions can be drawn from this apparent change but if it is real, and observations obtained between producing the diagram and the time of writing suggest that it is, then perhaps this is a result of the x-ray and radio flare that occurred in May 1975.

Fourier Analysis of the data

All the 1972-3 and 4 data have been subject to several Fourier analyses, both of all data and various subsets of it. This was to try to discover if variations with anything other than the orbital period were taking place, perhaps due to a third body in the system. All power spectra are dominated by power with half the orbital period, due to the double variation in each orbit. Removing this frequency and all its harmonics leaves no power at any frequency greater than 1%, which is about the noise level, between infinite period and half a day. The noise level at $\sim 1\%$ is some three times larger than that in one of the comparison stars, BD+34^o 3816, which is $0.9 m_b$ fainter

than HDE 226868 suggesting that real noise at about the 1% level is being generated by this star. At about the 1% level there are four systems of spikes in the power spectrum that could possibly be associated with real events. The periods are 1.04, 1.2, 2.94 or 2.18 days or their nearest aliases (due to the one day spacing of the observations). It will require more observations to decide on the reality of these variations.

Conclusions

A mean blue light curve has been presented that everywhere has a formal accuracy of better than 0.2% which should enable tighter limits to be put on possible models for the Cygnus X-I binary system. The blue light curve seems not to be constant on a time scale of years and models must take this into account. There have been no periodic variations in light with other than the orbital period and with amplitude greater than 1% and with periods between infinity and half a day during the first three years discussed here.

It is a pleasure to thank Angel Rolland Quintanilla of Granada University, Spain who made 27% of the observations discussed here and Mr Colin Buck and Dr Paul Murdin of the R.G.O. who produced the Fourier analysis program used here.

References

- Avni, Y. and Bahcall, J. N. 1975. *Ap. J.*, 197, 675.
Cherepashchuk, A. M., Lyutyi, V. M. and Sunyaev, R. A., 1972. *Soviet Astron. A. J.*, 17, No. 1.
Lester, D. F., Nolt, I. G. and Radostitz, J. V., 1973. *Nature*, 241, 125.
Lyutyi, V. M., Sunyaev, R. A. and Cherepashchuk, A. M., 1974. *Astron. Zh.* 51, 1150.
Walker, E. N., 1972. *Mon. Not. R. astr. Soc.*, 160, 9P.
Walker, E. N., and Rolland Q. A., 1974. *Mon. Not. R. astr. Soc.*, 169, 247.

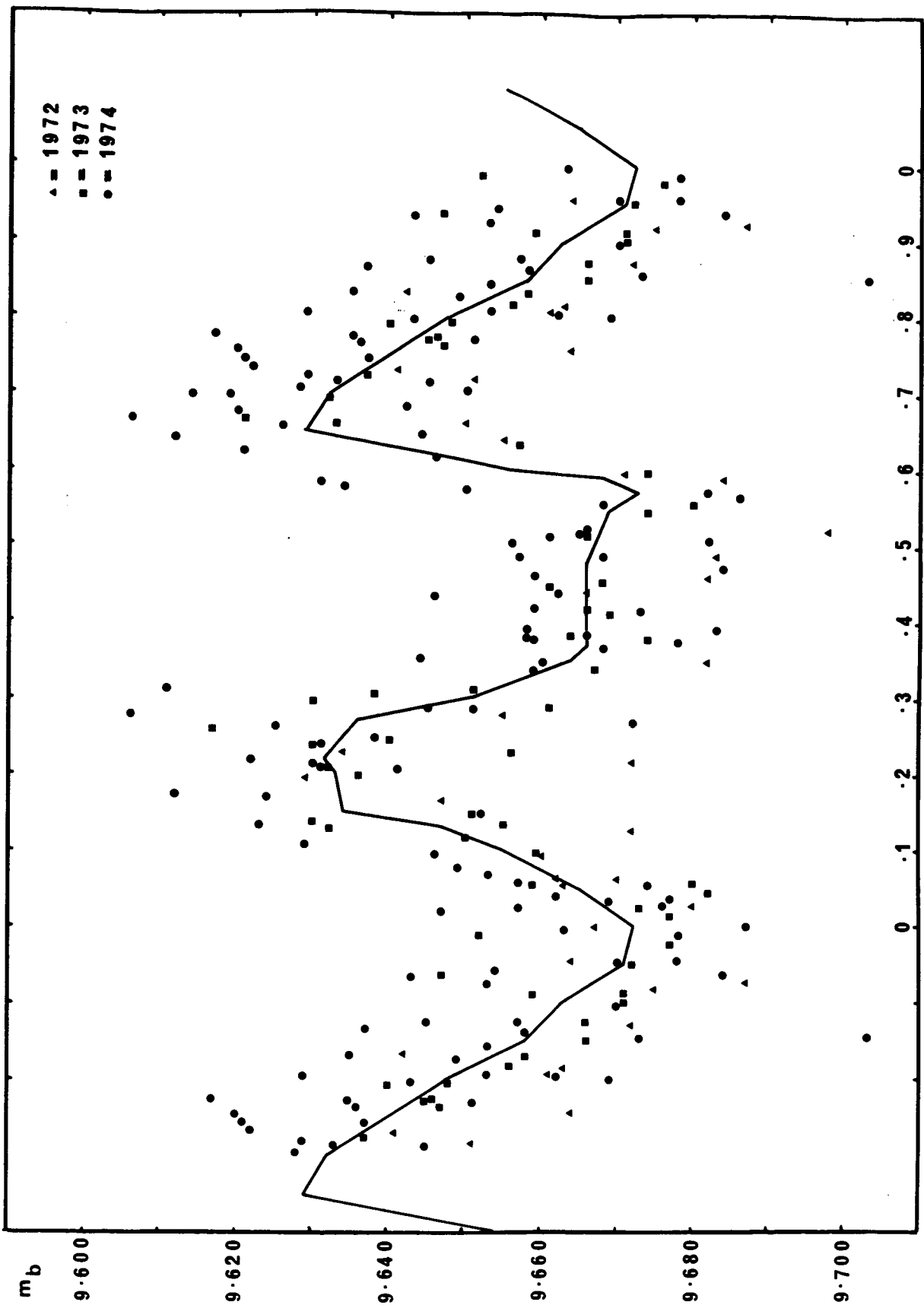


Figure 1 shows the mean curve drawn through all 1972, 3 and 4 observations.

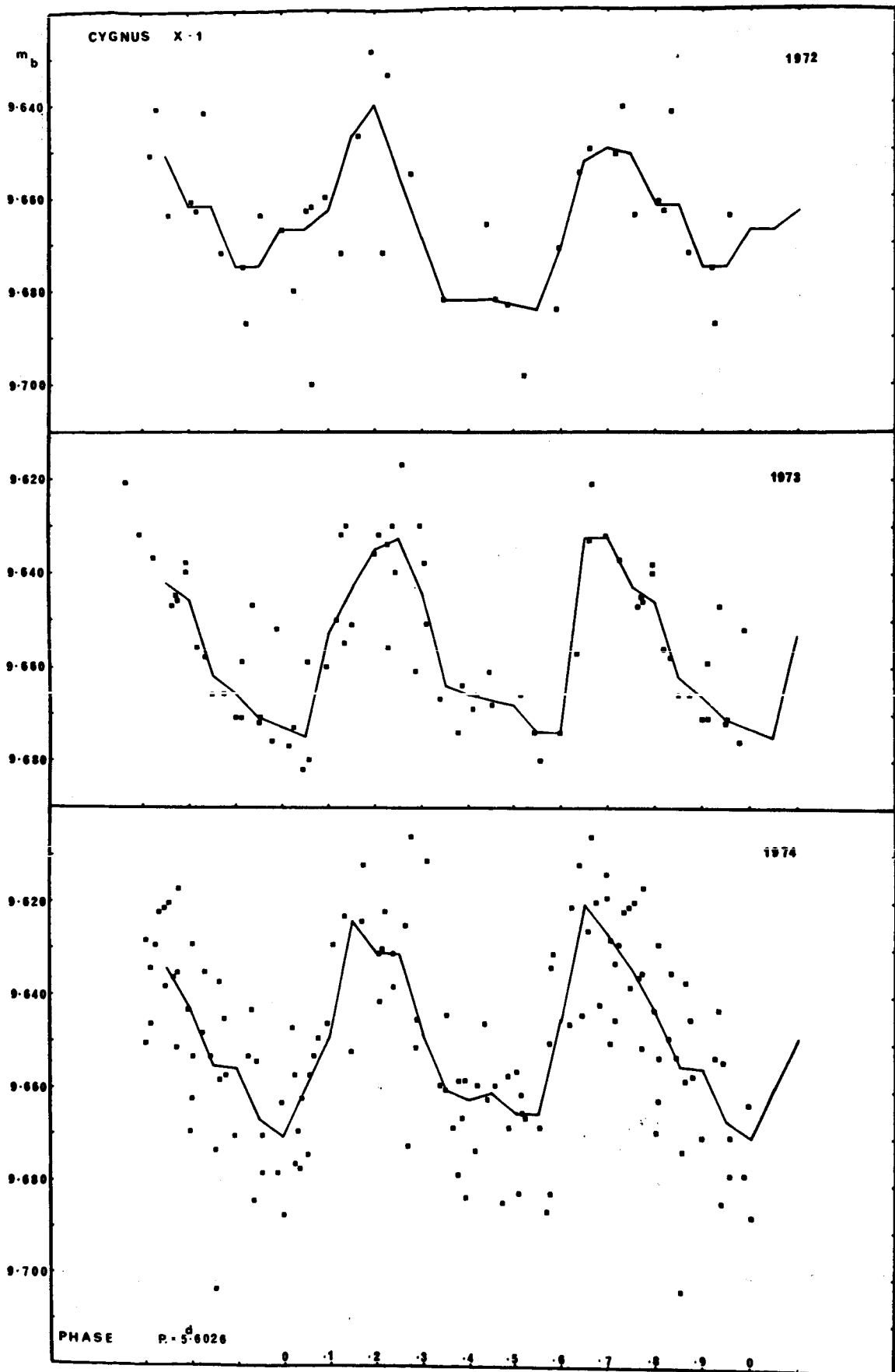


Figure 2 shows individual mean curves for the years 1972, 1973 and 1974.

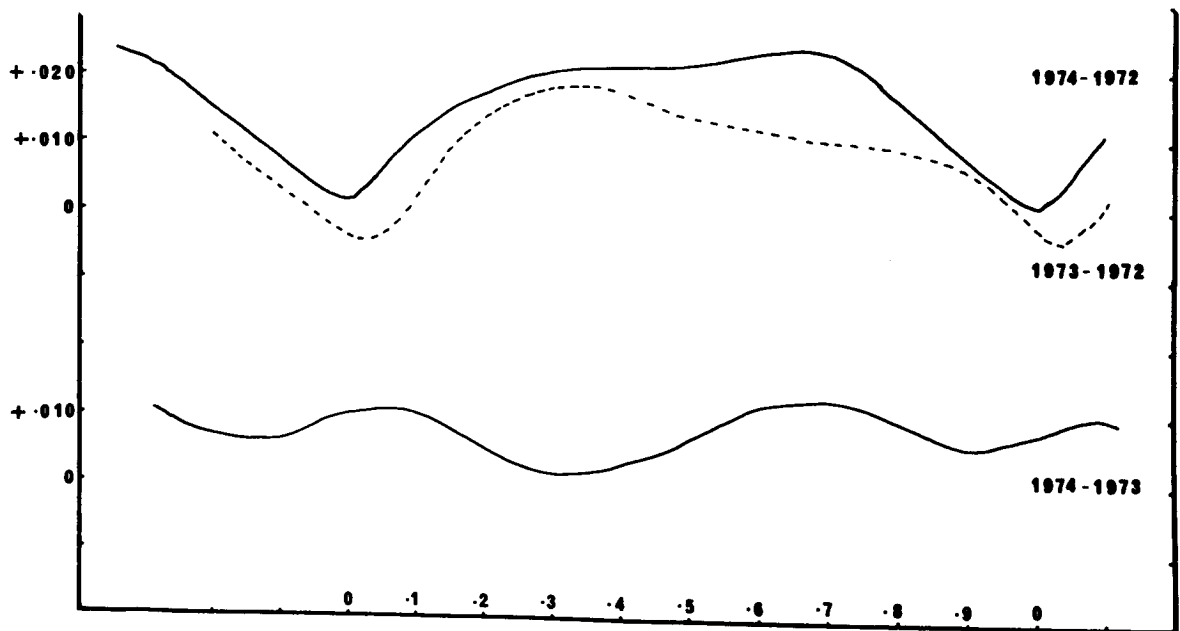
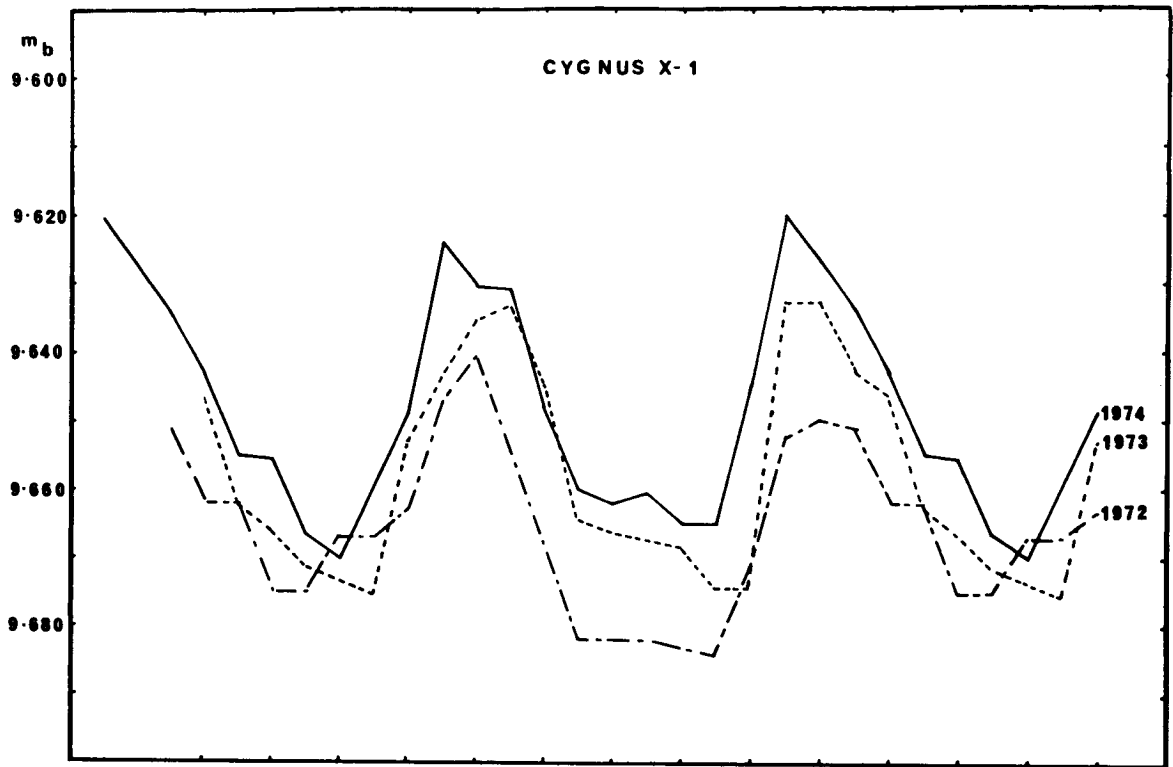


Figure 3. In the upper part we show the mean light curves for 1972, 3 and 4 superimposed while in the lower part we show the differences between the individual light curves.

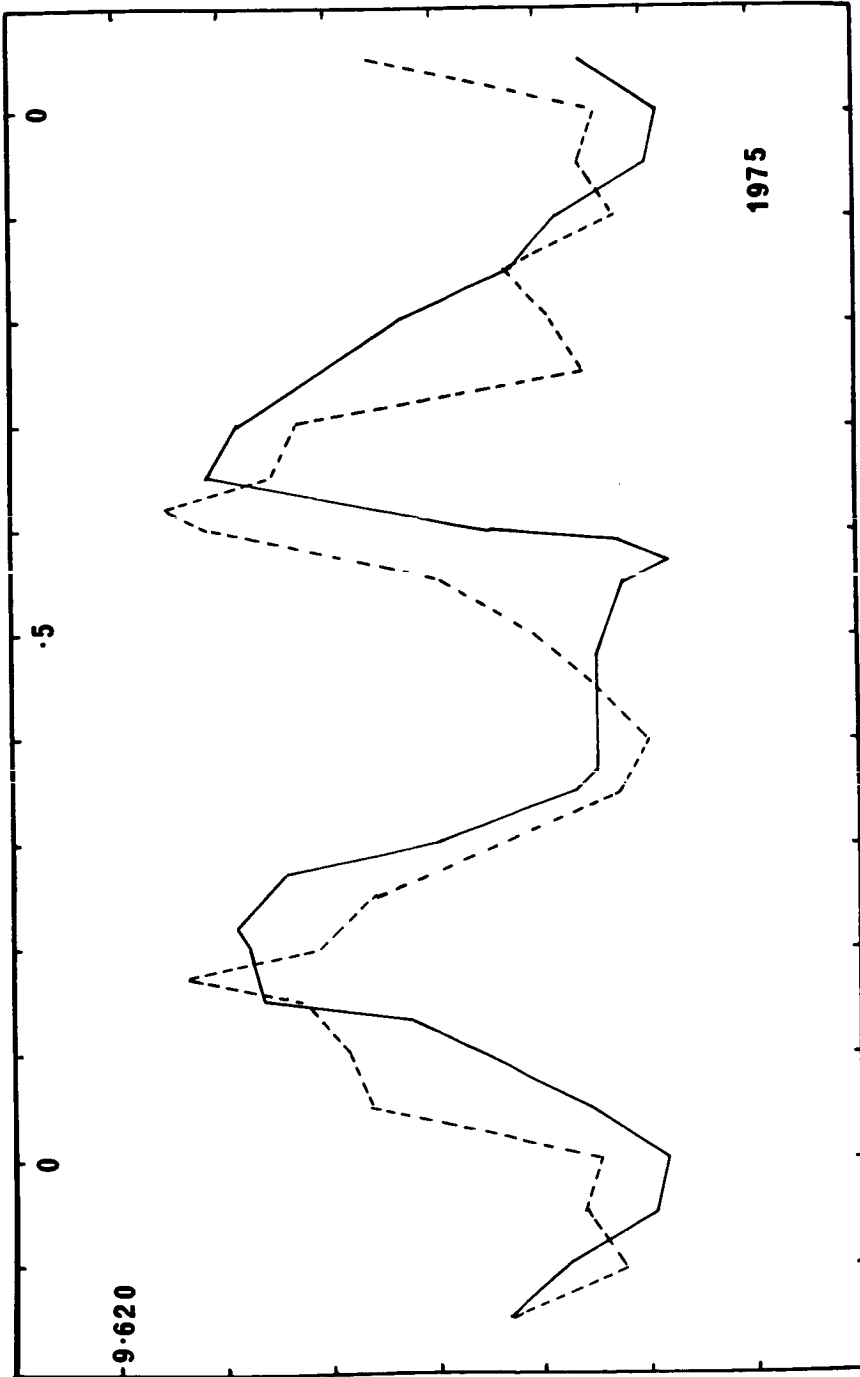


Figure 4 shows a provisional mean curve for 1975 superimposed on top of the mean curve for all previous observations.

INTERSTELLAR REDDENING ESTIMATE OF CYGNUS X-1 FROM THE ULTRAVIOLET

Chi-Chao Wu, R. J. van Duinen
Kapteyn Astronomical Institute, Dept. of Space Research
University of Groningen

G. Hammerschlag-Hensberge
Astronomical Institute, University of Amsterdam

ABSTRACT

Observations obtained by the University of Groningen experiment on board the Astronomical Netherlands Satellite (ANS) are used in the study of interstellar reddening towards the HDE 226868-Cygnus X-1 system. The ultraviolet instrument consists of a 22 cm aperture Cassegrain telescope and a five-channel spectro-photometer with central wavelengths at 1550, 1800, 2200, 2500 and 3300 angstroms. The response function of each channel is almost rectangular with full widths ranging from 100 to 200 angstroms. The field of view is 2.5×2.5 arc minutes with pointing accuracy of 0.5 arc minute.

In order to establish the interstellar reddening law for the region of the sky around Cyg-1, extinction curves for 20 stars within a circle of radius of about 10 degrees are derived. The result is: $E(\lambda-V)/E(B-V) = 5.28(\pm 0.07)$, $4.85(\pm 0.06)$, $6.78(\pm 0.10)$, $4.10(\pm 0.06)$ and $1.99(\pm 0.04)$ respectively for $\lambda = 1550, 1800, 2200, 2500$ and 3300 angstroms, the values inside the parentheses are probable errors for a given set of 20 data points. As it is well known, the extinction curve is strongly peaked at 2200 angstroms. Since the intrinsic spectral energy distribution of early type stars is smooth between 1800 and 2500 angstroms, we can estimate the amount of reddening without having to know the precise intrinsic colors of the object being studied. By adopting $R = 3.1$, then $A(\lambda)/E(B-V) = 3.1 + \{E(\lambda-V)/E(B-V)\}$, where $A(\lambda)$ is the total extinction at wavelength λ . $E(B-V)$ can be estimated by trial and error until a smooth energy distribution is obtained for the program star. Since $E(2200-V)/E(B-V)$ is 6.8, this method is very sensitive in estimating $E(B-V)$. Small over or under correction of reddening will give a hump or a dip respectively in the resulting spectrum.

The observed flux for the pointing centered at HDE 226868 (at orbital phase of 0.27) was first corrected for the presence of BD+34 3816 in the field of view, and then the dereddening process similar to that described above was applied. Our best estimate is $E(B-V) = 1.02$. Due to the facts that HDE 226868 is faint (large error bars) and highly reddened (large reddening correction), a smooth de-reddened spectrum cannot realistically be expected, rather, $E(B-V) = 1.02$ is the value which allows the resulting energy distribution of HDE 226868 to lie within the range set by a O9 Ib and a B0 Ib star. The ground-based value of $E(B-V) = 1.12$ gives a strong hump at 2200 angstroms, indicating that it is too high. This investigation provides an independent, and probably more accurate estimate of the interstellar reddening to Cyg X-1. Combined with the $E(B-V)$ vs distance relationship established from UBV photometry, the system is at 2.5 kpc or more. Therefore, in agreement with ground-based studies carried out by other investigators, HDE 226868 is a luminous and massive star, and Cyg X-1 is a probable candidate for a black hole.

HDE 226868 (CYG X-1)

Discussion

P. Murdin to C. T. Bolton:

Jay once fitted a spectroscopic binary orbit, quite successfully, to radial velocities of the pulsating giant, Mira. My point is that fitting a Keplerian orbit to a radial velocity cycle is relatively easy and the fact that a "good" orbit can be fitted to the HD226868 radial velocities does not, of itself, show that the velocities actually represent the orbit of the star. Although, personally, I agree it probably does--but that's just a feeling.

3U 1700-37 = HD 153919: Review

J.B. Hutchings

Dominion Astrophysical Observatory

Abstract. X-ray, spectroscopic, and photometric data for the source are reviewed briefly. A description is given of the generally accepted model and its important parameters derived. Some points of controversy and difficulty are discussed.

Introduction

The X-ray source 3U 1700-37 is moderately strong (~ 100 Uhuru counts) and shows a long eclipse, with a period of 3.412 days (Jones et al. 1973). In addition, the X-rays are attenuated near 0.5 phase, and show a very wide gradual decrease on either side of the total eclipse. The low-energy cutoff is the strongest of all the X-ray binaries. These characteristics are all qualitatively compatible with the optical star's, which represent an extreme in several ways: 1) the primary is an extreme Of star with large mass outflow through a spherically symmetric stellar wind (Hutchings 1974a); 2) it is the hottest of all X-ray binary primaries (with possible exception of Cen X-3); 3) the mass ratio is very high and the relative separation of the stars is low.

Spectroscopy

Spectroscopic analyses have been made by several workers (Walker 1973, Hutchings et al. 1973, Hensberge et al. 1973, Wolff and Morrison 1974, Hutchings 1974a, Conti and Cowley 1975), and all agree on these essential points. It is clear that in several ways the effect of the compact star on the primary is smaller than in the other systems. The stellar wind is basically unaffected by the companion. Indeed, the source is effectively buried in the wind and it seems very unlikely that an accretion disk can be formed. No sign is seen of emission from such a disk -- at least in comparison with the strong emission lines which come from the envelope as a whole. It has been claimed (Dachs and Schober 1974, Dachs 1975) that the H α emission varies in a phase dependent way, and this may be ascribed to a tidal modulation of the stellar wind, or X-ray absorption in the envelope near to the secondary. However, these results are not confirmed by Conti and Cowley (1975) and seem to me to be by no means certain.

The primary shows clear evidence of an outwardly accelerating envelope, similar to the Of star HD 152408 (Hutchings 1968). Table 1 shows how the mean velocity varies with excitation (and hence, in general, with distance from the photosphere). We also note that K decreases as we move away from the photosphere -- indicating that viscous or damping forces operate in the envelope. An interesting exception to the rule is C IV which has an apparently high recession velocity while having the expected high K for its (large) excitation. Possibly blending or an error in the line wavelengths could account for it, but no specific suggestions are obvious. It appears that K for the

underlying star is about 20 km/sec. The high negative value for V_o , even for the highest excitation lines is typical of this type of star (HD 108, 148937, 152408) and either they are all high velocity stars (all at ~ -50 km/sec!) or the lowest layers of the envelope are themselves expanding at this rate. Mass loss rates have been estimated at $2 \times 10^{-6} M_{\odot}/\text{yr}$ by Hensberge(1974). This is based on the wrong fitting of the He I 4471 profile and I must presently prefer my own estimate(Hutchings 1976) based on a comparative study of mass-loss indicators, of $1.5 \times 10^{-5} M_{\odot}/\text{year}$.

Recession velocities at the distance of the secondary ($\sim 1.5 R_*$) are probably about 100 km/sec. During phases just beyond 0.5, high velocity absorption components (-600 km/sec) are seen in He I $\lambda 5875$, the scatter in RV's increases, and emission in some lines tends to increase. These effects are all probably associated with the passage of the compact body through the moving outer envelope of the primary (see fig. 1). Finally, there are very broad emission features at $\lambda\lambda 4100$ and 4650, similar to those in HD 152408, which may arise in a very extended outer region, where velocities are some thousands of km/sec. This region, however, is probably little affected by X-radiation. The star is not known to be a radio emitter.

Photometry

The photometric behaviour shows a variation of 0.06^m with a large scatter (eg. Penny et al. 1973). Minima are seen at phases 0.1 and 0.5 from X-ray minimum. The 0.5^P minimum may be ascribable to gravitational darkening of the primary, but the cause of the minimum at 0.1^P rather than 0.0^P is not clear. A moderate eccentricity in the orbit could account for it, but would require many noticeable consequences (immersion of compact body in the primary photosphere, large changes in stellar wind behaviour, Roche lobe overflow, precession of orbit) and must probably be discounted. Closer study of the photometric behaviour is badly needed.

If the 0.06^m amplitude is ascribed to gravity darkening then an estimate can be made of the mass ratio (Hutchings 1974b). We must note an important new datum: the X-ray eclipse duration has been revised down to $\pm 44^\circ$ by Ariel data, from the $\pm 55^\circ$ deduced by the Uhuru workers (Fermi Summer School 1975). The reason is apparently increased sensitivity and the gradual nature of the eclipse cutoff. This relieves the difficulties noted e.g. by Sofia and Wilson (1975) of the primary apparently overflowing its Roche lobe and/or requiring an unrealistically high mass-ratio. Analysis of the light curve, eclipse duration, and spectroscopic mass functions (see eg. Hutchings 1975) yields masses of $M_1 = 27$, $M_2 = 1.3$, $q = 20 \pm 3$ and $i = 90^\circ \pm 5^\circ$. Table 2 shows my presently preferred parameters for the system. Reasonable values for the radius of an O7f supergiant ($\sim 20 R_{\odot}$) are fully compatible with these figures, and suggest that $V_{\text{rot}} \sim 300$ km/sec.

Rotation and Summary

This brings us to a second point of controversy. I have estimated V_{rot} from emission line widths, incorporating an expansion of ~ 100 km/sec, of ~ 300 km/sec. The absorption line widths, however, give $V_{\text{rot}} \sim 140$ km/sec and

some workers (Wolff and Morrison 1974, Conti and Cowley 1975) have placed more reliance on this number. If the absorption is formed through an extended region, or in a region significantly removed from the photosphere, then projection effects will cause an underestimate of V_{rot} . The factor of two in this case will occur for lines formed out to $1.3 R_*$ (or in a thin layer closer than this) if angular momentum is conserved in the envelope. Whether you believe this is so is a matter of which model of an expanding envelope you believe (see eg. Hutchings 1968, Castor et al. 1975).

If the rotation velocity is 140 km/sec it is impossible to achieve synchronous rotation without involving an X-ray occulting radius much larger than the photosphere and violating the surface temperature-luminosity relation. You have in any case trouble explaining the width of the emission lines, and must assume highly non-synchronous rotation of the primary. It should be possible to test between these alternatives by making predictions on wake and shock wave phenomena, and clearly this is an important point to pursue.

In summary, we have much to learn from a closer observational and theoretical study of this, the brightest X-ray binary system. We have (probably) a neutron star accreting from a wind rather than a disk, a primary star with an extreme stellar wind ($\dot{m} \sim 10^{-5} M_{\odot}/\text{year}$) with this probe immersed in it, and a system in a very interesting evolutionary state. For example, the primary has the luminosity and presumably radius of a $60 M_{\odot}$ star, but apparently has less than half this mass. It is also presumably -- as for all the X-ray binaries -- in the second stage of mass transfer in a system which may have lost a large fraction of its original mass. The star is bright enough for high quality observations and should be investigated further in all respects. X-ray observations should be investigated for signs and details of the wake and a search made for slow pulsations of the type (~ 280 sec) found in Vel X-1.

References

- Castor, J.I., Abbot, D.C., Klein, R.I. 1975 Ap.J. 195, 157.
- Conti, P.S. and Cowley, A.P. 1975 Ap.J. 200, 133.
- Dachs, J. 1975 A. & Ap. (in press)
- Dachs, J. and Schober, H.J. 1974 A. & Ap. 33, 49.
- Hensbege, G. 1974 A. & Ap. 36, 295.
- Hensbege G., van den Heuvel, E.P.J., Paes de Barros, M.H. 1973 Astr. & Ap. 29, 69
- Hutchings, J.B. 1968 M.N. 141, 219
- 1974a Ap.J. 192, 677.
- 1974b Ap.J. 188, 341.
- 1976 Ap.J. (in press)

- Hutchings, J.B., Thackeray, A.D., Webster, B.L., Andrews, P.J. 1973 M.N. 163, 13 P.
- Jones, C., Forman, W., Tananbaum, H., Schreier, E., Gursky, H., Kellogg, E., Giacconi, R. 1973 Ap.J. 181, L 43.
- Penny, A.J., Olowin, R., Penfold, J., Warren, P. 1973 M.N. 163, 7 P.
- Sofia, S. and Wilson, R.E. 1975 Bull. A.A.S. 7, 336.
- Walker, E.N. 1973 M.N. 162, 15 P.
- Wolff, S.C. and Morrison, N.D. 1974 Ap.J. 187, 69.

Table 1.

153919 line velocities in km/sec

<u>Absorption</u>	V_0	K	exc*	<u>Emission</u>	V_0	K	I.P.
N IV	-60	25:	94	He II 4686	18	13	54
He II	-64	19	76	Si IV 4116	-40	18:	45
O III	-65	22:	68	C III 5696	-74	16	48
Si IV	-83	--	57	N III 4640	-77:	15	47
He I	-87	12	21				
Balmer	-79	16	10				
H γ	-110	12:	10				
C IV	-117	22	85				
Mg II	-136	--	16				
H δ	-150	<10	10				

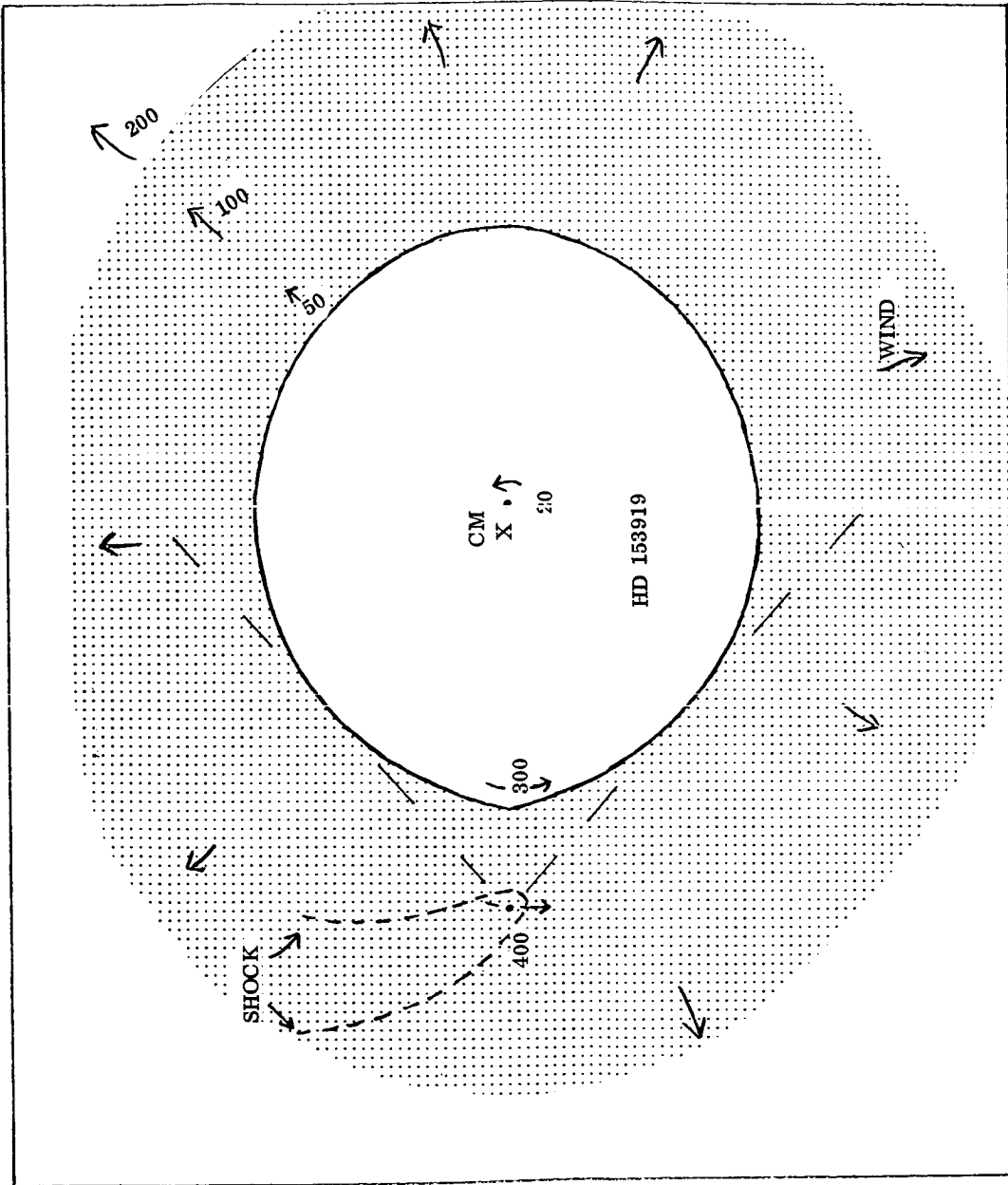
*I.P. of lower ion + e.p. of line lower level.

Table 2.

HD 153919 characteristics

$P = 3.4126 \pm .0003$ days	$V_{rot} = 300$ km/sec?
$K_1 = 20 \pm 2$ km/sec (greater if $e > 0$)	$K_2 = 400 \pm 70$ km/sec.
$V_0 = -65 \pm 2$ km/sec (or is the photosphere expanding?)	Sep/ $R_{primary} \sim 1.4$
$f(m) = .0027$	Light curve $\Delta m \sim 0^m.05$
$M_1 = 27 \pm 5 M_{\odot}$	Distance 1200 pc.
$M_2 = 1.3 \pm 0.2 M_{\odot}$	$M_V = -6.5$
$q = 20 \pm 3$	
$i = 90^\circ \pm 5^\circ$	

P
0.75



P
0.0

P
0.5

P
0.25

Figure 1: Scale drawing of model for HD 153919. Orbital, rotational and expansion velocities given in km/sec; shock front of wake indicated. Photometric phases shown on outside.

Summary of 3U1700-37 Panel Discussions

J.B. Hutchings

In our discussions we have established some new points about the system which I shall list briefly. We have also discussed possibilities and problems concerning the mechanism of accretion in a stellar wind, and the possible formation and detection of a wake.

The points established are: 1) the luminosity of the primary appears to be normal for its spectral type. Its position in the HR diagram is among the O supergiants where masses are thought to be $\sim 60 M_{\odot}$. It thus appears that the present mass is low and the star may have lost a large portion of its main sequence mass in its past evolution. 2) We still have seen no definite evidence of the secondary or its orbital motion -- either by periodic X-ray modulation or by optical line emission. We may still hope that more careful and accurate observations will reveal evidence of this nature. 3) The eclipse duration is shorter than indicated by the Uhuru data, but its exact value may still be uncertain, and important basic quantity to determine if we are fully to understand the orbit, wind and mass-exchange.

On the question of the wake, we have a number of curious and little understood phenomena near phase 0.7. These are the presence of high velocity absorptions in H β and He II λ 4541 as well as those previously seen in He I λ 5875, and the effects mentioned in my introduction. There is the possible identification of Fe XIV at λ 5303 which clearly needs to be confirmed or investigated further. Finally, we have seen that there are extra X-ray absorptions at phases near 0.7.

We do not see the clear evidence for a wake that is seen in Cen X-3, as these effects are variable in phase and strength. It seems likely that simultaneous optical and X-ray monitoring would be useful. It is by no means clear how the optical phenomena are associated with a wake and I commend the problem to the appropriate theoreticians. On the question of velocities and extent of the wake, it seems generally agreed that the X-ray source is moving through its local environment at velocities in excess of 100 km/sec, whatever we assume about the wind and rotation, so that wake formation is likely. More detailed information and interpretation would tell us a lot about accretion in a wind and much about the scale heights of winds in general. At present, theory and ad-hoc models based on the observations disagree on this point. Further investigation of this bright system thus seems very desirable from many astronomical points of view.

HIGH DISPERSION SPECTROSCOPIC OBSERVATIONS
OF HD153919 (3U 1700-37)

A. K. Dupree and J. B. Lester
Center for Astrophysics, Harvard College Observatory
and Smithsonian Astrophysical Observatory
Cambridge, Mass. 02138

ABSTRACT

A spectrogram of HD 153919 taken in June 1975 at phase $\phi = 0.79$ shows the following interesting features when compared to previously published line profiles: (i) increased central absorption or more extended blue wings for He II $\lambda 5411 \text{ \AA}$ and $\lambda 4541 \text{ \AA}$; (ii) a change in the P Cygni profile of H β ; (iii) a change in the relative intensities of N III and C III in the emission complex $\lambda\lambda 4630-4650 \text{ \AA}$; (iv) a previously unreported emission feature near $\lambda 5300 \text{ \AA}$. These observations indicate the presence of a variable stellar wind from the primary, changes in the emission measure of the line-forming region in the primary, and possible spectroscopic signatures of features in the extended expanding atmosphere of the primary or the "wake" of the secondary.

INTRODUCTION

HD153919 is a binary star that has been identified as the optical counterpart of the eclipsing X-ray source 3U1700-37 (Jones *et al.* 1973). The binary system contains an extreme Of star, O6f, making it the hottest of presently known binary X-ray sources, (Hensberge, van den Heuvel, and Paes De Barros 1973; Wolff and Morrison 1974). The Of primary appears to dominate the optical spectrum; no direct spectroscopic evidence of the secondary has been found. Line identifications and details of some spectral features have been presented by many authors (Hensberge *et al.* 1973; Hutchings *et al.* 1973; Walker 1973, 1974; Wolff and Morrison 1974; Conti and Cowley 1975).

Previous observations of the optical spectrum of HD153919 indicate that certain features may change in intensity and in line profile. The reported variability of emission features centers principally in the extremely broad (100 to 180 \AA wide) shallow emissions around H δ , H γ , C III and N III near $\lambda 4640 \text{ \AA}$, and He II $\lambda 4686 \text{ \AA}$ (Walker 1974; Hensberge *et al.* 1973) that may vary in strength in phase with the X-ray flux. These broad features have been attributed to the outflow of material

from the supergiant primary that is modulated by interaction or association with the X-ray source (Walker 1974). Stellar emission in H α , H γ , He I λ 5876 Å, and He II λ 4686 Å (P Cygni profile) has been reported to be variable during March-April 1973 from plates with 12-18 Å/mm dispersion (Hensberge *et al.* 1973) although spectroscopic observations during September 1973 and March 1974 (Conti and Cowley 1975) at 17 to 25 Å/mm indicated that variable intensities occurred only in H α and C III λ 5696 Å and possibly H β , and little or no variation was seen in H γ , and He II λ 5686 Å. The stellar absorption lines are generally reported not to vary in shape or intensity with the exception of an additional blue-shifted absorption feature and apparent line doubling that occurs near phase $\phi \sim 0.5$ to 0.8 in the He I λ 4471 Å transition (Walker 1974) and the absorption component of the He I λ 5876 Å line (Conti and Cowley 1975).

Here we report high resolution observations of selected line profiles in HD153919 that show asymmetric blue absorption wings that are more extensive than those found in 1973-1974. In addition, the N III and C III emission lines near λ 4650 Å have changed in relative intensity, and there are indications of high velocity absorptions in He II λ 5411 Å and λ 4541 Å at phase $\phi \sim 0.79$.

THE OBSERVATIONAL MATERIAL

The data were obtained with the cassegrain echelle spectrograph and Kron electronographic camera at the 60-inch telescope of the Mt. Hopkins Observatory on 25.27 June 1975. This time corresponds to a phase, $\phi = 0.787 \pm 0.075$, where the uncertainty in phase results from the extrapolation of the uncertainty in the center of the X-ray eclipse (Jones and Liller 1973).

The echelle format covered the spectral region from λ 4435 Å to λ 5840 Å with small gaps near both ends of the wavelength range where consecutive echelle orders do not overlap. The dispersion was 4 Å/mm providing a spectral resolution ~ 0.2 Å near the center of an order. The plate was traced on the David Mann microdensitometer at the Center for Astrophysics and the recorded data were handled on magnetic tape. Wavelengths were determined by means of a thorium-neon comparison source; in some of the following figures the wavelength scale is replaced by a velocity scale whose zero point is defined by the average velocity of the He II lines at λ 5411 Å and λ 4541 Å and represents a photospheric reference velocity. The ordinate of the figures is the residual flux that results when an average continuum from adjacent orders is subtracted from an order of interest so as to eliminate the effects of any

spatial variation in the response across the photocathode of the Kron tube.

Some line profiles of interest are presented below and discussed individually. The profiles are compared principally to those of Conti and Cowley (1975) who have published the most complete set of profiles with reasonably good phase coverage at dispersions of 17 to 25 Å/mm. Their observations were made in September 1973 and March 1974.

a) H β ; λ 4861 Å

The P-Cygni profile of H β (Figure 1) appears similar in velocity extent to the March 1974 profile (Conti and Cowley 1975) although the emission peak has increased by \sim 30 percent of the local continuum. Inspection of the profiles of September 1973, March 1974 and this one of June 1975 suggests increasing emission with time, since Conti and Cowley noted no apparent phase dependence in the line.

b) N III, λ 4634-4642 Å; C III, λ 4647-4651 Å

The N III, C III complex is shown in Figure 2 where the fluxes are referred to a local continuum. A most striking result here is the change in the relative intensity of the lines; the N III multiplet now appears comparable in intensity to the C III transition whereas N III was apparently a factor of 2 stronger in 1973 and 1974. The C III transition remained approximately constant at 20 to 25 percent of the local continuum. Now of course the agreement in C III may be fortuitous in view of the necessity to rely on a 'local' continuum since these features are superposed on a broad emission envelope that may be phase dependent. It is possible that the N III transitions remained constant and C III varied, in this case on the order of 50 percent in intensity. Since the lines have similar excitation energies and N III and C III appear to have the same average velocity variation, it is somewhat puzzling why a change in the relative intensities occurs. Provided that the emitting volumes are in correspondence for these transitions, it then would appear necessary to search for an explanation in the details of the line forming process. Perhaps this might be a density sensitivity in the dielectronic recombination process causing the emission or an interlocking radiative process that would affect one and not the other feature. It is interesting to note that the C III transition which is between triplet levels, has spontaneous emission coefficients that are equivalent for the upper levels of the three transitions shown in Figure 2; and the transition at λ 4647.40 arises from the 3P_2 level which has the highest statistical weight of the term. Thus it is perhaps surprising that this component of the C III

feature is not dominant in the multiplet. Taken at face value, this suggests that the densities in the extended envelope are not sufficient to ensure complete mixing of the levels in the term and with detailed calculations could perhaps be used to obtain limits on the density in the extended envelope.

c) He II; $\lambda 5411 \text{ \AA}$

This absorption line (Figure 3) is clearly asymmetric with a blue wing that extends to velocities of $\sim -400 \text{ km s}^{-1}$ in contrast to the observations of 1973-1974 (Conti and Cowley 1975) that show absorption to -200 km s^{-1} . There is also a suggestion of high velocity absorption near -700 km s^{-1} .

d) He II; $\lambda 4541.59 \text{ \AA}$

The profile of this He II transition (Figure 4) is not as asymmetric as the previously discussed $\lambda 5411 \text{ \AA}$ line and has a deeper central absorption than the profile measured in 1973-1974 (Conti and Cowley 1975). Here we also note the presence of a shallow absorption feature centered around -500 km s^{-1} . Such a high velocity is consistent with the possibly expanding absorption feature found in the He I $\lambda 5876 \text{ \AA}$ transition during 1973-1974.

e) Emission Line; $\lambda 5294 \text{ \AA}$

This spectrum shows a broad emission feature (Figure 5) at an apparent wavelength of $\lambda 5293.67 \text{ \AA}$. On this spectrum, the correction for zero velocity of the He II lines amounts to -92.7 km s^{-1} , suggesting a wavelength of $\lambda 5295.31 \text{ \AA}$ if the feature had the velocity of the He II transitions. The emission line is broad with a full width at half power of $\sim 3.4 \text{ \AA}$, a value that is comparable to the N III emission line at $\lambda 4634 \text{ \AA}$. Such a width suggests the feature is indeed associated with the binary system and differs from the narrow lines identified in another Of star, 9 Sagittae (Underhill 1958). A search through identification lists, and spectral studies for this source (Hensberge *et al.* 1973; Hutchings 1974) and other Of stars (Underhill 1966; Baschek and Scholz 1971) reveals no likely identification that is consistent in wavelength, or previously identified ion species. It is tempting to hypothesize that the emission feature could arise from a highly ionized atom that occurs as a result of photoionization by the X-ray source itself. Theoretical calculations (McCray 1974, 1975) have suggested that the X-ray source in HD 153919 can ionize an extended hemisphere of the expanding atmosphere of the primary and produce ions such as Fe XIV. The fine structure transition $3p^2 P_{1/2} - 3p^2 P_{3/2}$ of Fe XIV occurs at $\lambda 5303.4 \text{ \AA}$ (Jefferies, Orrall, and Zirker 1969) which leads to a velocity of $\sim -450 \text{ km s}^{-1}$. This velocity compares

favorably with other observed velocities associated with the disturbance of the "wake" of the X-ray source in the atmosphere of the primary. Obviously, more extensive observations of this feature are necessary to search for the intensity modulation that would be expected if the emission were associated with the X-ray source.

CONCLUSIONS

The line profiles presented in this paper give spectroscopic evidence for an increase by about 200 km s^{-1} in the outward velocities of the extended atmosphere of the primary star of HD153919 since 1973-1974. Additionally, there appear to be substantial (~ 50 percent) variations in the relative intensities of the strong N III and C III emission lines near $\lambda 4640 \text{ \AA}$ suggesting changes in physical conditions in the stellar atmosphere. A previously unreported emission feature near $\lambda 5295 \text{ \AA}$ is noted and its identification is discussed.

We are grateful to J. Hearnshaw of the Center for Astrophysics for obtaining the spectrum. This research is supported in part by NASA contract NAS5-20764.

REFERENCES

- Baschek, B. and Scholz, M. 1971, *Astron. and Ap.*, 15, 285.
- Conti, P. S. and Cowley, A. P. 1975, *Ap. J.*, 200, 133.
- Hensberge, G., van den Heuvel, E. P. J., and Paes De Barros,
M. H. 1973, *Astr. and Ap.*, 29, 69.
- Hutchings, J. B. 1974, *Ap. J.*, 192, 677.
- Hutchings, J. B., Thackeray, A. D., Webster, B. L., and
Andrews, P. J. 1973, *M. N. R. A. S.*, 163, 13P.
- Jefferies, J. T., Orrall, F. Q., and Zirker, J. B. 1969,
Forbidden Transitions in Stellar Spectra, Liege
Symposium No. 15, p. 235.
- Jones, C., Forman, W., Tananbaum, H., Schreier, E., Gursky,
H., Kellogg, E., and Giacconi, R. 1973, *Ap. J. (Letters)*,
181, L43.
- Jones, C. and Liller W. 1973, *Ap. J.*, 184, L 65.
- McCray, R. 1974, "Gas Flows in Binary X-Ray Systems",
International Conference on X-Rays in Space, U. of
Calgary, Canada, preprint.
- _____. 1975, personal communication.
- Underhill, A. B. 1958, *Pub. D.A.O.*, 11, 143.
- Walker, E. N. 1973, *M. N. R. A. S.*, 162, 15P.
- _____. 1974, *M. N. R. A. S.*, 169, 47P.
- Wolff, S. C. and Morrison, N. D. 1974, *Ap. J.*, 11, 143.

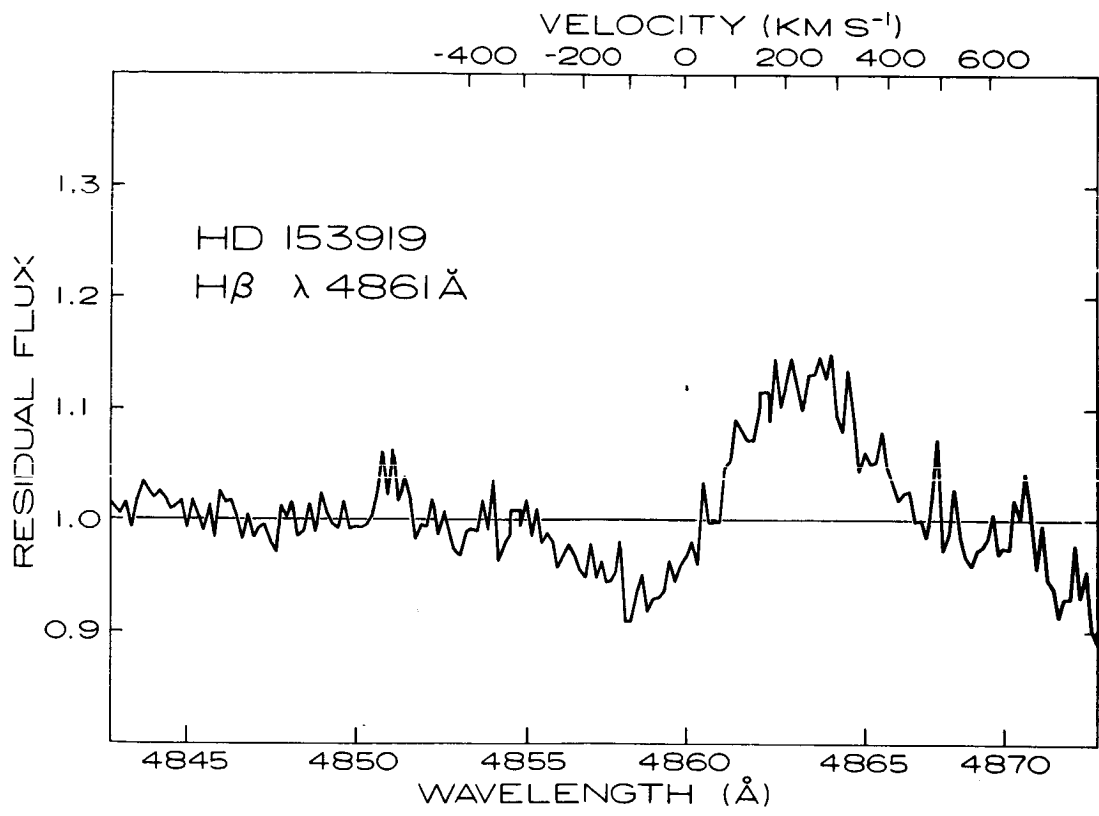


Fig. 1. - The P Cygni profile of Hβ in HD153919.

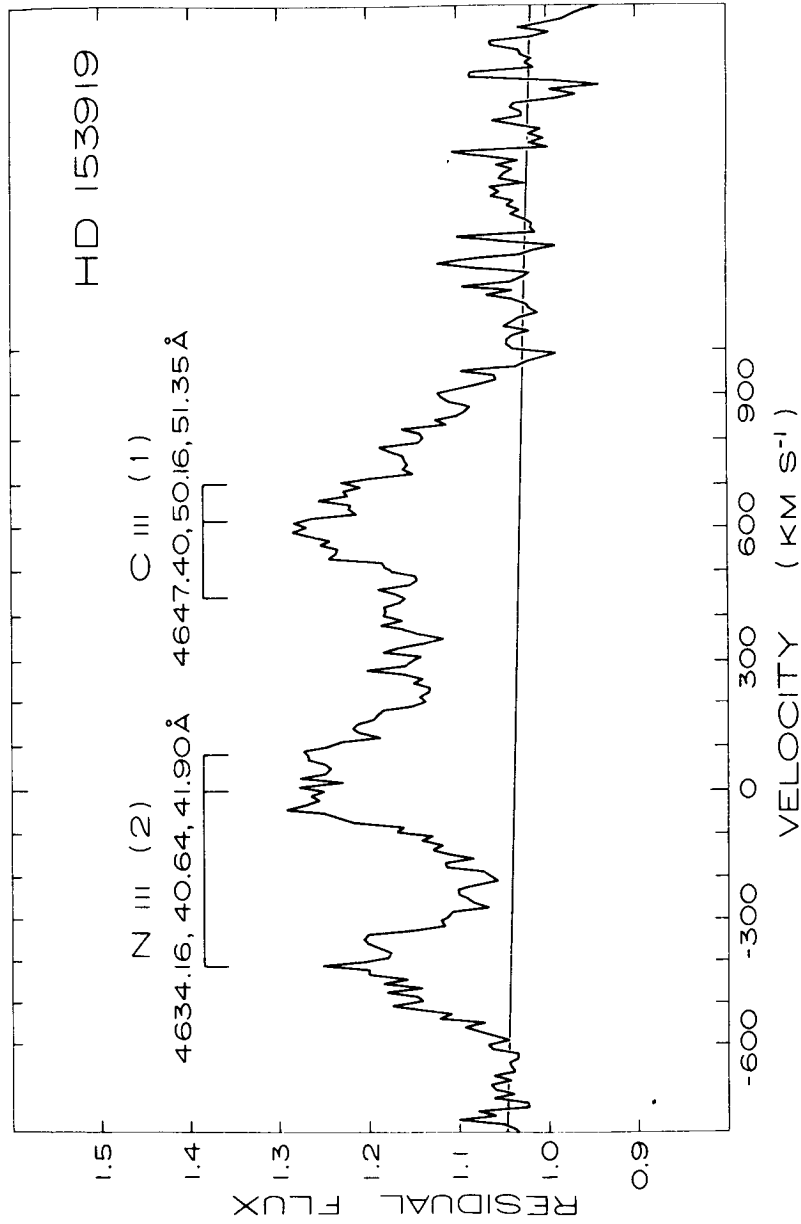


Fig. 2. - The N III and C III multiplets. The velocity scale has been set on the $\lambda 4640.64 \text{ \AA}$ line of N III with a zero point determined by the He II absorption lines.

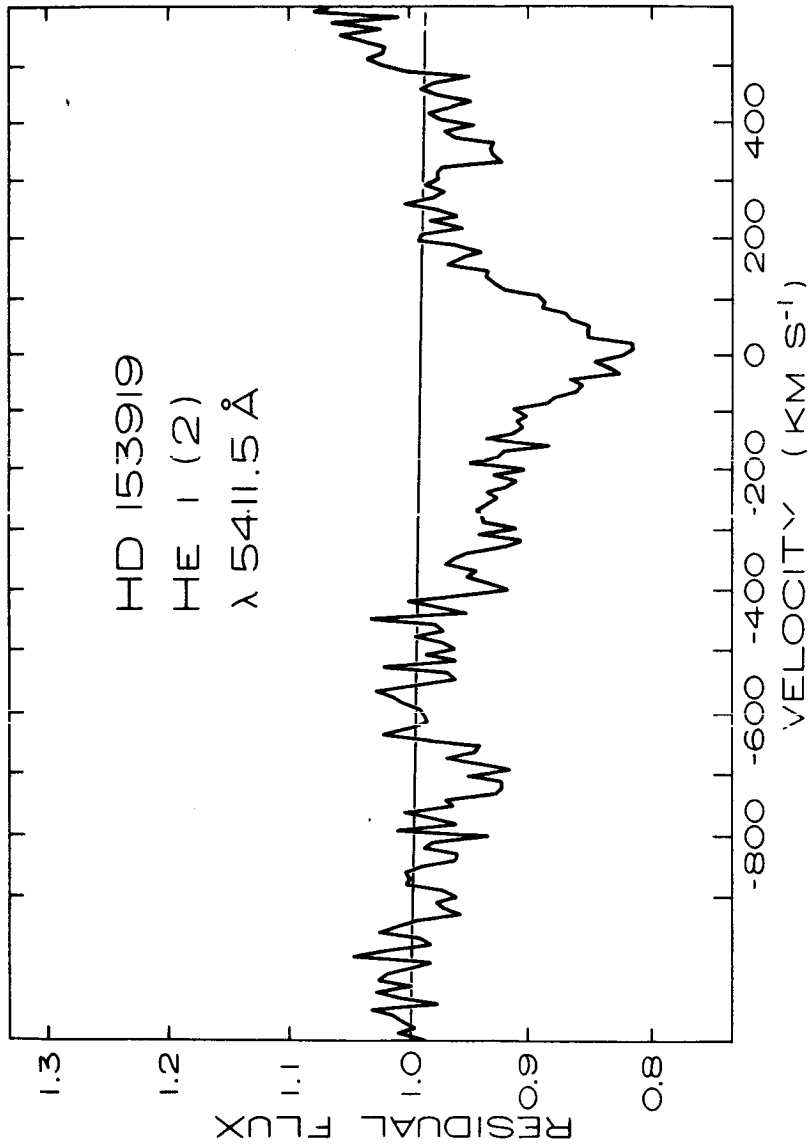


Fig. 3. - The He II λ 5411.5 Å transition. Note the extension of the blue wing to -400 km s^{-1} . In 1973-1974 the line was not as asymmetric and extended to $\sim -200 \text{ km s}^{-1}$.

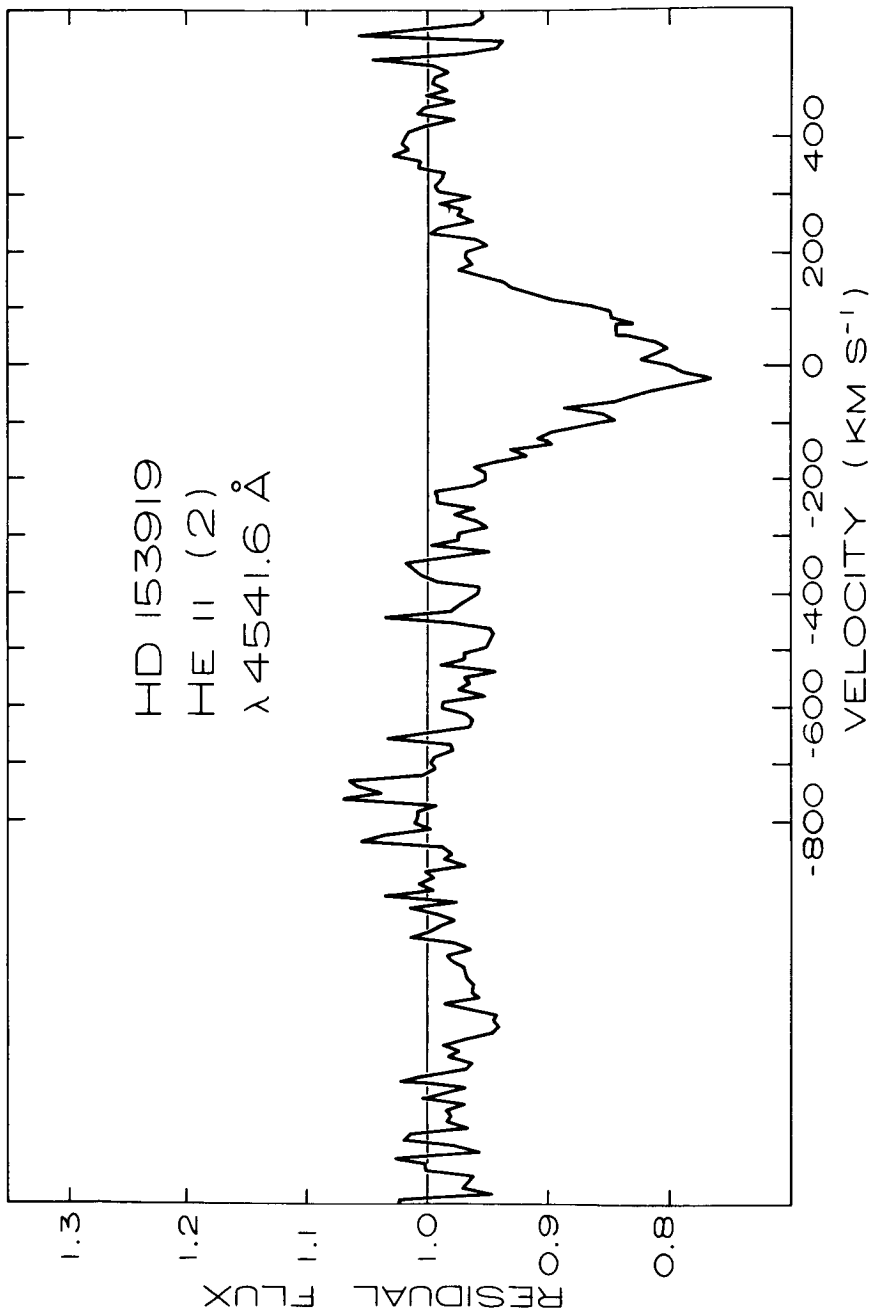


Fig. 4. - The He II λ 4541.6 Å transition. This line is not as extended on the blue wing as the λ 5411 Å line of He II; however there may be a high velocity absorption feature near -500 km s^{-1} .

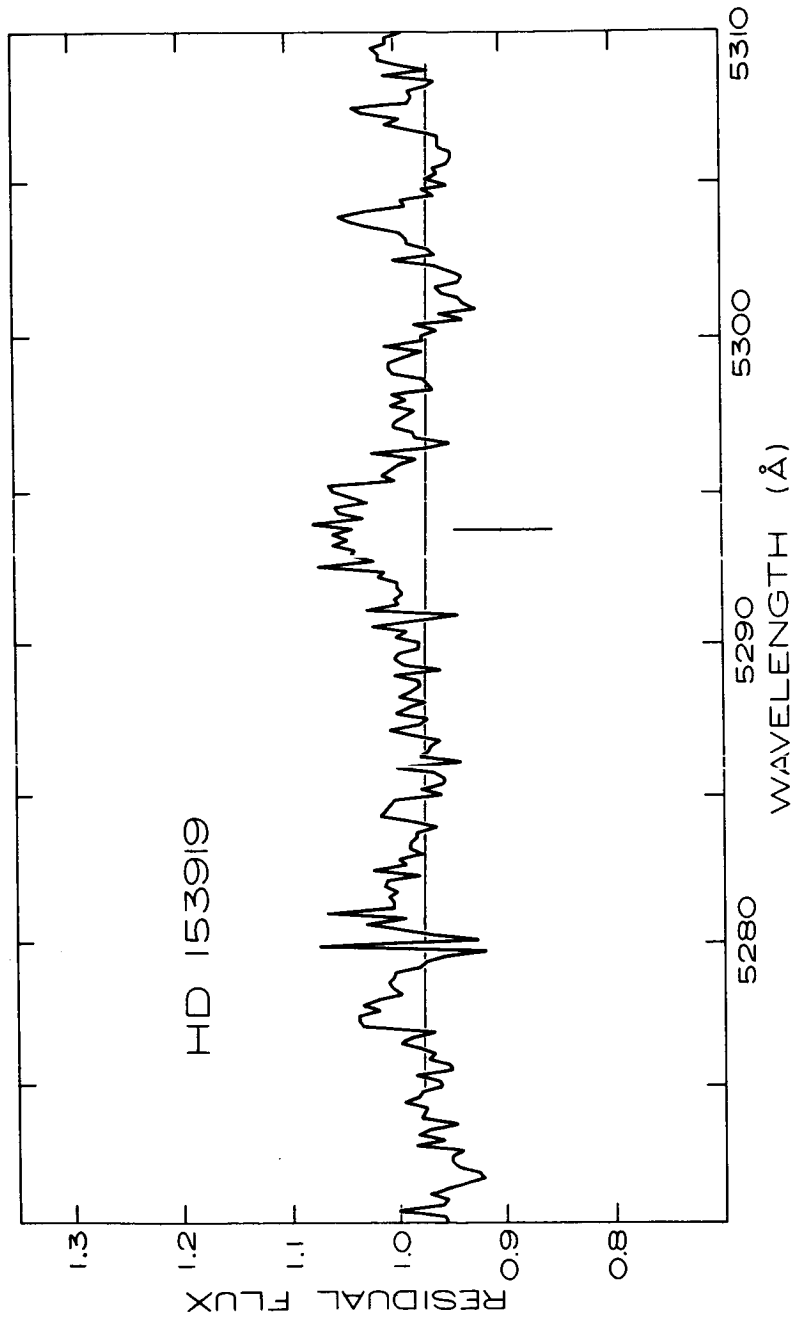
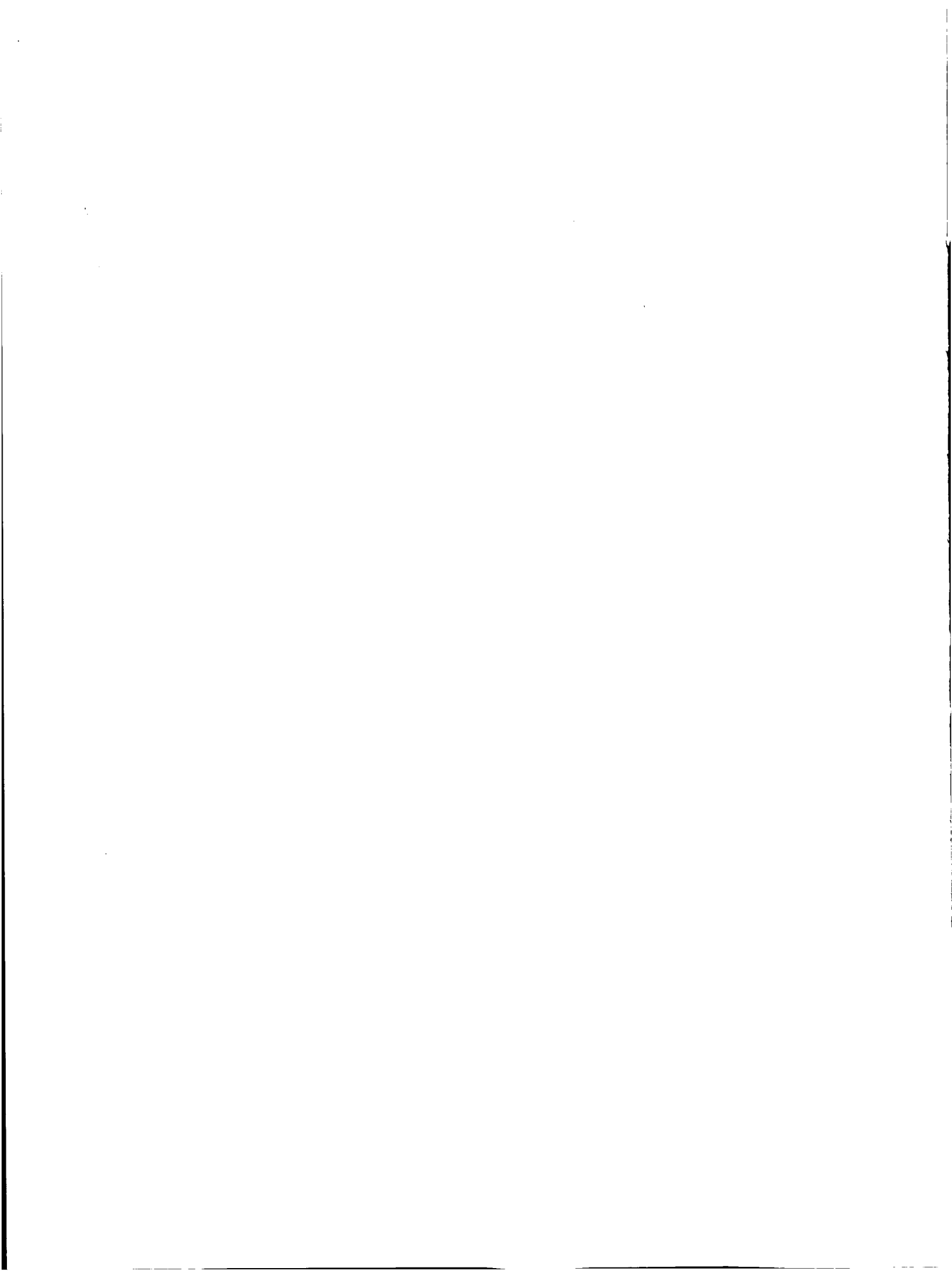


Fig. 5. - An unidentified emission feature at $\lambda 5293.67 \text{ \AA}$.



THE SKYLAB S019 ULTRAVIOLET SPECTRA OF
HD153919 (=3U1700-37) AND HDE226868 (=Cyg X-1)

Yoji Kondo
NASA Johnson Space Center
Houston, Texas 77058

S. B. Parsons, K. G. Henize*, J. D. Wray and G. F. Benedict
Astronomy Department
University of Texas
Austin, Texas 78712

Ultraviolet spectra of HD153919 (=3U1700-37) and HDE226868 (=Cyg X-1) have been obtained with the ultraviolet objective-prism spectrograph of Skylab Experiment S019 (Henize, et al., 1975a). The data shown in Figure 1 consist of unwidened spectra which extend to 1600Å for HD153919 and to 2400Å for HDE226868. The wavelength resolution is about 2Å at 1400Å and 12Å at 2000Å.

For HD153919 an unwidened spectrum of fair quality and extending to a wavelength of 1600Å was obtained at 22^h08^m on 1 September 1973. The energy distribution in this spectrum (see Figure 1) generally resembles that of other reddened O stars on our plates. However, a break in continuum intensity seems to occur at a wavelength of about 1720Å. We are unable to give an astrophysical explanation of such a break nor are we aware of any other star showing such a break. There is a suggestion of an emission line on the longward edge of the break but this could be either a chance clumping of grains or else a photographic edge-effect caused by the break. If real, this feature may be attributed to N IV λ1718 (or to Si IV λ1724), a line which occurs in emission in WN stars observed with this equipment (Henize, et al., 1975b). N IV λ1718 is observed in absorption in other O stars (see Figure 1). However, other ultraviolet emission lines observed in the WN stars, the strongest of which is He II λ1640, are not observed in HD153919. This spectrum was obtained during an X-ray eclipse, the mid-point of which occurred at 21^h50^m. A second spectrum of HD153919, obtained on 23 August, extends only to about 1900Å. It is similar in all respects to the corresponding region of the spectrum discussed above.

The spectrum of HDE226868 is visible only on the unwidened 4.5 minute exposure because of its faintness. No recognizable spectral features were identified longward of about 2400Å, which is the short wavelength limit reached. The spectral energy distribution is in agreement with that of a highly reddened O- or early B-type object.

*NASA Astronaut at Johnson Space Center.

REFERENCES

- Henize, K. G., Wray, J. D., Parsons, S. B., Benedict, G. F., Bruhweiler, F. C., Rybski, P. M., and O'Callaghan, F. G. 1975a, Ap. J. (Letters), 199, L119.
- Henize, K. G., Wray, J. D., Parsons, S. B., and Benedict, G. F. 1975b, Ap. J. (Letters), 199, L173.

Table 1 - Spectral Types and B-V Colors for Stars in Figure 1.

<u>Star</u>	<u>Spectral Type</u>	<u>B-V</u>
HR6672	07.5 II	+0.4
X Per	0 pe	+0.31
HDI53919*	06.5 Iaf ⁺	+0.27
HDI53426*	09 II-III	+0.14
HDE226868	09.7 Iab pv	+0.85

*same plate (SL3-201)

S-019 log I

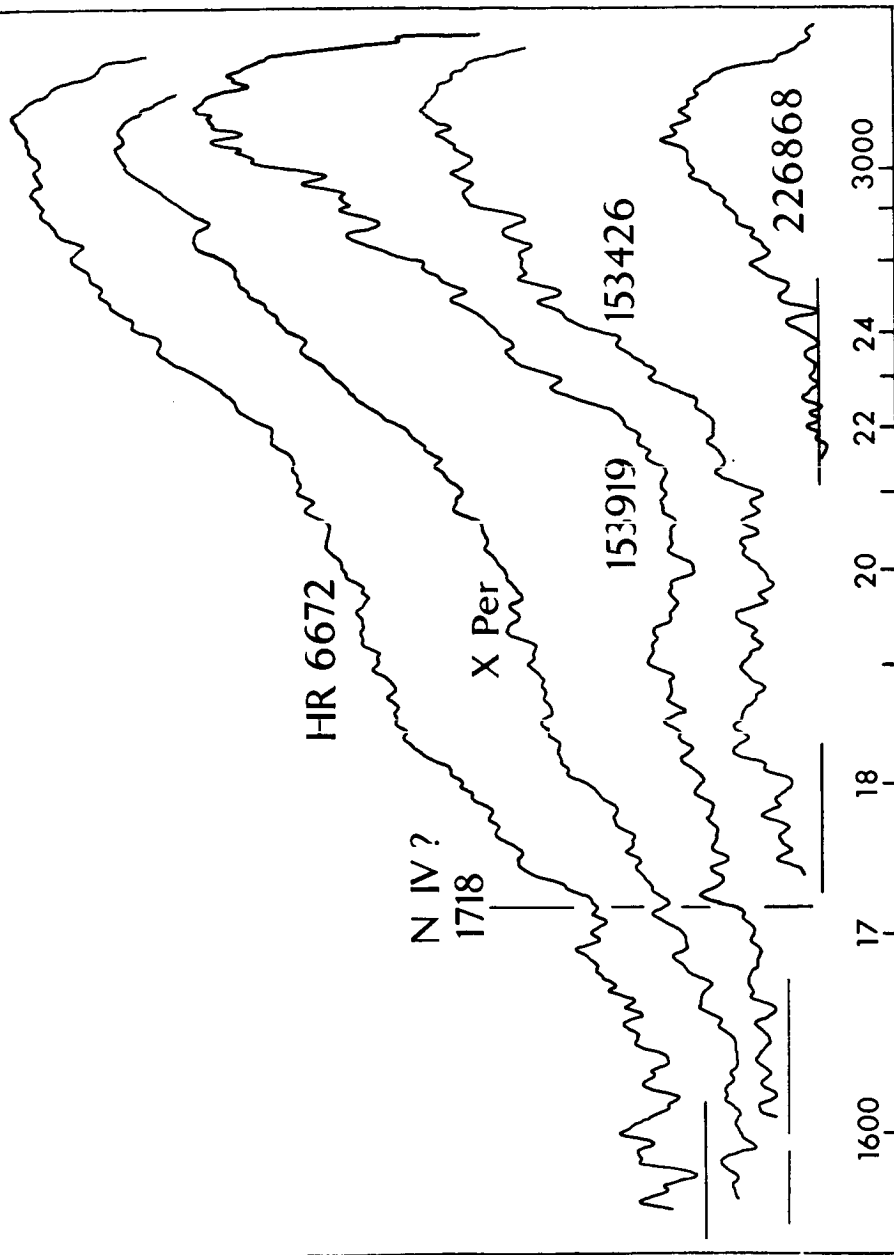


Figure 1 - Relative Intensity Tracings of HD153919, HDE226868 and Comparison Stars. Top two scans are from widened spectra, bottom three scans from unwidened spectra. Background level is indicated by a horizontal line for each tracing.

He II λ 4686 PHOTOMETRY OF HD 153919

W. Krzeminski
Institute of Astronomy, Polish Academy of Sciences
Al. Ujazdowskie 4, Warsaw, Poland

ABSTRACT

The optical component of the binary X-ray source 3U1700-37/HD 153919 has been observed with the interference filter centered on the He II λ 4686 emission. This photometry does not reveal any dependence of λ 4686 emission on the orbital phase thereby confirming earlier spectroscopic result that the region of formation of the ionized helium emission is confined to the envelope of the O6f primary.

INTRODUCTION

Soon after an optical identification of the X-ray binary 3U1700-37/HD 153919 was suggested (Jones et al. 1973), the author initiated in 1973 May He II λ 4686 photometry of this system. This was a search for phase-dependent photometric variability of the He II λ 4686 emission. If any such dependence were found it could provide us with some useful information on the extent of the emitting region in the system. It was found later (Dachs and Schober 1974; Hutchings 1974; Wolff and Morrison 1974; Conti and Cowley 1975) that the equivalent widths of the He II λ 4686 emission line show only small erratic changes independent of orbital phase and there is little variation in the emission profile, in contrast to large changes in this line seen in nearly all other X-ray binaries. This was explained (eg. Hutchings 1974) by confining the region of λ 4686 emission line formation solely to the primary envelope. Such explanation was confirmed by the radial velocity variations of He II λ 4686 emission which vary in phase with those of the photospheric absorption lines of the O6f primary (Hensberge et al. 1973; Wolff and Morrison 1974).

OBSERVATIONS

Photometry has been carried out on 39 nights between 1973 May 5 and October 11 (UT) using the 1-m and 50-cm ESO telescopes and the 40-inch (102-cm) reflector at the Las Campanas Observatory. Standard d.c., one-channel photometers were utilized on the La Silla telescopes; a two-channel, pulse-counting photometer was used at Las Campanas. Interference filters of 10Å halfwidth centered on λ 4686 and 4800 were used throughout this program; the latter was used for measurements of the continuum. Equivalent width of He II λ 4686 emission line in HD 153919 is around 2.7Å and FWHM is ~6Å (Conti and Cowley 1975). Stars BS 6327 and 6344 served as primary and secondary comparisons, respectively. A typical mean integration time was about one minute on each star in each spectral band and the nightly averages consisting of two or three observations were formed. The small corrections resulting from different telescope-photomultiplier spectral sensitivity were applied to the $h = -2.5 \log [I(4686)/I(4800)]$ indices to

bring them to the same instrumental system; extinction corrections were applied to the $\lambda 4800$ -filter observations. From repeated observations obtained on each night one gets the standard error ± 0.004 of a nightly average for h , and ± 0.003 for Δmag (4800).

Figure 1 shows the results; all the observations were folded modulo 3.412 days using the X-ray elements of Jones et al. (1973). Each point represents the nightly average; increased He II $\lambda 4686$ emission and $\lambda 4800$ luminosity are upwards. The filled circles refer to HD 153919, the open ones to the comparison stars. One may infer from the run of observations of the comparison stars in either panel that the scatter is larger than the errors quoted above. This is probably due to the lack of full compensation for different spectral sensitivity of the three instruments used.

DISCUSSION

It is readily seen from figure 1 that (i) the photometric strength of the He II $\lambda 4686$ emission does not depend on the orbital phase though scatter is $2\frac{1}{2}$ times greater than that for the comparison stars. It would be desirable to calibrate the ratio $I(4686)/I(4800)$ on early type stars with known He II $\lambda 4686$ equivalent widths, W , so that one could express the observed variation shown in figure 1 directly in the W values. (ii) The $\lambda 4800$ light curve shows a typical ellipsoidal-type light variations with roughly equal maxima and minima and a total amplitude of about 0.06 mag; the secondary minimum is shifted to phase -0.65 . This behavior agrees very well with the wide band photometry (eg. Penny et al. 1973).

From lack of correlation between the photometric strength of the He II $\lambda 4686$ emission and the orbital phase one may conclude that the region of formation of this emission line has to be ascribed to the primary envelope, in agreement with the results of high dispersion spectroscopy. The scatter in the photometric ratio He II $\lambda 4686$ /continuum is roughly three times larger than the estimated mean error of the nightly average. This is consistent with the small random changes found by Hutchings (1974) in the equivalent widths of He II $\lambda 4686$ and other Of emission lines.

The writer would like to express his thanks to Professors A. Blaauw and B. Westerlund for the invitation to spend several months at the European Southern Observatory, and to Dr. H. W. Babcock for Guest Investigator privileges at the Las Campanas Observatory of the Carnegie Institution of Washington.

REFERENCES

- Conti, P. S., and Cowley, A. P. 1975, *Ap.J.*, 200, 133.
Dachs, J., and Schober, H. J. 1974, *Astr. and Ap.*, 33, 49.
Hensberge, G., van den Heuvel, E. P. J., and Paes de Barros, M. H. 1973, *Astr. and Ap.*, 29, 69.
Hutchings, J. B. 1974, *Ap.J.*, 192, 677.
Jones, C., Forman, W., Tananbaum, H., Schreier, E., Gursky, H., Kellogg, E., and Giacconi, R. 1973, *Ap.J. (Letters)*, 181, L43.
Penny, A. J., Olowin, R. P., Penfold, J. E., and Warren, P. R. 1973, *M.N.R.A.S.*, 163, 7P.
Wolff, S. C., and Morrison, N. D. 1974, *Ap.J.*, 187, 69.

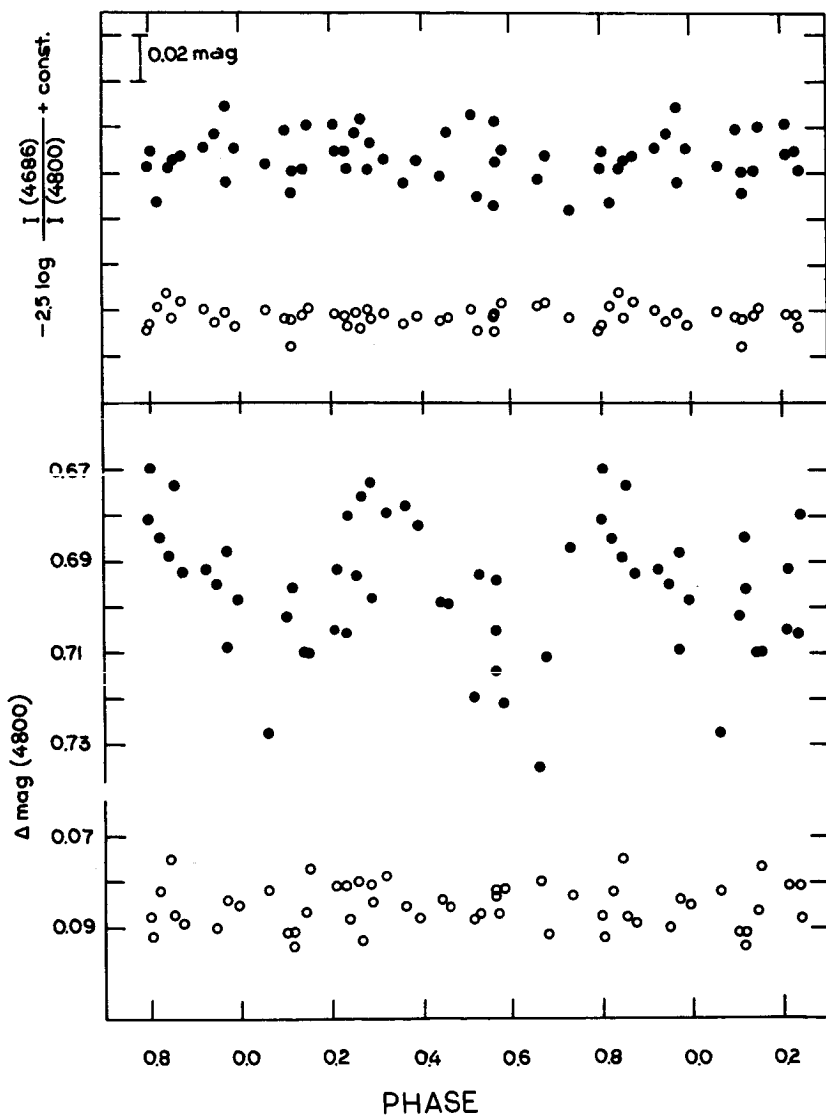


FIG. 1.- He II $\lambda 4686$ emission line photometry of HD 153919 (upper panel) and its differential light curve with respect to BS 6327 (lower panel) folded with a 3.412 period. Zero phase corresponds to the X-ray occultation center at JD 2,441,453.14 (Jones et al. 1973). The filled circles refer to HD 153919, the open ones to the comparison stars; each point represents the nightly average. Increased He II $\lambda 4686$ emission is upwards.

X-RAY OBSERVATIONS OF 3U 1700-37

Keith O. Mason, Graziella Branduardi
and Peter Sanford
Mullard Space Science Laboratory,
University College, London
Holmbury St. Mary, Dorking, Surrey, U.K.

ABSTRACT

X-ray observations with Copernicus reveal three categories of flux variability in 3U 1700-37. High amplitude hourly variations are energy independent in the 3-11 keV range while a change in the low energy absorbing column causes variations in flux level on an orbital timescale. This absorption is most severe prior to eclipse ingress, suggesting that the distribution of absorbing material around the X-ray source is asymmetrical with respect to the line of centers of the binary system. Further, the absorbing material may be identical with a high density region inferred from optical observations of HD 153919. In the third category, the maximum source intensity per binary cycle is variable by at least a factor of two between observations. Measurement of the eclipse duration on three occasions indicate that it is significantly less than when observed by Uhuru.

3U 1700-37 has been observed on two occasions by the M.S.S.L. X-ray instrumentation onboard Copernicus; in July 1974 and again in July 1975. The data from the first observation are shown in the lower section of figure 1 and extend over almost exactly one 3.4 day orbital cycle. When observing 3U 1700-37, the Copernicus detector also has the source 3U 1702-36 (Sco X-2) in its 3 degree FWHM field of view, and this contaminant signal (amounting to approximately 50 counts per minute) is subtracted out along with the charged particle background. The maximum range of variability seen in 3U 1702-36 during two control

observations immediately before and after that of 3U 1700-37 is marked in figure 1 and represents the dominant uncertainty in the background subtraction procedure. There are several points to notice about these data:-

1. The time spent by the X-ray source in eclipse is only 0.88 ± 0.06 compared with 1.10 ± 0.07 as seen by Jones et al (1973) with the Uhuru satellite. This shorter duration is confirmed by the 1975 data.
2. The transition into eclipse is gradual, with an indication of what might possibly be a pre-eclipse dip centered on 1974 day 182 21 hr. Exit from eclipse is relatively rapid.
3. The flux from 3U 1700-37 is highly variable, with on occasion fluctuations from a level consistent with zero up to 250 counts in only a few minutes. Indeed this is the most variable X-ray source on this timescale of which we are aware. The variability is best shown in the upper section of figure 1 where the most intense parts of the binary cycle have been plotted on the maximum time resolution available, 1.5 minutes. We have searched for a regular modulation of the X-ray flux similar to the 283 sec period seen in 3U 0900-40 (Rappaport and McClintock 1975). A power spectrum analysis revealed no such modulation in the range 2 to 50 minutes, with an upper limit to the peak to mean amplitude of 4% of the mean flux at the high frequency end of the range, increasing to 20% at the low frequency end.

To look for correlated changes in the intensity and energy spectrum of 3U 1700-37, we have taken the data from three periods, marked A, B and C in figure 1, and have binned them according to whether they fall above or below a threshold of 90 counts per minute. The Copernicus X-ray detector is fitted with a six channel Pulse Height Analyser (PHA) for energy resolution, and in figure 2 is plotted the PHA count distribution in the high and low intensity bins for each of the periods A, B and C. Also plotted is the ratio of the high to low intensity channels. In no case is there a significant deviation of these latter data from a horizontal line, indicating the absence of a detectable change in the energy spectrum of the source with intensity. This result is in contrast with that obtained for Sco X-1 (Culhane et al 1975 - this conference) which shows variability on a similar timescale during active periods, but a strong correlation between intensity and spectral slope.

Neither is it the behaviour expected if the fluctuations were caused by variable amounts of obscuring material, unless this material were completely ionized.

Figure 3 shows the Copernicus data integrated in bins of three hours duration, together with a spectral hardness index obtained by dividing the total counts in the four high energy PHA channels by those in the two low energy channels. Also shown on approximately the same intensity scale, for comparison, is the folded Uhuru data of Jones et al (1973) similarly binned. Note that the flux level at the time of the Copernicus observation is about twice that seen by Uhuru.

Model spectrum fits to our data indicate that it is consistent with a constant temperature throughout and variable low energy absorption (the converse is not true!). The variation of spectral hardness index in figure 3 can therefore be interpreted in terms of changing amounts of obscuring material, and the equivalent absorbing column is marked on the right hand ordinate of the diagram. It can be seen that the degree of absorption mirrors the asymmetric intensity profile discussed earlier, and the absorbing column is larger prior to eclipse ingress than it is after the source comes out of eclipse. This behaviour is again seen in the 1975 data (figure 4), where two and a half successive binary cycles were observed, and confirms that this is a phase dependant effect. The strength of the source in 1975 was less than that in 1974 and nearer the value seen by Uhuru.

In figure 5 we have drawn a schematic diagram of the 3U 1700-37 - HD 153919 binary system in which we have indicated the lines of sight along which high absorption columns are seen. Optical observers of HD 153919 (eg Hutchings 1974; Conti and Cowley 1975) have inferred from their data the presence of a high density region trailing the X-ray source in its orbit, and it is tempting to suggest that the optical observations may be explained by the same material which causes the anomalous X-ray absorption. It is difficult to model the phenomenon in terms of an accretion wake, since this would extend downwind relative to the X-ray source and produce a maximum in absorption between phase 0.5 and 0.75, not after phase 0.75 as in the present data (cf Charles et al 1975, figure 3 - this conference). Other possible explanations

include a gas stream in the binary system, or an asymmetry in the stellar wind of HD 153919. This is clearly an area in which coordinated X-ray/optical observations might prove useful.

REFERENCES

- Conti, P.S. and Cowley, A.P., 1975, Preprint.
Hutchings, J.B., 1974, Ap.J. 192, 677
Jones, C., Forman, W., Tananbaum, H., Schreier, E., Gursky, H., Kellogg, E.,
and Giacconi, R., 1973, Ap.J. 181, L43
Rappaport, S., and McClintock, J., 1975 IAU circular No. 2794

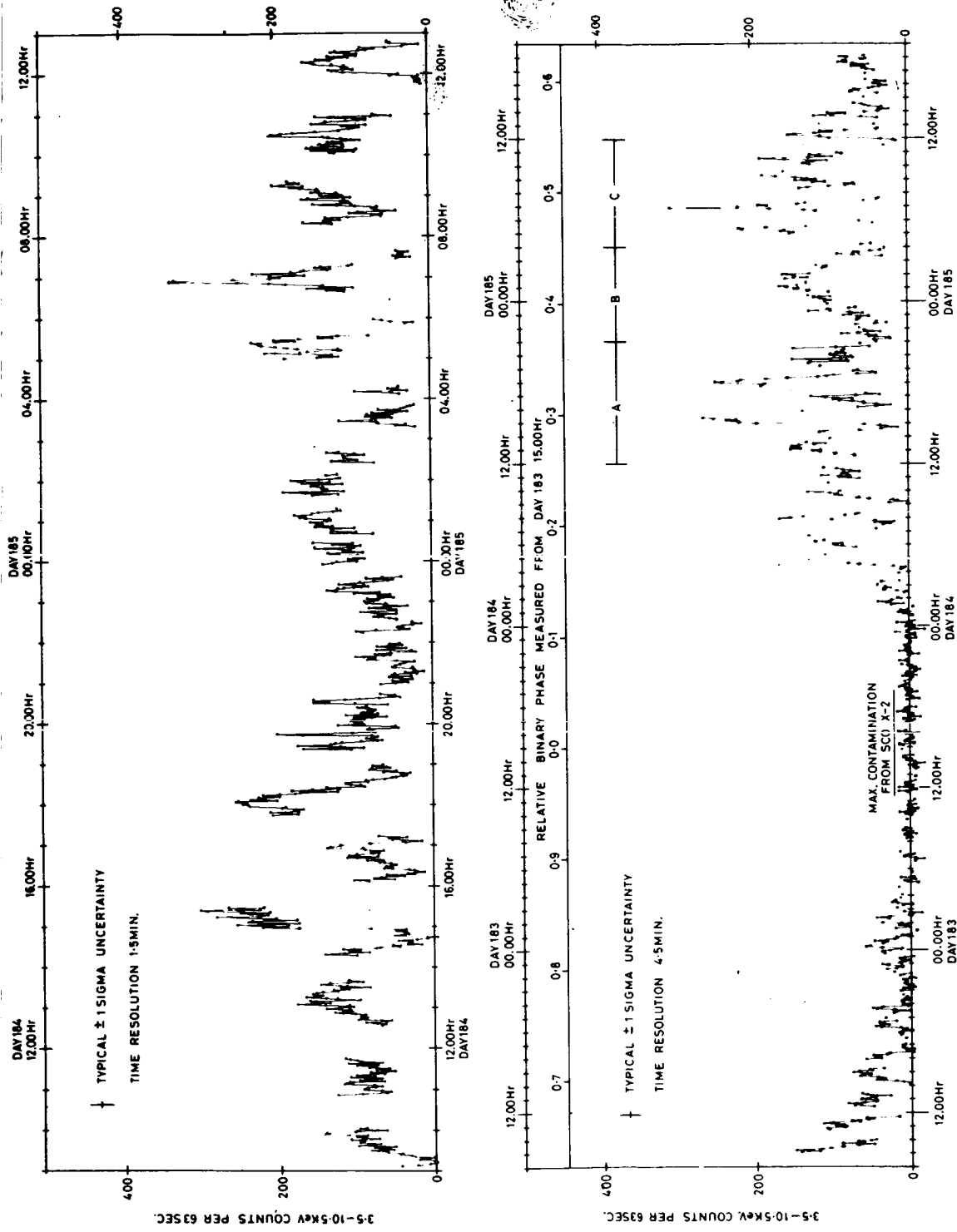


Figure 1 - Copernicus data on 3U 1700-57. The lower diagram shows the whole of the data with a 4.5 minute time resolution. In the upper diagram, part of the uneclipsed portion of the data is shown with a 1.5 minute time resolution. Consecutive data points are joined with straight lines.

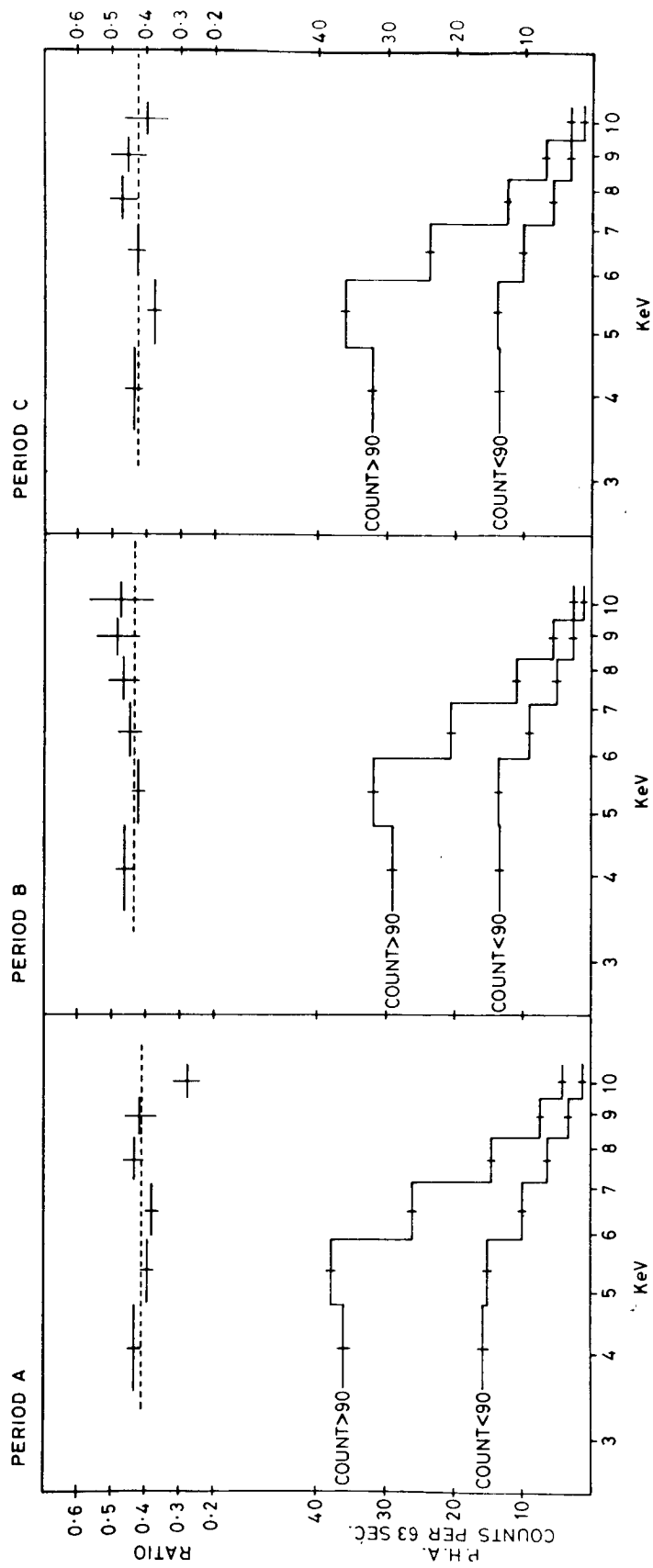


Figure 2 - Shows the PHA count distribution for three periods A, B and C (marked in figure 1) binned according to whether the integrated count per data frame is greater or less than 90 counts per minute. The upper section of the figure shows the ratio of the high and low count bins for each channel.

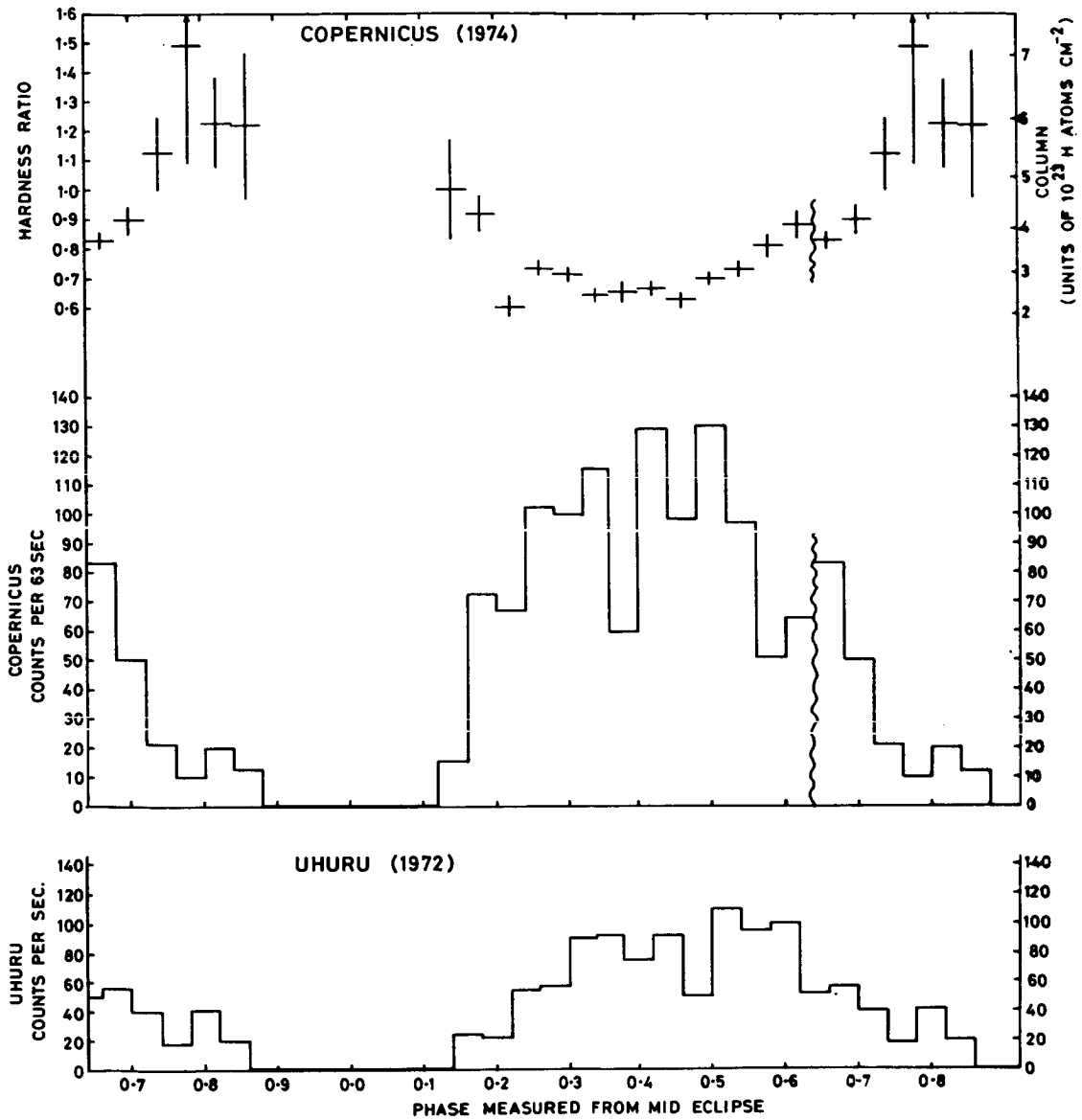


Figure 3 - The average Uhuru light curve (Jones et al 1973) and the light curve from the present observation are shown on the same absolute intensity scale. The spectral hardness index is plotted for each bin of the Copernicus data, and also marked is the equivalent absorbing column assuming a constant temperature thermal spectrum.

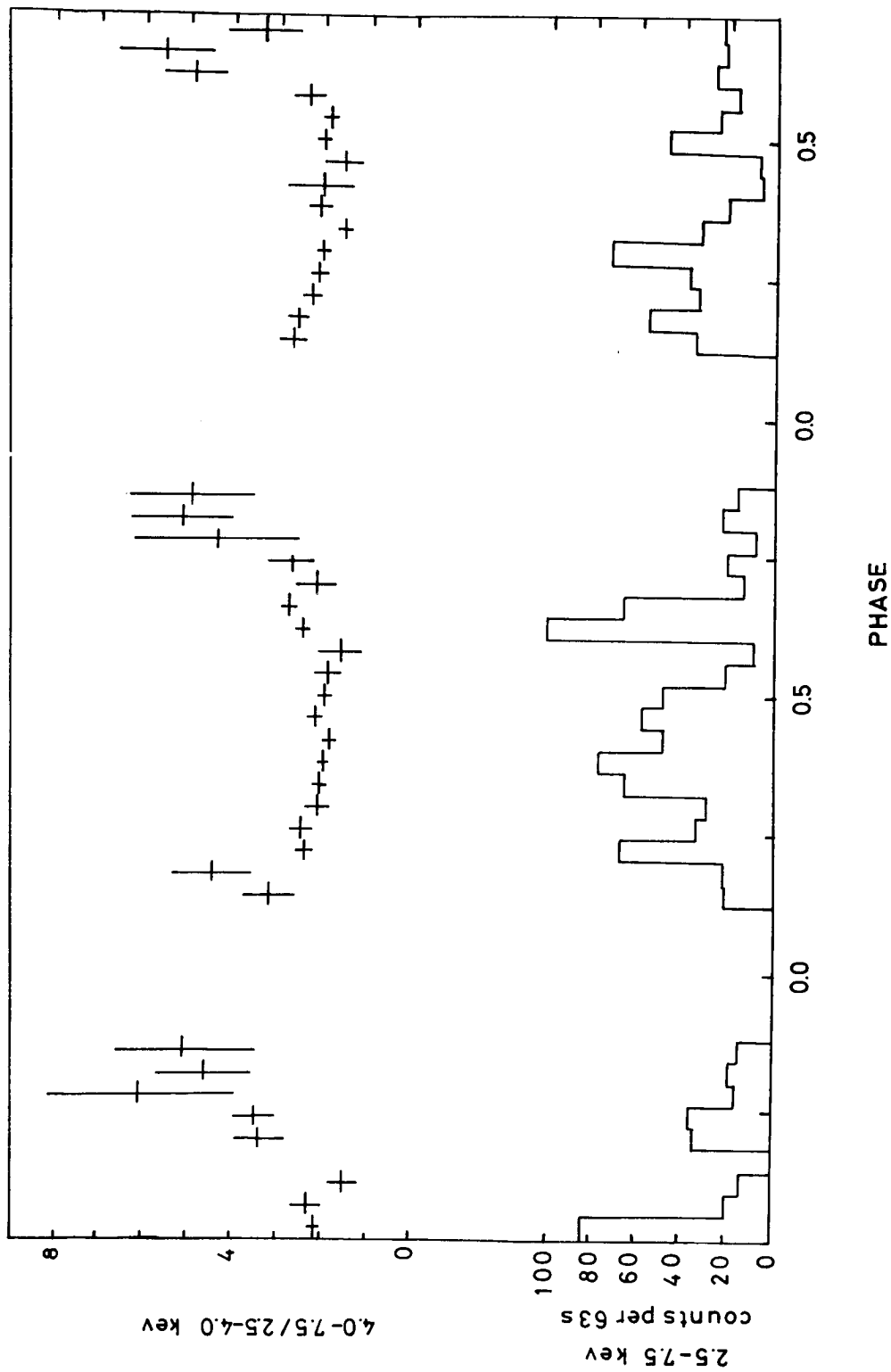


Figure 4 - A similar plot to figure 3, but for the 1975 Copernicus data. The observation started on 1975 day 195, 15 hr.

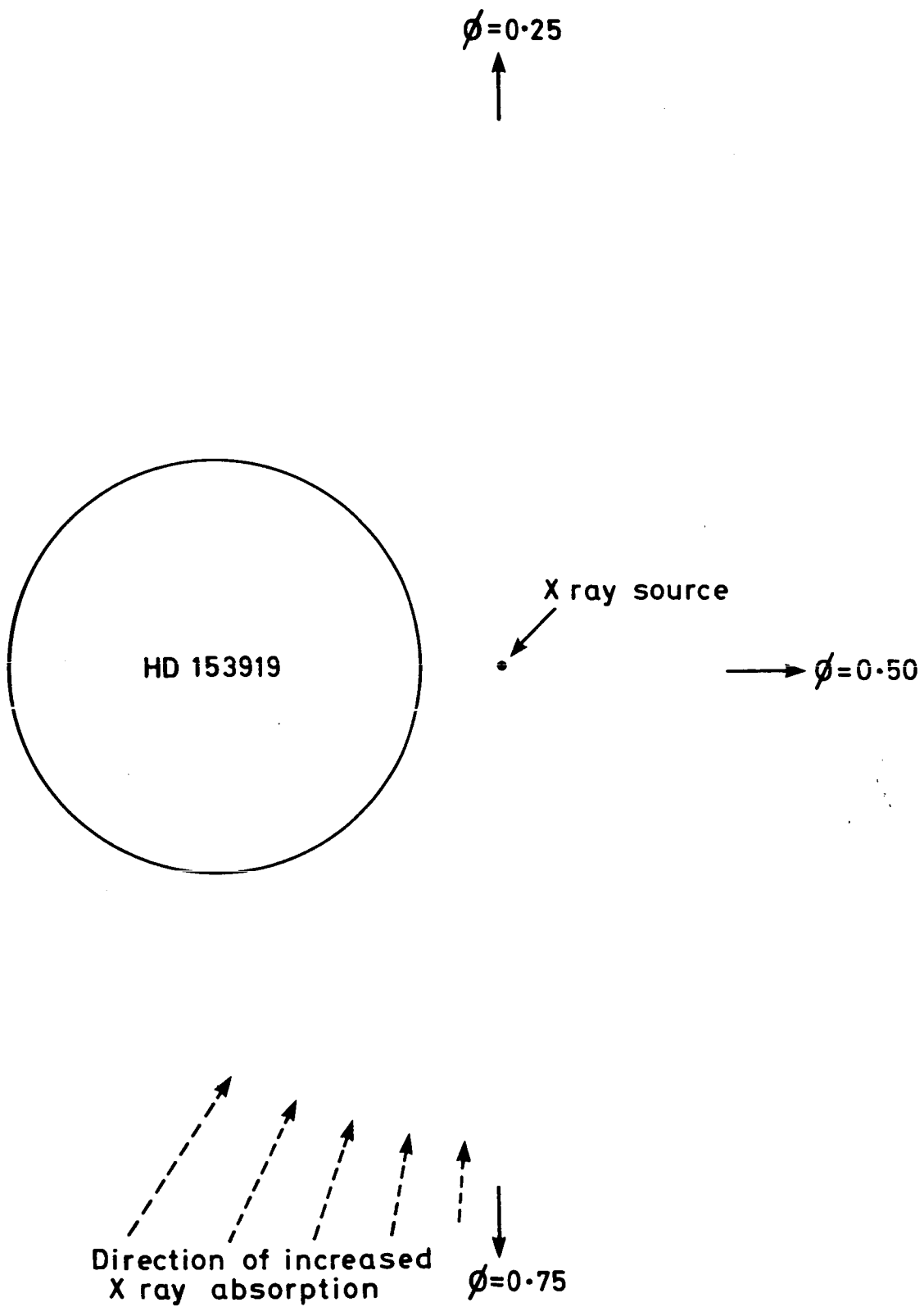


Figure 5 - Schematic diagram of the 3U 1700-37/HD 153919 binary system - see text.

The Broad Emission Features and "Wake" in HD 153919

E. N. Walker

Royal Greenwich Observatory,
Herstmonceux Castle,
Hailsham,
Sussex,
England.

Summary

It is shown that the broad emission features in the spectrum of HD 153919 are associated with the x-ray secondary and not significantly with the primary star. When the primary is at maximum velocity towards us the HeI line $\lambda 4471$ develops a blue shifted secondary component with a velocity of -470 km sec^{-1} relative to the primary.

Introduction

The star HD 153919 is the optical counterpart of the x-ray source 3U 1700-37. The identification is secure because both photometry and radial velocities of the star show similar periods to the x-rays which exhibit an 'off' phase for nearly one third of each orbit. Combination of x-ray and optical data shows that the secondary in this binary system is the source of x-rays and that eclipses of the secondary by the primary cause the dominant x-ray variation.

The first description of the spectrum of this star was given by Walker (1973) who showed that the star was $\sim O5.5f$ but with extreme features due to CIII $\lambda 4647$, 4650 and 4651 , not normally found in this spectral type, and a HeII emission line, $\lambda 4686$, among the strongest to be found at this spectral type. Various lines from different optical depths showed an expansion through the atmosphere of from zero to 200 km s^{-1} , a feature commonly found in extreme OB stars.

Underlying the main spectrum were found to be several very broad emission lines, which, if they were due to single narrow features and their widths due to either rotation or expansion, suggested velocities of between $6,000$ - $12,000 \text{ km s}^{-1}$. Such velocities would be extreme if associated with a non-compact object. The lines seemed to be centred on approximately $H\beta$, $H\gamma$ and $H\delta$. Their existence was confirmed by Hensberge et. al. (1973) who also found a similar feature underlying HeII $\lambda 4686$, although Bopp and Grupsmith (1974) failed to detect these features during five consecutive nights in June 1973.

There are two main problems associated with these features. One is to decide whether they are single, narrow features with some type of velocity broadening or are the broad features seen in Wolf Rayet stars. This latter

seems not to be the case, as the lines do not coincide with the Wolf Rayet features. The other problem is to decide whether these features are associated with the primary O5.5f star, in which case they are probably evidence for massive outflow from this star, or are associated with the x-ray emitting secondary, in which case their widths are probably due to the extreme gravitational field of a compact object.

The Analysis

The observational data were 18 E.S.O. spectra loaned to the author by Prof E.P.J. van den Heuvel and tracings of 34 Radcliffe spectra. Walker (1974) lists the data. Our analysis consisted in visually examining tracings of all spectra for the presence of the broad feature near H γ . This was chosen, as on the spectra available its detection was most certain. Figure 1 shows tracings of two Radcliffe spectra where the upper spectrum clearly shows the feature while the lower spectrum does not. The presence or absence of the H γ feature was estimated on a scale of from zero, meaning the line was not detectable to +2 meaning the line was present and strong. Figure 2 summarises some of the x-ray and optical features of this star while in the lower part the results on the H γ feature are shown. Although at any phase the line might be absent it is only ever seen as a strong feature when the x-ray secondary is visible. The line is never certainly present during x-ray eclipse, strongly suggesting that the broad features arise near the secondary. Inspection of spectra taken only ~ 1 hour apart shows that even when these lines are present and strong they are not permanent features and can go from maximum strength to being invisible in ~ 1 hour. The width of these lines, if interpreted as due to velocities, gives widths of $\pm 6,000 \text{ km s}^{-1}$. This is higher than the escape velocity from a white dwarf and if the material is in orbit about some object, that object must be more compact than a white dwarf. Without in any way being the only possibility, it is tempting to visualise these lines as arising in material circling either the neutron star or blackhole secondary, with their ephemeral nature being due to variations in the gas flow density in this region.

The Wake

During the course of the above investigation it was noticed that on some spectra the HeI $\lambda 4471$ line occasionally showed either a violet displaced wing or secondary component. This feature was only ever seen on the shortwards side of the line and never to its red. Further investigation showed the phenomenon to be phase dependent. Starting just after phase 0.5 a weak, violet wing is observed on $\lambda 4471$. This progressively increases in both strength and apparently in violet displacement until just after phase 0.7 the whole of $\lambda 4471$ is dominated by this feature. By phase 0.75 the wing has ceased to exist and has been replaced by a clearly resolved violet displaced line $\sim 470 \text{ km s}^{-1}$ from $\lambda 4471$. This displacement is sufficiently great to render impossible any confusion between this feature and the forbidden component of $\lambda 4471$. By phase 0.8 the whole feature has disappeared. Conti and Cowley (1975) have since discovered a very similar phenomenon at HeI $\lambda 5875$ and the reality of the effect seems beyond doubt.

The difficulty arises in deciding where in the binary system the material causing these absorption features lies. If the material lies between the primary and the observer then the feature is presumably due to a 'wake' created in the expanding atmosphere of the Of star by the passage of the secondary. However due to the phase of the phenomenon, i.e. maximum bluewards shift at the same phase as maximum bluewards shift of the primary then we have to hypothesise that the wake persists for 90° round the orbit despite the fact that within the parts of the photosphere accessible to the optical observers the outer parts are known to be moving outwards at 200 km s^{-1} relative to the inner parts. Alternatively, if the material is closely connected with the secondary then the 470 km s^{-1} blue shift just at the time the secondary will have $\sim 400 \text{ km s}^{-1}$ red shift is equally hard to understand.

Conclusions

A study of 42 spectra obtained over seven years suggests that the broad emission features arise close to the x-ray component of this binary system and when they do occur they are transient events with life times of the order of one hour. The violet displaced HeI absorption features which occur near phase 0.75 seem to be a stable feature in the orbit as they are always seen. However the location of the material causing these features in relation to the two components of the system is problematical.

The author would like to thank Prof E.P.J. van den Heuvel who provided all the E.S.O. spectra used here and Mr R.M. Catchpole who provided tracings of all the archival Radcliffe spectra.

References

- Bopp, B. W. & Grupsmith, G., 1974. Mon. Not. R. astr. Soc., 167, 65P.
Conti, P. S. & Cowley, A. P., 1975. Ap. J., 200, 133.
Hensberge, G., van den Heuvel, E. P. J. and Paes de Barros, M. H., 1973. Astr. Astrophys., 29, 69.
Walker, E. N., 1973. Mon Not. R. astr. Soc., 162, 15P.
Walker, E. N., 1974. Mon. Not. R. astr. Soc., 169, 47P.

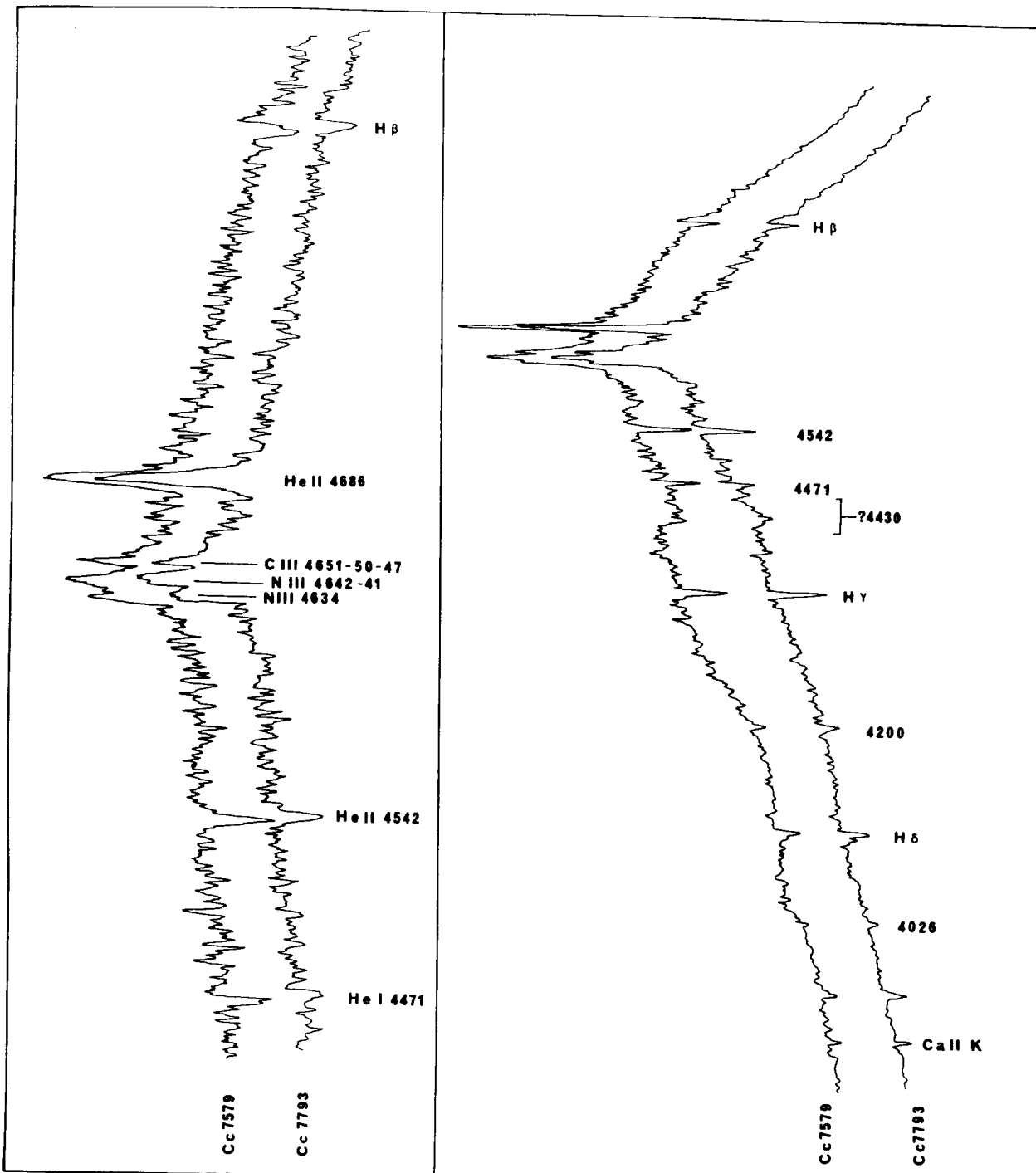


Figure 1 shows tracings of two Radcliffe spectra. The upper part shows the NIII, CIII, HeII lines in expanded scale while the lower part shows the difference between two spectra where the upper one shows the broad emission features and the lower one does not.

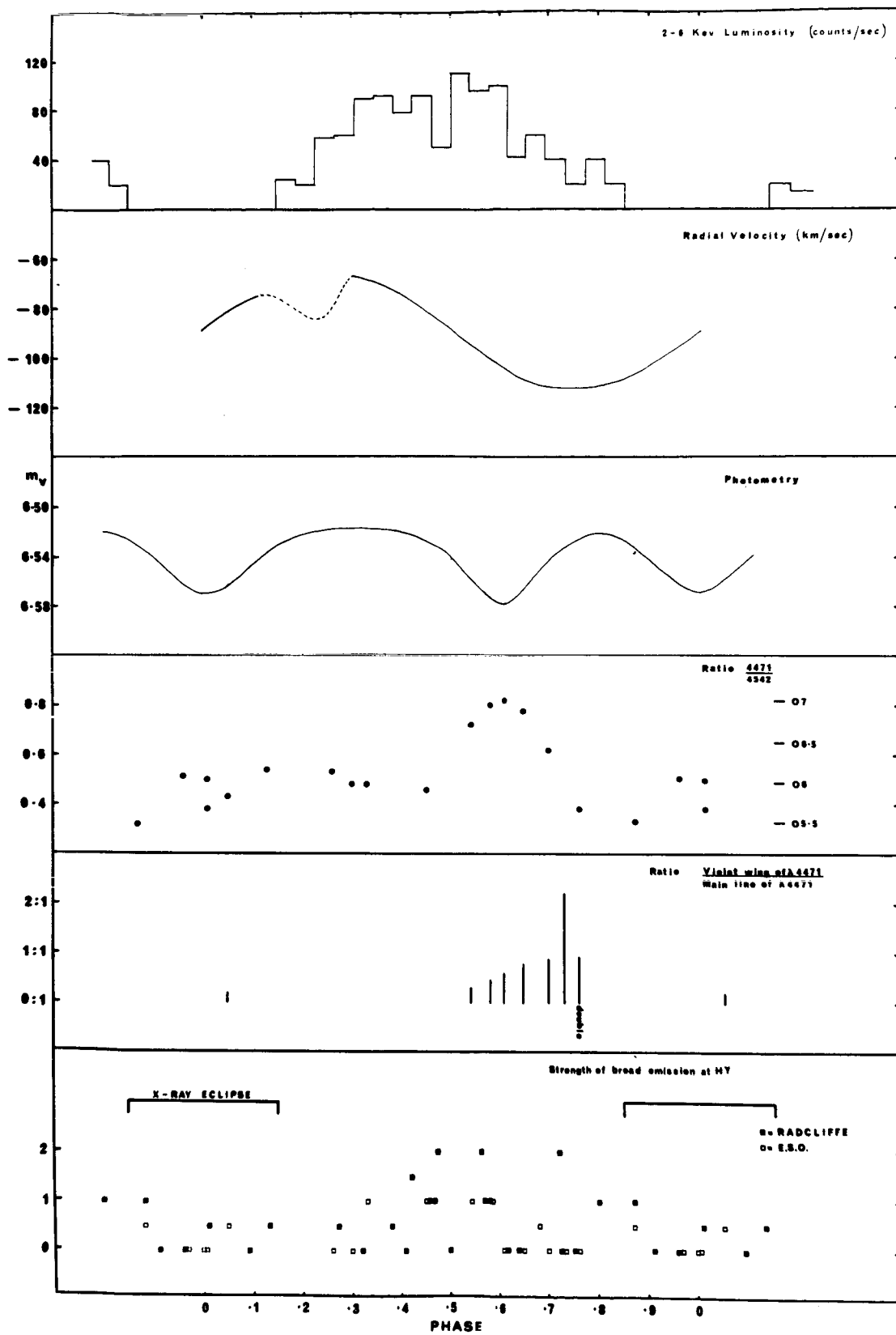


Figure 2 summarises some of the x-ray, radial velocity and photometric details of HD 153919. The bottom frame shows the phase relationship of the broad emission features while the frame above shows the phase dependence of the He I $\lambda 4471$ violet wing.

HD153919 (3U1700-37)

Discussion

P. Murdin to C. T. Bolton:

I'd be circumspect in putting X-ray sources into a reddening-distance relation. The field stars are selected down to an apparent magnitude so the more reddened stars are discriminated against, but the X-ray sources are selecting themselves with a high optical luminosity and are identifiable through more reddening. This is why this star, HD226868 and the Cen X-3 candidate are all more heavily reddened than the stars in the field. So the reddening distance is an upper limit to the true distance of the star.

THE X-RAY BINARY HD77581 + 3U 0900-40

N. V. VIDAL

Center for Astrophysics, Cambridge, Massachusetts, and
Weizmann Observatory, Israel

1. Introduction

3U 0900-40 (also known as Vel XR-1 and GX 263+3) was first detected by Chodil et al. (1967). In 1972, observations by the OSO-7 UCSD and the Uhuru satellites revealed an X-ray period of about 8.95 days (Ulmer et al. 1972, Forman et al. 1973). Through the photometric period, Hiltner (1973), Vidal et al. (1973, 1973b) and Jones and Liller (1973) established the identification with the early type supergiant HD 77581. For a detailed account with references to these early investigations, see Jones (1974).

Fig. 1 shows the X-ray position of 3U 0900-40. The 7th magnitude star HD 77581 is clearly inside the error box. The position, the identical periods at X-ray and optical frequencies, and the occurrence of the X-ray minimum during the shallower optical minimum establish this identification beyond doubts.

From spectroscopic and photometric studies, it was soon realized that the compact secondary X-ray companion is an "exotic" type star, since its mass was in the range $2 \lesssim M/M_{\odot} \lesssim 3$. Therefore the secondary could be a massive neutron star or a black hole (Wickramasinghe et al. 1974 (WD), Zuiderwijk et al. 1974 (ZE), Hutchings 1974 (HT)). Recently the SAS-3 group found a 283 sec period modulated by a Doppler shift (see Rappaport and McClintock 1975). This outstanding discovery gives us the first opportunity to study the physical parameters of an X-ray binary system in a fairly accurate manner, since both mass functions are now known. In particular, the mass estimate of the X-ray star would be the first of its kind (whether it is a white dwarf, a neutron star or a black hole).

In this review, I present the properties of the binary system in the different regions of the electromagnetic spectrum, from X-rays to the radio. Physical parameters and a model for the system are then derived.

2. The X-ray observations

Fig. 2 shows the Uhuru observations taken during May and June 1972 folded with an 8.95-day period (Forman et al. 1973). The total eclipse is an indication of a high inclination angle for the system. Its duration is 1.9 ± 0.05 days. The scatter is probably real: Fig. 3 shows an X-ray flare (a factor of 30 in intensity) of about 2 hours duration. Jones (1974) shows that at the peak of the flare, the time scale of these variations is less than 0.4 sec. Spada et al. (1974) also detected an X-ray flare (4.1 σ level) that reached about twice the average intensity level and lasted for a few seconds. Analysing 100 sec observations taken at phase 0.42, Spada et al. did not find any periodic pulsations on time scales of 10 sec to 2 ms.

Eadie et al. (1975) observed this source with the Ariel V satellite during almost two cycles. Fig. shows the count rate as function of both time and phase. They noticed four persistent relatively strong "dips" on top of the usual fluctuations found by Uhuru. The spectral hardness varies too and becomes lower during these dips, possibly indicating a varying circumstellar origin.

Ulmer (1974) shows the X-ray spectrum up to 100 keV. It is relatively flat and similar to several other X-ray binaries. From a power law fit, the low-energy cutoff varies between 2.2 and 4.4 keV and the spectral index from -0.2 to +0.7 (Jones 1974). This would correspond to a hydrogen column density between 3.7 and 3.2×10^{23} atoms per cm^2 . This is

remarkably higher than the neutral hydrogen column density of 6×10^{21} atoms as derived from the 21 cm line in that direction (Jones 1974), and it is likely to be of a varying circumstellar origin.

Recently the SAS-3 group (IAUC 2794 and IAUC 2833) reported the remarkable discovery of a double peaked 283 sec pulse modulated by a Doppler shift. They observed it in the 1.5 to 2.7 Kev range but the strongest pulses were found in the 8-18 Kev range. The best fit parameters are:

$$P = 282.8913 \pm 0.0004$$

$$asini = 109 \pm 4 \text{ light seconds}$$

$$K_x = 268 \pm 12 \text{ k/sec}$$

$$f(M) = 17.3 \pm 2.0 M_{\odot}$$

$$e = 0.15 \pm 0.05$$

$$\omega = 157^{\circ} \pm 26^{\circ}$$

These parameters, and especially the much awaited mass function and eccentricity opened the way to determine accurately the mass of an X-ray star. (For a more recent determination of these parameters, see McClintock; this symposium.)

3. The optical light curve

In two consecutive IAU circulars, Hiltner (1973) and Vidal et al. (1973) announced independently that the photometric period of HD 77581 is identical to the X-ray period of 2U 0900-40. (For previous investigations, see Jones 1974.) Several authors observed the optical light curve in U, B, and V but the most extensive sets of observations in V was done by Jones and Liller (1973) and by Vidal (1974). These two sets of observations are in good agreement and are therefore suitable for theoretical analysis (Fig. 5). Both were taken on several consecutive cycles, with several days of overlap between the two sets. Since the claimed accuracy is about 0.01^m , the scatter of about 0.05^m in the light curve seems to be intrinsic to the star. The X-ray activity mentioned above as well as the study of the circumstellar material around the system (see section 7) are consistent with this interpretation. Fig. 6 shows that the maximum that was due about March 3, 1973 did not show up and this obscuration is likely to be of circumstellar origin.

The double-peaked light curve is usually interpreted as arising from the ellipsoidal aspects of the primary as seen by the observer. However, the lower part of Fig. 6 does not show that these aspects have any observable effect on the colours (Temperature).

Due to the scatter, it is difficult to see any special asymmetries like the one arising from an eccentric orbit. However, the radial velocity curve and the X-ray pulses do show a definitive non-zero eccentricity of about 0.15. Therefore, it would be of great interest to look for a possible apsidal motion. Since there is much scatter in the light curve, the study of these variations should use statistical methods.

4. The optical spectrum

Several authors describe the spectrum as very similar to the B0Ia star ϵ Ori (Hiltner et al. 1972, WD, ZE). However, there is not yet a general agreement as to the precise spectral class and luminosity. In a detailed spectral and continuum analysis, WD found that HD 77581 is probably very similar to the B0.5Ia star HD 152234 in the Sco OB1 association. Apart from the structure of the H α line, the only difference found was the somewhat broadened lines of HD 77581 relative to HD 152234. They attributed this difference to a higher rotational velocity of about 90 km/sec. ZE classify it as B0.5Ia too, and give an even higher rotational velocity of about 130 km/sec. However, the presence of a binary companion and a critical Roche lobe may create an over-extended atmosphere imitating a lower gravity and thus giving the impression of a relatively higher luminosity class. Therefore, although the star looks like a B0.5Ia star, a direct derivation of its mass and other physical parameters like those for "true" Ia luminosity class stars would not be completely safe. On the other hand, the temperature and gravity as derived directly from continuum scans are more reliable parameters (Fig. 7) ($T = 25000^{\circ}$ and $\log g = 2.8$, WD).

Compared to other supergiants that are optical counterparts of X-ray binaries, the spectrum of HD 77581 looks very "naive": No peculiarities are found. The usual typical spectral lines of early type supergiants like He I, Si III, Si IV, N II, N III, C III and O II are all present. The band of C III, O II and N II at $\sim \lambda 4650$ is in absorption. No nitrogen or carbon anomalies

(Walborn 1970) are found. Tracings of several lines show sometimes a distorted profile which may be correlated with phase (ZE, (Fig. 8)). The He II 4686 line is probably filled in emission. A visual inspection of some forty spectral plates of 90 and 45 $\text{\AA}/\text{m}$ dispersion which the author took at Mt. Stromlo did not reveal He II 4686 above the continuum. Jones (1974) took scans (about 4 angstroms resolution) in this spectral region and concluded that "there is little or no measurable He II 4686 observed in HD 77581." (Fig. 9.). Hutchings (1974) reported a weak and sometimes sharp line in emission at different phases on his high dispersion spectra. Compared to other similar optical counterparts like HD 226868 and SK 160, the relative weakness of this line in HD 77581 is remarkable.

Interstellar diffuse bands are found at about $\lambda 4430$, 5792, 5797 and 6284. The H and K lines are relatively strong and are consistent with a distance of about 2 kpc (see section 5). ZE report an unidentified line at $\lambda 6290$ which is variable and therefore expected to be of circumstellar origin. It would be of interest to correlate this variability with phase and/or with the shape of the H α profile (see section 7).

5. The distance

Low gravity is not a sufficient condition to assert a high luminosity class. An underluminous low mass star may have a low gravity too. Thus the distance is an essential parameter to establish the intrinsic luminosity. There are several arguments in favor of a relatively distant and therefore a high intrinsic luminosity.

1. The reddening ($E(B-V) \sim 0.7^m$) corresponds to other reddened supergiants ($M_V \sim -7^m$) in the same direction and at an apparent distance modulus of about 14^m . For a $3E(B-V) = 2^m$ visual absorption, HD 77581 would be at a distance of ~ 2 Kpc (Fig. 10).

2. The equivalent width of the Ca II K line points to such a distance too (ZE).

3. Reddening and polarization ratios are all consistent with an interstellar origin rather than circumstellar.

However, due to the scatter in the calibration of the reddening and the equivalent widths as a function of distance, the absolute visual magnitude may be as low as $M_V = -5.5$.

For a distance of about 2 Kpc, the X-ray luminosity would be $\sim 10^{37}$ ergs/sec.

6. The radial velocity curve

Since the mass function of the X-ray companion is known, the mass function of the optical companion is now of utmost importance. Together, they may allow the mass determination of both companions, provided the inclination of the orbit can be derived from the light curve. As is well known, radial velocities of early type supergiants are difficult to measure. The H α studies in HD 77581 (section 7) revealed the fact that circumstellar material is playing an important role in the outer region of the system. ZE found a correlation between the distorted shape of H β and some He I line profiles as a function of phase (Fig. 8), and the profile of the H α line as well). These streams would produce asymmetrical profiles and would make radial velocity measurements less reliable. Furthermore, lines of different elements may be affected differently.

Three sets of extensive radial velocity observations are given by ZE, Petro and Hiltner (1974) and Wallerstein (1974). Although the first two sets agree with each other (within the observational errors) the work by Wallerstein shows that, at some periods, the radial velocities can be very discordant. Observations by Petro and Hiltner on two nights in common with Wallerstein show that, evidently, these two nights are in disagreement with the rest of their observations, although they were taken with the same equipment. Therefore we shall adopt the assumption that Wallerstein's observations are of non-orbital origins (Hutchings 1974, Petro and Hiltner 1974). Although there is a good basis for it, this assumption should be taken with great caution until more extensive observations are made. From the mean radial velocity curve, Petro and Hiltner derived the following

parameters (Fig. 13)

$$\begin{aligned}V_o &= -5.0 \pm 2 \text{ km/sec} & K &= 22.7 \pm 2 \text{ km/sec} \\e &= 0.19 \pm 2 & \omega &= 28^0 \pm 1 \\f(M) &= 0.011 M_o\end{aligned}$$

ZE found that the Balmer lines, the He I lines and the metal lines, although close to each other, give slightly different sets of parameters. For the hydrogen lines they find (Fig. 12)

$$\begin{aligned}V_o &= 3.6 \pm 0.6 \text{ km/sec} & K &= 26.0 \pm 0.7 \text{ km/sec} \\e &= 0.223 \pm 0.024 & \omega &= 13.4^0 \pm 7.8^0 \\f(M) &= 0.0147\end{aligned}$$

and for the metal lines (Paradijs et al. 1975) (V_o was not reported)

$$\begin{aligned}K &= 22.4 \pm 2.0 \text{ km/sec} & \omega &= 357^0 \pm 32^0 \\e &= 0.16 \pm 0.10 & f(M) &= 0.010 M_o\end{aligned}$$

At the moment, since all three sets of parameters are within the claimed observational errors, we regard all three as essentially identical. The main conclusion would be that the orbit is eccentric with a probable mass function of about 0.013.

7. The distribution of circumstellar material from H α studies

The multiple structure of the H α line in emission and in absorption shows that a rather complicated pattern of streams prevails in the outer regions of the system. According to the accretion model mechanism, such a dynamic extended atmosphere is expected to supply the material to the X-ray emitting disk around the collapsed secondary. Bessell et al. (1975) took high dispersion Coudé spectra of H α during several cycles and combined their observations with ZE's and Wallerstein's to look for a possible periodic flow pattern. They found two persistent absorption and one emission components that vary in position and intensity more or less according to phase. Fig. 13 is a schematic profile of the observed H α line. The velocity range of the "fast" blue shifted absorption is about 250-420 km/sec and it grows with phase from 0.6 to 0.85. The second, slower moving absorption is probably less than 100 km/sec. (Its exact values are difficult to estimate since it is overlapping with the slope of the emission line). The structure of the double peaked line may be interpreted as arising from a large extended static atmosphere on which is superimposed a slow moving stratum that "cuts" the blue side of the emission line (and produces the double peaked shape of the emission). Fig. 4 is a reproduction from Bessell et al. showing a schematic view of the gas-streaming model. (Note the absence of streams (absorptions) at phases \sim 0.3-0.5 and \sim 0.9-0.1). It may be interesting to note that two of the strong X-ray "dips" found by Eadie et al. (1975) do correspond to the phases \sim 0.26 and 0.65 where the streams are most active.

The picture derived from these H α studies and especially the presence of the high velocity stream suggests that the outer parts of HD 77581 atmosphere are close or above the escape velocity and, therefore, are unlikely to be confined to the Roche lobe limits. This conclusion lends support to theoretical models in which HD 77581 is in contact with its Roche lobe. Furthermore, this picture explains the distortions found in the line profiles of many lines in the spectrum, which, in turn, would yield discordant radial velocity curves and inaccurate mass functions. Finally, the streams model may explain the source of the scatter in the light curve, and more specifically, even the long term obscurations found for example on March 3, 1975 in Jones and Liller's (1973) observations.

8. Ultraviolet, Infrared and radio observations

Nandy et al. (1975) observed the UV flux over the wavelengths 1350-2500 Å⁰ and found that HD 77581 is very similar to other early type supergiants (Fig. 15). The broad absorption feature centered at 1920 Å⁰ is present and the continuum at the shorter wavelengths decreases systematically as compared to a main sequence star of the same spectral class. The continuum is very similar to that of the B0Ia supergiant ε Ori and thus lends support to a high temperature of about 25000⁰ K (WD). However, since both continua are depressed relative to main sequence stars of the same spectral type, the temperatures of both ε Ori and HD 77581 may have been overestimated by about 3000⁰ K (Humphries et al. 1975).

Nandy et al. (1975) discussed also the distance as derived from their estimates of the interstellar obscuration. They found that the system is at 1.3 ± 0.2 Kpc, as compared to about 3 Kpc derived previously from optical observations. However, due to the scatter in the optical calibrations, these two values for the distance may still be compatible.

Infrared observations in the region between 1.25 to 3.6μ by Hyland and Mould (1973) and Frogel and Persson (1973) show that the emitted infrared flux is normal for early type supergiants. Hyland and Mould followed the variations in the K band and found intensity modulations of about 0.1mm consistent with the optical and X-ray periods (Fig. 16). The variations can be interpreted in the same way as in the optical region, namely, that the light curve is the manifestation of limb and gravity darkening of the rotating ellipsoidal optical

primary. These small variations in the K band and especially when the secondary is between the optical primary and the observer do not support the existence of a large obscuring cloud around the collapsed secondary. This is also confirmed from H α studies (section 7).

No radio flux has been detected from this system (Tananbaum and Tucker 1974). Hjelmning (private communication, 1975) reports an upper limit of 0.004 Jy at 2695 and 8085 MHz.

9. Polarization observations

The recent discovery of the periodic pulsations of about 283 sec in the X-rays may suggest that the secondary companion is an unusually slowly rotating neutron star. Therefore the search for a relatively strong magnetic field would be of utmost importance to complement our knowledge of the character of the secondary. It is expected that the Zeeman effect would be manifested as circular polarization at the wings of the Balmer lines, whether from plasma emission around the system or directly from HD 77581. Furthermore, it is likely that the maximum amount of circular polarization, if any, would be detected when the neutron star is in between the observer and the optical primary. At this phase the rotating magnetic field is most exposed to the observer. If the circularly polarized power is high enough, a possible periodic pulsation of 283 sec may be detected.

Unfortunately, very few polarization observations have been made, and, furthermore, the results contradict each other. Kemp and Wolstencroft (1973) report a positive result, leading to a varying magnetic field of up to 10^4 Gauss on the primary. Angel et al. (1973) were not able to confirm this result and state that the 10^3 or less Gauss they detected are "consistent with random errors expected from photon statistics assuming no magnetic field".

In view of the importance of these polarization observations, it would be desirable to organize an extended observational program to put, at least, upper limits on the physical parameters involved.

Kemp and Wolstencroft report also a varying linear polarization component. If confirmed, it is likely to arise from electron scattering in the asymmetrical shape of the optical primary, and occasionally, from "tongues" of material (see section 7) around the system.

10. Parameters estimates for the binary system

Since both optical and X-ray companions have observed mass functions and the analysis of the optical light curve should yield the orbit inclination, both masses as well as other parameters of the system can be calculated. As in similar binary systems (where both companions are optically seen), streams of matter may distort the radial velocity curve and produce a similar large scatter in the light curve. Therefore, careful examination of the observations is needed before adopting mean observed values and their accuracies. We could adopt the extreme view that all observed deviations have equal weights and therefore should be included as uncertainties. Such an indiscriminatory attitude may be the safest but it neglects the physical insights that may help in "cleaning" the observations from side effects. We have already mentioned (section 6) that the radial velocity observations by Wallerstein may be affected by non-orbital components and may therefore be given a lower weight in deriving the orbital elements of the system. Other workers did find such anomalies (Hiltner et al. 1972; Petro and Hiltner 1974). In the case of the light curve the relatively large scatter prevents a straightforward determination of the amplitude. Here again the anomalies (like that found on March 3rd, 1972 by Jones and Liller) should not be included while folding all observations to estimate the mean amplitude. For example, in the extreme case, a free hand curve connecting such obscuration events would yield unrealistically small amplitudes that have nothing

to do with the true orbital revolution. Observations taken consecutively and in a long period of time allow the detection of anomalies, and the "cleaning" process is then reliable. Thus the mean of all amplitudes derived in each cycle separately would be a better representation than an amplitude derived by folding all data. Accordingly, isolated observations should be discarded from amplitude analyses. The amplitude derived from such a procedure is 0.110 ± 0.015 mag in V (Jones and Liller 1973, Vidal 1974).

The inclination of the orbit is usually derived using a Roche lobe analysis. (For a critique of this assumption, see Kondo (1974) and Kondo and McCluskey, this volume). It is assumed that the light curve is the manifestation of the different aspects of a distorted star during its orbital revolution. The light variations are determined by the orbital parameters and the atmospheric properties of the optical companion. Several computer programs exist now that generate such theoretical light curves. The input parameters that yield the best fit to the observations are then adopted as the parameters of the system. Wickramasinghe and Whelan (1975) gave an excellent analysis and comparison of several existing programs and found a good agreement between Wilson (1972), Strittmatter et al. 1973, Avni and Bahcall (1975) and their program. Their analysis (1974) for HD 77581 used full cycles data and yielded the following best fit parameters:

$$80^{\circ} < i < 90^{\circ}$$

$$e \sim 0.1$$

$$\omega \sim 0^{\circ}$$

$$q \sim 0.093$$

The three last parameters are consistent with the radial velocity constraints from X-ray and optical observations (Rappoport and McClintock 1975). Obviously, the inclusion of all existing data without discrimination (see discussion above) may yield a larger range for the inclination angle (Fig. 17, curve a, Petro and Hiltner 1974, Avni and Bahcall 1975).

The mass function of the X-ray companion is

$$\frac{M_p^3 \sin^3 i^3}{(M_p + M_x)^2} = (17.3 \pm 2.0) M_0$$

For the optical companion a mass function that is consistent with the observations of Petro and Hiltner, ZE, and Paradijs et al. (1975):

$$\frac{M_x \sin^3 i}{(M_p + M_x)^2} = (0.1025 \pm 0.0025) M_0$$

In Fig. 18 we plotted the possible range of masses for the two companions using the last two equations for $i = 90^{\circ}$ and 80° . Each equation yielded two limiting

lines (curves) corresponding to the given lower and upper limits. The mass ranges are (in solar units)

$$\begin{array}{lll}
 1.56 \leq M_x \leq 2.1 & 18.1 \leq M_p \leq 23.0 & \text{for } i = 90^\circ \\
 1.64 \leq M_x \leq 2.2 & 19.0 \leq M_p \leq 23.7 & \text{for } i = 80^\circ \\
 1.9 \leq M_x \leq 2.55 & 20.7 \leq M_p \leq 27.7 & \text{for the extreme case } i = 70^\circ
 \end{array}$$

Due to its mass, the safest conclusion about the secondary is that it is unlikely to be a white dwarf. However, the mass is at the very upper limits for a realistic model of a neutron star (Malone et al. 1975) and, in this respect, it is a little puzzling. According to current theories, the 283 sec periodicity rules out a black hole, if its origin is from a disk surrounding the X-ray object.

The mass estimates of the primary makes it a true supergiant, although not as massive as previously suggested (Wickramasinghe et al. 1974, ZE 1974, Hutchings 1974). This is also consistent with the calculated radius of about $30 R_\odot$ (Wickramasinghe and Whelan 1974). Due to the uncertainty in the distance, the absolute visual magnitude may be as low as $M_V = -5.5$. Fig. 19 shows that even such a low luminosity makes HD 77581 overluminous for its mass.

From the derived parameters, it seems that HD 77581 may not be in corotation with the orbit of the secondary. A more quantitative estimate (with the uncertainties involved) of its rotational velocity would be desirable. Wickramasinghe (1975) calculated light curves taking into account different degrees of departure from corotation. He found that, in general, for a given radial velocity amplitude, the value of the masses of both companions are overestimated if corotation is assumed.

11. Discussion

From the extensive and wide variety of observations it seems that the parameters of the binary system are now fairly well known. The accuracy given for each parameter is common to many other binary systems of this type. In the following we give the various parameters that fit best the X-ray and optical observations:

Orbital period = 8.96 days

I. X-rays:

Eclipse duration = 1.90 ± 0.05 days

$a \sin i = 109 \pm 4$ sec

$K_x = 268 \pm 12$ km/sec

$f(M) = (17.3 \pm 2) M_0$

$e = 0.15 \pm 0.05$

$\omega = 157^\circ + 24^\circ$

pulse period = 282.9 sec

II. Optical:

Spectral type Bo.5Ia, $T_e \sim 25000^\circ$ $\log \sim 2.8$

$K_p = 22-27$ km/sec

$V_o = -5$ km/sec

$f(M) = (0.0125 \pm 0.0025) M_0$

$80^\circ \leq i \leq 90^\circ$

$\omega \sim 0$

$e \sim 0.15$

$q \sim 0.093$

III. Mass ranges:

$$15.6 \leq M_x/M_\odot \leq 2.2$$

$$18.1 \leq M_p/M_\odot \leq 23.7$$

(for more recent values that are slightly different, see the following reports.)

As for the model of the system, studies in H α and X-rays show that various streams dominate the outer extended regions. A thorough study of these flow patterns is needed. Elimination of those active phases may help to give more reliable observable parameters.

Since the optical luminosity of HD 77581 may be as low as $\sim 5 \times 10^{38}$ ergs/sec, the ratio of the optical to the X-ray luminosity may be of the order of 100 (independent of distance). It would be even smaller during X-ray flares. Therefore it would be of great interest to try to detect the 283 sec pulsations in the optical region. As in polarization observations, these pulsations, if any, would be maximized when the X-ray secondary is in between the observer and HD 77581. Fortunately at this phase, the H α studies show little activity.

The origin of these pulsations is not well understood. The period is unusually long for a neutron star rotation. Transfer of angular momentum of opposite direction to the neutron star spin may have slowed it down to the present period. A rough calculation shows that if this process was 100 per cent efficient, then at a mass loss rate of $10^{-9} M_\odot/Y$ it would take 10^7 years to slow it down from 1 sec to 300 sec (a stream velocity of 400 km/sec is assumed, as from H α studies). This is larger than the whole main sequence age of HD 77581. It is possible that HD 77581 was more active in the past: With an average mass loss rate of $10^{-6} M_\odot/Y$,

10^4 years would be sufficient (all these estimates have been made with 100 per cent efficiency and no magnetic fields present). On the other hand, if the pulsations are from free precession origin then the expected spin periods would be in the range 0.1-0.01 sec (Brecher 1975). Spada et al. did not detect such pulsations in their 100 sec flight. It would be interesting to look again for such pulsations during an extended observation.

The author is grateful to Dr. W. Liller and the Center for Astrophysics for their hospitality and their help during the author's extended visit in September and October 1975.

This work has been supported in part by the National Science Foundation Grant MPS73-04987 A01 and by the Israel Commission for Basic Research.

References

- Angel, J.R.P., McGraw, J.T. and Stockman, H.S. 1973, Ap. J. (Letters),
184, L79.
- Avni, Y. and Bahcall, J.N. 1975, Ap. J., 197, 675.
- Bessell, M.S., Vidal, N.V. and Wickramasinghe, D.T. 1975, Ap. J. (Letters)
195, L117
- Brecher, K. 1975, Nature, 257, 203
- Chodil, G., Mark, H., Rodrigues, R., Seward, F.D. and Swift, C.D., 1967,
Ap. J. 150, 57
- Eadie, G., Peacock, A., Pounds, K.A., Watson, M., Jackson, J.C. and Hunt,
R. 1975, M.N.R.A.S., 172, 35P.
- Forman, W., Jones, C., Tananbaum, H., Gursky, H., Kellogg, E. and
Giacconi, R. 1973, Ap. J. (Letters), 182, L103.
- Frogel, J.A., and Persson, S.E. 1973, P.A.S.P., 85, 641.
- Hiltner, W.A., Werner, J. and Osmer, P. 1972, Ap. J. (Letters), 175, L19.
- Hiltner, W.A. 1973, IAU Circ. No. 2502.
- Humphries, C.M., Nandy, K. and Kontizas, E. 1975, Ap. J., 195, 111.
- Hutchings, J. 1974, Ap. J. 192, 685.
- Hyland, A.R. and Mould, J.R. 1973, Ap. J. 186, 993.
- Jones, C. and Liller, W. 1973, Ap. J. (Letters), 184, L121.
- Jones, C. 1974, Ph.D. Thesis, Harvard University, Cambridge, Massachusetts.
- Kemp, J.C. and Wolstencroft, R.D. 1973, Ap. J. (Letters), 182, L43.
- Kondo, Y. 1974, Astroph. and Sp. Sci. 27. 293.
- Malone, R.C., Johnson, M.B. and Bethe, H.A. 1975, Ap. J. 199, 741.

- Nandy, K.M.D., Napier, D. and Thompson, G.I. 1975, M.N.R.A.S., 171, 259.
- Paradijs, J.A., Hammerschlag-Hensberge, G., van den Heuvel, E.P.J.,
Zuiderwijk, E.J. and Takens, R.J. 1975, IAU Circ., No. 2841.
- Petro, L. and Hiltner, W.A. 1974, Ap. J., 190, 661.
- Rappaport, S. and McClintock, J. 1975, IAU Circ., No. 2833.
- Spada, G., Bradt, H., Doxsey, R., Levine, A. and Rappaport, S. 1974
Ap. J. (Letters), 190, L113.
- Strittmatter, P.A., Scott, J., Whelan, J., Wickramasinghe, D.T. and
Wolf, N.J. 1973, Astr. and Astrophys., 25, 275.
- Tananbaum, H. and Tucker, H. 1974, X-ray Astronomy, 207, Giacconi, R.
and Gursky, H. (D. Reidel Publishing Co., Dordrecht Holland).
- Ulmer, M.P., Baity, W.A., Wheaton, W.A. and Peterson, L.E. 1972,
Ap. J. (Letters), 178, L121.
- Vidal, N.V., Wickramasinghe, D.T. and Peterson, B.A., 1973, IAU Circ.,
No. 2503.
- Vidal, N.V., Wickramasinghe, D.T. and Peterson, B.A. 1973b, Ap. J. (Letters),
182, L77.
- Vidal, N.V. 1974, P.A.S.P., 86, 317.
- Wallerstein, G. 1974, Ap. J., 194, 451.
- Wickramasinghe, D.T., Vidal, N.V., Bessell, M.S., Peterson, B.A. and Perry,
M.E. 1974, Ap. J., 188, 167.
- Wickramasinghe, D.T. and Whelan, J. 1974, M.N.R.A.S., 167, 21P.
- Wickramasinghe, D.T. and Whelan, J. 1975, M.N.R.A.S., 172, 175.
- Wickramasinghe, D.T. 1975, M.N.R.A.S., 173, 21.
- Wilson, R.A. 1972, Ap. J. (Letters), 174, L27.
- Zuiderwijk, E.J., van den Heuvel, E.P.J. and Hensberge, G. 1974,
Astronomy and Astrophysics, 35, 353.

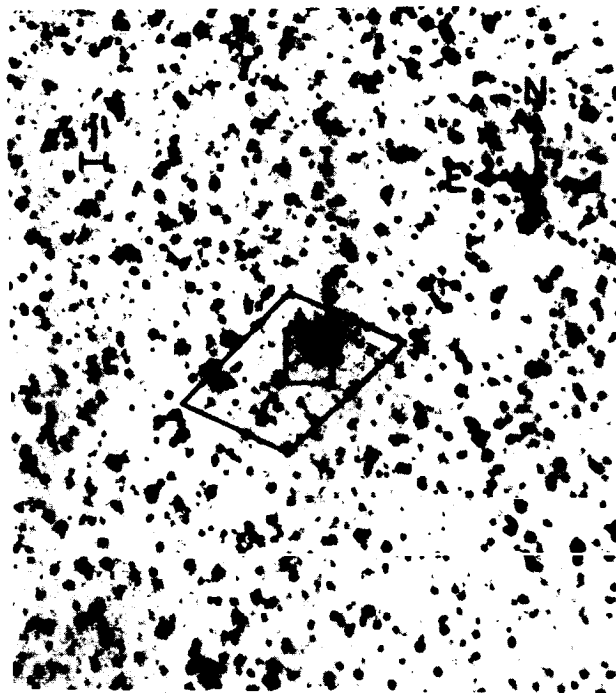


Fig. 1: Location of 3U 0900-40. The bright star inside the error box is the early type supergiant HD 77581 (Forman et al.1973).

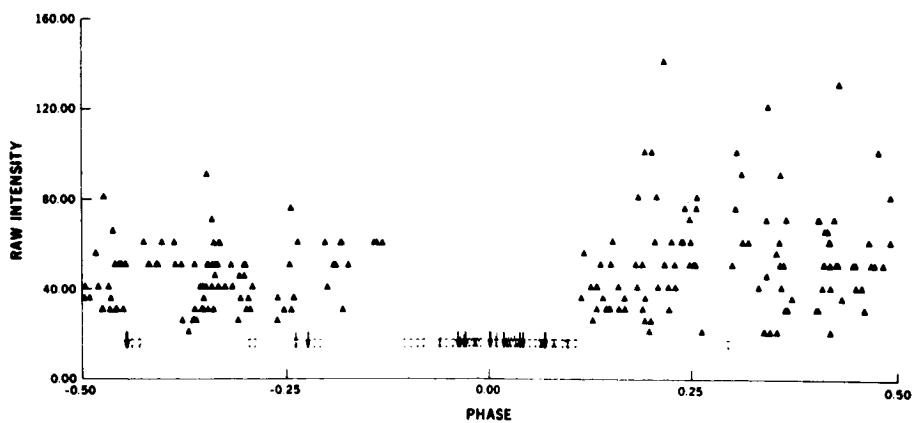


Fig. 2: Uhuru observations folded modulo 8.95 days (Forman et al. 1973).

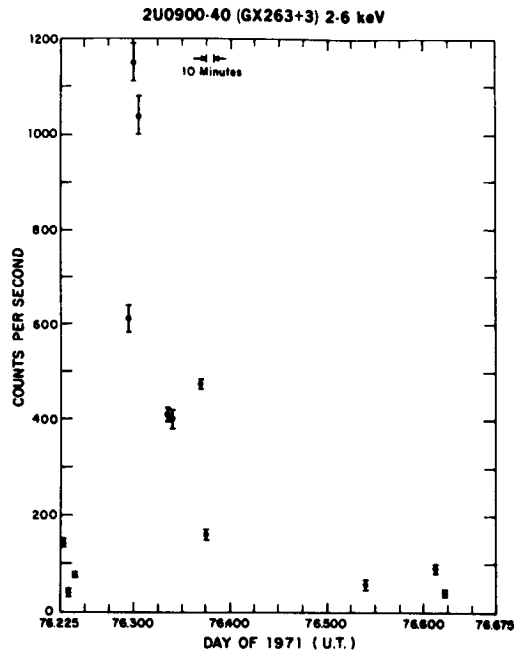


Fig. 3: An X-ray flare in 3 U 0900-40 (Forman et al. 1973).

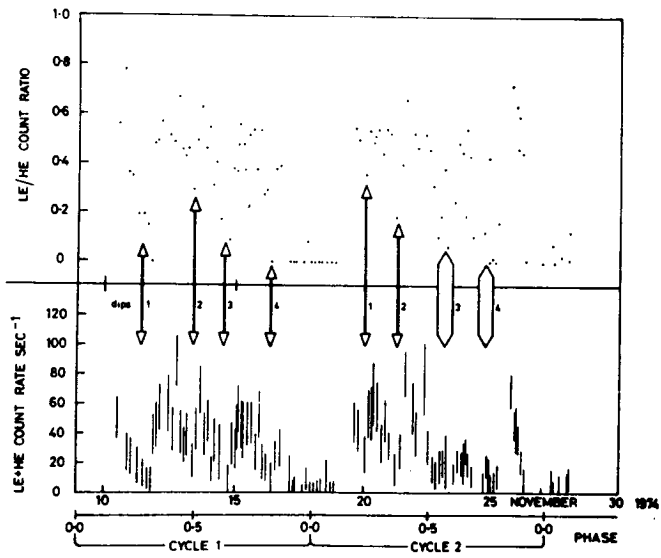


Fig. 4: X-ray light curve of 3U 0900-40 (Eadie et al. 1975).

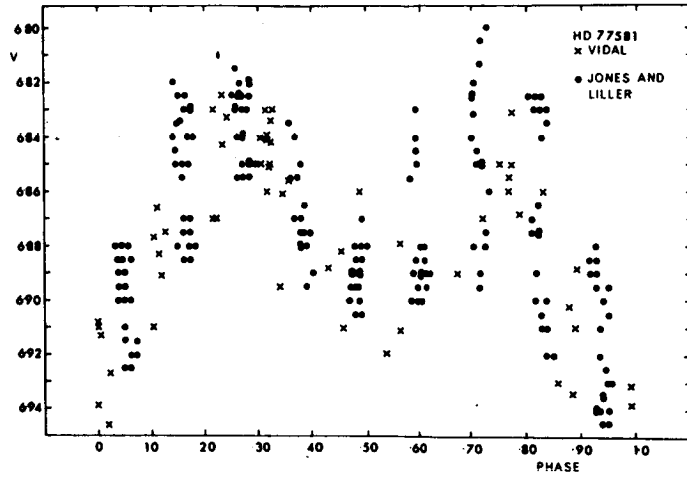


Fig. 5: Photoelectric observations in V folded 8.95 days (Vidal 1974).

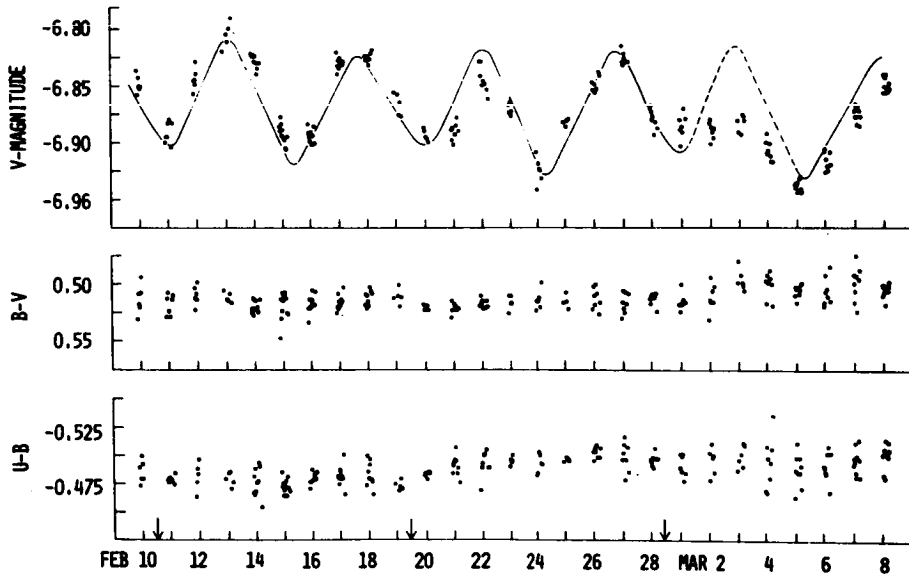


Fig. 6: Photoelectric observations by Jones and Liller (1973).

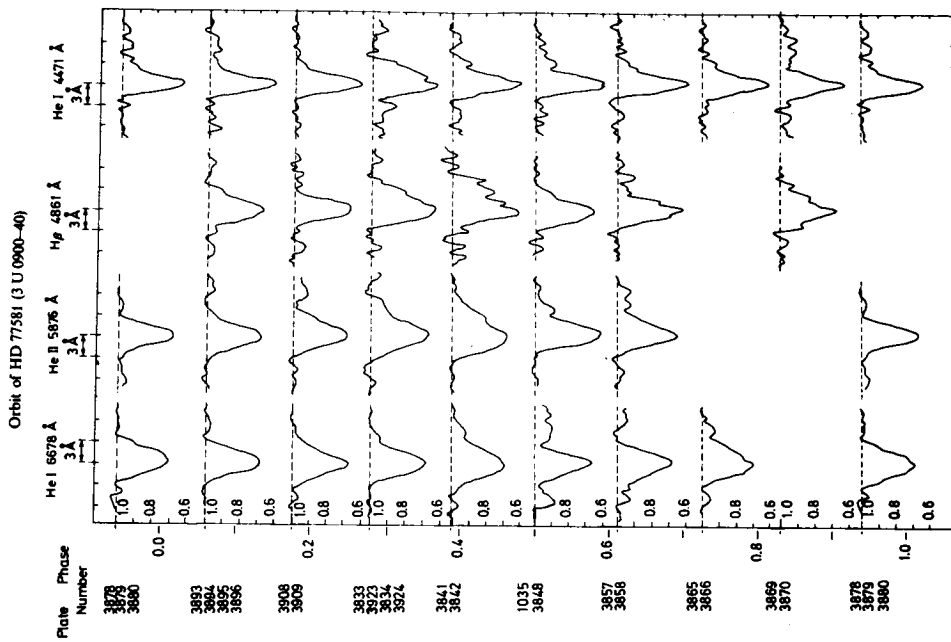


Fig. 8: Line profiles as function of phase (ZE).

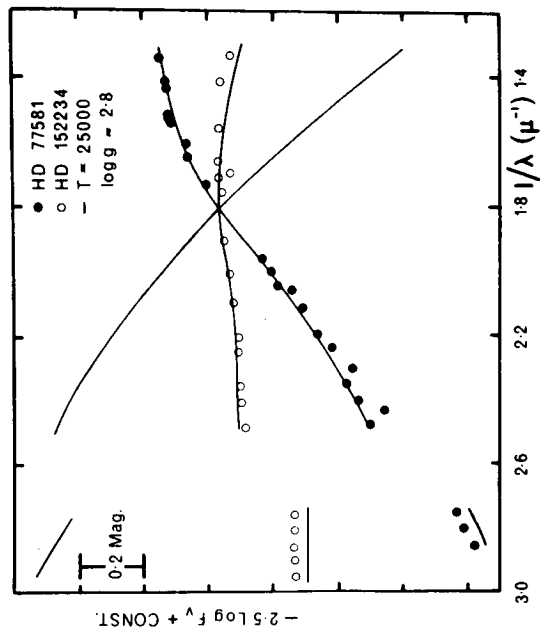


Fig. 7: Scans of HD 77581 and HD 152234. The solid curve is from theoretical model atmospheres. (WD).

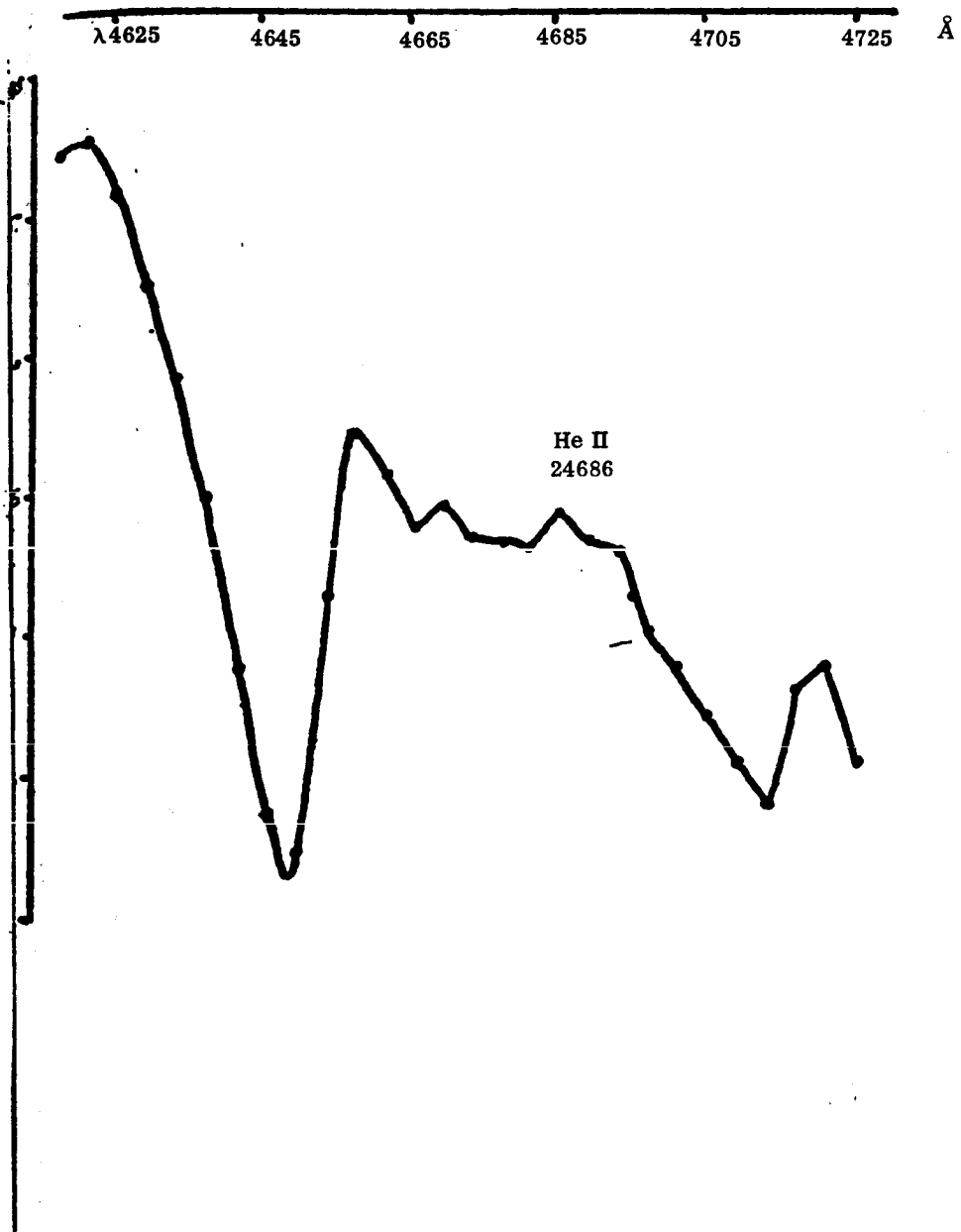


Fig. 9: Spectral scans at about $\lambda 4665$ added together (Jones 1974).

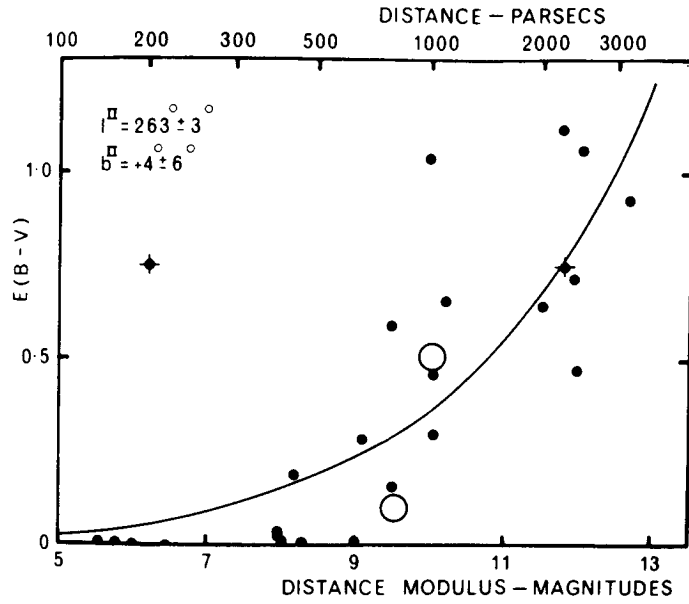


Fig. 10: Reddening as function of true distance modulus in the direction of HD 77581. The plus sign marks the position of HD 77581 (WD).

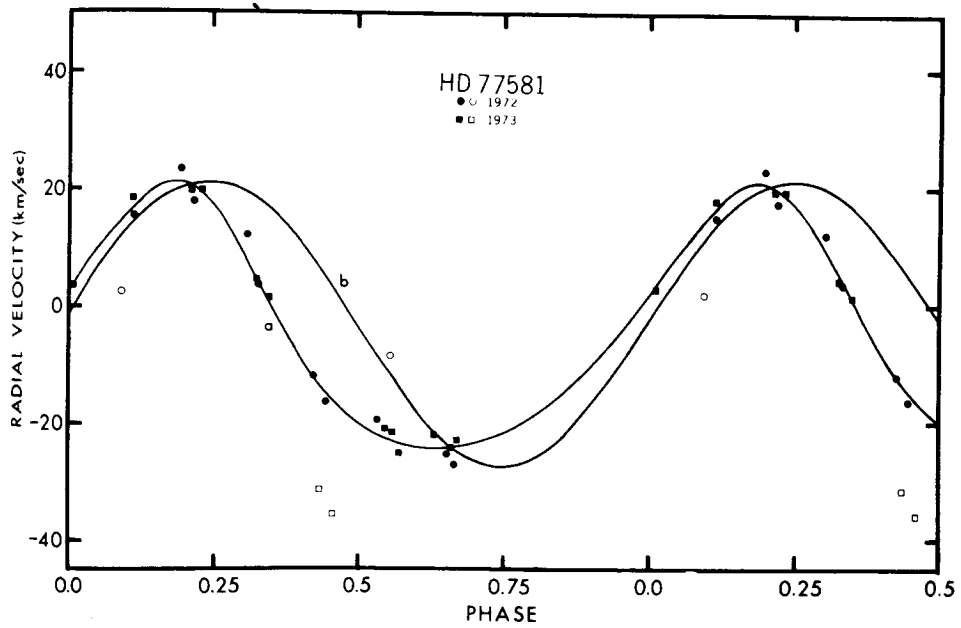


Fig. 11: Petro and Hiltner radial velocities observations (1974).

Orbit of HD 77581 (3 U 0900-40)

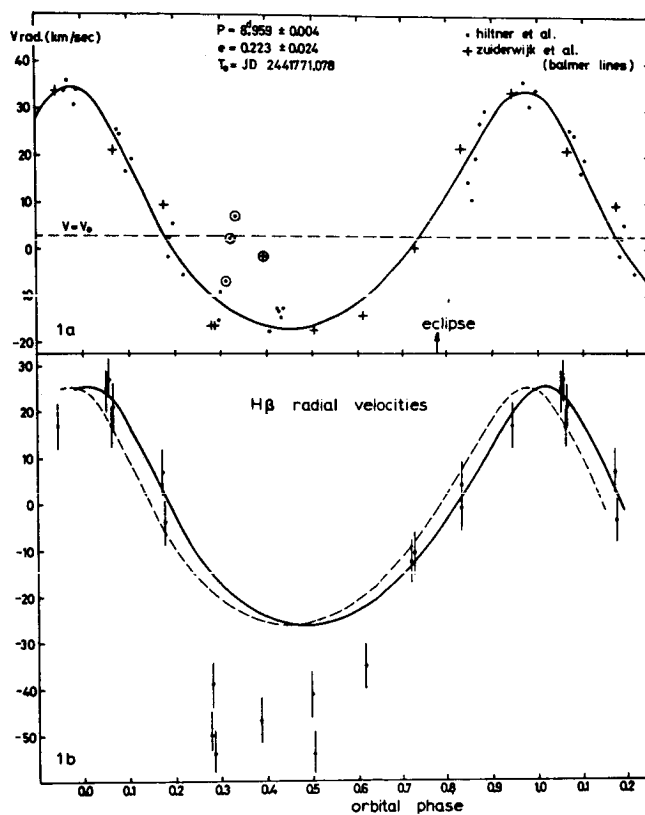


Fig. 12: ZE radial velocity curve for the Balmer lines. $H\beta$ shows systematically lower velocities between the phases 0.3-0.7.

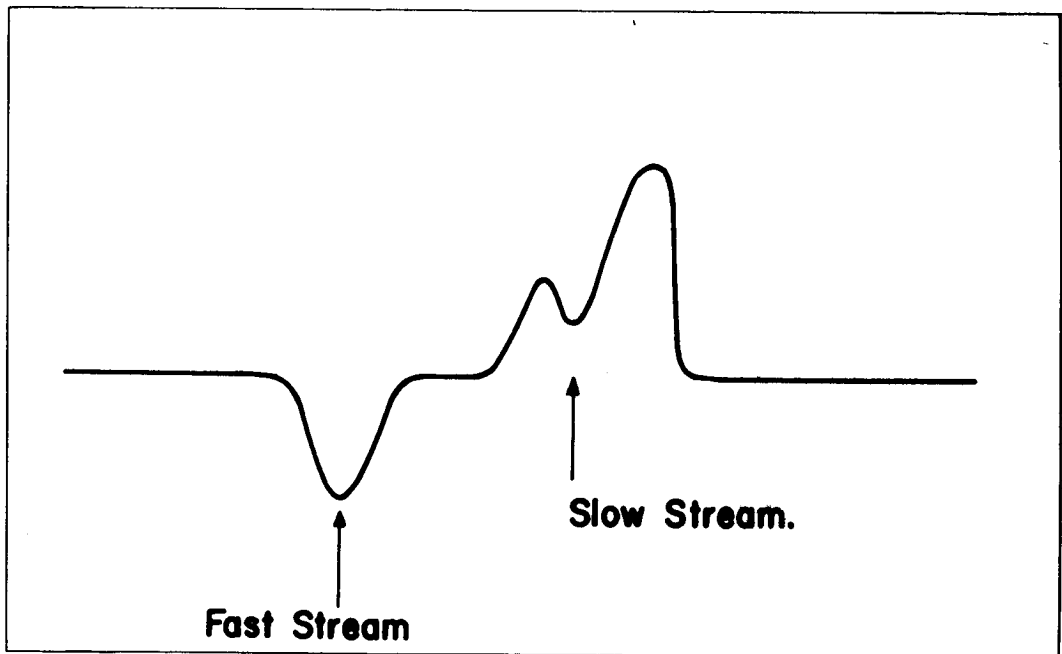


Fig. 13: Schematic profile of the H α line.

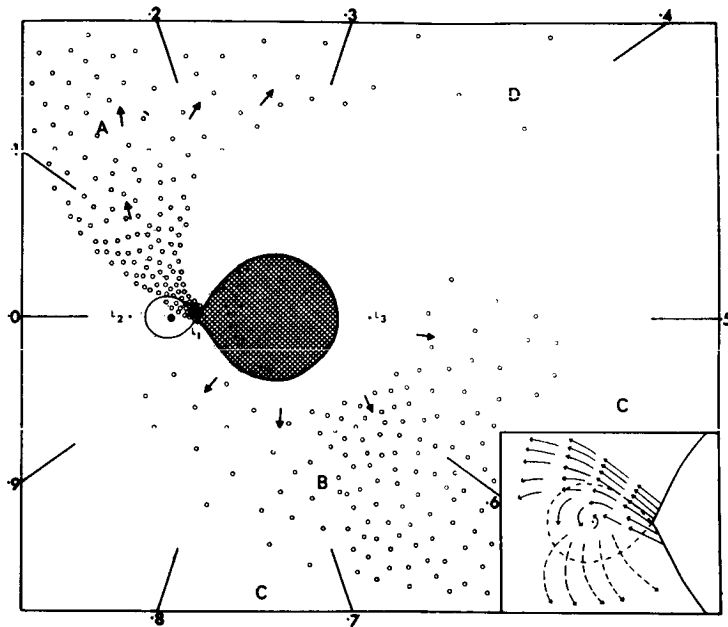


Fig. 14: A flow pattern model around HD 77581 + 3U 0900-40 (Bessell et al. 1975).
 The positions of the marked velocities do not represent actual distances from the system.

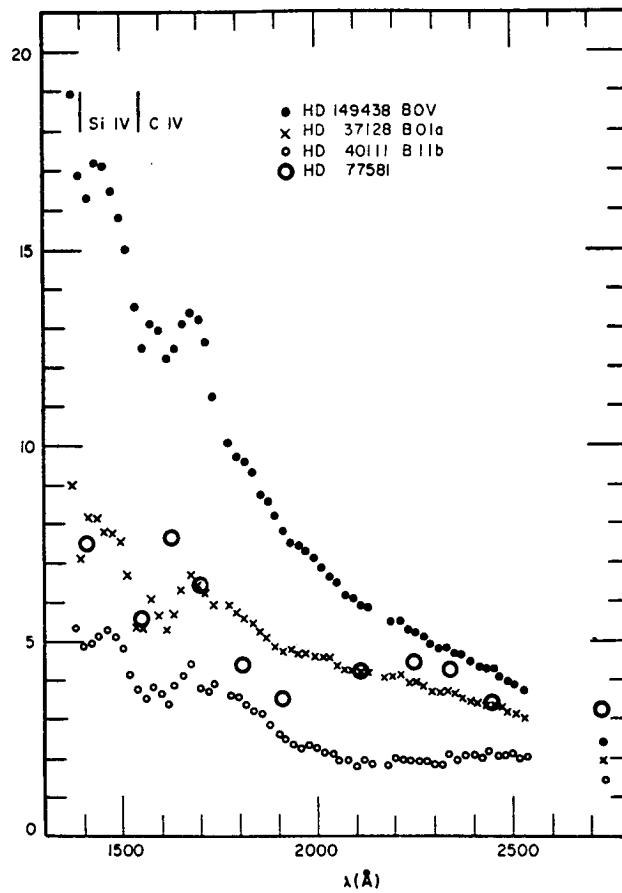


Fig. 15: The UV flux of HD 77581 and other early type stars (Nandy et al. 1975).

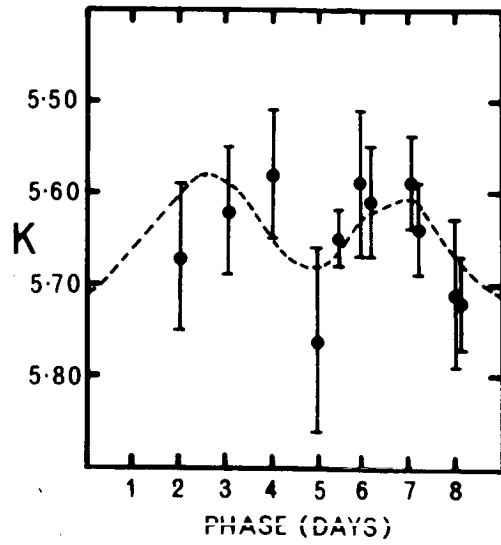


Fig. 16: K magnitude observations folded in 8.95 day period (Hyland and Mould 1973).

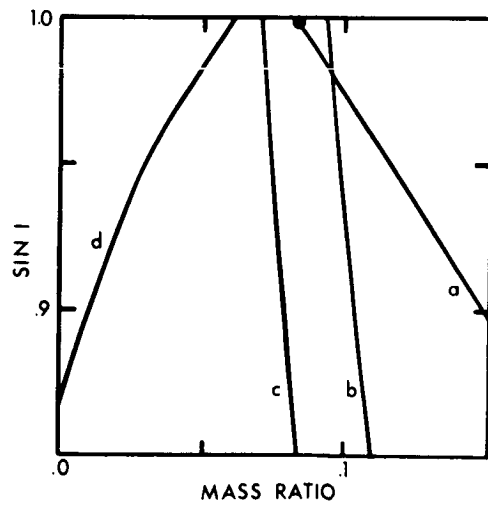


Fig. 17: Possible inclination angles as function of mass ratios (Petro and Hiltner 1974).

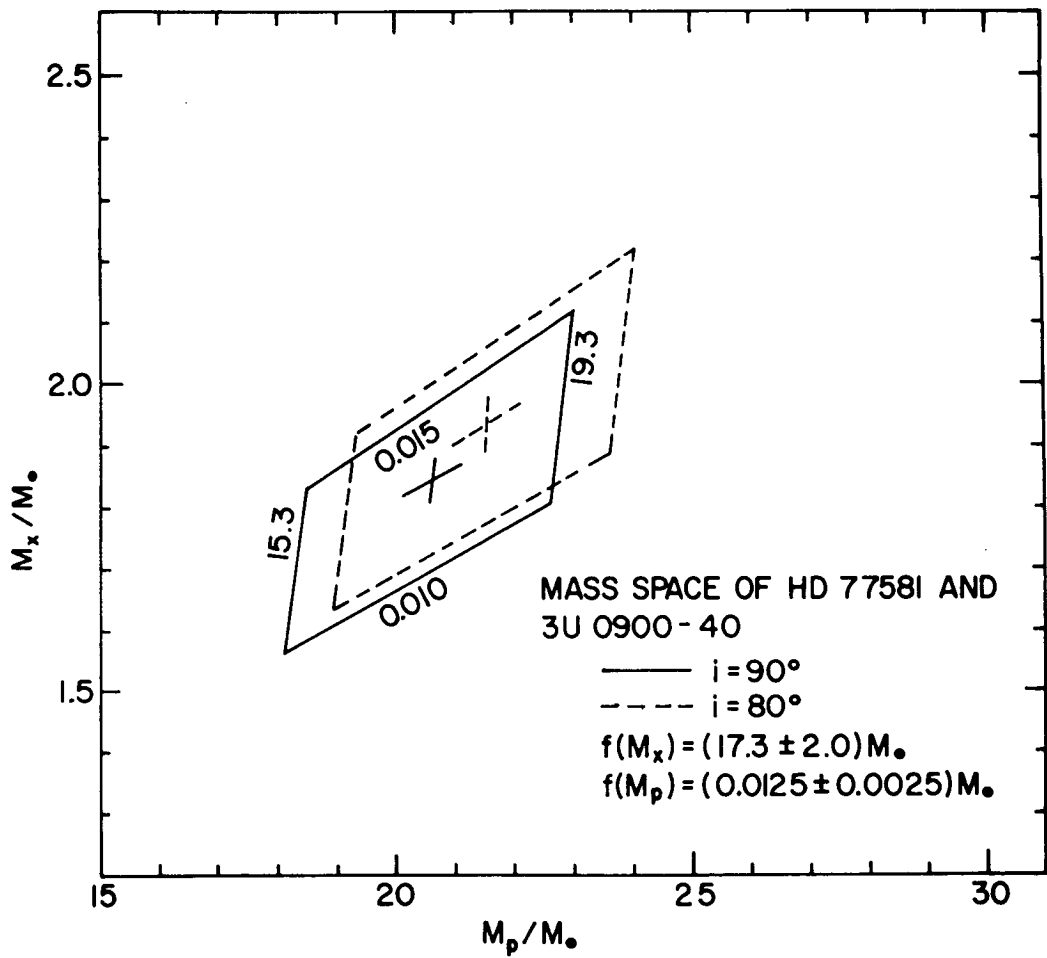


Fig. 18: Mass ranges of HD 77581 (M_p) and 3U 0900-40 (M_x) depending on orbital inclination i .

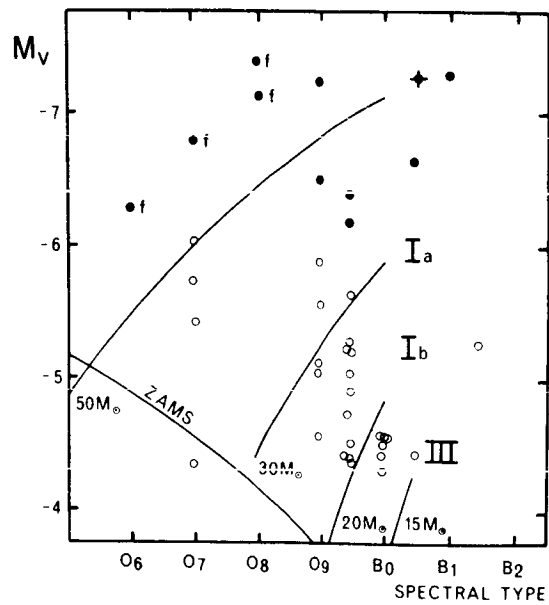


Fig. 19: Absolute visual magnitudes as function of spectral type. The solid curves are positions of single stars as calculated from stellar evolution theory. Circles denote the observed positions.



A symposium on X-ray binaries

HD 77581 + 3U0900-40 session (Wednesday morning)

Chairman Summary (N.V. Vidal)

The emergent picture is that we need better observational parameters to determine the orbital elements and masses of the system. The optical light curve is and will stay probably highly scattered and it will be difficult to improve the lower limit for the inclination angle. However long range observations in both X-rays and optical regions are still needed to detect a possible variation in ω , namely, the opsidal motion. The amplitude of the radial velocity curve is fairly known but its accurate value is much needed. More Coude spectra are highly desirable, but the study of the line profiles as well as the grouping of elements should be made with great caution to determine a reliable radial velocity curve. H α studies and X-ray variations in both soft and hard regions may help understand the streams and wake models of the system. Polarisation observations are highly needed to confirm the classical magnetic neutron star model, if any, for the collapsed secondary. More accurate rotational velocities of the primary are needed to check the corotational hypothesis used frequently in theoretical analysis.

It is intriguing that the properties of the secondary do not fit satisfactorily to any of the white dwarf, neutron star or black hole models: The relatively long pulsation period fits more a white dwarf

but the mass is unlikely to be so; the mass may fit a neutron star but then the origin of the long pulsation period will have to be explained. Finally the mass is high enough to suggest a black hole but the current accepted models of the accretion disk do not allow a stable pulsation phenomenon. Any of these models, if accepted, will have to explain the corresponding apparent puzzles.

STATUS OF THE STUDY OF ELLIPSOIDAL
LIGHT VARIATIONS IN 3U0900-40 AND OTHER
X-RAY BINARIES

Yoram Avni^{*,+}

Center for Astrophysics, Cambridge, Massachusetts, and
Institute for Advanced Study, Princeton, New Jersey 08540^{**}

and

John N. Bahcall

Institute for Advanced Study, Princeton, New Jersey 08540^{**}

ABSTRACT

Implications of recent observations of 3U0900-40 and other X-ray binaries on the standard picture of ellipsoidal light variations are discussed. Our estimates of system parameters and component masses are reviewed. The mass for the X-ray source in 3U0900-40 is found to be in the range $1.3M_{\odot} < M_X < 2.2M_{\odot}$. The importance of determining the X-ray eclipse duration in binary systems is explained. A list of important observations for testing and utilizing the standard picture is presented.

I. INTRODUCTION

The study of the ellipsoidal optical light curves of X-ray binaries is an important tool for estimating the masses of the components in these systems. The recent discovery of a 283 s periodicity in the X-ray intensity of 3U0900-40 (Rappaport and McClintok 1975a) provided the first real observational test of the theoretical framework for those estimates (for a description of the "standard picture" see Avni and Bahcall 1975a). We predicted, using the standard picture, that the radial velocity of the X-ray pulsar must be in the range of 200 to 300 km s⁻¹ (Avni and Bahcall 1975b). The measurement of $V_X \sin i$ by the MIT X-ray astronomy group (Rappaport and McClintok 1975b, McClintok 1975) has confirmed this

⁺Talk presented at the Symposium on X-Ray Binaries, Goddard Space Flight Center, October, 1975

* Permanent address: Weizmann Institute, Rehovot, Israel

** Research supported in part by NSF Grant No. 40768X

prediction, proving the consistency of the theoretical model with observations for that system. The above determination of the pulsar's radial velocity can be combined with a recent determination of the optical radial velocity (van Paradijs et.al. 1975) and with our analysis to yield the present estimate for the mass of the pulsar, $1.3 \leq M_x \leq 2.2 M_\odot (2\sigma)$.

In this talk we first describe our analysis of the 3U0900-40 system (§II); we then discuss in some detail the Cen X-3 system, which could provide another important observational test of the model (§III); and we review the status of the theoretical framework with regard to the other identified X-ray binary systems (§IV through VII). In the spirit of this conference, we stress the observational aspects of the subject and suggest some observations that are of great importance in determining the masses of the components. We summarize our conclusions in §VIII.

As a prelude to our discussion of specific systems we first make some general comments. Mass determinations that make use of the ellipsoidal light curves are model dependent. They are based on the interpretation that the periodic component of the light variations is due to the tidal deformation of the primary in the gravitational field of the secondary. (Some non-trivial intermediate interpretation of the optical observations may be required to extract the light amplitude associated with the tidal deformation in the presence of mass motion in the binary system that may create additional sources of light and of obscuration.) The calculation of this effect is performed by assuming that the star is in a hydrostatic and radiative equilibrium with respect to the combined gravitational and centrifugal potential (for a detailed discussion of the standard picture see Avni and Bahcall 1975a, Avni 1975b). Hence the importance of testing the theoretical framework in a number of systems and for a variety of observational aspects. In this talk we also report (see Avni and Bahcall 1975b) on a calculation of the color variations for the Cyg X-1 system that agrees with the recent observations of Lester et.al. (1975). We also describe a study of the 3U1700-37 system, from which we conclude that the standard picture may be applied also to this binary in view of the recent redetermination of the eclipse duration with the Copernicus satellite (Mason et.al., 1975, Mason 1975).

The X-ray eclipse duration (measured by the eclipse half angle θ_e) is an important parameter that enters the light curve analyses. The sensitivity of the derived masses to the value of θ_e , and the importance of correctly identifying the value of the photospheric eclipse duration, became evident as a result of our early work on the Cen X-3 system (Avni and Bahcall 1974). Apparently longer eclipses can result from absorption e.g. in a stellar wind. Due to changes in the density of the wind, the observed value of θ_e may be variable. A more detailed discussion of this point will be found in our summary of the Cen X-3 system (§III). It would be valuable if X-ray observers could compile histograms of eclipse durations (and their energy dependences) for the X-ray binaries. This would help enormously in identifying the photospheric eclipse more reliably.

The extraction of the amplitude of the ellipsoidal variations from the observed light curve presents serious difficulties as well. The scatter in the data

is larger than the observational error, and is typically a significant fraction of the full amplitude. This shows that in addition to the underlying ellipsoidal variations there exist additional sources of light and/or of obscuration in the binary system. These perturbations may be in part phase dependent. Therefore, the amplitude cannot be determined to an accuracy that is much better than the observational scatter at any given phase (without using further assumptions on the nature of the extrastatistical scatter).

In view of the above problems it is quite clear that point estimates ("best values") for the masses of the components cannot be made at present. Rather, we calculate and present acceptable ranges for these masses: values that are consistent with the observational data within their limits of uncertainties and that are subject to consistency checks as new observational ingredients become available.

II. AN OBSERVATIONAL TEST: 3U0900-40

We analyzed the 3U0900-40 system (Avni and Bahcall 1975b) making use of the following observational constraints:

(1) The X-ray eclipse duration is $\theta_e = 34^\circ$ to 40° . The Uhuru measurement was $\theta_e = 38^\circ \pm 2^\circ (2\sigma)$ (Forman et.al. 1975) and we have allowed for a value smaller by yet another 2σ to be prepared for a possible systematic uncertainty in θ_e due to absorption in a stellar wind, in analogy with a recent development in the Cen X-3 system (see §III below). Two new observations of θ_e were reported in this conference: $\theta_e = 39.8^\circ \pm 0.4^\circ$ (Charles 1975) on the long side, and $\theta_e = 36^\circ \pm 4^\circ$ (Pounds 1975) on the short side, the latter having a somewhat large uncertainty, but possibly indicating in fact a somewhat shorter eclipse.

(2) The amplitude of the ellipsoidal variations in the V band between maximum at quadratures and the minimum at phase zero is $\Delta A_m = 0.08 \pm 0.02$ (Jones and Liller 1973, Vidal et.al. 1973, Petro and Hiltner 1974). The scatter in the data is relatively large, and there is a wide dispersion in the values for the amplitude given by different observers; the range given above is consistent with all available observations.

(3) The spectral type is approximately B 0.5 Ib (Morgan et.al. 1955). This gives an effective temperature of $T = 22,500^\circ\text{K}$ and a limb darkening coefficient of $u = 0.30$ (Gingerich 1969). In order to estimate uncertainties in the derived parameters we also have calculated light curves for the extreme values of $T = 20,000^\circ\text{K}$ and $T = 30,000^\circ\text{K}$ and with the extreme slopes of the limb darkening functions of $u_e = 0.20$ and $u = 0.60$.

(4) The optical radial velocity is in the range of 18 to 39 km s^{-1} (Hutchings 1974, Petro and Hiltner 1974, Zuiderwijk, et.al. 1974, Wallerstein 1974). Some of the radial velocity curves show large irregular variations and different velocities for different lines. In some cases they are asymmetric and formally yield large values for the eccentricity. We have assumed that the orbit is approximately circular and that the asymmetry and variability are

mostly caused by instabilities in the observed stellar wind or by other mass motions in the system. The recent observations by SAS-3 give, in fact, a rather small eccentricity (McClintok 1975). The optical radial velocity was very recently redetermined (van Paradijs *et al.* 1975) by excluding the hydrogen lines that cause most of the variability, yielding $V_{\text{opt}} \sin i = 19.8 \pm 2.4 \text{ km s}^{-1} (2\sigma)$, and considerably reducing the scatter in the data. The new value is within the range that we have considered.

(5) The mass of the optical primary is $10 \leq M_1 \leq 30 M_{\odot}$. The lower mass limit is required by stellar models in order to produce the luminosity of a B0 supergiant (Giannone *et al.* 1968; Kippenhahn 1969). The upper mass limit was suggested from evolutionary models (Mikkelsen and Wallerstein 1974).

We searched the parameter space for orbital elements and masses that are consistent with all the above listed constraints. We found that there are no solutions unless the X-ray pulsar's radial velocity amplitude is in the range of 200 to 300 km s^{-1} , a strong prediction of the standard picture. This result did not depend on the actual value of $V_{\text{opt}} \sin i$: for any given value of $V_{\text{opt}} \sin i$, within the assumed range, the same restriction on $V_x \sin i$ followed independently. The MIT measurement of $V_x \sin i$ (Rappaport and McClintok 1975b, McClintok 1975) confirmed our prediction, proving consistency of the standard picture with observations for the 3U0900-40 system. The new determination of $V_{\text{opt}} \sin i$ neither strengthens nor weakens this observational test, as the theoretical limits on $V_x \sin i$ were independent of the value of $V_{\text{opt}} \sin i$ within the range considered.

Figure 1 summarizes the constraints imposed by ΔA and by θ_e , presenting them as functions of the inclination angle i and of the mass ratio $Q = M_x/M_1$. We have mapped the Q - i plane with lines of equal θ_e and with lines of equal ΔA , calculated with Roche geometry and with the star filling its Roche lobe. Allowing the star to be smaller than the Roche lobe does not add any new solutions.

Combining the recent values of $V_x \sin i = 274 \pm 9 \text{ km s}^{-1}$ and $V_{\text{opt}} \sin i = 19.8 \pm 2.4 \text{ km s}^{-1}$ we find from Figure 1 that $i > 70^\circ$. Therefore we obtain $1.3 \leq M_x \leq 2.2 M_{\odot} (2\sigma)$. The lower limit is thus very close to the upper mass limit for white dwarfs.

Vidal (these proceedings) has made special assumptions which involve "cleaning" the optical light curve data and thus obtained an amplitude of $0.110 \pm 0.015 \text{ mag}$ in the V band. He tries to use Wickramasinghe and Whelan's (1974) analysis of the light curve to obtain a mass ratio and a range of inclination angles. However, none of the solutions listed by Wickramasinghe and Whelan are consistent with Vidal's amplitude, and the minimum value of M_x obtained by them is $2.3 M_{\odot}$, larger than the maximum mass Vidal prefers. Vidal's remarks show that it is easy to make serious misinterpretations of the analysis of the ellipsoidal light variations if one is not sufficiently careful.

III. CEN X-3: THE NEXT TEST?

The Cen X-3 system may provide another important test for the theoretical framework, since the radial velocity of the X-ray pulsar is well known (Schreier *et al.* 1972), and the optical radial velocity we predict (~ 25 km/sec) is within reach (Osmer *et al.*, 1975). Most of our results for this system are already published (Avni and Bahcall 1974, 1975a; Avni 1975 a,b), and we refer the reader to these papers for numerical details and for the relevant references. In view of the special importance of this system for testing the standard picture, and also because the participants of this meeting may have been confused by some remarks regarding M_x made during the Cen X-3 session, we review the present overall status of the ellipsoidal variations.

The large sensitivity of the allowed range of M_x to the numerical value of θ_e , and the importance to the results of the identification of the photospheric eclipse duration, were evident from our early work on Cen X-3 (Avni and Bahcall 1974), and have been frequently pointed out by us ever since.

Figure 2 demonstrates the numerical sensitivity to θ_e . We have mapped the mass-ratio-inclination-angle plane with lines of equal θ_e and with lines of equal light amplitude, ΔA , calculated with Roche geometry and assuming that the star fills the critical Roche lobe (allowing the radius of the star to be smaller does not add any new solutions). One can clearly see that at $i = 90^\circ$, a change of θ_e by 1° induces a change of M_x by $\sim 0.3 M_\odot$.

The uncertainty in the identification of the photospheric eclipse duration stems from the observational facts that the eclipse duration is variable, and that there are variable, energy-dependent, transition regions. Therefore, some part of the eclipse is caused by absorption above the photosphere, e.g. in a stellar wind. [It also has been suggested (Giacconi 1975) that variations of the intensity of the wind are responsible for the extended low states in the X-ray intensity.] The best observational estimate for the photospheric eclipse duration is therefore the shortest eclipse ever observed. This is now 40° according to Uhuru observations (Schreier 1974) or $39^\circ \pm 2^\circ$ according to recent Copernicus results (Pounds *et al.* 1975). If X-ray observers provide enough observational material on the systematics of the occurrences of eclipse durations and their energy dependences, model-dependent evaluations of θ_e (photospheric) may be attempted.

The light amplitude presents yet another problem. Two independent observations, one by Krzeminski (1974) and the other by Petro (1975), yield amplitudes $\Delta A_{0.5} \approx 0.075$ with an uncertainty of about 0.02, and with the minimum at phase 0.5 being deeper than the minimum at phase 0.0, as expected from the standard picture. These two observations are consistent with the theoretical model and yield the range of masses that we discuss below. Mauder (1975) however observed an amplitude of 0.14 (no errors quoted), with the two minima being equal to each other. Such a behavior is inconsistent with the standard picture. Mauder has argued that the equality of the minima indicates the absence of X-ray heating on the facing side of the primary. But this cannot be the explanation because two equal and deep minima actually indicate an appreciable heating effect (Avni and Bahcall 1975b, Avni 1975b). It is also in apparent contradiction with the observed small value of ϕ_x/ϕ_{opt} in this system (one estimates the amount of X-ray energy falling on the optical star is only $\sim 10^{-3} L_{opt}$). The data of Mauder, therefore, cannot be used per se in quantitative estimates, with the standard picture, of the masses in Cen X-3.

The observational situation with regard to ΔA clearly calls for further work in order to clarify the above discrepancy. One would like to know whether the source of the trouble is purely observational, or whether real changes are taking place in the system. In the latter case, a systematic study of the variability will help to decide what is the amplitude that should be associated with the tidal deformation.

On the basis of the observations of Krzeminski and of Petro (and their uncertainties), and using the present observational estimates for θ_e , namely $\theta_e = 37^\circ$ to 40° , we deduce from Figure 2 that $M_x = 0.6$ to $1.8 M_\odot$, with Roche geometry. At present there is no need to invoke higher masses. Higher masses will become necessary only if future observations give a shorter eclipse duration and a light amplitude larger than 0.09 .

In our earlier paper (Avni and Bahcall 1974) we studied also the implications of using the "tidal lobe" (i.e., no rotation of the primary) instead of the Roche lobe. The lines of equal θ_e as well as the lines of equal ΔA move upward in the Q-i plane when the Roche geometry is replaced by tidal geometry. Therefore, the range of masses shifts to larger values, and the lower mass limit for $w_{rot} = 0$ is $1.1 M_\odot$.

Similarly, if the rotational angular velocity of the primary in the 3U0900-40 system is decreased by a small amount from that required for corotation, then M_x is underestimated when corotation is assumed. Vidal (these proceedings) claims that M_x in 3U0900-40 is overestimated if corotation is assumed. He failed to take account of the fact that for 3U0900-40 one knows both an approximate optical radial velocity and a more accurate X-ray radial velocity.

We wish to stress at this point that the rotational angular velocity (i.e., Roche vs. tidal geometry) is not directly correlated with the mass-loss mechanism (critical lobe overflow vs. stellar wind). Therefore, stellar wind models can be consistent with corotation and Roche geometry, and do not imply the larger masses that correspond to the tidal geometry.

An observation of crucial importance is the determination of the optical radial velocity. Osmer et al. (1975) have suggested an upper limit of $\sim 50 \text{ km s}^{-1}$ for the velocity amplitude. We believe, however, that due to the small number (6) of data points their limit may be too optimistic. Their observations nevertheless show that a determination of $v_{opt} \sin i$ (or at least of a useful limit) is close to being achieved. We predict $v_{opt} \sin i$ to be between -15 and 40 km/sec using the standard picture, with the present determination of θ_e . A measurement of the optical radial velocity will give directly the mass ratio (or a limit on it). It will yield valuable information on the masses of the components, even without recourse to theoretical estimates, in addition to providing an important test for the standard picture.

IV. CYG X-1

The principal result of our initial study of the Cyg X-1 system (Avni and Bahcall 1975a) is that the range of possible masses for the secondary is 8 to $\sim 15 M_\odot$, significantly wider than what had been claimed before. The main reasons for this difference is a fuller and realistic allowance for observational uncertainties and a more complete survey of parameter space.

We have recently tested our solutions by calculating color variations. We find ellipsoidal color-curves in B-V and in U-B with an amplitude of ~ 0.002 , with the star being redder at the light minima (Avni and Bahcall 1975b). This is consistent with new data of Lester *et.al.* (1975) who find a similar amplitude with the same sense.

A further consequence of our early work is that the optical light curve cannot help to distinguish between the binary model for the system and the triple-star model. In the optical continuum, a normal secondary that contributes 2% to 25% of the blue light cannot be distinguished from a black hole because the two reflection effects (on the optical primary and secondary) are roughly equivalent to a small change in ΔA , without a noticeable change in the ratio of the two minima. We also showed that the effect of most such normal secondaries on the spectral lines is too small to be visible on a single spectrum because of photon noise. We suggested, therefore, that one could test for the presence of such secondaries by combining line profiles from a number of observations taken all at the same orbital phase, and search for systematic variations as a function of the orbital phase. A preliminary study along these lines was recently taken up by Bolton (1975) who claims to rule out some, but not all, of the possible normal companions. It is important to conduct a systematic study of this sort, in order to derive realistic constraints on the triple star model.

Observationally, it is also desirable to clarify the situation with regard to the conflicting light amplitudes found by Walker (1975, and references quoted therein): 0.04 , and by Lester *et.al.* (1975, and references quoted therein): 0.06 . If these results indicate real changes in the system, one would like to know the systematics of these changes.

V. 3U1700-37

The original Uhuru determination of the eclipse duration (Jones *et.al.* 1973b) yielded a value of $\theta = 58^\circ \pm 4^\circ$. This requires very small mass ratios that are inconsistent with the observed amplitude of the optical light curve $\Delta A_o(v) = 0.05 \pm 0.01$, and in any case requires that $M_x/M_o \geq 100 M_\odot$ when combined with the observed optical mass function (for details see Bahcall 1975, Avni 1975b). In view of the possibility that the intense stellar wind observed in this system is responsible for a significant part of the eclipse duration, we have recently analyzed the light variations (Avni and Bahcall 1975b) in order to put limits on the length of the photospheric eclipse that are implied by the standard picture. We found that M_x/M_o must be ≥ 0.025 and that θ must be $\leq 46^\circ$. Recent Copernicus observations (Mason *et.al.* 1975, Mason 1975) yielded a short eclipse with $\theta = 47^\circ \pm 3^\circ$. Therefore the theoretical model is consistent also with observations for this system. In fact, one may regard the shorter Copernicus eclipse duration as a verification of a prediction from the standard picture.

VI. SMC X-1

The special interest in this system stems from the fact that the large X-ray flux that heats the facing side of the primary modifies significantly the ellipsoidal light variations and reverses the ratio between the two light minima (Avni and Bahcall 1975b). We have shown that the consideration of this effect is important in deriving the masses of the components, and that the resulting mass ratios are $Q = 0.10$ to 0.17 .

From our analysis it followed that the X-ray luminosity L_x must be approximately equal to the optical luminosity L_{opt} . A recent redetermination of both L_x and L_{opt} using the most up-to-date information on the X-ray spectrum and on the radius of the optical primary (Avni 1975b) has confirmed this prediction.

We have also shown (Avni 1975b) that if the primary is assumed to approximately fill the critical Roche lobe, the masses of the components are determined from the radius of the primary and from the optical radial velocity amplitude. With $R_1 = 18.6 R_\odot$ and $V_{opt} \sin i = 30$ to 50 km s^{-1} we obtain $M_x = 2$ to $4 M_\odot$. When better estimates for R_1 and $V_{opt} \sin i$ become available, refined estimates can be made for M_x by scaling M_x like R_1^3 and by scaling $V_{opt} \sin i$ like R_1 .

Observationally, an improved determination of $V_{opt} \sin i$ is clearly needed. Also, SMC X-1 is known to have extended low states (as observed from Earth). Since X-ray heating has a visible effect on the optical light curve, it would be very interesting to conduct simultaneous X-ray and optical observations in order to test whether the ratio of the two minima changes together with the X-ray flux. We admit that this is not an unambiguous test of the model, because the X-ray emission need not be isotropic (note the 35° behavior of Her X-1), and because even without X-ray heating there seems to be a large variability in the ellipsoidal light curves.

VII. HER X-1

The available data, from historical plates, on the ellipsoidal variations of HZ-Her in its extended low states (Jones *et al.* 1973a; Liller 1975) is not precise enough to yield significant constraints on the masses in this system (Avni and Bahcall 1974, cf. Whelan 1973).

When HZ-Her next goes into an extended low state, accurate data on the ellipsoidal light curve may be collected, in several colors, and the optical radial velocity will be hopefully unambiguously determined. These observations will provide a powerful test of the theoretical model of ellipsoidal variations, and will place strong constraints on the masses of the components.

VIII. CONCLUSIONS

We have reviewed the status of the theoretical framework used to determine the masses of the components in X-ray binaries, with the aid of ellipsoidal light curves. We have described the numerical sensitivity of the derived masses to the value of the X-ray eclipse duration and the uncertainty in the

identification of the photospheric eclipse. An intensive observational study of the systematics of eclipse durations and their energy dependences is required in order to eliminate this uncertainty, to make the mass estimates more precise, and the observational tests more powerful. We have also described the scatter in the values found for the light amplitudes and the implications that this uncertainty has for the masses.

The present situation is summarized in Table 1 for the six binary systems for which an analysis can be attempted. For all of the six systems we have found sets of parameters that are consistent with the standard picture and with all observational constraints available at present. In particular, the MIT measurement of $V_x \sin i$ in the 3U0900-40 system confirmed a prediction that had been made on the basis of the standard picture. Also, a recent re-determination of the eclipse duration in the 3U1700-37 system is consistent with limits on θ_e that have been derived from the model. The color variations calculated for the Cyg X-1 system are also consistent with recent observations.

Observational tests for the standard picture are of great importance since the mass determinations are model dependent. A potentially strong test would be a measurement of $V_{opt} \sin i$ in the Cen X-3 system, within the reach of present observational techniques.

Additional observations of interest would be simultaneous optical X-ray observations of SMC X-1 in order to test the effects of X-ray heating on the optical light curve, and measurements of the ellipsoidal light curve and optical radial velocity of HZ-Her when it next goes into an extended off state.

REFERENCES

- Avni, Y., 1975a, Proceedings of the Seventh Texas Symposium on Relativistic Astrophysics (New York: The New York Academy of Sciences).
- Avni, Y., 1975b, Proceedings of the Enrico Fermi Summer School on Physics and Astrophysics of Neutron Stars and Black Holes, Varenna, Italy, in press.
- Avni, Y., and Bahcall, J.N., 1974, Ap.J. (Letters) 192, L139.
- Avni, Y., and Bahcall, J.N., 1975a, Ap.J. 197, 675.
- Avni, Y., and Bahcall, J.N., 1975b, Ap. J. (Letters) 202, L___
- Bahcall, J.N., 1975, Proceedings of the Enrico Fermi Summer School on Physics and Astrophysics of Neutron Stars and Black Holes, Varenna, Italy, in press.
- Bolton, T., 1975, these proceedings.
- Charles, P.A., 1975, these proceedings.
- Forman, W., Jones, C., Tannanbaum, H., Gursky, H., Kellogg, E., and Giacconi, R., 1973, Ap. J. (Letters) 182, L103.
- Giacconi, R., 1975, Proceedings of the Seventh Texas Symposium on Relativistic Astrophysics, (New York: The New York Academy of Sciences).
- Giannone, P., Kohl, K., and Weigart, A., 1968, Z.Ap. 68, 107.
- Gingerich, O., 1969, ed., Theory and Observation of Normal Stellar Atmospheres (Cambridge: MIT Press).
- Hutchings, J.B., 1974, Ap.J. 192, 685.
- Jones, C.A., Forman, W., and Liller, W., 1973a, Ap.J.(Letters) 182, L109.
- Jones, C., Forman, W., Tananbaum, H., Schreier, E., Gursky, H., Kellogg, E. and Giacconi, R., 1973b, Ap.J. (Letters) 181, L43.
- Jones, C., and Liller, W., 1973, Ap.J. (Letters) 184, 121.
- Kippenhahn, R., 1969, Astron. and Ap. 3, 83.
- Krzeminski, W., 1974, Ap.J. (Letters) 192, L135.
- Lester, D.F., Nolt, I.G., Stearns, S.A., Straton, P. and Radostitz, J.V., 1975, Ap. J., in press.

- Liller, W., 1975, these proceedings.
- Mason, K.O., 1975, these proceedings.
- Mason, K.O., Branduardi, G., and Sanford, P., 1975, preprint.
- Mauder, H., 1975, Ap. J.(Letters) 195, L27.
- McClintok, J., 1975, these proceedings.
- Mikkelsen, D.R., and Wallerstein, G., 1974, Ap. J. 194, 459.
- Morgan, W.W., Code, A.D. and Whitford, A.E., 1955, Ap.J. Suppl. 2, 41.
- Osmer, P.S., Hiltner, W.A. and Whelan, J.A.J., 1975 Ap.J. 195, 705.
- van Paradijs, J.A., Hammerschlag-Hensberg, G., van den Heuvel, E.P.J., Takens, R.J., Zuiderwijk, E.J. and DeLoore, C., 1975, preprint, and these proceedings.
- Petro, L.D., 1975, Ap.J. 195, 709.
- Petro, L.D., and Hiltner, W.A., 1974 Ap.J. 190, 661.
- Pounds, K.A., 1975, these proceedings
- Pounds, K.A., Cooke, B.A., Ricketts, M.J., Turner, M.J. and Elvis, M., 1975, M.N.R.A.S., in press.
- Rappaport, S. and McClintok, J., 1975a, IAU Circ. No. 2794.
- Rappaport, S. and McClintok, J., 1975b, IAU Circ. No. 2833.
- Schreier, E., 1974, private communication.
- Schreier, E., Levinson, R., Gursky, H., Kellogg, E., Tananbaum, H., and Giacconi, R., 1972, Ap.J. (Letters) 172, L79 [Erratum, *ibid*, 173, L151].
- Vidal, N.V., Wickramasinghe, D.T., and Peterson, B.A., 1973, Ap.J. 182, L77.
- Walker, N., 1975, these proceedings.
- Wallerstein, G., 1974, Ap.J. 194, 451.
- Whelan, J., 1973, Ap.J. (Letters) 185, L127.
- Wickramasinghe, D.T., and Whelan, J.A.J., 1974, M.N.R.A.S., 167, 21P.
- Zuiderwijk, E.J., van den Heuvel, E.P.J., and Hensberg, G., 1974, Astron. and Ap. 35, 353.

Table 1. ANALYSES OF ELLIPSOIDAL LIGHT VARIATIONS

<u>Source</u>	<u>Ingredients</u>	<u>$M_x (M_\odot)$</u>	<u>$M_{opt} (M_\odot)$</u>	<u>Remarks</u>
3U0900-40	$\theta = 34^\circ$ to 40° $\Delta A = 0.08 \pm 0.02^m$ $K_x = 274 \pm 9 \text{ km s}^{-1}$ $K_{op} = 19.8 \pm 2.4 \text{ km s}^{-1}$	1.3 to 2.2	20 to 28	Recently measured K_x falls inside range predicted by model.
3U1700-37	$\theta = 47^\circ \pm 3^\circ$ $\Delta A = 0.05^m \pm 0.01^m$ $K_{op} = 18 \pm 5 \text{ km s}^{-1}$	uncertain	uncertain	A recent remeasurement of θ_e allows consistency with model.
Cyg X-1	No eclipse $\Delta A = 0.05^m \pm 0.01^m$ $K_{op} = 72 \text{ km s}^{-1}$	8.5 to 15	23 to 45	Calculated B-V and U-B are redder by -0.2% at light minima in agreement with recent observations.
Cen X-3	$37^\circ < \theta < 40^\circ$ $\Delta A = 0.075^m \pm 0.025^m$ $K_x = 415 \text{ km s}^{-1}$	0.6 to 1.8	16 to 20	Measurement of K_{op} (predicted to be 15 to 40 km s^{-1} with corotation and presently determined θ_e) would be a test of the model and would determine the masses.
SMC X-1	$\theta = 27.75^\circ$ $\Delta A = 0.11^m$ $K_{op} = 40 \text{ km s}^{-1}$	2.2 to 4.2	26 to 30	X-ray heating important (-0.02^m) An accurate determination of K_{op} needed. Correlated optical X-ray observations interesting.
Her X-1	$\theta = 25.4^\circ$ $\Delta A = 0.18^m \pm 0.12^m$ $K_x = 169 \text{ km s}^{-1}$	-1	-2	Radial velocity, ellipsoidal light variations, can be measured during an extended X-ray OFF period and will yield over-determined system of equations, i.e., all parameters plus a check on theory.

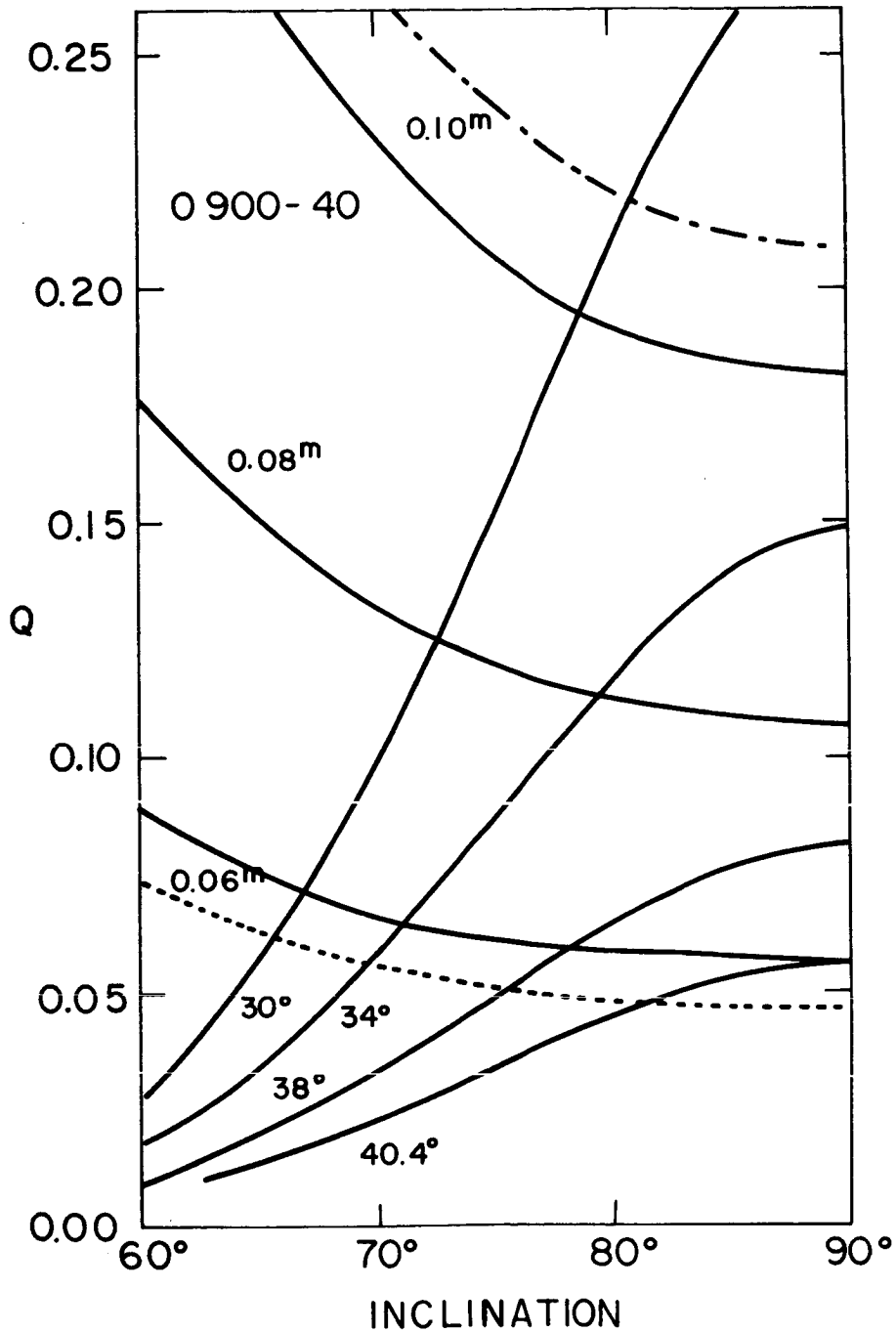


Figure 1. A mapping of the Q - i plane with lines of equal θ_e and with lines of equal $\Delta A_{o,o}$ for 3U0900-40 with Roche geometry and $R_{opt}/R_{crit} = 1$. Here Q is the mass ratio M_x/M_{opt} and R_{opt}/R_{crit} is the ratio of the radius of the optical star to the critical Roche radius. Solid lines: $T_e = 22,500^\circ$ and $u = 0.3$; dotted line: $T_e = 20,000^\circ$ and $u = 0.6$; solid-dotted line: $T_e = 30,000^\circ$ and $u = 0.2$.

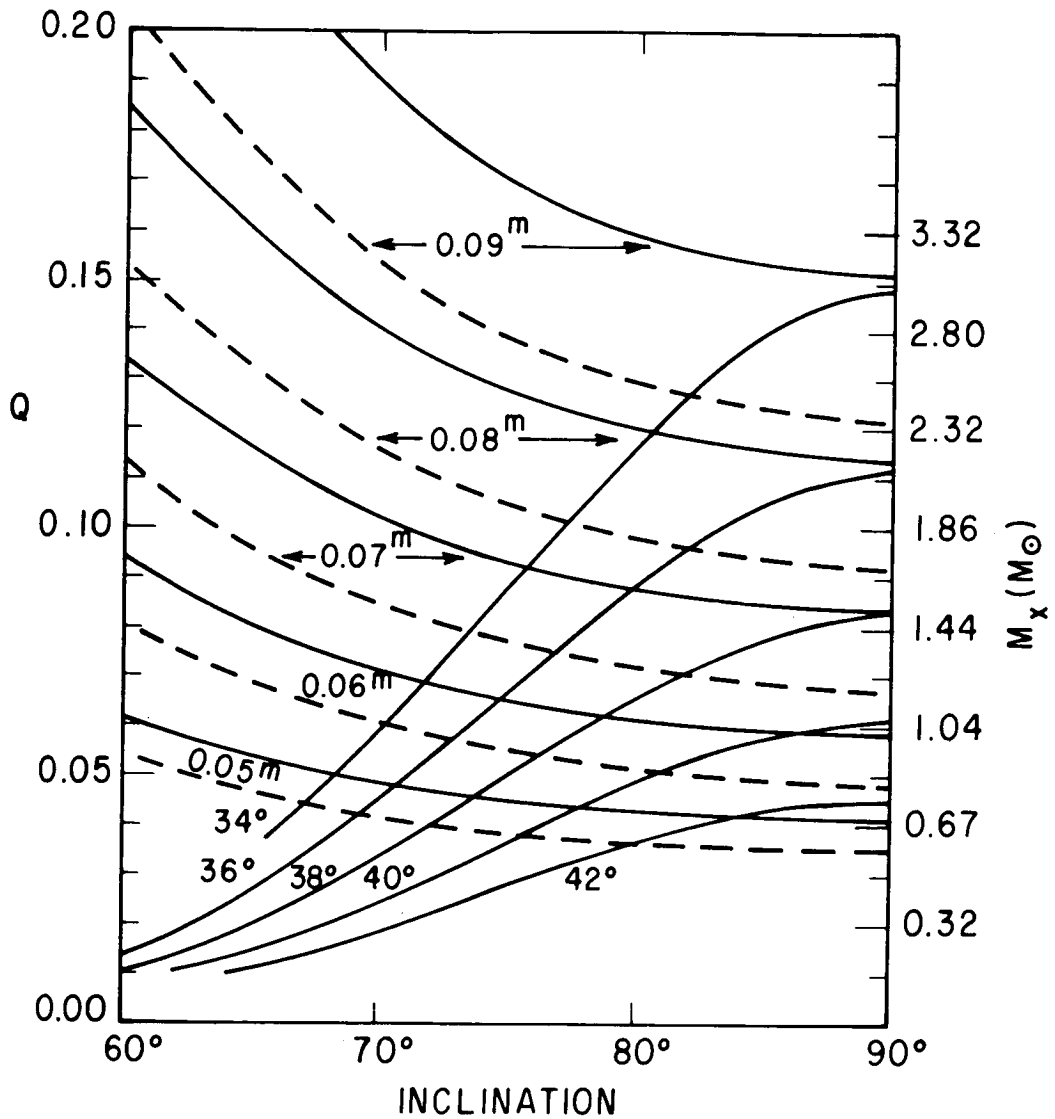


Figure 2. A mapping of the Q - i plane with lines of equal θ_e and with lines of equal $\Delta A_{o,o}$ for the Cen X-3 system, with Roche geometry and $R_{opt}/R_{crit} = 1$. Here Q is the mass ratio M_x/M_{opt} and R_{opt}/R_{crit} is the ratio of the radius of the optical star to the critical Roche radius. Solid line: $T_e = 30,000^\circ$ and $u = 0.3$; broken line: $T_e = 20,000^\circ$ and $u = 0.45$. The masses denoted on the right margin are for $i = 90^\circ$ only.

THE X-RAY VARIABILITY OF VELA X-1 (3U0900-40)

P. A. Charles, K. O. Mason, J. L. Culhane, P. W. Sanford, N. E. White

Mullard Space Science Laboratory

University College London

Holmbury St. Mary

Dorking

Surrey

England

Abstract

From observations of Vela X-1 with the MSSL 2.5-7.5 KeV detector onboard Copernicus, we note that the behaviour of the source can be characterized by three phases: (a) high intensity, (b) low intensity, (c) eclipse. Combining data from the 1972 UHURU observations with our eclipse observation yields a binary period of 8.963 ± 0.001 days with zero phase on 1975 Feb. 6.97 ± 0.04 UT. All our data is modulated by a period of $282^{\text{s}}.896 \pm 0^{\text{s}}.030$ (mean phase = 0.47) with a mean amplitude of 20-30%.

The low intensity phase is interpreted as being due to increased absorption in an accretion wake traveling across the line of sight (the spectral slope remains relatively constant throughout the cycle). Another period of enhanced absorption immediately after exit from eclipse may be due to a bow shock.

Comparison of our two observations suggests that these structures vary from cycle to cycle and, since the orbital period is long, probably during each cycle.

Introduction

The binary nature of the X-ray source 3U0900-40 (Vela X-1) was first noted by Ulmer et al (1972) with the UCSD OSO-7 X-ray telescope and has subsequently been observed by UHURU (Forman et al, 1973), Ariel 5 (Eadie et al, 1975) and OSO-7 (Ulmer, 1975). Another interesting facet of this source has very recently come to light with the discovery by SAS-3 (Rappaport and McClintock, 1975) that the source is pulsing with a period of 282.9 sec. By combining this information with detailed radial velocity observations of the optical counterpart HD77581, Paradijs et al (1975) derive masses of $1.6 \pm 0.2 M_{\odot}$ and $21 \pm 2 M_{\odot}$ for the components of the system.

The overall features of this source have been discussed by the above mentioned authors. It was, then, with a view to obtaining detailed information on the X-ray behavior during individual cycles that we observed Vela X-1 with the Copernicus X-ray instrumentation in February and again in May 1975.

Observational Details

The MSSL X-ray instrumentation has been discussed by Culhane et al (1975 - this conference) but briefly these observations were performed with a detector sensitive in the energy range 2.5-7.5 KeV equipped with a 6 channel pulse height analyzer (PHA) for spectral information. The geometrical area is 18 cm.², field of view is 29.5 x 30.0 (FWHM) and temporal resolution 62.5 secs. (1 frame). A more detailed description of the experiment and satellite can be found in Bowles et al (1974) and Hawkins (1974). The background counting rate is evaluated and removed as discussed by Sanford (1974) and Davison (1974).

Information concerning the observing program on 3U0900-40 is summarized in Table 1. The basic observed counting rates (summed in 5 frame bins) on each occasion are presented in figures 1a and 2a. We also display the variation of the spectral hardness ratio (when the statistics warrant it) as defined by -

$$\text{H.R.} = \frac{\sum_{E=5 \text{ KeV}}^{7.5 \text{ KeV}} I(E)}{\sum_{E=2.5 \text{ KeV}}^{5 \text{ KeV}} I(E)}$$

where the I (E) are the PHA count rates. It is immediately apparent from these diagrams that 3U0900-40 can be characterized by three phases:

- (a) "high intensity", for approximately half the cycle, during which time intensity variations are not mirrored by the hardness ratio plot; in particular, flares, such as that on day 138.6 where the flux doubled on a time scale of a few minutes, show no significant spectral changes. This behaviour is similar to that of

Observational Details (Cont)

flares in 3U1700-37 (see Mason et al, 1975 - this conference) although they occur more frequently in that source, and dissimilar to those seen during active periods in Sco X-1, during which the source intensity is strongly correlated with spectral slope (see Culhane et al, 1975 - this conference, and White et al, 1975).

- (b) "low intensity", again for approximately half the cycle, where the behavior of the hardness ratio implies the presence of significant absorption by cold material (hardness ratio increases for increased absorption);
- (c) "eclipse", lasting for $1^{\text{d}}.98 \pm 0^{\text{d}}.04$.

To investigate these variations in more detail we summed the data in 4^{h} bins so as to improve the statistics and fitted each one with standard power law X-ray spectra by means of the chi-square grid technique. All the data are well fit by $\alpha = 1.0$ (it was impossible to differentiate between power law and thermal spectra) together with a variable absorption term. This is illustrated in Figures 1b and 2b which show the summed data and the absorption column required to fit the data assuming a constant spectral slope. We have also plotted on Figure 1b the level expected (dotted lines) if there had been no (photo electric) absorption. The mean "low intensity" level is still lower than the mean "high intensity" level and indicates that some non energy dependant absorption may be taking place.

Observational Details (Cont)

By assuming that the period has remained constant since the 1972 UHURU observations, our mid-eclipse times yield a period of 8.963 ± 0.001 days with zero phase on 1975 Feb 6.97 \pm 0.04 U.T. This is in excellent agreement with the period as determined optically (Paradijs et al, 1975). The measurements we have made of the 282.9 second period (Table 2) agree well with those given by SAS-3.

Interpretation

The first point that is clear from a comparison of Figures 1 and 2 is that any structure or spectral feature in the light curve is variable from cycle to cycle and probably, owing to the long binary period, within each cycle.

The light curve of the February 1975 cycle shows spectral structure (in terms of the column variations) that we interpret as being due to passage of the X-rays through an accretion wake. The existence of an accretion wake in binary X-ray sources has now been established by a number of workers for the Cen X-3 system (Giacconi, 1974; Tuohy and Cruise, 1975; Pounds et al, 1975) and for the purposes of this discussion we shall use the sketch of the system in Figure 3. The points to note are:

- (1) the increase in absorption at phase 0.55 and the decrease at phase 0.85; this represents the boundaries of the accretion shock;
- (2) the intermediate decrease in absorption at phase 0.7;
- (3) the additional absorption dip around phase 0.15, almost exactly 180° in phase away from the accretion axis.

Interpretation (Cont)

Theoretical studies of the accretion process (Hunt, 1971; Jackson, 1975) show that material will fall in to the X-ray source leaving a line of relatively low density along the accretion axis itself. Also, in certain circumstances material may accumulate on the opposite side of the X-ray source to the accretion axis, giving rise to absorption along this line of sight (Eadie et al, 1975). Inside this wake the electron density may be high enough to provide the non energy dependant scattering visible in the light curve as mentioned earlier. Therefore this model accounts in a general way for most of the observed features of this source.

Using the orbital velocity of approx. 270 km. s^{-1} from the solution of Rappaport and McClintock (1975) we may combine this with the implied angle of 70° between the accretion axis and the line of centers to derive an upper limit to the stellar wind velocity in the vicinity of the X-ray source of about 100 km. s^{-1} .

The May 1975 light curve, although mainly of the high intensity phase, shows that this wake (if, indeed, the above interpretation is correct) is variable over many cycles.

Further studies of this system at both X-ray and optical wavelengths should permit a more detailed definition of both the accretion process and the nature of the stellar wind of the companion star.

Acknowledgements

The model presented here has benefited considerably from discussions with Drs. A. C. Fabian and J. E. Pringle. The encouragement of Prof. R. L. F. Boyd is appreciated, and the support of the Appleton Laboratory staff at the Goddard Space Flight Center in planning the satellite observations is gratefully acknowledged.

PAC, KOM and NEW acknowledge the financial support of the SRC.

References

- Bowles, J. A., Patrick, T. J., Sheather, P. H. and Eiband, A. M., 1974, J. Phys. E. Sci. Instr. 7, 183.
- Culhane, J. L., Mason, K. O., Sanford, P. W. and White, N. E., 1975 - this conference.
- Davison, P. J. N., 1974, Proceedings of the workshop on electron contamination in X-ray astronomy experiments, NASA-GSFC, Technical Information, X661-34-130.
- Forman, W., Jones, C., Tananbaum, H., Gursky, H., Kellogg, E., and Giacconi, R., 1973, Ap. J. 182, L103.
- Hawkins, F. J., 1974 Proc. Roy. Soc. A, 340, 397.
- Hunt, R., 1971, MNRAS, 154, 141
- Jackson, J. C., 1975, MNRAS, 172, 483.
- Mason, K. O., Branduardi, G., and Sanford, P. W., 1975 - this conference.
- Paradijs, J. A. van, Hammerschlag - Hensberge, G., Heuvel, E. P. J. vanden, Takens, R. J., Zuiderwijk, E. J. and Loore, C. de, 1975 (preprint).
- Pounds, K. A., Cooke, B. A., Ricketts, M. J., Turner, M. J. and Elvis, M., 1975; MNRAS 172, 473.
- Rappaport, S. and McClintock, J. 1975, IAU Circ. No. 2794.
- Rappaport, S. and McClintock, J. 1975, IAU Circ. No. 2833.

Sanford, P. W., 1974, Proc. Roy. Soc. A, 340, 411

Tuchy, I. R. and Cruise, A. M., 1975, MNRAS 171, 33P

Ulmer, M. P., 1975, Ap. J. 196, 827

Ulmer, M. P., Baity, W. A., Wheaton, W. A. and Peterson, L. E., 1972,
Ap. J. 178, L121

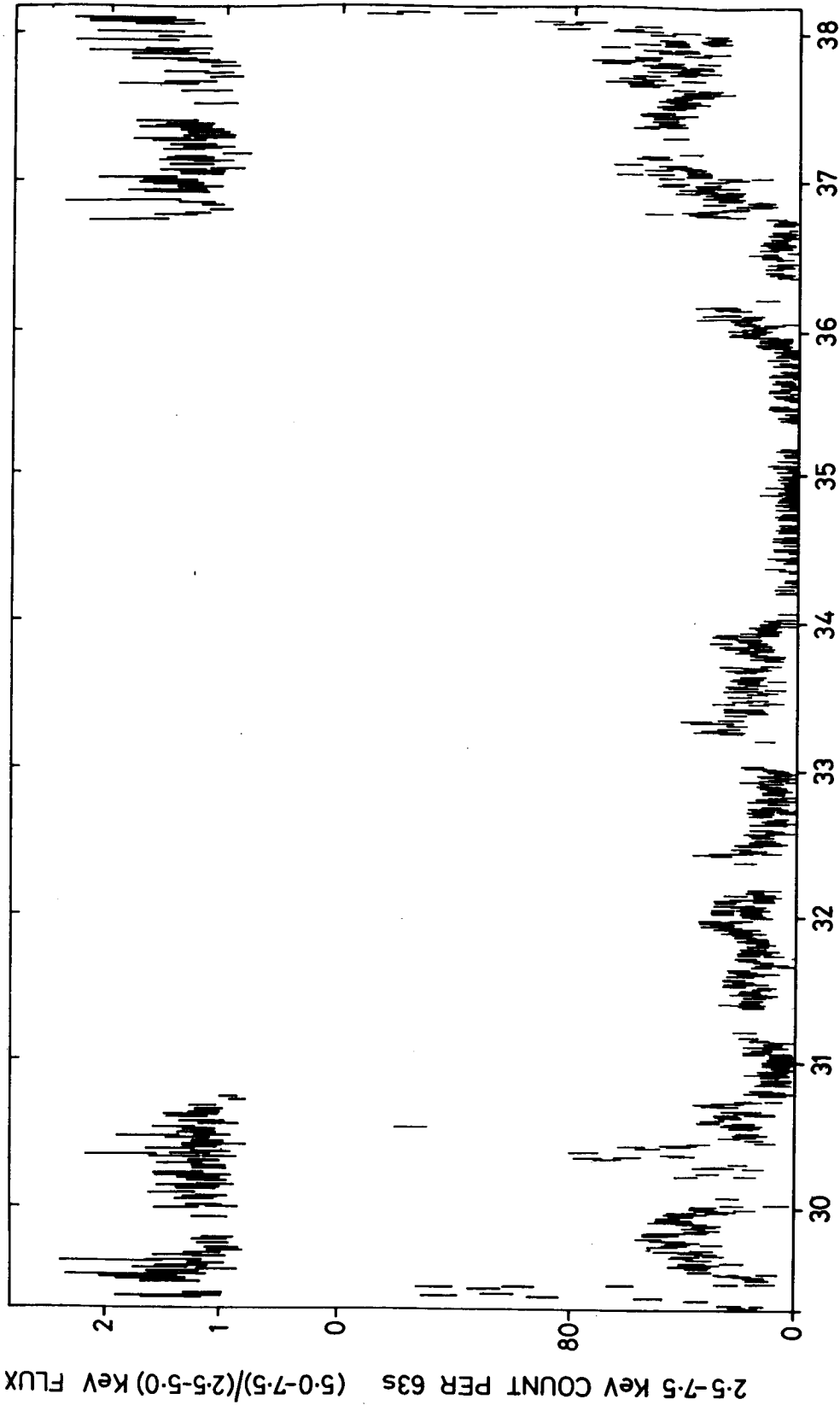
White, N. E., Mason, K. O., Sanford, P. W., Ilovaisky, S. and Chevalier,
C., 1976, MNRAS (in press)

TABLE 1. OBSERVATIONS

	<u>Date Start</u>	<u>Date Stop</u>
1.	1975 Feb 1	1975 Feb 10
2.	1975 May 17	1975 May 22

TABLE 2. SHORT PERIOD ANALYSIS

	<u>Feb. 75</u>	<u>May 75</u>	<u>Mean</u>
P sec.	282.9154	282.87657	282.896
error	0.0396	0.045	0.030
sample s.d.	0.198	0.130	-
mean phase	0.55	0.38	0.47



1975 DAY No.

Figure 1.a. Observed counting rates from Vela X-1 in the 2.5-7.5 KeV energy range in February 1975, each point being the mean of 5 frames. The spectral hardness ratio is also plotted (see text for definition). The length of the error bars represents 2 s.d.

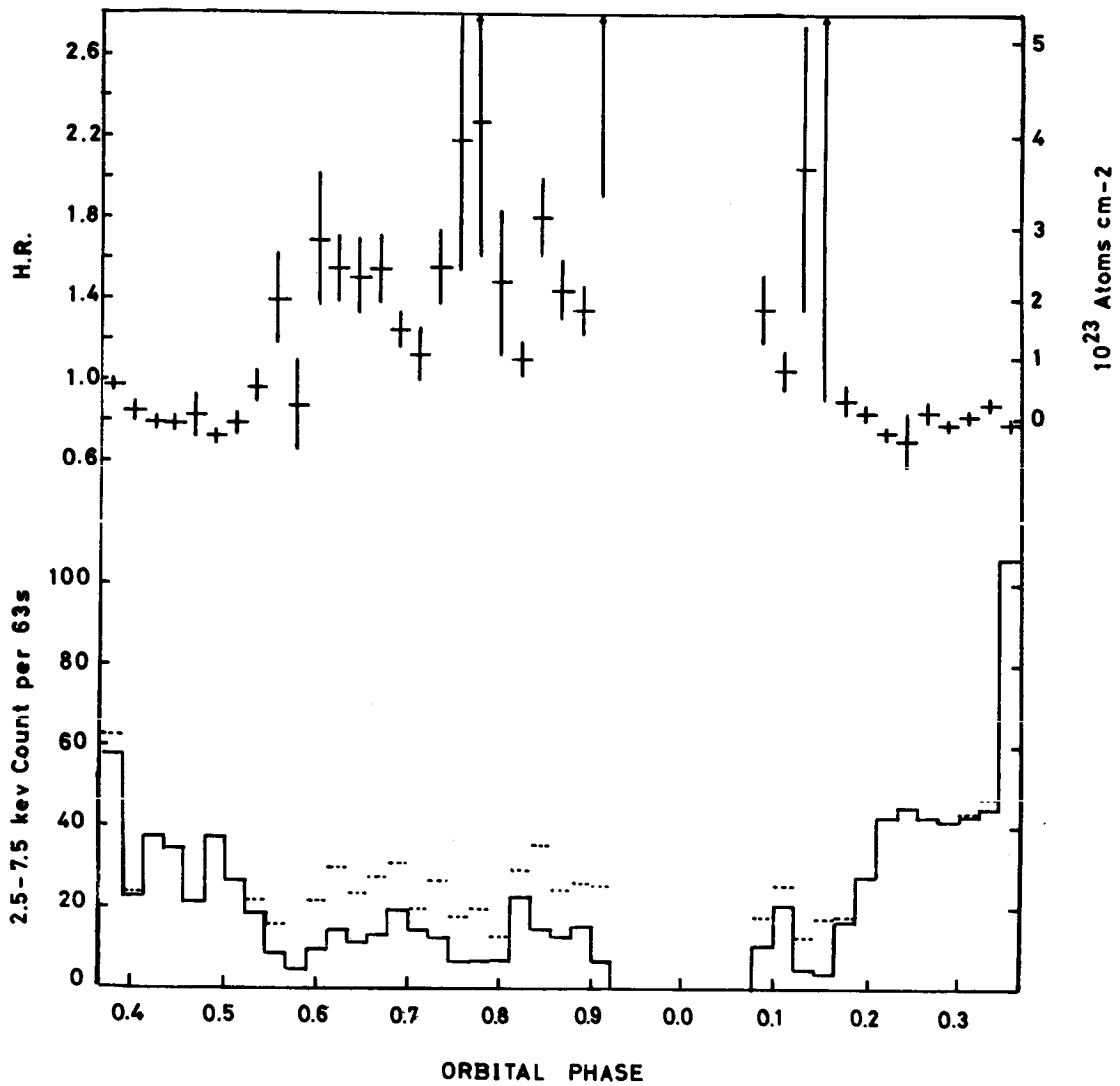


Figure 1.b. Same data as in 1a but summed instead in 4 hour bins and with the equivalent X-ray absorbing column density shown as obtained from a spectral analysis of the data.

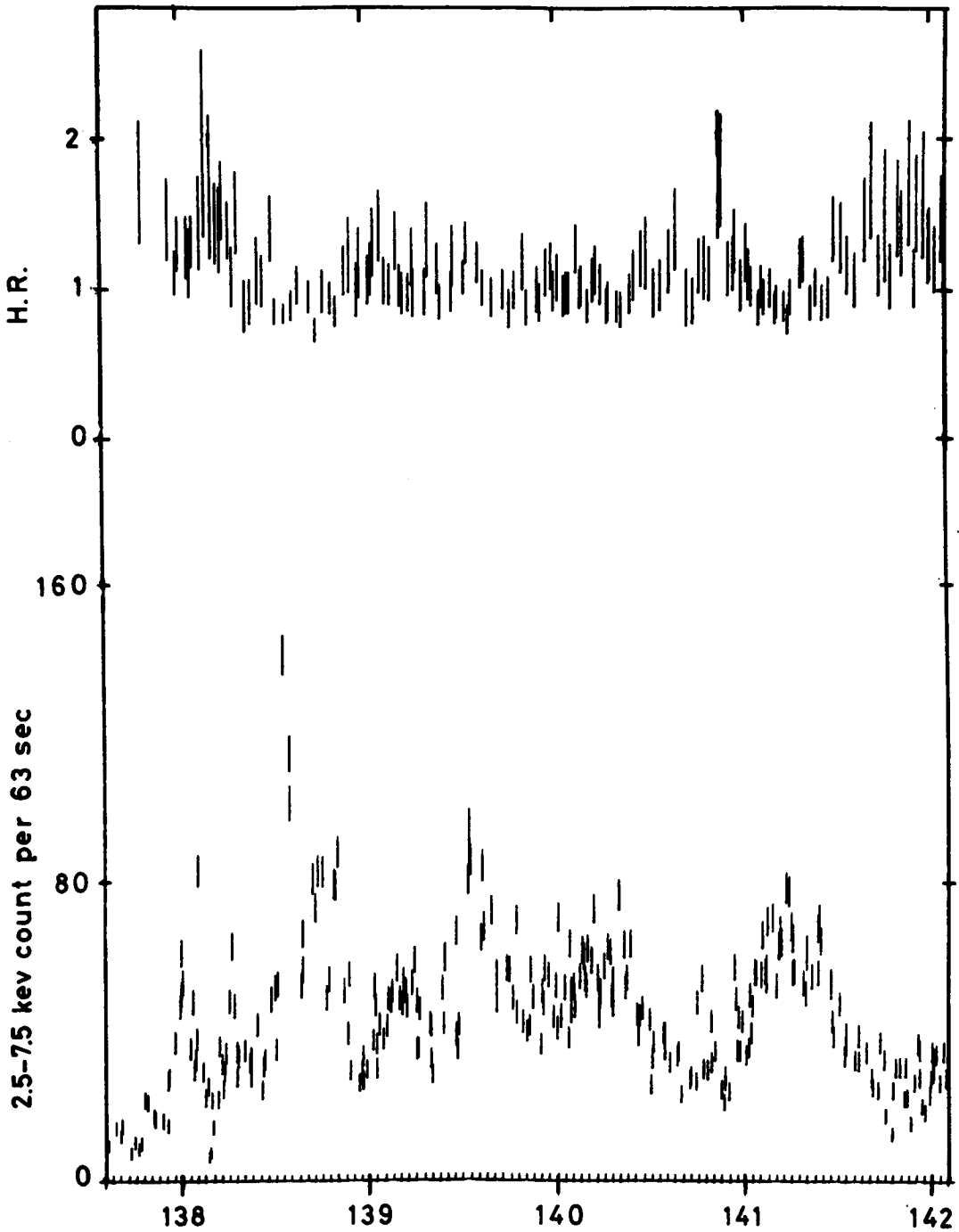


Figure 2.a. Observed counting rates from Vela X-1 in the 2.5-7.5 KeV energy range in May 1975, each point being the mean of 5 frames. The spectral hardness ratio is also plotted (see text for definition). The length of the error bars represents 2 s.d.

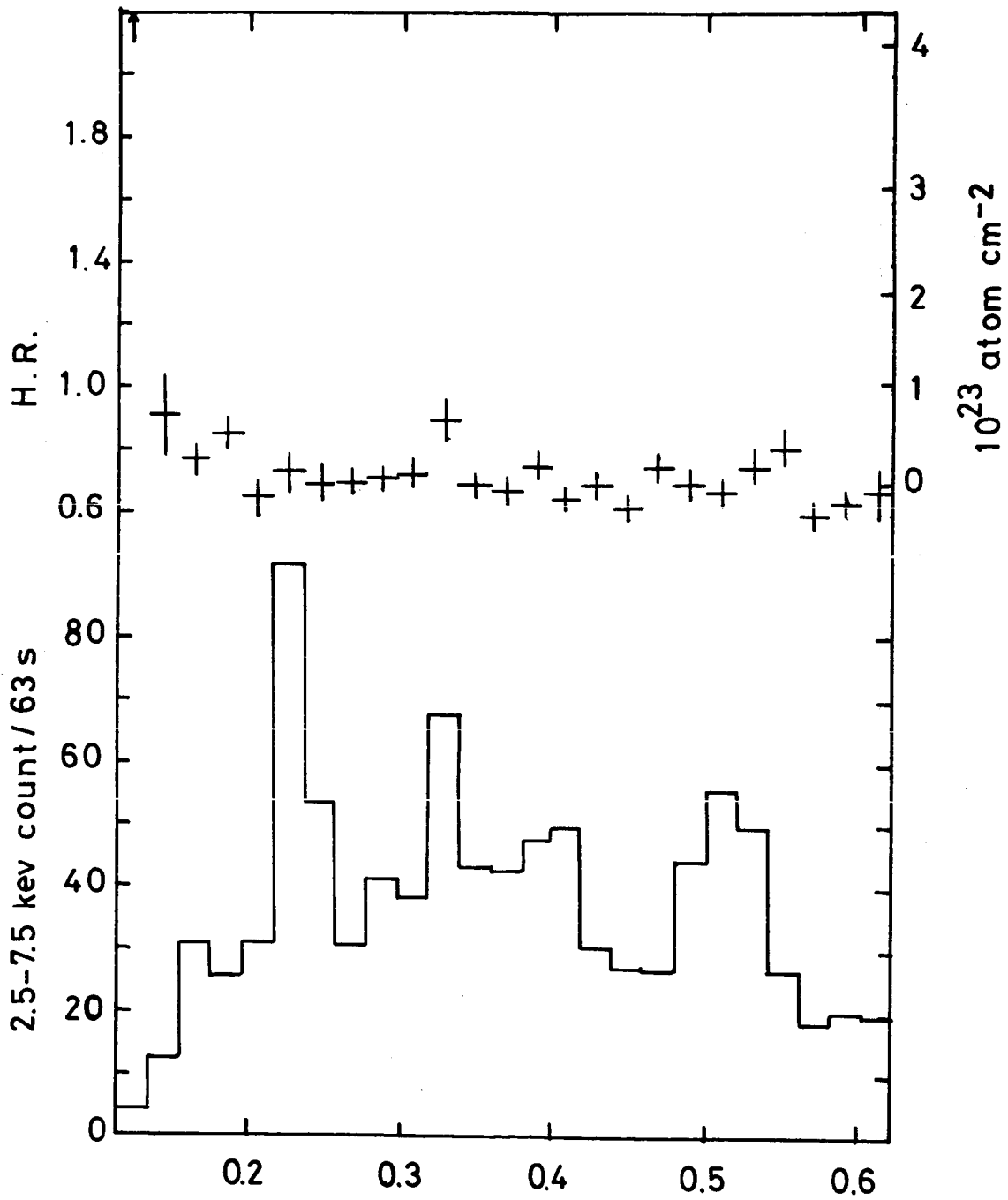


Figure 2.b. Same data as in 2a but summed instead in 4 hour bins and with the equivalent X-ray absorbing column density shown as obtained from a spectral analysis of the data.

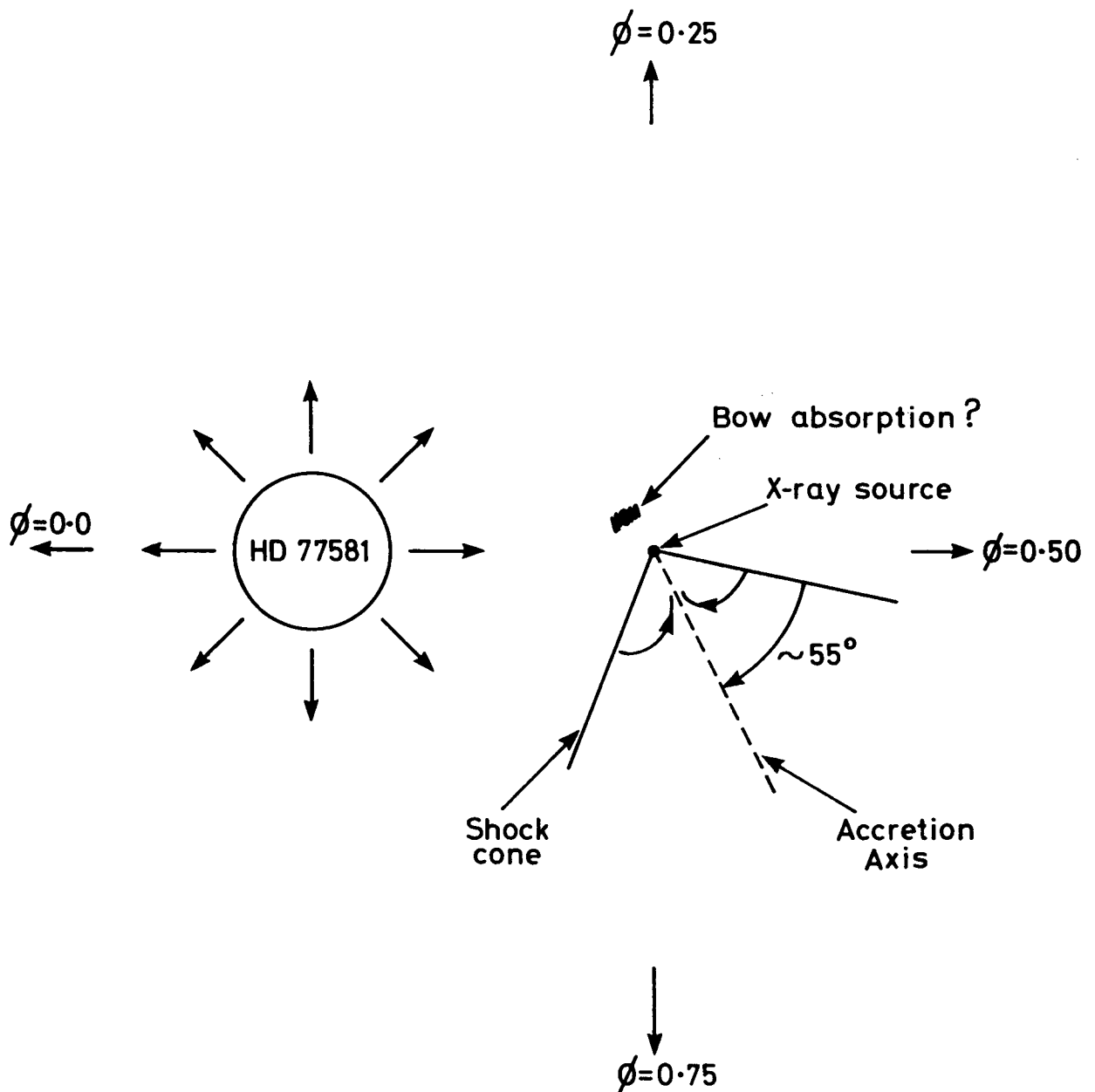


Figure 3. Rough outline of the Vela X-1 binary system (primary shown too small, for clarity) showing the accretion shock & wake around the X-ray source. The phases of the observer are also displayed.

MASS DETERMINATION FOR THE X-RAY BINARY SYSTEM
VELA X-1 (= 3U 0900-40)

J. A. van Paradijs, G. Hammerschlag-Hensberge,
E. P. J. van den Heuvel, R. J. Takens, and
E. J. Zuiderwijk

Astronomical Institute
University of Amsterdam
Amsterdam, The Netherlands

and

C. De Loore
Astrophysical Institute
Vrije Universiteit Brussel
Brussels, Belgium

ABSTRACT

From a radial velocity study of lines of He I and the heavier ions of HD 77581 (=Vela X-1) we derive orbital elements for this X-ray binary system. Together with the orbital elements given by Rappaport and McClintock from X-ray Pulsar results, this enables us to determine masses for both the X-ray and the early type supergiant component : $M_x = 1.61 \pm 0.22 M_\odot$ and $M_{opt} = 21.2 \pm 2.4 M_\odot$, respectively.

INTRODUCTION

The 6.9 mag B0.5 Ib supergiant HD 77581 has been identified as the optical counterpart of the X-ray eclipsing binary system 3U 0900-40 (Vela X-1) (Hiltner et al., 1972; Jones et al., 1973; Vidal et al., 1973). The system shows X-ray eclipses with a period of 8.95 ± 0.02 days (Forman et al., 1973). Rappaport and McClintock (1975) recently reported the discovery of regular X-ray pulses in Vela X-1. The mean pulse

period of 282.9 sec is periodically modified due to the radial velocity variation of the X-ray pulsar in its orbital motion. This makes Vela X-1 the third X-ray binary system in which the orbits of both the optical and the X-ray component can be studied. From an analysis of velocity variations of the X-ray pulsar Rappaport and McClintock (1975) derive the following orbital parameters : $e_X = 0.15 \pm 0.05$, $\omega_X = 157^\circ \pm 24^\circ$ and $K_X = 268 \pm 12$ km/s.

The two other eclipsing binary systems containing an X-ray pulsar (Cen X-3 and Her X-1) present severe difficulties to a standard analysis as a double lined spectroscopic binary. In Her X-1, the heating effect on one part of the optical component due to the proximity of the X-ray source makes an unambiguous interpretation of the radial velocity variations of the optical component difficult (Crampton, 1974; Bahcall et al., 1974). In Cen X-3 the radial velocity variations are difficult to determine, as the optical counterpart is very faint (Krzeminski, 1974) and its lines are extremely broad and weak (Osmer et al., 1975).

Analyses of the light curve of HD 77581 have shown that the heating effect is too small to be detected (Jones et al., 1973; Milgrom and Salpeter, 1975). Furthermore, the star is bright and the spectral lines are not extremely broad. This makes the Vela X-1 system at present the only one for which for the first time a relatively accurate direct mass determination of both the X-ray and the early-type supergiant component is feasible.

Earlier studies of the radial velocity variation of HD 77581 have given discrepant results (Zuiderwijk et al., 1974; Hutchings, 1974; Wallerstein, 1974). For the semi-amplitude K of the orbit values ranging between 19 and 40 km/s have been derived, and values for the eccentricity ranging from 0.00 to 0.54 have been given. According to Wallerstein (1974) the radial velocity data of HD 77581 do not allow a consistent solution of the orbit, due to mass transfer in the

system. In this paper we show that a consistent solution can be obtained, however, provided that the lines of hydrogen - expected to be most sensitive to gas motions in the system - are excluded from the analysis.

OBSERVATIONS AND REDUCTIONS

The present analysis of the radial velocity variations of HD 77581 is based on 26 coude spectrograms, obtained with the 152 cm telescope of the European Southern Observatory, La Silla, Chile, during 4 observing runs between April 1973 and June 1975. The spectra have been taken on IIA0 emulsion, and cover the wavelength region from 3600 to 4950 Å. The dispersion of the plates is 12 Å/mm or 20 Å/mm. The plates obtained during the first observing period have been analysed previously (Zuiderwijk et al., 1974), but have been remeasured independently for use in the present analysis. The observations are distributed evenly over the entire orbital cycle. The spectra were measured for line positions with the Grant Comparator of the Kapteyn Astronomical Laboratory of the University of Groningen. All absorption features visible in the spectrum were measured, without selecting beforehand a particular set of lines. In this way some very weak lines were missed on some plates, on the other hand especially for the weak lines it was considered to be an advantage to measure without a predetermined expectation of where the lines should be found. The wavelengths were determined by means of a dispersion curve of the third degree, obtained from the iron-arc comparison spectrum. After this the identifications were made using the Revised Multiplet Table (Moore, 1945). Lines of H I, He I, O II, N III, N II, Si III and Si IV are present in the measurements of at least half of the spectra. From the measurements of the radial velocity of the interstellar Ca II K-line we find $\bar{v}_{\text{Ca II}} = 16.1 \pm 0.6$ (m.e.) and

13.7 \pm 1.0 km/s for the 12 Å/mm and the 20 Å/mm spectra, respectively. In order to increase the homogeneity of the data we have reduced the measurements of the 20 Å/mm plates to the 12 Å/mm system, by applying the correction of 2.4 km/s. In order to have an impression of the internal accuracy of the present measurements five plates were measured twice. The differences in the mean velocity as obtained from two such measurements of one plate vary between 0.3 and 4.2 km/s; the standard deviations from the mean per line for one plate vary between 8.0 and 11.5 km/s.

In the analysis we have used mean values of the radial velocity as obtained from the He I lines and from the lines of heavier ions. These average radial velocities are given in Table 1. A full table of all individual line radial velocity measurements will be published elsewhere.

With the computer program "Orbit" based on a program of Wolfe et al. (1967) the best fitting radial velocity curve through the points was computed. This was done for all lines of He I and the heavier ions together. Also separate solutions for the He I lines and the heavier ion lines were made. The radial velocity measurements were weighted according to $w_i = 1/\sigma_i^2$, where σ_i is the standard deviation of the mean of the measurements. The average orbital period P determined in these solutions equals 8.966 \pm 0.005 days. This agrees well with Hutchings' (1974) result (P = 8.966 \pm 0.001 days), based on radial velocity determinations by several observers, over a time interval of 17 years. We have therefore subsequently made new orbital solutions with the period P = 8.966 days as a fixed parameter. These orbital elements, as derived from all lines together - except the hydrogen lines - are presented in Table 2. The best fitting radial velocity curve is shown in Fig. 1. The separate solutions for He I and the heavier ions are in good agreement with the mean solution (see Table 2 and Fig. 2 and 3). We have also made solutions for

individual lines of heavier elements which are somewhat less accurate, but consistent with the solution for all the lines together. Fig. 4 shows clearly that no consistent orbit can be obtained from the hydrogen lines. Therefore, those lines should be omitted in future attempts to determine orbital elements for this binary system.

DISCUSSION OF THE RESULTS

The values for the orbital parameters derived here are in good agreement with the X-ray pulsar data, which for convenience are also given in Table 2. In particular the values of the eccentricity and the angle of periastron, which should be 180° apart for the optical and the X-ray solution, agree well (within the quoted accuracy intervals). In our opinion this agreement lends confidence to the orbital character of the optical radial velocity variations; the non-orbital (gas-streams, stellar wind fluctuations) component does not seem to be very important for the results from He I and heavier elements. We find the following values for the system parameters :

$$\text{mass ratio : } M_{\text{opt}}/M_X = (a_X/a_{\text{opt}}) = 13.2 \pm 0.9$$

$$\text{total mass : } (M_{\text{opt}} + M_X) \sin^3 i = 21.5 \pm 2.2 M_\odot$$

$$M_X \sin^3 i = 1.52 \pm 0.19 M_\odot \quad \text{and} \quad M_{\text{opt}} \sin^3 i = 20.0 \pm 2.1 M_\odot.$$

From a detailed analysis of the optical light variations, Avni and Bahcall (1975) have found that the inclination i should be higher than 74° , in order to get a consistent picture of both the observed light curve and the X-ray eclipse duration. Taking 74° and 90° as lower and upper limits of the inclination angle we get

$$M_X = 1.61 \pm 0.22 M_\odot \quad \text{and} \quad M_{\text{opt}} = 21.2 \pm 2.4 M_\odot.$$

This result shows that the compact component is very probably

too heavy for being a white dwarf.

If it would be a white dwarf - its evolutionary history implies that it should consist mainly of carbon and oxygen (van den Heuvel, 1974, 1975); the upper mass limit for such white dwarfs is around $1.4 M_{\odot}$ (Hamada and Salpeter, 1961). Its most probable mass of $1.61 M_{\odot}$ is just consistent with the presently allowed theoretical masses of neutron stars ($M \lesssim 1.6 M_{\odot}$) (Cameron and Canuto, 1974). The mass determination of the supergiant allows a test of the theoretically computed evolution of massive stars through a comparison with theoretical evolutionary tracks. The luminosity of HD 77581 can be inferred in two ways. The spectral type and luminosity class (B0.5 Ib) provide in principle the absolute magnitude M_v , bolometric correction BC and effective temperature T_{eff} . Using the luminosity calibration of Blaauw (1963) or Keenan (1963) we derive $M_v = -5.9 \pm 0.4$ mag. For the bolometric correction values between 2.4 and 2.6 mag have been given (Morton and Adams, 1968; Schlesinger, 1969). This gives $M_{\text{bol}} = -8.4 \pm 0.5$ mag. For the orbital parameters given here and by Rappaport and McClintock (1975) and assuming a minimum observed eclipse angle of 34° Avni and Bahcall (1975) derive for the radius of HD 77581 $R = 30 R_{\odot}$. For the effective temperature values ranging from 22000 K (Osmer, 1973) to 29000 K (Auer and Mihalas, 1972) have been given for early B-type supergiants. Adopting $T_{\text{eff}} = 25000 \pm 4000$ K we find $M_{\text{bol}} = -9.0 \pm 0.75$ mag.

From a comparison with evolutionary tracks (Simpson, 1971; Stothers, 1972) we then find the following values of the evolutionary mass : $M/M_{\odot} = 22 \pm 7$ and 30 ± 10 , respectively; these values, although not very accurate, are consistent with the presently determined value of $21.2 \pm 2.4 M_{\odot}$. Therefore, the early type supergiant in this X-ray binary system does not seem to show signs of being particularly undermassive for its spectral type (as has been suggested by some authors for some of the X-ray binaries, particularly, Cygnus X-1

(Trimble et al., 1973)).

ACKNOWLEDGEMENTS

We thank Drs. J.Heise for presenting this paper for us at the Goddard conference.

We are indebted to the ESO Staff and Directorate for the use of observing facilities in Chile.

REFERENCES

- Auer, L.H., and Mihalas, D. 1972, *Astrophys. J. Suppl.* 24, 193.
- Avni, Y., and Bahcall, J.N. 1975, *Astrophys. J. Lett.* (in press)
- Bahcall, J.N., Joss, D.C., and Avni, Y. 1974, *Astrophys. J.*, 191, 211.
- Blaauw, A. 1963, in *Basic Astronomical Data*, ed. K. Aa. Strand, Univ. of Chicago Press, Chicago and London, p. 383.
- Cameron, A.G.W., and Canuto, V. 1974, in *Astrophysics and Gravitation, Proceedings of the 16th Solvay Conference on Physics*, Univ. of Brussels Press, p. 221.
- Crampton, D. 1974, *Astrophys. J.*, 187, 345.
- Forman, W., Jones, C., Tananbaum, H., Gursky, H., Kellogg, E., and Giacconi, R. 1973, *Astrophys. J. Lett.*, 182, L 103.
- Hamada, T., and Salpeter, E.E. 1961, *Astrophys. J.*, 134, 683.
- van den Heuvel, E.P.J. 1974, in *Astrophysics and Gravitation, Proceedings of the 16th Solvay Conference on Physics*, Univ. of Brussels Press, p. 119.
- van den Heuvel, E.P.J. 1975, Review presented at IAU Symp. Nr. 73 "Structure and Evol. of Close Binary Systems", to be published, Reidel, Dordrecht.
- Hiltner, W.A., Werner, J., and Osmer, P. 1972, *Astrophys. J. Lett.*, 175, L 19.
- Hutchings, J.B. 1974, *Astrophys. J.*, 192, 685.
- Jones, C., and Liller, W. 1973, *Astrophys. J. Lett.*, 184, L121.
- Keenan, P.C. 1963, in *Basic Astronomical Data*, ed. K. Aa. Strand, Univ. of Chicago Press, Chicago and London, p.78.
- Krzeminski, W. 1974, *Astrophys. J. Lett.*, 192, L 135.
- Milgrom, M., and Salpeter, E.E. 1975, *Astrophys. J.*, 196, 583.
- Moore, C.E. 1945, *Princeton Univ. Obs. Contrib.*, No. 20.
- Morton, D.C., and Adams, T.F. 1968, *Astrophys. J.*, 151, 611.
- Osmer, P. 1973, *Astrophys. J.*, 181, 327.
- Osmer, P. S., Hiltner, W.A., and Whelan, J.A.J. 1975, *Astrophys. J.*, 195, 705.
- Rappaport, S., and McClintock, J. 1975, *IAU Circ. No.* 2794.

- Rappaport, S., and McClintock, J. 1975, IAU Circ. No. 2833.
- Schlesinger, B. 1969, *Astrophys. J.*, 157, 533.
- Simpson, E.E. 1971, *Astrophys. J.*, 165, 295.
- Stothers, R. 1972, *Astrophys. J.*, 175, 431.
- Trimble, V., Rose, W.K., and Weber, J. 1973, *Mon. Not. Royal Astron. Soc.* 162, 1P.
- Vidal, N.V., Wickramasinghe, D.T., and Petterson, B.A. 1973, *Astrophys. J. Lett.*, 182, L 77.
- Wallerstein, G. 1974, *Astrophys. J.*, 194, 451.
- Wolfe, R.H.Jr., Horak, H.G., and Storer, N.W. 1967, in *Modern Astrophysics*, ed. M. Hack, Gauthiers-Villars, Paris, p. 251.
- Zuiderwijk, E.J., van den Heuvel, E.P.J., and Hensberge, G. 1974, *Astron. and Astrophys.* 35, 353.

Table 1. Journal of Observations.

plateno.	JD2440000+	phase ^x	v_{rad} (km/s)	m.e.	O-C
G3834	1773.626	.480	- 8.64	7.79	+ 8.00
G3842	1774.608	.590	-18.02	3.18	+ 4.77
G3848	1775.582	.699	-22.03	3.22	+ 1.76
G3858	1776.583	.810	-11.00	3.36	+ 9.25
G3866	1777.613	.925	- 7.72	4.14	+ 3.93
G3879	1779.535	.139	+16.74	5.24	+ 3.11
G3896	1780.632	.262	+13.85	3.35	+ 2.68
G3909	1781.631	.373	- 2.37	3.11	+ 2.18
G3923	1782.556	.476	-20.48	3.51	- 4.18
F1684	2169.522	.636	-32.65	3.33	- 8.88
F1694	2170.522	.747	-26.57	3.46	- 3.76
F1702	2171.477	.854	-14.37	4.06	+ 3.25
F1709	2173.593	.090	+ 5.68	5.52	- 2.80
F1717	2174.581	.200	+14.16	4.58	- 1.39
F1727	2175.594	.313	- 3.27	4.94	- 7.56
F1739	2176.559	.421	-13.00	6.06	- 2.36
F1750	2177.492	.525	-11.60	6.31	+ 8.22
F1765	2180.463	.856	-12.23	7.00	+ 5.23
G6480	2439.647	.763	-27.27	4.80	- 4.98
G6491	2440.710	.882	-23.62	6.72	- 8.12
G6497	2441.734	.996	- 8.92	3.82	- 5.24
G6505	2442.684	.102	+12.98	4.23	+ 3.03
G6511	2443.658	.211	+22.75	5.54	+ 7.51
G6519	2444.729	.330	+ 3.80	3.72	+ 2.08
F3116	2560.509	.243	+ 1.18	5.44	-11.90
F3124	2566.531	.915	-18.34	4.19	- 5.73

^xPhase zero corresponds to mid-eclipse time JD2441446.54 + n x 8.966 day.

Table 2. Orbital elements for HD 77581 = Vela X-1

	Optical Observations			X-ray Pulsar
	Mean values for He I and heavier elements	He I	heavier ions	
P	8.966	8.966	8.966	8.96 day
V_o	-7.97 ± 0.82	-8.45 ± 0.64	-7.16 ± 1.06	km/s
K	19.81 ± 1.19	20.54 ± 0.99	21.19 ± 1.42	268 ± 12 km/s
e	0.20 ± 0.06	0.23 ± 0.04	0.22 ± 0.07	0.15 ± 0.05
ω	$10^\circ \pm 17^\circ$	$18^\circ \pm 11^\circ$	$2^\circ \pm 19^\circ$	$157^\circ \pm 24^\circ$
asini	$2.4 \pm 0.2 \times 10^6$	$2.5 \pm 0.1 \times 10^6$	$2.6 \pm 0.2 \times 10^6$	$3.3 \pm 0.1 \times 10^7$ km

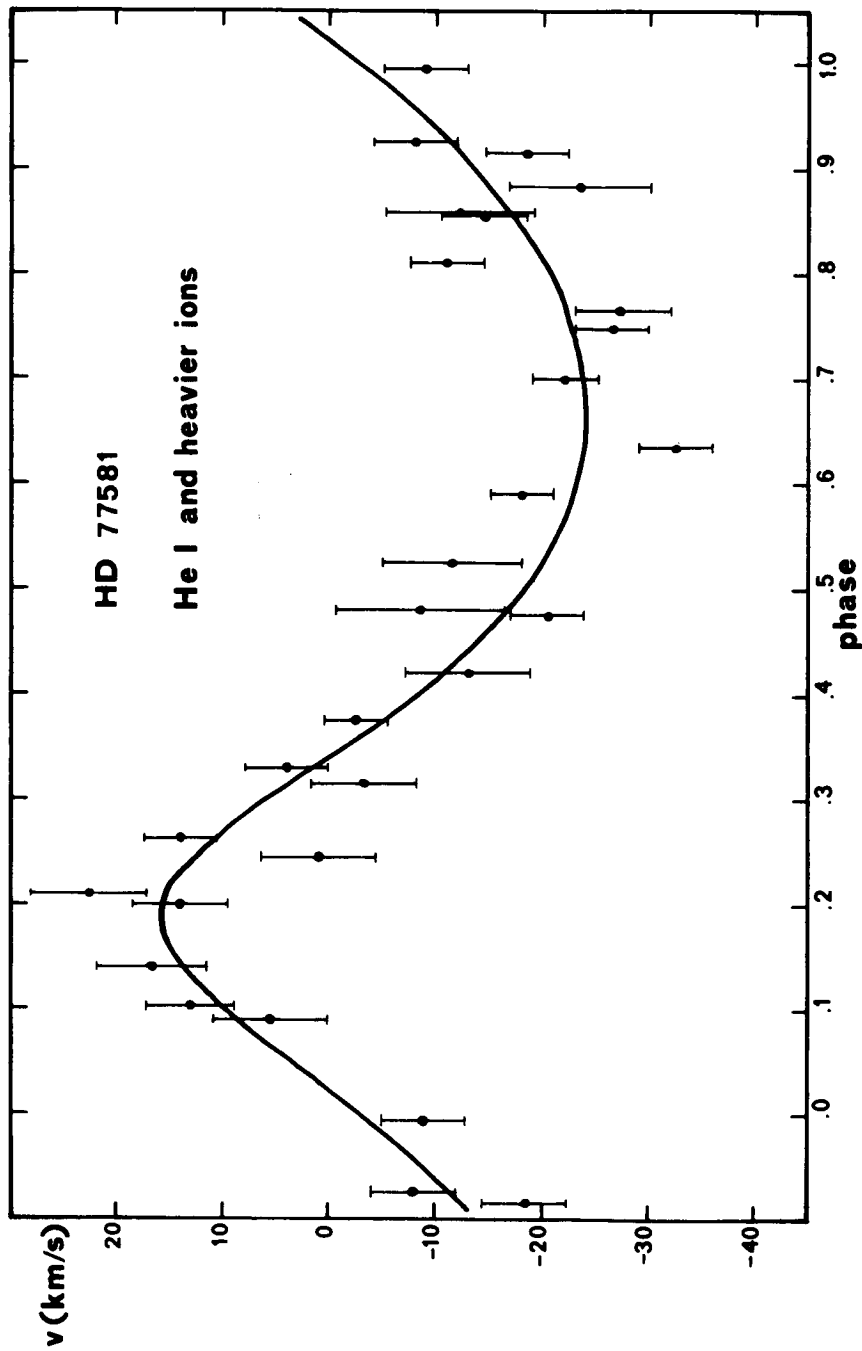


Fig. 1. Radial velocity curve of HD 77581 = Vela X-1 for a period of 8.966 days. Phase zero corresponds to mid-eclipse time. The points denote mean values of the measurements of lines of He I and heavier ions. Mean errors per plate are indicated by the length of the vertical bars.

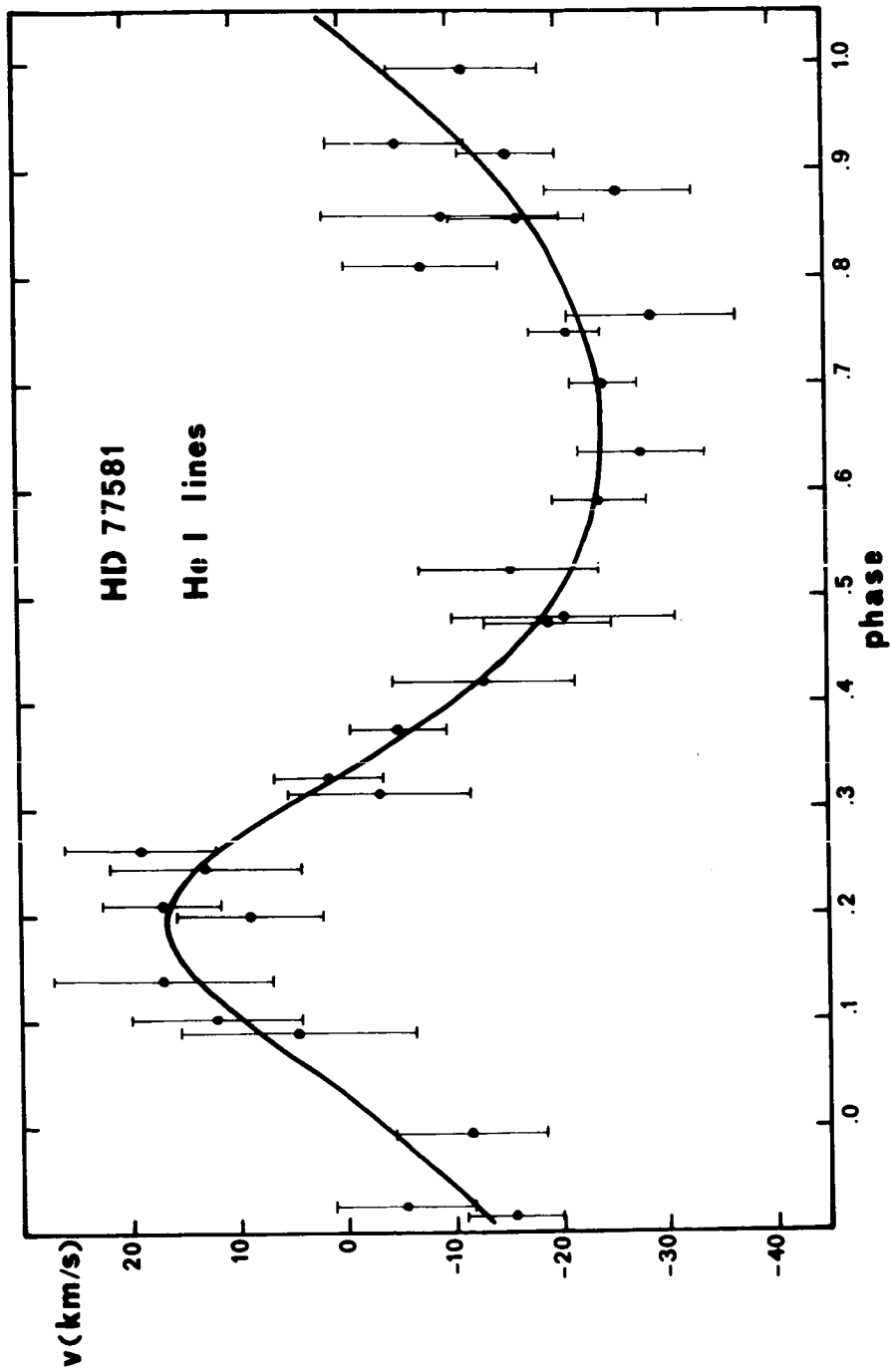


Fig. 2. Radial velocity curve of HD 77581 = Vela X-1. The points denote mean values of the measurements of lines of He I.

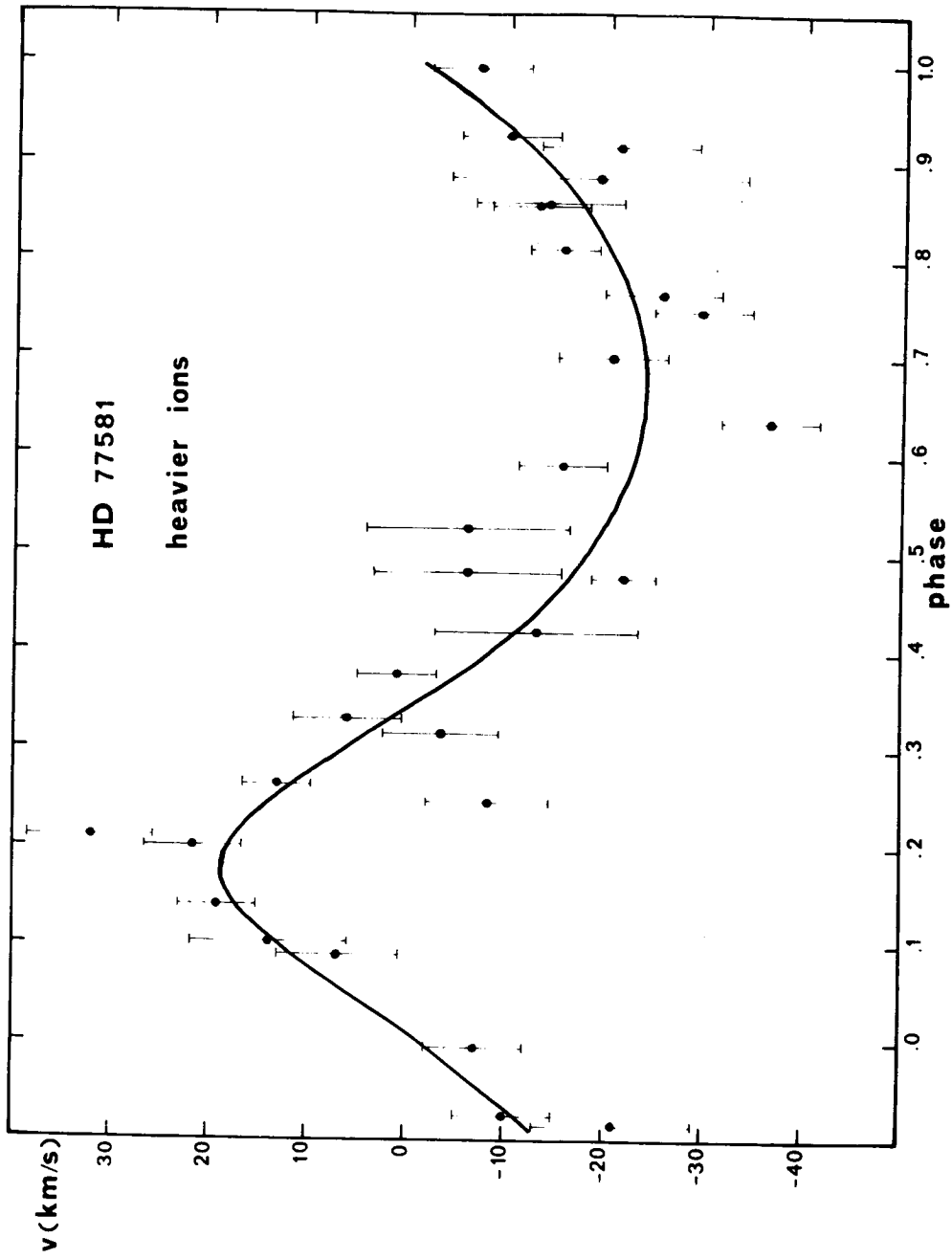


Fig. 3. Radial velocity curve of HD 77581 = Vela X-1. The points denote mean values of the measurements of lines of ions heavier than He.

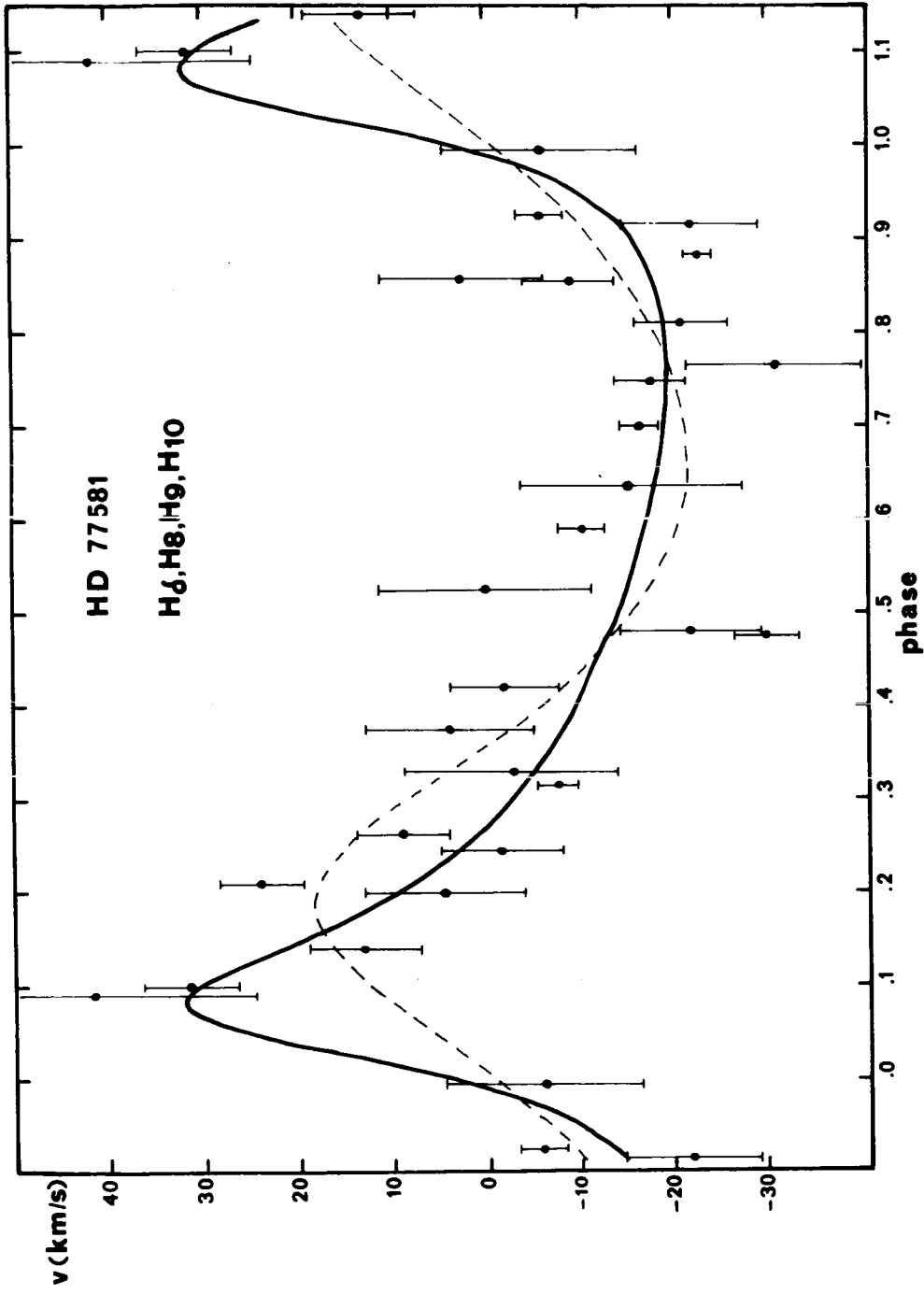


Fig. 4. Radial velocity measurements of lines of hydrogen. The solid line is the curve derived from the hydrogen lines; the dashed line is the curve derived from lines of He I and heavier ions.

VELA X-1 AND NEUTRON STAR ORIGINAL SPIN^{*}

D. Q. Lamb and F. K. Lamb[†]

Department of Physics
University of Illinois at Urbana-Champaign
Urbana, Illinois 61801

and

W. D. Arnett

Department of Astronomy
University of Illinois at Urbana-Champaign
Urbana, Illinois 61801

ABSTRACT

Usually it is assumed that neutron stars are formed spinning rapidly, with rotation periods as short as 10^{-3} - 10^{-4} s. In contrast with this picture, we propose that neutron stars are born with a wide range of initial rotation periods, some very long. Increasing observational evidence supporting this hypothesis includes the lack of correlation between pulsar spindown time scales and inferred distances from the galactic plane, and the detection of long period pulsating X-ray sources. We examine transfer of angular momentum from the degenerate core to the envelope of neutron star progenitors as one example of the ways in which such slowly spinning neutron stars might be formed. We discuss several implications of our suggestions.

^{*}This research was supported in part by the NSF under grants MPS75-08790, MPS74-20755 and by the A. P. Sloan Foundation.

[†]Alfred P. Sloan Foundation Research Fellow

AN X-RAY DETERMINATION OF THE ORBITAL ELEMENTS OF 3U0900-40

J. McClintock, P.C. Joss, and S. Rappaport
Center for Space Research
Massachusetts Institute of Technology
Cambridge, Massachusetts 02139

ABSTRACT

We have determined the orbital elements of the 3U0900-40 binary system by measuring the variations in the arrival times of the 283-second X-ray pulses. The best-fit values of the system parameters and their 95% confidence limits are listed in Table 1.

I. INTRODUCTION

On 18 June 1975 we discovered a 283-second periodicity in the X-ray intensity of 3U0900-40 = Vela X-1 (Rappaport and McClintock 1975), making it the third periodically pulsing X-ray source in an eclipsing binary system. The two other objects in this class are Centaurus X-3 (pulse period $P = 4.8^s$; Giacconi *et al.* 1971; Schreier *et al.* 1972) and Hercules X-1 ($P = 1.24^s$; Tananbaum *et al.* 1972). In addition, there are two pulsing, "transient" sources which have not been observed to have an eclipse cycle, and are not known to be in binary systems: A0535+26 ($P = 104$ s; Eyles *et al.* 1975) and All18-61 ($P = 6.755$ min; Ives *et al.* 1975).

II. OBSERVATIONS

The data were obtained using two proportional-counter detectors aboard the third Small Astronomy Satellite, SAS-3. The argon-filled detector has an effective area of 80 cm^2 and has three energy channels: 1-3 keV, 3-6 keV and 6-12 keV. The xenon-filled detector has an effective area of 115 cm^2 has four energy channels: 8-19 keV, 19-30 keV, 30-39 keV and 39-55 keV. The detectors view out along the azimuthal scan circle of the spacecraft through coaligned, 1.7° FWHM collimators. The data were recorded at 0.42 second time resolution. The SAS-3 observatory was operated in a pointed mode so that 3U0900-40 was nearly centered in the field of view of the detectors throughout each orbit. A more detailed description of the SAS-3 observatory and the two detectors is given elsewhere (Bradt *et al.* 1975).

During the non-earth-blocked portion of each satellite orbit, 3U0900-40 was observed continuously, netting about 3000 seconds of observation time per orbit. The discovery of the 283-second pulse period occurred during an observation on June 18 (Figure 1). Subsequently, we performed two extended observations during the intervals June 18.8-24.2 and July 19.3-

25.3 UT. Both observation intervals combined yielded a total of 35 satellite orbits of data which had a sufficiently good signal to noise ratio to be useful in determining the orbit of the X-ray star.

III. ORBITAL PARAMETERS

We folded the counting rate data for each satellite orbit separately, using an approximate pulse period of 282.9 seconds. For each orbit of data we determined the time of arrival of a fiducial feature in the pulse shape. We then carried out a minimum χ^2 fit to the 35 observations of pulse arrival time in June and July 1975. In performing the fit, we weighted the observations by the relative accuracy to which the arrival times could be measured. The fit had six free parameters: the heliocentric pulse period (P), the zero-point of pulse phase, the projected orbital amplitude ($a_x \sin i$), the orbital phase, the orbital eccentricity (e), and the longitude of periastron (ω). The orbital period (P_{orb}) is not well determined by our data alone; we therefore fixed the orbital period at the value of 8.9625 days, which is accurate to within an uncertainty of ± 0.005 days (Li 1975). The results of our fit are listed in Table 1 and illustrated in Figure 2.

From our fitted value of $a_x \sin i$, we obtain a mass function of $f(M) = 18.7 \pm 1.6 M_\odot$ (95% confidence). Unfortunately, optical observers (Wallerstein 1974; Hutchings 1974; Zuiderwijk, van den Heuvel, and Hensberge 1974; van Paradijs *et al.* 1975, 1976) have obtained widely varying results for the projected orbital velocity of the companion star, HD 77581. It is critically important to refine these measurements and to gain a better theoretical understanding of variations of optical radial velocity with time and among different spectral lines, in order to establish an accurate value for the mass of the X-ray star.

We are grateful to the members of the SAS-3 group and to the many persons who have contributed to the successful fabrication, launch, and operations of SAS-3. We thank the staffs of the Laboratory for Space Experiments and the Center for Space Research at M.I.T., the Applied Physics Laboratory of Johns Hopkins University, the Goddard Space Flight Center, and Centro Ricerche Aerospaziali.

REFERENCES

- Bradt, H., Mayer, W., Buff, J., Clark, G.W., Doxsey, R., Hearn, D., Jernigan, G., Joss, P. C., Laufer, B., Lewin, W., Li, F., Matilsky, T., McClintock, J., Primini, F., Rappaport, S., and Schnopper, H. 1975, Submitted to Ap. J. Lett.
- Eyles, C. J., Skinner, G. K., and Willmore, A. P. 1975, IAU Circ., No. 2787.
- Hutchings, J. B. 1974, Ap. J., 192, 685.
- Ives, J. C., Sanford, P. W., and Bell Burnell, S. J. 1975, Nature, 254, 578.
- Giacconi, R., Gursky, H., Kellogg, E., Schreier, E., and Tananbaum, H. 1971, Ap. J. Lett., 167, L67.
- Li, F. 1975, private communication.
- Rappaport, S., and McClintock, J. 1975, IAU Circ., No. 2794.
- Schreier, E., Levinson, R., Gursky, H., Kellogg, E., Tananbaum, H., and Giacconi, R. 1972, Ap. J. Lett., 174, L143.
- van Paradijs, J. A., Hammerschlag-Hensberge, G., van den Heuvel, E. P. J., Takens, R. J., and Zuiderwijk, E. J. 1976, this monograph.
- van Paradijs, J. A., Hammerschlag-Hensberge, G., van den Heuvel, E. P. J., Zuiderwijk, E. J., and Takens, R. J. 1975, IAU Circ., No. 2841.
- Wallerstein, G. 1974, Ap. J., 194, 451.
- Zuiderwijk, E. J., van den Heuvel, E. P. J., and Hensberge, G. 1974, Astron. and Ap., 35, 353.

TABLE 1

BEST-FIT PARAMETER VALUES
OF THE 3U0900-40 BINARY SYSTEM*

P	= 282 ^S 8916 ± 0 ^S .0004
a _x sin i	= 112 ± 3 light seconds
K _x	= 274 ± 9 km s ⁻¹
f(M)	= 18.7 ± 1.6 M _o
e	= 0.12 ± 0.04
ω	= 146° ± 23°

*Quoted errors are formal single-parameter 95% confidence limits.

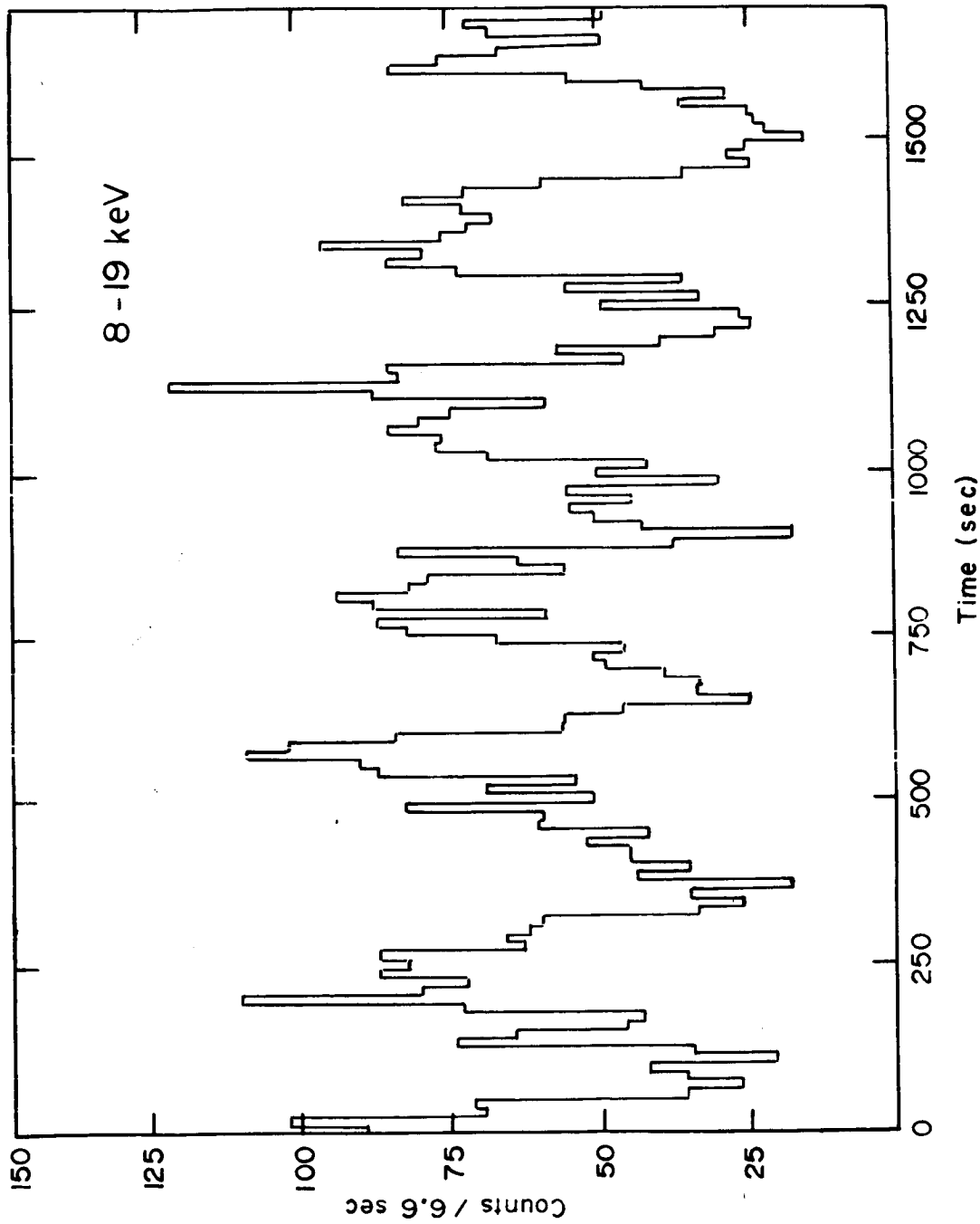


Figure 1: The X-ray intensity of 3U0900-40 during a 30-minute observation. A background counting rate of about 50 counts/6.6 sec has been subtracted.

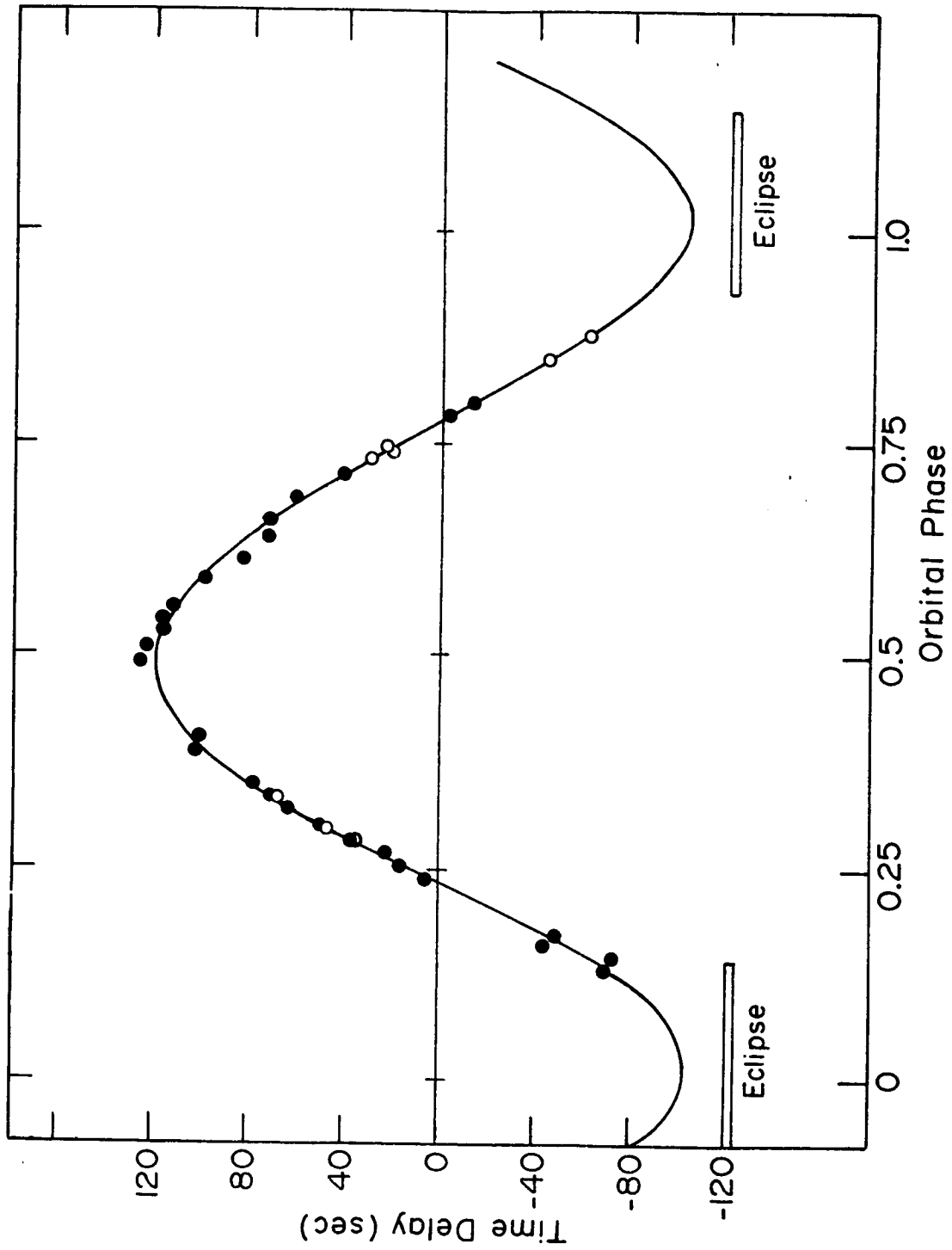


Figure 2: Doppler corrections to the pulse arrival times as a function of 8.96 orbital phase. The open circles are for the June 18.8-24.2 data, the solid circles are for the July 19.3-25.3 data, and the solid curve is the best-fit orbit.

3U0900-40 (HD77581)

Discussion

A. Bunner:

I'd like to urge everyone to refer to this X-ray source as 3U0900-40, or perhaps Vel XR-1, but not Vela X-1, to avoid confusion with the radio and X-ray supernova remnant Vela X, which is totally unrelated.

P. C. Joss to P. A. Charles:

There is evidence in the data presented in this talk and in the Ariel 5 data presented earlier by Dr. Pounds that Vela X-1 is brighter, on average, before mid-phase than after mid-phase. The source variability has been ascribed to attenuation of the X-rays as they pass through a bow shock and an accretion wake. However, the X-ray star has an appreciably eccentric orbit, with periastron occurring before mid-phase. When the X-ray star is nearer its companion, the local density of the stellar wind from the companion is higher and the mass accretion rate onto the X-ray star may be enhanced. It is thus possible that some fraction of the source variability is due to an intrinsic variation in source intensity, with maximum intensity occurring near periastron.

THE "OTHER" GALACTIC X-RAY SOURCES

by

Herbert Gursky
Center for Astrophysics
Harvard College Observatory/
Smithsonian Astrophysical Observatory
60 Garden Street
Cambridge, Massachusetts 02138

ABSTRACT

There is by now a "standard" model for X-ray sources comprising a binary system containing a compact star and powered by mass accretion. It can be argued that the majority and perhaps all the galactic X-ray sources are of this kind. In this paper I discuss three kinds of sources which may be qualitatively different from these; namely, low luminosity sources such as 3U0352 + 30 (= X Perseus?), the sources associated with the globular clusters, and the transient X-ray sources.

The outstanding result of the last several years in galactic X-ray astronomy has been the discovery of the binary X-ray stars, and the realization that the X-ray emitter is a neutron star or a black hole. These are strong X-ray sources with identified optical companions in which either the X-ray source or the optical star or both shows clear evidence of a binary system. There are nine such systems and they are listed in Table 1, along with certain characteristics.

These objects have been subject to intense study throughout the electromagnetic spectrum and the revealed characteristics can be summarized as follows:

1. The 1-10 keV X-ray luminosity is in the range 10^{36} - 10^{38} erg/sec.
2. The binary periods extend from 0.2 days to 10 days.
3. Three of the sources show regular pulsing of the X-ray emission of 1.2, 4.8 and 234 sec, respectively. These objects are likely rotating, magnetic neutron stars.
4. There is a variety of direct and indirect evidence for gas streaming and mass transfer between the binary members.

Furthermore, this is clear evidence for a distinct class of binary systems in which the optical member is an early type giant or supergiant star, including Cyg X-1, 0900-40, 1700-37, Cen X-3 and SMC X-1. Because of the rarity of this kind of star it is likely that there is a unique evolutionary sequence leading to its existence of the kind described by Van den Heuvel and his colleagues (cf. Van den Heuvel and Heise, 1972). The remaining X-ray sources have a companion of normal mass; however, only for Cyg X-2 and for Her X-1 is the companion star "seen" in any degree.

The standard model which has evolved for these X-ray stars is a binary system in which one member is a compact star, either a neutron star or a black hole (cf. Rees, 1974). The X-ray emission originates from heated matter falling onto the compact star. It is also possible that white dwarfs may be the compact star (Gursky, 1975).

The optical and X-ray characteristics of these X-ray sources have been reviewed recently (cf. Gursky and Schreier, 1975; Giacconi, 1974; Bahcall and Bahcall, 1974). The question I ask is simply, are all the galactic X-ray sources of this kind or are there other, very different kinds of objects present? The question is not so easy to answer because the X-ray sources do not offer an obvious "signature" as do, for example, the radio pulsars. There are a few X-ray sources which are clearly different; for example, the X-ray emission associated with the nearby bright stars Sirius and Capella (Mewe et al, 1975), and the X-ray emission from the supernova remnants (Gorenstein, 1974). Rather we are concerned with the 100 or so sources which are obviously galactic because of their concentration along the Milky Way, but which cannot be placed among the sources in Table 1. These sources are plotted in Figure 1. It is likely that most of these sources are similar to those in Table 1, however, there are indications that some are "different". There are three kinds of sources I wish to discuss. One is the low luminosity sources, the second is the globular cluster sources and the third is the transient sources.

As I stated, the binary X-ray sources in Table 1 lie in the range 10^{36} - 10^{38} erg/sec and it can be argued that the majority of sources plotted in Figure 1 have luminosities in this range (Gursky, 1973; Margon and Ostriker, 1974). However, there is evidence for weaker sources. χ - Perseus is coincident with the X-ray source 3U0352 + 30 within less than 1'. If this is the source, then the X-ray luminosity is about 3×10^{33} ergs/sec. The fact that the star is an early supergiant would make one believe it belongs to the category Cyg X-1, 0900-40, etc. However, the luminosity is three orders of magnitude below that of the others and there is no evidence that it is a close binary. The only evidence for duplicity is a 584 day periodicity found by Hutchings et al (1974). It is possible that this is simply a widely separated example of the other binary X-ray stars; however, it may be useful to look for other possibilities. The fact that the star itself emits $\sim 10^{38}$ erg/sec in optical and ultraviolet radiation and perhaps 10^{36} erg/sec in a solar wind makes it possible that some unlikely non-thermal process is operative which is giving rise to the observed X-rays.

Other evidence for low luminosity sources is the appearance of a number of X-ray sources in the back half of the galaxy ($100^\circ < l < 240^\circ$) in the intensity range 5 - 10 Uhuru c/s shown separately in Figure 2. For these sources to have a luminosity of 10^{36} erg/sec, their distance would need to be in the range 5 - 10 kpc; thus, it is very possible that they are nearer and of much lower luminosity.

The globular cluster sources were discovered in the Uhuru survey (Giacconi et al, 1974), and the MIT-OSO-7 survey (Clark et al, 1975; Markert et al, 1975). The luminosity and variability of these sources is similar to that of other strong galactic sources. Their significance as evidence that some of the X-ray sources such as Sco X-1 and Cyg X-2 were of extreme Population II was discussed by Gursky and Schreier (1975). Also, Clark (1975) has suggested that they are capture binaries. However, a qualitatively different possibility has been discussed by Bahcall and Ostriker (1975) and by Silk and Arons (1975); namely, that they are massive black holes formed at the centers of globular clusters during their early history. If this latter possibility turns out to be correct, we will have a new category of black hole to investigate.

The third kind of source - the transient sources - differs from the others in that there is a well-defined signature present; namely, a sudden increase in X-ray emission of at least 2 or 3 orders of magnitude and a gradual decline of from weeks to months. Within the past year important new information has emerged which may be the essential information in establishing their nature. Two transient sources have been found which have periodic emission. One, in Centaurus, was found to have a period of 6.75 minutes (Ives et al, 1975) and the other in Taurus with a periodicity of 104 sec (Eyles et al, 1975). Also, it is likely that one of the transient sources has been optically identified. A source in Monoceros, A0621-00, first reported by Elvis et al (1975) has apparently been identified optically by Boley and Wolfson (1975) based on a position from the SAS-3 experiment (Matilsky, 1975). Eachus (1975) has found from studying material in the Harvard plate stacks that the optical object erupted once in the past and may be a recurring novae. Especially because of this latter observation, there is a great temptation to fit the transient X-ray sources in with the classical novae and describe them as the explosive phase of a mass accreting white dwarf. However, there is no evidence for this, except the obvious analogy. An example of an alternate hypothesis as discussed by Van Horn and Hansen (1974) is that this is a classical novae in the sense that hydrogen rich

TABLE 1. CHARACTERISTICS OF IDENTIFIED X-RAY SOURCES

Name	Binary Period	Optical Companion	Remarks
3U1956 + 35	Cyg X-1	9 mag 0.97lb	
1118 - 60	Cen X-3	13 mag B0Ib-III	4.8 sec X-ray pulse period
0900 - 40	Vela XR-1	6 mag B0.5Ib	284 sec X-ray pulse period
1700 - 37		6 mag 07f	
0115 - 37	SMC X-1	13 mag B0Ib	
1617 - 15	Sco X-1	?	
1653 + 35	Her X-1	15m late A	HZ-Her. 1.2 sec pulse period
2030 + 40	Cyg X-3	-	Heavily obscured, seen only $\lambda \approx 1\mu$
2142 + 38	Cyg X-2	? 14 mag G	

material accretes onto a compact star and eventually burns explosively, however, instead of the compact star being a white dwarf, it is a neutron star. The optical emission would result from the explosively driven material and would closely mimic what is seen from traditional novae. The X-ray emission could simply result from the hot surface of the neutron star.

By now we have identified the following systems or conditions that lead to observable cosmic X-radiation; blast waves from supernova remnants, ultra-relativistic electrons in supernova remnants, radio pulsars, accretion onto neutron stars and black holes, flare stars, cataclysmic variables, stellar coronae, and hot white dwarfs. In addition there are literally dozens of other possibilities that have been proposed but not yet observed. It is likely that we have only just begun to unravel the diversity of physical conditions leading to X-ray emission from galactic objects.

REFERENCES

- Bahcall, J.N., and Bahcall, N.A., 1974, in "Astrophysics and Gravitation", Proceedings of the 16th Solvay Conference, Editions de L'Université de Bruxelles, Bruxelles, Belgique, p. 73.
- Bahcall, J.N., and Ostriker, J.P., 1975, *Nature* 256, 23.
- Boley, F. and Wolfson, R., 1975, IAU Circular #2819, August 19.
- Clark, G.W., Markert, T.H., and Li, F.K., 1975, *Astrophys. J.* 199, L93.
- Clark, G.W., 1975, *Astrophys. J.* 199, L143.
- Eacius, L.J., 1975, IAU Circular #2823, 27 August (reported by W. Liller).
- Elvis, M., Griffiths, C.G., Turner, M.J.L., and Page, C.G., 1975, IAU Circular #2814, August 8.
- Eyles, C.G., Skinner, G.K., Willmore, A.P., and Rosenberg, F.D., 1975, IAU Circular #2787, June 2.
- Giacconi, R., 1974, in "Astrophysics and Gravitation", Proceedings of the 16th Solvay Conference, Editions de L'Université de Bruxelles, Bruxelles, Belgique, p. 27.
- Giacconi, R., Murray, S., Gursky, H., Kellogg, E., Schreier, E., Matilsky, T., Koch, D., and Tananbaum, H., 1974, *Astrophys. J. (Suppl.)* 237, 27, 37.
- Gorenstein, P., 1974, in "Supernovae and Supernova Remnants" (C.B. Cosmovici, ed.), D. Reidel, Dordrecht, Holland, p. 223-242.
- Gursky, H., 1973, in "Black Holes" (DeWitt and DeWitt, eds.), Gordon and Breach, New York, p. 291.

- Gursky, H. , 1975, presented at IAU Symposium No. 73, Close Binary Systems, Cambridge, England, to be published.
- Gursky, H. and Schreier, E. , 1975, in "Black Holes, Neutron Stars, and Binary X-Ray Sources" (H. Gursky and R. Ruffini, eds.), D. Reidel, Dordrecht, Holland, p. 175.
- Hutchings, J.G. , Cowley, A.P. , Crampton, D. , Redman, R.O. , 1974, *Astrophys. J.* 191, L101.
- Ives, J.C. , Sanford, P.W. , and Burnell, S.J. , 1975, *Nature* 254, 578.
- Markert, T.H. , Backman, D.E. , Canizares, C.R. , Clark, G.W. , and Levine, A.M. , 1975, *Nature* 257, 32.
- Matilsky, T. , 1975, IAU Circular #2819, August 19.
- Mewe, R. , Heise, J. , Gronenschild, E.H.B.M. , Brinkman, A.C. , Schrijver, J. , and den Boggende, A.J.F. , 1975, *Astrophys. J.* (Letters) to be published.
- Rees, M. , 1974, in "Astrophysics and Gravitation", Proceedings of the 16th Solvay Conference, Editions de L'Université de Bruxelles, Bruxelles, Belgique, p. 97.
- Silk, J. , and Arons, J. , 1975, *Astrophys. J.* (Letters) 200, L131.
- Van den Heuvel, E. , and Heise, J. , 1972, *Nature Physical Sci.* 239, 67.

DISTRIBUTION OF LOW LATITUDE SOURCES 3U CATALOG

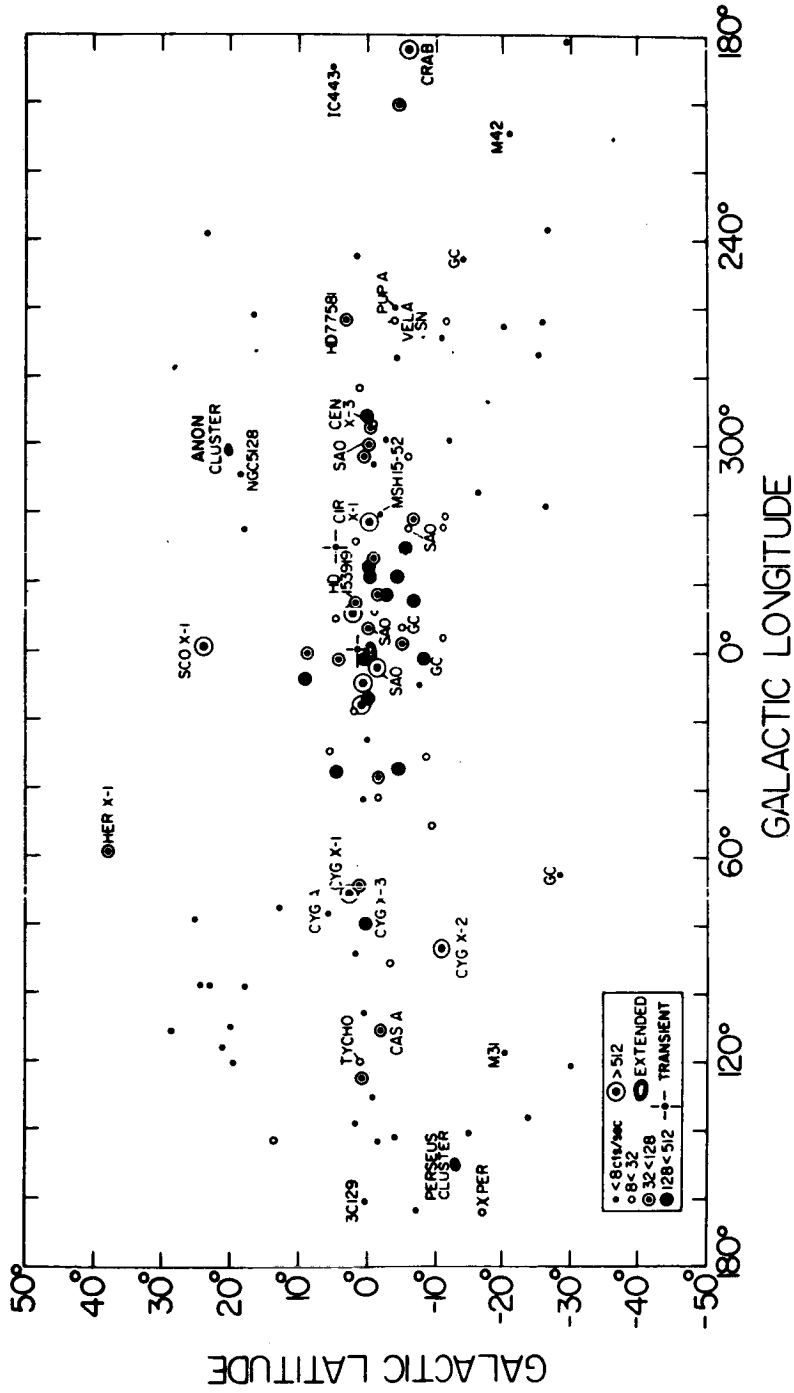


Figure 1. Plot of X-ray sources from the 3U catalog (Giacconi et al, 1975) in galactic coordinates. With the exception of Her X-1 only sources with $b < 30^\circ$ are plotted.

DISTRIBUTION OF WEAK, LOW-LATITUDE SOURCES
3U CATALOG

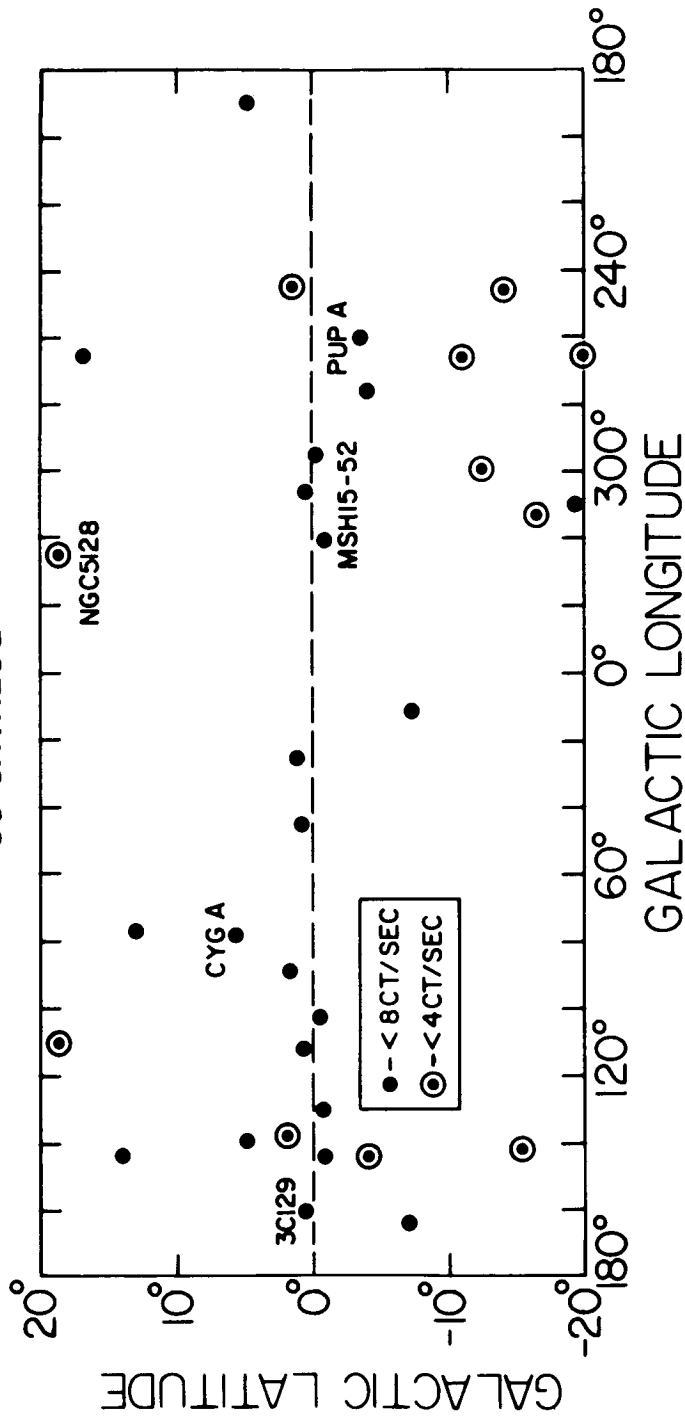


Figure 2. Plot of weak low latitude X-ray sources from the 3U catalog. There is a significant excess of sources between $5^\circ < b < -5^\circ$ which are likely of galactic origin.

OPTICAL OBSERVATIONS OF WRA 977
(3U 1223-62?)

D.J. Bord* and D.E. Mook*
Department of Physics and Astronomy
Dartmouth College
Hanover, New Hampshire 03755

and

L. Petro* and W.A. Hiltner*
Department of Astronomy
University of Michigan
Ann Arbor, Michigan 48104

ABSTRACT

UBV photometry of WRA 977 on 36 nights between January and July of 1974 shows that this object is active on a time scale of days at the 0.1 mag level, but that it remains quite constant during monitoring intervals lasting up to 1 hour. Periodogram analysis reveals no significant periodic variation in the brightness of this object.

INTRODUCTION

Although x-ray observations of 3U 1223-62 do not indicate that this source is part of a binary star system (Ricker *et al.* 1973 and McClintock *et al.* 1971), Mauder (1974) has reported that his observations of WRA 977, the optical object suggested for association with 3U 1223-62 (see Vidal 1973 and Jones *et al.* 1974), are consistent with a $\cos 2\theta$ variation of period 13^d5. In an attempt to confirm this result, we have observed WRA 977 photometrically during the period 1974 January-July, and we report our data to indicate the nature of the brightness variability of this star. As suggested above, it is of interest to look for periodic fluctuations in the light curve of this object since the majority of the identified x-ray sources have been shown to be members of binary systems whose brightness varies cyclically with time.

THE OBSERVATIONS

The data consist of 36 nights of differential photometry (see Hardie 1962) in the V band using a regional standard star whose constancy has been checked. Figure 1 shows a sample of monitoring of WRA 977 on 1974 April 19 UT. The magnitude difference, ΔV , is taken in the sense $\Delta V = V_{\text{WRA977}} - V_{\text{STANDARD}}$ and each point is a 5 s integration. The standard deviation of the points about the mean magnitude is 0.005 mag, and agrees with that expected for each point from a Poisson distribution, indicating that the scatter in the data is due primarily to photon statistics. This type of monitoring was carried out on 6 nights for intervals of up to 1 h, and all the observations confirm the results shown in

* Visiting Astronomers, Cerro Tololo Inter-American Observatory, which is operated by the Association of Universities for Research in Astronomy, Inc., under contract with the National Science Foundation.

Fig. 1. Our conclusion is that WRA 977 shows little activity at the 0.01 mag level on time scales of 1 h or less, in agreement with Mauder's (1974) findings.

LIGHT CURVE ANALYSIS

We have examined our data for evidence of a periodic component in the light curve of WRA 977. Using the technique of Gray and Desikachary (1973), we searched for periodicities in the nightly mean magnitudes in the range 0.05 to 0.25 cycles/day. Our analysis revealed a strong component in the periodogram with a frequency of 0.113 cycles/day and a corresponding period of 8.85 days. A least squares fit to the data using a sinusoid in this frequency gave an amplitude of 0.022 mag; the r.m.s. scatter of the data about the sine curve was 0.021 mag (see Fig. 2). Clearly, since the amplitude of the least squares fit is comparable to one standard deviation, the disagreement between the observations and the computed light curve shown in Fig. 2 is not surprising.

Although the results described above strongly suggest that there is no periodic variation of significant amplitude in our data, we performed one final check by folding the nightly means modulo 8^d85 . Our findings are shown in Fig. 3 where zero phase is taken to coincide with our first observation on JD 2442073.76. At any given phase, the scatter in the data is comparable to the amplitude of any mean curve one might be tempted to draw through the points, and argues against the existence of an 8^d85 variation in the light curve of WRA 977.

In order to determine whether WRA 977 exhibited any periodic fluctuations in brightness prior to the start of our observations in 1974, we also performed a periodogram analysis on van Genderen's (1973) data as read from a 2x enlargement of his graphical presentation. The results indicated the presence of a periodic component with a period of 11^d5 , but again, a comparison of the data with the best least squares fit to a sinusoid in the primary frequency revealed large differences between the two, not unlike those found in Fig. 2.

CONCLUSIONS

It would appear that van Genderen's characterization of WRA 977 as an irregular variable is correct in so far as neither the 13^d5 cycle reported by Mauder or any other significant periodic variation in either our data or that of van Genderen has been found. At best, there is a suggestion that this object may be varying in a quasi-periodic fashion such that low amplitude periodic fluctuations of a given frequency persist for a few cycles and then disappear. However, more observations will be needed before this behavior can be confirmed, especially if the time scale of the cyclic variations is of the order of 10 days.

The authors wish to thank the Astrophysical Journal (© by the American Astronomical Society. All rights reserved.) and the University of Chicago Press for granting permission to reproduce Figs. 1 and 2 from a paper by Bord *et al.* (1976).

REFERENCES

- Bord, D.J., Mook, D.E., Petro, L., and Hiltner, W.A. 1976, Ap.J. (in press).
- Gray, D.F., and Desikachary, K. 1973, Ap.J., 181, 523.
- Hardie, R.H. 1962, in Astronomical Techniques, ed. W.A. Hiltner (Chicago: University of Chicago Press), p. 178.
- Jones, C.A., Chetin, T., and Liller, W. 1974, Ap.J. (Letters), 190, L1.
- Mauder, H. 1974, I.A.U. Circ. No. 2673.
- McClintock, J.E., Ricker, G.R., and Lewin, W.H.G. 1971, Ap.J. (Letters), 166, L73.
- Ricker, G.R., McClintock, J.E., Gerassimenko, M., and Lewin, W.H.G. 1973, Ap.J., 184, 237.
- van Genderen, A.M. 1973, Info. Bull. on Var. Stars No. 856.
- Vidal, N.V. 1973, Ap.J. (Letters), 186, L81.

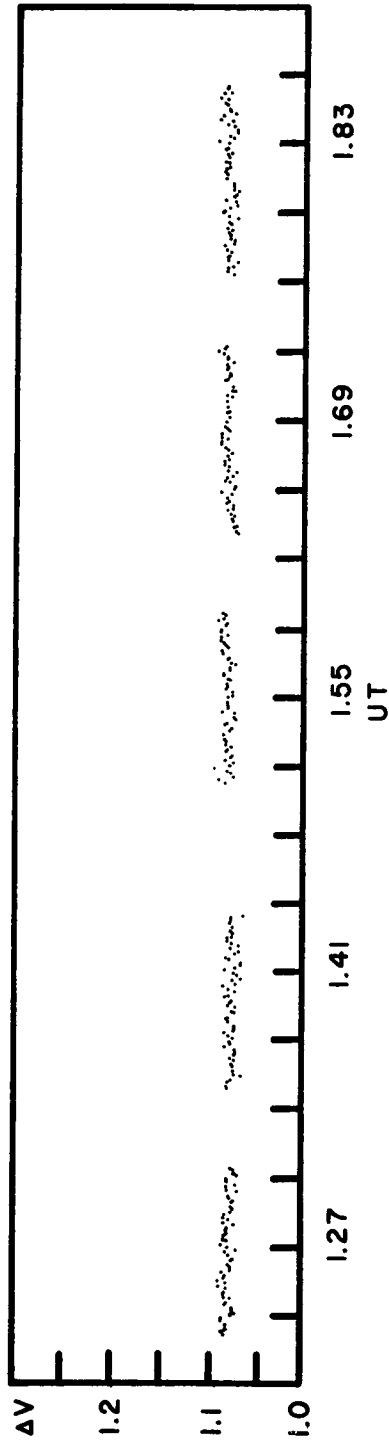


Figure 1. V-magnitude monitoring of WRA 977 on 1974 April 19 UT. Each point is a 5 s integration with a standard deviation (computed from Poisson statistics) of less than 0.004 mag.

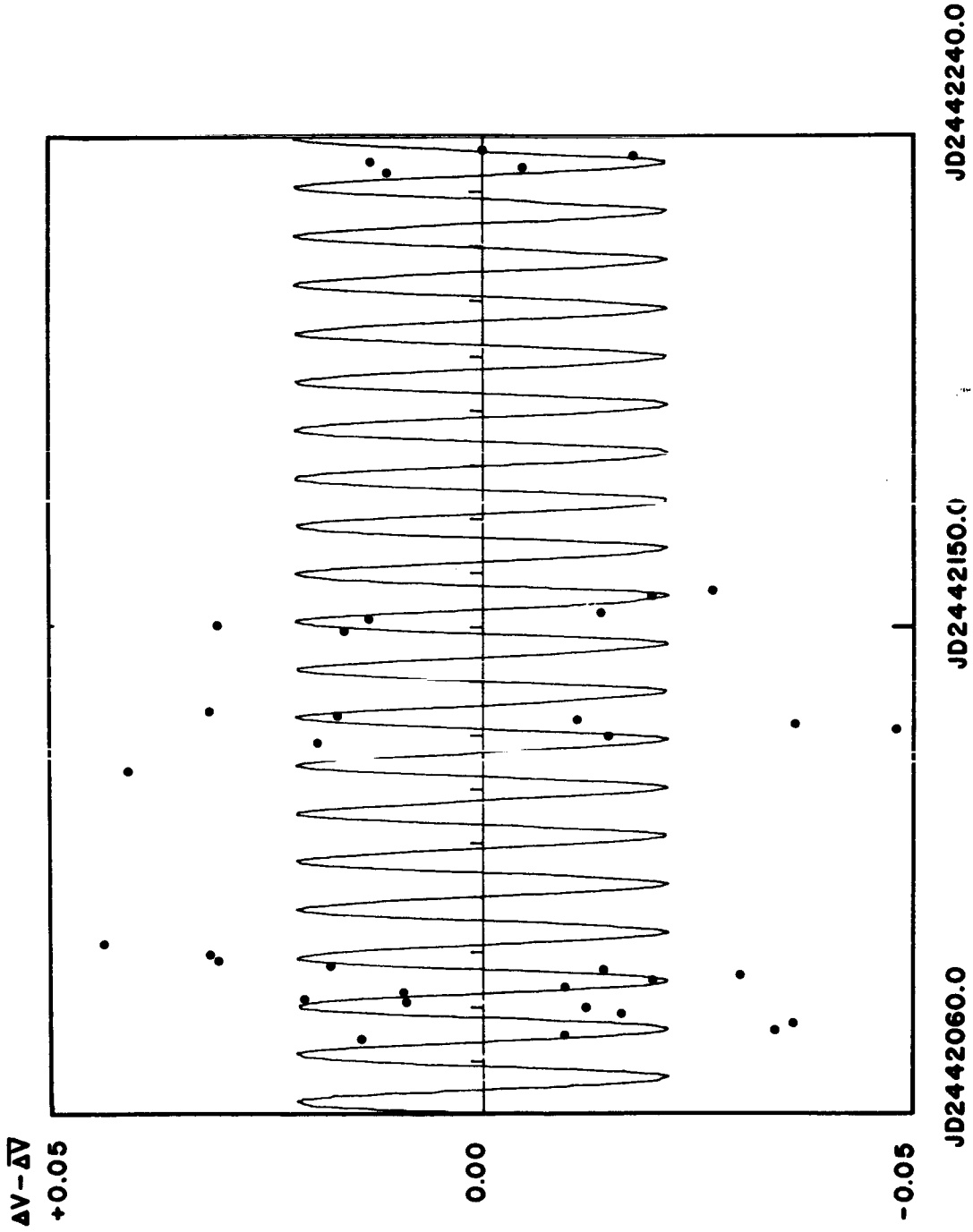


Figure 2. Least squares fit to our data using a sinusoid of frequency 0.113 cycles/day. $\Delta V - \overline{\Delta V}$ is the difference between the nightly mean values of ΔV and the average of this quantity for each data run. The amplitude of the sinusoid is 0.022 mag, and its phase on JD 2442114 is 67%.

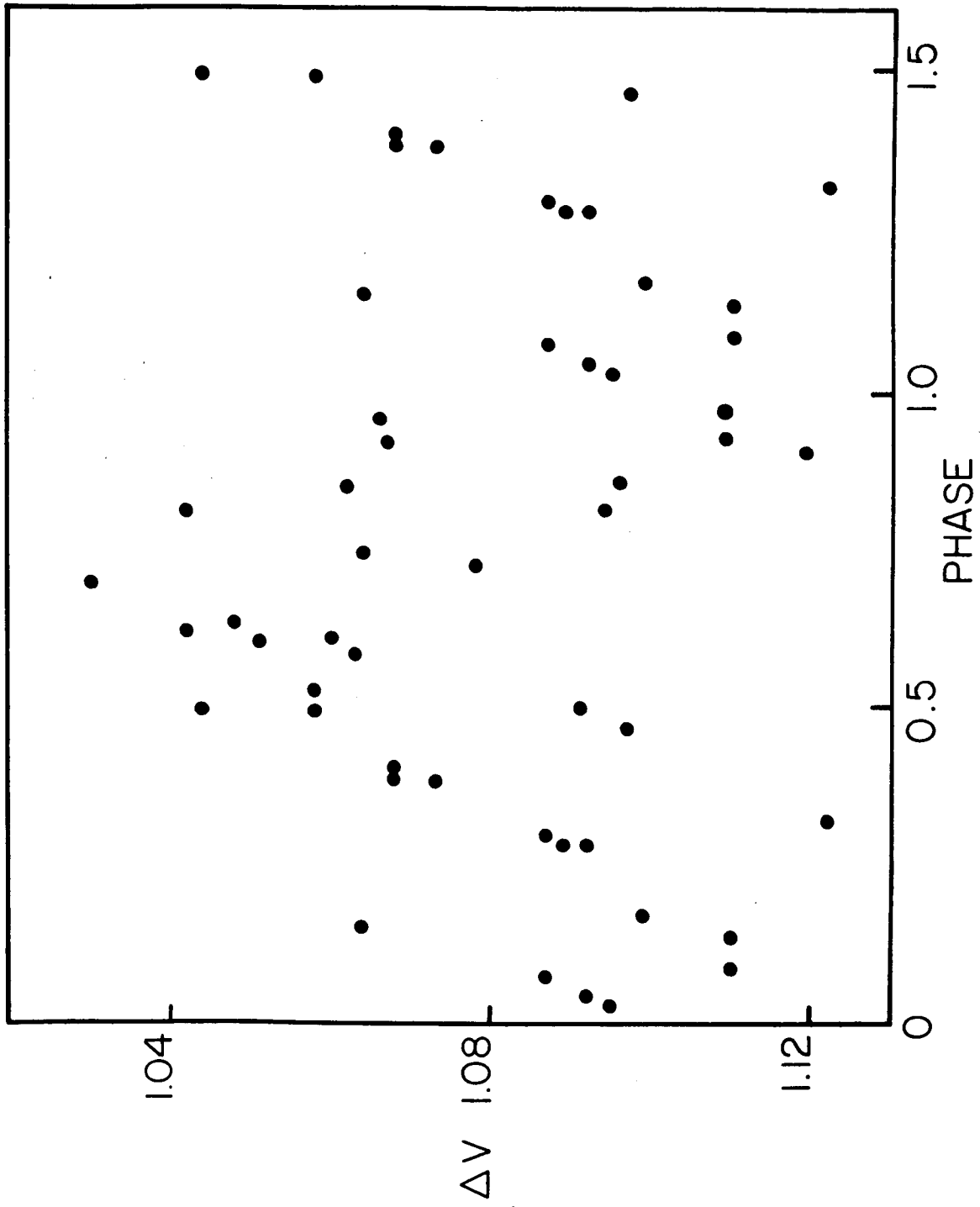


Figure 3. Nightly mean values of ΔV folded modulo 85. Zero phase is taken to occur on JD 2442073.76, and the accuracy of the magnitude differences is better than 0.01 mag in all cases.

THE INTERACTING BINARY SCO X-1

Anne P. Cowley and David Crampton
Dominion Astrophysical Observatory
R.R.#7, Victoria, B.C.
V8X 3X3.

ABSTRACT

New spectroscopic observations of Sco X-1 show conclusively that the emission lines vary in radial velocity with a period of $.787^d \pm .006$ and a full range of $\sim 120 \text{ km s}^{-1}$. The period is identical to that found by Gottlieb *et al* (1975) from photometric data; light minimum occurs when the emission line region is at superior conjunction. The observations indicate that the emission lines originate in an accretion disk surrounding a neutron star which is orbiting about a normal, although somewhat evolved companion. The light variation is due to a heating effect on the non-degenerate star, viewed at a small inclination angle. Various arguments are used to show that the most probable masses for the degenerate (neutron) star and the somewhat evolved companion are $\sim 1.4 M_{\odot}$ and $\sim 1.0 M_{\odot}$ respectively.

INTRODUCTION

A brief discussion of the results from recent spectroscopic observations are given in this paper; a more detailed account of this work is in press (Cowley and Crampton 1975; Crampton, Cowley, Hutchings and Kaat 1976). Approximately 70 spectrograms (42 Å/mm) were obtained at KPNO with the 2.1m telescope using the image tube spectrograph on the nights of 1975 June 2, 3, 4 and 8. These have been measured for radial velocity using the oscilloscope display machine at the DAO and rectified intensity tracings have been made to study the line profile and intensity variations.

SPECTRUM AND VELOCITIES

The spectrum consists of a blue continuum with strong emissions of He II ($\lambda 4686 \text{ \AA}$) and N III ($\lambda 4640-50$ blend) plus weaker emissions of H, He II, He I, C III, NV, Si IV, and others. The H emission is noticeably variable in intensity, at times being virtually absent. We find no evidence for any absorption features (other than interstellar) between $\lambda 3800-5000 \text{ \AA}$.

Figure 1 shows the measured velocities of He II $\lambda 4686 \text{ \AA}$, the strongest and least blended feature in the spectrum. Each point represents the velocity from one spectrogram. A sine curve is superimposed with $P = 0^d787$. A search was made for other periods which might fit this data -- no others were found in the range $0^d1 = 12^d0$. The observations are assembled in a velocity/phase diagram in fig. 2.

The hydrogen lines are considerably weaker and suffer serious blending problems with other features, but they do vary with the same period and phase and approximately the same amplitude and systemic velocity as He II 4686 \AA . We conclude these lines are formed around the same object as the He II.

MODEL AND MASSES

In Table 1, we present the formal orbital elements based on the He II emission velocities. A small eccentricity ($e = 0.12 \pm 0.04$) is derived when a solution for all six elements is made. We have fixed $e = 0$ (circular orbit), and suggest any formally derived eccentricity is probably spurious. We note that the more precise period found by Gottlieb *et al* ($P = .787313^d$) falls within the error of our determination.

Because the light curve (Gottlieb *et al*, 1975) shows one minimum at the conjunction when the emission object is behind, we infer that the $.2^m$ modulation is primarily due to a heating effect on the non-degenerate companion. Thus the emission lines are formed either (1) around the X-ray source itself or (2) on the heated face of its companion. However if (2) is correct, then the center of mass of the system must lie within the companion to Sco X-1. This requires a large mass ratio in turn implying either large values of i or very high masses, both of which can be excluded considering the small light amplitude and the relatively short period. We therefore conclude that the emissions are formed in a region (the accretion disk) about the X-ray source itself and move with it.

In Table 2 we list possible masses of the components for assumed values of i . We also compute the radius of the Roche lobe about the secondary star (R_2 Roche) for the given values of q and i , and the radius of a main sequence star of mass M_2 (R_{M_2}). We expect the secondary star fills its Roche lobe, and transfers material to the neutron star through the inner Lagrangian point (Tannanbaum and Hutchings 1974). The numbers in Table 2 indicate that no normal main sequence star, which would be faint enough not to be spectroscopically visible, comes close to filling its Roche lobe even for small inclinations. We therefore suggest the secondary is a slightly evolved star, having reached the Roche limiting surface only after leaving the main sequence. Mass transfer at this stage would be very rapid, perhaps accounting for the scarcity of such objects.

Limits to the value of i and the individual masses can be obtained in several ways. A value of $i < 65^\circ$ is inferred by the absence of eclipses, and even smaller values are suggested by the absence of phase-dependent variations of the weak emission spectrum and from the small amplitude of the light variations. On the other hand, the masses become unacceptably high if $i < 15^\circ$. The X-ray source itself is likely to be a neutron star, indicating a mass in the range $1 - 2 M_\odot$. The mass of the secondary is probably less than $1.5 M_\odot$, since a more massive star would be spectroscopically visible. Further, if one adopts a distance (best estimates are $1 - 2$ kpc), then the observed X-ray flux places limits on the mass, assuming the accretion rate is at the Eddington limit. Adopting a probable mass for the neutron star of $1.4 M_\odot$, we estimate the secondary lies between 1.0 and $1.2 M_\odot$. We emphasize the secondary must be evolved to fill its Roche lobe. Furthermore the small amplitude of the heating effect suggests that there could be considerable attenuation of the X-rays in the orbital plane, or that the accretion disk itself contributes a large percentage of the total light.

A HOT SPOT IN THE ACCRETION DISK

The He II 4686 line shows considerable structure at the peak. Crampton et al tabulate He II velocities for both the emission line center and the peak, and show that there is a systematic difference in these velocities. The velocity behaviour suggest that the peak of the line is formed in a hot spot on the following side of the accretion disk, where material streaming from the mass-losing star hits the accretion disk. The ΔV (velocity peak-center) implies an observed rotation of the disk at this height of $\sim 50 - 60 \text{ km s}^{-1}$. The total width of $\lambda 4686 \text{ \AA}$ implies a rotation of $\sim 700 \text{ km s}^{-1}$ closer to the neutron star. If $i \sim 30^\circ$, the true rotational velocities will be twice these values. At phase 0 (when the hot spot is viewed directly) the peak is central, and at phase .5 there is a reversal in the peak, perhaps implying self absorption when the hot spot is viewed on the far side of the accretion disk.

EMISSION LINE INTENSITIES

Equivalent widths and intensities have been measured for all of the lines. These are discussed in detail by Crampton et al. Because of the small amount of overlap in phase of this data, it is not possible to tell if the variations in strength are periodic. Further observations are needed to test this. In Fig. 3 we plot W_λ vs phase for this data from H γ , He II 4686, and N III blend. Because we do not have simultaneous photometry, these values have not been corrected for a probable change in the continuum strength. We find that the largest variations in strength occur when the emissions are strongest and that the H lines vary over a greater range than the He II and other lines.

SUMMARY

Details of the above work can be found in Cowley and Crampton (1975) and Crampton et al (1976). It is curious that the binary nature of this extremely bright X-ray source has been so elusive. The (lower quality) published velocities of Westphal et al (1968) and Crampton and Cowley (1975) do not fit this period. We suggest that there may be times when the star is more or less quiescent (not flaring) when these velocity variations are more easily detected, and that we were fortunate to observe the system at such a time.

We note that the systemic velocity is very high (-145 km s^{-1} with respect to the local standard of rest), so that Sco X-1 may belong to the old disk population, as do the spectroscopically similar old novae.

In summary this new data show that Sco X-1 is a short period ($P = .787^d$) spectroscopic binary consisting of a neutron star (assumed to be about $1.4 M_\odot$) with a dense accretion disk and a mass-losing, slightly evolved star of about $1 M_\odot$.

REFERENCES

- Cowley, A.P. and Crampton, D. 1975 Ap.J. (Letters) (Oct. 15).
- Crampton, D., and Cowley, A.P. 1975 Ap.J. 197, 467.
- Crampton, D., Cowley, A.P., Hutchings, J.B. and Kaat, C. 1976 Ap.J. (submitted)
- Gottlieb, E.W., Wright, E.L., and Liller, W. 1975 Ap.J. (Letters), 195, L33.
- Tananbaum, H.D. and Hutchings, J.B. 1974 Seventh Texas Symposium on Relativistic
Astrophysics
- Westphal, J., Sandage, A. Kristian, J. 1968 Ap.J. 154, 139.

TABLE 1

ORBITAL ELEMENTS FOR SCO X-1

$$P = 0.7874 \pm .0058^d$$

$$K = 58.2 \pm 3.0 \text{ km s}^{-1}$$

$$V_o = -138.5 \pm 3.0 \text{ km s}^{-1}$$

$$e = 0 \text{ (fixed)}$$

$$T_o = \text{JD } 2442565.741 \pm .013^d$$

standard deviation of fit = 15.9 km s^{-1}

number of observations = 62

TABLE 2.

Possible Masses and Radii of Sco X-1

	$q = M_1/M_2^*$	M_1	M_2	R_2 Roche (10^5 km)	R_{M_2} (10^5 km)
$i = 60^\circ$	1	.1	.1	5.4	.6
	2	.4	.2	6.8	1.3
	3	1.2	.4	8.1	2.7
	4	2.5	.6	9.4	4.1
$i = 45^\circ$	1	.2	.2	6.7	1.3
	2	.8	.4	8.3	2.7
	3	2.2	.7	10.0	4.8
	4	4.5	1.1	11.4	7.7
$i = 30^\circ$.5	.1	.3	8.3	2.0
	1	.5	.5	9.4	3.4
	2	2.3	1.2	11.8	8.5
	3	6.1	2.0	14.1	10.9
$i = 15^\circ$.1	.1	1.1	15.9	7.7
	.3	.5	1.6	15.5	9.1
	.5	1.1	2.1	16.1	11.2
	.8	2.4	3.0	17.3	15.0
	1	3.8	3.8	18.2	18.9

* M_1 defined as the emission line object

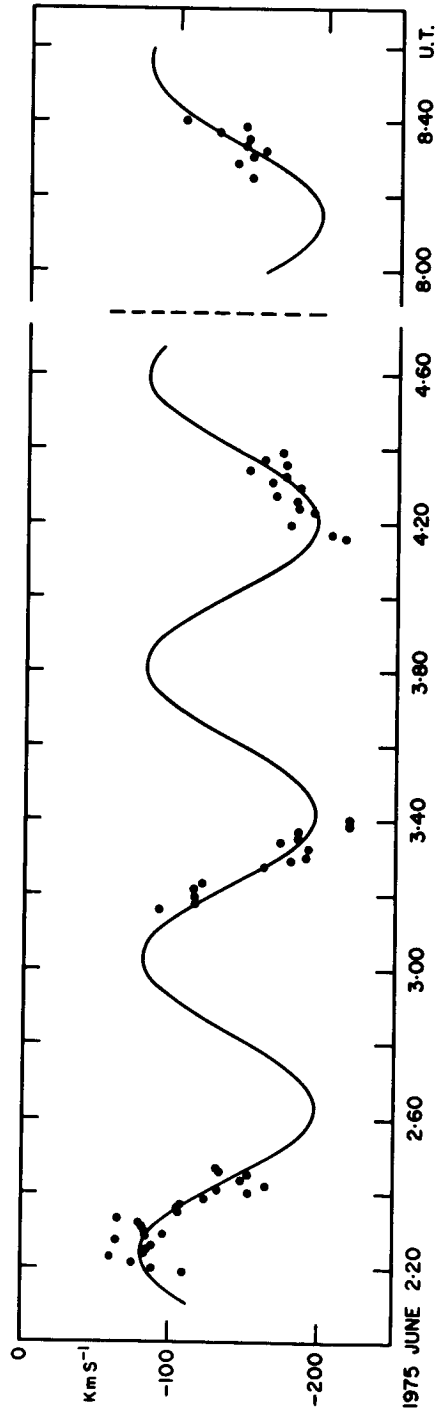


Fig. 1. Radial velocities of He II $\lambda 4686 \text{ \AA}$ plotted against UT. A sine curve with $P = 0.787$ is drawn through the points.

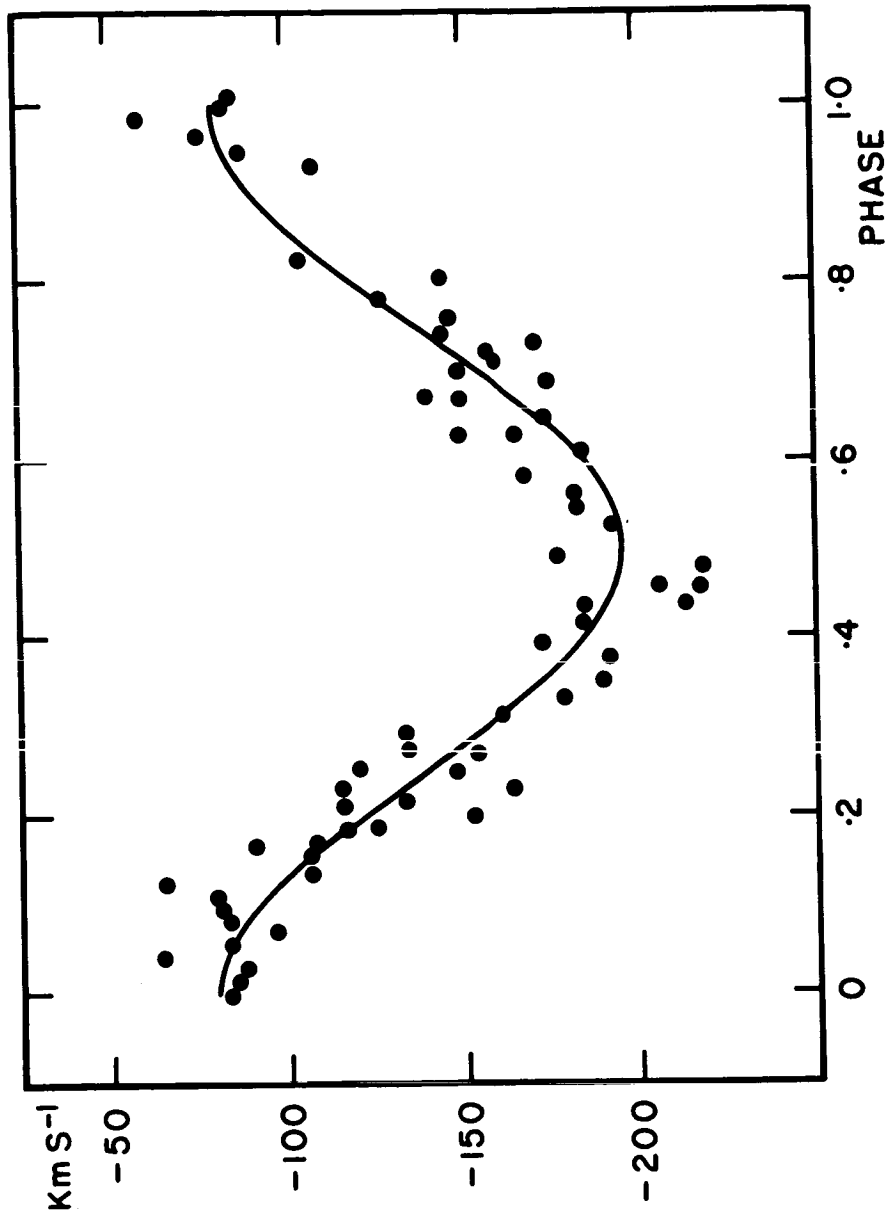


Fig. 2. The velocity/phase diagram for He II λ 4686 \AA with $P = 0^d.7874$.
The curve represents the fitted orbital elements (Table 1).

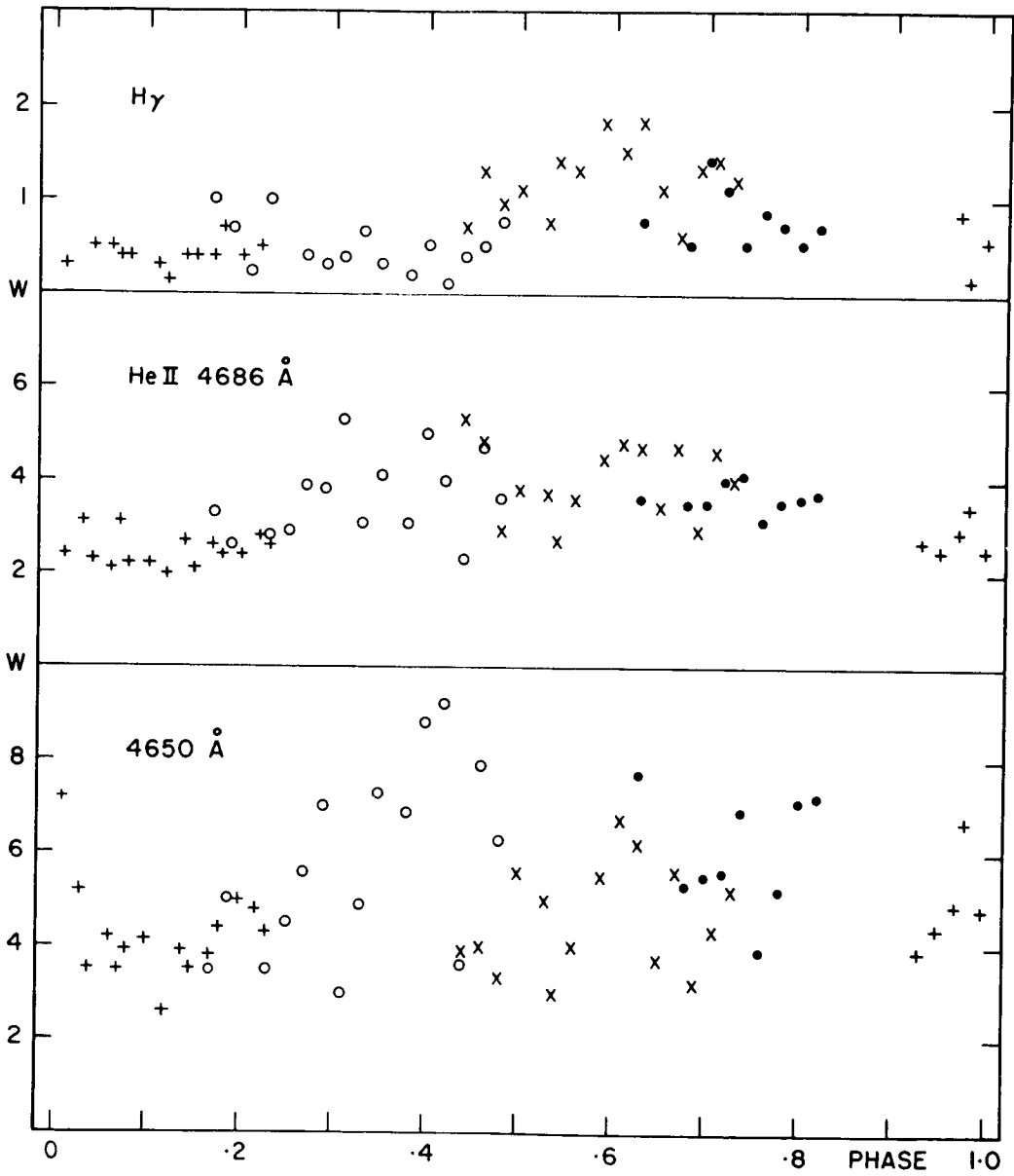


Fig. 3. Equivalent widths of various emission features plotted as a function of orbital phase. The observations from each night are shown by separate symbols.

SPECTROPHOTOMETRY OF THE UNUSUAL OPTICAL CANDIDATE

FOR 3U 1728-24 (=GX 2+5 = GX 1+4):

A RECURRENT NOVA ?

Arthur Davidsen
Department of Physics
The Johns Hopkins University
Baltimore, Maryland 21218

and

Roger Malina and Stuart Bowyer
Space Sciences Laboratory and Astronomy Department
University of California
Berkeley, California 94720

ABSTRACT

We have investigated the spectrum of the object suggested as a possible optical counterpart of GX 2+5 (Glass and Feast 1973), using the image tube scanner attached to the 3-m telescope of Lick Observatory. An improved x-ray error box obtained with Copernicus (Mason 1974) strongly supports this proposed identification. We find that the candidate displays all the characteristics of the symbiotic stars and the related recurrent novae. The spectrum reveals the presence of an M star together with a blue component and a large number of emission lines displaying a wide range of ionization. Among the emission lines identified or suspected are: H I, He I, O I, [O I], [O II], [O III], Na I, Fe II, [Fe VII], [Fe X], [A X], and [A XI]. There is evidence of variability of both the continuum and the line intensities.

This object provides strong support for the often proposed association of some x-ray sources with nova-like systems. We suggest that in GX 2+5 accretion on a compact companion of an M giant produces x-rays and ultraviolet radiation which ionizes a circumstellar nebula, perhaps ejected in a previous nova-like outburst.

INTRODUCTION

A hard x-ray source designated GX 1+4 was discovered by Lewin et al. (1971) and has subsequently been associated with the source 3U 1728-24 (Giacconi et al. 1974). This source has also been observed with the Copernicus x-ray telescope by Hawkins, Mason, and Sanford (1973), who derived an improved position and refer to it as GX 2+5. A further improvement of the position by Mason (1974) yields $\alpha = 17^{\text{h}} 28^{\text{m}} 58.3^{\text{s}}$, $\delta = -24^{\circ} 42' 50''$ (1950.0) with an error box smaller than 0.5 square arc min. This error box is shown along with several earlier ones in Figure 1, taken from Davidsen, Malina and Bowyer (1976).

Although 1728-24 is listed as non-variable in the 3U catalog (Giacconi et al. 1974), its flux in the 18-50 keV range is variable by factors of 2-4 over time scales of order one minute (Lewin et al. 1971). Lewin et al. suggest that the variation may be periodic with $P \approx 2.3$ minutes. The spectrum observed in 1970 could be fit by an exponential model with $kT = 28 \pm 12$ keV or by a power-law model with energy index $\alpha = 1.4 \pm 0.7$ (Lewin et al. 1971, Ricker et al. 1973). According to Ricker et al., the hard x-ray flux with $\alpha = 1.37 \pm 0.05$ in the range 23-400 keV observed by Johnson et al. (1972) in a wide-field balloon observation of the galactic center region may be due largely to GX 1+4. This object would then be the dominant hard x-ray source in the galactic center. No low energy x-ray spectrum has been reported for this source, but Hawkins et al. (1973) remark that it displays attenuation with respect to Sco X-1.

A bright infrared object displaying strong H α emission was discovered within the Hawkins et al. error circle by Glass and Feast (1973), who suggested it as a candidate for identification with the x-ray source on the basis of its peculiarity. The improved Copernicus error box, shown superposed on the red Palomar Sky Survey print in Figure 2, contains this object as the brightest image. It is the only object visible within the error box on the blue Sky Survey print of the field, which is very heavily reddened. Here we present spectrophotometry of this H α object, whose position and unusual spectrum now suggest quite strongly that it is the optical counterpart of 3U 1728-24.

OBSERVATIONS

Observations of the candidate were made with the image tube scanner (ITS) attached to the 3-m telescope of Lick Observatory on three nights in 1974 and 1975. Some details of the observations are given in Table 1. Although there is good evidence of variability, a weighted average of the three spectra has been formed in order to improve the detectability of weak features. The resulting spectrum is shown in Figure 3.

The overwhelming dominance of the spectrum by H α emission is the most striking feature of the data. The weighted mean flux in H α is $3.2 \times 10^{-13} \text{ erg cm}^{-2} \text{ s}^{-1}$. None of the other emission lines present has a flux which exceeds 0.03 F(H α). H β has a flux of $\sim 0.010 \text{ F(H}\alpha)$. After H α , the strongest lines present are He I $\lambda\lambda 5876, 6678, \text{ and } 7065$, and [Fe VII] $\lambda 5721$ and $\lambda 6086$. [O III] $\lambda\lambda 4959, 5007$ are clearly present and are weaker than H β . Numerous Fe II lines are also evident. A search for [Fe II] lines reveals no definite evidence of their presence, although there are some weak broad blends to which they might contribute. The He I lines increased in intensity by a factor of 2.6 between 1975 June and August while H α increased by a factor 1.6.

There is also evidence for lines of higher ionization states than [Fe VII]. The strong feature at $\sim \lambda 6370$ probably contains a contribution from [Fe X] $\lambda 6374$ in addition to Fe II $\lambda 6369$ and Si II $\lambda 6371$. These lines are unresolved in these observations, where the resolution is $\sim 10 \text{ \AA}$. The possible presence of [AX] $\lambda 5535$ and [A XI] $\lambda 6919$ supports the suggested presence of the [Fe X] coronal line. The [Fe XIV] $\lambda 5303$ coronal line is not present. Although accurate radial velocities cannot be obtained from these data, all of the suggested identifications are consistent with the radial velocity of $\sim -150 \text{ km s}^{-1}$ derived from the H and He lines. This is also in agreement with the H α velocity measured by Glass and Feast (1973).

In addition to emission lines displaying a wide range of ionization, the spectrum also reveals absorption features of an M star. Particularly evident is the strong blend of TiO and VO bands in the 7700 - 8000 \AA region. The TiO band at $\lambda 7054$ is also clearly present, although it is somewhat filled in by He I $\lambda 7065$ emission. The VO band at $\lambda 7345$ is also apparent. The presence of VO indicates the spectral type is M6 or later (Albers 1974). Comparison of the spectrum with those of RS Del (M6.5-7) and R Aql (M8.5), also obtained with the ITS, indicates a type \sim M6, although precise classification is hampered by the filling in due to emission lines and an underlying blue continuum. Luminosity classification is difficult based on these data, but an M dwarf can be ruled out. Our adopted type M6 III is consistent with the reddening and probable distance of this object discussed below.

REDDENING AND DISTANCE

The optical candidate for 3U 1728-24 is very heavily reddened. If we assume the intrinsic Balmer decrement is that appropriate to radiative recombination in Case B (Brocklehurst 1971), the observed ratio $H\alpha/H\beta \approx 100$ implies $E_{B-V} \approx 3.3$. This is almost certainly an upper limit since the true Balmer decrement may well be affected by collisional excitation and self-absorption.

Another estimate of the reddening can be obtained from the infrared colors measured by Glass and Feast and our result for the spectral type. The measured colors are $J-H = 1.54 \pm 0.13$ and $H-K = 0.75 \pm 0.11$. Using the intrinsic colors of M giants and the reddening relationships given by Lee (1970), we find $E_{B-V} = 1.7$. This result is illustrated in Figure 4. A value $E_{B-V} = 3.3$ would make the infrared colors inconsistent with an M type spectrum. We adopt $A_V = 3.6$ $E_{B-V} = 6.1$ (Lee 1970), which implies the intrinsic Balmer decrement is $H\alpha/H\beta \approx 17$.

The continuum observed in the yellow region of the spectrum cannot be provided by the M star, whose expected magnitude is $V(M6 III) = 20.7$. The observed values $V = 18.66$ and $V = 19.36$ then indicate that a variable blue component is responsible for most of the light observed in the V band. This component may be associated with the source of ionization for the high excitation emission lines.

The distance to the system can be derived from the spectral type and extinction found above. Assuming $M_V = -0.5$ for an M giant we find $d \approx 10$ kpc. Of course, this value is sensitive to A_V , which is not well determined. The corresponding x-ray luminosity, including both the Uhuru and 18-50 keV flux is $L_x \approx 4 \times 10^{37} d_{10}^2 \text{ erg s}^{-1}$, where d_{10} is the distance in units of 10 kpc. These results place the system very close to the galactic center and indicate an x-ray luminosity similar to that of other high luminosity x-ray sources (Margon and Ostriker 1973). The expected interstellar absorption corresponding to the observed reddening is $N_x \approx 1 \times 10^{22} \text{ cm}^{-2}$ (Ryter, Cesarky and Adouze 1975).

SYMBIOTIC STARS, RECURRING NOVAE, AND X-RAY SOURCES

The combination of high excitation emission features with an M type absorption spectrum is the defining characteristic of the symbiotic stars (Merrill 1950). The members of this class are all variable and include the recurring novae RS Oph and T CrB (cf. Swings 1970), whose spectra are very similar to that of the object discussed here (e.g. Joy and Swings 1945). T CrB has been established to be a binary, in which the M3 III component probably fills its Roche lobe and transfers matter toward a blue subdwarf companion (Kraft 1958). X-rays could be produced by such a system if the companion were a compact object. Photoionization of gas surrounding the system might then explain the occurrence of emission lines up to and including [Fe X].

Another line of argument also supports the connection between 3U 1728-24 and the nova-like optical object discussed here. The transient x-ray sources display a behavior quite similar to optical

novae. None of these sources has been optically identified until recently, when A 0620-00, by far the brightest transient x-ray source observed to date (Flavis et al. 1975, Matilsky 1975), was associated with a nova-like optical outburst (Boley and Wolfson 1975). The optical counterpart is apparently a recurrent nova which underwent a previous outburst in 1917 (Fachus, Wright and Liller 1975). Although its spectral characteristics at minimum light are as yet unknown, the pre-nova was a faint red object (Ward et al. 1975), suggesting a possible similarity to the 3U 1728-24 candidate discussed here.

That A 0620-00 might contain a red giant has been suggested at this symposium by Cowley (1975), who noted the redness of the pre-nova. Cowley suggested that the color indicates that most of the light from the system at minimum may be due to the red giant. However, analogy with the 3U 1728-24 candidate indicates the possibility that the very red color on the Sky Survey plates is due to strong H α emission. In that case the visual continuum might still come largely from the (presumably blue) compact component. We will have to wait until the system returns to minimum light to test these alternatives.

Our suggestion that 3U 1728-24 may be related to transient x-ray sources such as A 0620-00 implies that such sources are sometimes relatively quiescent x-ray emitters. An example of such an object is Aql X-1 (3U 1908+00), which underwent a large outburst in 1975 June (Buff 1975) after a long period of low activity (Davidsen et al. 1975). This source would have been classed as a transient if it had not previously been catalogued (Kaluziński et al. 1975).

CONCLUDING REMARKS

We have shown that the optical candidate for 3U 1728-24 is a composite object consisting of a red giant and a variable blue component. In addition, there are emission lines indicating a high degree of ionization which might be produced by photoionization of a shell of matter surrounding an embedded x-ray source. Such a shell could be the remnant of an earlier nova-like outburst. In view of these facts and the very small x-ray error box, the association of these two objects becomes extremely plausible. It would, of course, be desirable to observe correlated x-ray and optical variability in order to establish the relation conclusively. It would be particularly interesting to establish whether the optical object or the x-ray source have ever experienced a nova-like outburst. Such an outburst would provide an important link in the chain of arguments connecting "transient" x-ray sources and novae.

We are greatly indebted to Hy Spinrad for donating some observing time to this project and for his continuing interest and assistance.

REFERENCES

- Albers, H. 1974, Ap. J., 189, 463.
- Boley, F. and Wolfson, R. 1975, this symposium.
- Brocklehurst, M. 1971, M.N.R.A.S., 153, 471.
- Buff, J. 1975, I. A. U. Circ. No. 2788.
- Cowley, A. P. 1975, this symposium.
- Davidsen, et al. 1975, I. A. U. Circ. No. 2793.
- Davidsen, A., Malina, R., and Bowyer, S. 1976, Ap. J., 203, in press.
- Eachus, L. J., Wright, E. L., and Liller, W. 1975, this symposium.
- Elvis, M., Griffiths, C. G., Turner, M. J. L. and Page, C. G. 1975, I. A. U. Circ. No. 2814.
- Giacconi, R., Murray, S., Gursky, H., Kellogg, E., Schreier, E., Matilsky, T., Koch, D., and Tananbaum, H. 1974, Ap. J. Suppl., 27, 37.
- Glass, I. S., and Feast, M. W. 1973, Nature Phys. Sci., 245, 39.
- Hawkins, F. J., Mason, K. O., and Sanford, P. W. 1973, Nature Phys. Sci., 241, 109.
- Johnson, W. N. III, Harnden, F. R. Jr., and Haymes, R. C. 1972, Ap. J. (Letters), 172, L1.
- Joy, A. H., and Swings, P. 1945, Ap. J., 102, 353.
- Kaluzienski, L. J., Holt, S. S., Boldt, F. A. and Serlemitsos, P. J. 1975, this symposium.
- Kraft, R. 1958, Ap. J., 127, 625.
- Lee, Thomas A. 1970, Ap. J., 162, 217.
- Lewin, W. H. G., Ricker, G. R., and McClintock, J. E. 1971, Ap. J. (Letters), 169, L17.
- Margon, B. and Ostriker, J. 1973, Ap. J., 186, 91.
- Mason, K. O. 1974, private communication.
- Matilsky, T. 1975, I. A. U. Circ. No. 2819.

Merrill, P. 1950, Ap. J., 111, 484.

Ricker, G. R., McClintock, J. F., Gerassimenko, M., and Lewin, W. H. G.
1973, Ap. J., 184, 237.

Ryter, C., Cesarsky, C. J., and Adouze, J. 1975, Ap. J., 198, 103.

Swings, P. 1970, Spectroscopic Astrophysics, ed. G. Herbig, p.189
(Berkeley: Univ. of Calif. Press).

Ward, M. J., Penston, M. V., Murray, C. A., and Clements, E. D. 1975,
Nature, 257, 659.

Table 1

Spectrophotometry of the 3U 1728-24 Optical Candidate

Date	Wavelength Range \AA	V scanner	H α flux ($10^{-13} \text{ erg cm}^{-2} \text{ s}^{-1}$)
1974 July 14	4400-6700	18.66	3.0
1975 June 13	4800-7300	19.36	2.5
1975 August 12	5900-8250	-	3.9

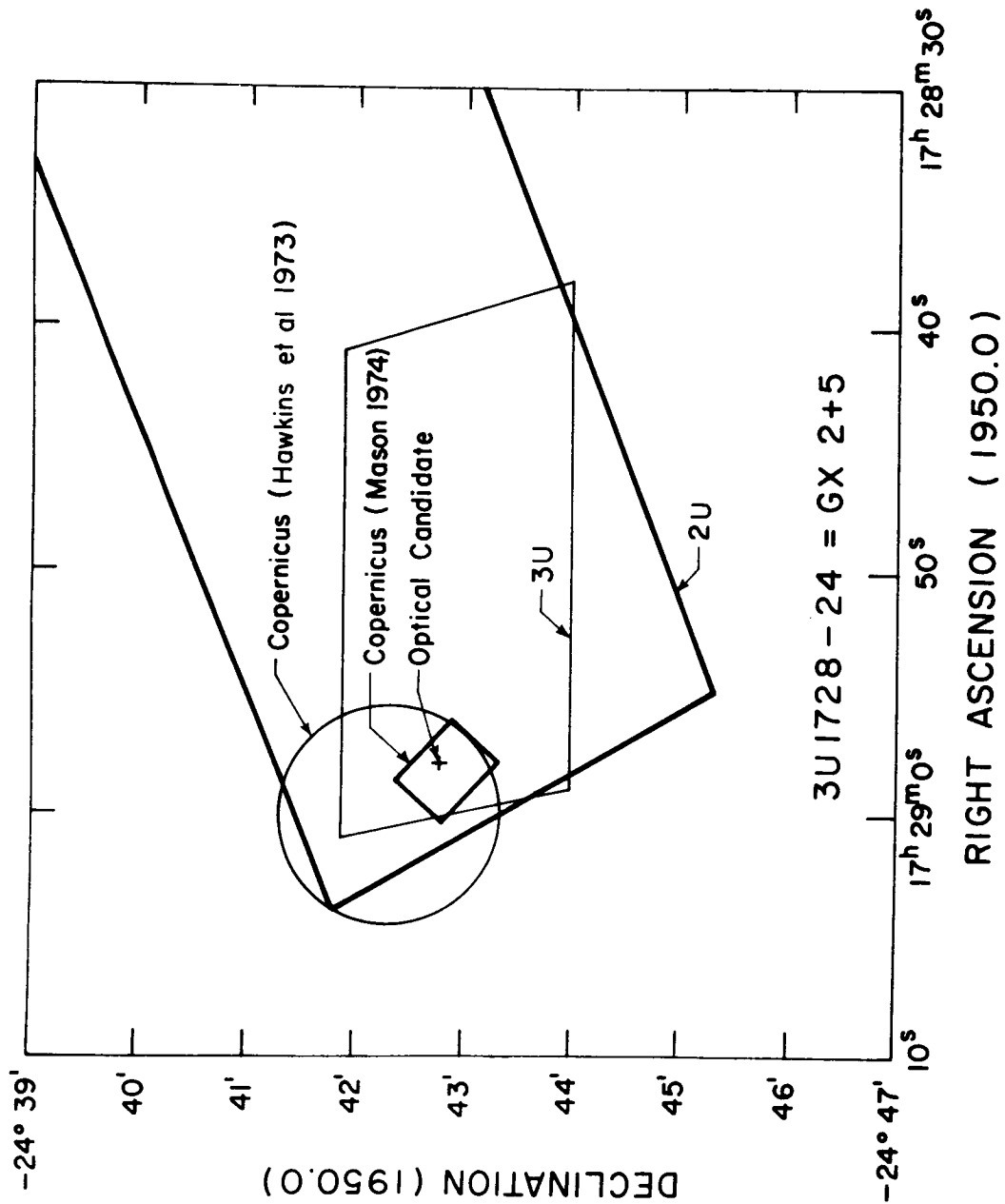
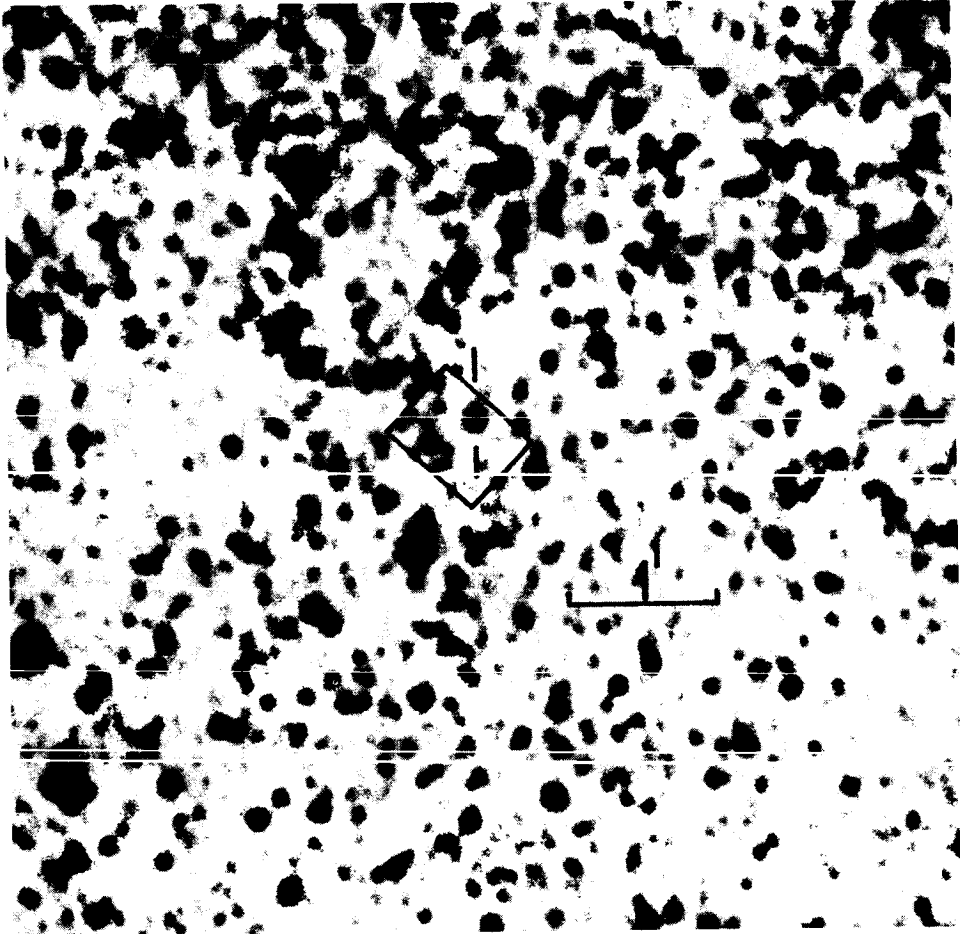


Figure 1 Error boxes for 3U 1728-24 (= GX 2+5 = GX 1+4). 90% confidence limits are shown. The position of the optical candidate discussed in the text is also indicated.



3U 1728-24

Figure 2 A finding chart for 3U 1728-24. The Copernicus error box is superposed on the red Palomar Sky Survey print, with north at the top and east to the left. The optical candidate is marked.

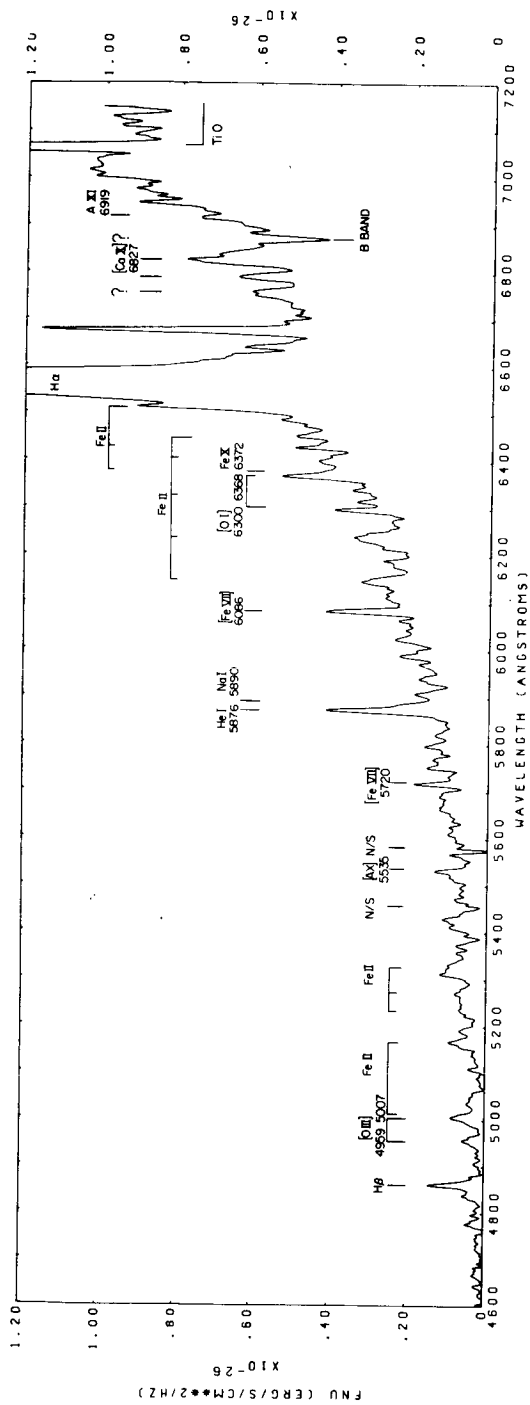


Figure 3a Spectrum of the 3U 1728-24 optical candidate in the wavelength range 4600-7200 Å. This is the weighted average of the three observations listed in Table 1, obtained with the Lick Observatory image tube scanner. Many of the most prominent emission lines have been labelled.

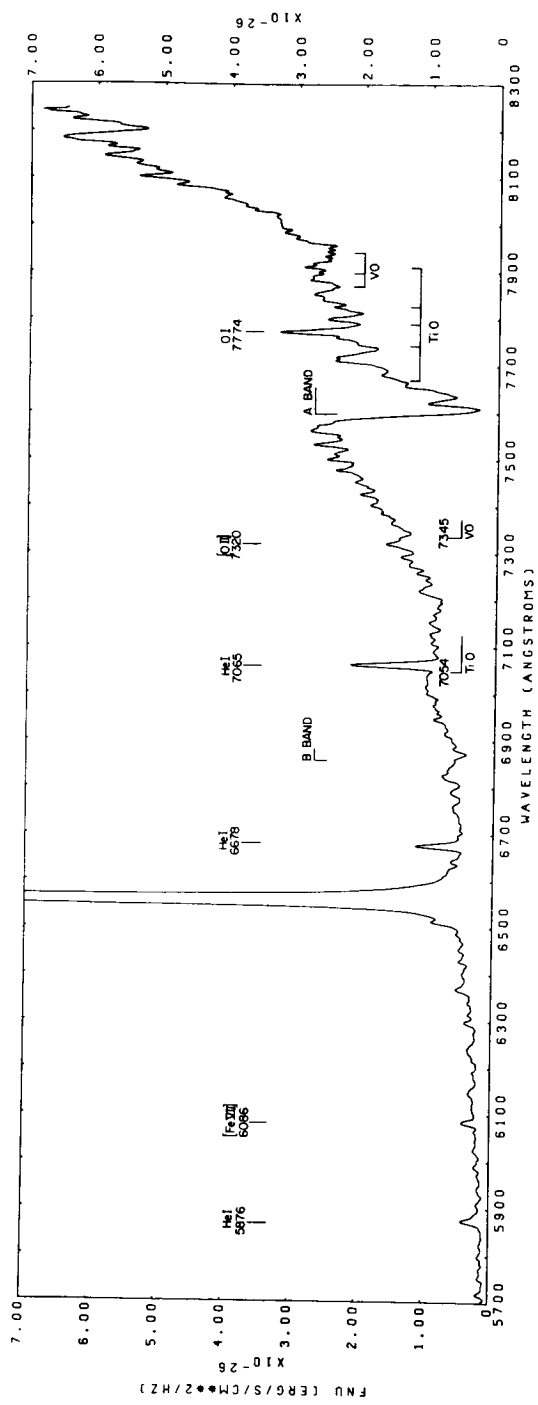


Figure 3b As in Figure 3a, but for the wavelength range 5700-8300 Å. In addition to the emission lines, the absorption bands of an M star are apparent, especially the large depression in the 7700-8000 Å region.

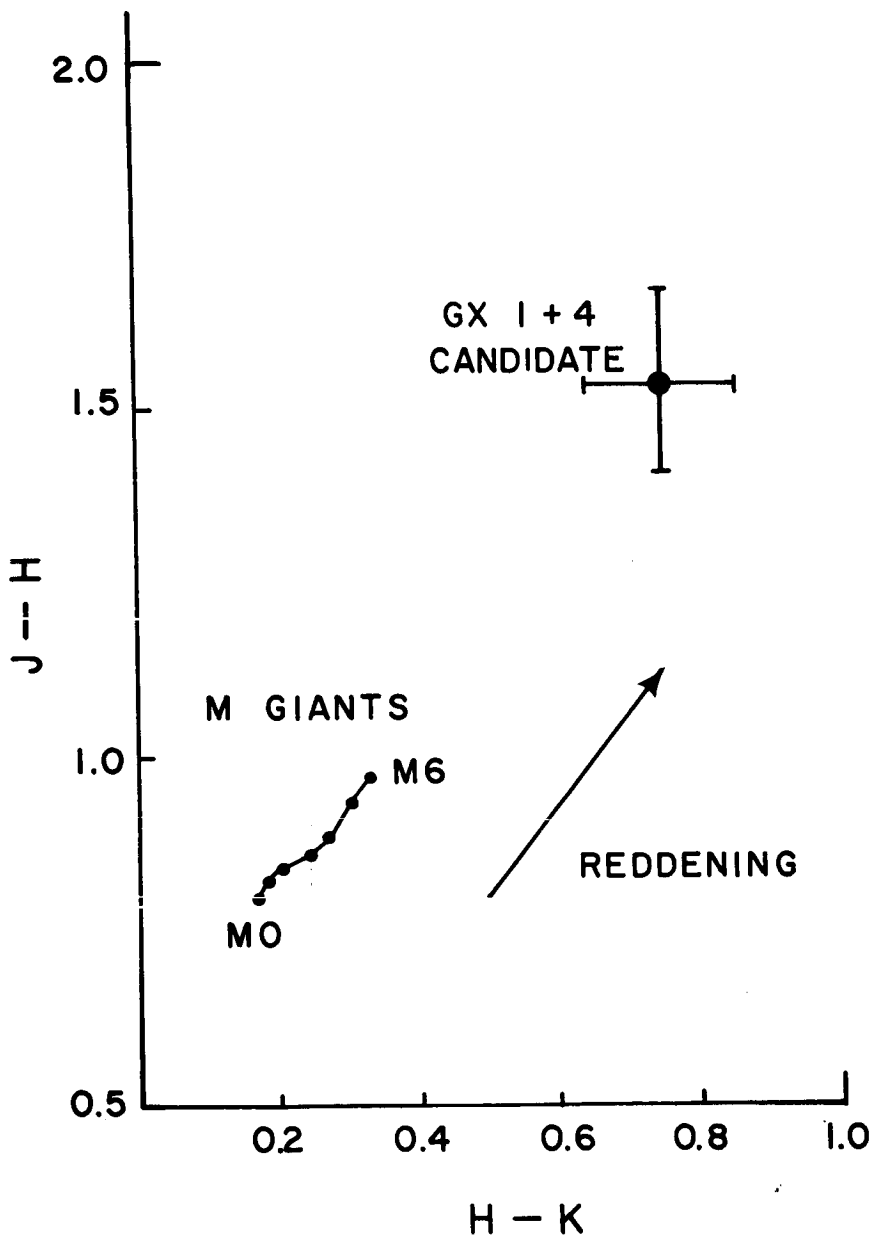


Figure 4 J-H vs. H-K for M giants and for the GX 1+4 optical candidate. The infrared colors for MO III to M6 III stars and the reddening line are from Lee (1970). The colors of the GX 1+4 candidate are from Glass and Feast (1973). For spectral type M6 III a reddening $E_{B-V} = 1.7$ is inferred.

Long-Term X-ray Studies of Sco X-1

S. S. Holt, E. A. Boldt and
P. J. Serlemitsos
NASA/Goddard Space Flight Center
Greenbelt, Maryland 20771

L. J. Kaluziński
University of Maryland
College Park, Maryland 20742

ABSTRACT

No modulation of the 3-6 keV x-ray intensity of Sco X-1 at a level of excess of 1% is observed at the optical period of .787313d. Evidence is found for shot-noise character in a large fraction of the x-ray emission. Almost all of the Sco X-1 emission can be synthesized in terms of ~ 200 shots per day, each with a duration of $\sim 1/3$ day.

Subject headings: x-ray sources -- binaries

I. INTRODUCTION

As Sco X-1 is, by far, the brightest x-ray source in the sky, searches for regularity in its temporal behavior have been undertaken for almost a decade. As yet, no reproducible regularity in x-rays has been observed on any timescale (c.f. Canizares, et al. 1975, Holt, et al. 1973, and included references).

More recently a convincing periodicity of 0.787313d has been discovered by Gottlieb, Wright, and Liller (1975) at optical wavelengths. The modulation amplitude of this effect in the optical is $\sim 25\%$. We report here an upper limit of 1% to any similar variation in x-rays.

The irregular variability of Sco X-1 in x-rays has long been noted, but no quantitative estimate of the extent or timescale of this variability (in general) has been available. The long-duration exposures to Sco X-1 reported here enable us to estimate this variability on timescales of hours or more, and allow for the

modeling of the temporal intensity profile of Sco X-1. It is found that a large fraction of the emission from the source can be sensibly associated with shot-like pulses of duration $\sim 1/3d$.

II. SEARCH FOR PERIODICITY

The present data are obtained with the Ariel-5 All-Sky Monitor, a scanning pinhole camera with efficiency-corrected area of 0.6cm^2 in the band 3-6 keV. The finest temporal resolution available is 100 minutes, during which time the duty cycle for source observation is $\sim 1\%$. Approximately 300 Sco X-1 counts are accumulated in each 100 minute orbit, in a background which is typically < 10 counts. A more extensive experiment description may be found in Holt (1975).

Figure 1 is a fold of one year of single orbit Sco X-1 data at the Gottlieb, Wright and Liller (1975) optical period of $0.787313d$. No single sinusoid at any phase with amplitude as large as 1% can be fit to the data. Any modulation of the x-ray intensity at this period must, therefore, be more than an order of magnitude below the corresponding optical modulation.

III. SHOT-NOISE ANALYSIS

The intensity measured each orbit from Sco X-1 is not consistent with a constant average. Some indication of this non-Poisson behavior is evident from Figure 2, where (b) contains a particularly variable sample of single-orbit Sco X-1 data. The intensity never drops substantially below $10\text{ cm}^{-2}\text{sec}^{-1}$ (3-6 keV) or above $\sim 30\text{ cm}^{-2}\text{sec}^{-1}$ over the first year of Ariel-5 operation (1974 October - 1975 October), although its average value over 3-month intervals decreases monotonically during the year (see Figure 1).

Of particular interest is the fact that intensity variations generally extend over several orbits, indicating that the totality of Sco X-1 variation cannot be ascribed to individual "flares" with duration ≤ 1 hour.

Terrell (1972) first pointed out that the intensity fluctuations in sources like Cyg X-1 on timescales of $<$ minutes could be reconciled with the mathematical formalism of classical shot-noise. This picture was pursued by Boldt, et al. (1975) and Weisskopf, Kahn and Sutherland (1975), with the result that the major fraction of the emission from Cyg X-1 can be represented by shot-noise with a shot duration of $\sim 1/2$ sec. Presumably, this timescale is characteristic of the x-ray emitting volume of Cyg X-1, and we attempt here to apply an analogous formalism to data obtained with the Ariel-5 All-Sky Monitor from Sco X-1.

The basic test we apply to the data is the extent to which the source variations, as a function of sampling time, are consistent with the statistical errors. We construct a "variance ratio" V_t , which is defined:

$$V_t = \left\langle \frac{(I_k - \bar{I})^2}{(\delta I_k)^2} \right\rangle, \quad (1)$$

where \bar{I} is the mean of the intensity values I_k (each obtained over a sampling time t , and each with statistical error δI_k). The expectation-value-brackets indicate that V_t represents the mean of each of the N values of the bracketed quantity in the total data sample. Clearly, if the scatter of the I_k about \bar{I} is statistical only, $V_t = 1$. Furthermore, if the errors δI_k have been underestimated, $V_t > 1$ but is independent of timescale t .

If we assume that the emission from a source is composed entirely of a constant baseline and a superposition of shots of several durations (τ_i) it may be shown that

$$V_t = \kappa^2 \left[1 + \eta \sum_i \frac{f_i^2}{\lambda_i} (A_i)_t \right], \quad (2)$$

where η is the number of counts detected in the smallest sampling interval ($t=1$), f_i is the fraction of η arising from the i 'th variety of shot noise, λ_i is the corresponding shot pulse rate (in units of $(t=1)^{-1}$) of duration τ_i (in units of $t=1$), and

$$\begin{aligned} (A_i)_t &= 1 \text{ for } t \gg \tau_i, \\ &= \frac{t}{\tau_i} \text{ for } t \ll \tau_i. \end{aligned} \quad (3)$$

κ is a possible correction factor if the statistical error has been incorrectly estimated ($\kappa = 1$ if the error is correct).

The method of investigation then involves an interrogation of three aspects of the V_t distribution. If we assume a Sco X-1 intensity composed of a constant baseline and two shot-noise components, one with $\tau_1 \ll (t=1)$ and one with $\tau_2 \gg (t=1)$, we obtain

$$\begin{aligned} V_1 &= \kappa^2 \left\{ 1 + \eta \left(\frac{f_1^2}{\lambda_1} + \frac{f_2^2}{\lambda_2 \tau_2} \right) \right\}, \\ V_2 - V_1 &= \kappa^2 \eta \frac{f_2^2}{\lambda_2 \tau_2}, \\ \text{and } V_\infty &= \kappa^2 \left\{ 1 + \eta \left(\frac{f_1^2}{\lambda_1} + \frac{f_2^2}{\lambda_2} \right) \right\}. \end{aligned} \quad (4)$$

The simultaneous solution of the above yields an unambiguous value of τ_2 (if the model is correct) since η is prescribed by the data, but the other parameters are not uniquely definable. In particular, f_1^2/λ_1 is not separable, and cannot be determined independently of κ . We can, however, construct an additional "measurable" quantity

similar to equation (1) from adjacent data elements only, i.e.

$$V^* = \left\langle \frac{(I_k - I_{k+1})^2}{(\delta I_k)^2 + (\delta I_{k+1})^2} \right\rangle. \quad (5)$$

This expression reduces to V_1 in the limit of either no shot noise or $\tau \ll (t = 1)$ and has the advantage of being relatively insensitive to variations on time scales much longer than $(t = 1)$.

Figure 3 is the distribution of V_t for $\sim 10^3$ orbits of data obtained between 1974 December and 1975 February. It is clear that no single shot-noise model can explain the V_t distribution because there is no apparent asymptote. Some insight into a possible recovery from this disappointment can be gleaned from Figure 3b, where the four quarters of the 10^3 orbits have each been analyzed separately. Only trial 3 is obviously inconsistent with the $\lambda = 10$, $\tau = 4$ trace of Figure 3a, and the reason may be apparent from Table I. A marked change in the average intensity \bar{I} occurred between trials 3 and 4 (actually during the duration of trial 3). As λ cannot be treated as a variable in the analysis as developed, any local variation in λ outside of Poisson statistics will invalidate the form of equation (1).

In order to determine the possible contribution of an underestimated error, two separate diagnostics were used. Crab Nebula data were analyzed in precisely the same way, with the result that V_t was always < 2 , with an average value of ~ 1.3 . This is an indication that some unrecoverable systematic errors are present in the data (associated with pointing errors and incorrect accumulation times), but the same value of κ ($\sim \sqrt{1.3}$) may not be appropriate to Sco X-1. A direct test is the value of V^2 , which

should be unity for both the limiting cases $\tau \ll 1$ and $\tau \gg 1$. Its value of ~ 4.4 indicates that in no case can the estimated error be incorrect by more than a factor of two, and it is probably much less than that. As we can determine τ_2 independently of κ , however, $4 < \tau_2 < 5$ (a shot duration of $\sim 1/3$ d) is apparently a firm result of this analysis.

We can solve (non-uniquely) for the remainder of the parameters, because κ is estimable and consistency with the data is achievable. If we adopt $1 \leq \kappa \leq \sqrt{2}$, we obtain $.7 \leq f_2 \leq .9$ for the situation $4 \leq \tau_2 \leq 5$ from V' alone, which is consistent with the overall picture of these long-duration shots dominating the source variation (in this case, f_1 plays no significant role in the determination of V'). The pulse rate λ_2 may vary considerably, ranging from ~ 8 ($f_2 = .7, \kappa = 1$) to ~ 27 ($f_2 = .9, \kappa = \sqrt{2}$).

IV. SUMMARY AND DISCUSSION

No discernable x-ray modulation of the Sco X-1 intensity is observed at the binary period of 0.787313d, with an upper limit of 1%. The only regularity in the x-ray emission for timescales in excess of a few hours appears to be the consistency of a large fraction of the emission with shot noise. The most likely parameters (in units corresponding to 100 min. orbits) are $\tau_2 = 4.5 \pm .5$, $\lambda_2 = 15 \pm 5$ and $f_2 = .8 \pm .1$. Variations on smaller timescales (or a constant baseline intensity) are not assignable from the present data. It should be noted, however, that "flares" with

duration ≤ 1 hour are explicitly required for complete consistency, with an expected average frequency $\leq 10 \text{ day}^{-1}$ contributing at most a few percent of the total source emission. The average pulse rate λ_2 can remain roughly constant for times of the order of a month (i.e. the actual number of shot pulses per orbit has a Poisson distribution about this mean), but can change by $\sim 10\%$ in a time < 1 week. These changes in λ_2 , although relatively small, make the V_t distribution uninterpretable for total sample times > 1 month.

The key features of this analysis with respect to a physical interpretation of the parameters are a multiplicity of pulses (i.e. not a single pulse present at one time), and a characteristic time of $\sim 1/3\text{d}$ (i.e. one-quarter to one-half of the binary period of the system). With respect to the former feature, the large number of shots present any time (~ 70) imply an emission region which is not well-localized. An accretion disk is the obvious candidate region for such a diffuse phenomenon, but we have no satisfactory a priori reason for expecting the deduced shot frequency. The consistency of the characteristic shot duration with \leq one-half the binary period might conceivably be interpreted as a distribution of hot spots which each have duration times longer than $1/3$ day, but which are intensity-modulated at the $.787\text{d}$ period of the binary system. This would suggest an expected $.787$ periodicity in the Sco X-1 intensity over a small number of cycles, but no such short-term behavior is apparent in Figure 2b. It would appear, therefore, that $\sim 1/3\text{d}$ is the true duration of the x-ray emission pulses.

The "model" we have presented here requires no detailed physical assumptions about Sco X-1: instead, it is a simple mathematical idealization (in terms of constant-amplitude, constant-duration shots) which can synthesize the temporal behavior of the source on timescales > 1 hour. Nevertheless, this overall consistency with a multiplicity of long-duration shots (rather than single flares superimposed on a baseline continuum) may be generally characteristic of accretion sources. Lamb, Pines and Shaham (1975) have suggested that the anomalous rotation period variations in Her X-1 and Cen X-3 may be explainable in terms of shot-like accretion variations in those sources, for example.

TABLE 1

"Measurable" Parameters in Shot-Noise Analysis

<u>Run</u>	<u>V_1</u>	<u>$V_2 - V_1$</u>	<u>Asymptote*</u>	<u>\bar{y}</u>	<u>\bar{I}</u>
1-4	10.7	4.1	--		17.2
1	8.7	3.6	~ 24	4.4	17.6
2	10.1	4.6	~ 23	5.5	17.9
3	9.8	5.1	--	4.3	17.6
4	8.3	4.2	~ 27	3.5	15.7

*The best value of asymptote is obtained for t between $\sim 3 \tau$ and $\sim 1/5$ of the total data record t_{\max}

References

- Boldt, E., Holt, S., Rothschild, R., and Serlemitsos, P. 1975,
Proc. Intl. Conf. X-Rays in Space, D. Venkatesan, ed., Univ.
of Calgary.
- Canizares, C. R., Clark, G. W., Li, F. K., Murthy, G. T., Bardas, D.,
Sprott, G. F., Spencer, J. H., Mook, D. E., Hiltner, W. A., Williams,
W. L., Moffett, T. J., Grupsmith, G., Vanden Bout, P. A., Golson,
J. C., Irving, C., Frohlich, A., and van Genderen, A. M. 1975,
Ap. J. 197, 457.
WM
- Gottlieb, E. W., Wright, E. L., and Liller, W. 1975, Ap. J. (Letters)
195, L33.
WM
- Holt, S. S. 1975, Proc. COSPAR Symp. Fast Transients X- and Gamma Ray
Astron., Ap. and Space Sci., in press.
- Holt, S. S., Boldt, E. A., Serlemitsos, P. J., and Briskin, A. F. 1975,
Ap. J. (Letters) 180, L69
WM
- Lamb, F. K., Pines, D., and Shaham, J. 1975, preprint.
- Terrell, N. J., Jr. 1972, Ap. J. (Letters) 174, L35.
WM
- Weisskopf, M. C., Kahn, S. M., and Sutherland, P. G. 1975, Ap. J.
(Letters) 190, L147.
WM

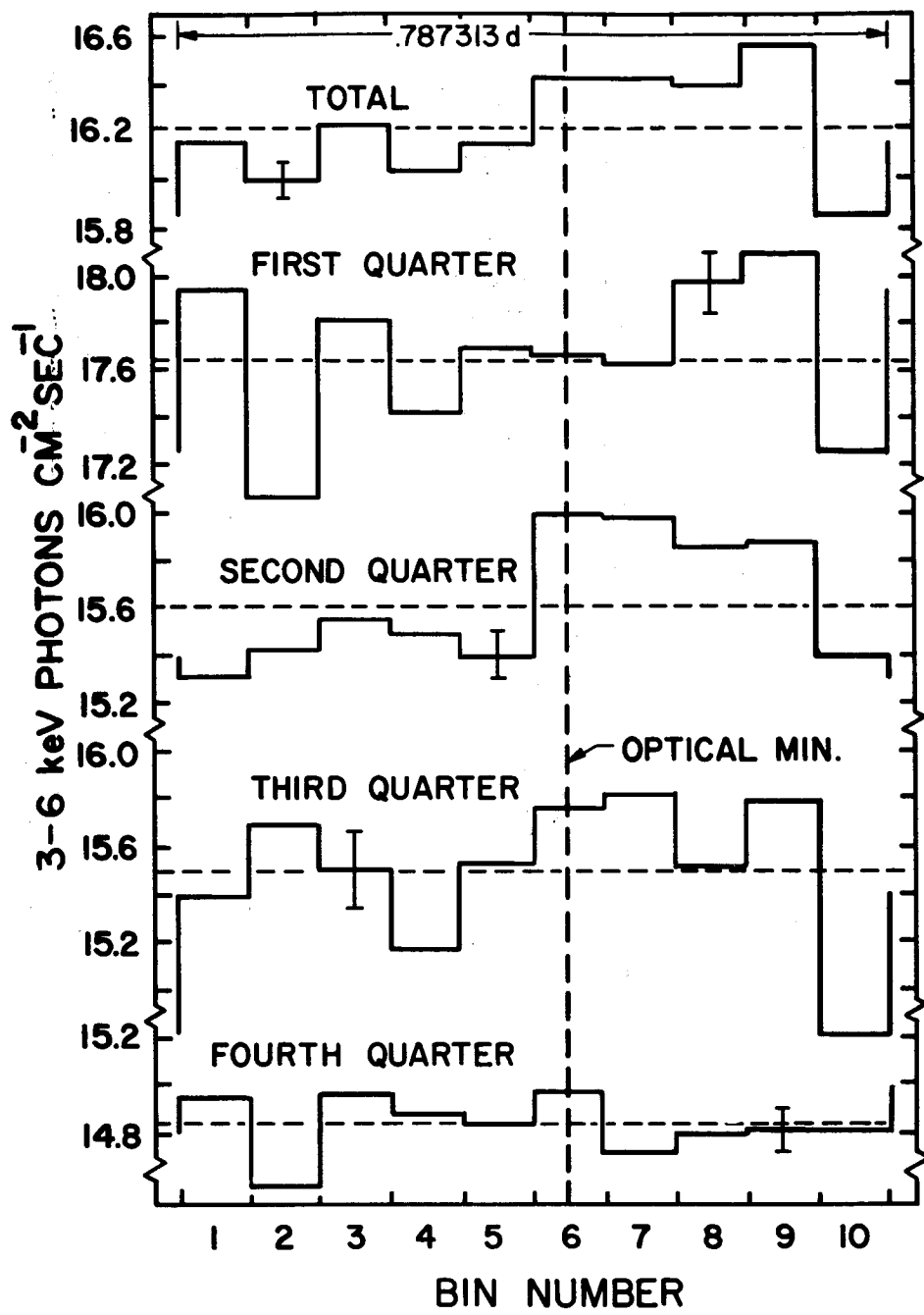
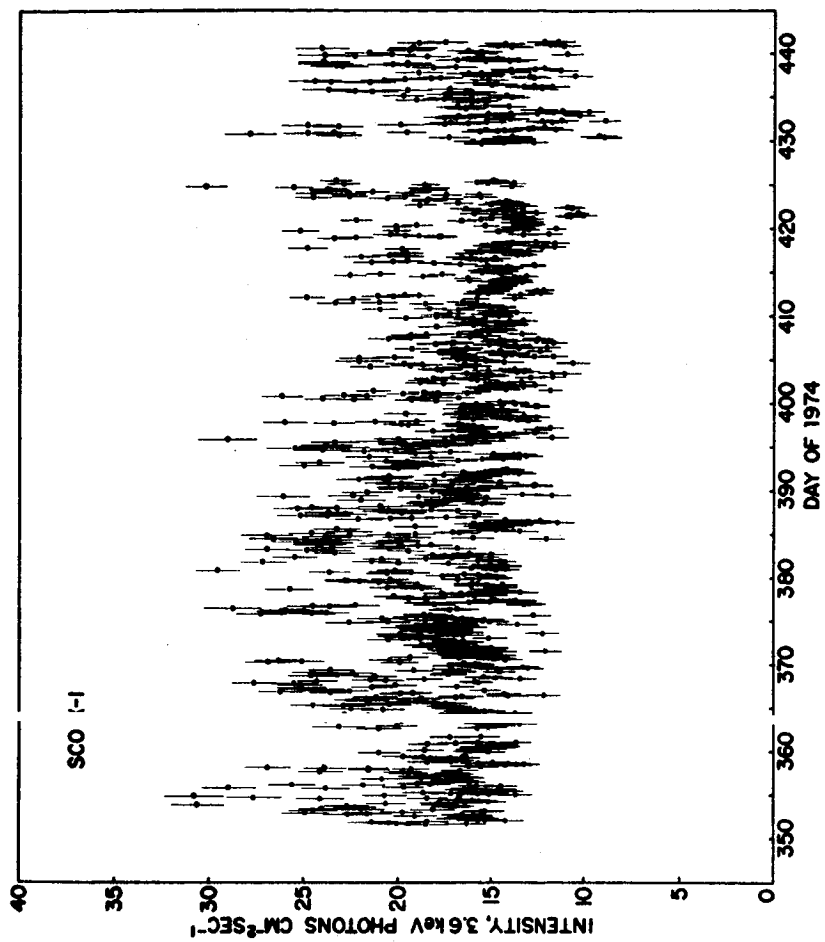
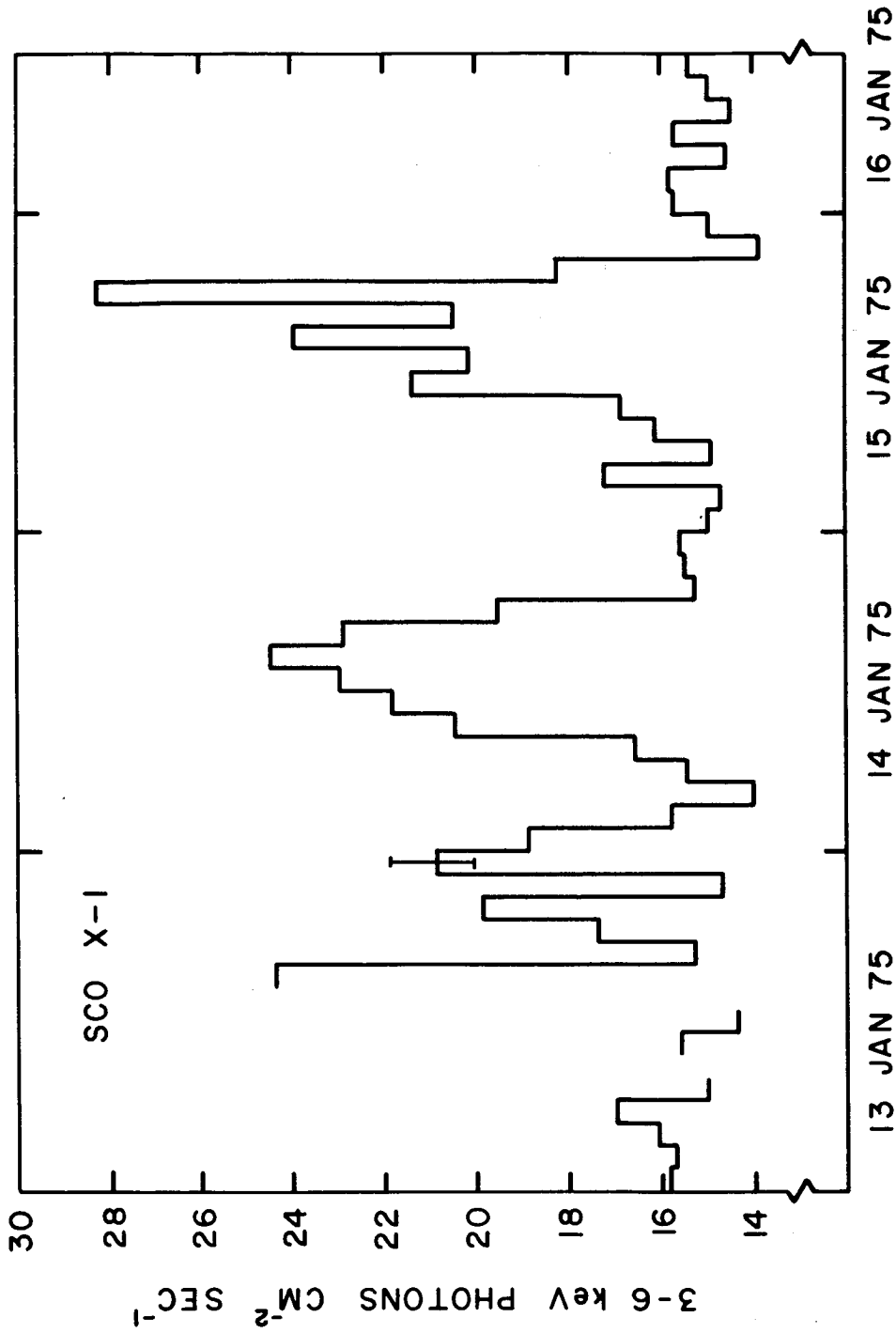


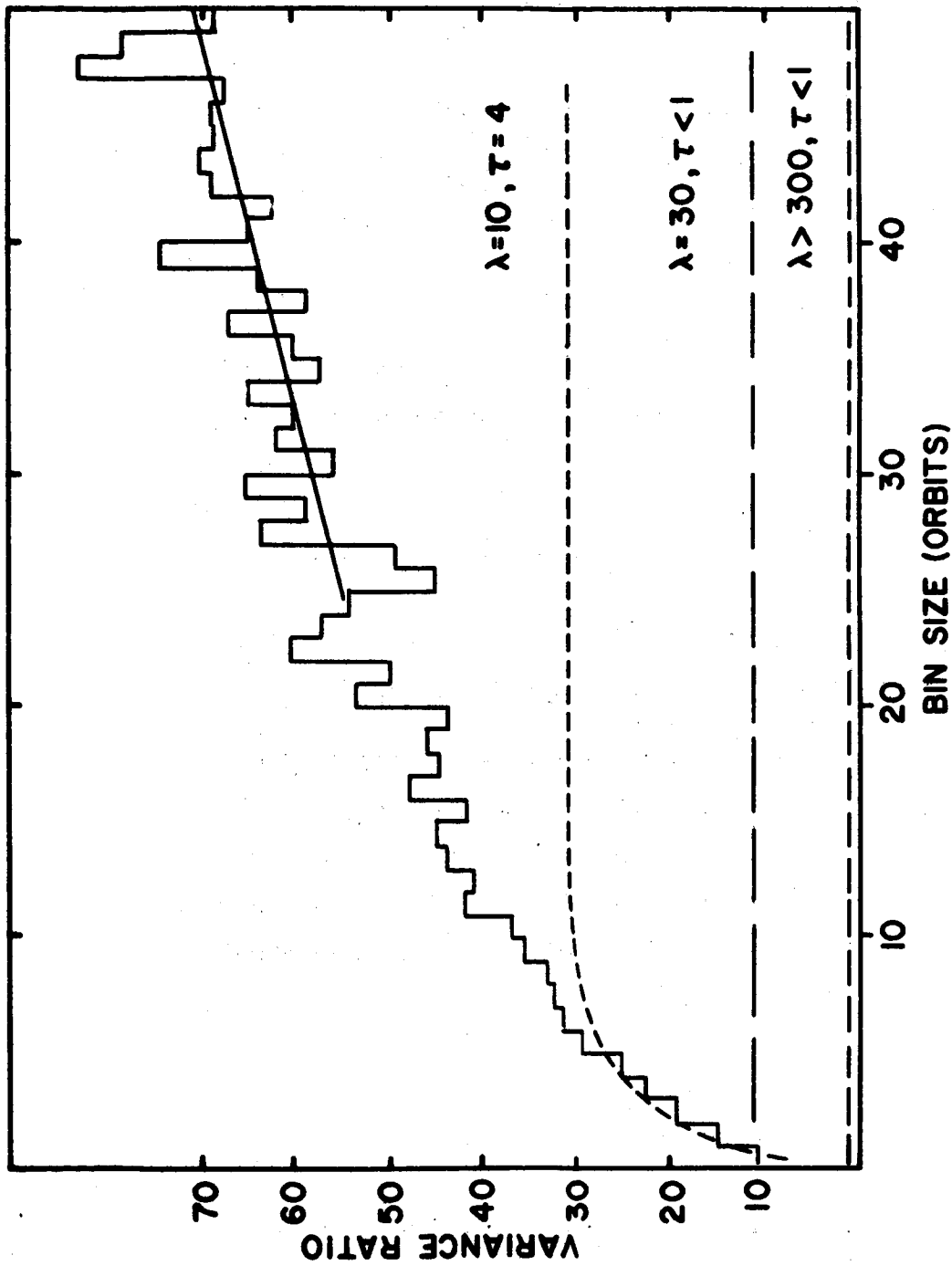
Figure 1. Sco X-1 single-orbit data folded modulo .787313d. The trace labelled "total" contains one year (1974 October - 1975 October) of data, while the other four are each approximately one-quarter of the data.



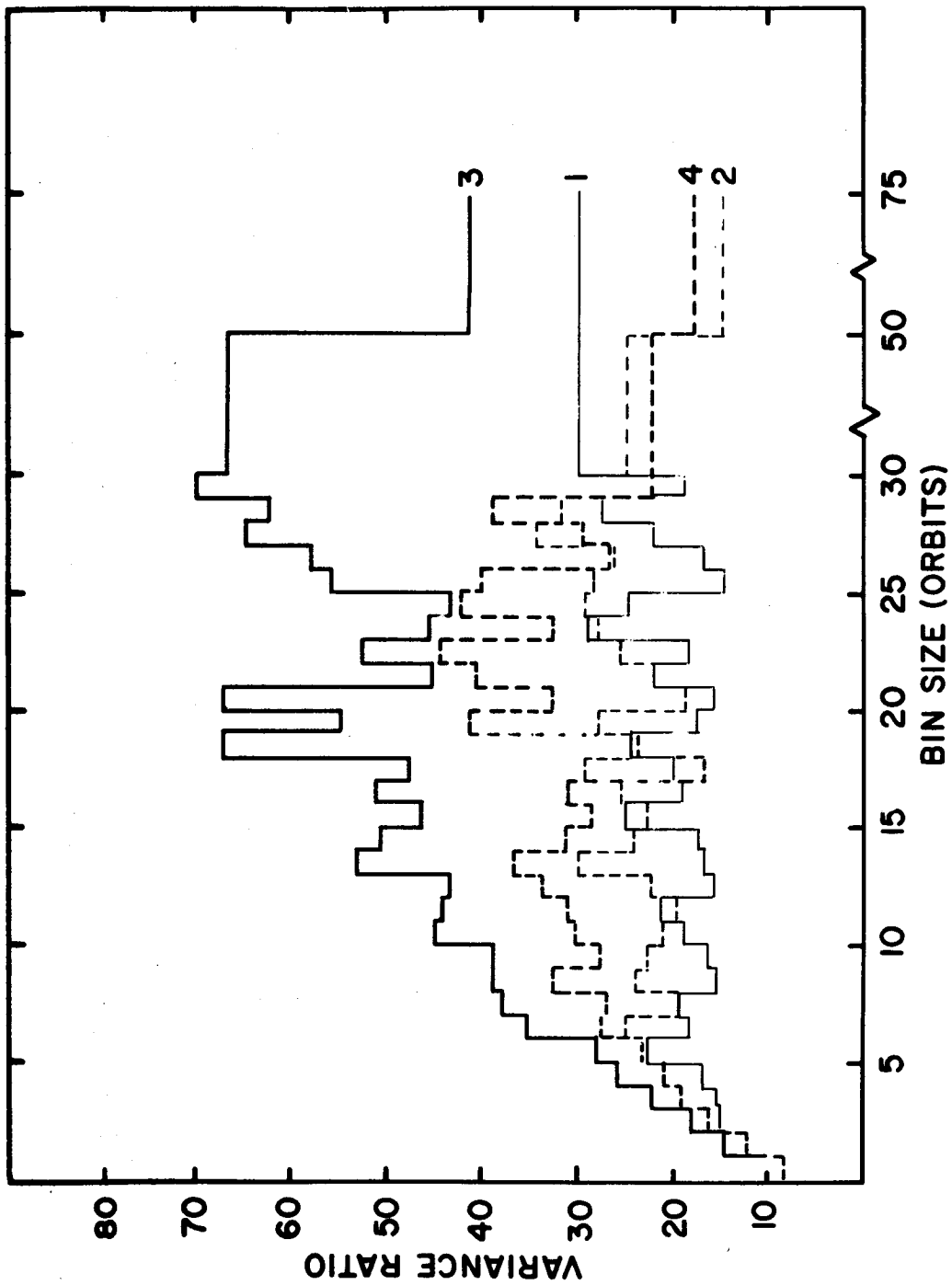
(a)
 Figure 2. Sample Sco X-1 single-orbit data. The first 10^3 orbits in the 90-day interval in a) are used in the shot-noise analysis. The apparent coherence of most intensity variations over several orbits displayed in b) is typical of the total Sco X-1 reorrd.



(b)
 Figure 2. Sample Sco X-1 single-orbit data. The first 10^3 orbits in the 90-day interval in a) are used in the shot-noise analysis. The apparent coherence of most intensity variations over several orbits displayed in b) is typical of the total Sco X-1 record.



(a)
 Figure 3. The variance ratio V_t as defined in the text for a) the total 10^3 orbits analyzed, and b) the four quarters of the 10^3 orbit record. The parameters of Table I are extracted from these data. Also shown in a) are the expected V_t for the annotated simple shot-noise cases.



(b)
 Figure 3. The variance ratio V_t as defined in the text for a) the total 10^3 orbits analyzed, and b) the four quarters of the 10^3 orbit record. The parameters of Table I are extracted from these data. Also shown in a) are the expected V_t for the annotated simple shot-noise cases.

EVIDENCE FOR A 13.6-DAY PERIOD IN CYGNUS X-2
FROM X-RAY AND OPTICAL OBSERVATIONS

CLAUDE CHEVALIER
Observatoire de Meudon

SERGIO A. ILOVAISKY
Observatoire de Meudon and Centre d'Etudes Nucléaires de Saclay

GRAZIELLA BRANTMARDI and PETER W. SANFORD
Mullard Space Sciences Laboratory, University College London

ABSTRACT

Analysis of photoelectric photometry of the Cygnus X-2 optical candidate obtained at the Haute Provence Observatory and of X-ray observations of this source made with OAO Copernicus in 1974 and 1975 indicates the available data are consistent with a period of 13.6 days. The optical light curve, which shows intrinsic scatter, exhibits two maxima and two minima per period and has an amplitude of 0.4 magnitude in the B filter. The 1974 X-ray light curve, whose amplitude is of a factor of two, shows a minimum which coincides in phase with one of the optical minima. The 1975 X-ray curve, based on 12 days of observations in June, shows a smooth 45% flux modulation with an intensity maximum at mid-phase ($\phi = 0.5$). Superposed on this are sharp X-ray "dips" during which the source drops in intensity by as much as a factor of two. The mean optical brightness of Cyg X-2 in the B filter decreased from 1974 to 1975 by 0.3 magnitude whereas the mean X-ray level increased by about 50%. Further correlated observations are planned.

SIMULTANEOUS X-RAY AND OPTICAL OBSERVATIONS
OF X PERSEI

Bruce Margon
Space Sciences Laboratory, University of California, Berkeley

ABSTRACT

Photoelectric photometry of X Persei was obtained on five out of seven consecutive nights in January 1975, from the Lick and Leuschner Observatories. The observations yield $B = 6.848 \pm 0.002$, $B-V = 0.139 \pm 0.001$, with no strong evidence for variability during the observing run. These are the faintest and bluest photoelectric magnitudes and colors ever reported for X Per; this change apparently occurred relatively uniformly during 1973-74 and is reminiscent of behavior last observed in ~ 1900 .

The suggested association of X Persei with the weak X-ray source 3U 0352+30 raises the possibility of detection of X-ray/optical covariability. We have successfully conducted a simultaneous optical/X-ray observation utilizing ground-based photometry and a satellite-borne proportional counter. On 1975 January 21, 7 hours of data were obtained from both observatories simultaneous with OAO Copernicus X-ray observations of 3U 0352+30. The X-ray data varied during this period by a factor of two, but there is no obviously correspondent optical activity, to a level of 0.02 mag. The optical data are also used to limit to 0.01 mag variations coincident with the X-ray periodicity reported by White et al.

1. Introduction

The peculiar Be star X Persei is of interest not only due to its unusual spectrum and variability, but also because of its possible association with the weak X-ray source 3U 0352+30. This association has been noted by many observers (e.g. Braes and Miley 1972; van den Bergh 1972; Brucato and Kristian 1972), but is currently based only on a positional coincidence of order 1 arcmin (Hawkins, Mason, and Sanford 1975). Verification of the identification is especially interesting because if it is valid, the X-ray luminosity of X Per is only $\sim 4 \times 10^{33}$ erg s^{-1} , several orders of magnitude less than any other identified X-ray source (Margon and Ostriker 1973).

It has been pointed out by Moffat *et al.* (1973) and Haupt and Moffat (1973) that another interesting candidate, ADS 2859B, is only 22.5 arcsec away from X Per. Because this spacing is beyond the spatial resolution capabilities for the current generation of X-ray astronomy experiments, it would seem that the only prospects for a conclusive identification in the immediate future lie in the detection of correlated X-ray and optical variability. Since the X-ray data of White *et al.* (1976) show the source to be variable by a factor of ~ 2 on timescales of hours, and also indicate an 11 or 22 hr periodicity, a search for such correlated optical activity seems profitable. In particular, a small amplitude 11 or 22-hr modulation could easily have escaped detection thus far, as most existing photometry has evaluated fluctuations on timescales of minutes and shorter, or weeks and longer (e.g. Richer *et al.* 1972; Mook *et al.* 1974; Frohlich and Nevo 1974), and the close coincidence of these timescales to the sidereal period makes it difficult to obtain uniform phase coverage.

2. Observations

Photoelectric photometry of X Per was obtained on 5 out of 7 consecutive nights in January 1975, utilizing the 76-cm Ritchey-Chretien reflector of the Leuschner Observatory, and the 61-cm Cassegrain reflector of the Lick Observatory. In both cases a 1P21 photomultiplier was employed. Integration times varied from 10-sec to several minutes; several adjacent points were typically averaged prior to data reduction. Filters which mimic the Johnson B and V bands were used alternately, resulting in a total of 320 magnitudes during the week of observing.

The data were reduced to standard Johnson B and V magnitudes through the observation of at least 3 different standard stars each night. To provide maximum discrimination against systematic effects, different standard stars and a different reduction programme were used at the two observatories. The resulting standardized magnitudes and colors are shown in Figure 1. The data show no strong evidence for variability within a night, with a standard error for each point (derived from the scatter in the data itself) of approximately 0.02 mag in B. The magnitudes and colors have therefore been averaged separately for each site for each night, and these data appear in Table 1. The uncertainties quoted in this table are the standard deviation of the mean of the data sample for each night.

Inspection of the table reveals that all of the B magnitudes are in agreement to within better than 3 standard deviations; we thus have no evidence for night-to-night variability. There is slightly more scatter

in the measured values of B-V, with two of the differences barely significant at the 3σ level. Although color changes in X Per have been suggested by several observers (e.g. Frohlich and Nevo 1974), we do not consider the small color differences in our data notable in view of the sky brightness at our two observing sites. We have therefore also provided in Table 1 the mean and standard deviation of the entire data set.

On January 21, 1975 from 0230 to 1000 UT, our photometry was simultaneous with 2.5 - 7.5 keV X-ray observations of 3U 0352+30 by the UCL collimated proportional counter aboard OAO Copernicus. The instrumentation and observing technique of this experiment have been described in detail elsewhere (Sanford 1974; Bowles et al. 1974). Facilities at both Lick and Leuschner Observatories were employed on this night, and the observing program was planned using a detailed OAO orbital ephemeris. This permitted us to maximize simultaneous coverage by obtaining observations of standard stars only while X Per was Earth-occulted for OAO, or while the X-ray experiment was off during passage through the South Atlantic Anomaly. This modified observing procedure accounts for the greatly increased density of data points near 55 hours elapsed time in Figure 1.

In Figure 2 we present on an expanded scale the individual magnitudes and colors obtained during this period of simultaneity with OAO. Through the kindness of P. Sanford and his colleagues, the figure also contains the background-corrected X-ray count rate on the source 3U 0352+30. The only gaps in the data are caused by OAO experiment shutdowns for the reasons discussed above. Each point of X-ray data is the sum of a 63-s integration period.

3. Discussion

The most obviously interesting feature of the photometry presented in Figure 1 and 2 is that the B magnitudes are substantially fainter, and the B-V colors substantially bluer, than any photoelectric measurements previously reported for X Per. The historical tabulation of Mook et al. (1974) indicates that no photoelectric magnitudes fainter than $B = 6.6$ have ever been recorded, nor colors bluer than $B-V = 0.24$. There are only scattered instances of X Per becoming as faint as the $V = 6.7$ we observe now, with no such occasions for the past 25 years.

Because Mook et al. obtained $B = 6.52 \pm 0.01$, $B-V = 0.28 \pm 0.01$ in January 1973, this latest decline must have occurred during the two year interval between our observations. The records of the American Association of Variable Star Observers (Mattei 1975) are consistent with a gradual decline in brightness of X Per during this time period, as is the preliminary report of Gottlieb and Liller (1975), based on photographic magnitudes from patrol plates. Two quite comparable steady decreases in the brightness of X Per occurred in 1895 and 1903 (cf. Mook et al. 1974), but certainly none since that time. Further photoelectric observations will be interesting in this regard.

We now examine the question of correlated X-ray and optical fluctuations. It is clear from Figure 2 that our data show no compelling evidence for such correlations. For example, the distinct peaks in the X-ray flux at UT 0319, 0455, and 0743 are not accompanied by analogous optical events. This statement can be made to an accuracy of the individual photometric brightness determinations, which is of order 0.02 mag.

It is interesting to predict the expected level of such correlated fluctuations, under the assumption that the identification of X Per with 3U 0352+30 is correct. The dominant cause of simultaneous variability on the timescales relevant to our data (i.e., minutes to hours) will be reprocessing into visible light of X-rays incident on the atmosphere of X Per. This same process is responsible for both the 1.7-day and 1.24-s optical variability of HZ Herculis (Davidsen *et al.* 1972; Davidsen, Margon, and Middleditch 1975). There are four factors which will affect the amplitude of the resulting optical modulation: the ratio of intrinsic X-ray to optical flux in the system, the physical reprocessing efficiency, the solid angle subtended by X Per at the X-ray source, and the extent to which fluctuations are smoothed by characteristic light travel times in the system.

The first quantity is directly computable from our data, and is a particularly useful ratio because it is distance independent. The visible flux we observe in the B-band ($\lambda\lambda$ 3800 - 5400 Å) corresponds to 2.5×10^{-8} erg cm⁻² s⁻¹ incident at the top of the Earth's atmosphere. The observed X-ray flux in the 2.5 - 7.5 keV band, equivalent to 10 OAO counts per 63-s integration period, is 2×10^{-10} erg cm⁻² s⁻¹. Thus the X-ray to optical flux ratio is of order 10^{-2} . For the second quantity, the efficiency of the physical process responsible for X-ray to optical reprocessing, we note that the inferred energy input needed to cause the 1.7-d variability of HZ Herculis is very close to the observed X-ray luminosity of Hercules X-1 (Milgrom and Salpeter 1975). Thus at least for some systems this efficiency is of order unity.

The remaining two parameters are dependent upon the geometry adopted for the system. If we consider the X-ray source to be in orbit about X Per with a 584 day period, as has been suggested by Hutchings *et al.* (1974), then only $\sim 10^{-4}$ of the X-ray flux is incident on the visible star. In addition, the light travel time from secondary to primary is of order of or greater than the timescale of the X-ray fluctuations in Figure 2. Thus under these assumptions we do not expect detectable covariability through this process.

If, however, we associate the 11/22-hr X-ray variability reported by White *et al.* (1976) with orbital motion of the X-ray source, the situation is quite different. In the case of this very close orbit, ~ 0.5 of the X-ray flux is incident on X Per, and the light travel times are negligible compared to the X-ray fluctuation times in Figure 2. Therefore we expect the the X-ray variations should appear in the optical data at a level diluted by the product of the inverse solid angle and the X-ray to optical intensity ratio, i.e., 5×10^{-3} . The variations of factor two on timescales of minutes indicated in Figure 2 should thus give rise to optical fluctuations of order 0.005 mag, slightly below the sensitivity threshold of the current work, but still easily attainable with existing instrumentation. Thus if continued simultaneous observations of improved sensitivity fail to reveal such covariability, the association of X Per with the X-ray source, or the X-ray modulation with an orbital period, may well be in doubt.

Finally, we consider constraints provided by our data on any 11/22-hr optical/X-ray covariability. It is clear from Table 1 that on individual nights our B magnitudes are in agreement to a level of ~ 0.003 mag. In our 150-hour observing period, we have sampled almost 7 22-hr periods, but only 60% of an entire 22-hr phase. A reasonably sinusoidal light curve, of the type caused by tidal distortion of the primary, would certainly not have escaped our attention if it had amplitude of 0.01 mag or greater. For the

purposes of comparison, the amplitude of the light curve of HDE 226868, the companion of Cygnus X-1, is 0.05 mag (e.g. Walker 1972), and that of Centaurus X-3, which has a similar mass function to that derived by Hutchings *et al.* for X Per, has amplitude 0.12 mag (Krzeminski 1974).

I am indebted to Messrs. R. Stone and G. Penegor for their competent assistance in obtaining some of the photometry, thank Ms. J. Mattei for providing AAVSO records, and am grateful to Messrs. P. Sanford and K. Mason for helping to arrange the simultaneous OAO observations and providing their data prior to publication. This work has been supported by NASA Grants NSG 5057 and NSG 7139.

Day of Jan 1975 (UT)	Table 1. Photometry of X Persei			n
	Telescope cm	B	B-V	
19	76	6.850±0.002	0.143±0.002	28
20	76	6.851±0.002	0.143±0.001	39
21	76	6.845±0.003	0.139±0.001	72
21	61	6.844±0.009	0.115±0.008	6
23	61	6.850±0.005	0.131±0.003	7
25	61	6.857±0.003	0.137±0.002	8
All data	--	6.848±0.002	0.139±0.001	160

References

- Bowles, J. A., Patrick, T. J., Sheather, P. H., and Eiband, A. M. 1974, *J. Phys. E.*, 7, 183.
- Braes, L. L. E., and Miley, G. K. 1972, *Nature*, 235, 273.
- Brucato, R. J., and Kristian, J. 1972, *Ap. J. (Letters)*, 173, L105.
- Davidson, A., Henry, J. P., Middleditch, J., and Smith, H. E. 1972, *Ap. J. (Letters)*, 177, L97.
- Davidson, A., Margon, B., and Middleditch, J. 1975, *Ap. J.*, 198, 653.
- Frohlich, A., and Nevo, I. 1974, *M.N.R.A.S.*, 167, 221.
- Gottlieb, E. W., and Liller, W. 1975, *I.A.U. Circ. No.* 2774.
- Haupt, W., and Moffat, A. F. J. 1973, *Ap. Letters*, 13, 77.
- Hawkins, F. J., Mason, K. O., and Sanford, P. W. 1975, *Ap. Letters*, 16, 19.
- Hutchings, J. B., Cowley, A. P., Crampton, D., and Redman, R. O. 1974, *Ap. J. (Letters)*, 191, L101.
- Krzeminski, W. 1974, *Ap. J. (Letters)*, 192, L135.
- Mattei, J. A. 1975, private communication.
- Margon, B., and Ostriker, J. P. 1973, *Ap. J.*, 186, 91.
- Milgrom, M., and Salpeter, E. E. 1975, *Ap. J.*, 196, 589.
- Moffat, A. F. J., Haupt, W., and Schmidt-Kaler, T. L. 1973, *Astr. and Ap.*, 23, 433.
- Mook, D. E., Boley, F. I., Foltz, C. B., and Westpfahl, D. 1974, *P.A.S.P.*, 86, 894.
- Richer, H. B., Auman, J. R., Isherwood, B. C., Steele, J. P., and Ulyrch, T. J. 1972, *Nature Phys. Sci.*, 238, 131.
- Sanford, P. W. 1974, *Proc. Roy. Soc. Lond. A*, 340, 411.
- van den Bergh, S. 1972, *Nature*, 235, 273.
- Walker, E. N. 1972, *M.N.R.A.S.*, 160, 9p.
- White, N. E., Sanford, P. W., Mason, K. O., and Murdin, P. 1976, *M.N.R.A.S.*, in press.

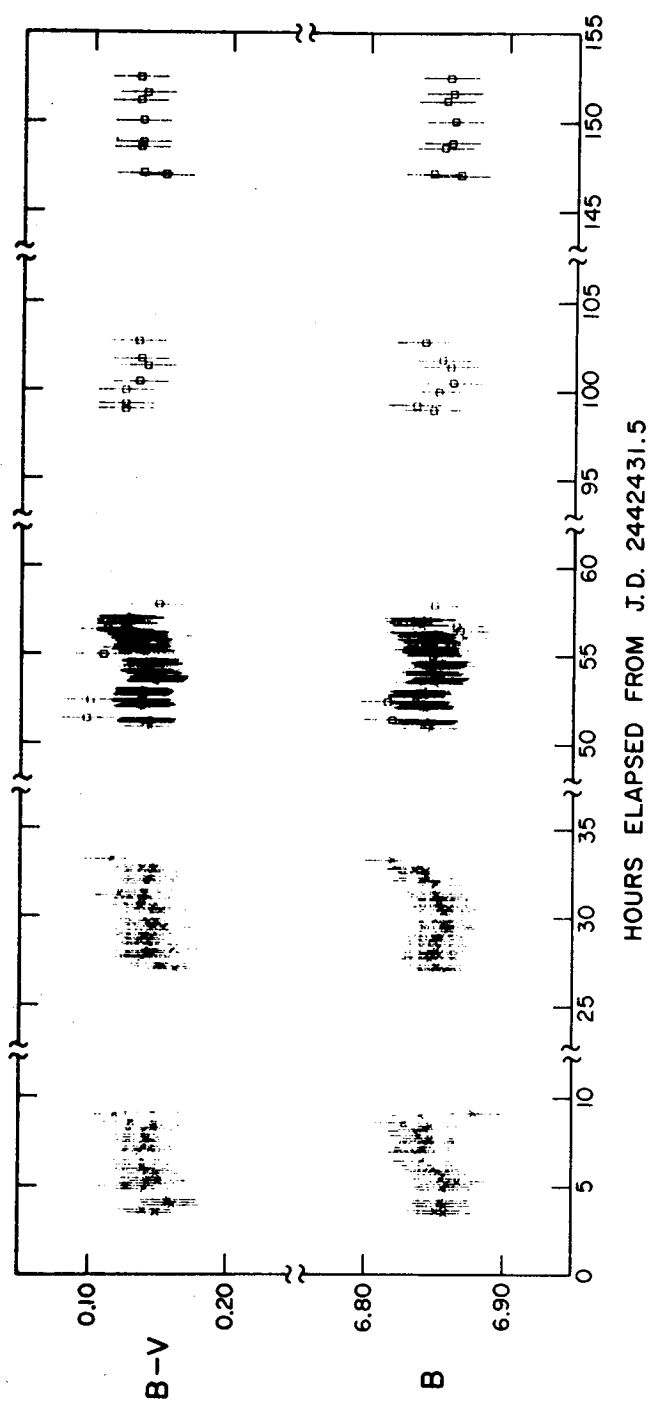


Figure 1. Photoelectric photometry of X Persei starting at 0^h UT January 19, 1975. Crosses, points obtained at Leuschner Observatory; Squares, points obtained at Lick Observatory. The individual, unaveraged data points are shown here to aid in a search for short timescale variability; nightly averages appear in Table I.

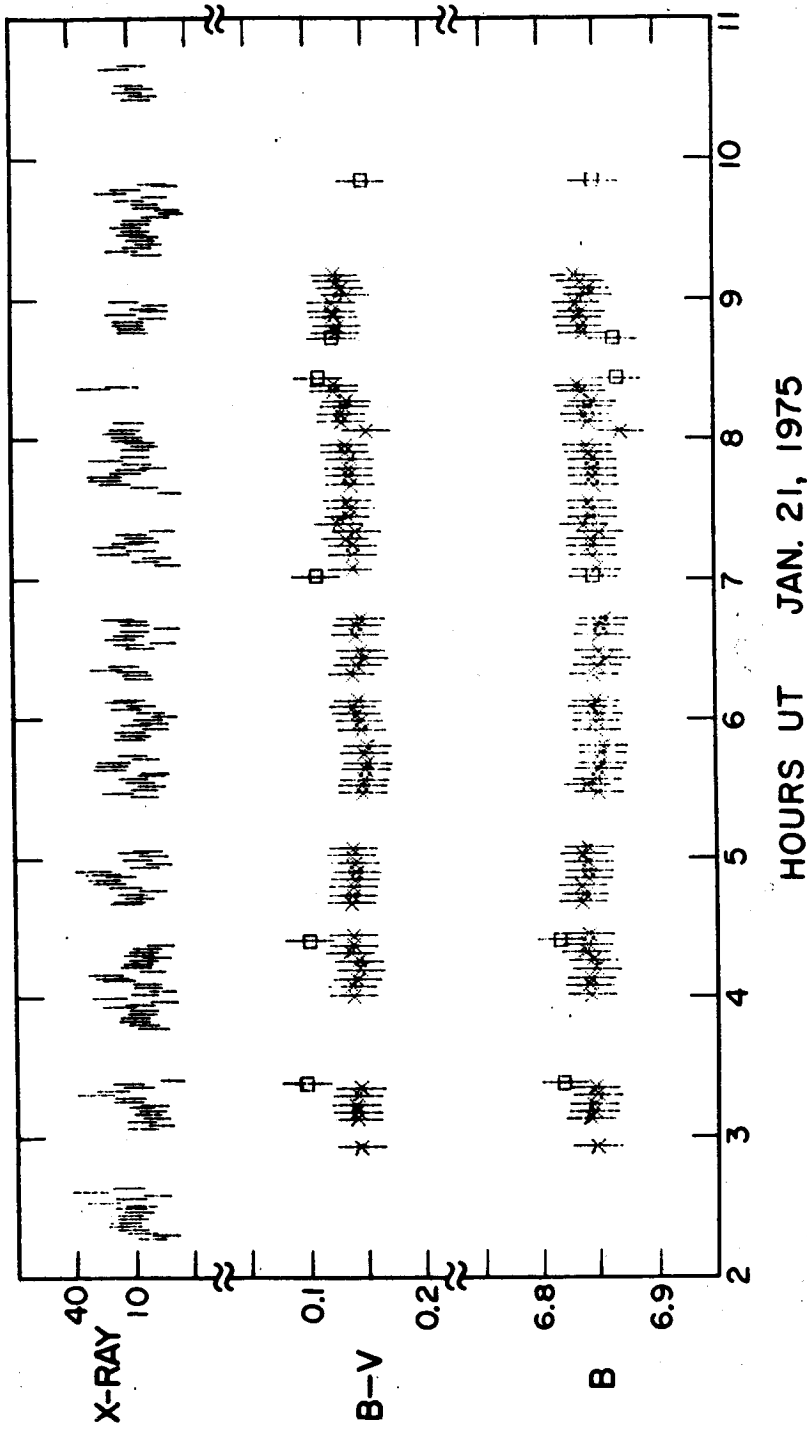


Figure 2. Simultaneous optical and X-ray photometry of X Persei and 3U 0352+30 on January 21, 1975. All error bars are $\pm 1\sigma$ statistical uncertainties. The X-ray data are background-subtracted, and in units of counts per 63-sec integration period. Gaps in the X-ray data are due to Earth occultation of the source or spacecraft passage through the South Atlantic Anomaly; gaps in the optical data are due to observations of standard stars. Observatory symbols same as Figure 1.

OTHER POSSIBLE X-RAY BINARIES

Discussion

N. V. Vidal to D. Bord:

1. I collected some 27 image tube spectroscopic plates of WRA 977 in the blue and in the red regions at 50 and 100 Å/mm dispersion. Line profiles change frequently and absorption lines sometimes are completely filled in emission (HeI 4922). Any radial velocities measurements will be unreliable. The P Cygni profile at H β and H α keeps changing. The separation between the absorption and the emission components is ~400 km/sec in both H α and H α .

2. On inspection of the photoelectric data by Van Genderen we found that period of 13.5 days (Mauder, H. 1974, IAUC 2673) may be fitted but the scatter is high. The best defined minimum is on July 10, 1973.

W. Baity:

I wish to draw attention to the source Circinus X-1. Good evidence for a 12.3^d period has been presented by Jones, Forman and Tananbaum (Ap. J., 1975), but this was not found by the MIT and UCSD instruments on board OSO-7, nor does there appear to be a periodicity at small multiples of 12.3^d. However, the source does flare up for periods of 1 or more days, with at least three of these flares separated by ~ 200 days.

X-RAY ASTRONOMY PROGRAM AT CIT

G. P. Garmire
Department of Physics
California Institute of Technology
Pasadena, CA 91125

ABSTRACT

The X-ray Astronomy program at CIT includes a rocket borne Wolter type I telescope with associated position sensitive detectors, ground based observations in the optical and infrared spectral bands, an experiment on the HEAO-A spacecraft, and a rocket borne test flight of the HEAO-A concept jointly with the GSFC group using a modified detector flown on their rocket to study Cyg X-1 millisecond pulse structure and spectra.

The Caltech program is currently expending most of its time on the development of a focusing Wolter type I telescope (Wolter, 1952) to be carried by an Astrobee F early next year; the modification of the Goddard rocket payload to include a low energy detector to study Cygnus X-1 with a launch in mid-April of 1976; the calibration, testing and development of data handling programs for the low energy portion of the HEAO A-2 experiment; the development of high resolution position and energy sensing scintillation detectors; and the development of a mass production technique for fabricating Wolter type I telescopes with angular resolution better than one arc minute. Finally, a ground based observing program is being initiated by Bill Friedhorsky, a graduate student, to study the spatial distribution and intensity of corona lines in supernova remnants, photometry and time variability of binary X-ray sources and high resolution spectrophotometry of binary sources to study gas motion and excitation. There is continuing interest in the infrared emission from compact X-ray sources, particularly Cyg X-3.

The scientific objectives of the rocket program are summarized below:

- 1) Positioning, identification and mapping of clusters of galaxies.
- 2) The mapping and spectral study of supernova remnants.
- 3) The photometry of potential EUV stars in several bands.
- 4) Positioning and identification of high latitude X-ray sources.
- 5) Scattering by interstellar dust.

The program consists of about three or four flights of a nested pair of Wolter type I telescopes on an Astrobee F vehicle to be followed by a similar number of flights of a much larger telescope of the Wolter type I design for an Aries vehicle. The latter program is a joint effort with the Columbia Astrophysics Laboratory, while the Astrobee program has been in

collaboration with Dr. Guenter Riegler formerly at the Bendix Aerospace Corporation and now with JPL. The Aries program is envisioned as a preparation for Space Shuttle Missions. The physical parameters of the two systems are listed below.

	<u>Astrobee F</u>	<u>Aries</u>
Geometrical area	200 cm ²	1450 cm ² (2 mirrors)
Focal length	50 inches	85 inches
Angular resolution	20 arcseconds	30 arcseconds
Sensitivity		
0.5 - 1.5 keV	3×10^{-3} ph/cm ² sec ΔE	5×10^{-4} ph/cm ² sec ΔE
0.15 - 0.28 keV	1.4×10^{-3} ph/cm ² ΔE	2×10^{-4} ph/cm ² sec ΔE
0.060 - 0.075 keV	8×10^{-3} ph/cm ²	1×10^{-3} ph/cm ² sec ΔE
Field of View	2°	3°

The high energy cut-off of the Aries telescope can be increased by including a third set of mirrors with smaller angles of incidence within the currently planned nested pair. This would increase the geometrical area by about 500 cm² and the weight by another 300 lbs. The choice of focal length is determined by what will fit into a Space Shuttle pallet rather than the Aries capability. This length may change depending on a better understanding of limitations imposed by the Space Shuttle.

This work is supported by NASA grants: NAS 5-23315, NGR 5-002-284 and NGL 05-002-207.

Reference

Wolter, H., 1952, Ann. Physik, 10, 94.

OSO-8 OBSERVING SCHEDULE FOR X-RAY BINARIES

Roger J. Thomas
Laboratory for Solar Physics
and Astrophysics
Goddard Space Flight Center
Greenbelt, Maryland 20771

ABSTRACT

Six different instruments on OSO-8 have observed several binary x-ray sources between energies of 0.13 keV and 1 MeV at various times since 21 June 1975. The schedule for these observations is given, as well as the present plan for such future observations through July 1976. Included is the OSO-8 observing schedule for the transient x-ray source A0620-00.

Although the eighth Orbiting Solar Observatory (OSO-8) launched on 21 June 1975 was not primarily designed for cosmic investigations, it does include six instruments in the rotating wheel section of the spacecraft that are capable of studying binary x-ray sources. Instrumental parameters of these experiments are listed in Table 1. Together, they cover the entire energy range from 0.13 keV to over 1 MeV with good resolution and sensitivity.

Due to operational constraints, the observing schedules of the cosmic x-ray experiments on OSO-8 must be planned long in advance. A baseline plan has already been generated with a lead-time of more than twelve months, presently running through July 1976. In addition detailed schedules for every satellite orbit (each 90 minutes of time) are negotiated from one to four months before the actual observations.

From these two types of schedules, I have extracted the times during which binary x-ray sources were (or are planned to be) in the nominal field of view of each OSO-8 instrument. These times are listed in Table 2, which gives the month and day (U.T.) for the start and end of each observing interval included in the detailed schedules to date; they should be accurate to a tenth of a day. Dates after 4 December 1975 (shown in parentheses in Table 2) are from the general baseline plan, and are only accurate to within a few days even in the absence of major schedule revisions. Also listed in Table 2 is the angular separation between the source and the sun ($+5^\circ$) for each observation. The OSO-8 observing schedule for the strong, transient source A0620-00 is included as well, due to the considerable interest in this remarkable object.

TABLE 1

OSO-8 COSMIC X-RAY PAYLOAD

INSTRUMENT	INSTITUTION	DETECTORS	ENERGY RANGE (keV)	AREA (cm ²)	F.O.V. (FWHM)	OFFSET FROM SPIN AXIS
X-Ray XTAL Spectrometer	Columbia U.	8 prop. count.	2-8	2170*	3°X80°	90°
Stellar X-Ray Polarimeter	Columbia U.	2 prop. count.	2.6, 5.2	800*	2°X2°	180°
Cosmic X-Ray Spectroscopy	GSFC (Serlemitsos)	Prop. counter	2-60	244	5°X5°	0°
		Prop. counter	2-60	271	5°X5°	175°
		Prop. counter	2-20	76	3°X3°	180°
Hard X-Ray Telescope	GSFC (Frost)	CsI(Na) scintillation xtals	20-5000	25	5°X5°	175°
Mapping X-Ray Heliumeter	Lockheed	6 prop. count.	2-30	185	2'X 120**	90°
Soft X-Ray Telescope	Wisconsin	3 prop. count.	0.13- 50	155	3.5° X 3.5°	0°
		3 prop. count.	0.13- 50	155	3.5° X 3.5°	175°

*Area of analyzing xtal.

**Three systems at 0°, ±60° relative orientations.

TABLE 2 (cont.)
OSO-8 Observing Schedule for X-ray Binaries (cont.)

	Columbia Polarimeter	Columbia Spectrometer	GSFC Front	GSFC Srinivasan	Lockheed	Wisconsin	Solar Separation
<u>3U1700-37</u>			9/11.1 9/11.4	9/11.1 9/14.1		9/11.1 9/11.4	90°
			9/12.8 9/14.1		10/11.1 10/12.2 11/5.5 12/5.0	9/13.0 9/14.1	90° 62° 30° 90°
		(5/20/76)		(3/9/76)		(3/9/76)	90°
		(6/9/76)			(5/20/76)		156°
					(6/9/76)		156°
							165°
							165°
<hr/>							
<u>Cen X-3</u>			7/16.1 7/18.4	7/16.1 7/26.6		7/16.1 7/18.4	90°
			7/18.4 7/26.5	7/26.5 7/26.6		7/26.5 7/26.6	90° 90° 90° 90° 90° 90°

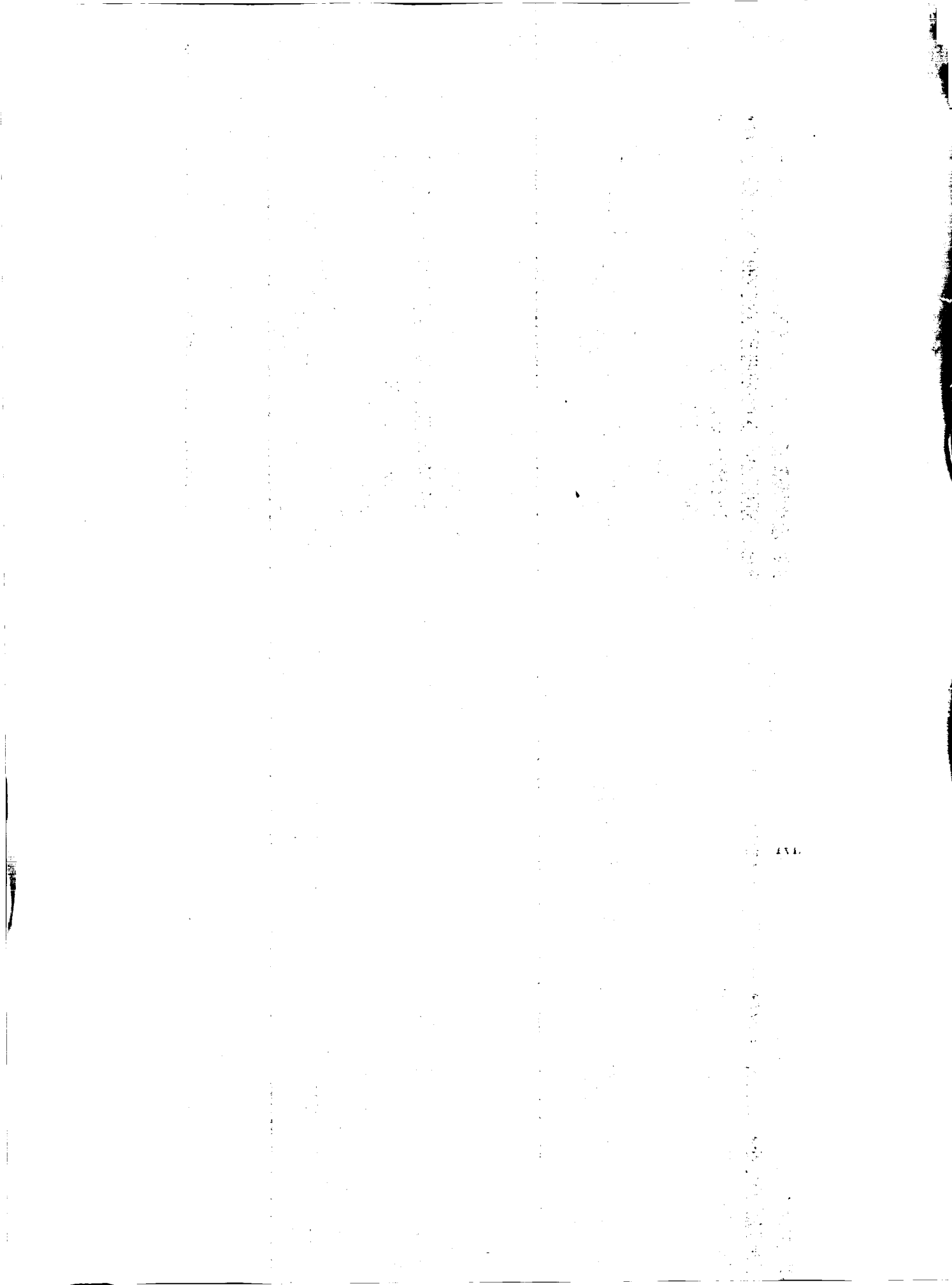
TABLE 2 (cont.)
OSO-8 Observing Schedule for X-ray Binaries (cont.)

	<u>Columbia Polarimeter</u>	<u>Columbia Spectrometer</u>	<u>GSFC Front</u>	<u>GSFC Serlemitsos</u>	<u>Lockheed</u>	<u>Wisconsin</u>	<u>Solar Separation</u>
<u>Can X-3</u>		8/10.9 8/11.9			8/10.5 8/19.4		80°
		9/25.4 9/27.9			9/4.9 9/6.2 9/23.9 10/2.4		80° 88° 80° 80°
		(4/1/76)		(1/19/76)		(1/19/76)	90° 90°
		(8/21/76)			(4/1/76)		122° 122°
					(6/21/76)		106° 106°
<u>SMC X-1</u>				10/27.3 10/30.5			90°
						10/27.5 10/30.3	90°
<u>SU0352-30</u>				(2/22/76)		(2/22/76)	90° 90°

TABLE 2 (cont.)
 OGO-8 Observing Schedule for X-ray Binaries (cont.)

	Columbia Polarimeter	Columbia Spectrometer	GSFC Front	GSFC Sidelenses	Lockheed	Wisconsin	Solar Separation
<u>SU0032-24</u>				(1/5/76)		(1/5/76)	90°
				(7/10/76)		(7/10/76)	90°
<u>SU0918-55*</u>							90°
<u>SU0527-05*</u>							90°
<u>SU1820-30</u> (SEP X-4)			9/20.4 9/21.8	9/20.4 9/21.8		9/20.6 9/21.6	90°
			(6/26/76)			(6/26/76)	173°
<u>A0630-00</u>				9/30.5 10/2.5		9/30.7 10/3.3	90°
					10/16.4 11/1.3		110°
	10/17.3 10/18.3						110°
	10/26.1 10/27.3						110°

*the observations of these sources are scheduled through July 1976.



THE OBSERVATION PROGRAM FOR THE GSFC
COSMIC X-RAY SPECTROSCOPY EXPERIMENT

R. H. Becker, E. A. Boldt, S. S. Holt, S. H. Pravdo,
R. E. Rothschild, P. J. Serlemitsos, J. Swank
NASA/Goddard Space Flight Center
Greenbelt, Maryland 20771

ABSTRACT

The GSFC cosmic x-ray spectroscopy experiment on OSO-8 will observe seven x-ray binary sources in its first six months of operation. If possible, each of these sources will be observed for one or more binary orbits so that we can observe the x-ray spectrum of each object through all phases of its orbit. For the two pulsing binaries, Her X-1 and Cen X-3, we will study spectral variations over the pulse period. We have arranged for simultaneous radio observations of Cyg X-1 and Cyg X-3 to search for any correlation between radio and x-ray emission. During the first year of operation, the GSFC detectors will observe over 50% of the known x-ray sources. The large number of x-ray sources included in this program could result in the discovery of new x-ray binary sources.

The OSO-8 satellite has been operational since June 21, 1975. Since then, extensive observations have been made of the binary sources Her X-1, Cen X-3, 3U1700-37, and most recently SMC X-1. The GSFC x-ray detectors have produced detailed spectra for these objects in the energy range 2-60 keV. In the next two months the OSO-8 observational program will include three additional binary x-ray sources, Cyg X-1, Cyg X-3, and 3U0900-40. Our primary objective with regard to the binary x-ray sources is to search for spectra variability over a wide range of temporal regimes. Each x-ray binary will be studied for one or more binary periods, allowing observations of each binary in every phase of its orbital motion.

Our analysis of quick look data from Cen X-3 and Her X-1 (the only type of data available thus far) confirms that the spectra of these sources change on time scales of both the pulse and orbital period. With the availability of all the data, we anticipate studying the spectral differences between pulsed and non-pulsed emission, the effects of varying amounts of absorption on the x-ray spectrum as a compact x-ray source approaches and exits eclipse by its primary, and the spectra of low intensity periods such as during eclipse and intensity dips.

When possible, we want to add an extra dimension to our study of binary sources by arranging simultaneous observations in other bandwidths. This is achieved automatically in some instances in so far as OSO-8 carries a NASA-GSFC hard X-ray telescope and a soft X-ray experiment from the University of Wisconsin. In addition, for some sources it is important to obtain simultaneous radio and infrared observations. As an example of the type of cooperation possible, last summer Cen A, an extragalactic x-ray emitter, was observed by our x-ray experiment, the NASA-GSFC hard x-ray telescope, three southern hemisphere

infrared observatories, and the millimeter wavelength radio telescope at the University of Texas. Our plans for the future include simultaneous observations of Cyg X-1 and Cyg X-3 in November, 1975, with the NRAO 4-element interferometer at centimeter wavelengths.

A final aspect of the OSO-8 observational program is a search for previously undetected binary sources. Our sensitivity and time resolution allows us to examine very weak sources for evidence of periodicity. In the first year of operation, the GSFC detectors aboard OSO-8 will view over 50% of the known x-ray sources in the sky. However, since OSO-8 occasionally spends as few as three hours on some sources, we are not always assured of detecting a binary source. None the less, looking forward to possibly 2 years of successful operation and the large number of x-ray sources that will be included in the observations, this program could result in the discovery of new binary x-ray sources.

A STUDY OF THE COSMIC SOURCES OF HARD X-RAYS

B. R. Dennis, J. Beall[†], C. J. Crannell,
K. J. Frost and L. E. Orwig
Laboratory for Solar Physics and Astrophysics
NASA-Goddard Space Flight Center
Greenbelt, Maryland 20771

ABSTRACT

An actively-shielded, high-energy x-ray telescope was launched on-board OSO-8 on 21 June 1975. The primary objectives of this experiment are the measurements of the energy spectrum of discrete cosmic x-ray sources in the range 20 keV to 3 MeV and of the temporal variations in the intensity of each source detected with a time resolution of 0.3 msec. This detector provides the highest duty factor and the finest time resolution of any of its kind for observations over a period of up to 10 days. The background spectrum of this detector in orbit has been monitored continuously since shortly after launch. The minimum detectable source strength is estimated to be between 10^{-4} and 10^{-5} photons/cm²-sec keV, limited primarily by the effects of induced radioactivity. From 16 July through 18 July 1975 the x-ray binary, Cen X-3, was observed with the hard x-ray telescope. For this source, complete data coverage is needed before statistically significant results can be reported on the high-energy x-ray spectrum and the energy dependence of the pulsed fraction. With the partial data coverage presently available, statistically significant results have been obtained from observations of Cen A (27 July through 4 August 1975) and Sco X-1 (6 through 9 September 1975). Some of the hard x-ray sources which will be the observational objectives of this experiment during the period from October 1975 through June 1976 are Cyg X-1, Cyg X-2, Per X-1, Tau X-1, Vel X-1, Com X-1, Vir X-1, and 3C273.

The primary objectives of the High-Energy Celestial X-Ray Experiment on OSO-8 are:

To measure the spectrum of cosmic x-ray sources in the energy range from 20 keV to 3 MeV, and

To search for both periodic and aperiodic time variations in the intensity of the sources detected.

In order to achieve these objectives we have built a detector designed to minimize and to monitor continuously the detector background spectrum. The detector covers a broad energy range and has continuous in-flight calibration. The relatively narrow field of view of (5° FWHM) enables closely

[†] Department of Physics, University of Maryland, College Park, Maryland

spaced sources to be resolved. Very precise timing capability (312.5 μ s for each photon) has been incorporated in the design of the experiment so that periodic sources can be detected and the details of their time history studied.

The high-energy x-ray detector is an actively shielded scintillation telescope of the type originally designed by Frost et al (1966). The center of the detector consists of two optically isolated CsI(Na) crystals each 1.27 cm thick. These crystals are shielded by a large active collimator made up of 5 CsI(Na) crystals. (See Figure 1.) Seventeen parallel holes 1.435 cm in diameter and 13.34 cm long drilled through the top shield crystal to one of the two central crystals allows the unimpeded passage of a fraction of X-rays from the forward direction while x-rays from all other directions are attenuated by a shield thickness of at least 5 cm. This configuration provides a total sensitive area of 26.2 cm² and an aperture with a FWHM of 5°. The second completely shielded central crystal serves to monitor the internal background of the instrument. Two 2.5 cm photomultipliers (RCA C31016F) view each central crystal from the side and a total of 13 photomultipliers (RCA C31016F and C70132B) view the shield crystals. A 0.635 cm thick plastic scintillator positioned over the 17 holes serves to reject low-energy charged particles incident on the open central crystal. Two charged particle monitors are used to turn off the high voltage to the other photomultipliers during passages through the South Atlantic Anomaly.

X-ray events are recorded when a signal is detected from either one of the two central crystals in anticoincidence with any signals from the shield crystals and from the plastic scintillator over the collimation holes. Each acceptable x-ray pulse from either central crystal is pulse-height-analyzed into 256 linear channels which can, by command from the ground, cover one of 16 energy ranges extending from 0-200 keV to 0-3 MeV. The central crystal and shield discriminator threshold levels can also be adjusted independently by command to achieve the optimum levels consistent with minimum dead time and efficient x-ray selection. Currently, the central crystal energy range is \approx 20-275 keV and the shield threshold levels are set at \approx 100 keV. The parameters which determine the energy ranges are continuously monitored in orbit using in-flight calibration systems. The central crystals are calibrated with the 59.6 keV x-rays from Am²⁴¹ tagged by the 5 MeV coincident α -particles detected by two solid-state detectors. The shield crystals are calibrated with the light from Am²⁴¹ α -particles produced in NaI(Tl) pellets.

The detector efficiency as a function of photon energy is shown in Figure 2. The decrease at low energies is caused by the material in front of the central crystal including an approximately 70 micron non-scintillating layer on the CsI(Na) crystal itself resulting from the action of water vapor before launch (Goodman, 1975). The time of arrival of each accepted x-ray event is also recorded to a resolution of 312.5 μ s. The spacecraft clock is very stable - < 1 part in 10⁹ per 24 hours - and it is time tagged with respect to Universal Time once per day to an accuracy of < 100 μ s. Thus, data for periodic x-ray sources can be phase folded for long periods \leq 10 days and compared in phase with other observations.

The pulse amplitude and time of arrival of an acceptable x-ray event are read out in the telemetry once every 20 msec. Thus, this information on a maximum of 50 events/second can be read out. The overall instrument live time is read out once every 160 msec allowing a constant determination of the "true" rate of events.

The x-ray detector is mounted in the wheel section of OSO-8 with its field-of-view pointed in the aft direction, i.e. away from the sail section of the spacecraft. The detector axis is offset from the wheel spin axis by 5° so that as the wheel rotates at ≈ 6 rpm the detector axis sweeps out a small circle on the celestial sphere. Any celestial x-ray source close to the circumference of this circle will pass into and out of the detector field of view every ten seconds. In this way regular measurements are made of the detector counting rate both with and without the source in the field of view. This source modulation is very important since it provides a continual monitor of the detector background rate in addition to the monitor provided by the second central crystal. The spin axis of the spacecraft is opportunistically re-oriented to bring different x-ray sources into the 5° circle swept out by the detector axis. Since launch the following sources with significant fluxes above 20 keV have been observed: Cen X-3, Cen A, Sco X-1 and sources near the galactic center. A complete analysis of the data has not yet been made but preliminary analysis of the 2-4 orbits/day of quick-look data has shown that we have clearly detected Cen A at about the same intensity as that observed by Hall et al. (1975) at energies up to 150 keV. We have also detected Sco X-1 up to 50 keV and possibly Cen X-3. A sample of the data on Sco X-1 is shown in Figure 3, in which the counting rate of 20-30 keV x-ray events from the open central crystal is plotted as a function of the wheel azimuth angle. The triangular response of the detector which in this representation is about 100° wide at the base is clearly seen in the data. The source intensity obtained from these data is in agreement with values obtained previously.

The limit in source detectability of this instrument is set by the detector background rate which is dominated by the induced radioactivity produced during passage through the high proton fluxes in the South Atlantic Anomaly. This detector background spectrum is shown in Figure 4 in which the various peaks resulting from the decay of various isotopes originating in the detector material can be clearly seen. Only those sources with fluxes which will contribute significantly above this background spectrum can be detected by this instrument. With the constant monitoring of this background spectrum, both by the second completely shielded central crystal and by the source modulation, we expect to be able to detect sources which contribute anything more than a few percent to the total spectrum. From Figure 4 this would mean that a source with a flux above 20 keV of 10^{-4} - 10^{-5} photon/cm²-sec keV should be detectable by this instrument, provided the wheel spin axis is held 5° away from it for a period of 10 days or more.

In the coming months the spin axis will be moved to bring the following sources of interest into our field of view for some period of time generally less than 10 days: Cyg X-1, Cyg X-3, Per X-1, Tau X-1, Vela, Vir X-1 and 3C273. Each of these sources will be observed by the GSFC/Serlemitsos and the Wisconsin instruments during the same interval giving a combined x-ray coverage from 0.25 keV to the maximum detectable energy of our instrument.

REFERENCES

- Frost, K. J., Rothe, E. D., and Peterson, L. E. 1966, JGR, 71, 4079.
- Goodman, N. B. 1975, NASA-GSFC X-682-75-201.
- Hall, R. C., ~~Heegan~~, C. A., Walraven, G. D., Djuth, F. T., Shelton, D. H., and Haymes, R. C. 1975, Proc. 14th Int. Cosmic Ray Conf., OG 3-1 (to be published).
- Laros, J. G., Matteson, J. L., and Pelling, R. M., 1973, Nature Phys. Sci., 246, 109.
- McBreen, B., Ball, S. E., Jr., Campbell, M., Greisen, K., and Koch, D., 1973, Ap. J., 184, 571.

OSO-8 20keV - 5MeV. X-RAY DETECTOR

PARAMETERS OF DETECTORS	
SENSITIVE AREA	26.2cm ²
MAXIMUM ACCEPTANCE ANGLE	5.9°
F.W.H.M	5.1°
AREA X SOLID ANGLE FACTOR	0.25cm ² sr
MINIMUM SHIELD THICKNESS	2"

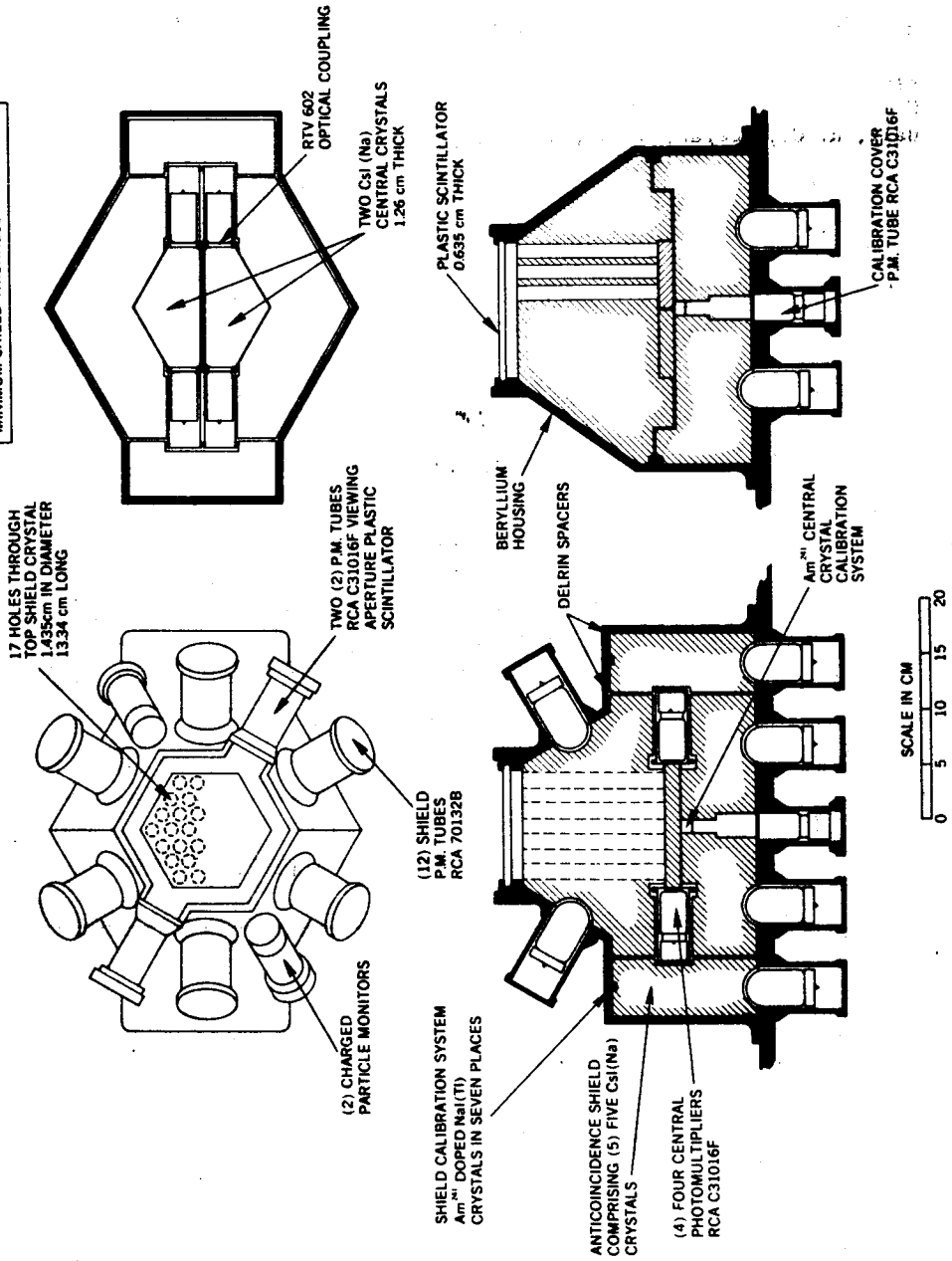


Figure 1. An outline drawing of the High-Energy Celestial X-Ray Detector on OSO-8.

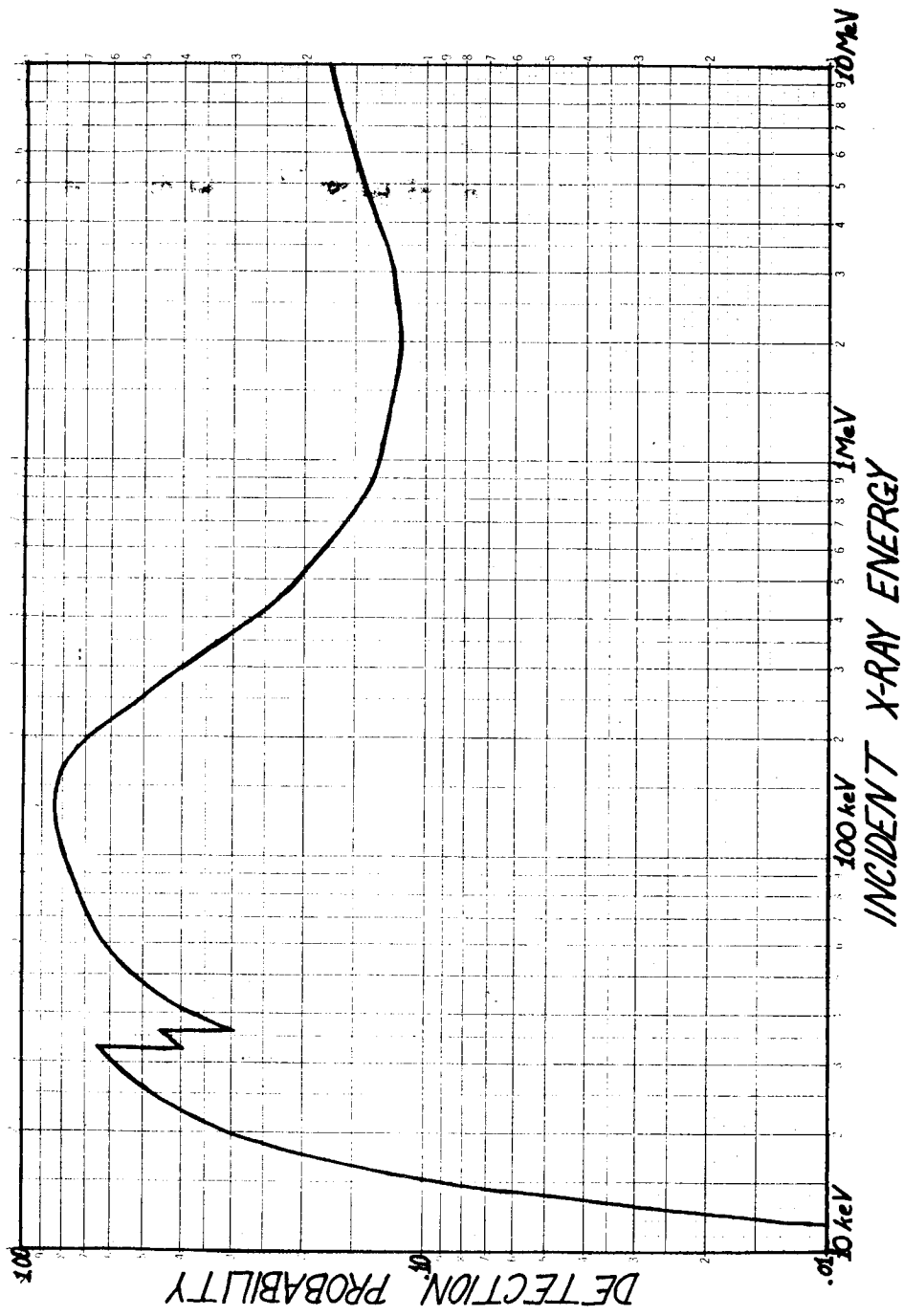


Figure 2. The detector efficiency as a function of photon energy.

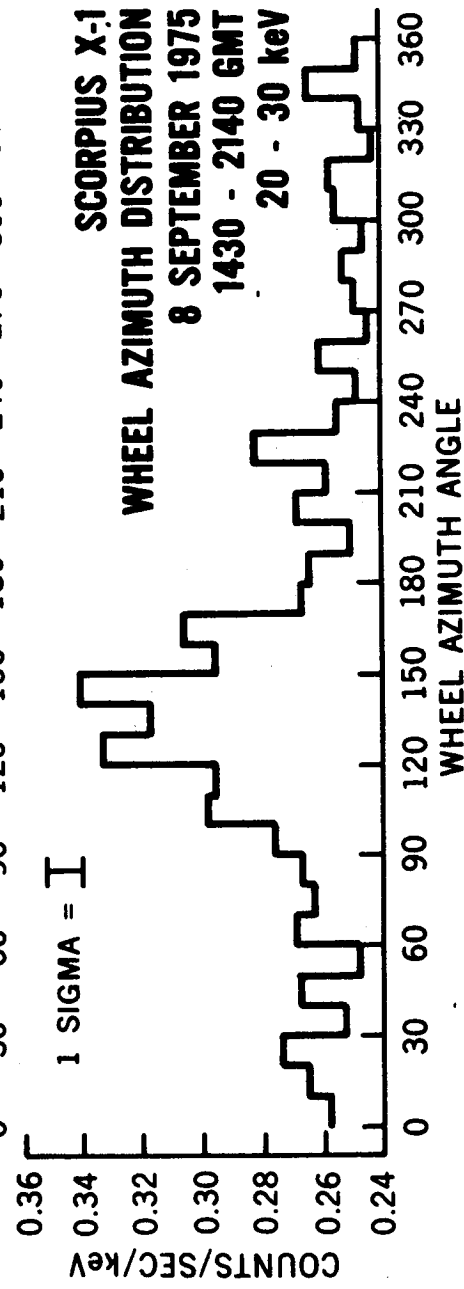
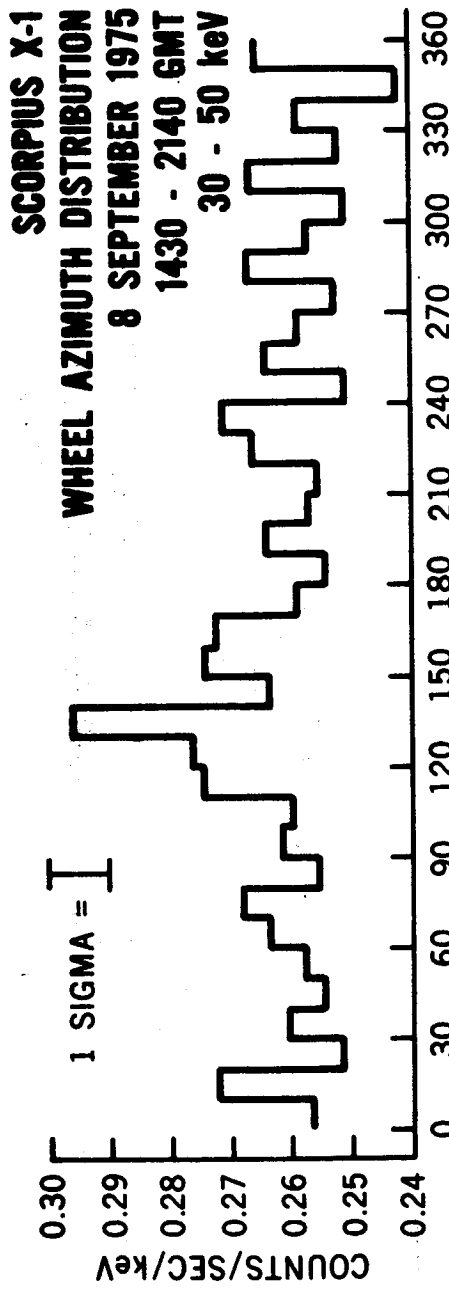


Figure 3. Distribution of counting rates for Sco X-1 as a function of detector wheel-azimuth angle.

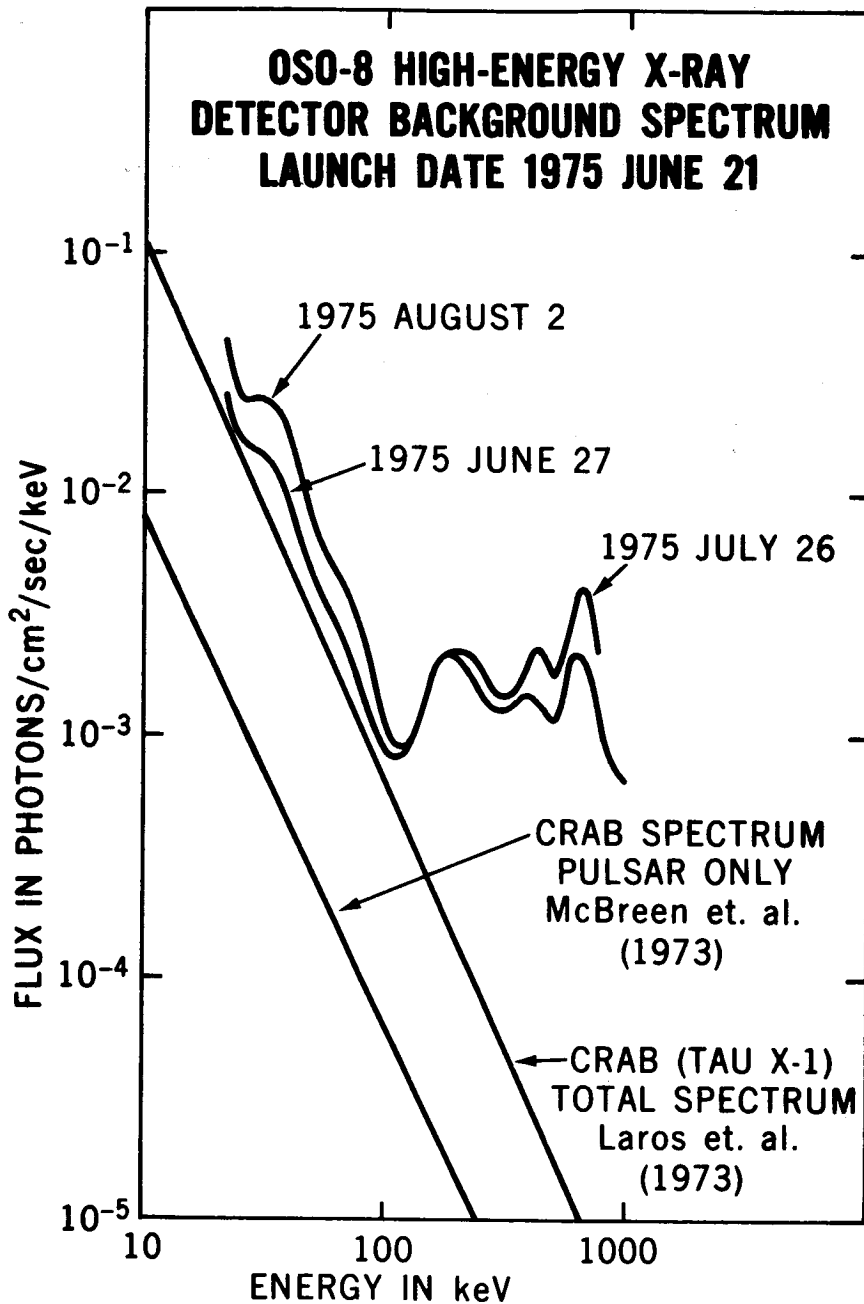


Figure 4. X-ray detector background spectra corrected for detector efficiency measured at different times after launch. The Crab spectra (total and pulsed) are also included for comparison.

ULTRAVIOLET OBSERVATIONS FROM IUE

A. K. DUPREE

Center for Astrophysics, Harvard College Observatory
and Smithsonian Astrophysical Observatory

The launch of the International Ultraviolet Explorer (IUE) Satellite in 1977 will allow the first ultraviolet spectroscopy of X-ray sources. The 45-cm aperture telescope will have two echelle spectrographs covering the wavelength region $\lambda\lambda$ 1135 - 3255 Å with both high and low dispersion. The high dispersion format gives a resolving power $\lambda/\Delta\lambda$ of 10^4 to 1.5×10^4 ; the low dispersion format has a resolution of ~ 6 Å. I.U.E. will be operated under a Guest Observer program which includes both U. S. and European astronomers.

Some scientific goals of ultraviolet observations will be outlined; the cooperative monitoring program will be described.

OBSERVATIONAL PROGRAMS

Discussion

A. Bunner to R. Thomas:

I would just like to say a few words concerning the capabilities of the Wisconsin Soft X-Ray experiment on OSO-8 to add to the information put on X-ray Binaries. This experiment covers the spectrum from 0.13 keV to about 50 keV with 16 energy channels, including 6 channels below 1.5 keV. So we are looking forward, when our data tapes finally begin to arrive, to testing spectral models in the soft X-ray region for the source mechanism and temperature and for line-of-sight absorption such as might help settle the question of the distance to Nova Monocerotis, for example, or the question of how low the Cen X-3 cut-off energy gets.

CLOSING WORDS

Yoji Kondo
NASA Johnson Space Center
Houston, Texas 77058, U.S.A.

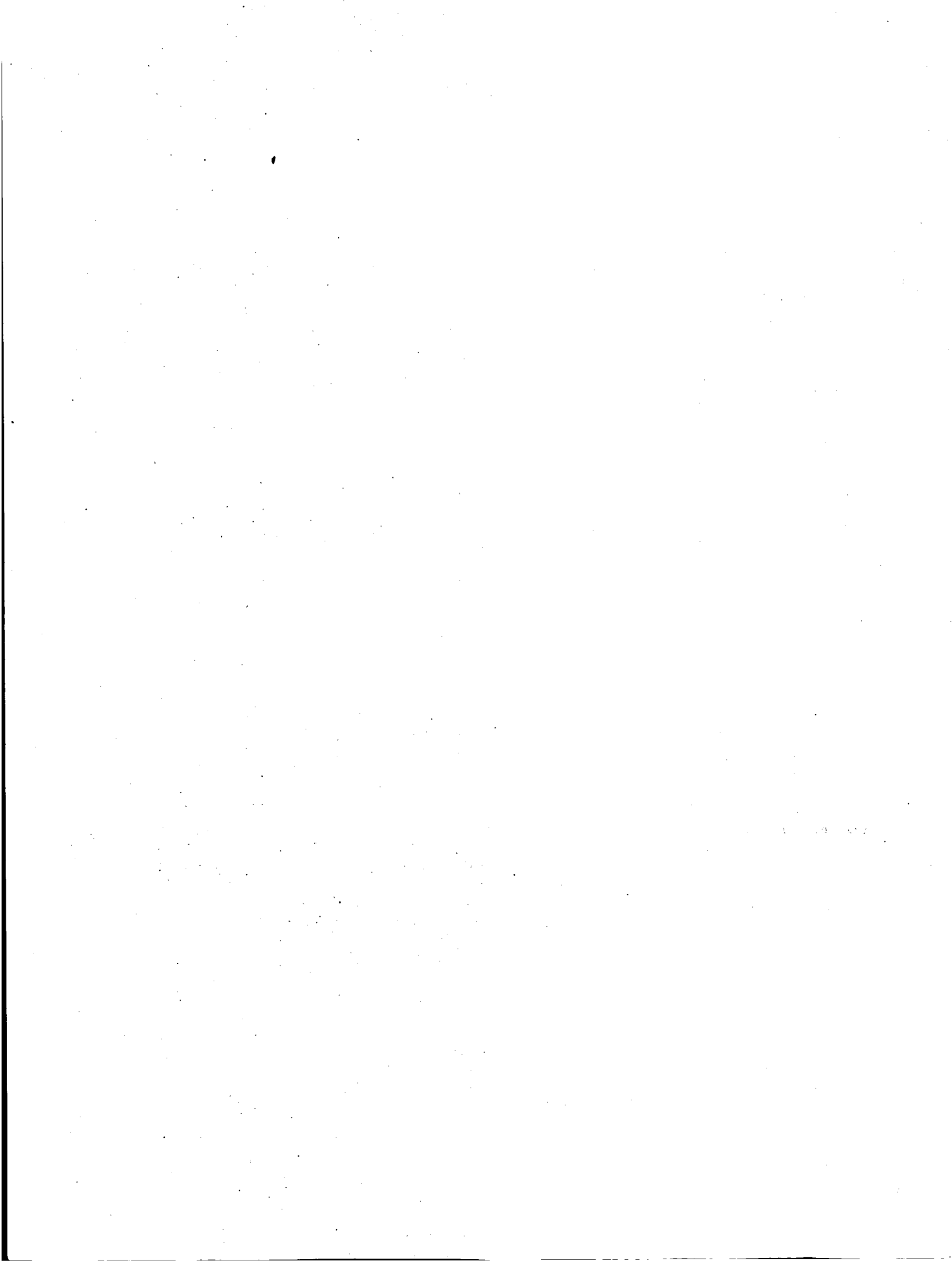
The symposium was attended by some 150 participants including X-ray experimenters, ground-based optical and radio observers, theorists and satellite ultraviolet experimenters. During these three days, numerous recent results were presented and interesting and sometimes heated discussions were exchanged. We feel that the original objectives of the workshop were satisfactorily fulfilled; that is to say, the meeting provided an arena for exchange of information and an opportunity for the workers from different disciplines and/or from different corners of the world to become acquainted with each other.

The very popularity of the meeting, which resulted in a rather crowded schedule for each session, necessitated limitations on the length of discussions following each paper. This is not very uncommon, of course, and, hopefully, the summaries given by the chairman after each session have partially compensated for it.

Regarding coordinated (simultaneous) observations of X-ray binaries, it seems to me a more practical and realistic idea to designate an individual to manage a campaign on a specific object. (There have been some precedents, e.g., the campaign to observe Cyg X-3 organized by Dr. Hjellming last year). Such an individual would of course be better acquainted with specific problems involved and know what sort of observations are critical. Dr. Hjellming indicated an interest in Cyg X-3; similarly, Dr. Bolton has an interest in Cyg X-1.

In closing, I wish to express my personal appreciation to those who participated in the symposium and made it such a stimulating and rewarding experience. I should also like to acknowledge, in behalf of all the participants, our gratitude to Dr. E. Boldt who gave a great deal of himself to make this conference such a resounding success.

18 November 1975.



A SYMPOSIUM ON X-RAY BINARIES
Workshop Program for Coordinated Campaign - IAU Commissions 42 and 44

Goddard Space Flight Center, Greenbelt, Maryland
October 20-22, 1975

Registered Participants

S. P. S. Anand
Code 680
NASA/GSFC
Greenbelt, MD 20771

Giulio Auriemma
Laboratorio di Astrofisica
Casella Postale 67
Frascati, Italy

Yoram Avni
Dept. of Physics
Weizmann Institute
Rehovot, Israel

John Bahcall
Institute for Advanced Study
Princeton, New Jersey 08540

William Baity
Univ. of California
Mail Code C-011
LaJolla, California 92093

Jim Beall
Code 682
NASA/GSFC
Greenbelt, MD 20771

Robert H. Becker
Code 661
NASA/GSFC
Greenbelt, MD 20771

P. L. Bernacca
Osservatorio Astrofisico
36012 Asiago
(Vicenza) Italy

Richard Bleach
13131 Larchdale Road
Laurel, Maryland 20811

Nancy W. Boggess
Code SG
NASA Headquarters
Washington, DC 20546

C. T. Bolton
David Dunlap Observatory
University of Toronto
Richmond Hill, Ontario
Canada L4C 4Y6

Donald J. Bord
Dept. of Physics
Dartmouth College
Hanover, New Hampshire 03755

Hale Bradt
37-581, M.I.T.
Cambridge, Massachusetts 02139

Kenneth Brecher
Room 6-201
M.I.T.
Cambridge, Massachusetts 02139

A. C. Brinkman
Astronomical Institute
Space Research Laboratory
Beneluxlaan 21, Utrecht
The Netherlands

Alan N. Bunner
Dept. of Physics
Univ. of Wisconsin
Madison, Wisconsin 53706

Claude R. Canizares
37-501
M.I.T.
Cambridge, Massachusetts 02139

R. C. Catura
Lockheed Research Lab.
Bldg. 202, Dept. 52-12
3251 Hanover Street
Palo Alto, California 94304

P. A. Charles
Mullard Space Science Lab.
Univ. College London
Holmbury St. Mary
Dorking, Surrey, England

Talbot Chubb
5023 N. 38th Street
Arlington, Virginia

George Clark
37-611
M.I.T.
Cambridge, Massachusetts 02139

G. G. Cohen
Columbia Astrophysics Lab.
538 W. 120th Street
New York, NY 10027

A. P. Cowley
Astronomy Department
Univ. of Michigan
Ann Arbor, Michigan 48104

David Crampton
Astronomy Department
Univ. of Michigan
Ann Arbor, Michigan 48104

C. J. Crannell
Code 682
NASA/GSFC
Greenbelt, MD 20771

R. Cruddace
Naval Research Laboratory
Washington, DC 20375

J. L. Culhane
Mullard Space Science Lab.
Univ. College London
Holmbury St. Mary
Dorking, Surrey, England

Arthur F. Davidsen
Dept. of Physics
Johns Hopkins University
Baltimore, Maryland 21218

B. Dennis
Code 682
NASA/GSFC
Greenbelt, MD 20771

E. J. Devinney, Jr.
Code 673
NASA/GSFC
Greenbelt, MD 20771

J. F. Dolan
Warner & Swasey Obs.
1975 Taylor Road
E. Cleveland, Ohio 44112

Robert F. Doolittle
1290 Monument Street
Pacific Palisades
California 90272

A. K. Dupree
Center for Astrophysics
60 Garden Street
Cambridge, Massachusetts 02138

Douglas M. Eardley
Physics Department
Yale University
New Haven, Connecticut 06520

Andrew Endal
Code 671
NASA/GSFC
Greenbelt, MD 20771

L. Fisk
Code 660
NASA/GSFC
Greenbelt, MD 20771

Brian P. Flannery
Institute for Advanced Study
Princeton, New Jersey 08540

Gordon P. Garmire
320-47 Cal Tech
Pasadena, California 91125

Jonathan Grindlay
Center for Astrophysics
Smithsonian Obs.
60 Garden Street
Cambridge, Massachusetts 02138

H. Gursky
Center for Astrophysics
60 Garden Street
Cambridge, Massachusetts 02138

Michael G. Hauser
Code 661
NASA/GSFC
Greenbelt, MD 20771

John Heise
Space Research Laboratory
Beneluxlaan 21, Utrecht
The Netherlands

Richard C. Henry
Physics Department
Johns Hopkins University
Baltimore, Maryland 21218

T. J. Herczeg
Dept. Physics & Astronomy
Univ. of Oklahoma
Norman, Oklahoma 73069

Robert M. Hjellming
Rte. 3, Box 127
Charlottesville, Virginia 22901

S. Holt
Code 661
NASA/GSFC
Greenbelt, Maryland 20771

J. B. Hutchings
Dominion Astrophysical Obs.
RR 7
Victoria, B.C., Canada

Sergio A. Ilovaisky
DPh-EP Cen Saclay
B.P. No. 2
91190 Gif sur Yvette
France

W. Neil Johnson
Code 7128
Naval Research Laboratory
Washington, DC 20375

W. V. Jones
Code 660
NASA/GSFC
Greenbelt, MD 20771

Paul C. Joss
Rm. 6-314
M.I.T.
Cambridge, Massachusetts 02139

Louis J. Kaluziński
Code 661
NASA/GSFC
Greenbelt, MD 20771

Jonathan Katz
Institute for Advanced Study
Princeton, New Jersey 08540

Howard Kestenbaum
Columbia Astrophysics Lab.
538 W. 120th Street
New York, NY 10027

Robert H. Koch
Dept. of Astronomy
Univ. of Pennsylvania
Philadelphia, Pa. 19174

Y. Kondo
Astrophysics Section
TN 23
Johnson Space Center
Houston, Texas 77058

Wojciech Krzeminski
Institute of Astronomy
Al. Ujazdowskie 4
Warsaw, Poland

James D. Kurfess
Naval Research Laboratory
Washington, DC 20375

D. Q. Lamb
Dept. of Physics
Univ. of Illinois
Urbana, Illinois 61801

F. K. Lamb
Dept. of Physics
Univ. of Illinois
Urbana, Illinois 61801

Richard C. Lamb
Code 662
NASA/GSFC
Greenbelt, MD 20771

William Liller
Center for Astrophysics
60 Garden Street
Cambridge, Massachusetts 02138

Knox S. Long
Columbia Astrophysics Lab.
1038 W. 120th Street
New York, N.Y. 10027

Robert Lucke
Naval Research Laboratory
Washington, DC 20375

John Mack
Geosciences Department
State College
1300 Elmwood
Buffalo, New York 14222

R. K. Manchanda
Tata Institute
Bombay, India

Steve Maran
Code 683
NASA/GSFC
Greenbelt, Maryland 20771

Bruce Margon
Space Sciences Lab.
Univ. of California
Berkeley, California 94720

K. O. Mason
Mullard Space Science Lab.
Univ. College London
Holmbury St. Mary
Dorking, Surrey, England

T. Matilsky
Center for Space Science
M.I.T.
Cambridge, Massachusetts 02139

James L. Matteson
Physics Dept. C-011
Univ. of Calif., San Diego
La Jolla, California 92037

Horst Mauder
D-7400 Tuebingen
Waldhaeuser Strasse 64
West Germany

Jeffrey E. McClintock
Rm. 37-521, M.I.T.
Cambridge, Massachusetts 02139

George E. McCluskey, Jr.
Div. of Astron./Math Dept.
Lehigh University
Bethlehem, Pennsylvania 18015

Richard Messina
Amos Tuck School
Dartmouth College
Hanover, New Hampshire 03755

William Muney
Code 683
NASA/GSFC
Greenbelt, Maryland 20771

Paul Murdin
Royal Greenwich Observatory
Hailsham, Sussex
United Kingdom

R. Novick
Columbia Astrophysics Lab.
538 West 120th Street
New York, N.Y. 10027

Kenichiro Ohki
Code 682
NASA/GSFC
Greenbelt, Maryland 20771

J. Ormes
Code 661
NASA/GSFC
Greenbelt, Maryland 20771

Frazer Owen
N.R.A.O.
Edgemont Road
Charlottesville, Virginia 22901

William S. Paciesas
Physics Department
Code C-011, Univ. of Calif.
LaJolla, California 92037

D. Parsignault
Am. Science & Engr., Inc.
955 Massachusetts Avenue
Cambridge, Massachusetts 02139

Jacques Paul
DPh-EP Cen Saclay
B.P. No. 2 91190 Gif
sur Yvette
France

J. A. Petterson
Physics Department
Yale University
New Haven, Connecticut

K. A. Pounds
Univ. of Leicester
Dept. of Physics
Leicester LR1 7RH
United Kingdom

Steven H. Pravdo
Code 661
NASA/GSFC
Greenbelt, Maryland 20771

Reuven Ramaty
Code 660
NASA/GSFC
Greenbelt, Maryland 20771

George Ricker
M.I.T.
Cambridge, Massachusetts 02139

Guenther R. Riegler
183-701, Jet Prop. Lab.
Pasadena, California 91103

William K. Rose
Astronomy Program
Univ. of Maryland
College Park, Maryland 20742

Jeffrey D. Rosendhal
NASA Headquarters
Code SG
Washington, D.C. 20546

Richard Rothschild
Code 661
NASA/GSFC
Greenbelt, Maryland 20771

Charles E. Ryter
Code 661
NASA/GSFC
Greenbelt, Maryland 20771

J. Saba
Code 661
NASA/GSFC
Greenbelt, Maryland 20771

Richard St. John
Dept. Physics & Astronomy
Univ. of New Mexico
Albuquerque, New Mexico 87131

Wolfgang Schmidt
Code 661
NASA/GSFC
Greenbelt, Maryland 20771

H. Schnopper
Center for Astrophysics
60 Garden Street
Cambridge, Massachusetts 02138

E. Schreier
Center for Astrophysics
60 Garden Street
Cambridge, Massachusetts 02138

Peter J. Serlemitsos
Code 661
NASA/GSFC
Greenbelt, Maryland 20771

Seth Shulman
Naval Research Laboratory
Code 7125
Washington, D.C. 20375

Robert Silverberg
Code 661
NASA/GSFC
Greenbelt, Maryland 20771

C. L. Smith
TRW Systems
Bldg. R5, Rm. 1010
1 Space Park
Redondo Beach, Calif. 90278

Toon Snijders
Code 671
NASA/GSFC
Greenbelt, Maryland 20771

T. Snow
Princeton Univ. Observatory
Payton Hall
Princeton, New Jersey 08540

William Snyder
Dept. of Physics
Johns Hopkins University
Baltimore, Maryland 21218

S. Sobieski
Code 673
NASA/GSFC
Greenbelt, Maryland 20771

S. Sofia Code SG NASA Headquarters Washington, D. C. 20546	M. S. Vardya Code 671 NASA/GSFC Greenbelt, Maryland 20771	Richard Wolfson Dept. Physics & Astronomy Dartmouth College Hanover, New Hampshire 03755
Warren Sparks Code 671 NASA/GSFC Greenbelt, Maryland 20771	N. V. Vidal Center for Astrophysics 60 Garden Street Cambridge, Massachusetts 02138	Bruce Woodgate NASA/GSFC Code 683 Greenbelt, Maryland 20771
Rudiger Staubert 74 Tubingen Astronom. Institut of Univ. Tubingen Waldhauserstr. 64 Germany	E. N. Walker (permanent address) Royal Greenwich Observatory Hailsham, Sussex England until January 1976 Observatorio Univ. DeCartuja Paseo De Cartuja Apartado 32 Granada, Spain	Chi-Chao Wu Dept. Space Research Univ. of Groningen P.O. Box 800 Groningen The Netherlands
T. P. Stecher Code 672 NASA/GSFC Greenbelt, Maryland 20771	Martin C. Weisskopf Columbia Astrophysics Lab. 538 W. 120th Street New York, N.Y. 10027	Daryl Yentis Naval Research Laboratory Code 7129.2 Washington, D. C. 20375
George Strougylis Univ. of Maryland 2204 Phelps Road, Apt. 205 College Park, Maryland	Charles Wende Code 601 NASA/GSFC Greenbelt, Maryland 20771	
Jean Swank Code 661 NASA/GSFC Greenbelt, Maryland 20771	John A. Wheeler Dept. of Physics Princeton University Princeton, New Jersey 08540	
Roger J. Thomas Code 682 NASA/GSFC Greenbelt, Maryland 20771	A. P. Willmore Dept. of Space Research Univ. of Birmingham P.O. Box 363 Edgbaston, Birmingham B152TT England	
Virginia Trimble Astronomy Program Univ. of Maryland College Park, Maryland 20742	P. Frank Winkler Middlebury College Middlebury, Vermont	
J. Trumper Astron. Institut of Univ. Tubingen 74 Tubingen Waldhauserstr. 64 Germany	George W. Wolf Physics Department Southwest Missouri State Univ. Springfield, Missouri 65802	
I. R. Tuohy Physics Department Caltech Pasadena, California 91125	Richard Wolff Columbia Astrophysics Lab. Box 129 Pubin Hall 538 W. 120th Street New York, N.Y. 10027	Elihu Boldt Code 661 NASA/GSFC Greenbelt, Maryland 20771
Anne B. Underhill Code 670 NASA/GSFC Greenbelt, Maryland 20771		

AUTHOR INDEX

A

Aalders, J. W. G., 353
 Acton, L. W., 119
 Angel, J. R. P., 53
 Arnett, W. D., 659
 Auriemma, G., 485
 Avni, Y., 615

B

Bahcall, J. N., 99, 615
 Ballantine, J. E., 279
 Beall, J., 739
 Becker, R. H., 67, 161, 207, 737
 Benedict, G. F., 551
 Bernacca, P. L., 101
 Boldt, E. A., 67, 113, 161, 207, 245, 311
 369, 391, 443, 703, 737
 Boley, F., 327
 Bolton, C. T., 465
 Bord, D. J., 677
 Bowyer, S., 691
 Bradt, H., 317, 373
 Branduardi, G., 559, 717
 Brecher, K., 359
 Brinkman, A. C., 27, 241, 349
 Buff, J., 373
 Bunner, A. N., 187

C

Canizares, C. R., 373
 Capps, R. W., 355
 Cardini, D., 485
 Catura, R. C., 119
 Charles, P. A., 629
 Chevallier, C., 717
 Cohen, G. G., 53, 81
 Costa, E., 485
 Cowley, A. P., 683
 Crampton, D., 683
 Crannell, C. J., 739
 Culhane, J. L., 1, 629

D

Davidson, A. F., 127, 285, 691
 De Loore, C., 643
 Delvaille, J. P., 49
 den Boggende, A. J. F., 241, 349
 Dennis, B. R., 739
 Deviney, E. J., 361
 Dolan, J. F., 493
 Doty, J. P., 279
 Duerbeck, H. W., 343
 Dupree, A. K., 539, 747

E

Eardley, D. M., 379
 Elvis, M., 245
 Endal, A. S., 361
 Epstein, A., 49

F

Fabbiano, G., 197
 Friedman, H., 127, 285
 Fritz, G., 127, 285
 Frost, K. J., 739

G

Garmire, G. P., 727
 Giovannelli, F., 485
 Grindlay, J. E., 49, 267, 429
 Gronenschild, E., 241, 349
 Gulden, S. L., 499
 Gull, T. R., 347
 Gursky, H., 49, 267, 429, 669

H

Hammerschlag-Hensberge, G., 529, 643
 Heise, J., 27, 241, 349
 Henize, K. G., 347, 551

- Henry, R. C., 127, 285
Hiltner, W. A., 677
Hjellming, R. M., 229, 233, 495
Holt, S. S., 67, 113, 161, 207, 245, 311,
391, 443, 703, 737
Hutchings, J. B., 531,
- I
- Ilovaisky, S. A., 717
Ives, J., 255
- J
- Joss, P. C., 661
Joyce, R. R., 355
- K
- Kalata, K., 49
Kaluzienski, L. J., 245 311, 391, 703
Kendziorra, E., 277
Kestenbaum, H. L., 53, 81
Kester, D., 353
Kleinmann, S. G., 355
Kondo, Y., 499, 551,
Kriss, G. A., 279
Krzemiński, W., 555
- L
- Lamb, D. Q., 659
Lamb, F. K., 141, 659
Landecker, P. B., 53, 81
Laros, J. G., 407
Laufer, B., 373
Lester, J. B., 539
Lewin, W. H. G., 279
Liller, W., 155, 335, 513
- Mc
- McClintock, J., 661
McCluskey, G. E., Jr., 499
- M
- Malina, R., 691
Maran, S. P., 293
Margon, B., 719
Mason, K. O., 1, 255, 559, 629
Matilsky, T., 317
Matteson, J. L., 407
Mauder, H., 173, 177, 179
Mewe, R., 241, 349
Mook, D. E., 677
Morrison, P., 359
Murdin, P., 425
Mushotzky, R. F., 407
- N
- Novick, R., 53, 81
- O
- Orwig, L. E., 739
- P
- Paciesas, W. S., 407
Parsignault, D. R., 49, 267, 429
Parsons, S. B., 551
Peacock, A., 245
Petro, L., 677
Petterson, J. A., 159
Pietsch, W., 277
Pines, D., 141
Pounds, K. A., 245
Pravdo, S., H., 67, 161, 207, 245, 737
- R
- Ranieri, M., 485
Rappaport, S., 661
Regener, V. H., 171
Ricker, G. R., 279
Rothschild, R. E., 67, 113, 161, 207, 443, 737
Ryckman, S. G., 279
Ryter, C., 189

S

Sanders, W. T., 187
 Sanford, P. W., 1, 255, 559, 629, 717
 Scheepmaker, A., 279
 Schnopper, H. W., 49, 267, 429
 Schreier, E. J., 49, 197, 267, 429
 Schrijver, H., 241, 349
 Serlemitsos, P. J., 67, 113, 161, 207, 245,
 311, 391, 443, 703, 737
 Shaham, J., 141
 Shulman, S., 127, 285
 Snow, T. P., Jr., 347
 Snyder, W. A., 127, 285
 Sofia, S., 361
 Sohval, A. R., 49
 Staubert, R., 277
 St. John, R. H., 169, 171
 Swank, J. H., 67, 161, 207, 737

T

Takens, R. J., 643
 Thomas, R. J., 729
 Truemper, J., 277
 Tuohy, I. R., 219

V

van den Heuvel, E. P. J., 643
 van Duinen, R. J., 353, 529
 van Paradis, J. A., 643
 Vidal, N. V., 575,

W

Walker, E. N., 521, 569
 Walter, K., 343
 Watson, M. G., 245
 Weisskopf, M. C., 53, 81, 453
 Wesselius, P. R., 353
 White, N. E., 1, 629
 Wolff, R. S., 53, 81
 Wolfson, R., 327
 Wray, J. D., 551
 Wu, Chi-Chao, 353, 529

Y

Yentis, D., 285
 York, D. G., 347

Z

Zuiderwijk, E. J., 643